

STUDY ON PERFORMANCE OF SUBMERGED VANES WITH COLLAR

A THESIS

*Submitted in fulfilment of the
requirements for the award of the degree*

of

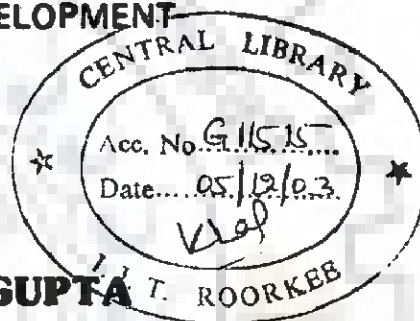
DOCTOR OF PHILOSOPHY

in

WATER RESOURCES DEVELOPMENT

By

UMESH PRASAD GUPTA



WATER RESOURCES DEVELOPMENT TRAINING CENTRE
INDIAN INSTITUTE OF TECHNOLOGY ROORKEE
ROORKEE-247 667 (INDIA)

MAY, 2003



INDIAN INSTITUTE OF TECHNOLOGY ROORKEE
ROORKEE

CANDIDATE'S DECLARATION

I hereby certify that the work which is being presented in the thesis entitled "STUDY ON PERFORMANCE OF SUBMERGED VANES WITH COLLAR" in fulfilment of the requirement for the award of the Degree of Doctor of Philosophy and submitted in the Water Resources Development Training Centre, Indian Institute of Technology, Roorkee, is an authentic record of my own work carried out during a period from January 2001 to May 2003 under the supervision of Dr. Nayan Sharma, Professor, Water Resources Development Training Centre, Indian Institute of Technology, Roorkee, and Dr. C.S.P. Ojha, Associate Professor, Department of Civil Engineering, Indian Institute of Technology, Roorkee.

The matter presented in this thesis has not been submitted by me for the award of any other degree of this or any other institute/university.

(UMESH PRASAD GUPTA)

This is to certify that the above statement made by the candidate is correct to the best of our knowledge.

Dr. C.S.P. Ojha
Associate Professor
Dept. of Civil Engineering

Dr. Nayan Sharma
Professor
Water Resources Development
Training Centre

Indian Institute of Technology, Roorkee

Dated: May 27, 2003

The Ph.D Viva-Voce examination of Umesh Prasad Gupta, Research Scholar, has been held on _____

Signature of Supervisor(s) Signature of H.O.D. Signature of External Examiner



INDIAN INSTITUTE OF TECHNOLOGY ROORKEE, 2003

ALL RIGHTS RESERVED

ABSTRACT

Increasing capital costs, emerging environmental concerns and rising maintenance expenses of the conventional river training works around the world have led to the development of submerged vanes in practice. Submerged vanes are being favoured for control of sediment movement, scour and deposition. The submerged vane functions through generation of secondary circulation for bringing about desired sediment redistribution within the channel cross-section. The strength of secondary circulation is profoundly influenced by the magnitude of the incident angle of vane to the approach flow direction. Most of the studies on submerged vanes are restricted to the incident angle in the range of 15° to 20° . In recent years, researchers have been experimenting with higher incident angles in their search for an optimal angle of a submerged vane for to extract optimal level of secondary circulation. However, the major impediment in the use of an optimal angle from the standpoint of secondary circulation hinges on occurrence of destabilizing local scour phenomenon especially around the leading edge of the vane. Research forays into the problem of scour reduction around a submerged vane for ensuring its stability have not yet been reported by the investigators so far. The main thrust of the present study is centered around the use of collar as an effective device to restrict the incidence of destabilizing scour phenomenon around a submerged vane.

In this study, elaborate experimentations have been conducted to investigate the problem in depth with different collar and submerged vane configurations to determine the optimal angle of attack. Most of the earlier investigators experimented with Froude numbers falling between 0 to 0.25. Therefore, two Froude numbers were selected for the study, one was 0.25 and other was kept in the middle range of it as 0.13. The local scour around the different types of submerged vanes such as rectangular, trapezoidal, double

curve type I, double curve type II, J1 and J2 type were studied without collar for Froude numbers 0.13 and 0.25.

The maximum scour depth was observed to have taken place in the case of rectangular vanes. Therefore, scour influencing variables were identified for rectangular vanes and also the model was developed for scour depth considering the rectangular vane. It was observed from the model that flow Froude number is more important than the densimetric Froude number. Cost analysis was carried out for the conventional method of riprap with filter and the collar for retardation of scour hole formation at the leading edge of rectangular vane for two Froude numbers of 0.13 and 0.25. The collar was found to be better option economically.

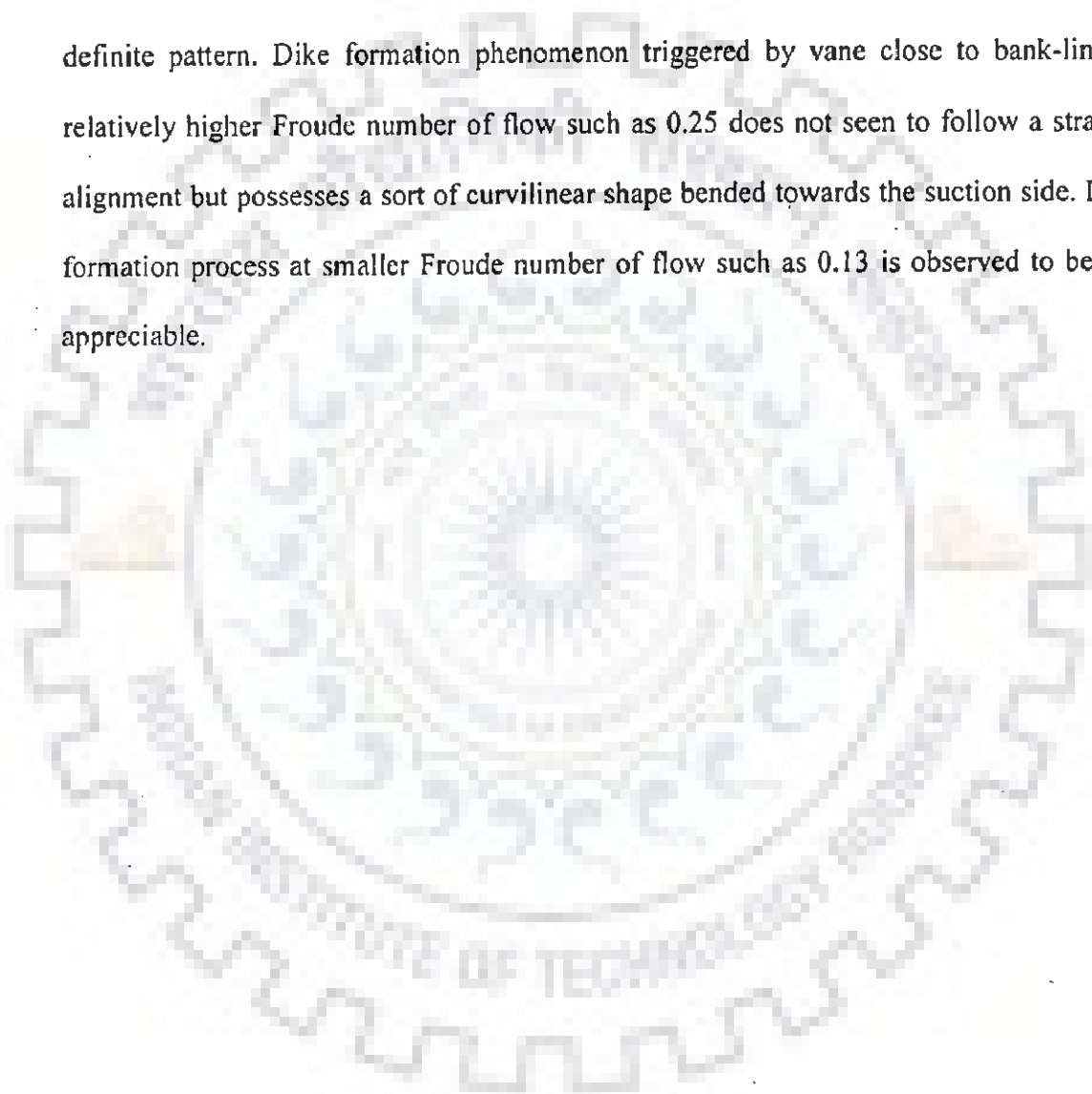
The most effective performance of the collar device was found for rectangular and trapezoidal vanes at the two Froude numbers of 0.13 and 0.25 with two representative median size sediments considered in the study namely 0.225 mm and 0.405 mm. Field study in the Solani river near Roorkee was carried out and it was found that the collar is highly effective in reduction the local scour around the vane, without any material impairment of its hydraulic function.

Optimal angle of attack for rectangular vane with collar considering three different degrees of submergence was investigated and its value lies close to 40° as reported by other researchers. It could be seen that the optimal angle of attack remains insensitive to degree of submergence and also remains unaffected by collar. Optimal angle of attack was also determined in case of curved vanes such as double curve type I, double curve type II, J1 and J2 type and its value in these cases was found to lie close to 45° .

Tapering of leading edge of rectangular vane with collar (called trapezoidal vane here) is found to noticeably influence the strength of vane induced secondary circulation

at the same angle of attack and similar hydraulic condition. Also the aspect ratio was seen to wield considerable influence on the rectangular vane induced secondary circulation at the optimal angle of attack, 40° and for the similar hydraulic condition.

A dimensionless moment of momentum (MOM) concept has been introduced in this work to study the vane induced secondary circulation. Streamwise decay of vane induced secondary circulation for rectangular and trapezoidal vane is not found to exhibit definite pattern. Dike formation phenomenon triggered by vane close to bank-line at relatively higher Froude number of flow such as 0.25 does not seem to follow a straight alignment but possesses a sort of curvilinear shape bended towards the suction side. Dike formation process at smaller Froude number of flow such as 0.13 is observed to be not appreciable.



ACKNOWLEDGEMENT

I take this opportunity to record my sincere gratitude and indebtedness to Dr. Nayan Sharma, Professor, W.R.D.T.C. and Dr. C.S.P. Ojha, Associate Professor, Dept. of Civil Engineering I.I.T. Roorkee, for their expert guidance, constant encouragement, constructive criticism and very fruitful discussions at various stages of the research work presented in this thesis.

I am indebted to Prof. M.K. Mittal, Dept. of Civil Engineering, I.I.T. Roorkee for the fruitful discussions during my research work.

I am very much thankful to Chairman, Central Water Commission, Government of India who permitted me to pursue this research work.

I owe my gratitude to Dr. Fredrick Marelius, Royal Institute of Technology, Stockholm (Sweden) for the help extended during my research work.

I am highly thankful to all faculty and staff of WRDTC specially Prof. Gopal Chauhan, Prof. G.C. Mishra and Dr. B.N. Asthana, Professor Emeritus for their continuous and moral encouragement during this research work.

The assistance rendered by Sri Beer Singh Chauhan, Sri Ram Dular, Sri Hari Singh, Sri Anurag Kumar and Sri Yogendra Sharma during the experimental investigations is thankfully acknowledged.

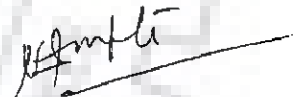
I am also thankful to Prof. P.K. Swamee, Prof. K.G. Ranga Raju, Sri A.D. Pandey, Dr. N.K. Samadhiya (I.I.T. Roorkee); Mr. T.S. Patil, Dr. Naresh Kumar (C.W.C.); Mr. M.G. Sharma, Mr. K. Venkatesh (R/S); Miss Shailza Verma (R/A) Dr. S.K. Sinha (USA) and Neeraj (Computer Operator) who helped me in different ways during research work.

On the top of every thing, I extremely grateful to my Late Parents Sri Awadh Lal Gupta and Smt. Tara Devi, Late grandmother Smt. Dairani Devi and Late father in-law Sri Manohar Gupta, who had always given me blessings and dreamed in me to make me responsible to complete this research work. I am also grateful to my pious mother in-law Smt. Drupadi Devi for her help through her divine eyes during the research work.

Love, affections, encouragement shown by my elder brothers and lovely sisters Urmila, Leela are also acknowledged. Thanks are also due to my niece Miss Manu Manisha for her cooperation during the research work.

The last and never the least, the immense love, encouragement and sacrifice given by my wife and manager of my experimental data Smt. Binita Gupta is gratefully acknowledged

But in my whole effort the angelic soul who suffered most: at my hands elder son Abhinav (Johnty) and younger son Monty who could not get enough love and care from my side which was due to them at their very small ages.



(UMESH PRASAD GUPTA)

CONTENTS

	Page No.
<i>Candidate's Declaration</i>	(i)
<i>Abstract</i>	(ii)
<i>Acknowledgement</i>	(v)
<i>Contents</i>	(vii)
<i>List of Tables</i>	(xi)
<i>List of Figures</i>	(xvi)
<i>List of Plates</i>	(xxiii)
<i>Notations</i>	(xxvi)
Chapter 1	
INTRODUCTION	1
1.1 GENERAL	1
1.2 LOCAL SCOUR REDUCTIONS WITH COLLAR IN CASE OF SUBMERGED VANES	4
1.3 OBJECTIVES OF THE STUDY	5
1.4 ORGANISATION OF THESIS	6
Chapter 2	8
REVIEW OF LITERATURE	
2.1 GENERAL	8
2.2 SOME SECONDARY CURRENT GENERATING STRUCTURES	8
2.2.1 Bandalling	8
2.2.2 Surface Panels	9
2.2.3 Bottom Panels	10
2.3 PRINCIPLE OF SUBMERGED VANES AND GENERAL GUIDE LINES	11
2.3.1 Case Study on Performance of Submerged Vanes	15
2.4 LOCAL SCOUR AROUND SUBMERGED VANES	17
2.5 COLLAR AS SCOUR RETARDER	18
2.6 VARIABLES INFLUENCING SUBMERGED VANES PERFORMANCE	20
2.6.1 Shapes of Submerged Vanes	20
2.6.2 Optimal Angle of Attack	21
2.6.3 Degree of Submergence	21

2.6.4	Streamwise Spacing of Submerged Vanes	22
2.6.5	Tapering of Leading Edge of Submerged Vanes	24
2.6.6	Aspect Ratio of Submerged Vanes	24
2.7	SUMMARY	25
Chapter 3	EXPERIMENTAL PROGRAMME	27
3.1	GENERAL	27
3.2	LABORATORY FLUME	28
3.2.1	Sediments Used	30
3.2.2	Other Equipment	30
3.3	EXPERIMENTAL PROCEDURE	33
3.4	PHASE ONE MODEL EXPERIMENTS	34
3.5	PHASE TWO MODEL EXPERIMENTS	38
3.6	PHASE THREE MODEL EXPERIMENTS	55
3.7	PHASE FOUR MODEL EXPERIMENTS	58
3.8	PHASE FIVE PROTOTYPE FIELD EXPERIMENTS	59
Chapter 4	PERFORMANCE EVALUATION OF SUBMERGED VANES WITHOUT COLLAR	62
4.1	GENERAL	62
4.2	SCOUR AROUND SUBMERGED VANES WITHOUT COLLAR	62
4.3	FUNCTIONAL RELATIONSHIPS FOR SCOUR	69
4.4	COST COMPARISON	74
Chapter 5	PERFORMANCE EVALUATION OF SUBMERGED VANES WITH COLLAR	81
5.1	GENERAL	81
5.2	COLLAR AS SCOUR RETARDER	83
5.3	LOCATION OF COLLAR	83
5.4	MOST EFFECTIVE COLLAR	84
5.4.1	Experiments at Froude Number 0.13 and d_{50} as 0.225 mm	85
5.4.1.1	Rectangular vane	85
5.4.1.2	Trapezoidal vane (3H:2.5V)	96
5.4.2	Experiments at Froude Number 0.25 and d_{50} as 0.225 mm	113

	5.4.2.1 Rectangular vane	113
	5.4.2.2 Trapezoidal vane (3H:2.5V)	113
	5.4.3 Experiments at Froude Number 0.25 and d_{50} as 0.405 mm	118
	5.4.3.1 Rectangular vane	118
	5.4.3.2 Trapezoidal vane (3H:2.5V)	144
	5.4.4 Experiments at Froude Number 0.13 and d_{50} as 0.405 mm	154
	5.4.4.1 Rectangular vane	154
	5.4.4.2 Trapezoidal vane (3H:2.5V)	154
5.5	RESULTS	159
5.6	PROTOTYPE FIELD STUDY	161
5.7	SUMMARY	167
Chapter 6	VARIATION OF STRENGTH OF VORTEX	168
6.1	GENERAL	168
6.2	ASSESSMENT OF STRENGTH OF VORTEX	168
6.3	OPTIMAL ANGLE OF ATTACK	171
	6.3.1 Rectangular Vanes	171
	6.3.1.1 Dimensional considerations	175
	6.3.2 Vanes with Alternative Shapes	178
6.4	EFFECT OF ASPECT RATIO	182
6.5	EFFECT OF TAPER ANGLE	182
6.6	CHANGE OF PRESSURE SIDES IN CURVED VANES	185
6.7	SUMMARY	186
Chapter 7	DIKE FORMATION AND DECAY OF STRENGTH OF VORTEX WITH DOWNSTREAM	187
7.1	GENERAL	187
7.2	FORMATION OF DIKES	188
	7.2.1 Formation of Dikes Downstream of Vane	188
	7.2.2 Formation of Dike along the Vane in Suction side	194
7.3	STREAMWISE DECAY OF STRENGTH OF VORTEX	196
7.4	SUMMARY	202

Chapter 8	GENERAL REMARKS, CONCLUSIONS & FUTURE WORK	203
8.1	GENERAL REMARKS	203
8.2	CONCLUSIONS	205
8.3	FUTURE SCOPE OF WORK	207
REFERENCES		208
APPENDIX - A	COST COMPARISON OF RIPRAP WITH FILTER VIS A VIS COLLAR	217
A.1	COMPUTATIONS RELATED TO FROUDE NUMBER 0.13	217
APPENDIX - B	EXPERIMENTAL DATA RELATING TO PERFORMANCE EVALUATION OF SUBMERGED VANES WITH COLLAR	219
APPENDIX - C	EXPERIMENTAL DATA RELATING TO VARIATION OF STRENGTH OF VORTEX	263
APPENDIX - D	EXPERIMENTAL DATA RELATING TO DIKE FORMATION AND DECAY OF STRENGTH OF VORTEX WITH DOWNSTREAM	281

LIST OF TABLES

Table No.	Title	Page No.
Table 2.1	Aspect ratio used or recommended by different investigator	24
Table 3.1	The sieve analysis of the sediment material of $d_{50} = 0.225$ mm	31
Table 3.2	The sieve analysis of the sediment material of $d_{50} = 0.405$ mm	31
Table 3.3	Phase one experiments	35
Table 3.4	Phase two experiments	54
Table 3.5	Dimensions of trapezoidal vane	56
Table 3.6	Phase three experiments	57
Table 3.7	Phase four experiments	58
Table 3.8	The sieve analysis of the bed material of river Solani at the vane construction spot	60
Table 4.1	Data relating to scour hole with rectangular vane (aspect ratio = 0.33)	77
Table 4.2	Estimation of filter area and volume of scour hole (rectangular vane, d_{50} as 0.225 mm)	78
Table 4.3	Cost of riprap with filter	78
Table 5.1	Froude numbers used by different investigators	82
Table 5.2	Summary of most effective collars	160
Table 6.1	Moment of Momentum at different nodes	172
Table 6.2	Computations of optimal α for rectangular vane	175
Table 6.3	Computations of optimal α for curved vane	181
Table 7.1	Distance of protected area from trailing edge of vanes	188
Table 7.2	Modelled equations for dike formation for different taper angles	189
Table B.1	Experimental data for rectangular vane ($F_r = 0.13$, $d_{50} = 0.225$ mm, Collar size AF1.1)	220
Table B.2	Experimental data for rectangular vane ($F_r = 0.13$, $d_{50} = 0.225$ mm, Collar size AF1.2)	221

Table B.3 Experimental data for rectangular vane ($F_r = 0.13$, $d_{50} = 0.225$ mm, Collar size AF1.3)	222
Table B.4 Experimental data for rectangular vane ($F_r = 0.13$, $d_{50} = 0.225$ mm, Collar size AF1.4)	223
Table B.5 Experimental data for rectangular vane ($F_r = 0.13$, $d_{50} = 0.225$ mm, Collar size AF1.5)	224
Table B.6 Experimental data for rectangular vane ($F_r = 0.13$, $d_{50} = 0.225$ mm, Collar size AF1.6)	225
Table B.7 Experimental data for rectangular vane ($F_r = 0.13$, $d_{50} = 0.225$ mm, Collar size AF1.7)	226
Table B.8 Experimental data for rectangular vane ($F_r = 0.13$, $d_{50} = 0.225$ mm, Collar size AF1.8)	227
Table B.9 Experimental data for trapezoidal vane (3H:2.5V) ($F_r = 0.13$, $d_{50} = 0.225$ mm, Collar size BF1.1)	228
Table B.10 Experimental data for trapezoidal vane (3H:2.5V) ($F_r = 0.13$, $d_{50} = 0.225$ mm, Collar size BF1.2)	229
Table B.11 Experimental data for trapezoidal vane (3H:2.5V) ($F_r = 0.13$, $d_{50} = 0.225$ mm, Collar size BF1.3)	230
Table B.12 Experimental data for trapezoidal vane (3H:2.5V) ($F_r = 0.13$, $d_{50} = 0.225$ mm, Collar size BF1.4)	231
Table B.13 Experimental data for trapezoidal vane (3H:2.5V) ($F_r = 0.13$, $d_{50} = 0.225$ mm, Collar size BF1.5)	232
Table B.14 Experimental data for trapezoidal vane (3H:2.5V) ($F_r = 0.13$, $d_{50} = 0.225$ mm, Collar size BF1.6)	233
Table B.15 Experimental data for trapezoidal vane (3H:2.5V) ($F_r = 0.13$, $d_{50} = 0.225$ mm, Collar size BF1.7)	234
Table B.16 Experimental data for trapezoidal vane (3H:2.5V) ($F_r = 0.13$, $d_{50} = 0.225$ mm, Collar size BF1.8)	235
Table B.17 Experimental data for trapezoidal vane (3H:2.5V) ($F_r = 0.13$, $d_{50} = 0.225$ mm, Collar size BF1.9)	236
Table B.18 Experimental data for trapezoidal vane (3H:2.5V) ($F_r = 0.13$, $d_{50} = 0.225$ mm, Collar size BF1.10)	237

Table B.19 Experimental data for trapezoidal vane (3H:2.5V) ($F_r = 0.13$, $d_{50} = 0.225$ mm, Collar size BF1.11)	238
Table B.20 Experimental data for trapezoidal vane (3H:2.5V) ($F_r = 0.13$, $d_{50} = 0.225$ mm, Collar size BF1.12)	239
Table B.21 Experimental data for trapezoidal vane (3H:2.5V) ($F_r = 0.13$, $d_{50} = 0.225$ mm, Collar size BF1.13)	240
Table B.22 Experimental data for trapezoidal vane (3H:2.5V) ($F_r = 0.13$, $d_{50} = 0.225$ mm, Collar size BF1.14)	241
Table B.23 Experimental data for rectangular vane ($F_r = 0.25$, $d_{50} = 0.225$ mm, Collar size AF2.12)	242
Table B.24 Experimental data for trapezoidal vane (3H:2.5V) ($F_r = 0.25$, $d_{50} = 0.225$ mm, Collar size BF2.5)	243
Table B.25 Experimental data for rectangular vane ($F_r = 0.25$, $d_{50} = 0.405$ mm, Collar size AF2.1)	244
Table B.26 Experimental data for rectangular vane ($F_r = 0.25$, $d_{50} = 0.405$ mm, Collar size AF2.2)	245
Table B.27 Experimental data for rectangular vane ($F_r = 0.25$, $d_{50} = 0.405$ mm, Collar size AF2.3)	246
Table B.28 Experimental data for rectangular vane ($F_r = 0.25$, $d_{50} = 0.405$ mm, Collar size AF2.4)	247
Table B.29 Experimental data for rectangular vane ($F_r = 0.25$, $d_{50} = 0.405$ mm, Collar size AF2.5)	248
Table B.30 Experimental data for rectangular vane ($F_r = 0.25$, $d_{50} = 0.405$ mm, Collar size AF2.6)	249
Table B.31 Experimental data for rectangular vane ($F_r = 0.25$, $d_{50} = 0.405$ mm, Collar size AF2.7)	250
Table B.32 Experimental data for rectangular vane ($F_r = 0.25$, $d_{50} = 0.405$ mm, Collar size AF2.8)	251
Table B.33 Experimental data for rectangular vane ($F_r = 0.25$, $d_{50} = 0.405$ mm, Collar size AF2.9)	252
Table B.34 Experimental data for rectangular vane ($F_r = 0.25$, $d_{50} = 0.405$ mm, Collar size AF2.10)	253
Table B.35 Experimental data for rectangular vane ($F_r = 0.25$, $d_{50} = 0.405$ mm, Collar size AF2.11)	254

Table B.36 Experimental data for rectangular vane ($F_r = 0.25$, $d_{50} = 0.405$ mm, Collar size AF2.12)	255
Table B.37 Experimental data for trapezoidal vane (3H:2.5V) ($F_r = 0.25$, $d_{50} = 0.405$ mm, Collar size BF2.1)	256
Table B.38 Experimental data for trapezoidal vane (3H:2.5V) ($F_r = 0.25$, $d_{50} = 0.405$ mm, Collar size BF2.2)	257
Table B.39 Experimental data for trapezoidal vane (3H:2.5V) ($F_r = 0.25$, $d_{50} = 0.405$ mm, Collar size BF2.3)	258
Table B.40 Experimental data for trapezoidal vane (3H:2.5V) ($F_r = 0.25$, $d_{50} = 0.405$ mm, Collar size BF2.4)	259
Table B.41 Experimental data for trapezoidal vane (3H:2.5V) ($F_r = 0.25$, $d_{50} = 0.405$ mm, Collar size BF2.5)	260
Table B.42 Experimental data for rectangular vane ($F_r = 0.13$, $d_{50} = 0.405$ mm, Collar size AF1.8)	261
Table B.43 Experimental data for trapezoidal vane (3H:2.5V) ($F_r = 0.13$, $d_{50} = 0.405$ mm, Collar size BF2.14)	262
Table C.1 3D velocity components for rectangular vane ($T/d = 0.60$)	264
Table C.2 3D velocity components for rectangular vane ($T/d = 0.67$)	266
Table C.3 3D velocity components for rectangular vane ($T/d = 0.75$)	268
Table C.4 3D velocity components for double curve type I vane ($T/d = 0.67$)	270
Table C.5 3D velocity components for double curve type II vane ($T/d = 0.67$)	272
Table C.6 3D velocity components for J1 type vane ($T/d = 0.67$)	274
Table C.7 3D velocity components for J2 type vane ($T/d = 0.67$)	276
Table C.8 3D velocity components for rectangular vane with different aspect ratio (Angle of attack = 40° , $T/d = 0.67$)	278
Table C.9 3D velocity components for trapezoidal vane with different taper angles (Angle of attack = 40° , $T/d = 0.67$)	279
Table D.1 Experimental data relating to dike formation for rectangular and trapezoidal vanes	283

Table D.2	Experimental data relating to dike formation along the rectangular vane in suction side(Angle of attack = 40° , $F_r = 0.25$, $T/d = 0.57$)	283
Table D.3	3D velocity components for rectangular vane without collar (Angle of attack = 40° , $F_r = 0.13$, $T/d = 0.57$)	284
Table D.4	3D velocity components for rectangular vane with collar (Angle of attack = 40° , $F_r = 0.13$, $T/d = 0.57$)	285
Table D.5	3D velocity components for trapezoidal vane (1H:1V) (Angle of attack = 40° , $F_r = 0.13$, $T/d = 0.57$)	286
Table D.6	3D velocity components for trapezoidal vane (3H:2.5V) (Angle of attack = 40° , $F_r = 0.13$, $T/d = 0.57$)	287
Table D.7	3D velocity components for trapezoidal vane (4H:2V) (Angle of attack = 40° , $F_r = 0.13$, $T/d = 0.57$)	288
Table D.8	3D velocity components for rectangular vane without collar (Angle of attack = 40° , $F_r = 0.25$, $T/d = 0.57$)	289
Table D.9	3D velocity components for rectangular vane with collar (Angle of attack = 40° , $F_r = 0.25$, $T/d = 0.57$)	290
Table D.10	3D velocity components for trapezoidal vane (1H:1V) (Angle of attack = 40° , $F_r = 0.25$, $T/d = 0.57$)	291
Table D.11	3D velocity components for trapezoidal vane (3H:2.5V) (Angle of attack = 40° , $F_r = 0.25$, $T/d = 0.57$)	292
Table D.12	3D velocity components for trapezoidal vane (4H:2V) (Angle of attack = 40° , $F_r = 0.25$, $T/d = 0.57$)	293

LIST OF FIGURES

Figure No.	Title	Page No.
Fig. 1.1	Definition sketch of submerged vane	2
Fig. 3.1	Plan of tilting flume and its components used in experiments	29
Fig. 3.2	Cummulative frequency curve for sand $d_{50} = 0.225$ mm	32
Fig. 3.3	Cummulative frequency curve for sand $d_{50} = 0.405$ mm	32
Fig. 3.4(a)	Shape and size of double curve type I vane	36
Fig. 3.4(b)	Shape and size of double curve type II vane	36
Fig. 3.5(a)	Shape and size of J1 vane	37
Fig. 3.5(b)	Shape and size of J2 vane	37
Fig. 3.6(1)	Collar size AF1.1	39
Fig. 3.6(2)	Collar size AF1.2	39
Fig. 3.6(3)	Collar size AF1.3	39
Fig. 3.6(4)	Collar size AF1.4	39
Fig. 3.6(5)	Collar size AF1.5	40
Fig. 3.6(6)	Collar size AF1.6	40
Fig. 3.6(7)	Collar size AF1.7	40
Fig. 3.6(8)	Collar size AF1.8	40
Fig. 3.7(1)	Collar size BF1.1	41
Fig. 3.7(2)	Collar size BF1.2	41
Fig. 3.7(3)	Collar size BF1.3	41
Fig. 3.7(4)	Collar size BF1.4	41
Fig. 3.7(5)	Collar size BF1.5	42

Fig. 3.7(6) Collar size BF1.6	42
Fig. 3.7(7) Collar size BF1.7	42
Fig. 3.7(8) Collar size BF1.8	42
Fig. 3.7(9) Collar size BF1.9	43
Fig. 3.7(10) Collar size BF1.10	43
Fig. 3.7(11) Collar size BF1.11	43
Fig. 3.7(12) Collar size BF1.12	43
Fig. 3.7(13) Collar size BF1.13	44
Fig. 3.7(14) Collar size BF1.14	44
Fig. 3.8(1) Collar size AF1.1	45
Fig. 3.8(2) Collar size AF1.2	45
Fig. 3.8(3) Collar size AF1.3	46
Fig. 3.8(4) Collar size AF1.4	46
Fig. 3.8(5) Collar size AF1.5	47
Fig. 3.8(6) Collar size AF1.6	47
Fig. 3.8(7) Collar size AF1.7	48
Fig. 3.8(8) Collar size AF1.8	48
Fig. 3.8(9) Collar size AF1.9	49
Fig. 3.8(10) Collar size AF1.10	49
Fig. 3.8(11) Collar size AF1.11	50
Fig. 3.8(12) Collar size AF1.12	50
Fig. 3.9(1) Collar size BF1.1	51
Fig. 3.9(2) Collar size BF1.2	51
Fig. 3.9(3) Collar size BF1.3	52
Fig. 3.9(4) Collar size BF1.4	52

Fig. 3.9(5) Collar size BF1.5	53
Fig 3.10 Trapezoidal vane	56
Fig. 3.11 Cumulative frequency curve for sand $d_{50} = 0.200$ mm (Field trial in Solani river)	60
Fig. 4.1 Variation of D_{50}/d_{50} with F_D at different d/d_{50}	72
Fig. 4.2 Variation of D_{50}/d with F_D at different d/d_{50}	72
Fig. 4.3 Variation of D_{50}/d_{50} with F_D at different d/d_{50}	73
Fig. 4.4 Variation of D_{50}/d_{50} with F_r at different d/d_{50}	73
Fig. 4.5 Comparison of computed data with observed data	74
Fig. 4.6 Definition sketch around rectangular submerged vane ($F_r = 0.25$, $d_{50} = 0.225$ mm)	76
Fig. 4.7 Idealised typical scour hole at the leading edge of rectangular submerged vane	78
Fig. 5.1 Scour pattern for rectangular vane with collar AF1.1 ($d_{50} = 0.225$ mm, $F_r = 0.13$, contour interval in cm)	86
Fig. 5.2 Scour pattern for rectangular vane with collar AF1.2 ($d_{50} = 0.225$ mm, $F_r = 0.13$, contour interval in cm)	87
Fig. 5.3 Scour pattern for rectangular vane with collar AF1.3 ($d_{50} = 0.225$ mm, $F_r = 0.13$, contour interval in cm)	88
Fig. 5.4 Scour pattern for rectangular vane with collar AF1.4 ($d_{50} = 0.225$ mm, $F_r = 0.13$, contour interval in cm)	89
Fig. 5.5 Scour pattern for rectangular vane with collar AF1.5 ($d_{50} = 0.225$ mm, $F_r = 0.13$, contour interval in cm)	90
Fig. 5.6 Scour pattern for rectangular vane with collar AF1.6 ($d_{50} = 0.225$ mm, $F_r = 0.13$, contour interval in cm)	91
Fig. 5.7 Scour pattern for rectangular vane with collar AF1.7 ($d_{50} = 0.225$ mm, $F_r = 0.13$, contour interval in cm)	92
Fig. 5.8 Scour pattern for rectangular vane with collar AF1.8 ($d_{50} = 0.225$ mm, $F_r = 0.13$, contour interval in cm)	94
Fig. 5.9 Scour pattern for trapezoidal vane with collar BF1.1 ($d_{50} = 0.225$ mm, $F_r = 0.13$, contour interval in cm)	97

Fig. 5.10	Scour pattern for trapezoidal vane with collar BF1.2 ($d_{50} = 0.225$ mm, $F_r = 0.13$, contour interval in cm)	98
Fig. 5.11	Scour pattern for trapezoidal vane with collar BF1.3 ($d_{50} = 0.225$ mm, $F_r = 0.13$, contour interval in cm)	99
Fig. 5.12	Scour pattern for trapezoidal vane with collar BF1.4 ($d_{50} = 0.225$ mm, $F_r = 0.13$, contour interval in cm)	100
Fig. 5.13	Scour pattern for trapezoidal vane with collar BF1.5 ($d_{50} = 0.225$ mm, $F_r = 0.13$, contour interval in cm)	101
Fig. 5.14	Scour pattern for trapezoidal vane with collar BF1.6 ($d_{50} = 0.225$ mm, $F_r = 0.13$, contour interval in cm)	102
Fig. 5.15	Scour pattern for trapezoidal vane with collar BF1.7 ($d_{50} = 0.225$ mm, $F_r = 0.13$, contour interval in cm)	103
Fig. 5.16	Scour pattern for trapezoidal vane with collar BF1.8 ($d_{50} = 0.225$ mm, $F_r = 0.13$, contour interval in cm)	104
Fig. 5.17	Scour pattern for trapezoidal vane with collar BF1.9 ($d_{50} = 0.225$ mm, $F_r = 0.13$, contour interval in cm)	105
Fig. 5.18	Scour pattern for trapezoidal vane with collar BF1.10 ($d_{50} = 0.225$ mm, $F_r = 0.13$, contour interval in cm)	106
Fig. 5.19	Scour pattern for trapezoidal vane with collar BF1.11 ($d_{50} = 0.225$ mm, $F_r = 0.13$, contour interval in cm)	107
Fig. 5.20	Scour pattern for trapezoidal vane with collar BF1.12 ($d_{50} = 0.225$ mm, $F_r = 0.13$, contour interval in cm)	108
Fig. 5.21	Scour pattern for trapezoidal vane with collar BF1.13 ($d_{50} = 0.225$ mm, $F_r = 0.13$, contour interval in cm)	109
Fig. 5.22	Scour pattern for trapezoidal vane with collar BF1.14 ($d_{50} = 0.225$ mm, $F_r = 0.13$, contour interval in cm)	111
Fig. 5.23	Scour pattern for rectangular vane with collar AF2.12 ($d_{50} = 0.225$ mm, $F_r = 0.25$, contour interval in cm)	114
Fig. 5.24	Scour pattern for trapezoidal vane with collar BF2.5 ($d_{50} = 0.225$ mm, $F_r = 0.25$, contour interval in cm)	116
Fig. 5.25	Scour pattern for rectangular vane with collar AF2.1 ($d_{50} = 0.405$ mm, $F_r = 0.25$, contour interval in cm)	120

Fig. 5.26	Scour pattern for rectangular vane with collar AF2.2 ($d_{50} = 0.405$ mm, $F_r = 0.25$, contour interval in cm)	122
Fig. 5.27	Scour pattern for rectangular vane with collar AF2.3 ($d_{50} = 0.405$ mm, $F_r = 0.25$, contour interval in cm)	124
Fig. 5.28	Scour pattern for rectangular vane with collar AF2.4 ($d_{50} = 0.405$ mm, $F_r = 0.25$, contour interval in cm)	126
Fig. 5.29	Scour pattern for rectangular vane with collar AF2.5 ($d_{50} = 0.405$ mm, $F_r = 0.25$, contour interval in cm)	128
Fig. 5.30	Scour pattern for rectangular vane with collar AF2.6 ($d_{50} = 0.405$ mm, $F_r = 0.25$, contour interval in cm)	130
Fig. 5.31	Scour pattern for rectangular vane with collar AF2.7 ($d_{50} = 0.405$ mm, $F_r = 0.25$, contour interval in cm)	132
Fig. 5.32	Scour pattern for rectangular vane with collar AF2.8 ($d_{50} = 0.405$ mm, $F_r = 0.25$, contour interval in cm)	134
Fig. 5.33	Scour pattern for rectangular vane with collar AF2.9 ($d_{50} = 0.405$ mm, $F_r = 0.25$, contour interval in cm)	136
Fig. 5.34	Scour pattern for rectangular vane with collar AF2.10 ($d_{50} = 0.405$ mm, $F_r = 0.25$, contour interval in cm)	138
Fig. 5.35	Scour pattern for rectangular vane with collar AF2.11 ($d_{50} = 0.405$ mm, $F_r = 0.25$, contour interval in cm)	140
Fig. 5.36	Scour pattern for rectangular vane with collar AF2.12 ($d_{50} = 0.405$ mm, $F_r = 0.25$, contour interval in cm)	142
Fig. 5.37	Scour pattern for trapezoidal vane with collar BF2.1 ($d_{50} = 0.405$ mm, $F_r = 0.25$, contour interval in cm)	145
Fig. 5.38	Scour pattern for trapezoidal vane with collar BF2.2 ($d_{50} = 0.405$ mm, $F_r = 0.25$, contour interval in cm)	147
Fig. 5.39	Scour pattern for trapezoidal vane with collar BF2.3 ($d_{50} = 0.405$ mm, $F_r = 0.25$, contour interval in cm)	149
Fig. 5.40	Scour pattern for trapezoidal vane with collar BF2.4 ($d_{50} = 0.405$ mm, $F_r = 0.25$, contour interval in cm)	151
Fig. 5.41	Scour pattern for trapezoidal vane with collar BF2.5 ($d_{50} = 0.405$ mm, $F_r = 0.25$, contour interval in cm)	152
Fig. 5.42	Scour pattern for rectangular vane with collar AF.8 ($d_{50} = 0.405$ mm, $F_r = 0.13$, contour interval in cm)	155

Fig. 5.43	Scour pattern for trapezoidal vane with collar BF.14 ($d_{50} = 0.405$ mm, $F_r = 0.13$, contour interval in cm)	157
Fig. 6.1	Grid points for the collection of data	169
Fig. 6.2	Definition sketch for velocity vectors	169
Fig. 6.3	Optimal angle of attack for rectangular vane ($T/d = 0.60$)	173
Fig. 6.4	Optimal angle of attack for rectangular vane ($T/d = 0.67$)	173
Fig. 6.5	Optimal angle of attack for rectangular vane ($T/d = 0.75$)	174
Fig. 6.6	Optimal angle of attack for rectangular vane at different T/d	174
Fig. 6.7	Comparison of MOM* for rectangular vane at different T/d	177
Fig. 6.8	Comparison of MOM** for rectangular vane at different T/d	177
Fig. 6.9	Optimal angle of attack for double curve type I vane ($T/d = 0.67$)	179
Fig. 6.10	Optimal angle of attack for double curve type II vane ($T/d = 0.67$)	179
Fig. 6.11	Optimal angle of attack for J1 type vane ($T/d = 0.67$)	180
Fig. 6.12	Optimal angle of attack for J2 type vane ($T/d = 0.67$)	180
Fig. 6.13	Comparison of MOM* for different types of vanes ($T/d = 0.67$)	183
Fig. 6.14	Effect of aspect ratio on MOM* ($\alpha = 40^\circ$, $T/d = 0.67$)	183
Fig. 6.15	Effect of taper angle on MOM* ($\alpha = 40^\circ$, $T/d = 0.67$)	184
Fig. 6.16	Change of pressure sides in curved vanes	185
Fig. 7.1	Definition sketch of origin for measurement of dike formation downstream of vane	189
Fig. 7.2	Dike alignment across the flow with different taper angles	191
Fig. 7.3	Dike alignment across the flow with different taper angles	191
Fig. 7.4	Dike alignment across the flow with vertical leading edge vane	192
Fig. 7.5	Dike alignment across the flow with taper angle (1H:1V)	192
Fig. 7.6	Dike alignment across the flow with taper angle (3H:2.5V)	193

Fig. 7.7	Dike alignment across the flow with taper angle (4H:2V)	193
Fig. 7.8	Definition sketch of origin for formation of dike formation along the vane	194
Fig. 7.9	Dike alignment along the rectangular vane in suction side (in vertical plane)	195
Fig. 7.10	Streamwise variation of MOM* for rectangular vane without collar at F_r 0.13	197
Fig. 7.11	Streamwise variation of MOM* for rectangular vane with collar at F_r 0.13	197
Fig. 7.12	Streamwise variation of MOM* for trapezoidal (1H:1V) vane with collar at F_r 0.13	198
Fig. 7.13	Streamwise variation of MOM* for trapezoidal (3H:2.5V) vane with collar at F_r 0.13	198
Fig. 7.14	Streamwise variation of MOM* for trapezoidal (4H:2V) vane with collar at F_r 0.13	199
Fig. 7.15	Streamwise variation of MOM* for rectangular vane without collar at F_r 0.25	199
Fig. 7.16	Streamwise variation of MOM* for rectangular vane with collar at F_r 0.25	200
Fig. 7.17	Streamwise variation of MOM* for trapezoidal vane (1H:1V) with collar at F_r 0.25	200
Fig. 7.18	Streamwise variation of MOM* for trapezoidal vane (3H:2.5V) with collar at F_r 0.25	201
Fig. 7.19	Streamwise variation of MOM* for trapezoidal vane (4H:2V) with collar at F_r 0.25	201
Fig. B.1	Definition sketch of origin for measurement of scour pattern	219
Fig. C.1	Definition sketch of origin for three dimensional velocity measurements	263
Fig. D.1	Definition sketch of origin for measurement of dike formation downstream of vane	281
Fig.D.2	Definition sketch of origin for measurement of dike formation along the vane	282
Fig.D.3	Definition sketch of origin for three dimensional velocity measurements	282

LIST OF PLATES

Plate No.	Title	Page No.
Plate 4.1	Local scour with rectangular vane at $F_r = 0.13$ ($d_{50} = 0.225$ mm)	63
Plate 4.2	Local scour with rectangular vane at $F_r = 0.25$ ($d_{50} = 0.405$ mm)	63
Plate 4.3	Local scour with trapezoidal vane(3H:2.5V) at $F_r = 0.13$ ($d_{50} = 0.225$ mm)	64
Plate 4.4	Local scour with trapezoidal vane(3H:2.5V) at $F_r = 0.25$ ($d_{50} = 0.405$ mm)	64
Plate 4.5	Local scour with double curve type I vane at $F_r = 0.13$ ($d_{50} = 0.225$ mm)	65
Plate 4.6	Local scour with double curve type I vane at $F_r = 0.25$ ($d_{50} = 0.405$ mm)	65
Plate 4.7	Local scour with double curve type II vane at $F_r = 0.13$ ($d_{50} = 0.225$ mm)	66
Plate 4.8	Local scour with double curve type II vane at $F_r = 0.25$ ($d_{50} = 0.405$ mm)	66
Plate 4.9	Local scour with J1 type vane at $F_r = 0.13$ ($d_{50} = 0.225$ mm)	67
Plate 4.10	Local scour with J1 type vane at $F_r = 0.25$ ($d_{50} = 0.405$ mm)	67
Plate 4.11	Local scour with J2 type vane at $F_r = 0.13$ ($d_{50} = 0.225$ mm)	68
Plate 4.12	Local scour with J2 type vane at $F_r = 0.25$ ($d_{50} = 0.405$ mm)	68
Plate 5.1	Scour pattern for rectangular vane with collar AF1.7 ($F_r = 0.13$, $d_{50} = 0.225$ mm)	93
Plate 5.2	Scour pattern for rectangular vane with collar AF1.8 ($F_r = 0.13$, $d_{50} = 0.225$ mm)	95
Plate 5.3	Scour pattern for trapezoidal vane (3H:2.5V) with collar AF1.13 ($F_r = 0.13$, $d_{50} = 0.225$ mm)	110
Plate 5.4	Scour pattern for trapezoidal vane (3H:2.5V) with collar AF1.14 ($F_r = 0.13$, $d_{50} = 0.225$ mm)	112
Plate 5.5	Scour pattern for rectangular vane with collar AF2.12 ($F_r = 0.25$, $d_{50} = 0.225$ mm)	115

Plate 5.6 Scour pattern for trapezoidal vane (3H:2.5V) with collar BF2.5 ($F_r = 0.25$, $d_{50} = 0.225$ mm)	117
Plate 5.7 Scour pattern for rectangular vane with collar AF2.1 ($F_r = 0.25$, $d_{50} = 0.405$ mm)	121
Plate 5.8 Scour pattern for rectangular vane with collar AF2.2 ($F_r = 0.25$, $d_{50} = 0.405$ mm)	123
Plate 5.9 Scour pattern for rectangular vane with collar AF2.3 ($F_r = 0.25$, $d_{50} = 0.405$ mm)	125
Plate 5.10 Scour pattern for rectangular vane with collar AF2.4 ($F_r = 0.25$, $d_{50} = 0.405$ mm)	127
Plate 5.11 Scour pattern for rectangular vane with collar AF2.5 ($F_r = 0.25$, $d_{50} = 0.405$ mm)	129
Plate 5.12 Scour pattern for rectangular vane with collar AF2.6 ($F_r = 0.25$, $d_{50} = 0.405$ mm)	131
Plate 5.13 Scour pattern for rectangular vane with collar AF2.7 ($F_r = 0.25$, $d_{50} = 0.405$ mm)	133
Plate 5.14 Scour pattern for rectangular vane with collar AF2.8 ($F_r = 0.25$, $d_{50} = 0.405$ mm)	135
Plate 5.15 Scour pattern for rectangular vane with collar AF2.9 ($F_r = 0.25$, $d_{50} = 0.405$ mm)	137
Plate 5.16 Scour pattern for rectangular vane with collar AF2.10 ($F_r = 0.25$, $d_{50} = 0.405$ mm)	139
Plate 5.17 Scour pattern for rectangular vane with collar AF2.11 ($F_r = 0.25$, $d_{50} = 0.405$ mm)	141
Plate 5.18 Scour pattern for rectangular vane with collar AF2.12 ($F_r = 0.25$, $d_{50} = 0.405$ mm)	143
Plate 5.19 Scour pattern for trapezoidal vane (3H:2.5V) with collar BF2.1 ($F_r = 0.25$, $d_{50} = 0.405$ mm)	146
Plate 5.20 Scour pattern for trapezoidal vane (3H:2.5V) with collar BF2.2 ($F_r = 0.25$, $d_{50} = 0.405$ mm)	148
Plate 5.21 Scour pattern for trapezoidal vane (3H:2.5V) with collar BF2.3 ($F_r = 0.25$, $d_{50} = 0.405$ mm)	150
Plate 5.22 Scour pattern for trapezoidal vane (3H:2.5V) with collar BF2.5 ($F_r = 0.25$, $d_{50} = 0.405$ mm)	153

Plate 5.23	Scour pattern rectangular vane with collar AF.8 ($F_r = 0.13$, $d_{50} = 0.405$ mm)	156
Plate 5.24	Scour pattern for trapezoidal vane (3H:2.5V) with collar BF1.14 ($F_r = 0.13$, $d_{50} = 0.405$ mm)	158
Plate 5.25	Trapezoidal Vane with Collar before installation in Solani River	162
Plate 5.26	Trapezoidal Vane without Collar before installation in Solani River	162
Plate 5.27	Augured end of pipe to facilitate driving in Solani River	163
Plate 5.28	Pipe is being driven in Solani River to support the vanes	163
Plate 5.29	Trapezoidal vane with collar in the process of installation in Solani River	164
Plate 5.30	Bed Profile in the vicinity of vane is being measured by dumpy level in Solani River	164
Plate 5.31	Trapezoidal vanes with and without collar installed in Solani River	165
Plate 5.32	Availability of water in Solani River on the day vanes installed	165
Plate 5.33	Vanes are fully submerged during the flood in Solani River	166
Plate 5.34	Sediment deposited on vanes after flood in Solani River	166
Plate 7.1	Scour hole at trailing edge of rectangular vane and dike formation along it in suction side ($F_r = 0.25$, $d_{50} = 0.405$ mm)	190
Plate 7.2	Dike formation in downstream of vane ($F_r = 0.25$, $d_{50} = 0.405$ mm)	190

NOTATIONS

A	cross sectional area of grid;
A_c	cross sectional area of collar;
A_f	cross sectional area of filter;
B	channel width;
B/d	channel width-depth ratio;
b	spur-dike width;
b_1	vane design section width;
C_c	cost of collar;
C_f	cost of filter;
C_{rf}	cost of riprap with filter;
c_L	lift coefficient;
d	pre-vane flow depth;
d_m	maximum flow depth;
d_v	vane induced flow depth;
d_{50}	median diameter of sediment;
d_{sc}	equilibrium scour depth in case of pier fitted with collar;
d_{sp}	equilibrium scour depth in case of pier without appurtenances;
\bar{d}	cross sectional average flow depth;
D	scour depth;
D_{sc}	computed scour depth;
D_{so}	observed scour depth;
D_1	pier diameter;
D_2	diameter of collar in case of bridge pier;

f	Darcy-Weisbach friction factor;
F	function;
F_D	sediment Froude number;
F_r	flow Froude number;
g	acceleration due to gravity;
H	vane height;
H/L	aspect ratio of the vane;
HP1	high pressure side of zone I;
HP2	high pressure side of zone II;
h	depth of collar below free water surface;
h_1	depth of idealized scour hole;
h_2	depth of bottom tip of idealized cone from the bottom of actual scour hole.;
$\bar{i}, \bar{j}, \bar{k}$	unit vectors in along X, Y, Z axes;
k	ratio of critical near-bed velocity to critical shear velocity;
L	vane length;
LM	linear momentum;
LP1	low pressure side of Zone I;
LP2	low pressure side of Zone II;
l	channel length along the flow;
l_1	inclined height of the cone;
l_2	inclined height of the bottom cone having radius R_1 ;
MOM	moment of momentum;
MOM*	dimensionless moment of momentum; (ratio of MOM and d times LM)

MOM^{**}	dimensionless moment of momentum; (ratio of MOM and H times LM)
m	mass;
m_1	resistance parameter;
N	number of vanes in lateral arrays;
n	exponent of power law velocity profile;
\bar{R}	location vector;
R_1	average radius of top circular shape of cone;
R_2	radius of bottom circular shape of cone;
R_a	top distance of extended scour hole in suction side from the leading edge of submerged vane;
R_b	top distance of extended scour hole in pressure side from the leading edge of submerged vane;
R_c	top distance of extended scour hole in upstream side from the leading edge of submerged vane;
r	channel radius (radius of curvature);
r/B	channel radius-width ratio;
r_c	mean channel radius;
r_f	rate of filter per unit area;
r_r	rate of riprap;
r_s	cost per unit weight of steel;
S	specific gravity of sediment;
T	water depth above the top of vane;
T/d	degree of submergence;
t	thickness of vane;
t_1	thickness collar;
U	mean flow velocity;

V_x, V_y, V_z time-average velocity components in X, Y, Z directions, respectively;

\bar{V}_x cross sectional average value of V_x ;

Vol_c volume of collar;

Vol_s volume of scour hole;

X, Y, Z cartesian axes; and

x, y, z streamwise, transverse and vertical coordinates, respectively.

Symbols

β angle of inclination of spur-dike;

ϕ bend angle;

μ dynamic viscosity of fluid;

ξ shape parameter describing geometry of spur;

σ standard deviation;

θ taper angle of vane;

α vane angle of attack;

α' vane angle with channel centerline;

κ Von Karman's constant (0.4);

$\Delta\gamma$ difference in specific weights between water and air;

$\Delta\gamma_s$ difference in specific weights between sediment and water;

ρ, ρ_s fluid and sediment density;

α_1 projected area/volume ratio for particle;

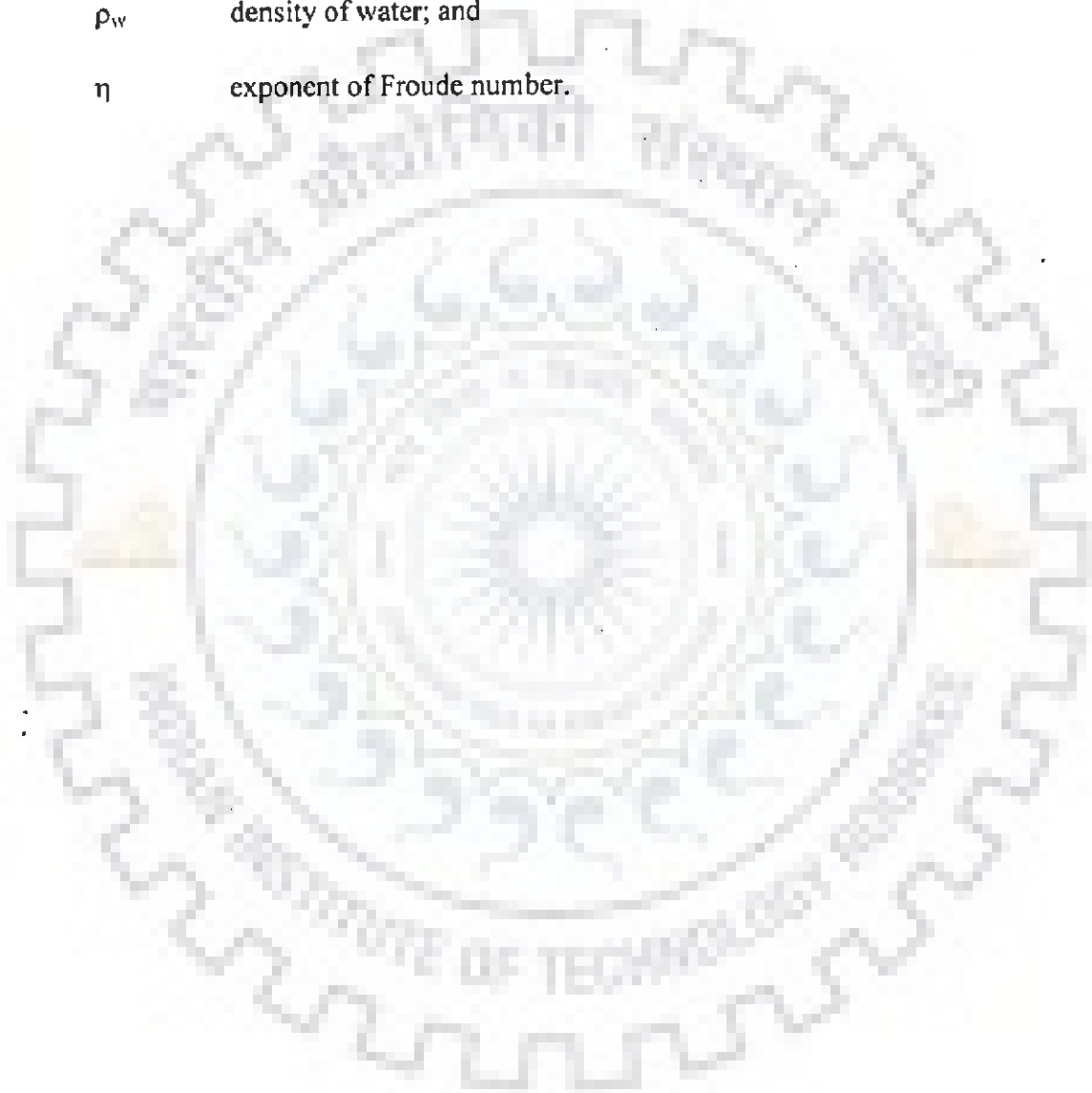
θ_1 Shield factor;

δ_b vane-to-bank distance;

Δd maximum change in flow depth = $d - \bar{d}$;

σ_g geometric standard deviation;

- δ_b vane to bank distance;
- δ_n vane spacing across the stream;
- δ_s streamwise spacing of the vanes;
- ω_o settling velocity of sediment;
- γ_{st} density of structural steel;
- ρ_w density of water; and
- η exponent of Froude number.



INTRODUCTION

1.1 GENERAL

Sediment control in alluvial channels, in particular the control of sediment movement, scour, and deposition, is one of the most difficult problems encountered by river engineers. Bed scour along the outer bank of river bends frequently causes undermining of the banks and loss of land. Deposition of sediment in the river bed often reduces flood-conveyance capacity of river and interferes with navigation. The diversion of flow from one channel to another or to a water intake or to reduce sediment entrainment at water intakes requires sediment management. The thalweg in a braided stream often switches from one side to other. Vertical wall bridge abutment of single span bridge is also affected by deep scour hole around it. The main difficulty in the treatment of these problems is the absence of cost-effective, low-maintenance and environmentally acceptable sediment control structures with a wide range of applications. One of the principal obstacles to amelioration of the sediment control problem is the affordable cost and inadequacy of the currently available conventional sediment control structures. The submerged vanes have been developed to meet the above problems and these have been successfully employed in other countries.

The submerged vanes (Fig. 1.1) are small and submerged foils aligned at an angle to the flow to modify the near-bed flow pattern and redistribute flow and sediment transport within the channel cross section.

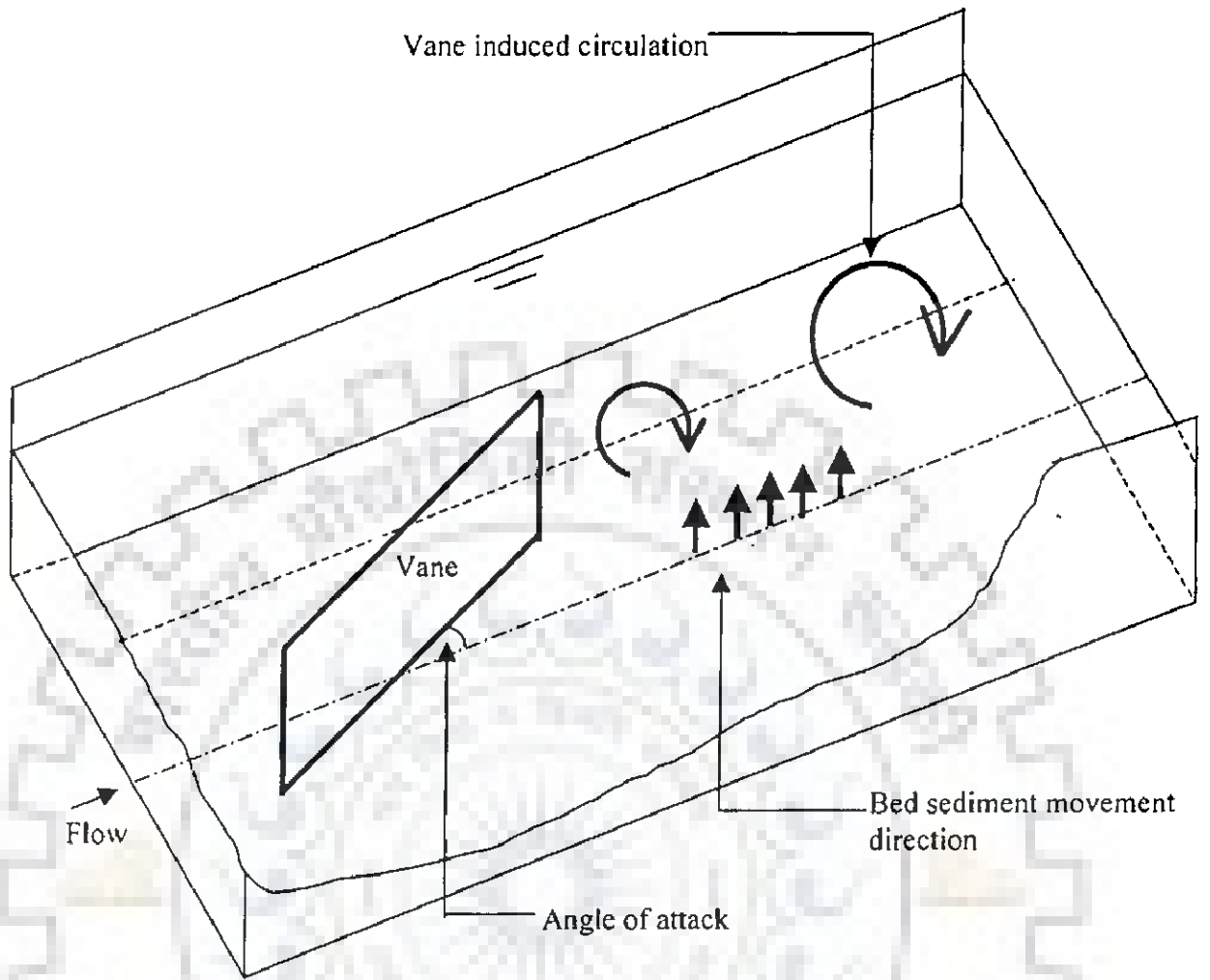


Fig. 1.1 Definition sketch of submerged vane

Submerged vanes are frequently used as vortex generating devices that have several applications, such as protection against bank erosion (Jansen et al. 1979; Odgaard and Kennedy, 1983; Odgaard and Mosconi, 1987; Odgaard and Wang, 1991 a,b); maintaining depth in navigation channel (Odgaard and Spoljaric, 1986); maintaining the pump-intake bays sediment free (Nakato et al.,1990), sediment control at lateral diversions (Barkdoll et al., 1999), sediment control at water intakes (Wang et al., 1996) and control of scour at vertical wall abutments (Johnson et al., 2001).

In the last two decades, there has been an increase in the use of submerged vanes as sediment management devices as opposed to the traditional sediment control structures (such as dikes and groins). Smaller vane dimension and the relatively better alignment with the flow field (compared to dikes and groins etc) lead to the required modification of the flow field at less flow resistance and low structural as well as low maintenance cost and these are some of the reasons behind their increased popularity. The vanes can be laid out to make the water and sediment move through a curve as if it were straight. As per Odgaard and Spoljaric (1986), significant changes in depth can be achieved without causing significant changes in cross-sectional area, energy slope, roughness and downstream sediment transport. As per literature, number, size and layout of the vanes depend on the channel morphology, velocity and depth at a meander bend. Vanes stabilize a channel reach without inducing changes upstream or downstream of that reach. Vanes may not be visible in time as they become buried by depositing sediment, and aid the stream in doing the work by redistributing the flow energy to produce a more uniform cross-section without an appreciable increase in the energy loss through the reach.

The submerged vanes function by generating secondary circulation in the flow, which alters the magnitude, and direction of the bed shear stresses and causes a change in the distributions of velocity, depth and sediment transport area affected by vanes. They are constructed on a river or stream bed and set with an angle of attack to the direction of flow to create secondary current. The strongest circulation will give the maximum effects of submerged vanes at optimal angle of attack and at the same time local scour holes might develop around the submerged vanes, which may dislodge the submerged vanes.

1.2 LOCAL SCOUR REDUCTIONS WITH COLLAR IN CASE OF SUBMERGED VANES

Odgaard and Kennedy (1983) proposed that the optimum angle of attack, for which the vanes are still effective in reducing the secondary current, but do not produce scour which might endanger their stability, is between 10° and 17° . For values of angle of attack $\geq 20^{\circ}$, flow separation has been found to occur around a third or more of the vane length and has led to the development of a persistent scour hole near the upstream end of each vane. Odgaard and Spoljaric (1986) proposed that when angle of attack is greater than 15° , flow separation becomes significant and causes excessive unacceptable local scour around the vane. Odgaard and Mosconi (1987) proposed that the optimum angle of attack, α , is generally about 20° . Odgaard and Wang (1991 a,b) performed the laboratory test using vane angle 15° for the curved channel and 20° for straight channel.

Marelius and Sinha (1998) proposed that the optimum vane angle lies between 36° and 45° and for flat plate it is very close to 40° , where the strength of vortex is maximum. They found that the scour hole which practically undermines the vane, requires large installation depth.

All the above researchers except Marelius and Sinha (1998) related the optimum angle of attack to the local scour hole so that significant local scour may not develop to dislodge the vanes. But Marelius and Sinha (1998) related the optimal angle of attack to the maximum strength of vortex, which looks more acceptable. However, all the researchers are silent as to how the local scour hole be reduced to install the submerged vanes at optimal angle of attack to get maximum effect of submerged vanes. There is a complete lack of studies on submerged vanes in respect of local scour. It can also be seen from the review of literature that so far there are hardly any detailed investigations conducted on the use of different shapes of submerged vanes in the context of reduction of local scour around the vane.

With the above background, the following objectives are set for the present study.

1.3 OBJECTIVES OF THE STUDY

- (1) To perform experimental runs on rectangular as well as different shapes of submerged vanes. Based on analysis of data, identification of key variables influencing the scour phenomena is to be achieved. Also, suitable relationships are to be evolved for describing the local scour around the rectangular submerged vanes without collar.
- (2) Study of collar as scour retarder and optimization of collar shape and size for rectangular and trapezoidal vanes at optimal angle of attack and at two Froude numbers such as 0.13 and 0.25.
- (3) Investigation of optimal angle of attack for rectangular vane with collar at different degree of submergence. A dimensional analysis

approach for dimensionless strength of vortex in terms of moment of momentum is also to be developed.

- (4) Investigation of optimal angle of attack for different shapes of submerged vanes such as double curve type I, double curve type II, J1 type and J2 type vanes. Details of these shapes are given later.
- (5) Effect of aspect ratio of rectangular submerged vanes on vane induced secondary circulation.
- (6) Effect of taper angle (trapezoidal vane) on the strength of vane induced secondary circulation.
- (7) Decay of strength of vane induced secondary circulation generated by rectangular and trapezoidal vanes at optimal angle of attack along the downstream region of the vane.
- (8) Investigation of the alignment of dike formation due to the rectangular and trapezoidal vanes at optimal angle of attack.
- (9) Field trials of the optimized shape and size of collar with trapezoidal vane (taper angle 3H:2.5V)

1.4 ORGANISATION OF THESIS

To meet the above objectives, the present study is organised as follows:

Chapter 1: It introduces the topic of investigation, underlying objectives and the layout of the thesis.

Chapter 2: The literature review relevant to submerged vanes are included here.

Chapter 3: It provides the details of experimental program.

Chapter 4: It presents the performance evaluation of submerged vanes of different shapes and sizes without collar. It also deals with the

development of appropriate relationships for predicting scour around rectangular vanes. In addition, it also outlines an approach for the cost analysis of riprap vis a vis a collar.

Chapter 5: It includes the optimization of collar shape and size for rectangular and trapezoidal vanes at different Froude number. In addition, it also includes the field verification of the tapering vane with optimized collar.

Chapter 6: It presents the optimal angle of attack at the different degree of submergence for the rectangular vanes with collar having the leading edges vertical and tapered. It also includes the optimal angle of attack for different shapes of submerged vanes. In addition, it also outlines dimensional analysis approach for dimensionless moment of momentum. It also describes the effect of scour hole on the strength of vortex.

Chapter 7: It includes the decay of vane-induced strength of vortex with downstream. It also includes the dike formation due to submerged vanes.

Chapter 8: It includes the general remarks, results of present investigation and outlines the main findings and provides framework for future work

REVIEW OF LITERATURE

2.1 GENERAL

Use of submerged vanes is found to be effective in a variety of solutions, as described in chapter 1. However, it is appropriate to know certain issues related to submerged vanes. In this Chapter, details of various studies related to other secondary current generating structures are provided along with submerged vanes. Salient findings of different investigators with regard to submerged vanes are also covered here. Among other issues, scour around submerged vanes, shapes of submerged vanes, role of collar and factors influencing the performance of vanes are also addressed in this chapter.

2.2 SOME SECONDARY CURRENT GENERATING STRUCTURES

Prior to introduction of vanes, a variety of secondary current generating devices including bandalling, surface panels, bottom panels were used.

2.2.1 Bandalling

In comparison to submerged vanes, bandalling is quite an old technique, which was successfully used as a palliative measure in Assam (India), mainly to improve navigation conditions (Remillieux, 1970). The bandalling system comprising of a mat placed oblique to the flow was developed in the Ganga-Brahmaputra river area and is still applied there to a certain extent. Bandalls are vertical mats or screens made of bamboo, supported on bamboo poles driven into the bed. The effect of bandalling is due to the generation of secondary currents. They are erected at mid water after the flood, with their upper edges rising clear of the water and their lower edges penetrating below the surface for about one third to one half the depth. They are set at an angle to the stream to divert

the surface currents towards the navigation channel, and have the secondary effect of encouraging deposition of the stream bed load, thereby indirectly deepening the navigation channel. In order to prevent deviation of the sediment transport from the sand banks towards the channel, a small opening is left between mat and sand bank gets diverted away from the sand bank deposits, while the bottom flow deposits. As a consequence, the surface flow together with bed load passes under the mat. The resulting helical flow transports the sediment away from the desired channel.

2.2.2 Surface Panels

According to Jansen et al. (1979), the system of surface panels was developed in the USSR by Potapov and his associates in 1936. According to the unpublished report on "method of transverse circulation complements relative to the surface panels" (1962), the surface panels is composed of an assembly of deflectors linked to four wings connected to a barge fitted with an anchor. This unit gives rise to a double helical circulation which extends downstream along the channel to get deeper. This report also concludes that the size distribution of the deposits, which from the sills and the flowing speeds due to the surface panels, may affect the movement of deposits. Surface panels, placed obliquely in the current, cause deviation of surface flow and due to acceleration under the panel, deviation of the bottom flow in the other direction. The result is a helical flow downstream of the panel. The increased sediment transport follows the bottom flow. According to Jansen et al. (1979), the principle mentioned above has also been applied by French engineers for scouring channel. They grouped a number of surface panels together in a so-called scouring barge.

2.2.3 Bottom Panels

The principle of bottom panels is also based on the generation of helical flow. The panels are placed at an angle of about 45° to the current at the edge of the channel to be eroded. According to Jansen et al. (1979), bottom panels have not only been applied for the creation of navigation channels, but have also been used for the closure of secondary river branches. The bottom panel does not have gap between the river bed and the panel unlike bandalling, surface panel and scouring barge. The bottom panel is submerged excepting the first panel of the system of bottom panels. The first panel of the system of bottom panels is placed in a water depth where the channel does not need to be deepened. Other panels such as bandalling, surface panel scouring barge are not submerged in flowing water and projected above it. Bottom panels are temporary regulation structures only, and their effect is local and much dependent on the stability of river channel (Jansen et al., 1979). According to Remillieux (1970), bandals have to be renewed each year after the flood, bottom panels remain in place, and effect, initially even greater than bandals, increases each year, the asymptotic limit usually being reached after three annual floods. According to the unpublished report on method of transverse circulation complements relative to the surface panels (1962), bottom panels gives larger and longer deepening in comparison to surface panels. Jansen et al. (1979) also states that "their efficiency is usually low and success can never be guaranteed". The common objective of all the above secondary current generating panels is to accentuate the effect of secondary current. But the strength of secondary current in quantitative terms was not explicitly explored and examined.

2.3 PRINCIPLE OF SUBMERGED VANES AND GENERAL GUIDE LINES

For a channel bend flow, the idea for submerged vanes was suggested based on the research findings by Zimmermann and Kennedy (1978) and Falcon (1979), which examines the torque (including the flux of moment of momentum) exerted on the flow about a streamwise axis at the channel bed or centroid. According to Zimmerman and Kennedy (1978), the centrifugal force per unit mass exerted on the fluid as a result of channel and streamline curvature increases upward from the bed, as the square of the tangential component of the local fluid velocity, and is greatest at or near the water surface. Consequently, the fluid in the upper portion of the channel is driven outward to the concave bank, and as a result of continuity requirements, the fluid at the lower levels moves to the inner bank. Thereby, a spiral motion or secondary flow is imparted to the fluid as it moves around a channel bed. Near the bed where the concentration of transported sediment is higher, the secondary current moves sediment inward across the channel and deposits some of it near the inside of the bend, while the concave bank is subjected to the erosive attack of sediment deficient fluid from the upper layers of the stream and thereby the bed near the outside bank is scoured.

The first known attempts to develop a theoretical design basis for submerged vanes were made by Odgaard and Kennedy (1983), and Odgaard and Spoljaric (1986). They proposed through the theoretical and physical model, that short vertical submerged vanes, installed at incidence to the channel axis in the outer half of a river-bend channel significantly reduce the secondary currents and the attendant undermining and high-velocity attack of the outer bank.

Odgaard and Kennedy (1983) concluded that submerged vanes are very effective in nullifying the secondary currents produced in the channel bends, which often lead to undermining and accelerated erosion of river banks and submerged vanes do not increase

the local channel roughness as do others, presently used means for reduction of the near-bank velocity. They also suggested that submerged vanes are attractive alternative to riprap and other structural types of bank protection in mitigating an intriguing natural phenomenon.

Odgaard and Spoljaric (1986) concluded that the change in flow depth induced by vane is proportional to the vane-induced transverse velocity component near the bed, which is a function of the angle of attack. They found changes in flow depth by transporting sediment sideward rather than downstream, while many traditional structures for sediment control produce a streamwise redistribution of sediment and a change in the flow. With the change in the energy conditions of the flow (slope, roughness), the vane system designed redistributes the bed sediment in the transverse direction without changing overall channel characteristics. Also they reported that the vanes do not change the cross-sectional area of the channel and the strength of vane-induced helical motion varied little, when H/d varied within the range $0.2 \leq H/d \leq 0.5$, where, H = Vane Height ; d = flow depth. They also suggested that the vane height, H , should be chosen such that the ratio H/d remains within the range $0.2 < H/d < 0.5$ at all erosion causing flow rates and the vane length, L , should be of the order of 3-4 times the vane height. They also suggested that the vanes should form an angle α , with channel centreline such that of $\alpha' = 10-15^\circ$ with the mean flow direction at bankfull flow; and the lateral spacing of the vanes and the distance from the outermost vane to the bank should be less than about twice the water depth at bankfull flow.

Based on field data, Odgaard and Mosconi (1987) concluded that submerged vane technique is a feasible and realistic alternative to the traditional techniques, e.g., rock riprap and spur dikes. Also, the design produced a reduction of the high flow transverse bed slope of at least 50% and a reduction of the near bank velocity of, generally 10-20%,

moving velocity maximum toward the centre of channel. They also concluded that the technique is notable by its simplicity in both design and construction, and the system did not cause any measurable change in the longitudinal slope of the water surface nor in the average depth for a given discharge. In other words, as per them the vane system should not interfere with the overall sediment balance and stability of channel.

Odgaard and Wang (1991a) carried theoretical studies of the vanes for non-separated flow and concluded that vanes are applicable to channels with any shape and plan form and vanes are installed at any angle of attack between $15-25^{\circ}$ with the flow, and their initial height is 0.2 – 0.4 times local water depth at design stage. The circulation alters magnitude and direction of bed shear stresses and causes a change in the distributions of velocity, depth, and sediment transport in the area affected by the vanes. As a result, the river bed aggrades in one portion of the channel cross section and degrades in another. They also concluded that by introducing relatively small changes in the bed shear stresses, arrays of vanes could generate local changes in the bed elevation of the order of the vane height. The major controlling parameters are vane height, vane aspect ratio, angle of attack, vane density (spacing), channel resistance, and sediment Froude number. An increase of any of these parameters causes the induced changes in bed elevation to increase.

Odgaard and Wang (1991b) have prepared a number of graphs showing maximum changes in flow depth, $d_m - d_v$, as a function of vane flow and sediment parameters, where, d_m equals maximum flow depth, and d_v equals vane induced flow depth.

They concluded the following vis a vis design guidelines.

- (i) In both the curved and straight flume, the vane induced changes occurred without causing significant changes of the area of the cross sections and of the longitudinal slope of the water surface. The changes in slope were less

than 10%. Thus, vanes will not cause any changes of the streams sediment-transport capacity upstream and downstream from the vane field and, therefore, should not alter the overall characteristics of the streams.

(ii) Vane-induced redistribution of sediment within a cross section is an irreversible process in the sense that a reduction of discharge does not lead to recovery of original distributions. A reduction in discharge does not result in a reduction in the volume of sediment accumulated in the vane field, because at the lower discharge the sediment-transport capacity in the vane field is too low to remove the sediment that accumulated at the higher discharge.

(iii) In most applications, the vane height will be between 0.2 and 0.4 times local bank-full flow depth, and vane length will be two to three times vane height. The submergence of the vanes will be as much as 100% of the average flow depth. The vanes will be placed in arrays along the bank of the river. Each array will contain two or more vanes. The vanes in an array will be spaced laterally at a distance of two to three times vane height. The streamwise spacing between the arrays will be 15 to 30 times vane height. The vane-to-bank distance should not exceed four times the vane height.

The first (most upstream) array in the vane system must be located at a distance of at least three array spacing upstream from the property to be protected or flow area to be improved and there must be at least three arrays in the system for it to be effective at and downstream from third array.

Johnson et al. (2001) performed laboratory experiments to evaluate the effectiveness of vanes for preventing scour at single-span bridges with vertical wall abutments. They used the rock vanes, which are single-arm structures angled to the flow

with a pitch into the streambed such that the tip of the vane is submerged even during low flow. Following conclusions were made by them based on the scaled experiments:

- (i) Vanes appropriately placed in a stream channel upstream of a vertical wall bridge abutment with setback move the abutment scour away from the bank and abutment toward the centre of the channel. The vane forces the flow to separate from the channel bank at the vane, causing reduced velocities and shear stress at the bank and increased velocities in the centre of the channel.
- (ii) If the vane is placed such that the abutment is within the influence of the vanes, then scour is greatly reduced in the lower velocity area along the abutment. Although scour is reduced along the abutment wall, scour still occurs in the channel away from the abutment.
- (iii) For higher flows, the maximum scour depth occurred about one-third the channel width away from the abutment, or about 20% further away from the abutment than for the no-vane use.
- (iv) The vanes do not armour against scour or significantly reduce scour overall; rather, they use the scouring to occur toward the centre of channel, away from the abutment.

2.3.1 Case Study on Performance of Submerged Vanes

Wang et al. (1996) demonstrated the utility of the vane technique for sediment management at water intakes. They used the design basis for the vane technique developed by Odgaard and Wang (1991a). The design process consists of selecting values of vane height H , vane length L , angle of incidence α , vane submergence T , vane spacings δ_n and δ_s , and vane-to-bank distance δ_b , using the following basic flow and sediment parameters: (i) prevane average flow depth d ; (ii) velocity U and resistance

parameter m_1 ($m_1 = \kappa \sqrt{\frac{8}{f}}$) where, κ = von Karman constant and f = Darcy-Weisbach friction factor (iii) channel width-depth ratio B/d and radius-width ratio r/B ; and (iv) the sediment Froude number F_D ($F_D = U / \sqrt{gd_{s0}}$). They also described the submerged vane technique used for solving sediment problems at the water intake at the Duane Arnold Energy Centre (DAEC) located on the Cedar River in Palo, Iowa and at the Byron Station water intake located on the Rock River in Byron, Ill. The DAEC intake velocity was about 0.04 m/s and Byron station intake velocity was 0.08 m/s, and river flow velocities at the DAEC intake and Byron Station intake were 0.5 m/s and 0.4 m/s respectively.

Since the start of operation in 1972, the DAEC intake had experienced recurring sediment problems, which were partly due to an unexpected shift in the flow pattern in the river. Considerable amount of sediment were being drawn into the cooling system, leading to maintenance problems; sediment was accumulating within the intake structure, and the gates at the entrance to the intake were repeatedly buried and made inoperable. At low flow, a sand bar typically was visibly in front of the downstream portion of the intake. The sandbar connected with the intake structure blocked the flow into part of the intake. Sediment deposition at the intake being as much as 1 m above the sill elevation.

The bed was lowered by 0.6 m in front of the intake after one year installation of submerged vanes.

The sediment problem at Byron Station water intake was partly due to the intake being on the inner bank of a river curve. In 1980, a channel was built into the river bottom to connect the intake opening with the deep portion of the river near the outer bank of the river across from the intake. This channel had to be dredged at very frequent intervals. In 1990, the bed elevation at the intake was about 1.3 m above the sill elevation of intake. Sediment deposits blocked a considerable portion of the intake opening.

The solution that was developed consisted of (i) removal of a shallow spur on the left bank upstream from the intake structure, (ii) reshaping of the riverbank downstream from the intake structure; (iii) installation of eight arrays of five vanes each in front of intake structure; and (iv) construction of two submerged wing-dams (submerged groins) upstream from the intake structure on the opposite bank.

The vanes were located to intercept the approaching bed load and divert it away from the face of the intake.

It was reported that the vane system very effectively developed a deep channel in front of the intake. In both the cases, the ratio of withdrawal velocity to river flow velocity was less than 0.2.

2.4 LOCAL SCOUR AROUND SUBMERGED VANES

Odgaard and Kennedy (1983) performed laboratory experiments with angle of attack of 15° , sediment mean diameter of 0.30 mm, its geometric standard deviation of 1.45 and H/d ratio as 1/3 in a curved flume at the Iowa Institute of Hydraulic Research of the University of Iowa. They also conducted experiments to determine the optimal angle of attack (α) for vane, which produces minimum scour hole. They suggested that for values of $\alpha > \cong 20^\circ$, flow separation occurred around a third or more vane length and produced a persistent scour hole near the upstream end of each vane. As α was reduced, the number of vanes producing objectionable scouring also decreased.

All the investigators agree that local scour depth increases with the increase of angle of attack. Probably for this reason vanes have not been used practically at the angle of attack beyond 20° .

Marelius and Sinha (1998) conducted laboratory experiments and found that the effect of vanes, i.e. strength of secondary flow in terms of moment of momentum induced

by submerged vanes is maximum at angle of attack very close to 40° . The graphical plot provided by Marelius and Sinha (1998) shows that there is significant variation of strength of vortex created by submerged vanes between the angle of attack 20° and 40° . However, the way to deploy the submerged vane at the optimal angle of 40° to drive its maximum beneficial effect for given hydraulic conditions remains to be investigated. Obviously, this will presuppose checking the occurrence of local scour around the submerged vanes by a suitable local scour retarder method.

2.5 COLLAR AS SCOUR RETARDER

In the last few decades, collars have been frequently used as scour retarder in case of bridge piers and abutments. Chiew (1992) performed laboratory experiments to reduce the local scour around the bridge piers using collars. He studied the effect of the size and position of a collar on the equilibrium scour depth around a cylindrical bridge pier based on experimental data in clear water condition. Following are his findings.

- (i) A collar can reduce the scour depth significantly.
- (ii) When the collar was placed below the mean bed level, scour development was arrested when the base of the scour hole coincided with the surface of collar.
- (iii) In general, the use of collars appears to be effective, especially when the undisturbed velocity is small enough that there is no lateral sediment transport or migration of bed forms past the pier. However, when general sediment transport occurs, the trough of migrating bed form may expose the pier beneath the collar under such condition, it loses its effectiveness.
- (iv) When a slot placed near the bed is combined with a collar, the combination is capable of eliminating scouring altogether.

- (v) There is zero scour for the combination of $0.25D_1$ slot and $3.0D_1$ collar at bed on a solid pier.

Vittal et al. (1994) performed laboratory experiments in clear water condition to investigate the clear-water scour around the bridge pier group. The sediments used were of mean sizes 0.775mm, 1.183mm, 1.543mm and 1.844mm. They reported the collar to be very effective for the bridge pier group. The collar was kept at a height of 1.50cm above the bed. They also reported that the 30° orientation of bridge pier group with approach flow as the best orientation.

Kumar et al. (1999) performed laboratory experiments on scour reduction around bridge piers under clear-water conditions. They used uniform-size sands having median diameters of 0.78mm, 1.18mm and 1.54mm. They suggested that a collar at any level above the bed, divides the flow into two regions above and below the collar. For region above the collar, it acts as an obstacle against the downflow due to which the downflow loses its strength on impingement at the bed. For the region below the collar, the downflow and horseshoe vortex are reduced. They also mentioned that the efficacy of collar depends on its size and the location on the pier with respect of bed. They presented the following equations

$$\frac{ds_p - ds_c}{ds_p} = f\left(\frac{D_2}{D_1}, \frac{h}{d}\right) \quad (2.1)$$

$$\frac{ds_p - ds_c}{ds_p} = 0.057 \left(\frac{D_2}{D_1}\right)^{1.612} \left(\frac{h}{d}\right)^{0.837} \quad (2.2)$$

for $h < d$

where,

ds_p = equilibrium scour depth in case of pier without appurtenances; ds_c = equilibrium scour depth in case of pier fitted with collar; D_1 = diameter of pier without

appurtenances; D_2 = diameter of collar;; h = depth of collar below free water surface; and d = depth of flow.

According to them, an additional parameter, like ratio of collar thickness to flow depth should also appear in eq. 2.1, but it was not introduced because their study was restricted to collars of negligible thickness. Kumar et al. (1999) claimed that performance of eq. 2.2 falls within $\pm 40\%$ error. Eq. 2.2, nevertheless, provides a means of estimating the reduction of scour that can be achieved by the use of a circular collar around the circular bridge pier. They suggested that eq. 2.2 should be used only for $h \leq d + ds_p$. They also concluded through eq. 2.2 that the larger diameter collars at or below the bed are more effective.

2.6 VARIABLES INFLUENCING SUBMERGED VANES PERFORMANCE

2.6.1 Shapes of Submerged Vanes

Odgaard and Wang (1991) used the shape of submerged vane as double-curved foils with slight twist in their experimental study. The curves were like J shape vane with slight twist curve at the leading edge on its top in horizontal plane. But they did not report the reason behind this shape.

Barkdoll et al. (1999) used the double vane with the aim to enhance its effects. It comprised a upper vane, set at opposite angle of attack, with the same dimensions and placed just under the water surface. The idea was that the upper vane would cause more flow to enter the diversion from the upper region of flow and thereby, decrease the amount drawn from near the bed. They concluded that the double vane increased the amount of turbulence at the diversion entrance and thereby increased sediment movement into the intake over that of a single vane.

2.6.2 Optimal Angle of Attack

Initially, optimal angle of attack for submerged vanes was related by the researchers to the dislodgement of vanes due to scour. Odgaard and Kennedy (1983) concluded that the optimal angle of attack, for which the vanes are still effective in reducing the secondary current but do not produce scour which might endanger their stability, is between 10° and 17° .

Odgaard and Spoljaric (1986) concluded that optimal angle of attack is 15° since flow separation becomes significant and causes excessive scour around the vane when angle of attack is greater than 15° .

Odgaard and Mosconi (1987) proposed that the optimal angle of attack for bend channel is generally about 20° .

For the first time, Marelius and Sinha (1998) related the optimal angle of attack to the vane induced circulation. They concluded that optimal angle of attack is very close to 40° , where the vane produces the strongest circulation. However, in the literature there has not been any work reported on the optimal angle of attack for vane with any scour retarding device like collar. There is also an imperative need to find the effect of local scour on the vane induced strength of vortex.

2.6.3 Degree of Submergence

According to Odgaard and Spoljaric (1986), the strength of vane induced helical motion varied little when T/d varied within the range $0.5 \leq T/d \leq 0.8$. They performed laboratory experiments with vanes for degree of submergence (T/d) as 0.5.

Odgaard and Mosconi (1987) gave the following relationship in terms of T/d :

$$\frac{NLH}{r\phi b_1} = \frac{2d}{c_L r} \left[\frac{d}{H} \right]^2 \left[(n+1) - (n+2) \frac{H}{d} \right]^{-1} \quad (2.3)$$

where, N = Number of vanes; L = vane length; H = vane height; r = radius of curvature; ϕ = bend angle; b_1 = vane design section width; d = flow depth; c_L = lift coefficient; n = power law exponent and function $F = \left[(n+1) - (n+2) \frac{H}{d} \right]^{-1}$

They suggested that F is relatively insensitive to the variations of H/d over the large range of H/d values. H/d indirectly refers T/d ($T/d = 1-H/d$). They also concluded that vanes function optimally if vane height (H) is less than about half the water depth at flow rates at which bank erosion occurs.

Odgaard and Wang (1991) provided a number of graphs to facilitate design at different degree of submergence such as 0.5, 0.7 and 1.0.

Wang and Odgaard (1993) performed laboratory experiments on rectangular vane with degree of submergence as 0.5.

Marelius and Sinha (1998) performed laboratory experiments to investigate the optimal angle of attack for rectangular vane with degree of submergence as 0.7.

Barkdoll et al. (1999) conducted laboratory experiments with submerged vanes of degree of submergence as 0.79 to investigate the effect of flow field and bed-sediment movement at a diversion, limit of their effectiveness for sediment control and their effectiveness by the use of additional devices and intake-entrance modifications.

2.6.4 Streamwise Spacing of Submerged Vanes

Odgaard and Kennedy (1983) suggested the following relationship for the evaluation of centreline spacing (streamwise spacing) of the vanes by analytical model:

$$\frac{\delta_s}{L} = \pi \frac{r_c}{B} (\sin \alpha) \left[(n+1) - (n+2) \frac{H}{d} \right] \left[\frac{H}{d} \right]^{(2+n)/n} \quad (2.4)$$

Where, δ_s = centreline spacing of the vanes; L = vane length; r_c = mean channel radius; α = vane inclination; n = exponent in the power-law velocity profile $\left(n \approx \frac{1}{\sqrt{f}} \right)$; H = vane height; d = depth of channel (flow depth); B = width of the channel; and f = Darcy-Weisbach friction factor.

The eq. 2.3 gives centreline spacing of $S = 95$ m for two-row array of vanes as per the data they used which appears to be sufficiently large to be practical. However, they used the centreline spacing of $S = 62$ m for the prototype model study in Sacramento River, California for verification of the findings of laboratory model study carried out in the curved flume.

For desired change in flow depth and given flow characteristics, Odgaard and Spoljaric (1986) suggested the following relationship for streamwise spacing between each lateral vane array and the number of vanes per lateral array:

$$\frac{\Delta d}{d} = \frac{NK_0}{\pi} \exp \left(- \frac{2\kappa}{\sqrt{\frac{8}{f} + \frac{1}{\kappa}}} \frac{\delta_s}{d} \right) \quad (2.5)$$

Where, Δd = maximum change in flow depth = $d - \bar{d}$; d = flow depth; \bar{d} = cross-sectional average flow depth; $K_0 = a \bar{V}_x \tan \alpha_1$; $a = (3 \alpha_1 / 2) (\sqrt{\theta_1 / k}) / \sqrt{gd_{50} (\rho_s - \rho) / \rho}$;

α_1 = projected area/volume ratio for particle normalized by that for sphere ($\alpha \approx 1.27$ for ordinary river sand); θ_1 = Shields' factor ($\cong 0.06$)(1936); k = ratio of critical near-bed velocity to critical shear velocity ($\cong 1$); d_{50} = grain size; ρ , ρ_s = fluid and sediment density; \bar{V}_x = cross-sectional average value of V_x ; V_x = time-averaged velocity component in the x direction; β = vane angle of incidence with flow; κ = von Karman's

constant 0.4; N = number of vanes in lateral arrays; δ_s = streamwise spacing of the vanes; and f = Darcy-Weisbach friction factor.

2.6.5 Tapering of Leading Edge of Submerged Vanes

Submerged vanes with tapered leading edge are installed in Wapsipinicon river bend in the U.S.A. and outside a new water intake in Nepal. In a personal communication with one of the supervisors (Prof. Nayan Sharma), Prof. A. J. Odgaard ascribed the rationale behind tapering the leading edge of the submerged vanes to deflect floating debris impinging on the vane. Also, possibly stuck up debris etc. at the leading edge in low to medium flows is more readily removed with the rising stage if the edge is tapered than vertical. In countries where rivers are ice covered in the winter, the taper facilitates natural ice removal. The effect of tapering the leading edge of submerged vanes on the strength of vane-induced secondary currents has not been investigated so far. Thus it is important to investigate the effect of tapering the leading edge of the vanes on the vane-induced secondary current.

2.6.6 Aspect Ratio of Submerged Vanes

Table 2.1 gives the summary of aspect ratio used by different investigators.

Table 2.1: Aspect ratio used or recommended by different investigators

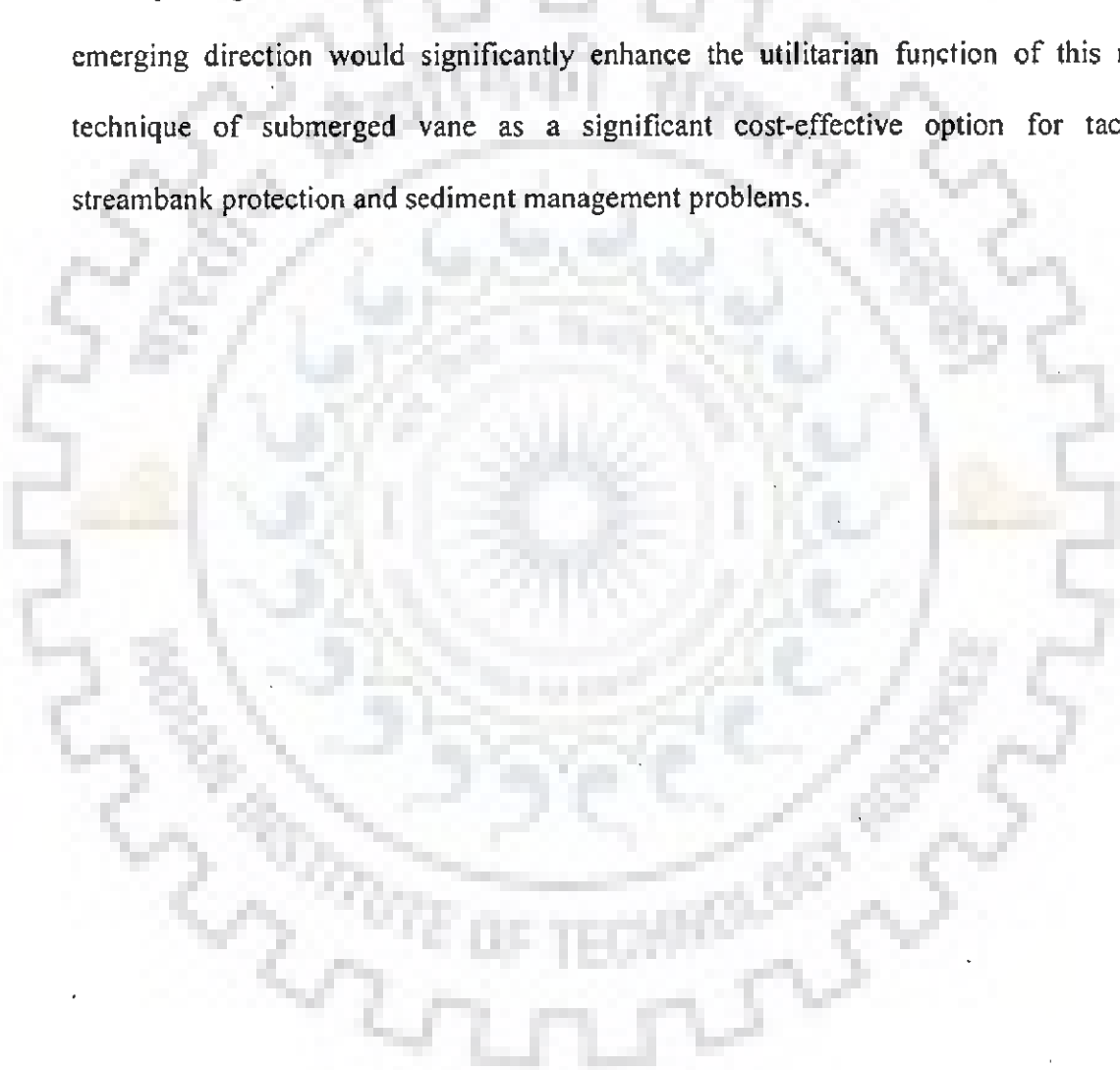
Name of investigators	Aspect ratio
Odgaard and Spoljaric (1986)	0.4
Odgaard and Mosconi (1987)	0.25 to 0.33
Odgaard and Wang (1991a)	0.3
Odgaard and Wang (1991b)	0.5
Wang and Odgaard (1993)	0.5
Wang et al.(1996)	0.33
Marelius and Sinha (1998)	0.5
Barkdoll et al. (1999)	0.32

2.13 SUMMARY:

From the preceding review of development of the submerged vane technique, it has become apparent that the researchers have been experimenting with the use of different angle of attack over the years along with other related parameters of design. Evidently, the main thrust of the research veers primarily around the optimal angle of attack without triggering a destabilizing scour, which would afford the largest vane-induced circulation of secondary flow to enhance vane performance substantially. While some significant headway has already been made by researchers in narrowing down the search for the optimal angle of incidence, there still remains the unresolved issue of preventing dislodgement of the vane due to large attendant scour depths at higher angles of attack especially around the leading edge of the vane. In this context, there is now an imperative need to undertake further research endeavour for evolving effective scour retarding mechanism especially around the vulnerable leading edge region for ensuring stability of the submerged vane at higher but optimal angle of incidence.

Further from the literature review, it could be discerned that with recently emerging prospect on the possibility of adopting higher angle of attack for a vane, the renewed direction of research enterprise may desirably now concentrate on ensuring stability of a vane against scour by devising a suitable scour retarding mechanism which should be optimised for realistic flow conditions. In its wake, it will also be pertinent to investigate the influence of such a scour retarding mechanism on the growth and decay of vane-induced vortex with respect to stream-wise spacing of a vane. From the above emerging scenario, it also seems imperative that supplementary experimental study is called for assessing the flow behaviour of tapering the leading edge of a vane with a scour retarding device. In the event of possible introduction of the aforesaid scour retarding mechanism in a vane, experimental analysis on its impact on the vital design parameters

at a vane such as aspect ratio, degree of submergence etc. will be pertinent from the standpoint of vane performance. It thus, transpires from the review that sustained experimental studies by several researchers have yielded significant development pertaining to lateral and longitudinal spacings of multi-vane array scenario. However, absolutely no forays have been made so far in the virgin research area for harnessing the high optimal angle for a vane with an optimized scour retarding mechanism encompassing all its related ramifications. A breakthrough in research in this newly-emerging direction would significantly enhance the utilitarian function of this novel technique of submerged vane as a significant cost-effective option for tackling streambank protection and sediment management problems.



EXPERIMENTAL PROGRAMME

3.1 GENERAL

From the preceding chapter, it is apparent that few types of submerged vanes have come into existence. It is obvious that certain preliminary studies on the performance of submerged vanes are necessary in order to identify the submerged vanes with minimum scour hole around it without material reductions in strength of vortex. The effect of different shapes and sizes of vanes on the strength of vane induced vortex and on the reduction of local scour around them is also to be studied. With this in view, the experimental programme was organized in five phases. In the first phase of experiment, the effect of different shapes and sizes of submerged vanes in context to local scour was investigated.

In the second phase, experiments were performed in a 50 cm wide mobile bed flume using collar as the local scour retarder for the two types of plastic plates with varying angle of attack, degree of submergence. In this phase of laboratory experiments, primarily it was endeavoured to gain an insight into the optimization of size and shape of collar for the assessment of a suitable one for the intensive lab experiments to be followed subsequently. The vanes were made of plastic plates. The trapezoidal shape is because of tapering the leading edge of the vane, to facilitate the smooth deflection of debris, ice and any other floating materials.

In the third phase of experiments, different shapes of the submerged vanes such as double curve type I, double curve type II, J1 and J2 type were tried.

The angles of attacks were varied in the third phase of experiments, which yielded the desired experimental data for undertaking the required analysis of data.

In the fourth phase of experiments, the study on the formation of dike due to rectangular and trapezoidal vane and decay of vane induced vortex with downstream of vane were carried out.

In the fifth phase of experimental study, the chosen configurations of laboratory model trapezoidal vane were faithfully reconstructed with identical size and shape of optimized collar configurations at optimum angle of attack in the Solani river near Roorkee to elicit actual field informations on their behaviour. The main aim of this study is to investigate the local scour hole and its retardation by collar in case of vanes with and without collar, which are founded in non-uniform sediment and subject to clear water live bed conditions. Therefore, experiments were conducted to examine the effects in local scour around the vanes, flow depth, discharge intensity, vane, height and length, their shape and sediment size, in clear water conditions. With this background, the details of the experimental programme are presented below.

3.2 LABORATORY FLUME

The flume used was eleven metre long tilting flume, made of mild steel with side walls made of transparent perspex sheet. Flume has an in-built upstream tank of 40 cm x 90 cm x 115 cm dimensions. The depth of flume is 50 cm and the width is 50 cm. Diagrammatic scheme is given in Fig. 3.1. The bed of flume is supported on angle iron sections, the lower ends of which are connected to a shaft, placed length-wise parallel to the central portion of flume below it. Shaft is movable horizontally backwards and forwards with the help of a gearbox

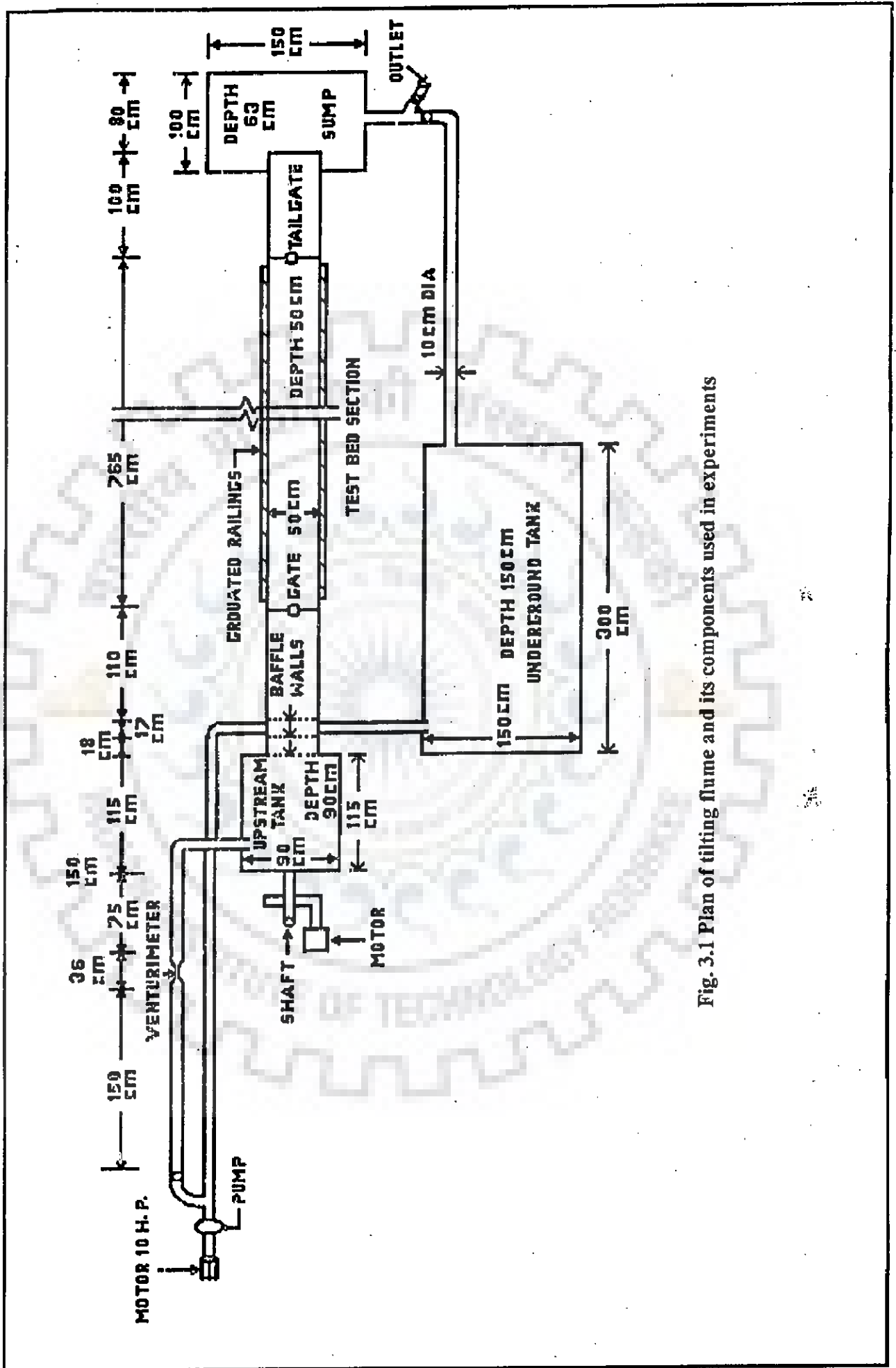


Fig. 3.1 Plan of tilting flume and its components used in experiments

and electric motor such that if the shaft moves towards the direction of flow, the front portion of flume moves upwards and lower portion moves downward and vice-versa. This is the mechanism of changing the required slope. The water flowing in the flume falls into a sump, which is connected to an underground tank of 1.5 m x 1.5 m x 3 m dimensions. From the underground, tank water is lifted with the help of a pump of 10HP capacity. 10 cm diameter pipes carry water from the underground tank to the upstream tank. The discharge is regulated with the help of a gate valve placed after the pump. A venturimeter is placed at a distance of 180 cm from the gate valve and 70 cm before the bend pipe leading to the top of upstream tank. The venturimeter is attached to the mercury manometer.

3.2.1 Sediments Used

Experiments were performed with two types of sediments having median diameter as 0.225 mm (geometric standard deviation 1.42)(as shown in the Table 3.1 and Fig. 3.2) and 0.405 mm (geometric standard deviation 1.37) (as shown in the Table 3.2 and Fig. 3.3). The relative densities of all sands were 2.65.

3.2.2 Other equipment

The depth of flow along the length of flume and the scour pattern around the submerged vanes were measured with the help of a pointer gauge, which could be moved along the hand rails fitted at the top of flume. The three-dimensional (3D) components of velocity were measured by means of an Acoustic Doppler Velocimeter (ADV). The velocimeter was capable of measuring all of the three components of the velocity with an accuracy of 0.25% of the velocity magnitude or 0.0025m/s (whichever was greater).

The sampling rate used in the experiment was 20Hz. A minimum of 800 values was taken at each measured point, and the mean value of these measurements was taken as representative velocities. The technique employed in ADV is superior to the other conventional methods, since the actual sampling volume is located at a lower depth (0.05m below the probe, in the present case) than the probe, and hence, is less disturbed.

Table 3.1: The sieve analysis of the sediment material of $d_{50} = 0.225$ mm

Size of sieves in mm	Weight retained on sieves in gm	% weight retained	Cummulative finer in gm	Cummulative % finer in gm
0.600	7.625	0.7625	992.375	99.2375
0.425	41.525	4.1525	950.85	95.085
0.300	149.825	14.9825	801.025	80.1025
0.225	298.475	29.8475	502.55	50.255
0.150	314.825	31.4825	187.725	18.7725
0.075	149.625	14.9625	38.1	3.81
0.063	31.625	3.1625	6.475	0.6475
0.050	6.475	0.6475	0	0

Table 3.2: The Sieve Analysis of the sediment material of $d_{50} = 0.405$ mm

Size of sieves in mm	Weight retained on sieves in gm	% weight retained	Cummulative finer in gm	Cummulative % finer in gm
0.600	0	0	1000	100
0.5	294.5	29.45	705.5	70.55
0.425	160.2	16.02	545.3	54.53
0.400	70.3	7.03	475	47.5
0.355	274	27.4	201	20.1
0.300	201	20.1	0	0

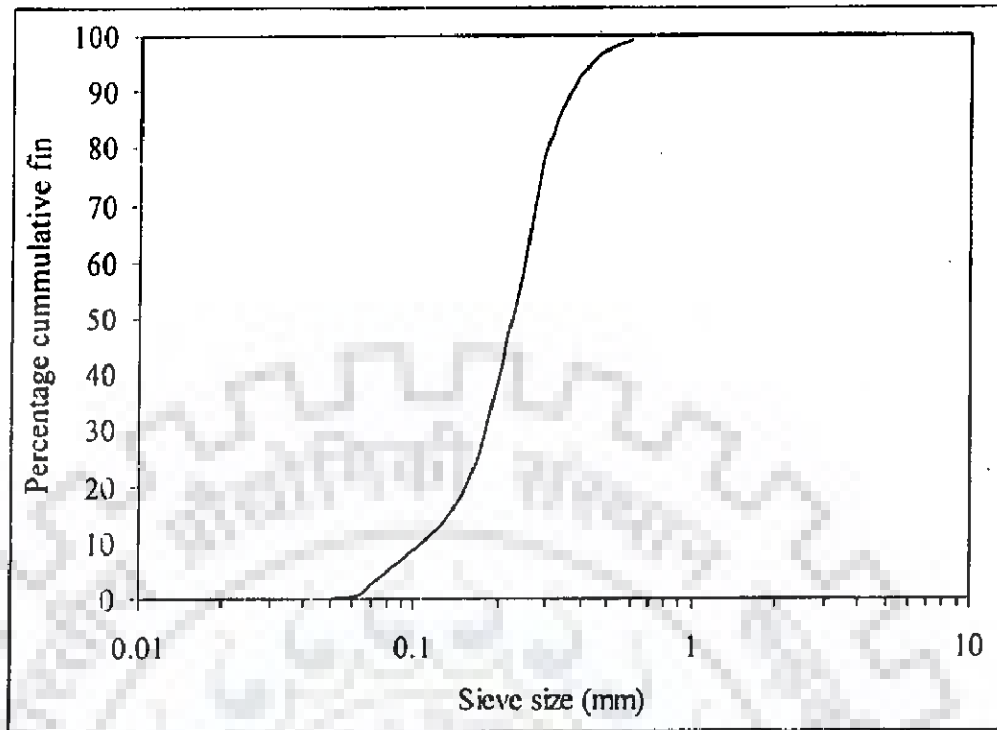


Fig. 3.2 Cumulative frequency curve for sand $d_{50} = 0.225$ mm

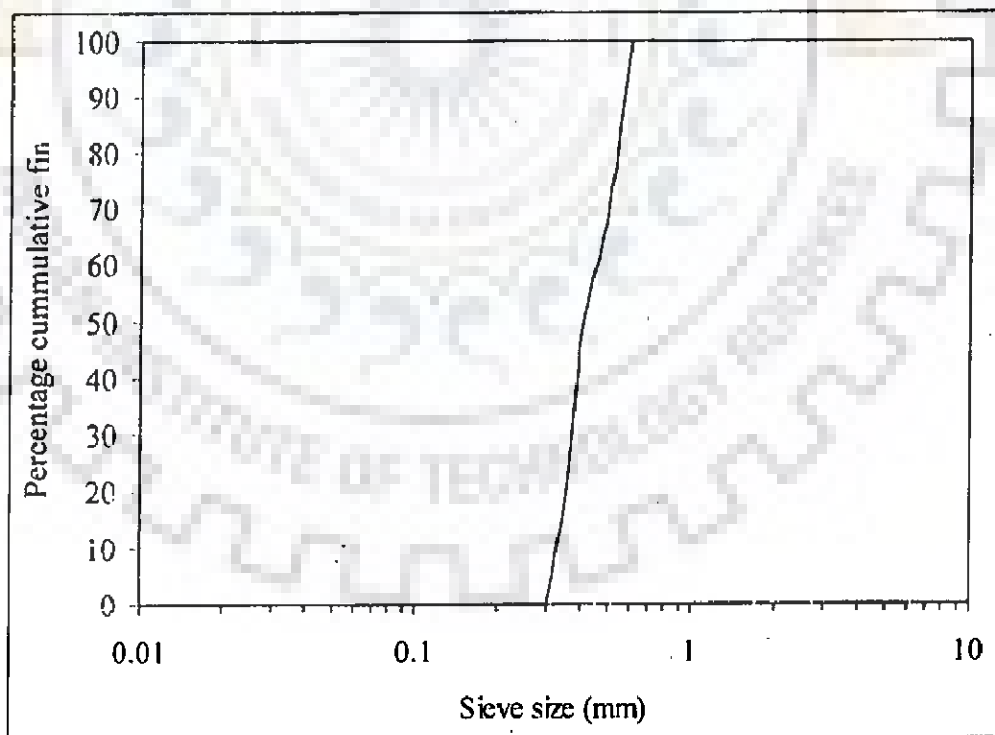


Fig. 3.3 Cumulative frequency curve for sand $d_{50} = 0.405$ mm

3.3 EXPERIMENTAL PROCEDURE

Experiments were conducted in the following steps:

- (i) The experiments were carried out in the River Engineering Laboratory, WRDTC of Indian Institute of Technology, Roorkee, India.
- (ii) First flume was adjusted to required slope.
- (iii) The depth of sediment bed layer of the test section was fixed at 15 cm. Uniform flow without sediment motion corresponding to a selected discharge was established with the help of tailgate.
- (iv) Before placement of submerged vanes, the sediment bed of flume was levelled.
- (v) After placement of submerged vanes, the sediment bed of flume was again levelled around the submerged vanes.
- (vi) Flow was introduced in the flume very slowly by closing the tail gate so that no scouring occurred around the submerged vanes due to operation.
- (vii) Temporal variation of scour was measured and the runs were carried out until such time as the scour bed not change by more than 1mm over a period of 4 hour. The corresponding scour depth was taken as equilibrium scour depth.
- (viii) Different sizes and shapes of collars at bed level were tried to reduce the local scour around the submerged vanes.

- (ix) After the experiment was over, the scour pattern was measured with the help of pointer gauge to see the effect of that size and shape of collar on the local scour around the submerged vanes.
- (x) All three components of velocities were measured by ADV at a distance of 15 cm from the centre of the vane to calculate the downstream strength of vortex in terms of moment and momentum. Near both the vertical walls of the flume, velocity measurements were not taken to avoid the effects of walls on secondary flow.
- (xi) Photographs were taken of the developed profiles, after the termination of the run.

3.4 PHASE ONE MODEL EXPERIMENTS

It was intended at the first instance to try out the different shapes of submerged vanes such as rectangular, double curve type I, double curve type II, J1 and J2 type in context of local scour at two Froude numbers such as 0.13 and 0.25 (Table 3.3). Double curve type I vane has curve shape at leading edge both in horizontal and vertical planes (Fig. 3.4a). The double curve type II has curve shape at leading edge in horizontal plane and curve shape at its top throughout its length in vertical plane (Fig. 3.4b). J1 and J2 type vanes are curved only at leading edge in horizontal plane (Figs. 3.5a and 3.5b). J1 type vane has smaller radius than that of J2 type vane. All the different shapes of submerged vanes were made of plastic sheets and having 6 cm height, 18 cm length and 4 mm thickness.

Table 3.3: Phase one experiments

Expt. No.	Rate of flow (m ³ /s)	Flow depth (cm)	d ₅₀ (mm)	Froude Number	T/d	Vane Type
A1	0.0154	18	0.225	0.13	0.67	Rectangular
A2	0.0203	14	0.405	0.25	0.57	Rectangular
A3	0.0154	18	0.225	0.13	0.67	Trapezoidal (3H:2.5V)
A4	0.0203	14	0.405	0.25	0.57	Trapezoidal (3H:2.5V)
A5	0.0154	18	0.225	0.13	0.67	Double curve type I
A6	0.0203	14	0.405	0.25	0.57	Double curve type I
A7	0.0154	18	0.225	0.13	0.67	Double curve type II
A8	0.0203	14	0.405	0.25	0.57	Double curve type II
A9	0.0154	18	0.225	0.13	0.67	J1 type
A10	0.0203	14	0.405	0.25	0.57	J1 type
A11	0.0154	18	0.225	0.13	0.67	J2 type
A12	0.0203	14	0.405	0.25	0.57	J2 type
A13	0.0157	18	0.225	0.13	0.67	Rectangular
A14	0.0170	18	0.225	0.14	0.67	Rectangular
A15	0.0179	18	0.225	0.15	0.67	Rectangular
A16	0.0188	18	0.225	0.16	0.67	Rectangular
A17	0.0198	18	0.225	0.17	0.67	Rectangular
A18	0.0203	14	0.225	0.25	0.57	Rectangular
A19	0.0150	14	0.405	0.18	0.57	Rectangular
A20	0.0168	14	0.405	0.20	0.57	Rectangular
A21	0.0186	14	0.405	0.23	0.57	Rectangular
A22	0.0200	14	0.405	0.24	0.57	Rectangular
A23	0.0215	14	0.405	0.26	0.57	Rectangular

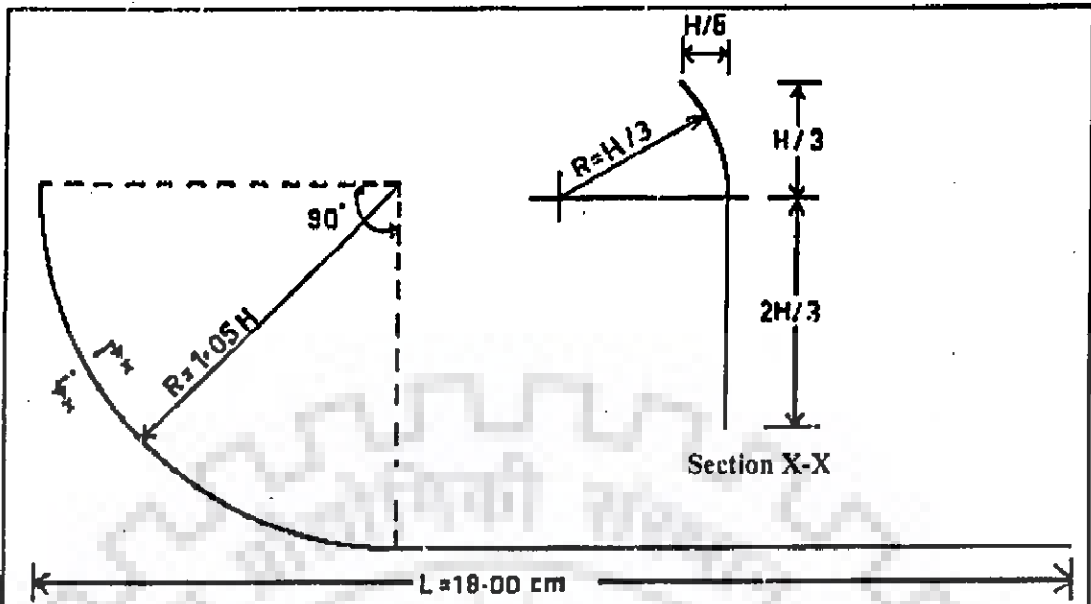


Fig. 3.4(a) Plan of double curve type I vane

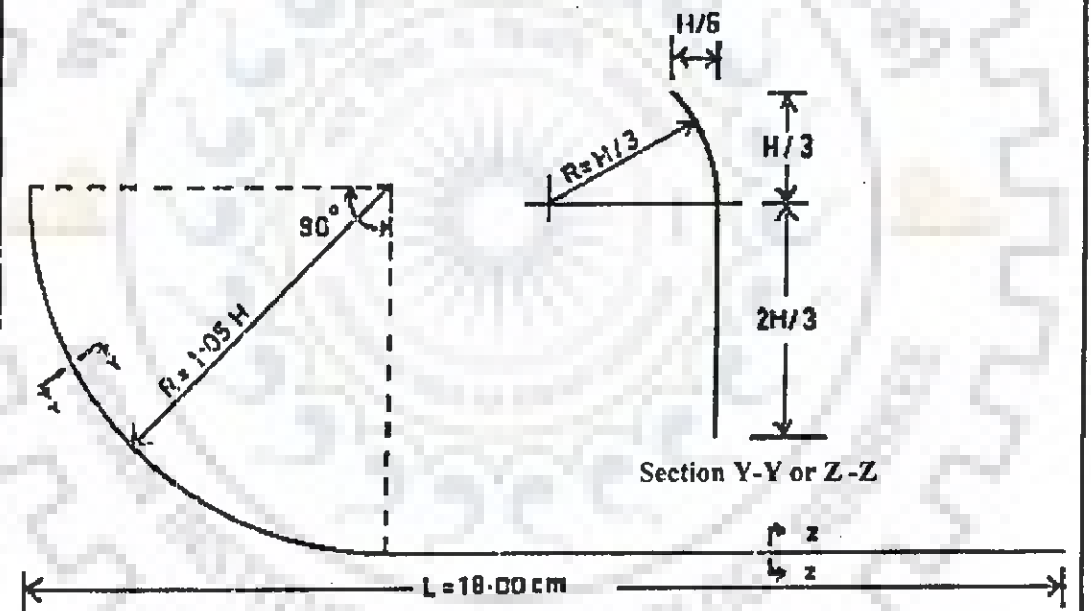


Fig. 3.4(b) Plan of double curve type II vane

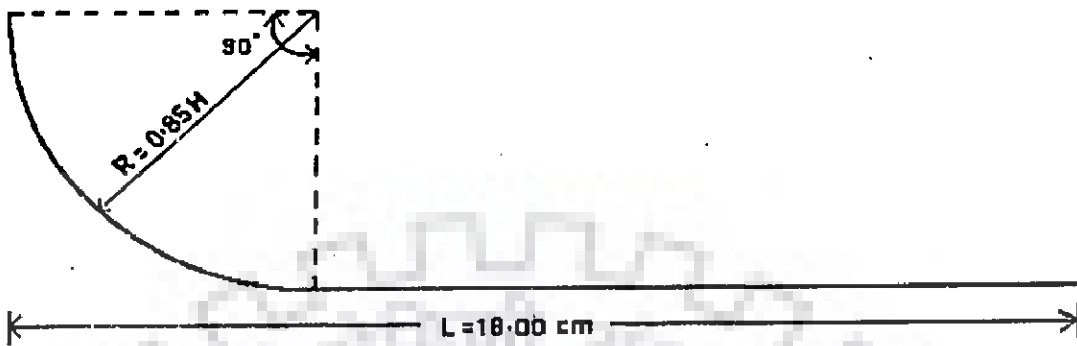


Fig. 3.5(b) Plan of J1 type vane

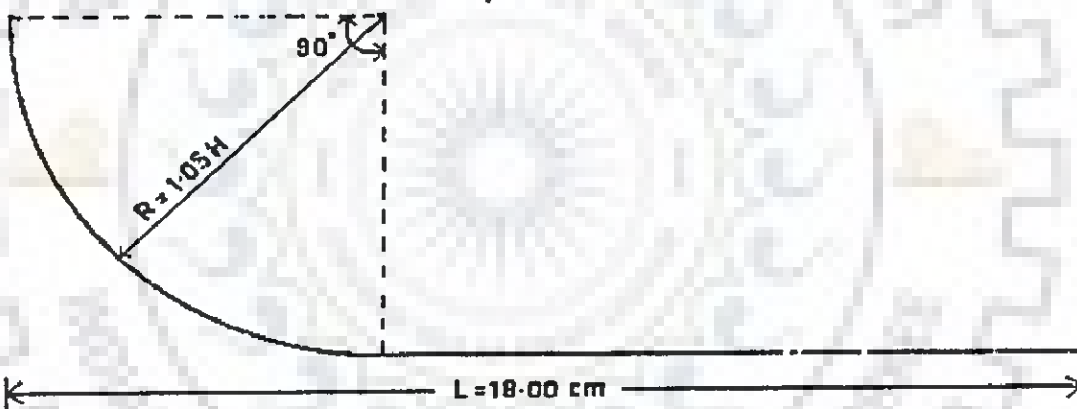


Fig. 3.5(b) Plan of J2 type vane

3.5 PHASE TWO MODEL EXPERIMENTS

It was intended at the first instance to try out the collar as scour retarder and optimization of shape and size of collar for the rectangular and trapezoidal vanes at two Froude numbers such as 0.13 and 0.25. At Froude number 0.13, eight nos. of different shapes and sizes of collar at $0.05H$ below the bed level were tried for rectangular vanes (Fig. 3.6(1) to 3.6(8)) and fourteen nos. of different shapes and sizes of collars at $0.05H$ below the bed were tried for trapezoidal submerged vanes (Fig. 3.7(1) to 3.7(14)). At Froude number 0.25, twelve numbers of different shapes and sizes of collar at $0.05H$ below bed level were tried for rectangular (Fig. 3.8(1) to 3.8(12)) and five numbers for trapezoidal vanes (Fig. 3.9(1) to 3.9(5)). Plastic sheet made rectangular submerged vanes were of height 6 cm and length of 18 cm. The trapezoidal vane used for optimization of collar had taper angle $3H:2.5V$ and its height and length were 6 cm and 18 cm respectively. Experiments relating to Phase two have been summarised in Table 3.4 and related experimental data have been presented in Appendix B.

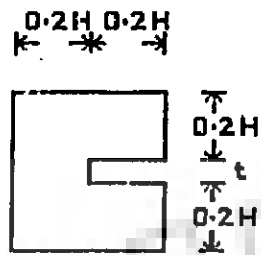


Fig. 3.6(1) Collar size AF1.1

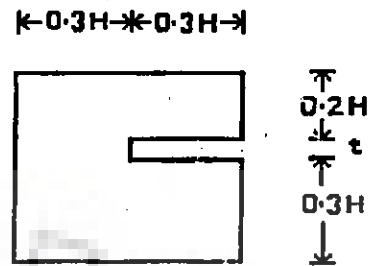


Fig. 3.6(2) Collar size AF1.2

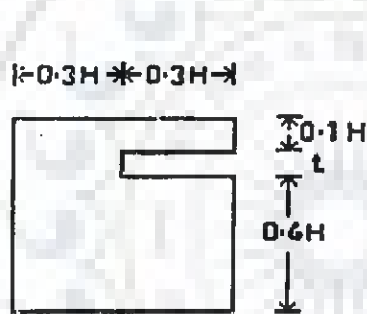


Fig. 3.6(3) Collar size AF1.3

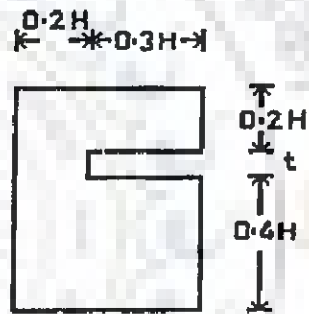


Fig. 3.6(4) Collar size AF1.4

$\leftarrow 0.3H \text{---} * 0.3H \text{---} \rightarrow$

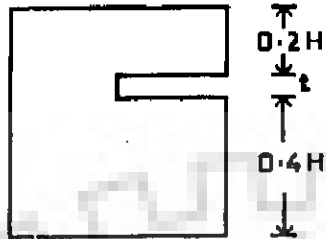


Fig. 3.6(5) Collar size AF1.5

$\leftarrow 0.3H \text{---} * 0.3H \text{---} \rightarrow$

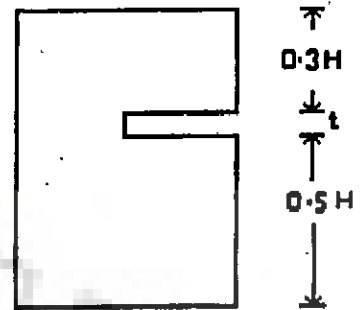


Fig. 3.6(6) Collar size AF1.6

$\leftarrow 0.3H \text{---} * 0.3H \text{---} \rightarrow$

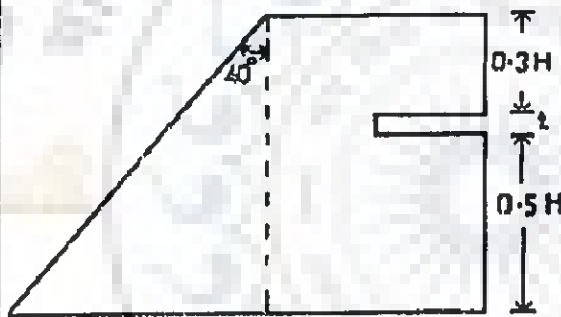


Fig. 3.6(7) Collar size AF1.7

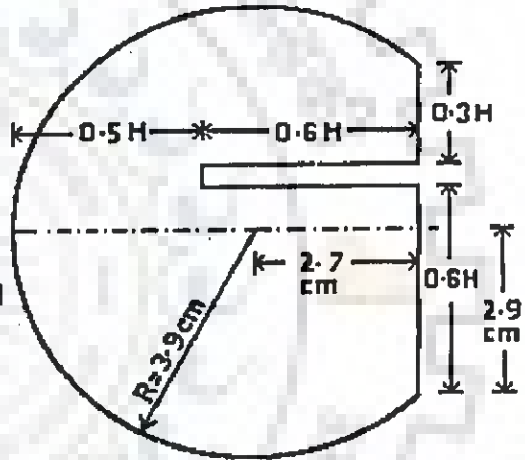


Fig. 3.6(8) Collar size AF1.8

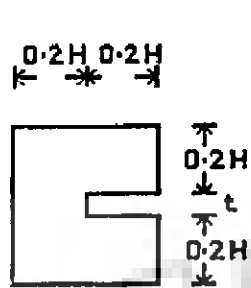


Fig. 3.7(1) Collar size BF1.1

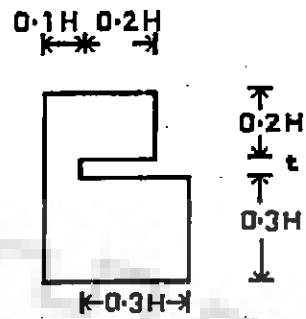


Fig. 3.7(2) Collar size BF1.2

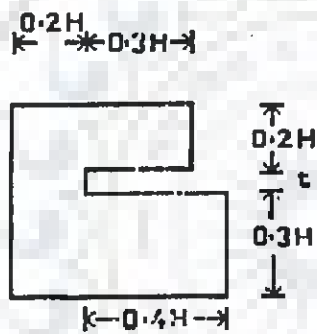


Fig. 3.7(3) Collar size BF1.3

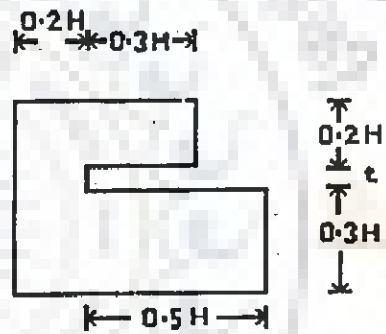


Fig. 3.7(4) Collar size BF1.4

$0.2H$
* $0.3H$ *

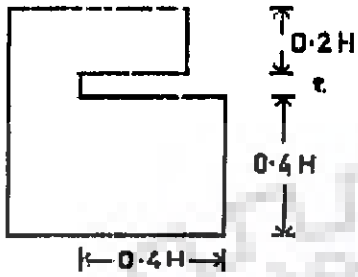


Fig. 3.7(5) Collar size BF1.5

$0.2H$
* $0.3H$ *

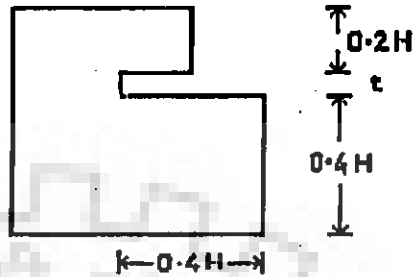


Fig. 3.7(6) Collar size BF1.6

* $0.3H$ *
* $0.3H$ *

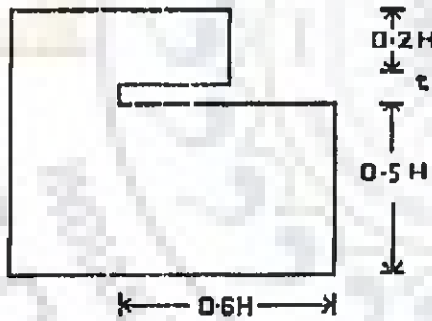


Fig. 3.7(7) Collar size BF1.7

* $0.3H$ *

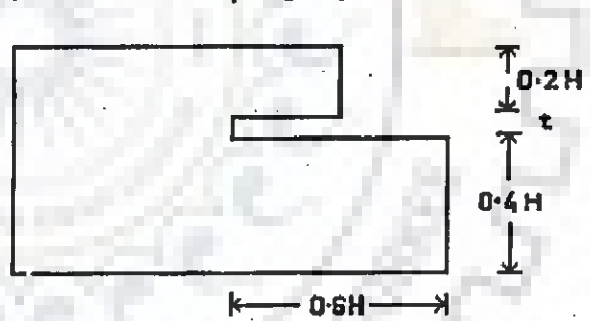


Fig. 3.7(8) Collar size BF1.8

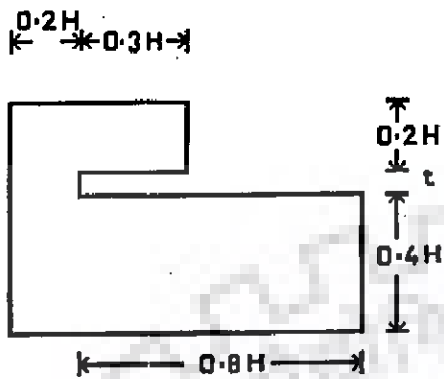


Fig. 3.7(9) Collar size BF1.9

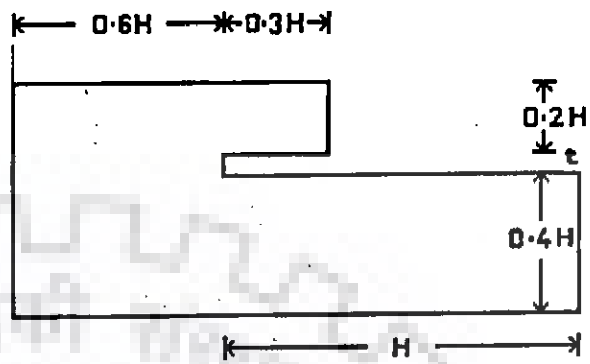


Fig. 3.7(10) Collar size BF1.10

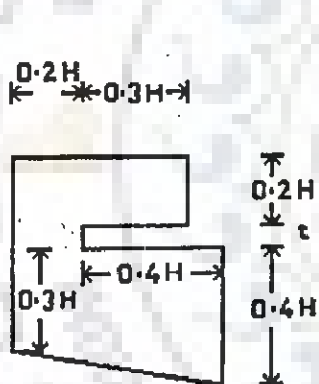


Fig. 3.7(11) Collar size BF1.11

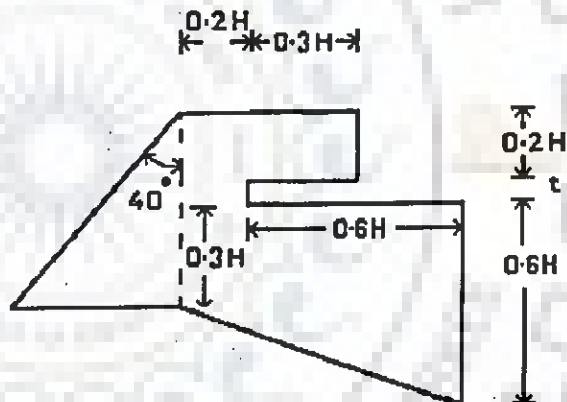


Fig. 3.7(12) Collar size BF1.12

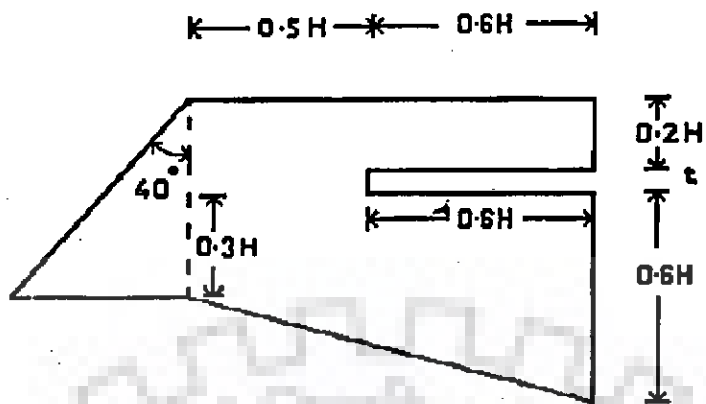


Fig. 3.7(13) Collar size BF1.13

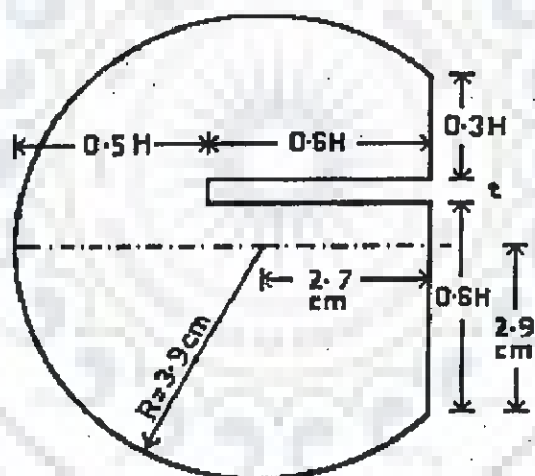


Fig. 3.7(14) Collar size BF1.14

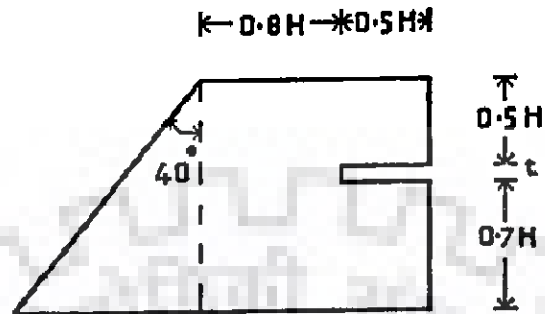


Fig. 3.8(1) Collar size AF2.1

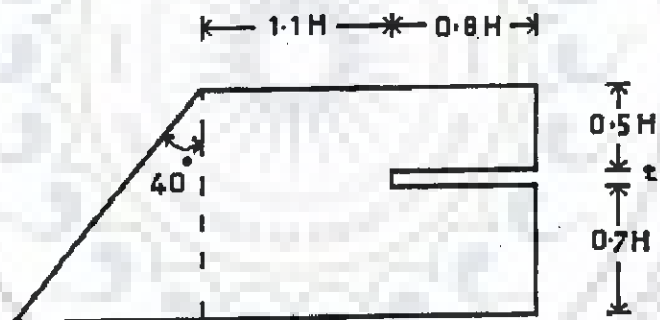
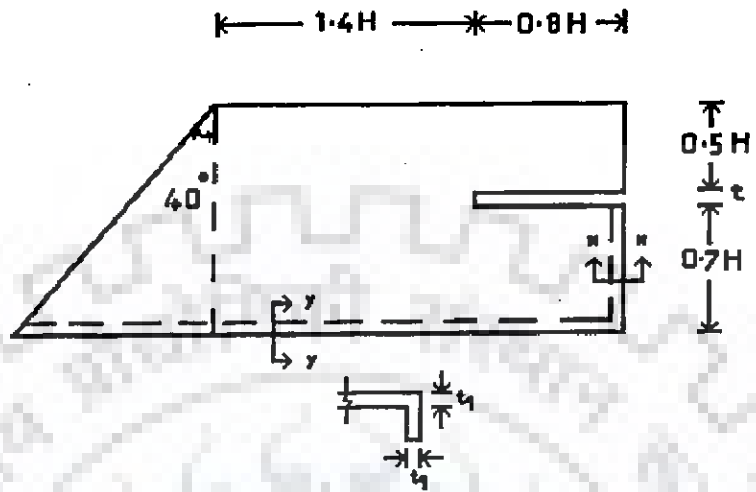
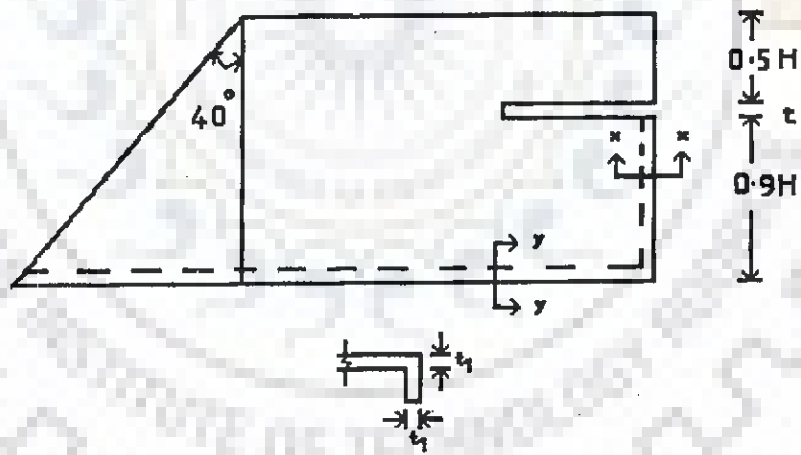


Fig. 3.8(2) Collar size AF2.2



Section X-X or Y-Y

Fig. 3.8(3) Collar size AF2.3



Section X-X or Y-Y

Fig. 3.8(4) Collar size AF2.4

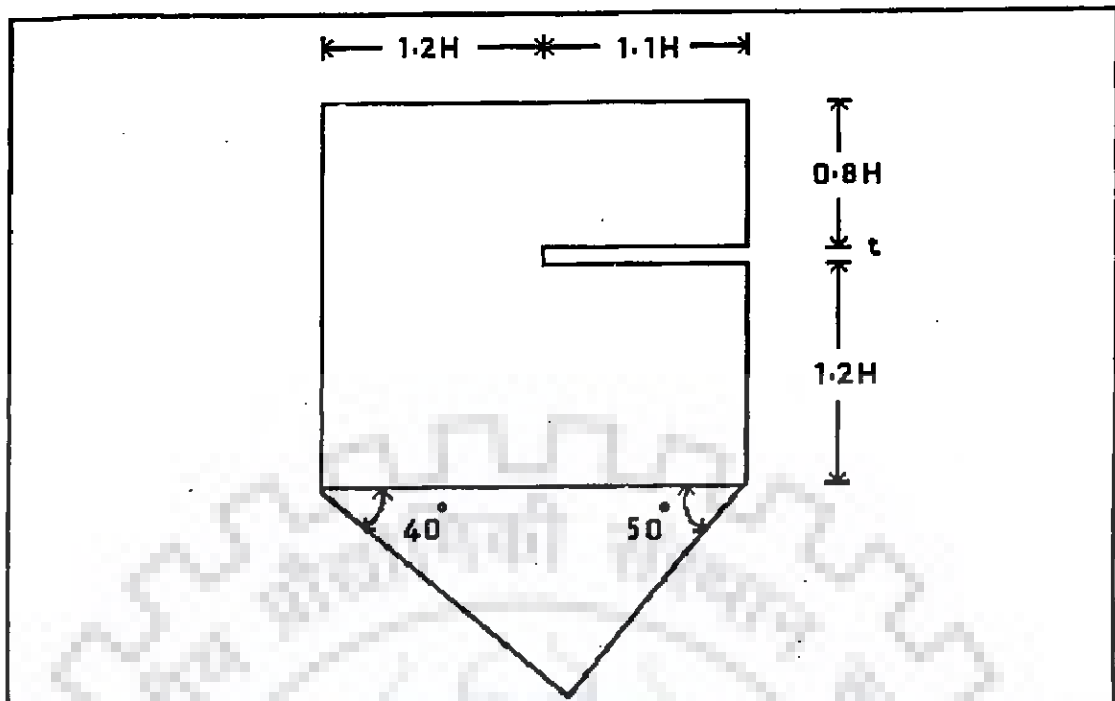


Fig. 3.8(7) Collar size AF2.7

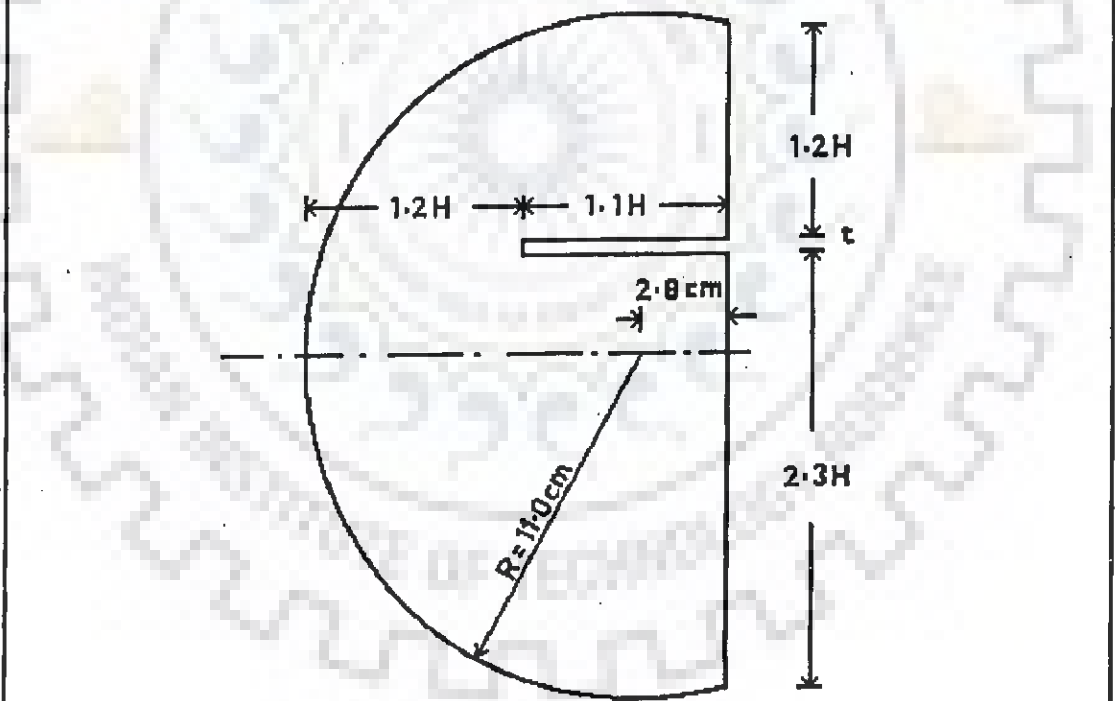


Fig. 3.8(8) Collar size AF2.8

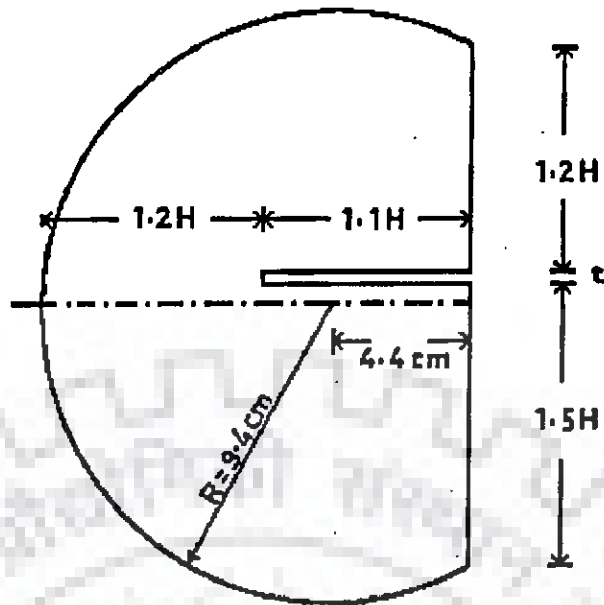


Fig. 3.8(9) Collar size AF2.9

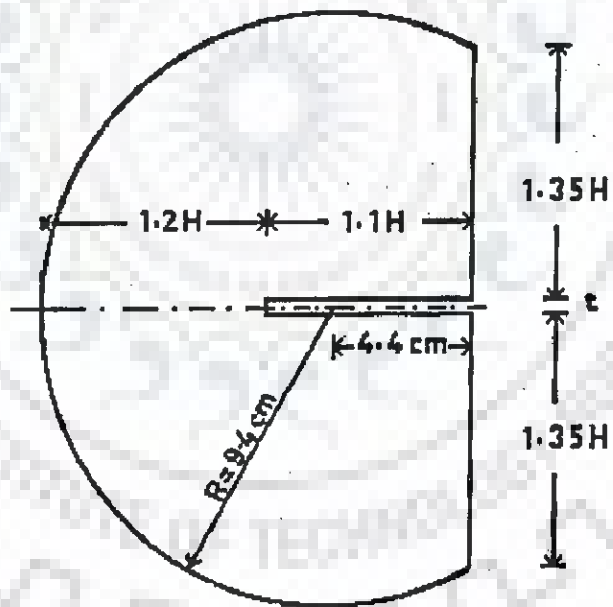


Fig. 3.8(10) Collar size AF2.10

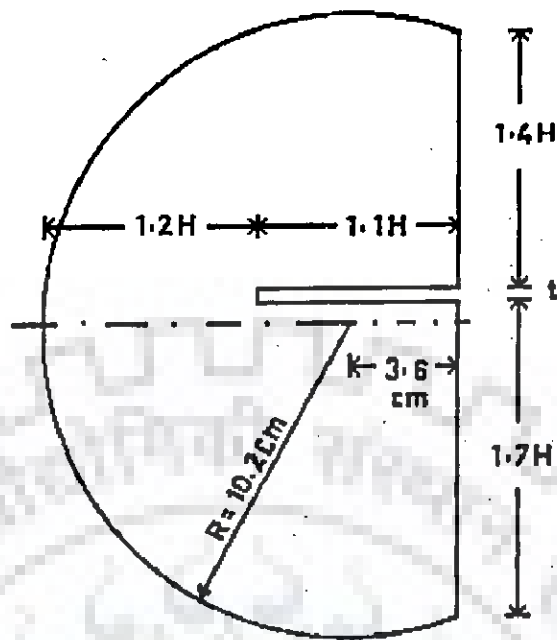


Fig. 3.8(11) Collar size AF2.11

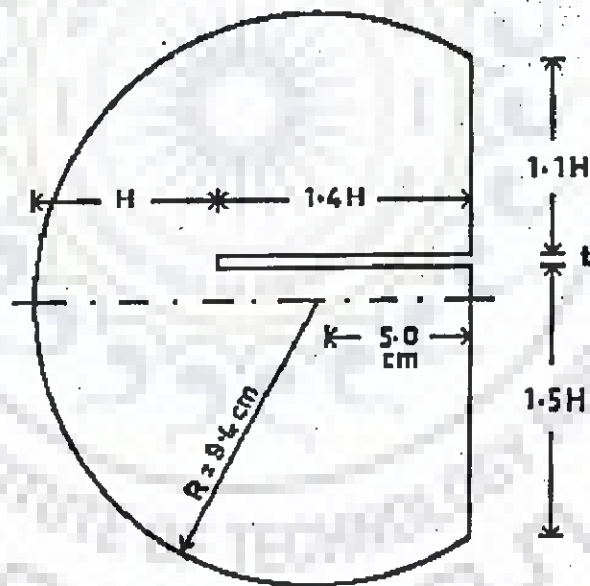
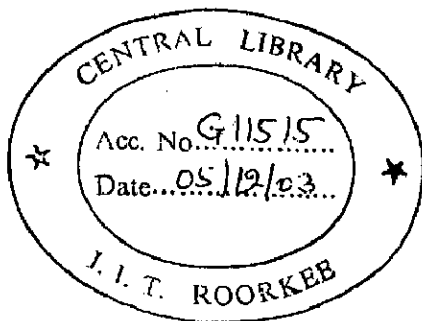


Fig. 3.8(12) Collar size AF2.12



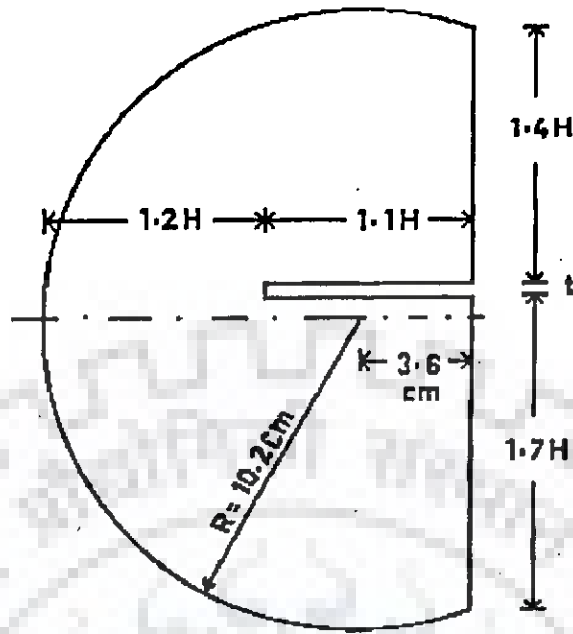


Fig. 3.9(1) Collar size BF2.1

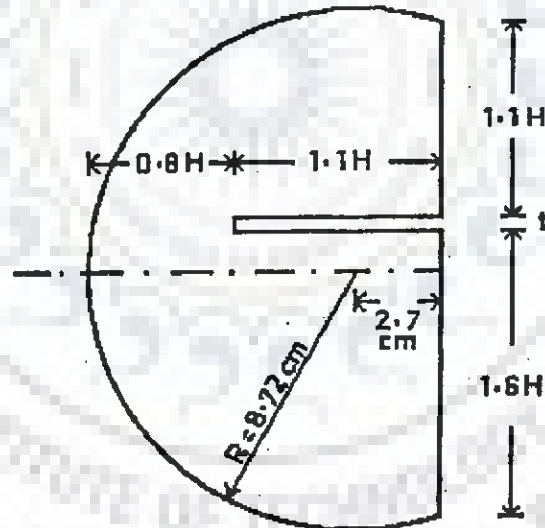


Fig. 3.9(2) Collar size BF2.2

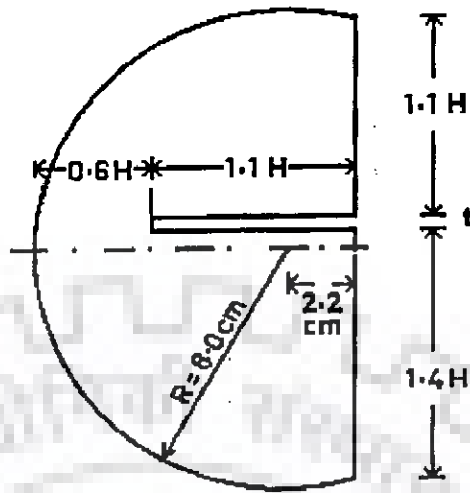


Fig. 3.9(3) Collar size BF2.3

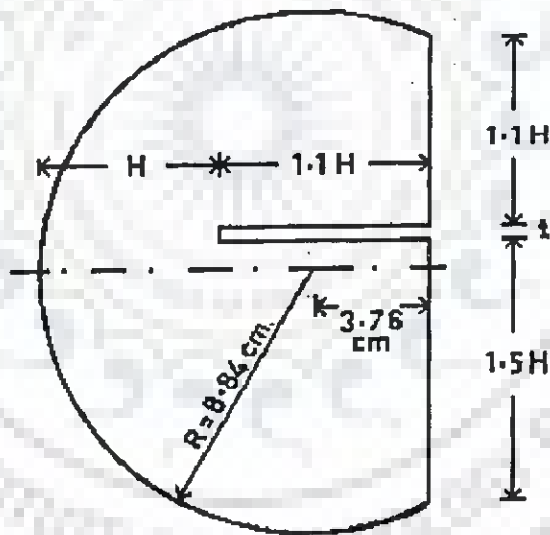


Fig. 3.9(4) Collar size BF2.4

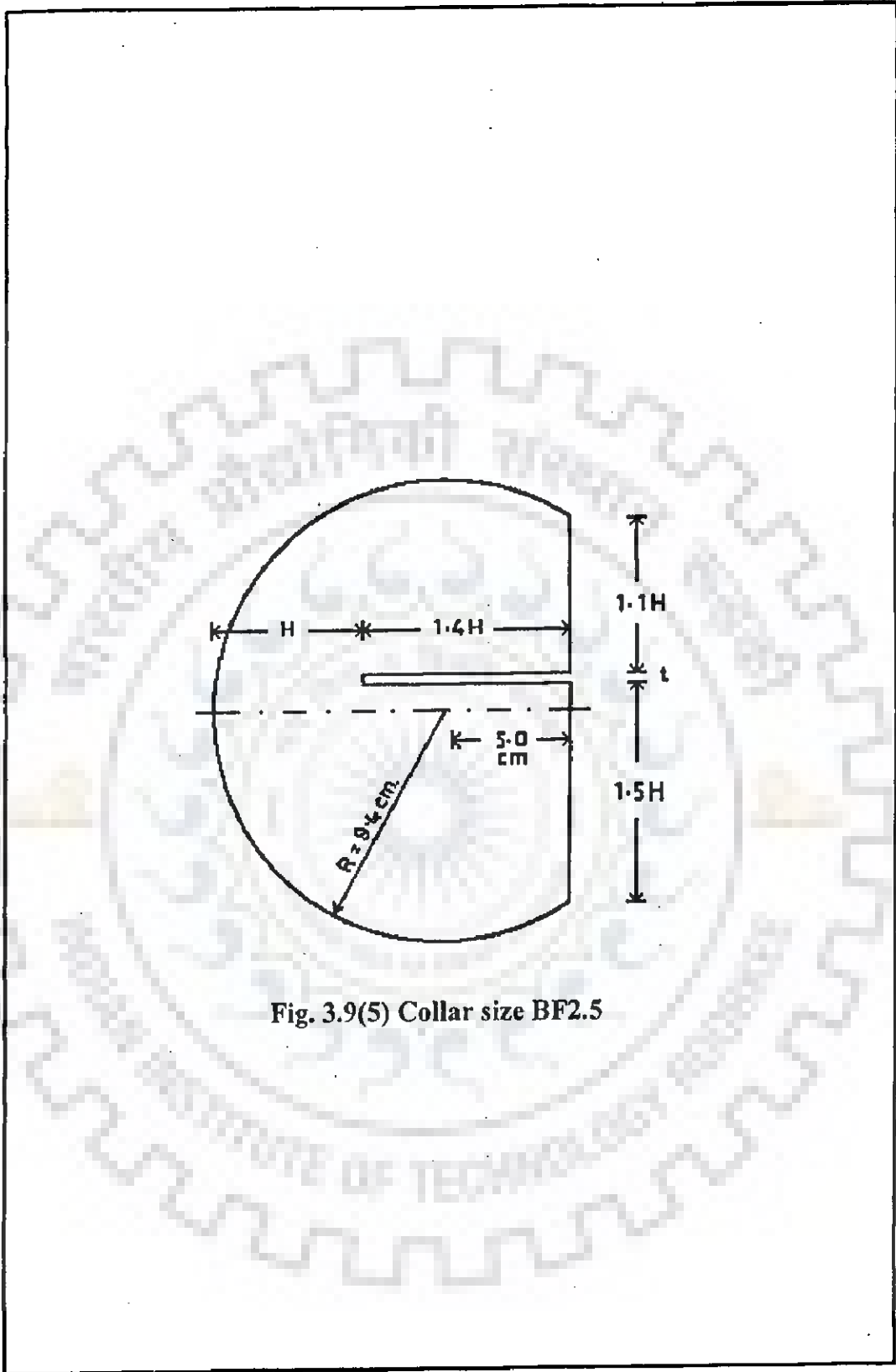


Fig. 3.9(5) Collar size BF2.5

Table 3.4: Phase two experiments

Expt. No.	Rate of flow (m ³ /s)	Flow depth (cm)	Fr. No.	(T/d)	d ₅₀ (mm)	Vanes type	Collar as given in Fig.
B1	0.0154	18	0.13	0.67	0.225	Rectangular	AF1.1
B2	0.0154	18	0.13	0.67	0.225	Rectangular	AF1.2
B3	0.0154	18	0.13	0.67	0.225	Rectangular	AF1.3
B4	0.0154	18	0.13	0.67	0.225	Rectangular	AF1.4
B5	0.0154	18	0.13	0.67	0.225	Rectangular	AF1.5
B6	0.0154	18	0.13	0.67	0.225	Rectangular	AF1.6
B7	0.0154	18	0.13	0.67	0.225	Rectangular	AF1.7
B8	0.0154	18	0.13	0.67	0.225	Rectangular	AF1.8
B9	0.0154	18	0.13	0.67	0.405	Rectangular	AF1.8
B10	0.0154	18	0.13	0.67	0.225	Trapezoidal (3H:2.5V)	BF1.1
B11	0.0154	18	0.13	0.67	0.225	Trapezoidal (3H:2.5V)	BF1.2
B12	0.0154	18	0.13	0.67	0.225	Trapezoidal (3H:2.5V)	BF1.3
B13	0.0154	18	0.13	0.67	0.225	Trapezoidal (3H:2.5V)	BF1.4
B14	0.0154	18	0.13	0.67	0.225	Trapezoidal (3H:2.5V)	BF1.5
B15	0.0154	18	0.13	0.67	0.225	Trapezoidal (3H:2.5V)	BF1.6
B16	0.0154	18	0.13	0.67	0.225	Trapezoidal (3H:2.5V)	BF1.7
B17	0.0154	18	0.13	0.67	0.225	Trapezoidal (3H:2.5V)	BF1.8
B18	0.0154	18	0.13	0.67	0.225	Trapezoidal (3H:2.5V)	BF1.9
B19	0.0154	18	0.13	0.67	0.225	Trapezoidal (3H:2.5V)	BF1.10
B20	0.0154	18	0.13	0.67	0.225	Trapezoidal (3H:2.5V)	BF1.11
B21	0.0154	18	0.13	0.67	0.225	Trapezoidal (3H:2.5V)	BF1.12
B22	0.0154	18	0.13	0.67	0.225	Trapezoidal (3H:2.5V)	BF1.13
B23	0.0154	18	0.13	0.67	0.225	Trapezoidal (3H:2.5V)	BF1.14
B24	0.0154	18	0.13	0.67	0.405	Trapezoidal (3H:2.5V)	BF1.14
B25	0.0203	14	0.25	0.57	0.405	Rectangular	AF2.1
B26	0.0203	14	0.25	0.57	0.405	Rectangular	AF2.2
B27	0.0203	14	0.25	0.57	0.405	Rectangular	AF2.3
B28	0.0203	14	0.25	0.57	0.405	Rectangular	AF2.4
B29	0.0203	14	0.25	0.57	0.405	Rectangular	AF2.5
B30	0.0203	14	0.25	0.57	0.405	Rectangular	AF2.6
B31	0.0203	14	0.25	0.57	0.405	Rectangular	AF2.7
B32	0.0203	14	0.25	0.57	0.405	Rectangular	AF2.8
B33	0.0203	14	0.25	0.57	0.405	Rectangular	AF2.9
B34	0.0203	14	0.25	0.57	0.405	Rectangular	AF2.10
B35	0.0203	14	0.25	0.57	0.405	Rectangular	AF2.11
B36	0.0203	14	0.25	0.57	0.405	Rectangular	AF2.12
B37	0.0203	14	0.25	0.57	0.225	Rectangular	AF2.12
B38	0.0203	14	0.25	0.57	0.405	Trapezoidal (3H:2.5V)	BF2.1
B39	0.0203	14	0.25	0.57	0.405	Trapezoidal (3H:2.5V)	BF2.2
B40	0.0203	14	0.25	0.57	0.405	Trapezoidal (3H:2.5V)	BF2.3
B41	0.0203	14	0.25	0.57	0.405	Trapezoidal (3H:2.5V)	BF2.4
B42	0.0203	14	0.25	0.57	0.405	Trapezoidal (3H:2.5V)	BF2.5
B43	0.0203	14	0.25	0.57	0.225	Trapezoidal (3H:2.5V)	BF2.5

3.6 PHASE THREE MODEL EXPERIMENTS

In this phase of experiments, five shapes of submerged vanes such as rectangular, double curve type I, double curve type II, J1 type and J2 type were deployed to investigate the optimal angle of attack. The optimal angle of attack for rectangular vane with collar was investigated. The effect of degree of submergence on the optimal angle of attack for rectangular vanes with collar was also investigated. The optimal angle of attack for double curve type I, double curve type II, J1 type and J2 vanes were also investigated. Further, the effect of aspect ratio and taper angle on the strength of vane induced vortex were also studied. All these shapes have the height 6 cm and length 18 cm. The experiments were run for 8 hrs. All the experiments were conducted in clear water conditions. The flow was adjusted to less than critical conditions. All the three components of velocities were measured at a distance of 15 cm downstream from the centre of the vanes. The grid was taken 3 cm × 3 cm. Experiments were conducted at the angle of attack of 30°, 35°, 40°, 45° and 50° to evaluate optimal angle of attack for all shapes. The effect of aspect ratio of rectangular submerged vanes was investigated. The effect of taper angle at the leading edge of rectangular submerged vanes on the vane-induced vortex was also investigated. Three types of taper angles were taken for the investigations (Fig. 3.10 and Table 3.5). Table 3.6 describes the summary of phase two experiments. Experimental data relating to this phase have been presented in Appendix C.

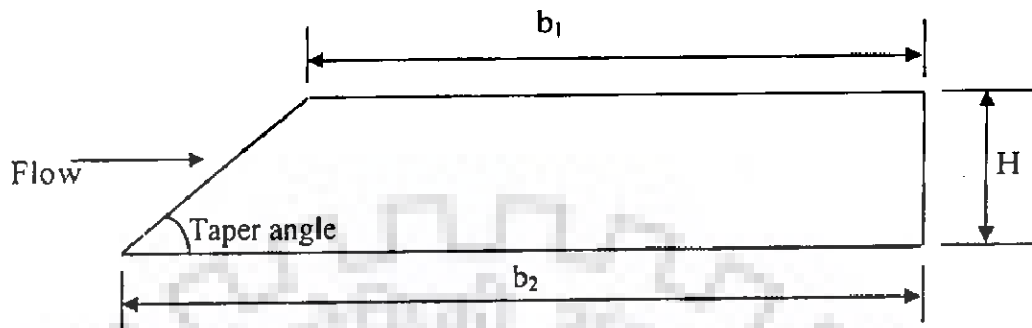


Fig. 3.10 Trapezoidal vane

Table 3.5: Dimensions of trapezoidal vane

Taper angle	Top length (b_1) in cm	Bottom length (b_2) in cm	Average length $(b_1 + b_2)/2$ in cm
1H:1V	15	21	18
3H:2.5V	14.4	21.6	18
4H:2V	12	24	18

Table 3.6: Phase three Experiments

Expt. No.	Rate of flow (m ³ /s)	d (cm)	F _r	T/d	H/L	α	Vane Type
C1	0.0128	15	0.14	0.6	0.33	30 ⁰	Rectangular with collar
C2	0.0128	15	0.14	0.6	0.33	35 ⁰	Rectangular with collar
C3	0.0128	15	0.14	0.6	0.33	40 ⁰	Rectangular with collar
C4	0.0128	15	0.14	0.6	0.33	45 ⁰	Rectangular with collar
C5	0.0128	15	0.14	0.6	0.33	50 ⁰	Rectangular with collar
C6	0.0154	18	0.13	0.67	0.33	30 ⁰	Rectangular with collar
C7	0.0154	18	0.13	0.67	0.33	35 ⁰	Rectangular with collar
C8	0.0154	18	0.13	0.67	0.33	40 ⁰	Rectangular with collar
C9	0.0154	18	0.13	0.67	0.33	45 ⁰	Rectangular with collar
C10	0.0154	18	0.13	0.67	0.33	50 ⁰	Rectangular with collar
C11	0.0205	24	0.11	0.75	0.33	30 ⁰	Rectangular with collar
C12	0.0205	24	0.11	0.75	0.33	35 ⁰	Rectangular with collar
C13	0.0205	24	0.11	0.75	0.33	40 ⁰	Rectangular with collar
C14	0.0205	24	0.11	0.75	0.33	45 ⁰	Rectangular with collar
C15	0.0205	24	0.11	0.75	0.33	50 ⁰	Rectangular with collar
C16	0.0154	18	0.13	0.67	0.50	40 ⁰	Rectangular with collar
C17	0.0154	18	0.13	0.67	0.25	40 ⁰	Rectangular with collar
C18	0.0154	18	0.13	0.67	0.33	40 ⁰	Rectangular without collar
C19	0.0154	18	0.13	0.67	0.33	40 ⁰	Trapezoidal (1H:1V)*
C20	0.0154	18	0.13	0.67	0.33	40 ⁰	Trapezoidal (3H:2.5V)*
C21	0.0154	18	0.13	0.67	0.33	40 ⁰	Trapezoidal (4H:2V)*
C22	0.0154	18	0.13	0.67	0.33	30 ⁰	Double curve Type I
C23	0.0154	18	0.13	0.67	0.33	35 ⁰	Double curve Type I
C24	0.0154	18	0.13	0.67	0.33	40 ⁰	Double curve Type I
C25	0.0154	18	0.13	0.67	0.33	45 ⁰	Double curve Type I
C26	0.0154	18	0.13	0.67	0.33	50 ⁰	Double curve Type I
C27	0.0154	18	0.13	0.67	0.33	30 ⁰	Double curve Type II
C28	0.0154	18	0.13	0.67	0.33	35 ⁰	Double curve Type II
C29	0.0154	18	0.13	0.67	0.33	40 ⁰	Double curve Type II
C30	0.0154	18	0.13	0.67	0.33	45 ⁰	Double curve Type II
C31	0.0154	18	0.13	0.67	0.33	50 ⁰	Double curve Type II
C32	0.0154	18	0.13	0.67	0.33	30 ⁰	J1 Type
C33	0.0154	18	0.13	0.67	0.33	35 ⁰	J1 Type
C34	0.0154	18	0.13	0.67	0.33	40 ⁰	J1 Type
C35	0.0154	18	0.13	0.67	0.33	45 ⁰	J1 Type
C36	0.0154	18	0.13	0.67	0.33	50 ⁰	J1 Type
C37	0.0154	18	0.13	0.67	0.33	30 ⁰	J2 Type
C38	0.0154	18	0.13	0.67	0.33	35 ⁰	J2 Type
C39	0.0154	18	0.13	0.67	0.33	40 ⁰	J2 Type
C40	0.0154	18	0.13	0.67	0.33	45 ⁰	J2 Type
C41	0.0154	18	0.13	0.67	0.33	50 ⁰	J2 Type

* with collar

3.7 PHASE FOUR MODEL EXPERIMENTS

In this phase, the formation of dike due to rectangular and trapezoidal vane was studied. The streamwise decay of vane induced vortex was also studied. In this phase all the experiments were conducted at sediment size 0.405mm and Froude number 0.25. The strength of vortex in terms of moment of momentum was examined at 10H, 20H, 30H and 40H distance from the vane. All three components of velocity were measured using ADV. Table 3.7 describes the summary of phase four experiments. Experimental data relating to this phase have been presented in Appendix D.

Table 3.7: Phase four experiments

Expt. No.	Rate of flow (m ³ /s)	d (cm)	F _r	T/d	H/L	α	Vane Type
D1	0.0106	14	0.13	0.57	0.33	40 ⁰	Rectangular without collar
D2	0.0106	14	0.13	0.57	0.33	40 ⁰	Rectangular with collar
D3	0.0106	14	0.13	0.57	0.33	40 ⁰	Trapezoidal (1H:1V)*
D4	0.0106	14	0.13	0.57	0.33	40 ⁰	Trapezoidal (3H:2.5V)*
D5	0.0106	14	0.13	0.57	0.33	40 ⁰	Trapezoidal (4H:2V)*
D6	0.0203	14	0.25	0.57	0.33	40 ⁰	Rectangular without collar
D7	0.0203	14	0.25	0.57	0.33	40 ⁰	Rectangular with collar
D8	0.0203	14	0.25	0.57	0.33	40 ⁰	Trapezoidal (1H:1V)*
D9	0.0203	14	0.25	0.57	0.33	40 ⁰	Trapezoidal (3H:2.5V)*
D10	0.0203	14	0.25	0.57	0.33	40 ⁰	Trapezoidal (4H:2V)*

* with collar

3.8 PHASE FIVE PROTOTYPE FIELD EXPERIMENTS

In this phase of prototype field experiments, two numbers of steel-made trapezoidal vanes, one with collar and another without collar were constructed in the Solani river 7 Km away from the place of study. The size and shape of collar was assembled with the trapezoidal vane at its leading edge. The aim of this experiment was to verify in actual river the optimal shape and size of collar as local scour retarder, which was earlier optimized in the laboratory experiment. The collar was located at $0.05H$ below bed level of Solani River.

The height and bottom length of both these vanes were 40 cm and 120 cm, respectively. The thickness of collar and vanes were 4mm. Two numbers of steel pipes of 5 cm diameters were tightened by nut and bolts with the vane. The grip length of the pipes was 1m to 1.5m depending upon the simple refusal for further driving. The bottom ends of the pipes were welded with auger so that simple rotation of the pipe in horizontal plane will penetrate into the river bed.

Bed levels and water levels were measured around the submerged vanes vis a vis discharge in the river.

Following measurements were also taken:-

1. The grain size distribution of the bed material was checked by the standard methods. Samples taken were dried in electrical oven for 5 days to 6 days. Everywhere around both the bamboo vanes, the river bed grains were found nonuniform of size $d_{50} = 0.200\text{mm}$ with σ , standard deviation 1.4. Table 3.8 and Fig. 3.11 show the sieve analysis of the bed material of this river at the construction spots.

Table 3.8: The sieve analysis of the bed material of river Solani at the vane construction spots

Size of sieves in mm	Weight retained on sieves in gm	% weight retained	Cummulative finer in gm	Cummulative % finer in gm
0.85	0.211	0.021	999.789	99.979
0.425	0.903	0.090	998.886	99.889
0.3	0.091	0.009	998.795	99.880
0.15	733.943	73.395	264.852	26.485
0.75	240.752	24.075	24.100	2.410
Pan	24.10	2.41	0.000	0.000

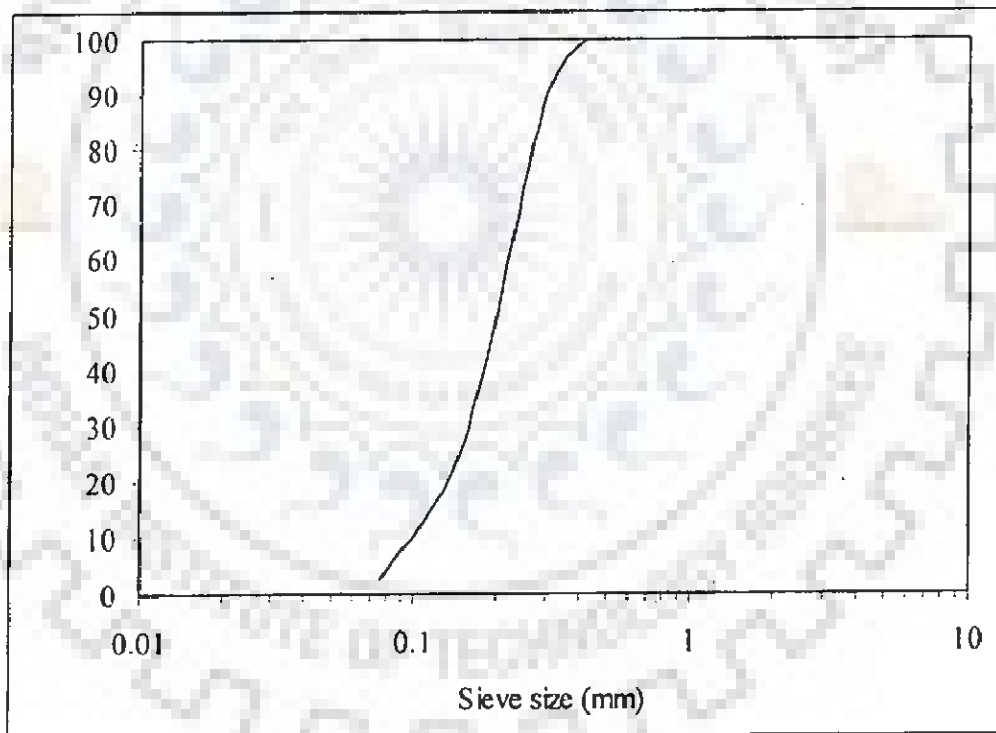


Fig. 3.11 Cummulative frequency curve for sand d_{50} as 0.200 mm (Field trial in Solani river).

2. The initial bed levels of the river and the scour depth after every 24 hours were measured against a bench mark with the help of dumpy level around both the trapezoidal submerged vanes.
3. Discharge variations were measured throughout this duration by the measurement of velocities and depths at every one metre distance along the river cross sections near the submerged vanes.
4. The slope of the river was calculated with the help of Dumpy level by reading the difference in level of water surface at different sections over a distance of 500m which showed the slope of river as in thousand.



PERFORMANCE EVALUATION OF SUBMERGED VANES WITHOUT COLLAR

4.1 GENERAL

Considering the fact that submerged vanes of different shapes are to be used in field conditions, the objective of these experiments was to identify the submerged vanes in which the minimum scour occurred at the leading edge of submerged vanes. For identical conditions of flow, aspect ratio (H/L) as 0.33 and degree of submergence (T/d) as 0.67, the pattern of local scour around the submerged vanes was used to identify the submerged vanes corresponding to minimum local scour hole at different Froude numbers. For modelling of local scour around the submerged vanes at optimal angle of attack 40° (Marelius and Sinha, 1998), certain existing models have been considered relevant. To reduce the local scour, the collar as scour retarder device can also be tried. It is relevant to compare the cost of most effective collar to that of the granular or riprap material along with geo-filter in order to reduce the local scour at the leading edge of rectangular submerged vanes.

4.2 SCOUR AROUND SUBMERGED VANES WITHOUT COLLAR

To study this, a set of experiments involving different types of vanes has been conducted. To have idea about the extent of scour around spurs, a series of Plates are included here. It can be seen that local scour around the leading edges of submerged vanes are different for rectangular and curved vanes (see Plates 4.1 to 4.12).

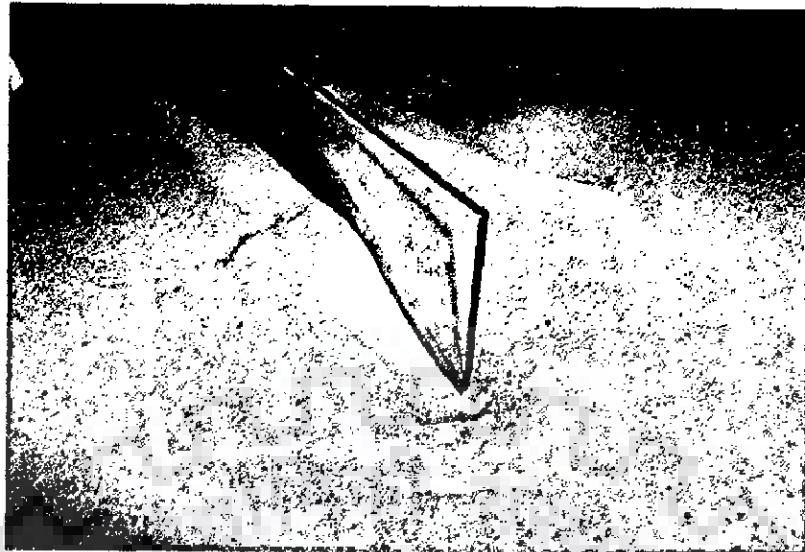


**Plate 4.1 Local scour with rectangular vane at Fr 0.13
($d_{50} = 0.225$ mm)**

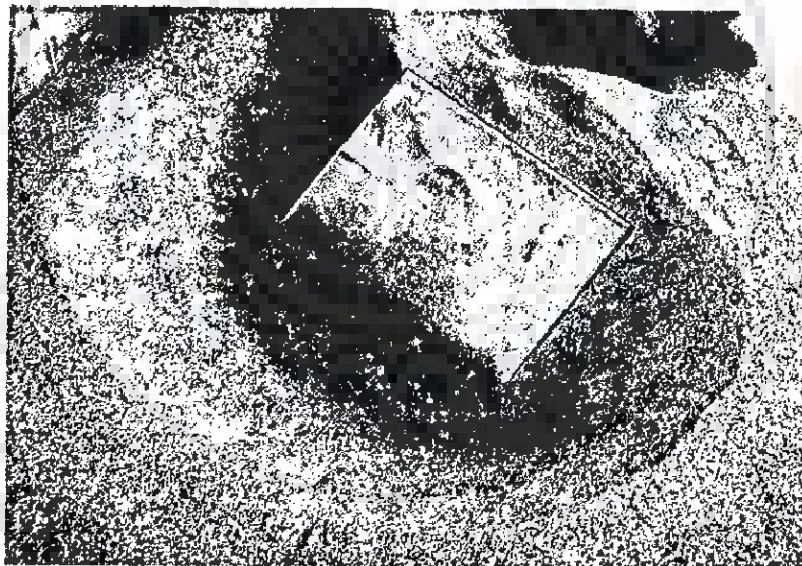


**Plate 4.2 Local scour with rectangular vane at Fr 0.25
($d_{50} = 0.405$ mm)**



**Plate 4.3 Local scour with trapezoidal vane (3H:2.5V) at Fr 0.13
($d_{50} = 0.225$ mm)**

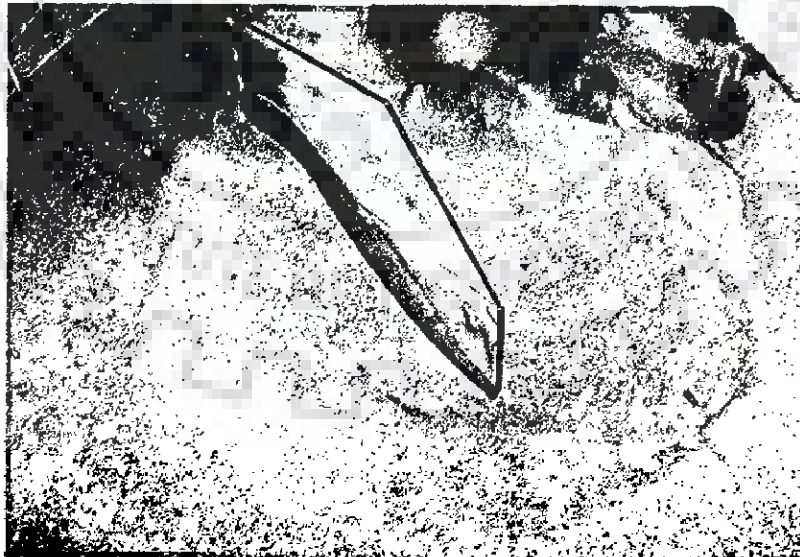


**Plate 4.4 Local scour with trapezoidal vane (3H:2.5V) at Fr 0.25
($d_{50} = 0.405$ mm)**

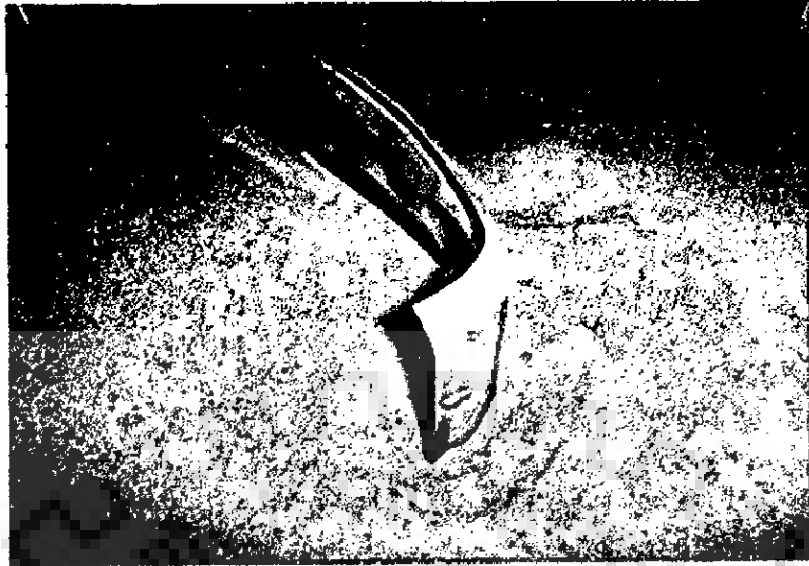


**Plate 4.5 Local scour with double curve type I vane at Fr 0.13
($d_{50} = 0.225$ mm)**

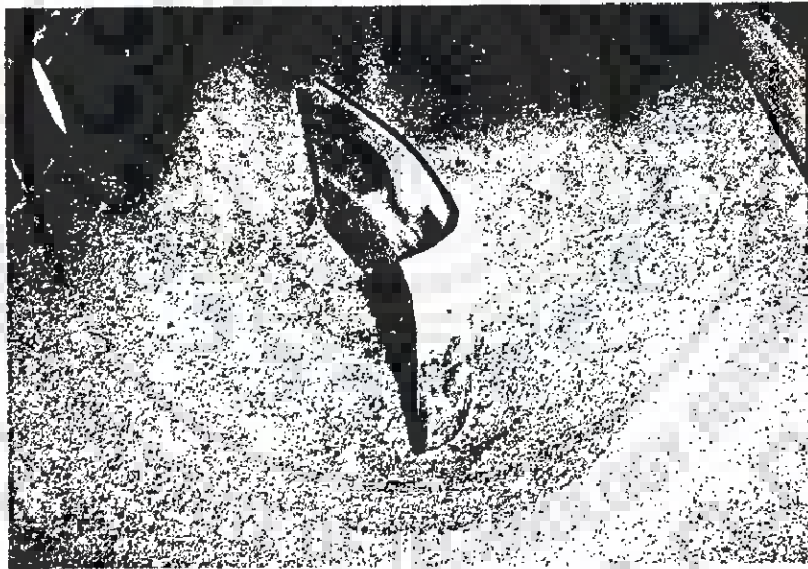


**Plate 4.6 Local scour with double curve type I vane at Fr 0.25
($d_{50} = 0.405$ mm)**



**Plate 4.7 Local scour with double curve type II vane at Fr 0.13
($d_{50} = 0.225$ mm)**



**Plate 4.8 Local scour with double curve type II vane at Fr 0.25
($d_{50} = 0.405$ mm)**

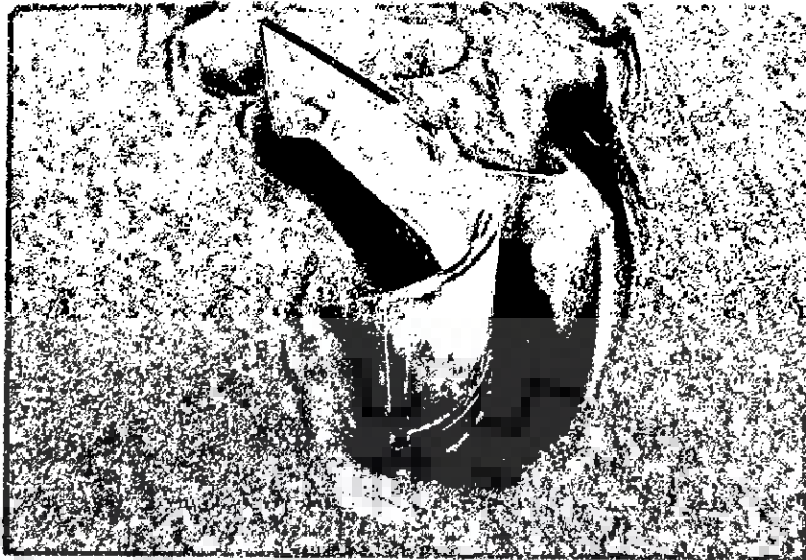


**Plate 4.9 Local scour with J1 type vane at Fr 0.13
($d_{50} = 0.225$ mm)**

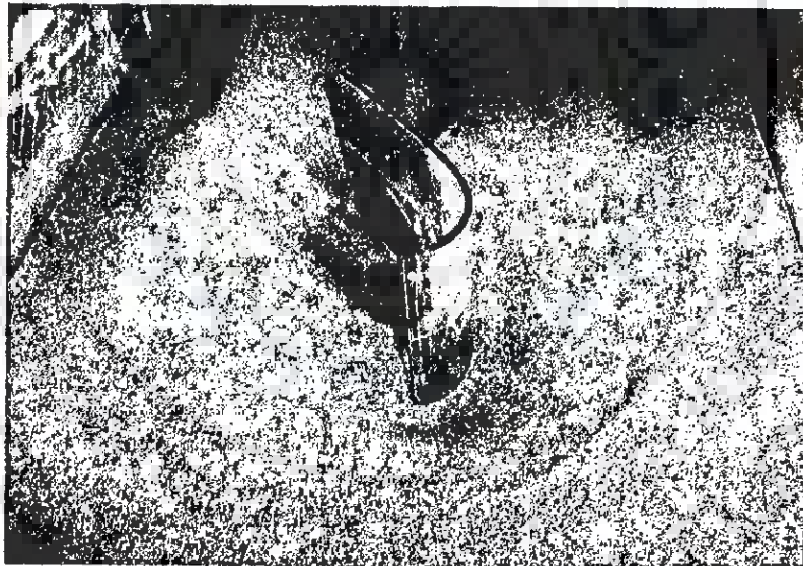


**Plate 4.10 Local scour with J1 type vane at Fr 0.25
($d_{50} = 0.405$ mm)**



**Plate 4.11 Local scour with J2 type vane at Fr 0.13
($d_{50} = 0.225$ mm)**



**Plate 4.12 Local scour with J2 type vane at Fr 0.25
($d_{50} = 0.405$ mm)**

The local scour at the leading edges of the vanes is smaller at Froude number 0.13 than that of at Froude number 0.25. With the same installation depth, the rectangular vane was dislodged by flow at Froude number 0.25, where as it was stable at Froude number 0.13. The local scour at the leading edges of curved type submerged vanes such as double curve type I, double curve type II, J1 and J2 type is smaller than that of rectangular vanes at Froude number 0.13. Thus, rectangular vane experiences maximum scour depth under similar condition of flow. For this reason, only the scour around rectangular vanes has been monitored for the provision of collar. However, huge local scour around all submerged vanes are formed at Froude number 0.25. Tapering the leading edge of rectangular vane is not effective to reduce the local scour around the vanes (Plates 4.1 to 4.4).

4.3 FUNCTIONAL RELATIONSHIPS FOR SCOUR

The local scour around bridge piers, deal with an obstructed flow situation, it is logical to assume that the local scour around rectangular submerged vanes will have similar dependency on variables describing flow, fluid, sediment and geometry.

For describing scour around spurs, Garde (1961) identified the pertinent variables as follows: mean flow velocity U , average depth of flow d , mass density of water ρ_w , difference in specific weights between water and air $\Delta\gamma$, dynamic viscosity μ , median size of sediment d_{50} , standard deviation σ , difference in specific weights between sediment and water $\Delta\gamma_s$, channel width B , width of spur-dike b , settling velocity of sediment ω_0 , shape parameters describing geometry of spur cross section ξ , and angle of inclination of spur-dike, β . In terms of these parameters, the following expression of scour depth, D ; relative to water surface was proposed by Garde (1961) as

$$D = f(U, d, \rho, \Delta\gamma, \mu, d_{50}, \sigma, \Delta\gamma_s, w_0, B, b, \xi, \beta) \quad (4.1)$$

In case of submerged vanes, neglecting B and b and replacing β by α , one can write

$$D = f(U, d, \rho, \Delta\gamma, \mu, d_{50}, \sigma, \Delta\gamma_s, \xi, \alpha) \quad (4.2)$$

Using dimensional analysis, equation (4.2) can be written as

$$\frac{D}{d} = f\left(\frac{d_{50}}{d}, \frac{\sigma}{d}, \frac{U}{\sqrt{gd}}, \alpha, \frac{4}{3} \frac{\Delta\gamma_s d}{w_o^2 \rho}, \xi\right) \quad (4.3)$$

In equation (4.3), some of the dimensionless terms including $\left(\frac{d_{50}}{d}\right)$ and $\left(\frac{\sigma}{d}\right)$ have been found to be not very important and for these reasons they have been ignored. A simplified form of the dimensionless relationship for the scour depth has been proposed as follows.

$$\frac{D}{d} = k F_r^n \quad (4.4)$$

In equation (4.4),

$$F_r = \frac{U}{\sqrt{gd}} \quad (4.5)$$

Considering the works of several investigators and eqs. 4.1 to 4.5, it appears logical to relate observed scour depth, D_{50} using a variety of functional relationships, as follows

$$\frac{D_{50}}{d_{50}} = f\left(\frac{U}{\sqrt{g(S-1)d_{50}}}\right) \quad (4.6)$$

$$\frac{D_{50}}{d} = f\left(\frac{U}{\sqrt{g(S-1)d_{50}}}\right) \quad (4.7)$$

$$\frac{D_{50}}{d_{50}} = f\left(\frac{U}{\sqrt{gd}}\right) \quad (4.8)$$

$$\frac{D_{50}}{d} = f\left(\frac{U}{\sqrt{gd}}\right) \quad (4.9)$$

The experimental data have been processed using eqs. 4.6 to 4.9 and the representative plots are given in Figs. 4.1 to 4.4. It can be seen from Figs. 4.1 to 4.4 that

the representation of scour depth is well described by Fig. 4.4. The functional relationships as per Fig. 4.4, can be expressed as follows

$$\frac{D_{sc}}{d} = 3.5675 F_r^{1.3761}. \quad (4.10)$$

where, D_{sc} = computed scour depth

Using eq. 4.10, the agreement between computed and observed scour is shown in the Fig. 4.5. From Figs. 4.1 to 4.4, it is apparent that despite the importance of densimetric Froude number $\left(\frac{U}{\sqrt{g(S-1)d_{50}}} \right)$, as represented by Zimmermann and Kennedy (1978), one cannot ignore the importance of flow Froude number in preference to densimetric Froude number (as apparent from Fig. 4.4).

Thus, for the planning of subsequent experiments, flow Froude number has been given a major consideration.

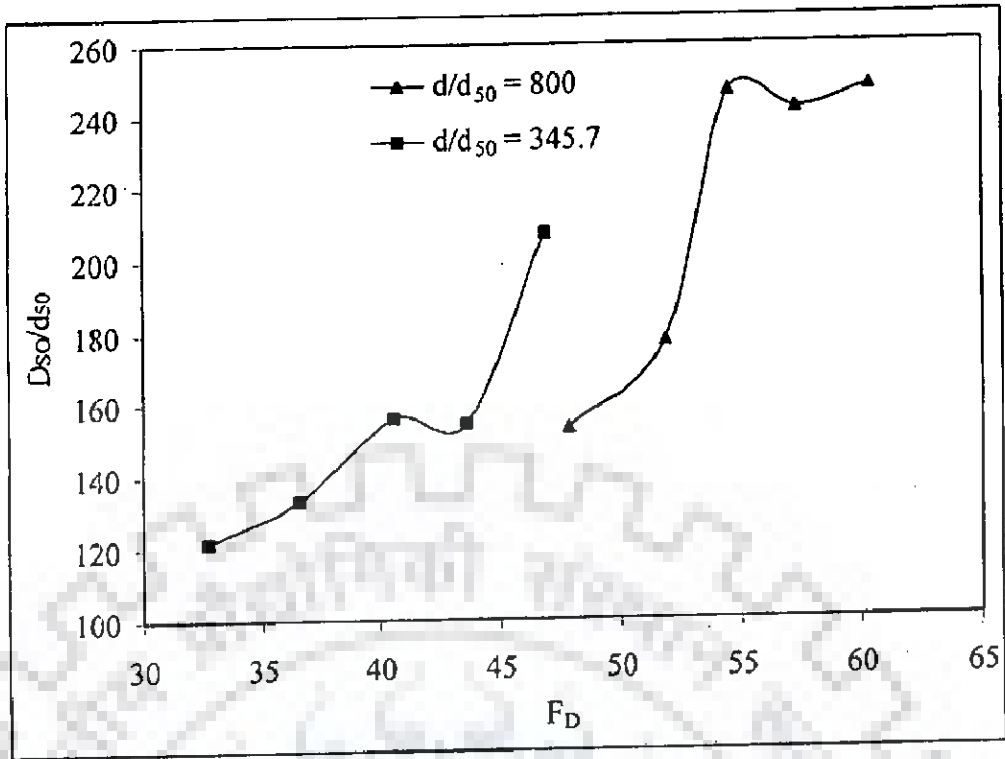


Fig. 4.1 Variation of D_{50}/d_{50} with F_D at different d/d_{50}

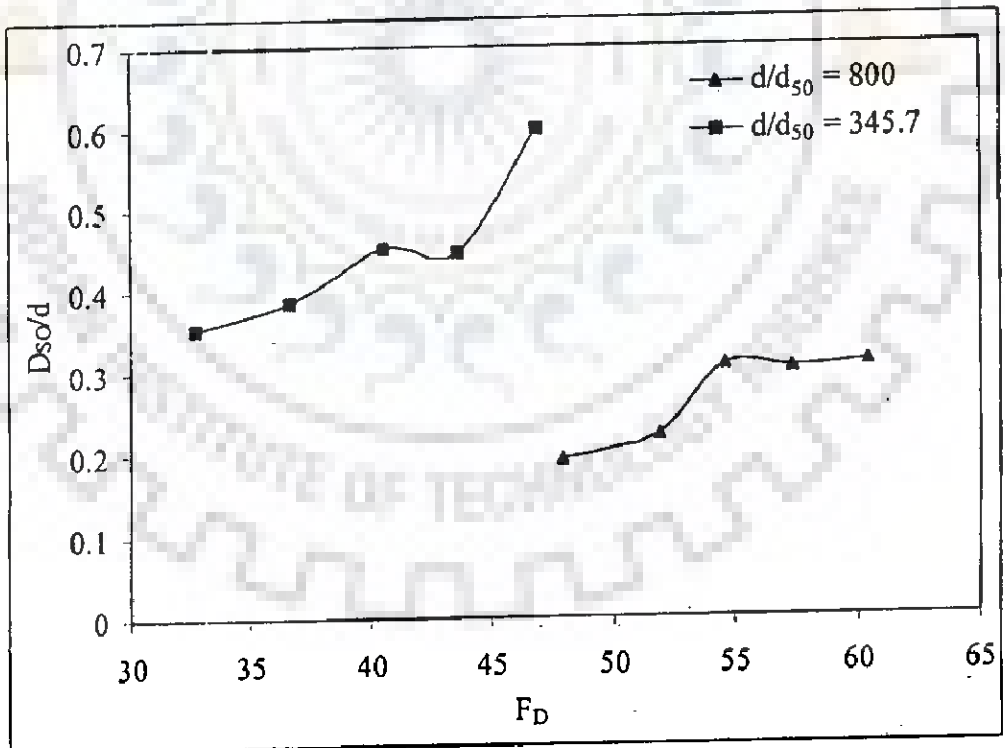


Fig. 4.2 Variation of D_{50}/d with F_D at different d/d_{50}

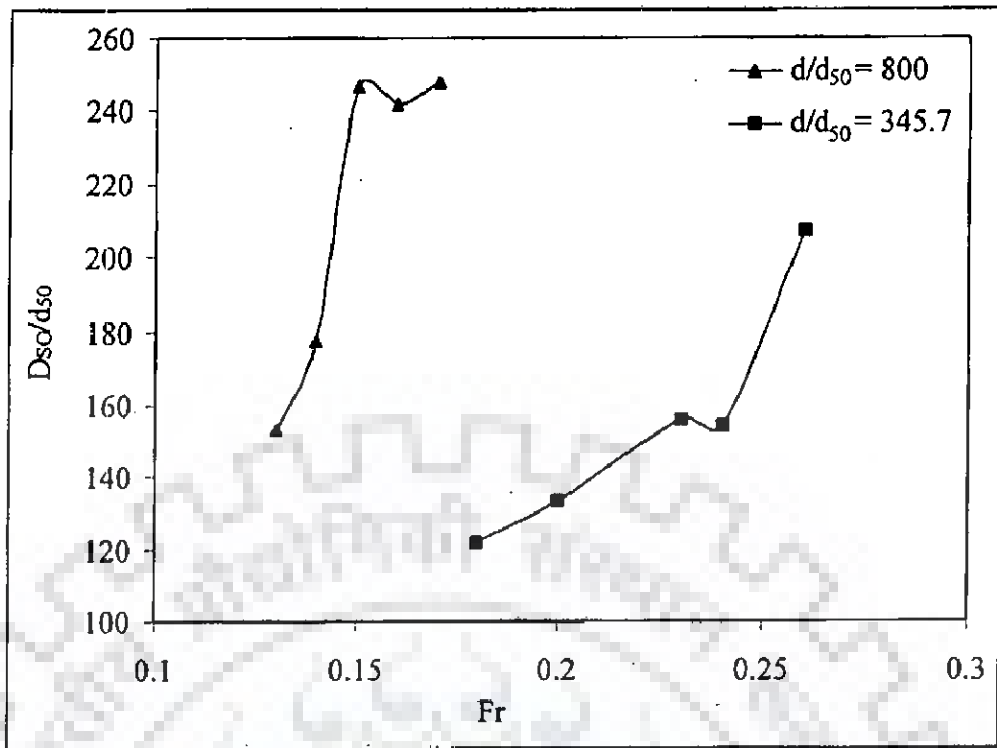


Fig. 4.3 Variation of D_{50}/d_{50} with Fr at different d/d_{50}

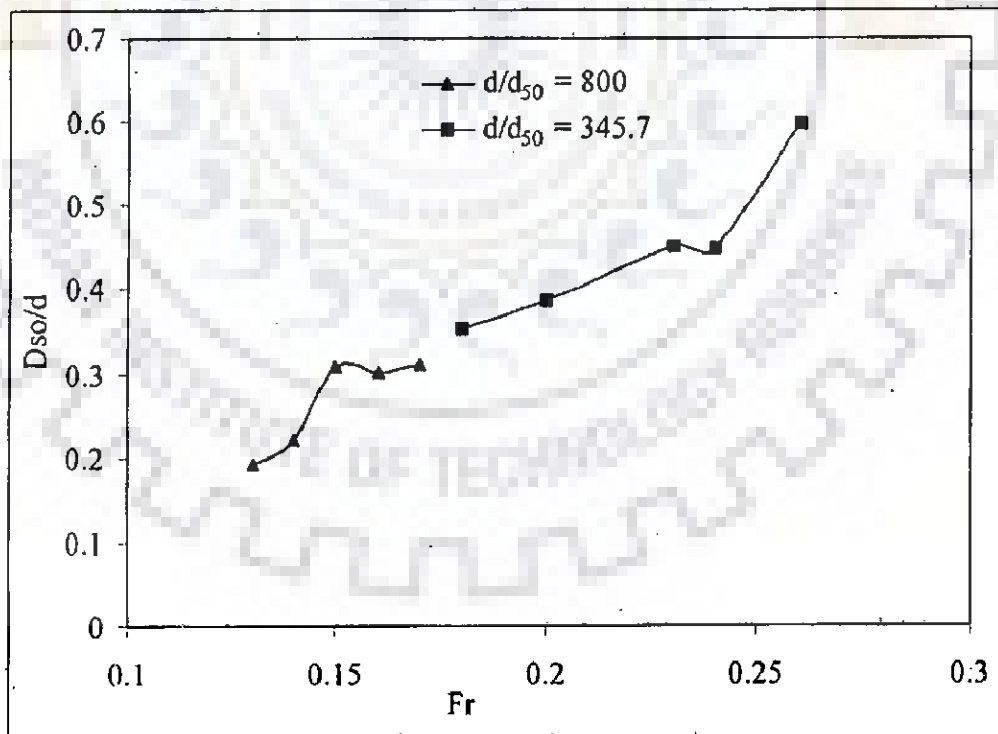


Fig. 4.4 Variation of D_{50}/d with Fr at different d/d_{50}

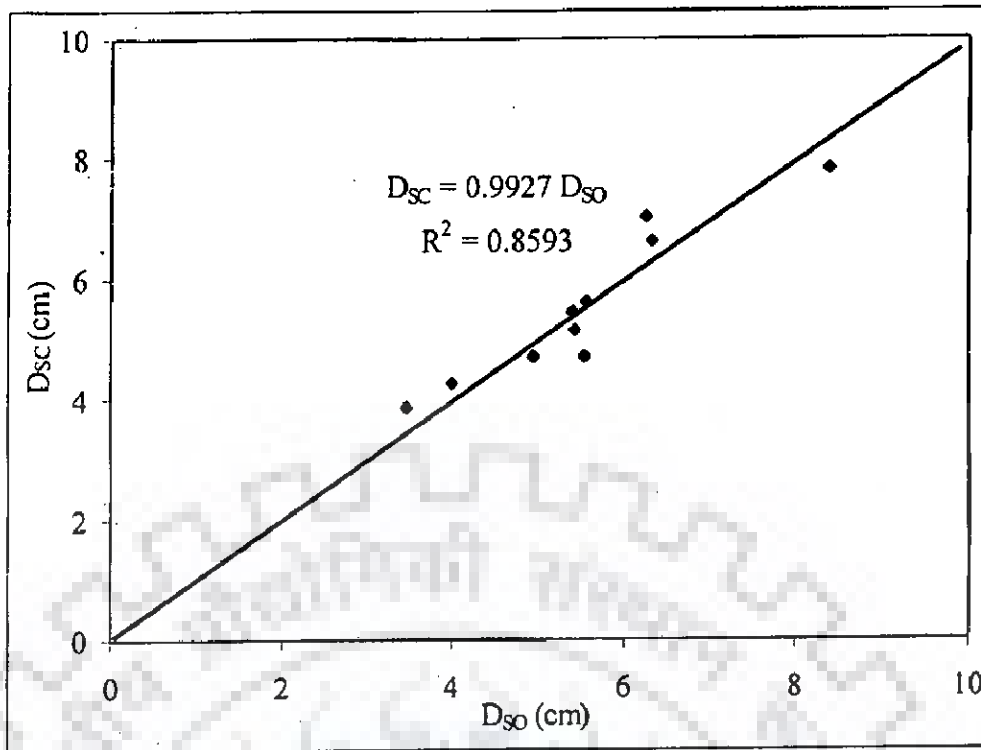


Fig. 4.5 Comparison of computed data with observed data

4.4 COST COMPARISON

It has been observed that development of local scour starts from the leading edge of submerged vane and its development takes place three dimensionally with the passage of time. The local scour at the leading edge of a submerged vane can be reduced either by using collar or granular material. Chiew (1992) studied the scour protection at bridge piers. It is important to compare the cost of granular material or riprap with the cost of collar as scour retarder device. In recent times, for bridge piers, riprap material is to be underlain with filters to prevent leaching of soil from the bed material. According to Chiew (1992), the objective of placing a filter for scour protection was found to be very effective in model experiments. However, it is difficult to place filters accurately as per design specifications in under water condition. According to Worman (1989), field investigations often displayed that riprap protection was generally defective.

An alternative method for provision of filter is to use synthetic geo-filters on the channel bed to be overlain by riprap. Compared to conventional gravel filters, synthetic geo-filters can be conveniently laid on the scour bed even in under water condition. Cost is normally insensitive to the size of boulders.

A definition sketch of formation of typical local scour hole around the submerged vane at Froude number 0.25 with median size of sediment as 0.225 mm has been shown in the Fig. 4.6. Experimental observations (Fig 4.6) revealed that scour hole could be best described as a frustum of cone. A typical top portion plan view of scour hole is schematically given in Fig 4.6. Fig. 4.6 shows that edge of the top portion of scour hole is not equidistant from the leading edge of submerged vane. Data relating to scour hole with rectangular vane have been presented in Table 4.1. Fig. 4.7 depicts the idealization of a typical scour hole at the leading edge of a rectangular submerged vane for the purpose of present cost comparison on a rational basis. Tables 4.2 and 4.3 present a comparison of cost of riprap along with filter with that of the cost of collar for the rectangular submerged vane at Froude numbers 0.13 and 0.25. The cost of mild steel plate to be used for collar is taken as Rs.20,000 per tonne based on local rates.

Thus, maximum area of collar as scour retarder is to be provided as per the following limiting condition given by

$$\text{Cost of collar} = \text{Cost of riprap with filters} \quad (4.11)$$

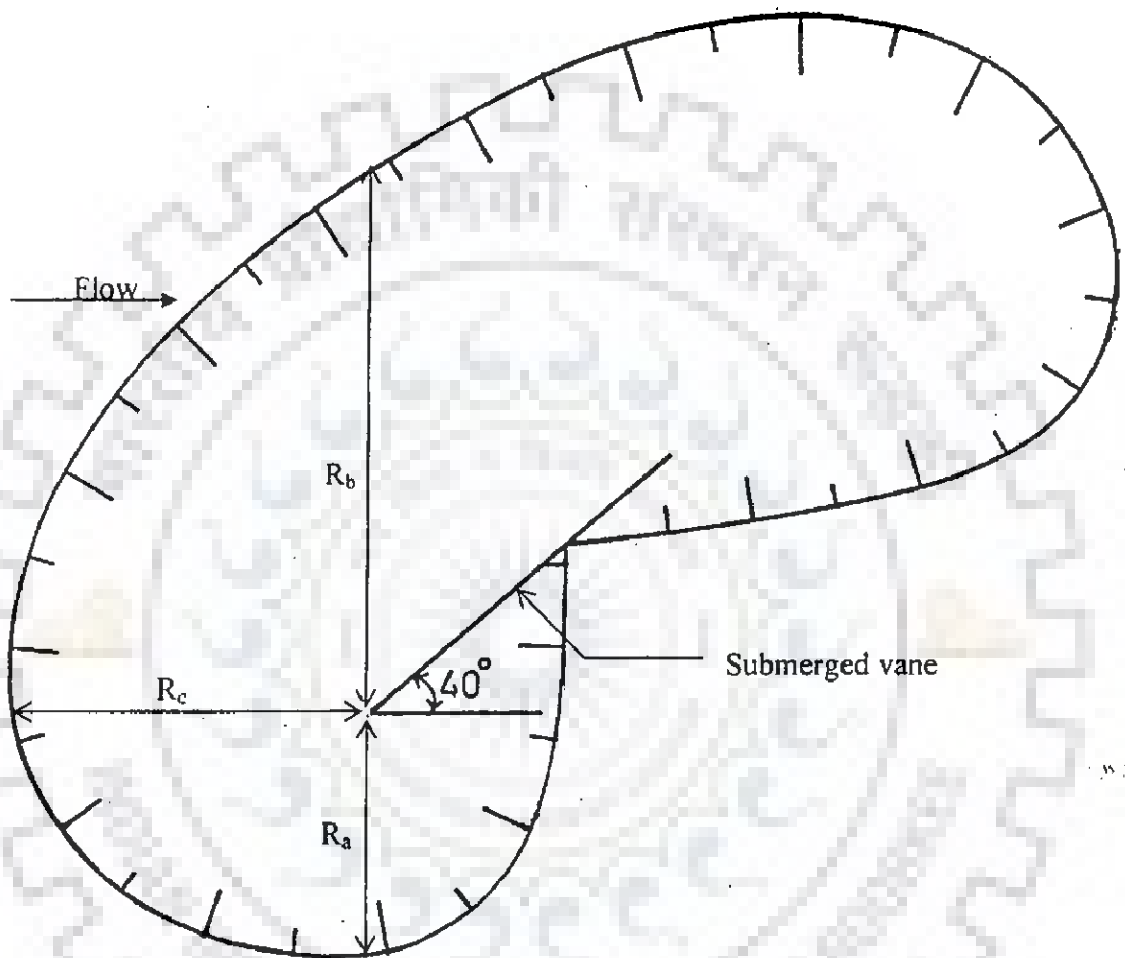


Fig. 4.6 Definition sketch showing plan of local scour hole around rectangular submerged vane ($F_r = 0.25$, $d_{50} = 0.225$ mm)

Table 4.1: Data relating to scour hole with rectangular vane (aspect ratio = 0.33)

Fr. No.	d_{50} (mm)	R_a (cm)	R_b (cm)	R_c (cm)	$R_1 = \left(\frac{R_a + R_b + R_c}{3} \right)$ (cm)	D_{os} (cm)	d/d_{50}	T/d
0.13	0.225	6.4	9.3	7.5	7.73	3.453	800	0.67
0.14	0.225	8.1	10.4	9.25	9.25	3.99	800	0.67
0.15	0.225	8.5	14.0	10.25	10.92	5.547	800	0.67
0.16	0.225	9.3	15.5	10.75	11.86	5.438	800	0.67
0.17	0.225	8.7	15.4	9.5	11.2	5.575	800	0.67
0.25	0.225	11	24.3	16.5	17.26	9.45	622.2	0.57
0.18	0.405	8.6	14.85	9.0	10.82	4.936	345.7	0.57
0.20	0.405	8.2	15.75	9.5	11.15	5.4	345.7	0.57
0.23	0.405	9.55	18.4	11.25	13.07	6.325	345.7	0.57
0.24	0.405	9.65	18.6	11.5	13.25	6.265	345.7	0.57
0.25	0.405	12.55	22.4	14.0	16.32	8.3875	345.7	0.57

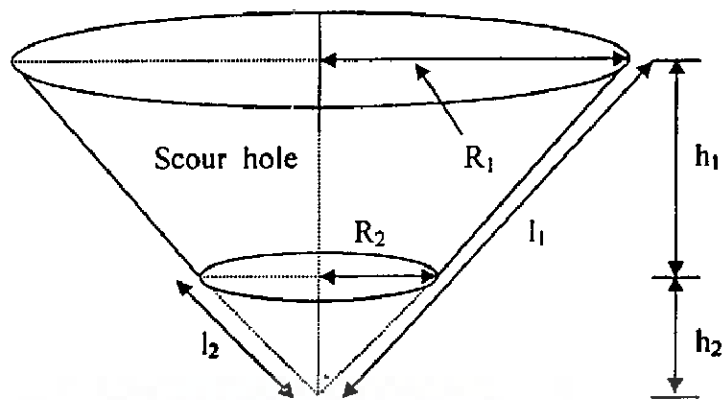


Fig. 4.7 Idealised typical scour hole at the leading edge of rectangular submerged vane.

Table 4.2: Estimation of filter area and volume of scour hole (rectangular vane, d_{50} as 0.225 mm)

Fr. No.	R_1	$R_2 = 0.4R_1$	h_1	$h_2 = \frac{h_1 R_2}{R_1 - R_2}$	$l_1 = \sqrt{(h_1 + h_2)^2 + R_1^2}$	$l_2 = \sqrt{h_2^2 + R_2^2}$	Total area of filter = $\pi\{(R_1 l_1 - R_2 l_2) + R_2^2\}$	Volume of Scour hole = $\frac{1}{3} \pi\{R_1^2 (h_1 + h_2) - R_2^2 h_2\}$
	(cm)	(cm)	(cm)	(cm)	(cm)	(cm)	(cm ²)	(cm ³)
0.13	7.7	3.1	3.5	2.4	9.7	3.9	226.9	342.2
0.25	17.26	6.9	9.45	6.3	23.4	9.3	1216.8	4599.4

Table 4.3: Cost of riprap with filter

Type of vane	Fr. No.	Volume of riprap (10 ⁻⁶ m ³)	Filter area (10 ⁻⁴ m ²)	Cost of riprap @ Rs.1000/m ²	Cost of filter @ Rs.35/m ²	Total cost (Rs.)
Rectangular	0.13	342.2	226.9	0.34	0.79	1.13
Rectangular	0.25	4599.4	1216.8	4.60	4.26	8.86

To compute cost of collar, one needs to know its volume (Vol_c) and cost per unit weight, which is rate of steel (r_s). Volume of collar can be expressed as

$$Vol_c = t_1 A_c \quad (4.12)$$

where, t_1 = thickness of collar and A_c = cross sectional area of collar.

Using eq. 4.12, the cost of collar, C_c can be expressed as

$$C_c = r_s \gamma_{st} Vol_c \quad (4.13)$$

where, γ_{st} = density of structural steel (7.85 ton/m^3)

The local scour, which develops at the leading edge of rectangular vane, can be idealized in conical shape. Assuming that riprap is provided in a circular manner, as shown in Fig. 4.7. One can compute the cost as follows. With R_1 as average radius of the top circular shape of cone; R_2 as radius of bottom circular shape of cone (which was found approximately $0.4R_1$); h_1 as depth of idealised scour hole; and h_2 as depth of the bottom tip of idealized cone from the bottom of actual scour hole (see Fig. 4.6), the volume of scour hole, Vol_s , can be expressed as

$$Vol_s = \frac{1}{3} \{ R_1^2 (h_1 + h_2) - R_2^2 h_2 \} \quad (4.14)$$

In Table 4.1, R_1 has been calculated as the average values of R_a , R_b and R_c where, R_a = top distance of extended scour hole in suction side of vane from its leading edge, R_b = top distance of extended scour hole in pressure side of vane from its leading edge and R_c = top distance of extended scour hole in upstream side of vane from its leading edge.

Riprap will be provided to fill the scour hole also. Thus one has to consider the provision of filter below the riprap. The cost of riprap with filter (C_{rf}) will consist of cost of riprap (C_r) and cost of filter (C_f), as given by

$$C_{rf} = C_r + C_f \quad (4.15)$$

Using eq. 4.14 and rate of riprap, r_r , one can write the following equation.

$$C_r = \text{Vol}_s r_f \quad (4.16)$$

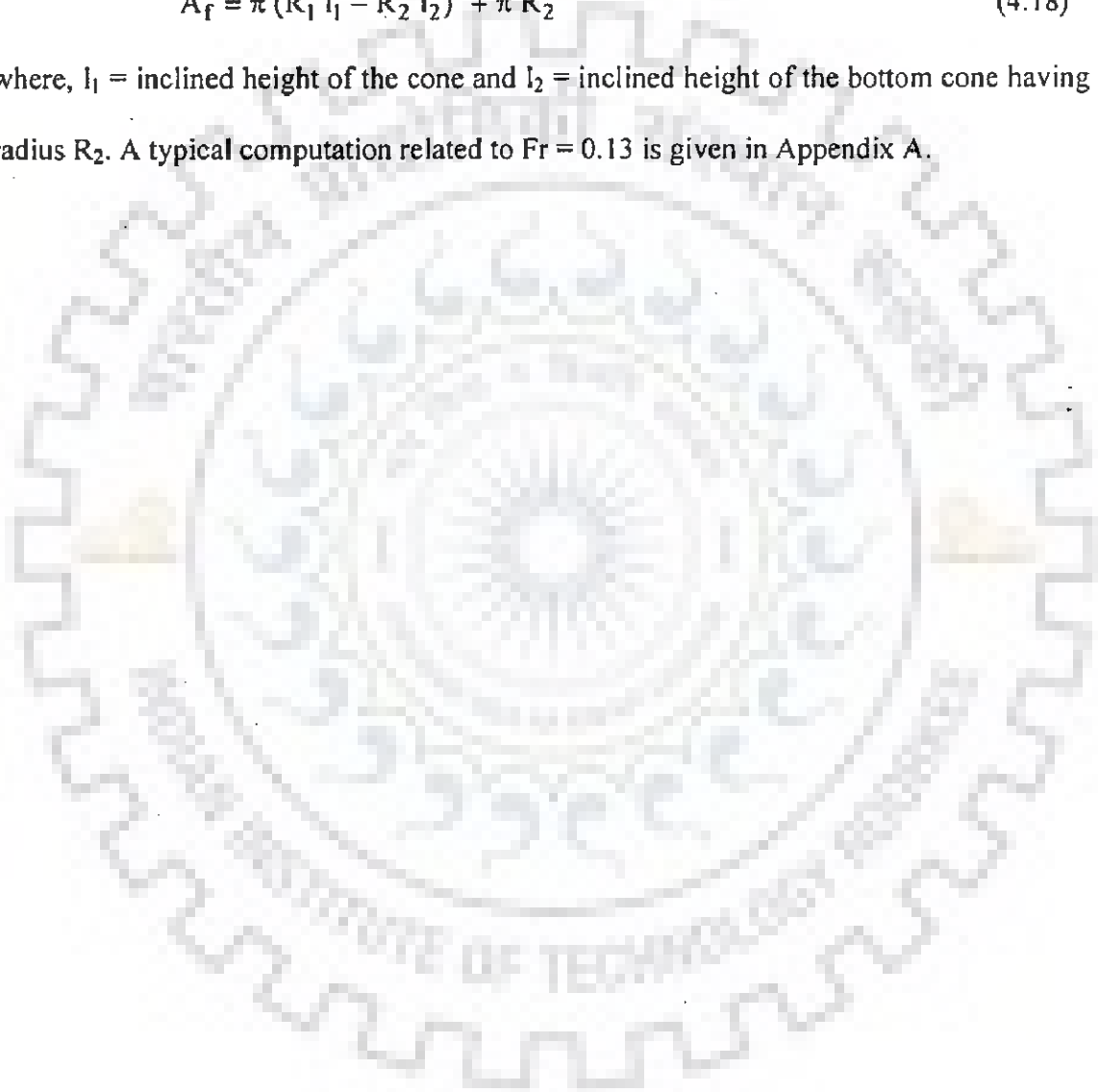
Similarly, the cost of filter can be obtained in terms of area of filter, A_f and rate of filter per unit area, r_f . For this purpose, one can use the following expression

$$C_f = A_f r_f \quad (4.17)$$

The expression of A_f for the scour hole for the Fig. 4.6 is as follows

$$A_f = \pi (R_1 l_1 - R_2 l_2) + \pi R_2^2 \quad (4.18)$$

where, l_1 = inclined height of the cone and l_2 = inclined height of the bottom cone having radius R_2 . A typical computation related to $Fr = 0.13$ is given in Appendix A.



PERFORMANCE EVALUATION OF SUBMERGED VANES WITH COLLAR

5.1 GENERAL

Considering the fact that in field conditions, submerged vanes of rectangular and trapezoidal shapes have been used, a set of 43 experiments were performed in phase II of this study to monitor the behaviour of local scour around submerged vanes with collars. As indicated earlier, the use of collar has been investigated in this study as a scour retarding device for the vane so that destabilising local scour could be kept at bay to enable use of optimal incident angle, for submerged vane orientation. The objective of these experiments has been to identify the collar in which the occurrence of local scour is the minimum or negligible at the leading edge of the vanes. For two Froude numbers and at two different sediment sizes, the pattern of local scour around the submerged vanes with collar have been compared to identify the most effective shape and size of collars corresponding to incidence of minimum local scour. It is also apparent from different plates, shown in Chapter 4, that huge destabilising local scour holes formed in case of rectangular submerged vanes without any scour retarding device. Based on the review of literature, it could be found that no research so far has been conducted on the reduction of local scour around the submerged vanes. However, it is apparent from the literature that on the basis of experimentations, collar had been recommended by several researchers in the past as scour retarder in case of bridge piers. Therefore, it has been preassumed here that the collar can also be gainfully used as scour retarder device in case of submerged vanes. The efficacy of using collar as local scour retarder has been examined in this chapter. Later, some of the bed profiles are shown in this chapter to highlight the most

effective shape and size of collar at different Froude numbers such as 0.13 and 0.25. The commonly used range of Froude numbers in existing studies (Table 5.1) is between 0 and 0.25. For this reason, only two values of Froude numbers have been considered in this study. The idea is that one can use the results based on these Froude numbers to plan the suitable collar shape and size for any intermediate value of Froude number.

Table 5.1: Froude numbers used by different investigators

Name of Investigators	Froude number
Odgaard and Spoljaric (1986)	0.185 to 0.28
Odagaard and Mosconi (1987)	0.27 to 0.31
Odgaard and Wang (1991 b)	0.31 (for curve channel), 0.25 (for straight channel)
Wang and Odgaard (1993)	0.18 to 0.27
Wang et al. (1996)	0.172
Johnson et al. (2001)	0.17 to 0.24

5.2 COLLAR AS SCOUR RETARDER

Local scour around the vane can be reduced by one of the following ways:

- (i) Introduction of collar throughout the submerged vane at bed level but it may prove too costlier.
- (ii) Introduction of collar at the trailing edge of submerged vane at bed level. It was observed that formation of scour hole starts from the leading edge of vane and its development takes place vertically, laterally and towards downstream. From Chapter 4, it has become apparent that huge destabilising scour hole can form at the leading edge of submerged vanes. Therefore, even after the introduction of collar at the trailing edge, development of scour hole at the leading edge of the submerged vanes and its development towards downstream can not be arrested which leads ultimately to failure of collar and hence dislodgement of vanes will occur.
- (iii) Thus, in view of (i) and (ii), introduction of collar at the leading edge of submerged vane appear to be probably the most reasonable choice.

5.3 LOCATION OF COLLAR

Vittal et al. (1994) performed laboratory experiments with collar at a height of 1.50 cm above the bed to safeguard the bridge pier from scour in clear water condition. Kumar et al. (1999) performed laboratory experiments on the reduction of local scour around bridge piers using collars in clear water condition and concluded that large diameter collar at or nearer the bed are more effective. Singh et al. (2000) concluded that the best location of the collar in case of bridge pier is at $0.1 D_1$ below the average bed level where D_1 is diameter of pier. Since the main thrust of the research was focused on evolution of an optimal collar configuration for scour retardation around a vane, various potential locations of the collar were investigated for appraisal of best performance. For

narrowing down the present search for optimal location of the collar, the experiences drawn by the past researchers on studies pertaining to a collar around a bridge pier were carefully collated at the time of planning of the present clear-water flume experimentations. To effectively cut off the strength of scour-producing downflow phenomenon, initially, the collar was experimented with locations above the bed level, and resulting scour pattern was observed. Subsequent series of experimental runs were performed at the bed level and also below it with alternative potential locations and the magnitude and extent of the consequent scour in the vicinity of the leading edge was critically observed. From the aforementioned series of experimentations, it was found that the collar at a location $0.05H$ below the initial bed level is the most effective and optimal as revealed, in the present studies.

5.4 MOST EFFECTIVE COLLAR

The most effective collar size may be defined as the minimum size of the collar, which will produce minimum or negligible scour hole at the leading edge of submerged vanes. Initially, optimization of shape and size of collar was done for two Froude numbers such as 0.13 and 0.25. Selection of different shapes and sizes of collars tried in laboratory experiments were based on location of formation of first scour hole, its development and extension. The initial bed level prior to the experimental run at the leading edge of submerged vane was taken as the origin for the measurement of scour pattern developed for all the cases in this chapter.

5.4.1 Experiments at Froude Number 0.13 and d_{50} as 0.225 mm

5.4.1.1 Rectangular vane

As there was no idea regarding the collar shape, an arbitrary smaller noncircular collar size AF1.1 was tried for rectangular vane. It can be seen from Fig. 5.1 that it was totally ineffective. Therefore, shape and size of the collar was further improved one by one from AF1.2 to AF1.6 (Figs. 5.2 to 5.6). It was observed that first scour hole formed into just downstream of the collar in low pressure side. After certain hours, this scour hole was observed to extend to the upstream corner of the collar in low pressure side and then further extends to the upstream edge of the collar. When the scour hole extends to the upstream edge of the collar, sediments starts moving below the collar and, it leads to ultimate failure of the collar. Probably, because of this reason, the dimension of the most effective collar is more in low pressure side than that of in high pressure side. In Fig. 5.7 and Plate 5.1, the upstream edge of collar was made perpendicular to the flow direction at Froude number 0.13 so that upstream corner of the collar in suction side of vane has somewhat more distance from the point of formation of first scour hole.

Collar size AF1.7 was found most effective for rectangular vane at Froude number 0.13 (Fig. 5.7 and Plate 5.1). Some of the circular shapes of collar were also tried and circular collar size AF1.8 (Fig. 5.8 and Plate 5.2) was found most effective for rectangular vane at Froude number 0.13 with median size of sediment as 0.225mm.

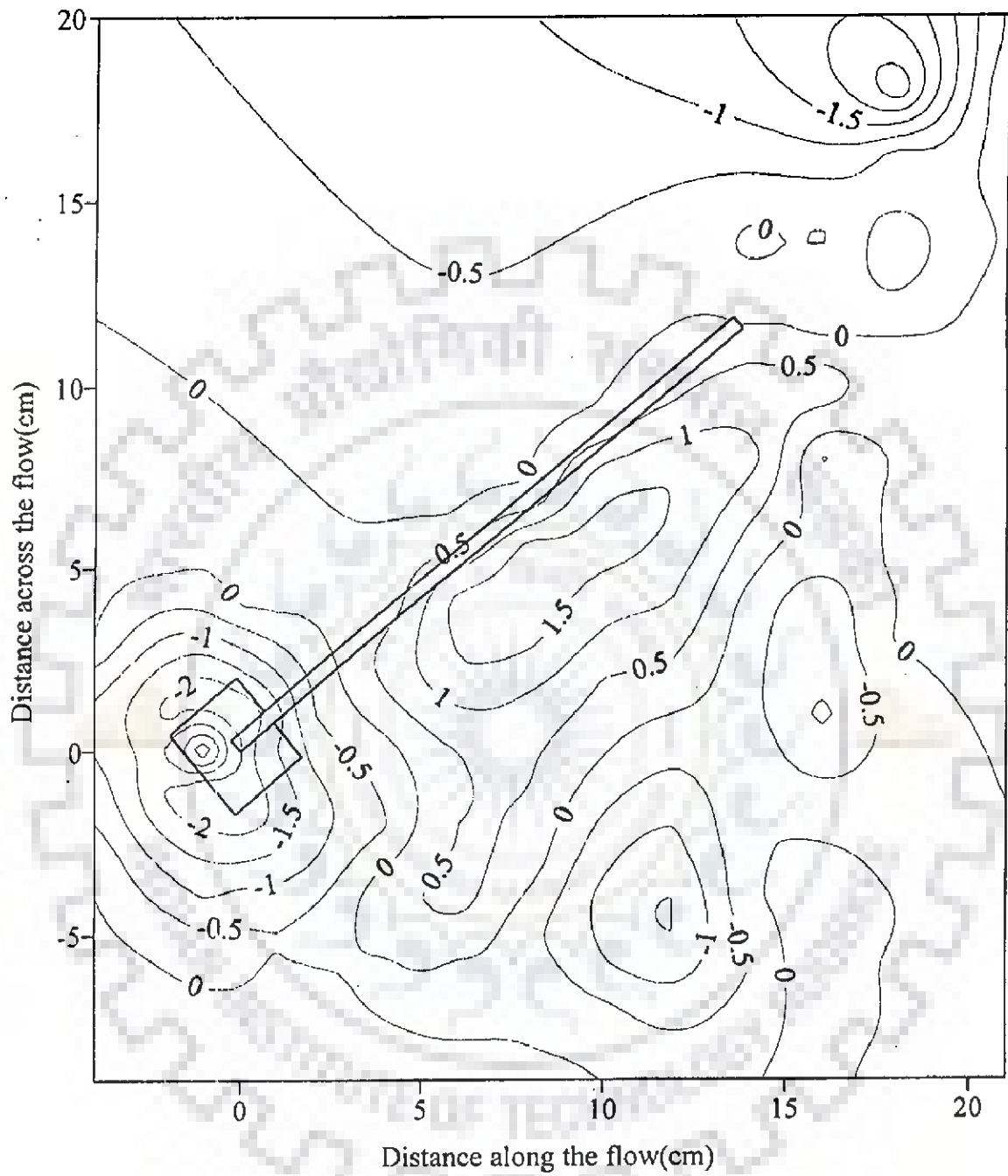


Fig. 5.1 Scour pattern for rectangular vane with collar AF1.1
 ($F_r = 0.13$, $d_{50} = 0.225$ mm, contour interval in cm)

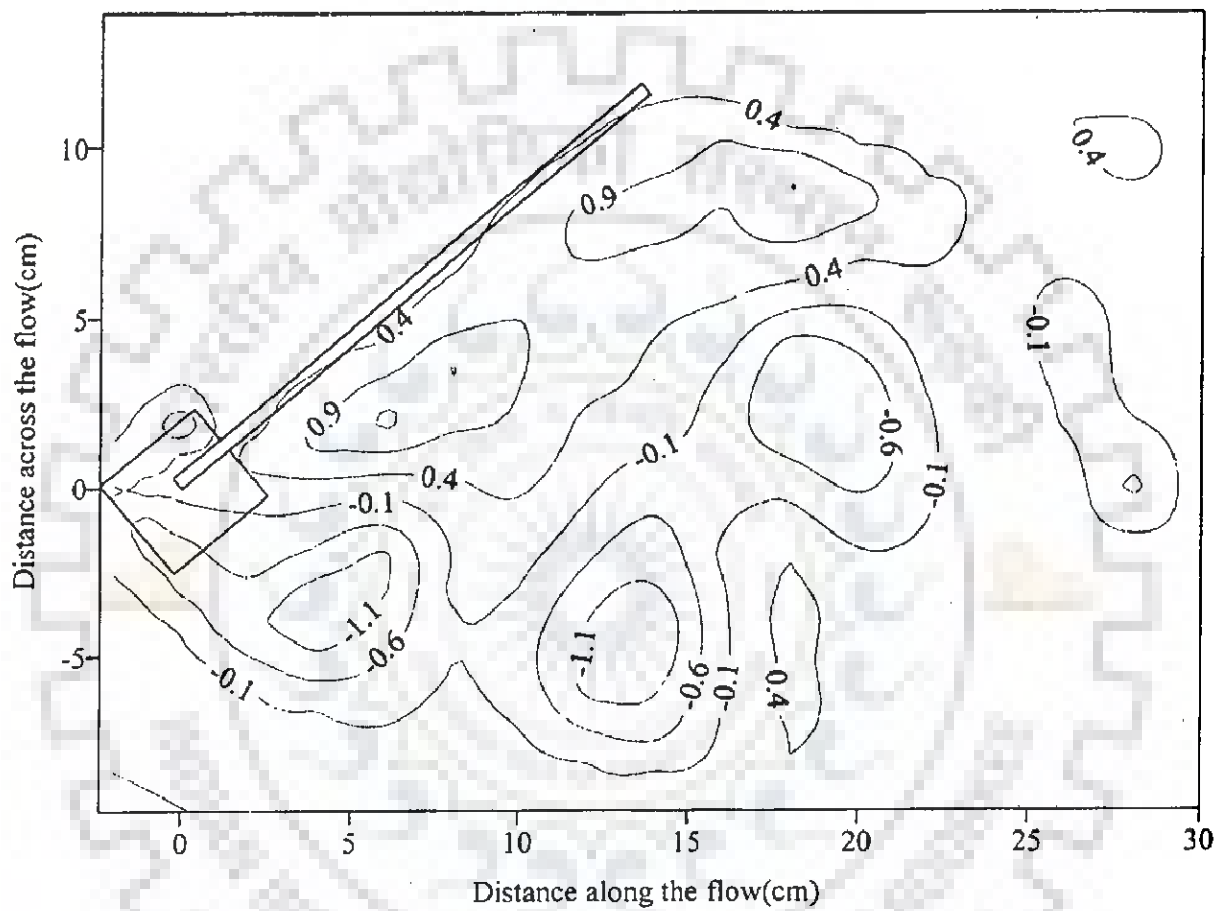


Fig. 5.2 Scour pattern for rectangular vane with collar AF1.2
 ($F_r = 0.13$, $d_{50} = 0.225$ mm, contour interval in cm)

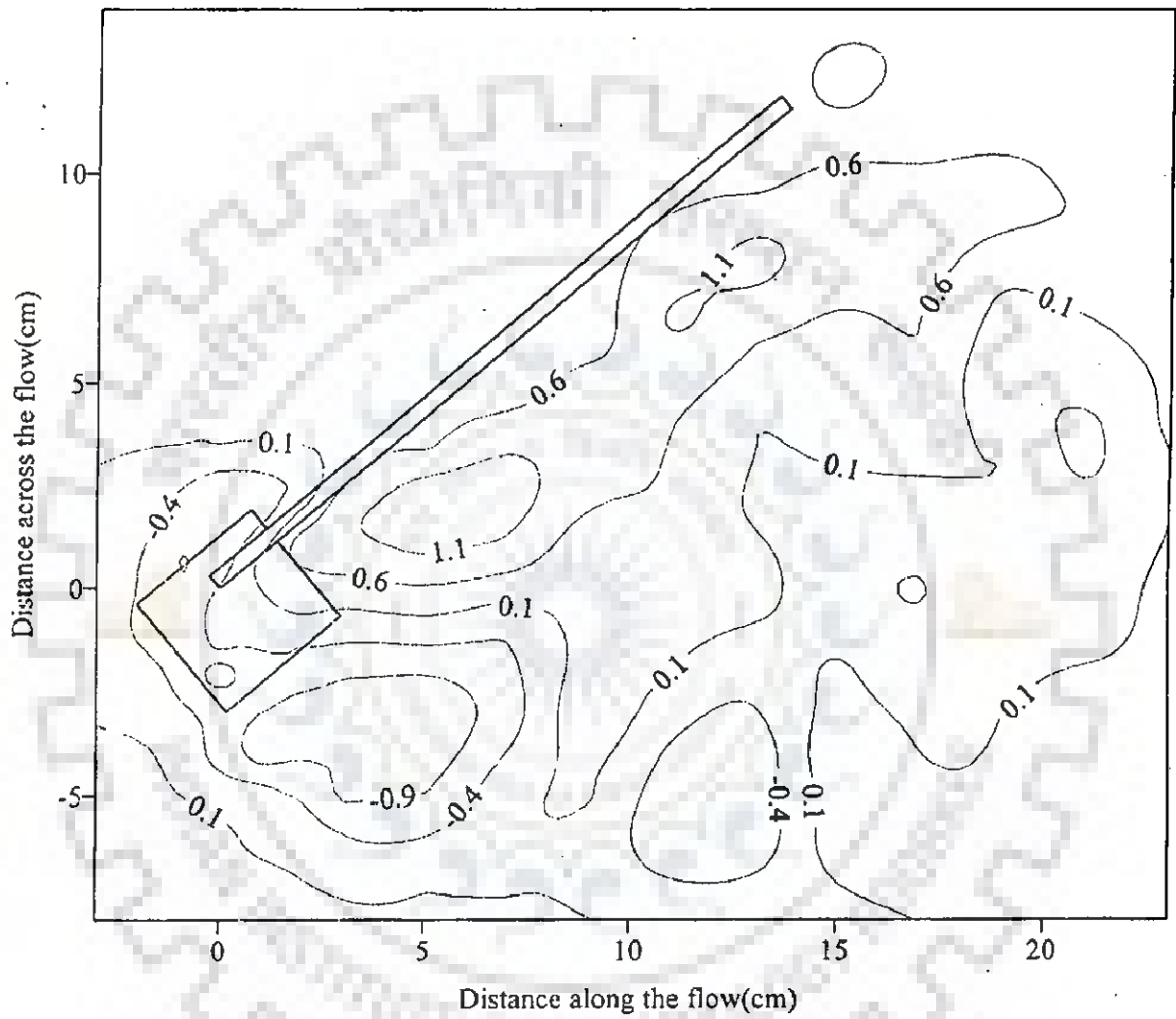


Fig. 5.3 Scour pattern for rectangular vane with collar AF1.3
 ($F_r = 0.13$, $d_{50} = 0.225$ mm, contour interval in cm)

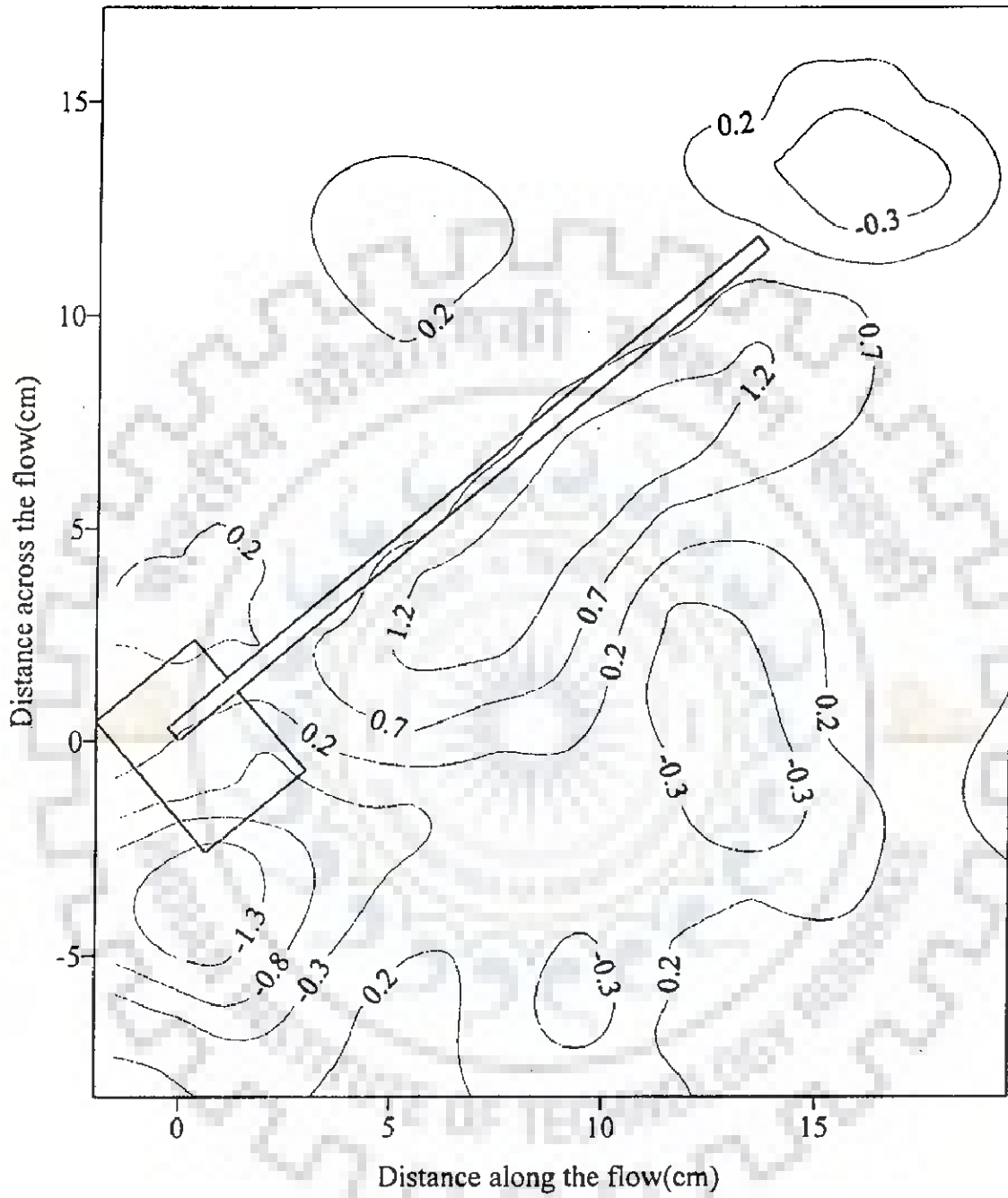


Fig. 5.4 Scour pattern for rectangular vane with collar AF1.4
 ($F_r = 0.13$, $d_{50} = 0.225$ mm, contour interval in cm)

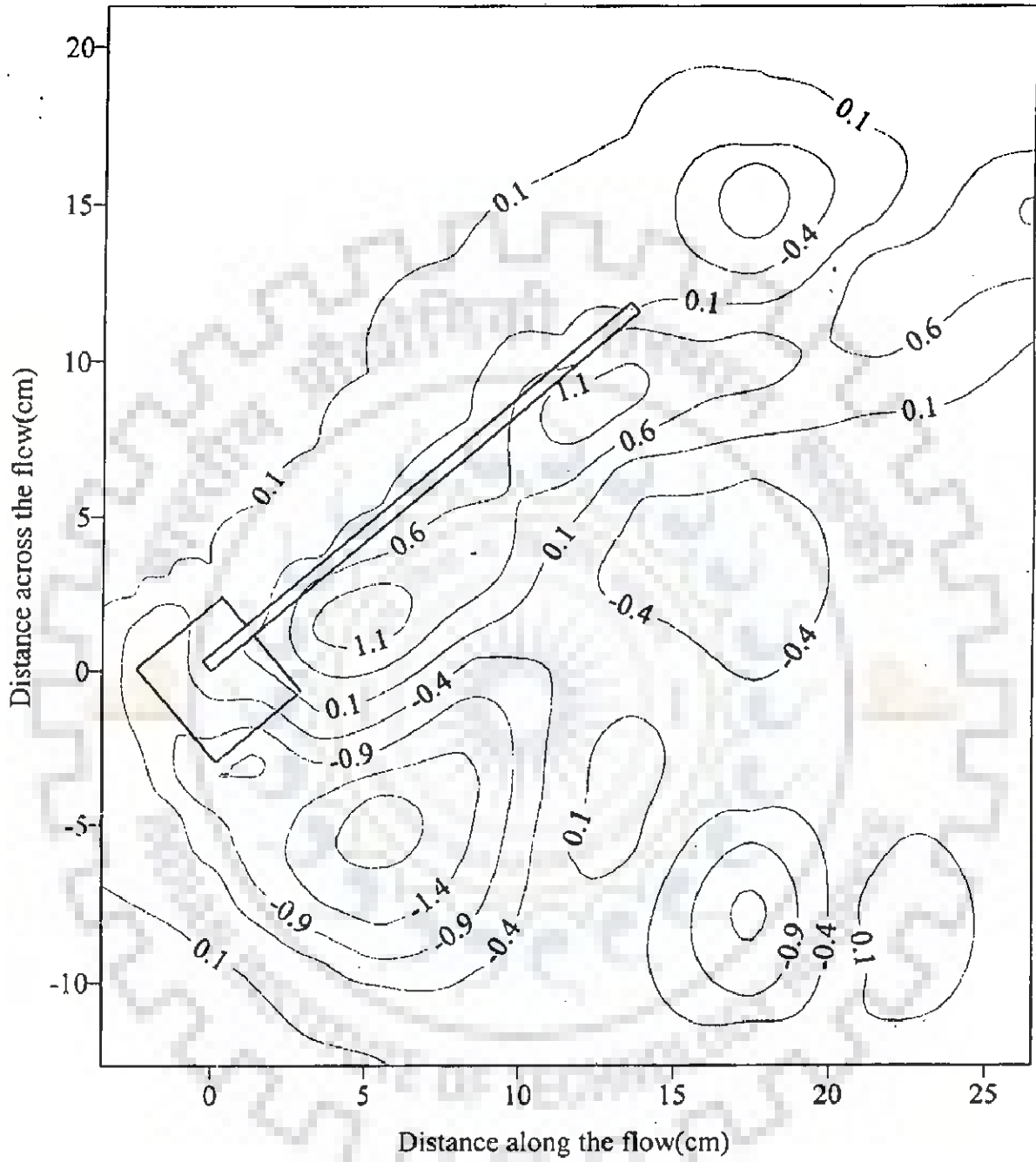
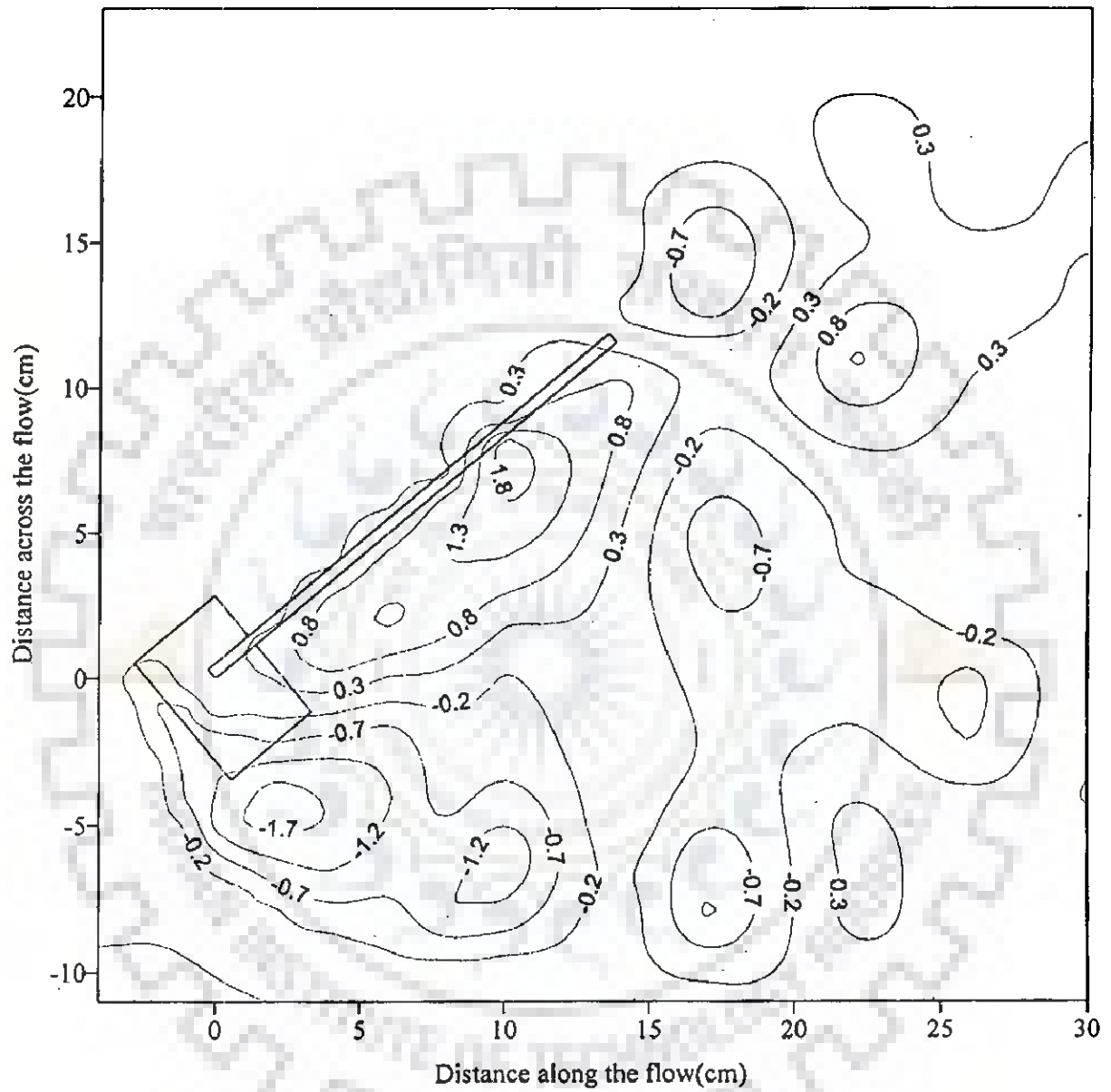
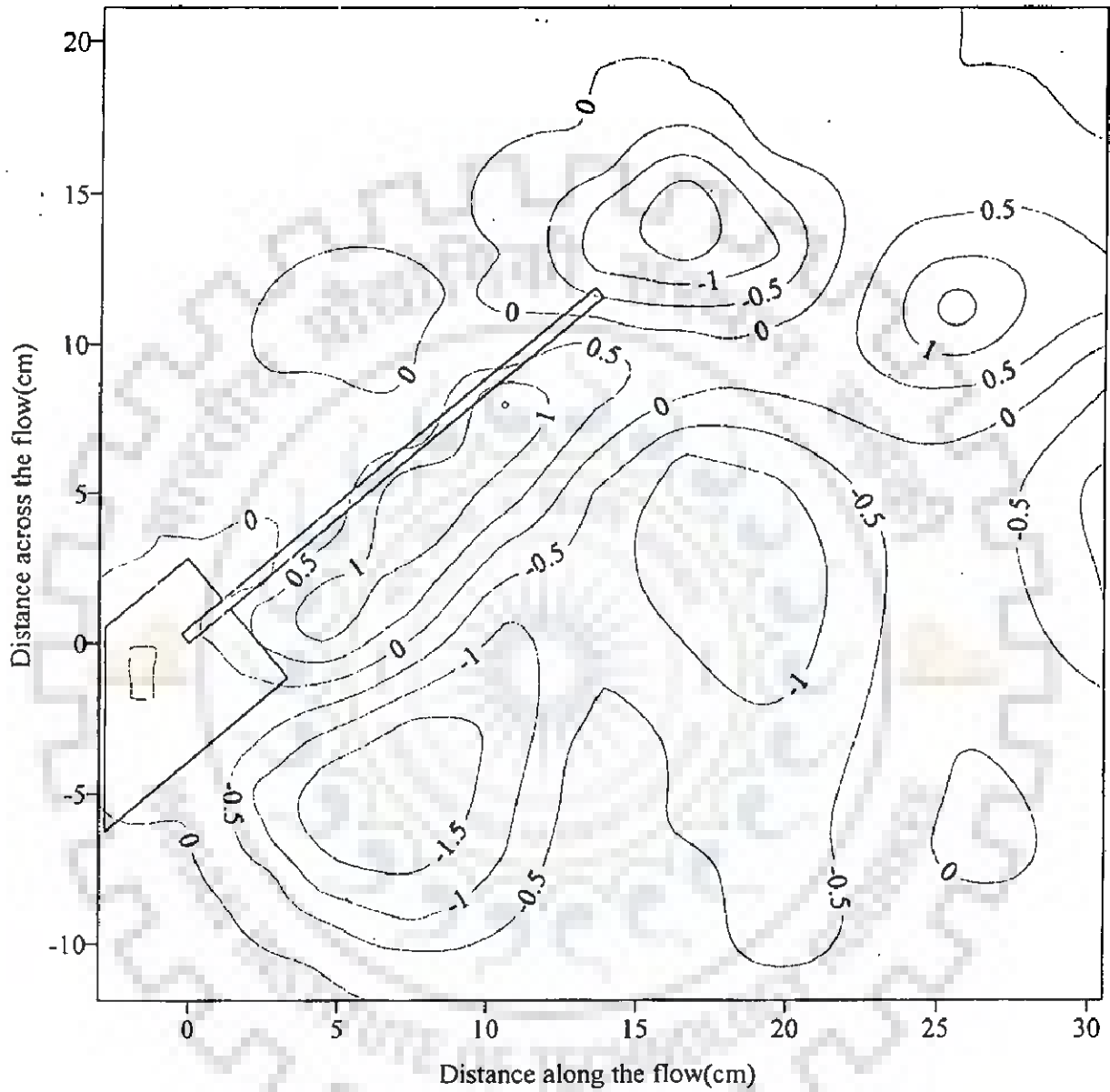


Fig. 5.5 Scour pattern for rectangular vane with collar AF1.5
 ($F_r = 0.13$, $d_{50} = 0.225$ mm, contour interval in cm)



**Fig. 5.6 Scour pattern for rectangular vane with collar AF1.6
 ($F_r = 0.13$, $d_{50} = 0.225$ mm, contour interval in cm)**



**Fig. 5.7 Scour pattern for rectangular vane with collar AF1.7
 ($F_r = 0.13$, $d_{50} = 0.225$ mm, contour interval in cm)**

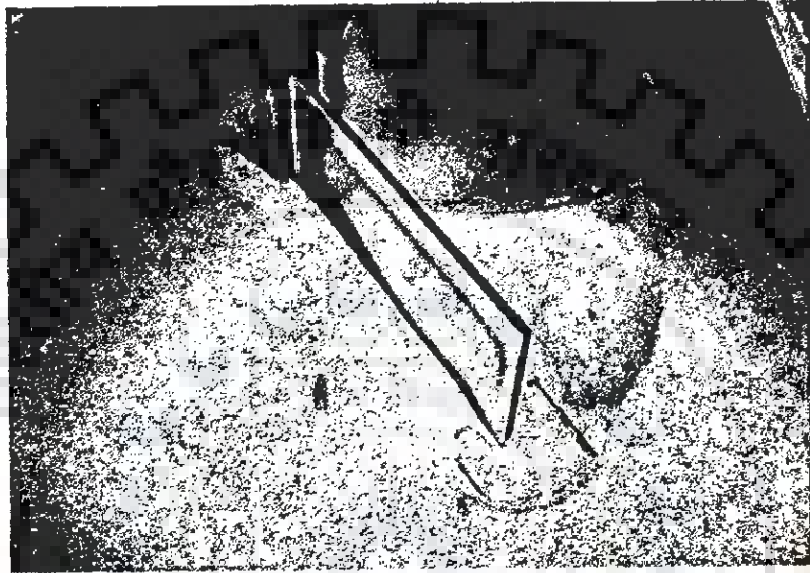


**Plate 5.1 Scour pattern for rectangular vane with collar AF1.7
($F_r = 0.13$, $d_{50} = 0.225$ mm)**

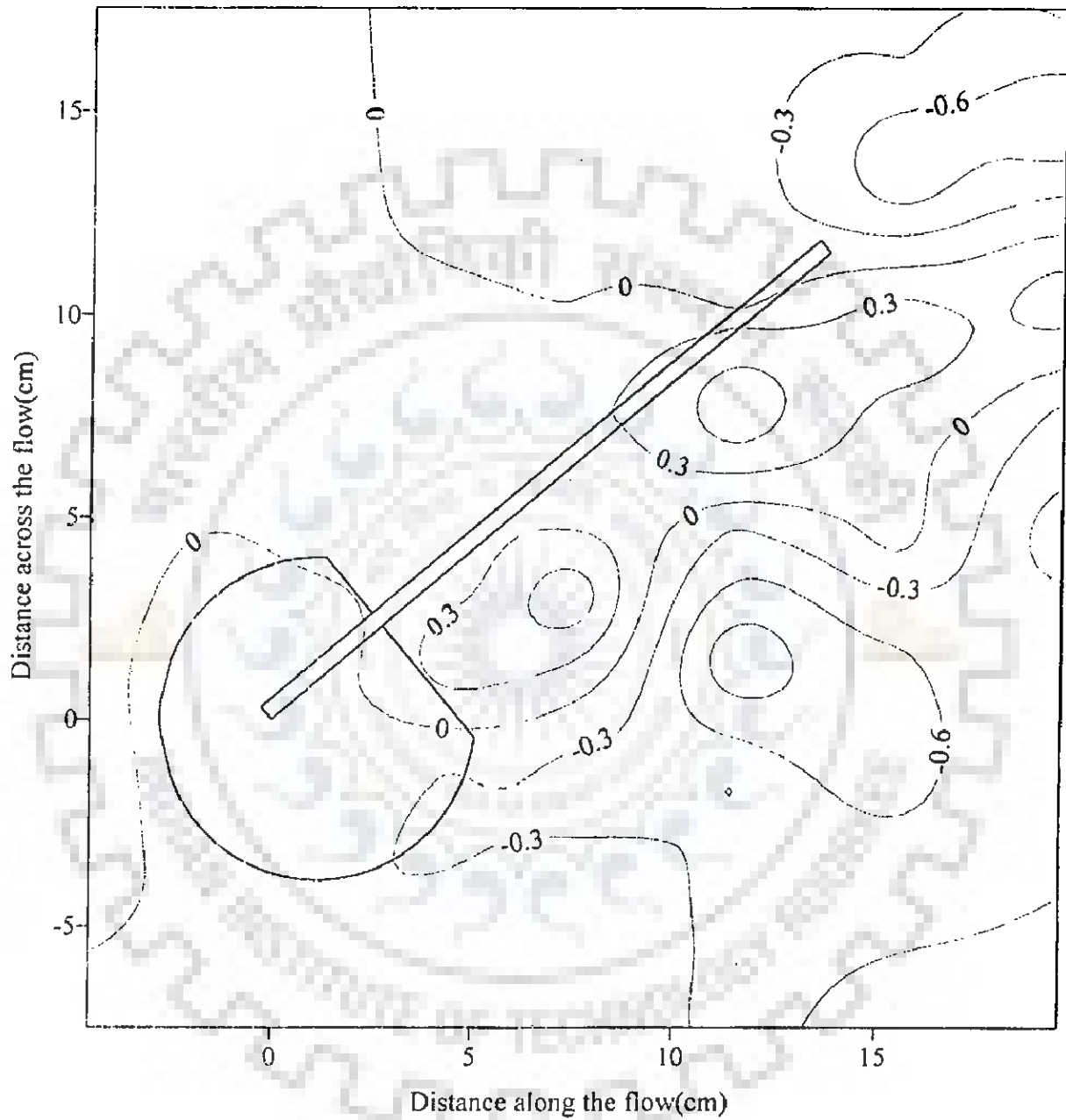
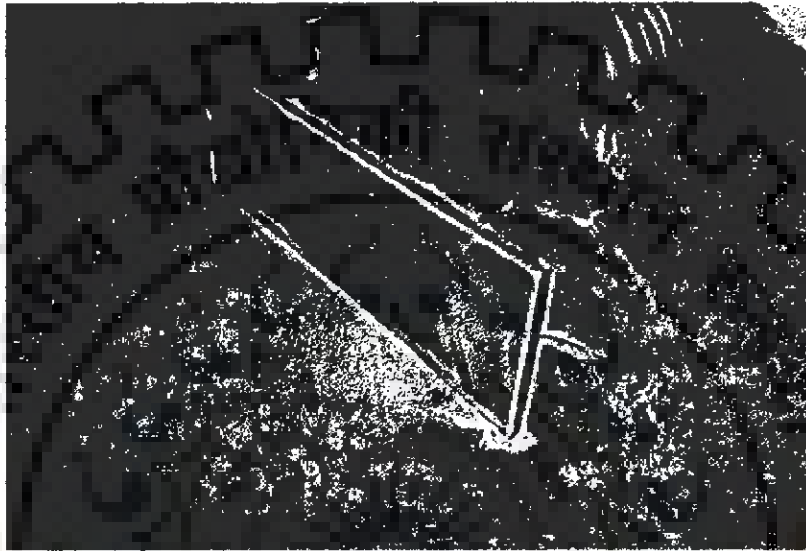


Fig. 5.8 Scour pattern for rectangular vane with collar AF1.8
 ($F_r = 0.13$, $d_{50} = 0.225$ mm, contour interval in cm)



**Plate 5.2 Scour pattern for rectangular vane with collar AF1.8
($F_r = 0.13$, $d_{50} = 0.225$ mm)**

5.4.1.2 Trapezoidal vane (3H:2.5V)

For trapezoidal vane (3H: 2.5V), an arbitrary noncircular smaller size of collar BF1.1 was tried and it was found totally ineffective (Fig. 5.9). Therefore, size of the collar was further improved one by one from BF1.2 to BF1.12 (Figs. 5.10 to 5.20). The formation of first scour hole, its extension and failures in case of trapezoidal vane (3H:2.5V) were similar to that of the rectangular vane as explained earlier. In Fig. 5.21 and Plate 5.3, the upstream edge of the collar was made perpendicular to the flow direction.

The collar size BF1.13 was found most effective. Some of the circular shapes of collar were also tried and circular collar size BF1.14 (Fig. 5.22 and Plate 5.4) was found most effective for trapezoidal vane (3H:2.5V).

From presentation point of view, I will prefer the case of Froude number as 0.25 and d_{50} as 0.225 mm to be written here.

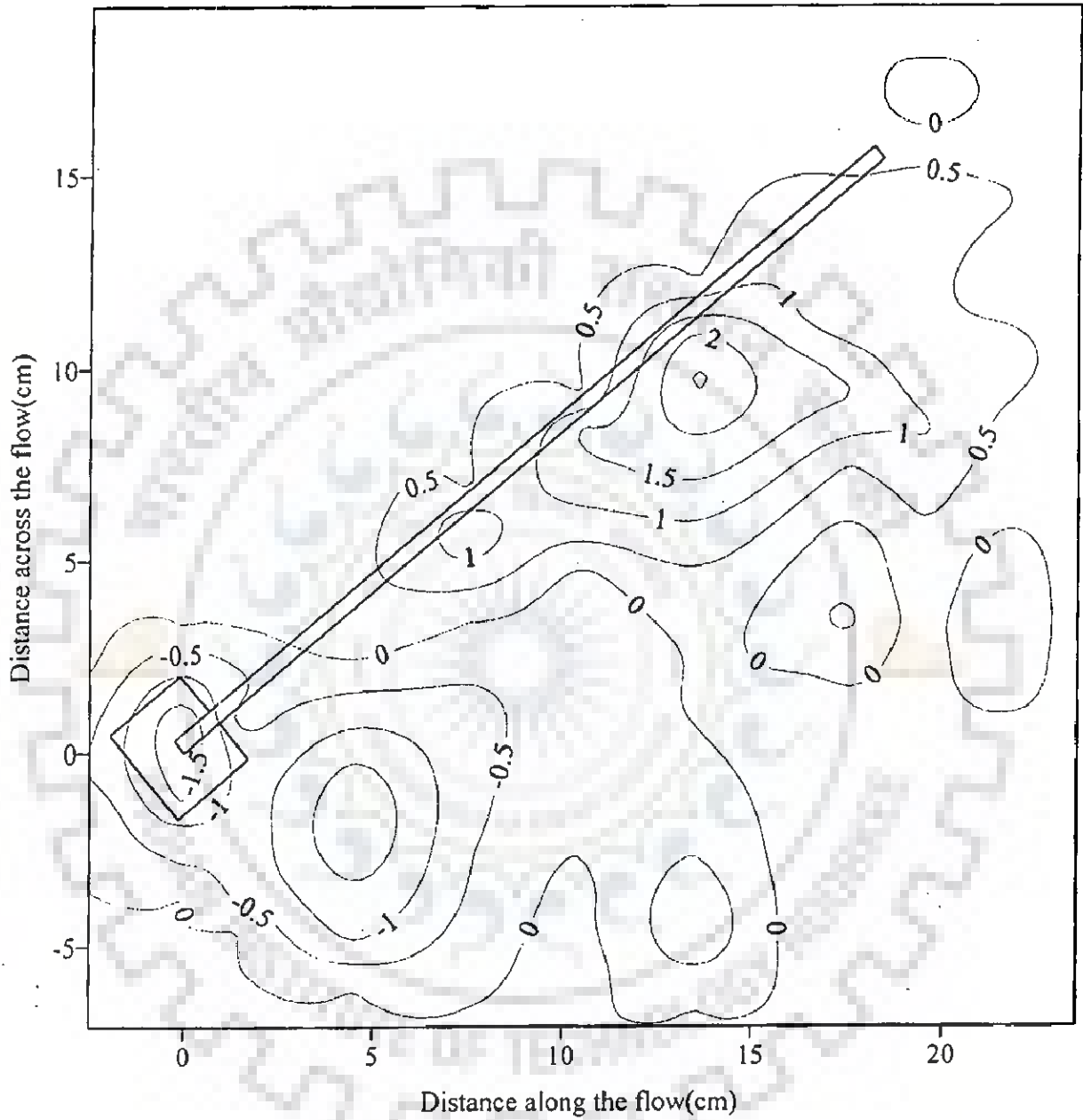


**Fig. 5.9 Scour pattern for trapezoidal vane (3H:2.5V) with collar BF1.1
 ($F_r = 0.13$, $d_{50} = 0.225$ mm, contour interval in cm)**

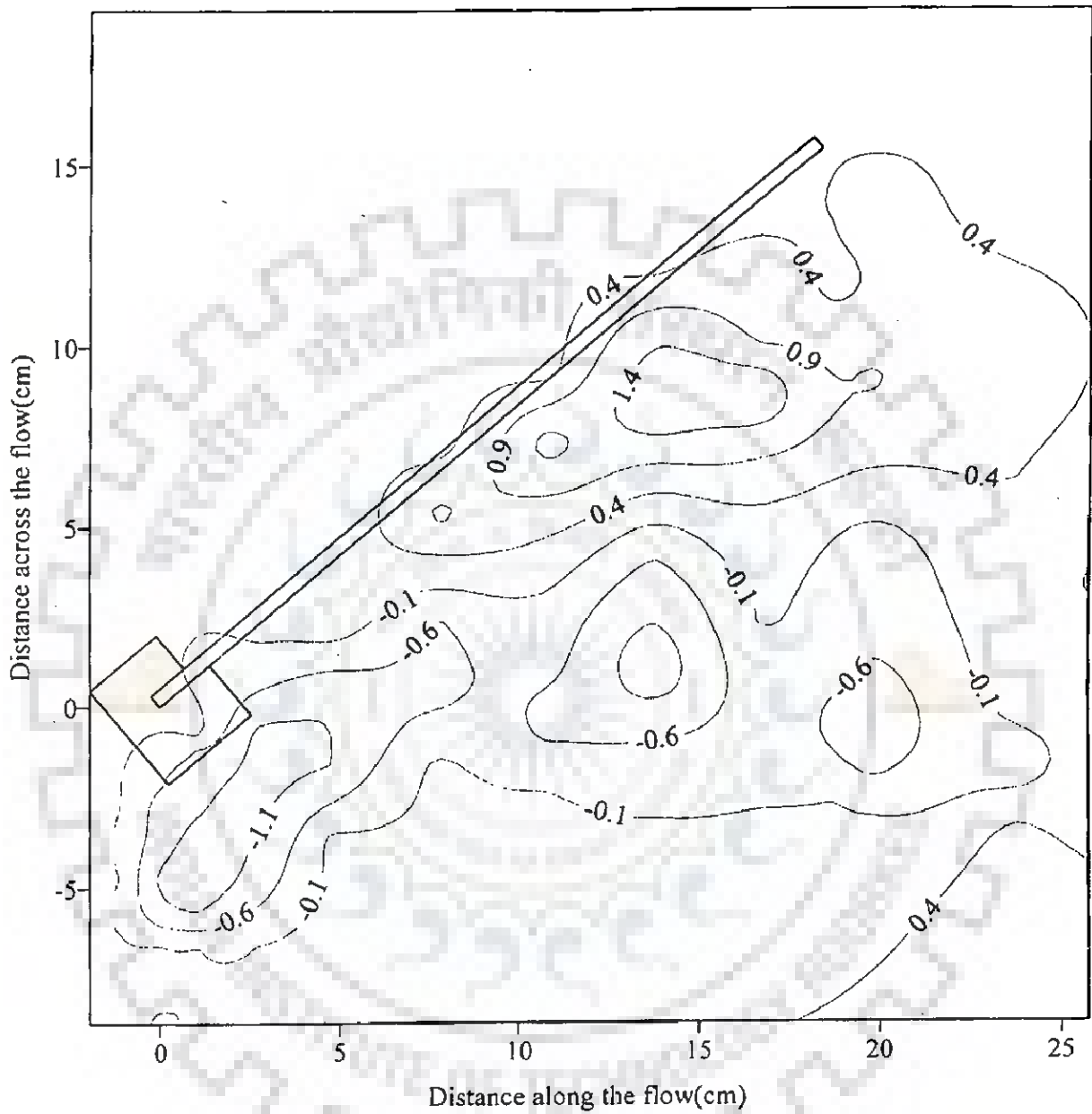


Fig. 5.10 Scour pattern for trapezoidal vane (3H:2.5V) with collar BF1.2
 ($F_r = 0.13$, $d_{50} = 0.225$ mm, contour interval in cm)

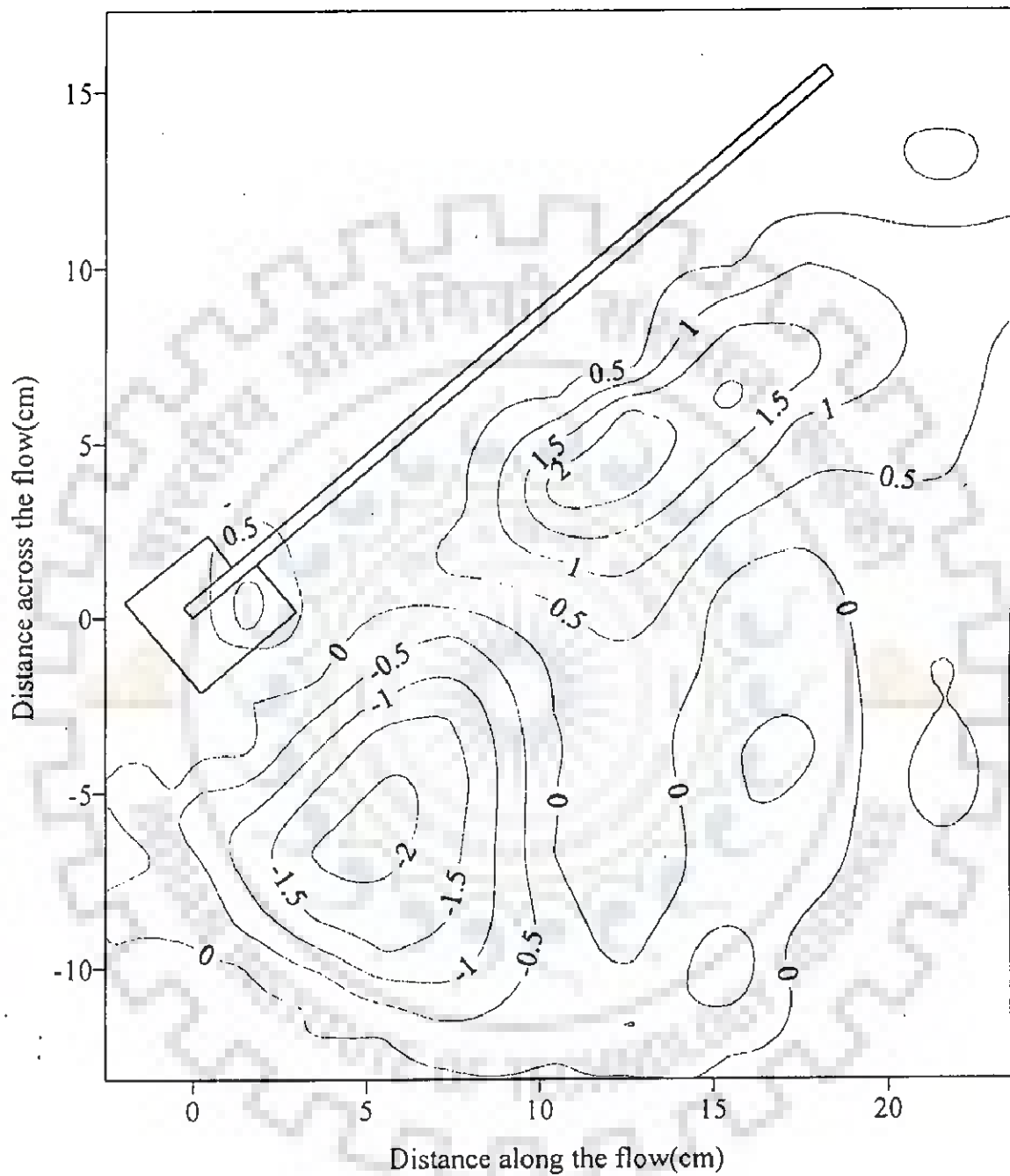


Fig. 5.11 Scour pattern for trapezoidal vane (3H:2.5V) with collar BF1.3
 ($F_r = 0.13$, $d_{50} = 0.225$ mm, contour interval in cm)

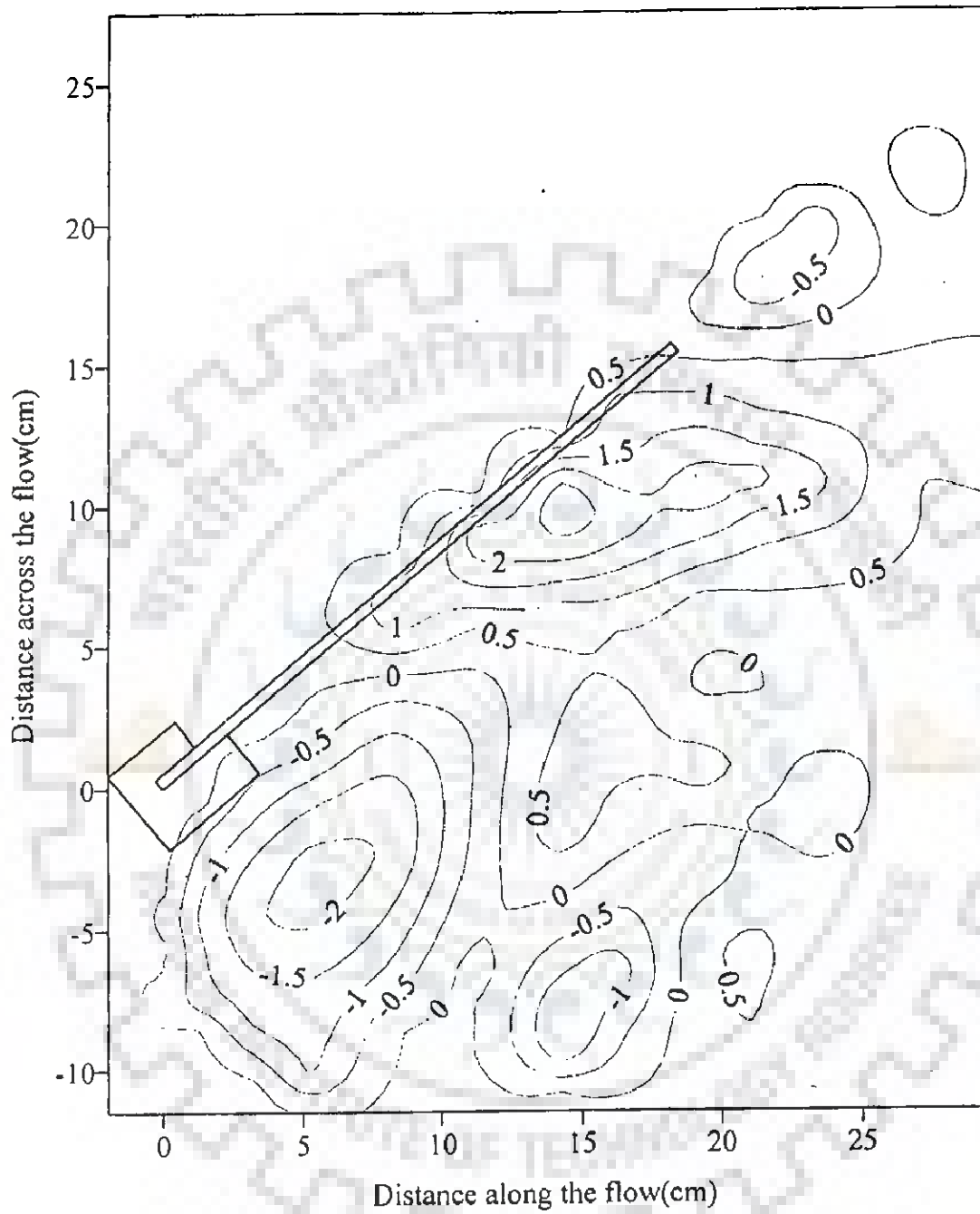


Fig. 5.12 Scour pattern for trapezoidal vane (3H:2.5V) with collar BF1.4
 ($F_r = 0.13$, $d_{50} = 0.225$ mm, contour interval in cm)

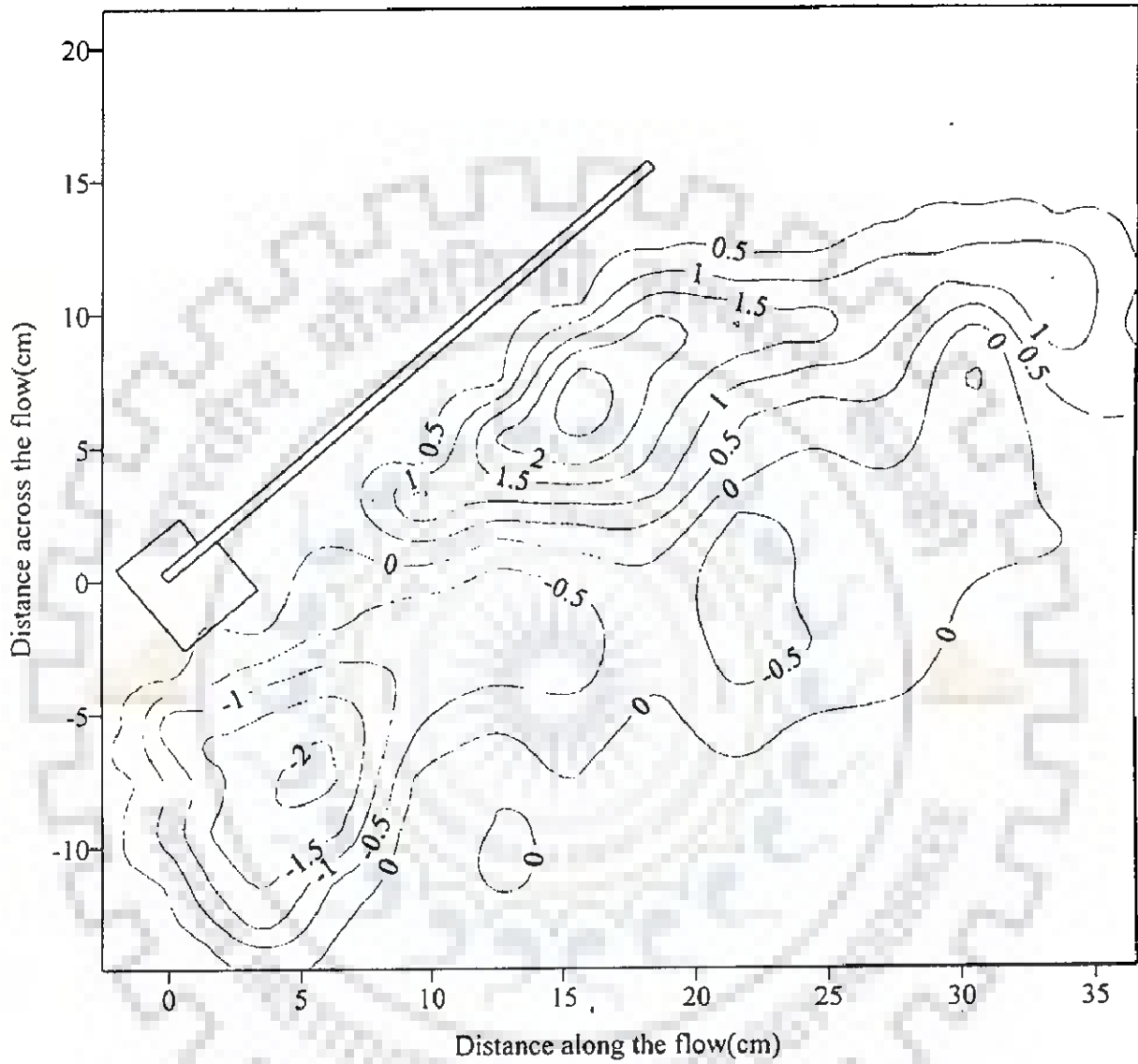


Fig. 5.13 Scour pattern for trapezoidal vane (3H:2.5V) with collar BF1.5
 ($F_r = 0.13$, $d_{50} = 0.225$ mm, contour interval in cm)

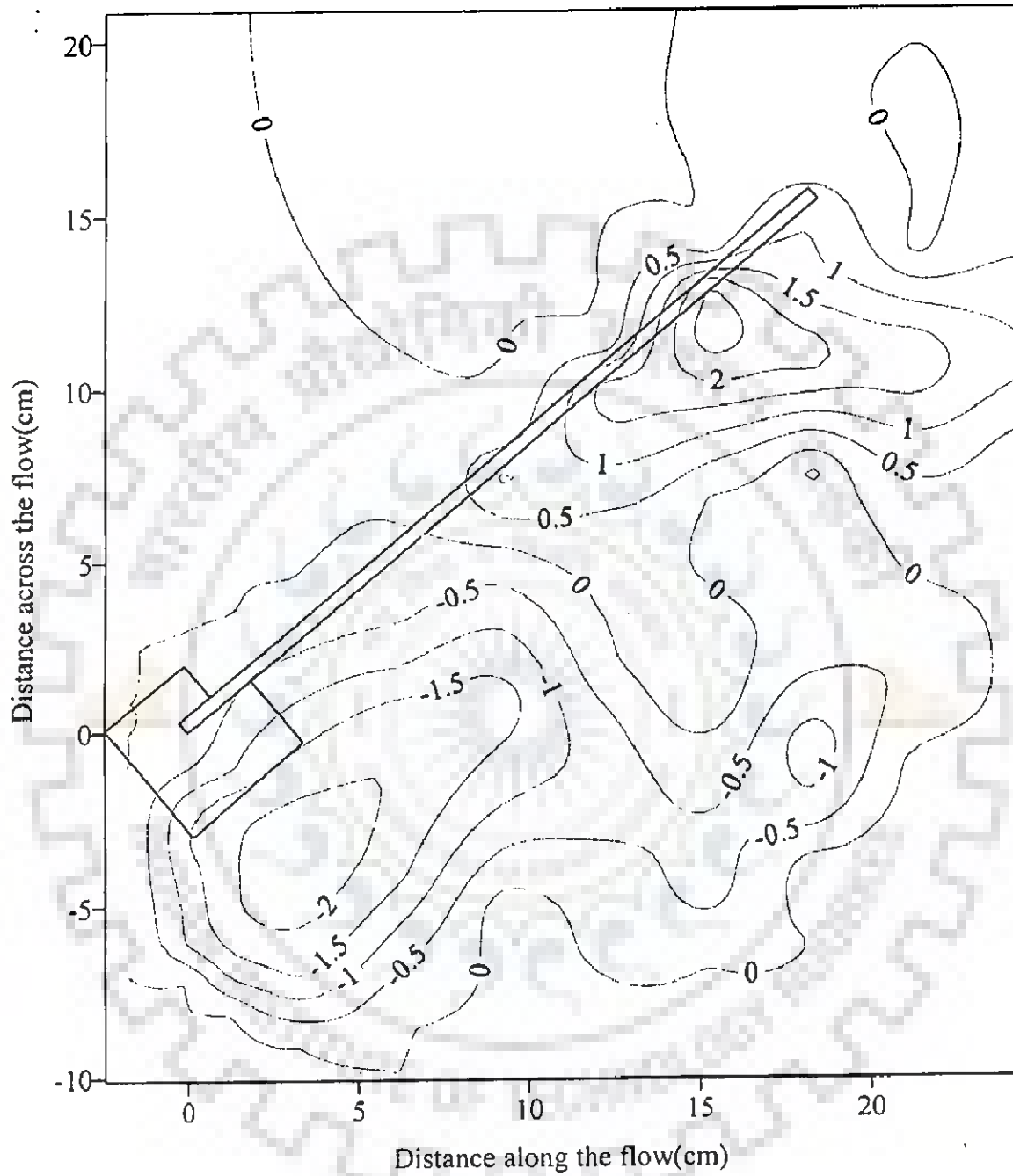


Fig. 5.14 Scour pattern for trapezoidal vane (3H:2.5V) with collar BF1.6
 ($F_r = 0.13$, $d_{50} = 0.225$ mm, contour interval in cm)

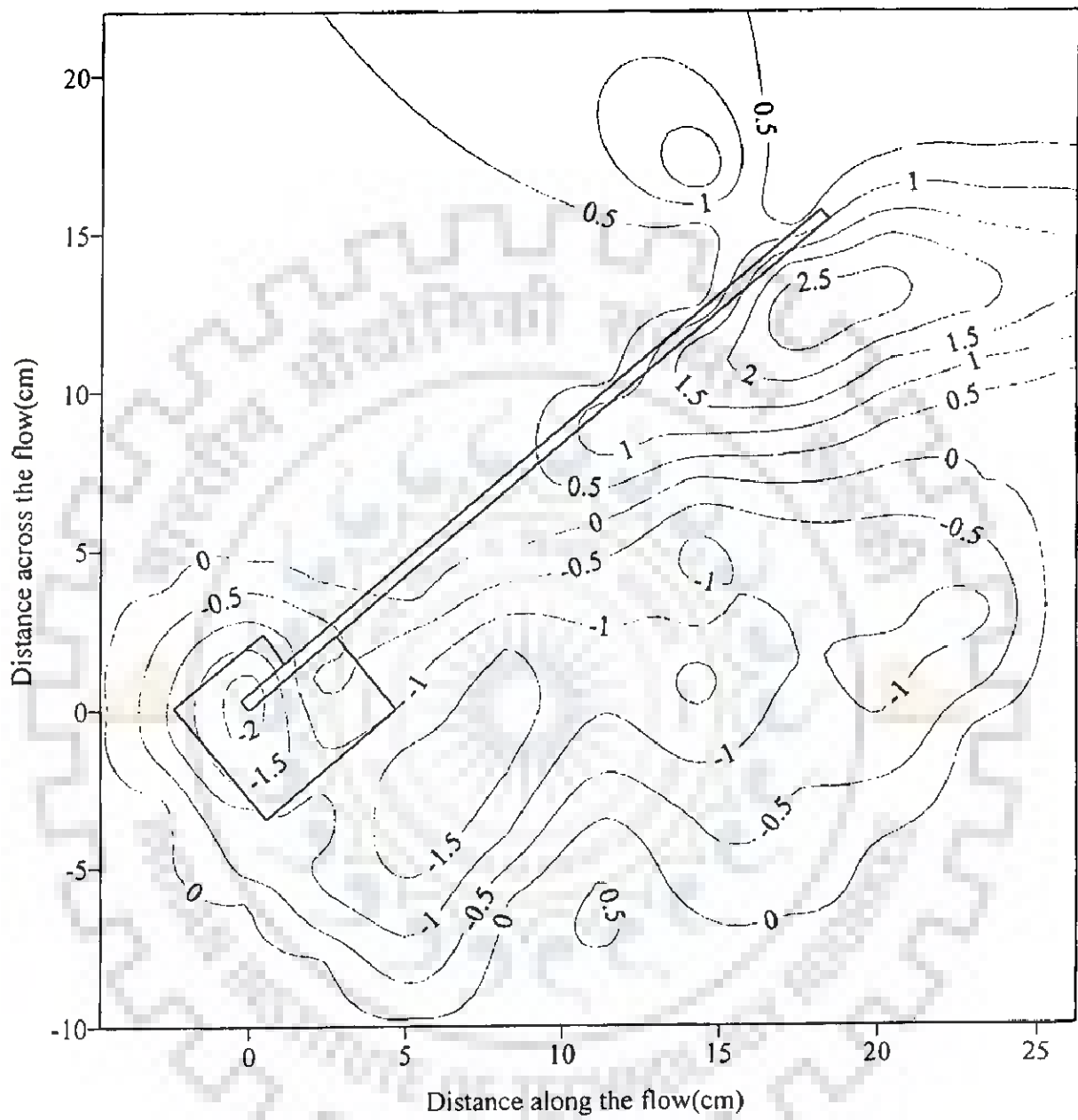


Fig. 5.15 Scour pattern for trapezoidal vane (3H:2.5V) with collar BF1.7 ($F_r = 0.13$, $d_{50} = 0.225$ mm, contour interval in cm)

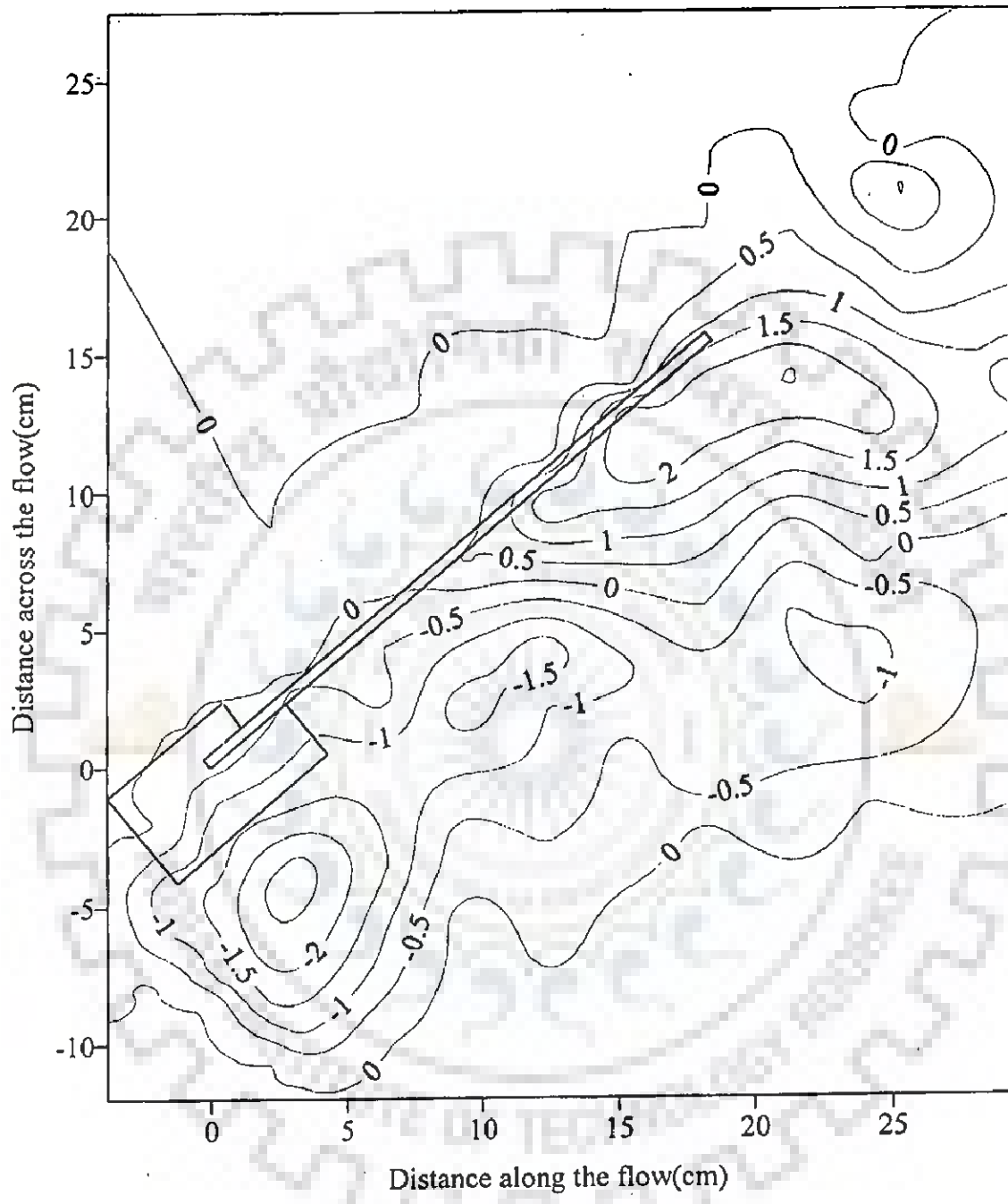


Fig. 5.16 Scour pattern for trapezoidal vane (3H:2.5V) with collar BF1.8
 ($F_r = 0.13$, $d_{50} = 0.225$ mm, contour interval in cm)

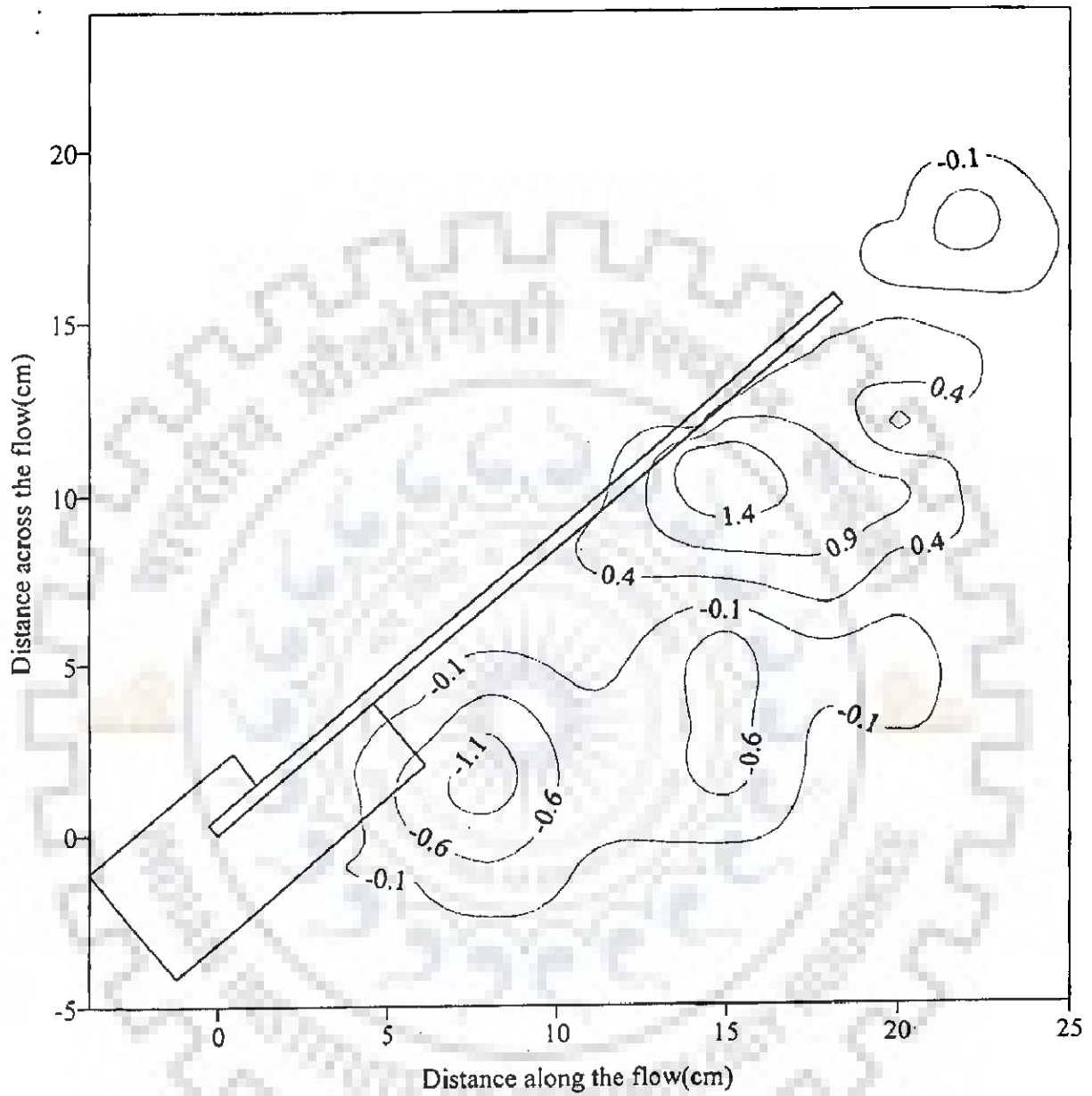


Fig. 5.17 Scour pattern for trapezoidal vane (3H:2.5V) with collar BF1.9
 ($F_r = 0.13$, $d_{50} = 0.225$ mm, contour interval in cm)

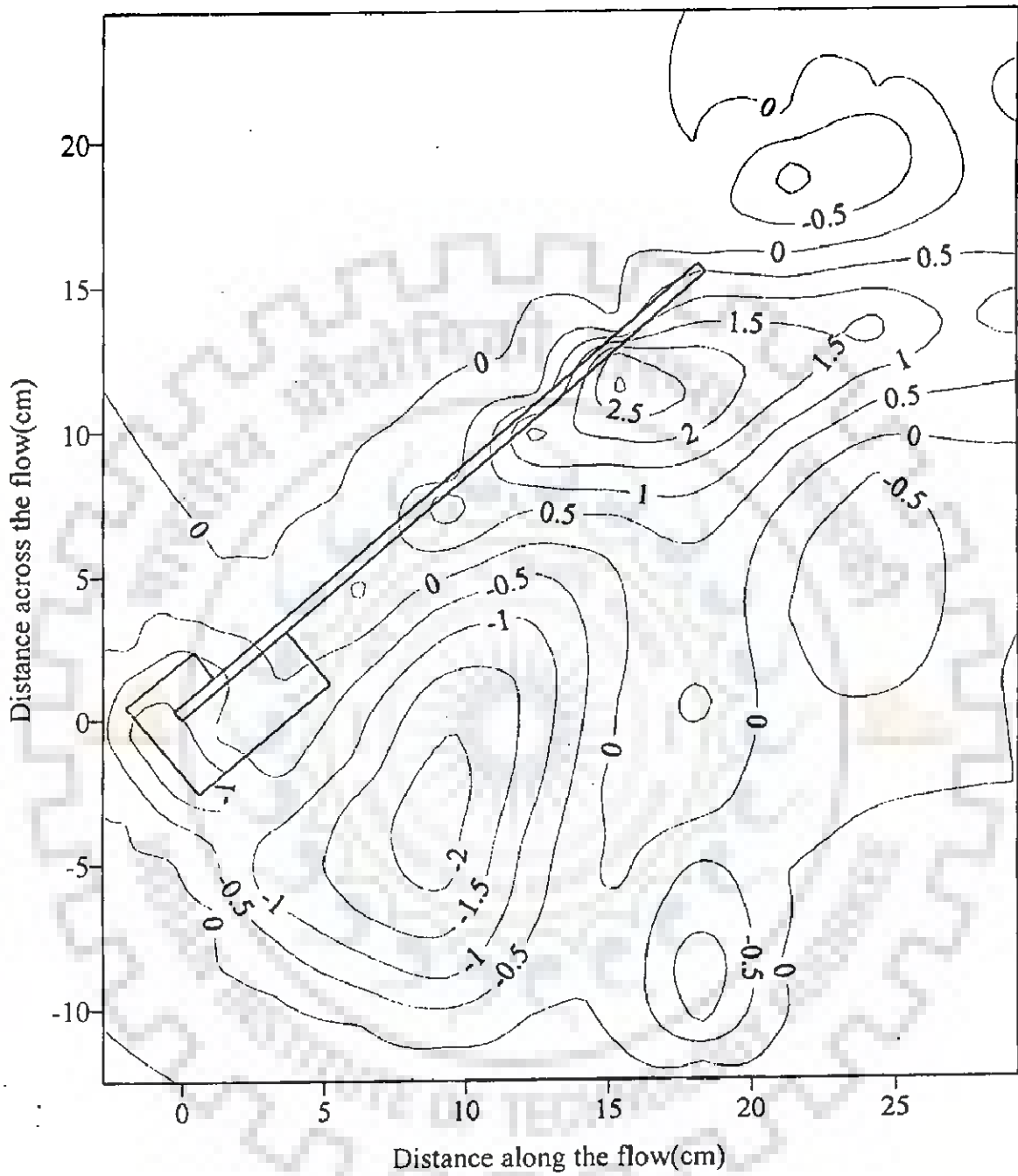
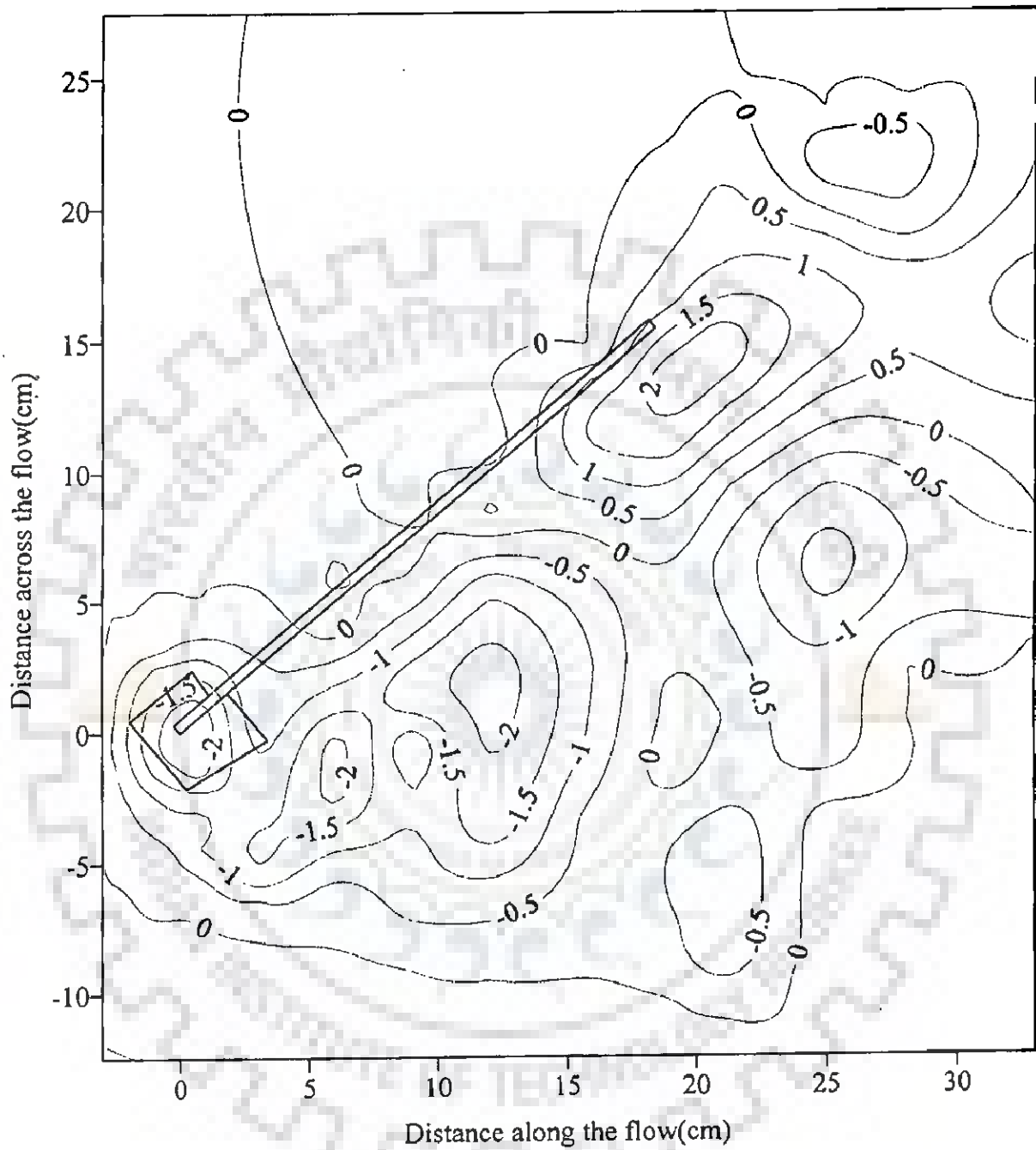


Fig. 5.18 Scour pattern for trapezoidal vane (3H:2.5V) with collar BF1.10
 ($F_r = 0.13$, $d_{50} = 0.225$ mm, contour interval in cm)



**Fig. 5.19 Scour pattern for trapezoidal vane (3H:2.5V) with collar BF1.11
($F_r = 0.13$, $d_{50} = 0.225$ mm, contour interval in cm)**

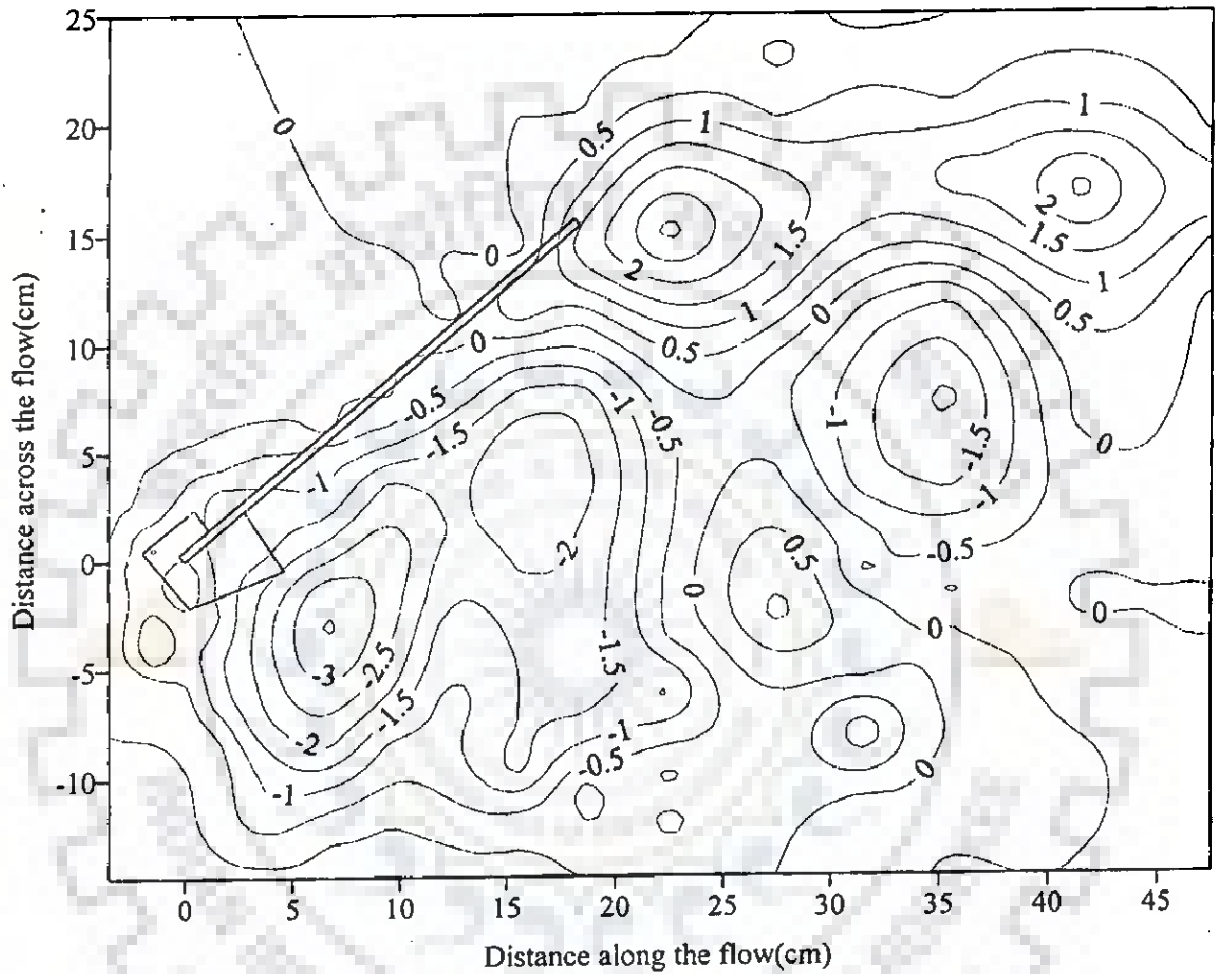


Fig. 5.20 Scour pattern for trapezoidal vane (3H:2.5V) with collar BF1.12
 ($F_r = 0.13$, $d_{50} = 0.225$ mm, contour interval in cm)

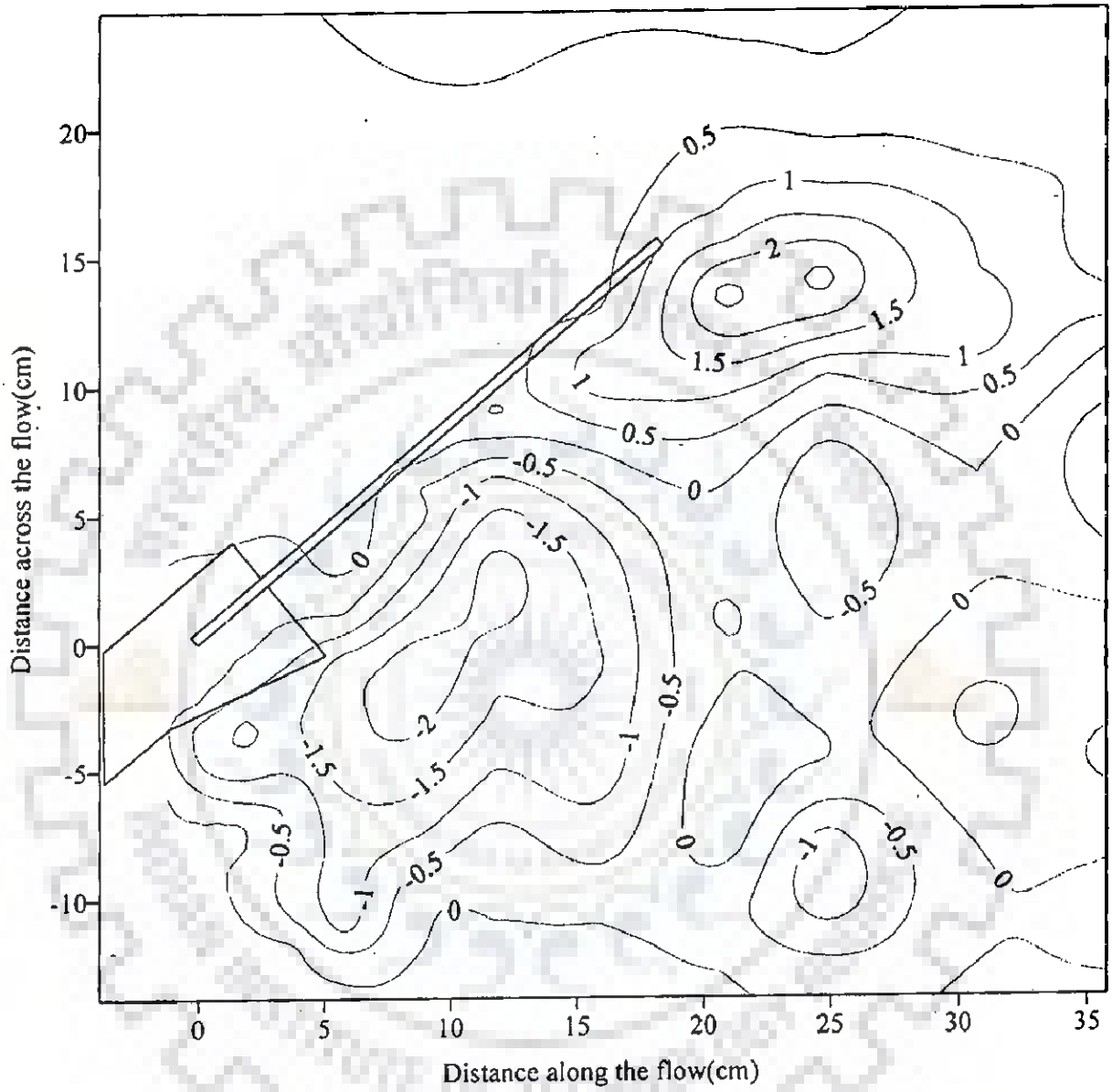
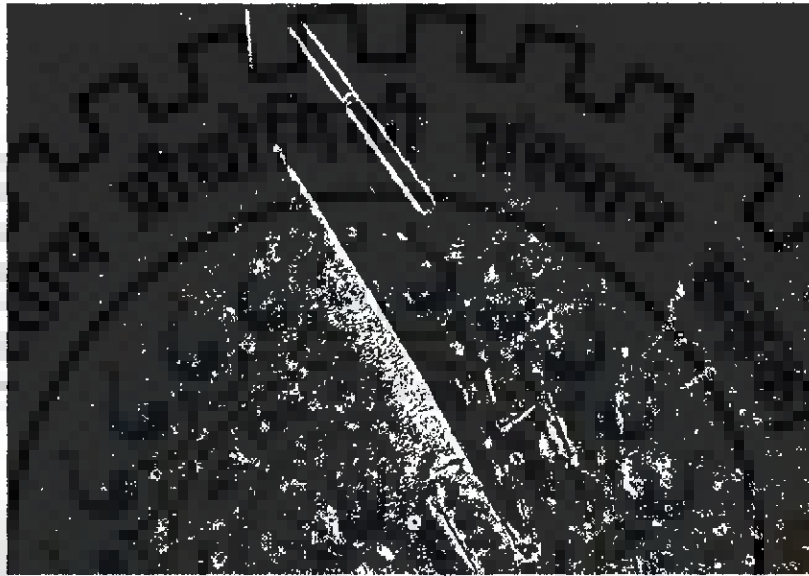


Fig. 5.21 Scour pattern for trapezoidal vane (3H:2.5V) with collar BF1.13
 $(F_r = 0.13, d_{50} = 0.225 \text{ mm}, \text{ contour interval in cm})$



**Plate 5.3 Scour pattern for trapezoidal vane (3H:2.5V) with collar BF1.13
($F_r = 0.13$, $d_{50} = 0.225$ mm)**

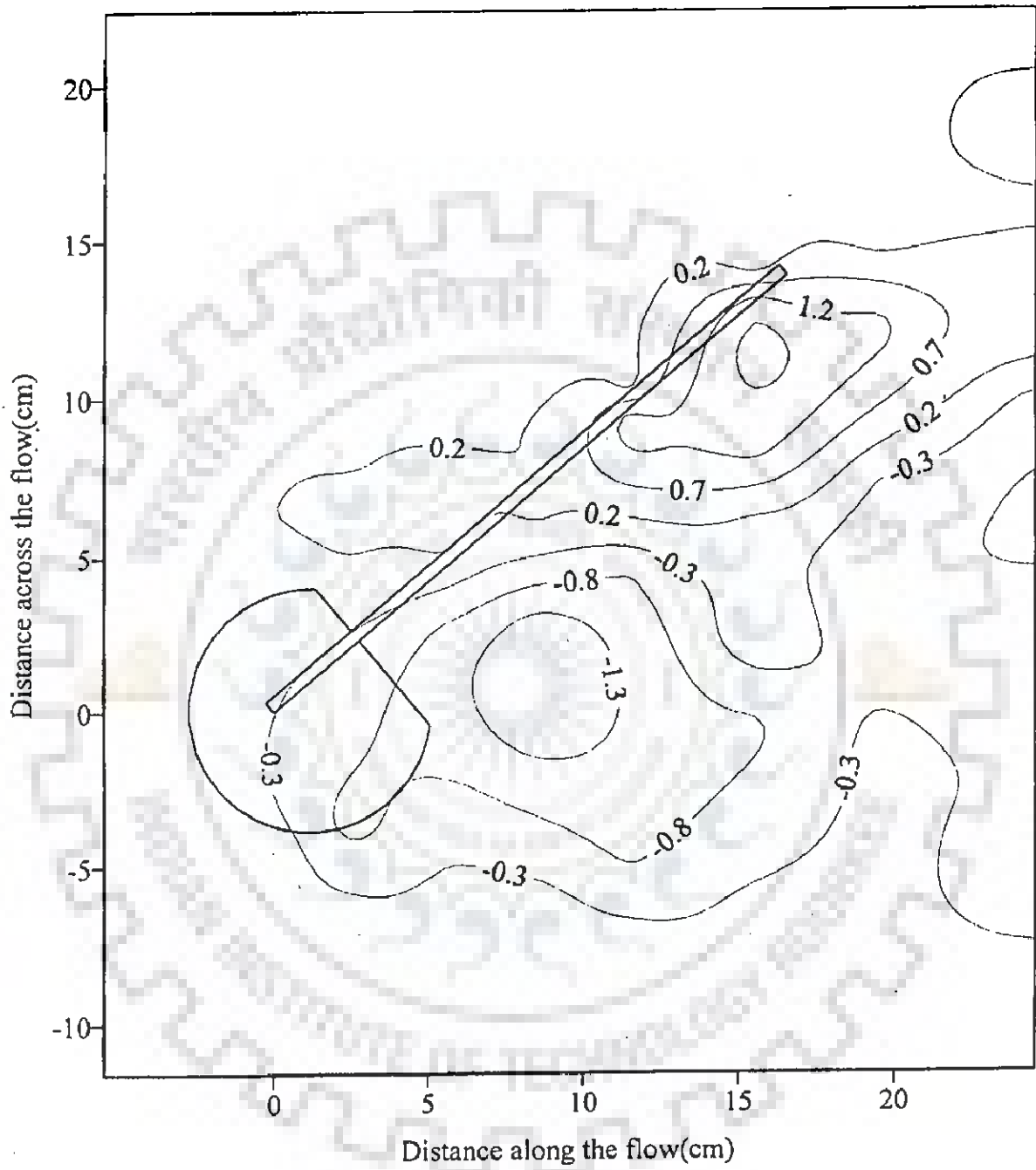


Fig. 5.22 Scour pattern for trapezoidal vane (3H:2.5V) with collar BF1.14
 ($F_r = 0.13$, $d_{50} = 0.225$ mm, contour interval in cm)



**Plate 5.4 Scour pattern for trapezoidal vane (3H:2.5V) with collar BF1.14
($F_r = 0.13$, $d_{50} = 0.225$ mm)**

5.4.2 Experiments at Froude Number 0.25 and d_{50} as 0.225 mm

5.4.2.1 Rectangular vane

This most effective collar size AF2.12 was further tested for rectangular vane at Froude number 0.25 with median size of sediment as 0.225mm and was found to be equally effective (Fig. 5.23 Plate 5.5). Afterwards no attempts were made for further refining of the collar shape since satisfactory performance has been provided by the use of above collar.

5.4.2.2 Trapezoidal vane (3H:2.5V)

The most effective collar size BF2.5 was further tested for trapezoidal vane (3H:2.5V) at Froude number 0.25 and median size of sediment 0.225mm and it was again found to be equally effective (Fig. 5.24 and Plate 5.6). Thus, no further attempts were warranted for further fine tuning of the above collar shape due to satisfactory performance.

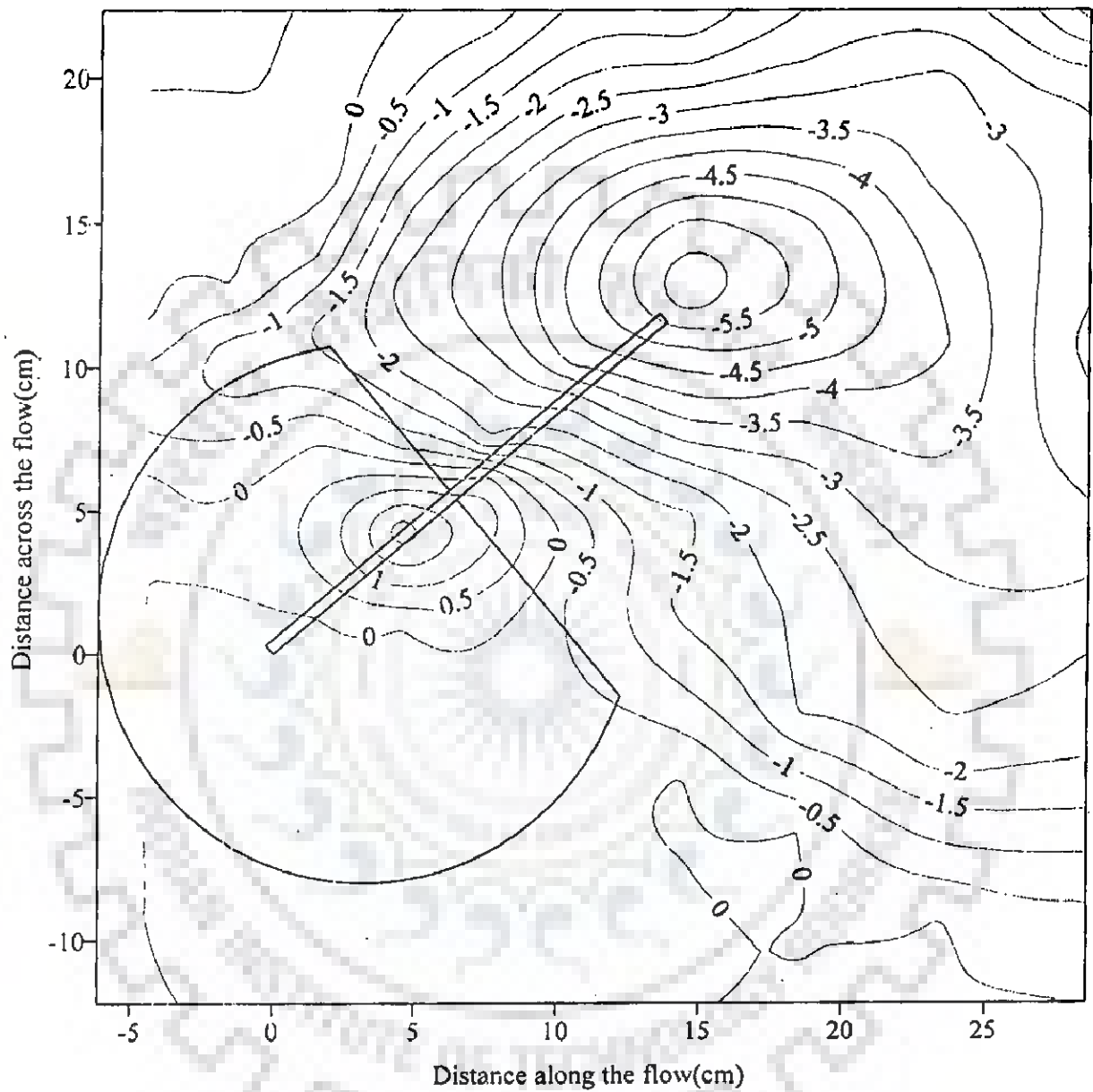
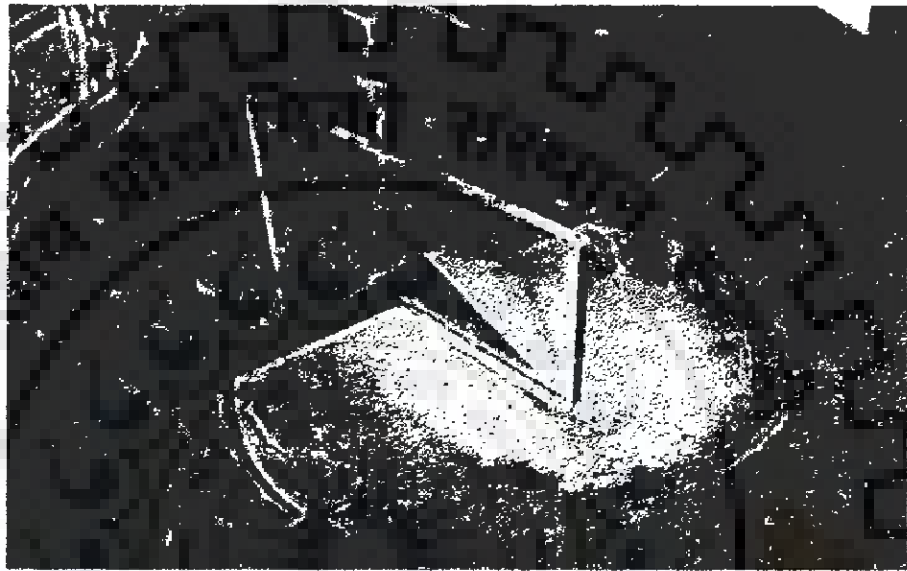


Fig. 5.23 Scour pattern for rectangular vane with collar AF2.12
 ($F_r = 0.25$, $d_{50} = 0.225$ mm, contour interval in cm)



**Plate 5.5 Scour pattern for rectangular vane with collar AF2.12
($F_r = 0.25$, $d_{50} = 0.225$ mm)**

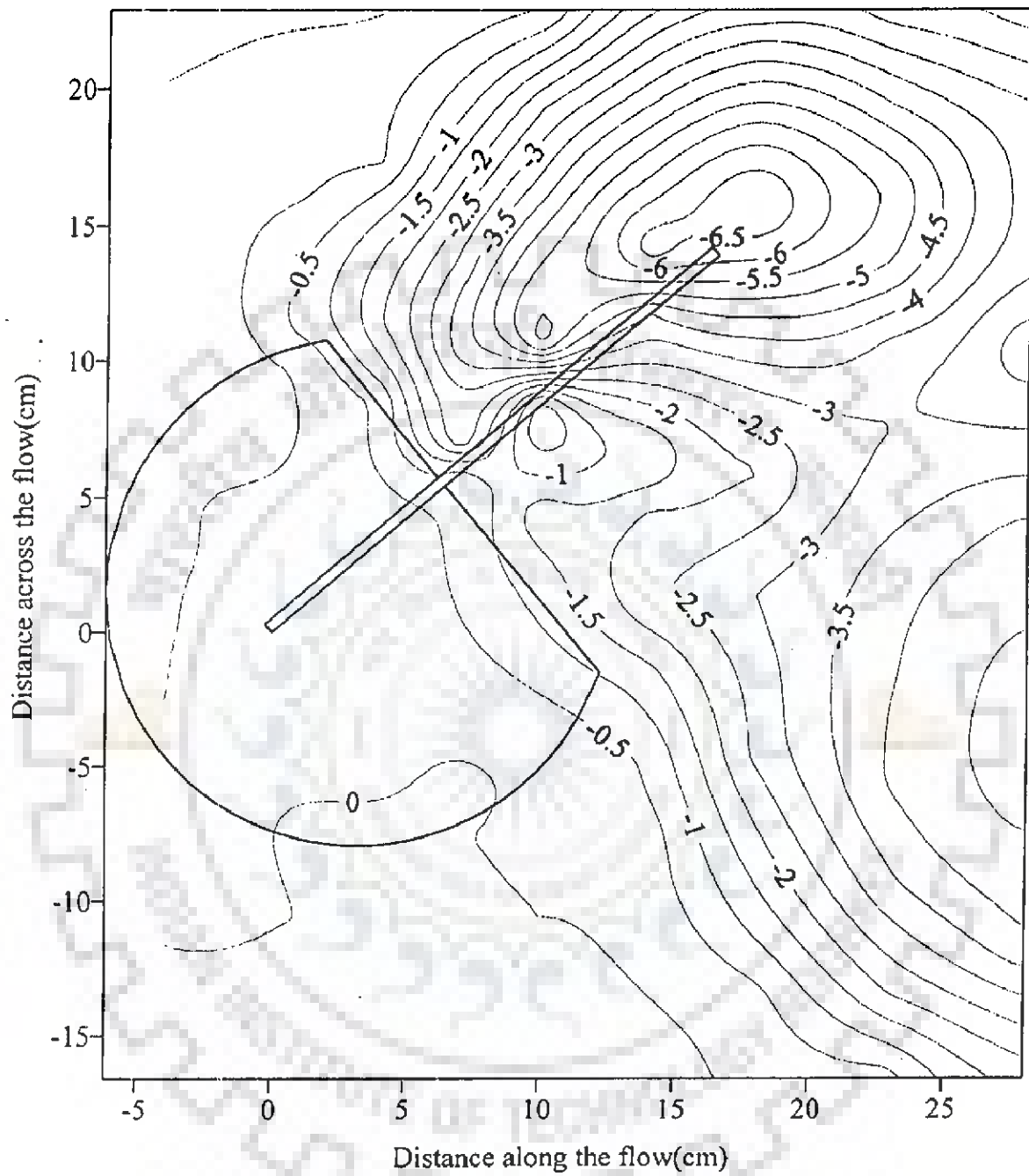
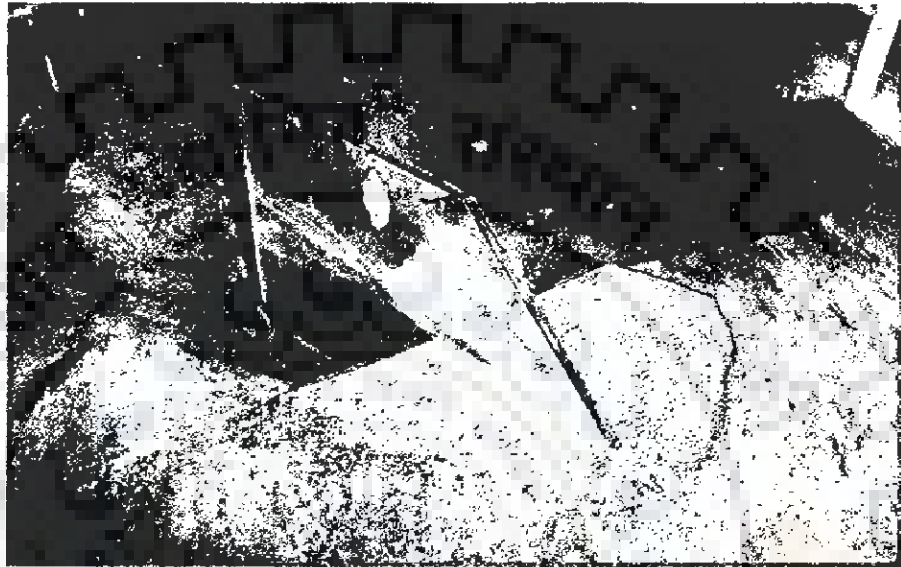


Fig. 5.24 Scour pattern for trapezoidal vane (3H:2.5V) with collar BF2.5
 ($F_r = 0.25$, $d_{50} = 0.225$ mm, contour interval in cm)



**Plate 5.6 Scour pattern for Trapezoidal vane (3H:2.5V) with collar BF2.5
($F_r = 0.25$, $d_{50} = 0.225$ mm)**

5.4.3 Experiments at Froude Number 0.25 and d_{50} as 0.405 mm

5.4.3.1 Rectangular vane

It was observed that the most effective collar size found for rectangular vane at Froude number 0.13 was not suitable at Froude number 0.25. Therefore, size of collar had to be again improved as AF2.1 and AF2.2 (Figs. 5.25 to 5.26 and Plates 5.7 to 5.8) and again it was found ineffective. It can be noted that shape of the noncircular collar size AF2.1 and AF2.2 are similar to that obtained most effective at Froude number 0.13 in case of rectangular vane. Initially, the major scour hole developed in the suction side near the collar, which further extended to the upstream edge of collar and sediment below the collar, was removed. In order to stop the scour below the edges of collar in suction side, the small vertical wall of height as $0.2H$ and thickness 3mm was provided at that edges in suction side (Collar size AF2.3, Fig. 5.27 and Plate 5.9) and this attempt was again in vain. Further, dimensions of collar in suction side were improved (Collar sizes AF2.4 to AF2.5, Figs. 5.28 to 5.29 and Plates 5.10 to 5.11), but still the collar was found to be ineffective. Now, collar was given different shapes (Collar size AF2.6, Fig. 5.30 and Plate 5.12) in which one of the edges of collars was made parallel to the direction of flow and again the collar was ineffective. This shape was further improved (Collar size AF2.7, Fig. 5.31 and Plate 5.13) and scour hole developed was still not acceptable. Circular shape of collar of arbitrary size AF2.8 (Fig. 5.32 and Plate 5.14) based on past experimental experience was tried and it was found to be better option in the context of shape than the earlier shapes experimented. However, there was still some scour below the collar. Once more its dimension was improved to AF2.9 (Fig. 5.33 and Plate 5.15) as per the location, development and extension of scour hole and again it was not seen to be acceptable as the most effective collar.

In this way, some more circular shapes of different sizes (Collar sizes AF2.10 to AF2.12, Figs. 5.34 to 36 and Plates 5.16 to 5.18) were experimented.

It was found that collar size AF2.12 (Fig. 5.36 and Plate 5.18) was the most effective size of collar. This finding also suggests that circular shape of collar is a better option than noncircular shapes.



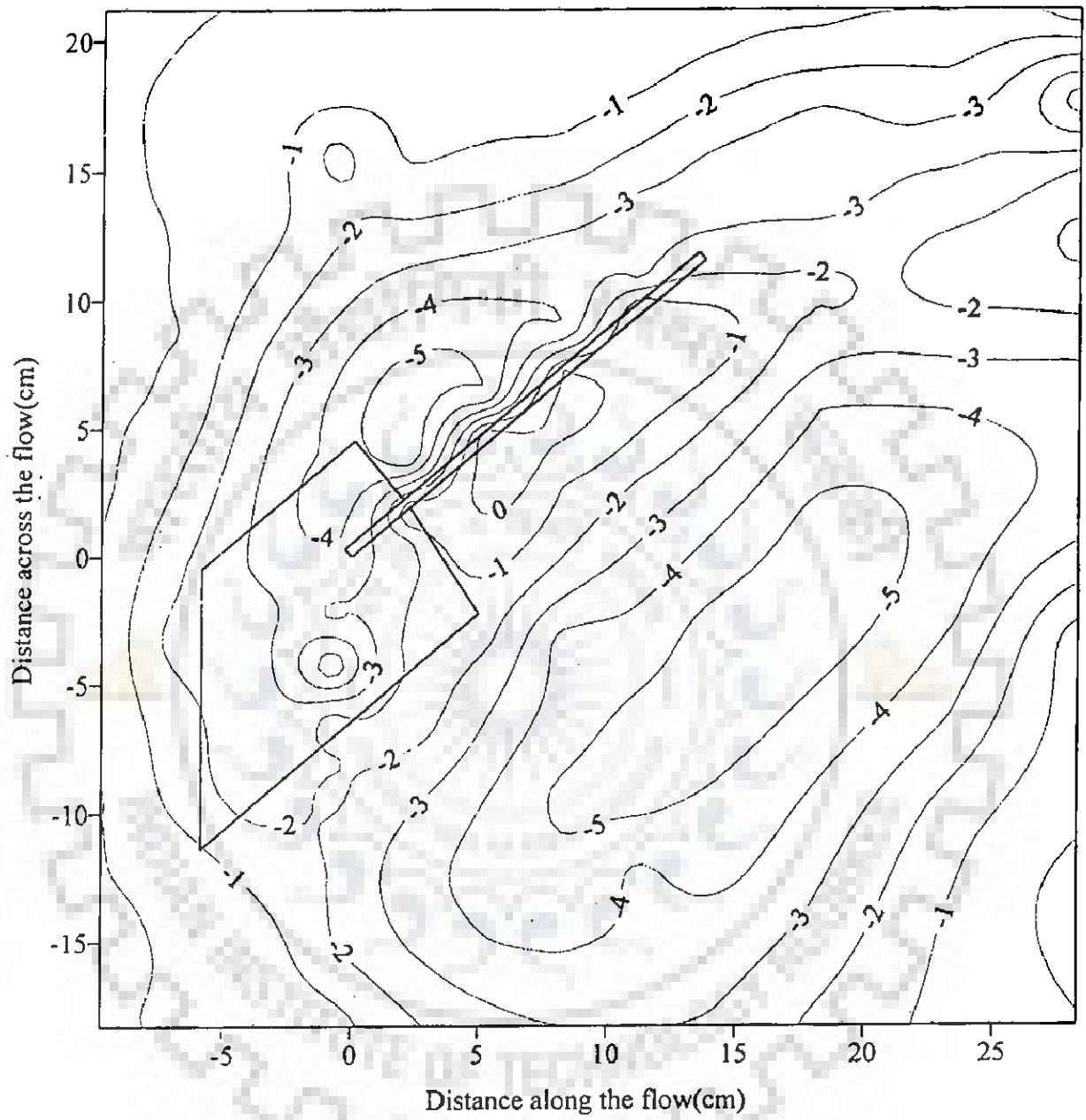


**Fig. 5.25 Scour pattern for rectangular vane with collar AF2.1
 ($F_r = 0.25$, $d_{50} = 0.405$ mm, contour interval in cm)**

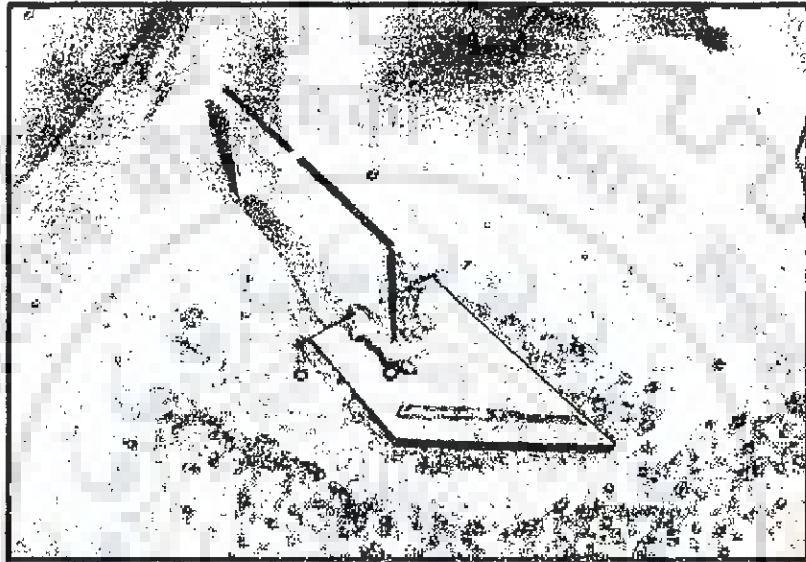


**Plate 5.7 Scour pattern for rectangular vane with collar AF2.1
($F_r = 0.25$, $d_{50} = 0.405$ mm)**

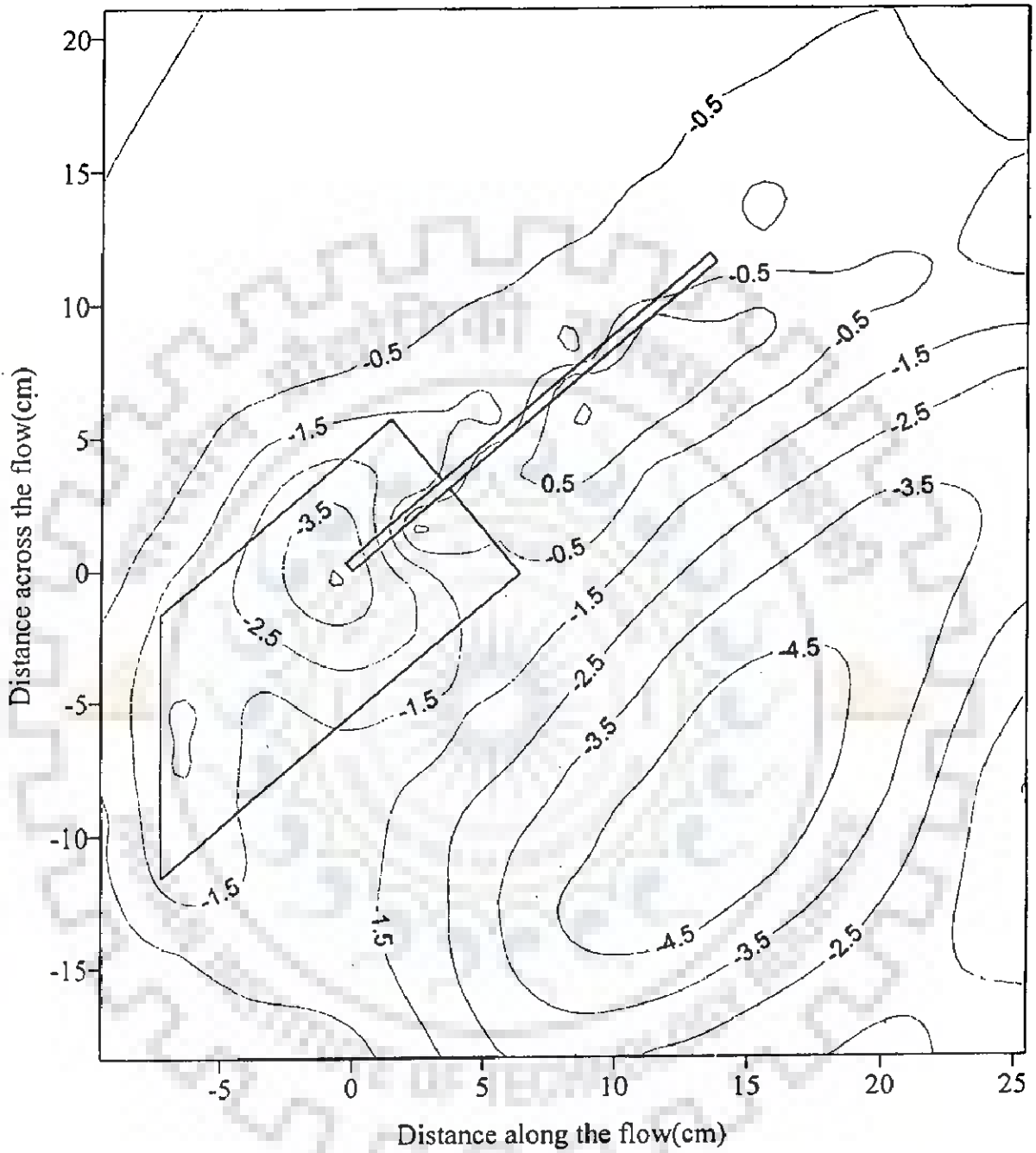
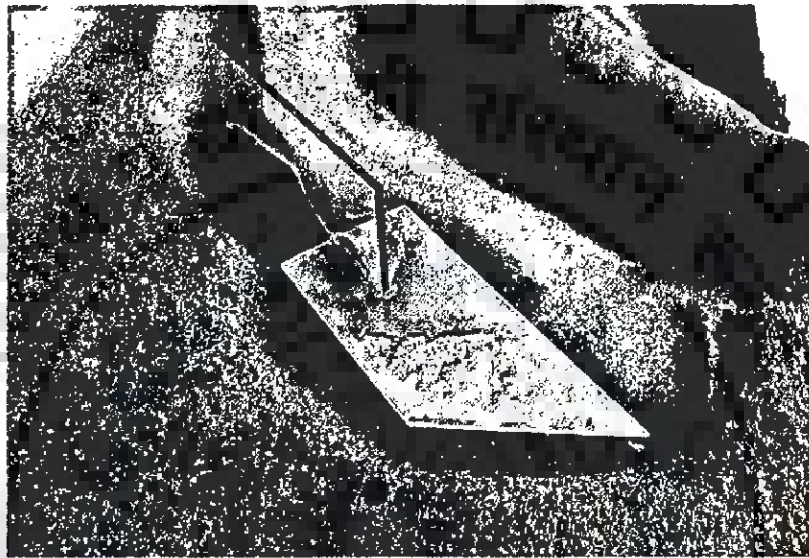


Fig. 5.26 Scour pattern for rectangular vane with collar AF2.2
 ($F_r = 0.25$, $d_{50} = 0.405$ mm, contour interval in cm)



**Plate 5.8 Scour pattern for rectangular vane with collar AF2.2
($F_r = 0.25$, $d_{50} = 0.405$ mm)**

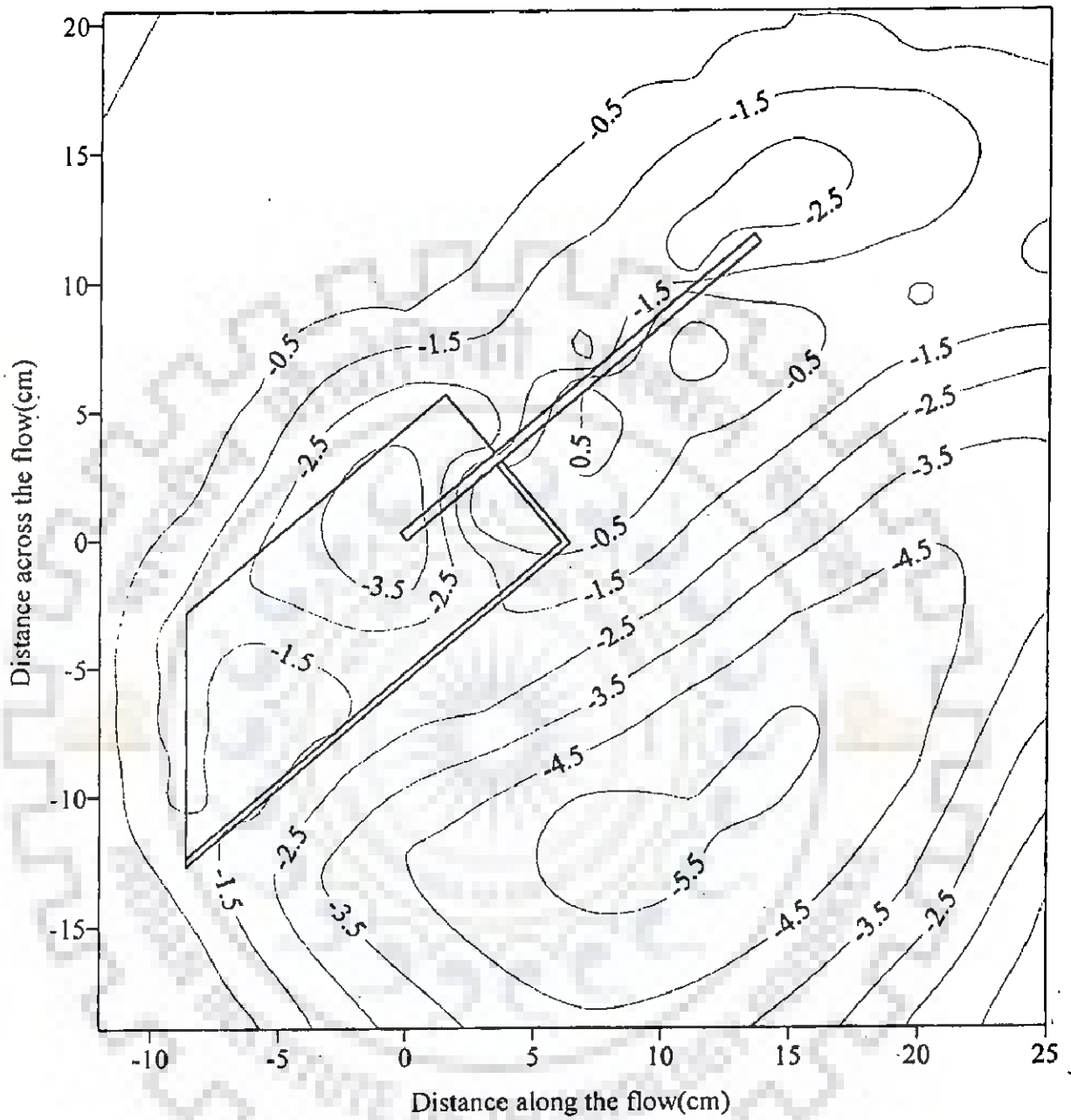
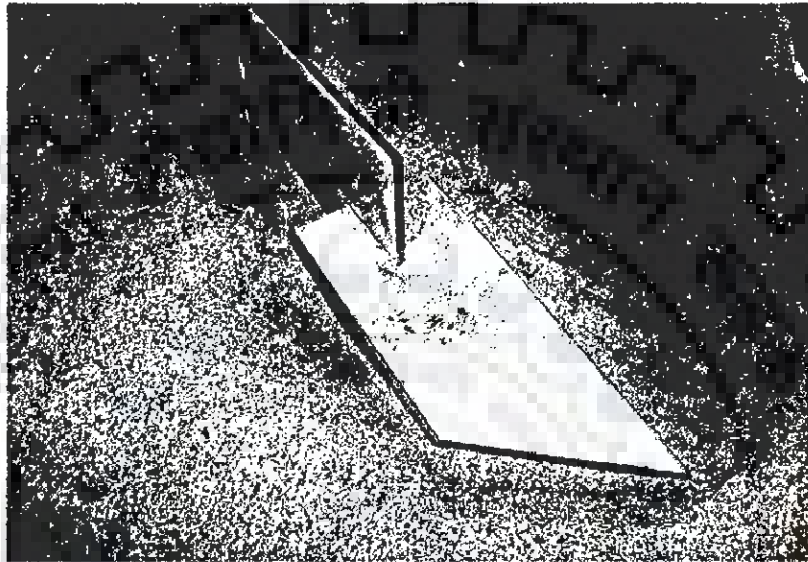


Fig. 5.27 Scour pattern for rectangular vane with collar AF2.3
 ($F_r = 0.25$, $d_{50} = 0.405$ mm, contour interval in cm)



**Plate 5.9 Scour pattern for rectangular vane with collar AF2.3
($F_r = 0.25$, $d_{50} = 0.405$ mm)**

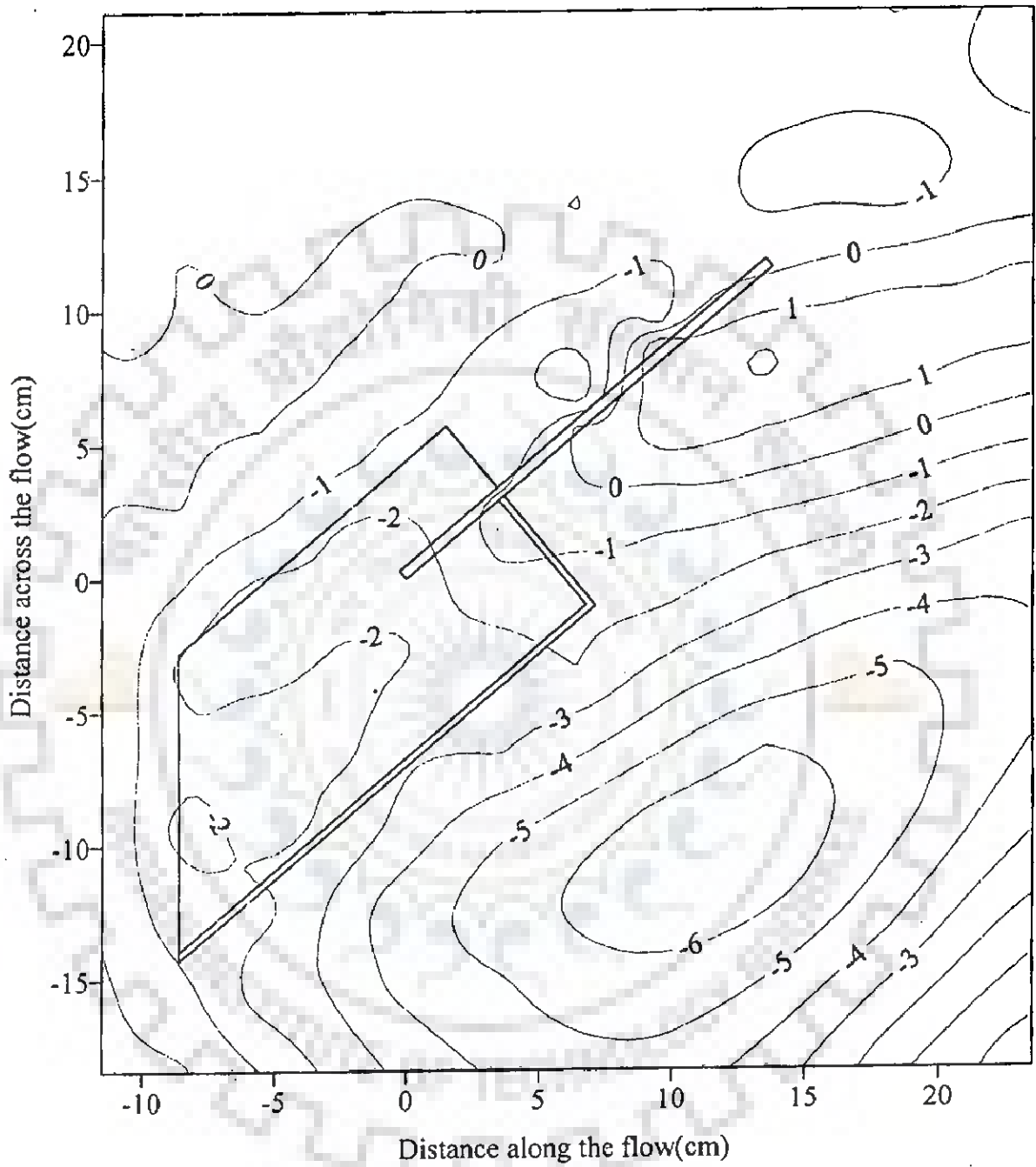


Fig. 5.28 Scour pattern for rectangular vane with collar AF2.4
 ($F_r = 0.13$, $d_{50} = 0.405$ mm, contour interval in cm)



**Plate 5.10 Scour pattern for rectangular vane with collar AF2.4
($F_r = 0.25$, $d_{50} = 0.405$ mm)**

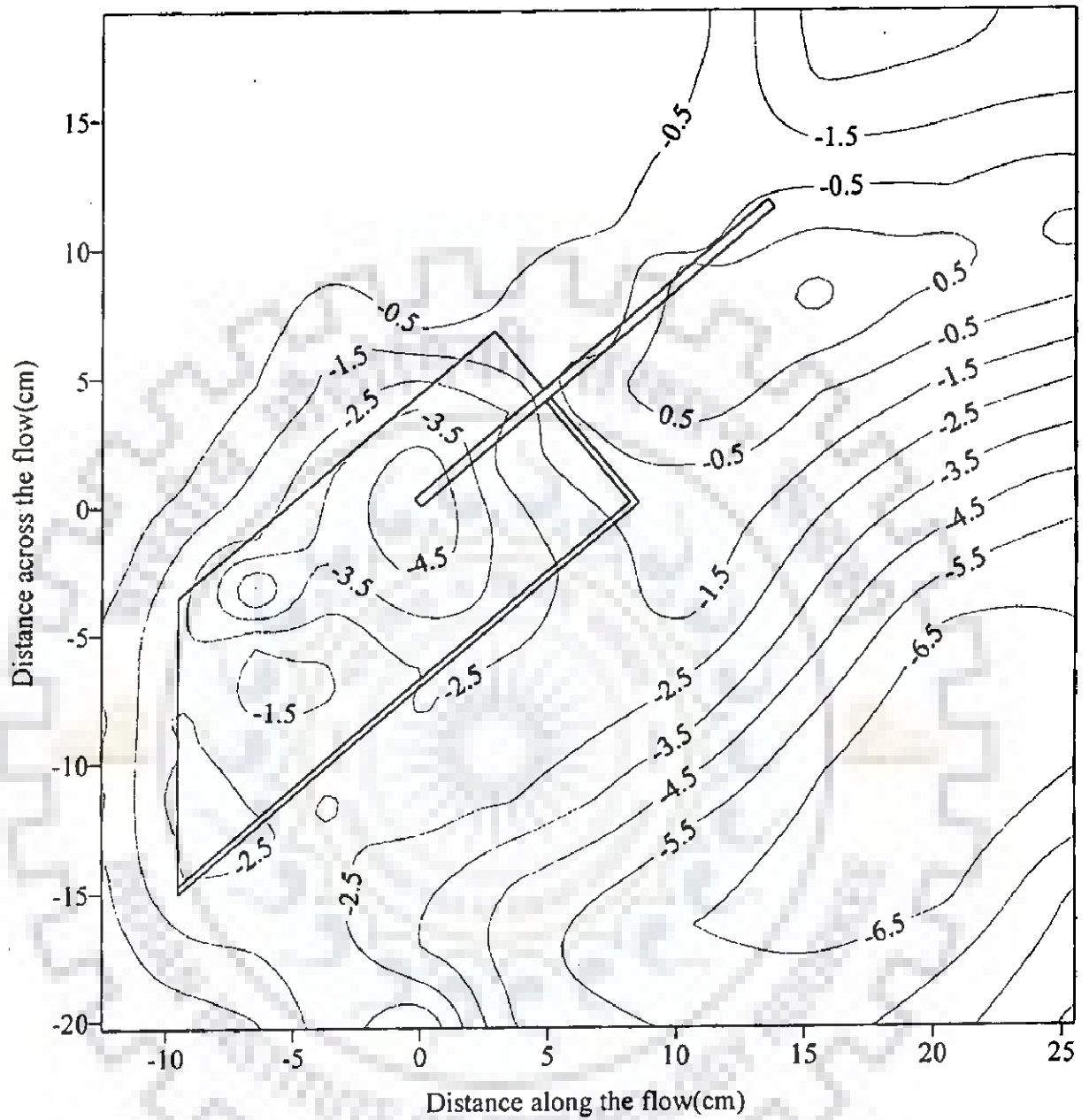
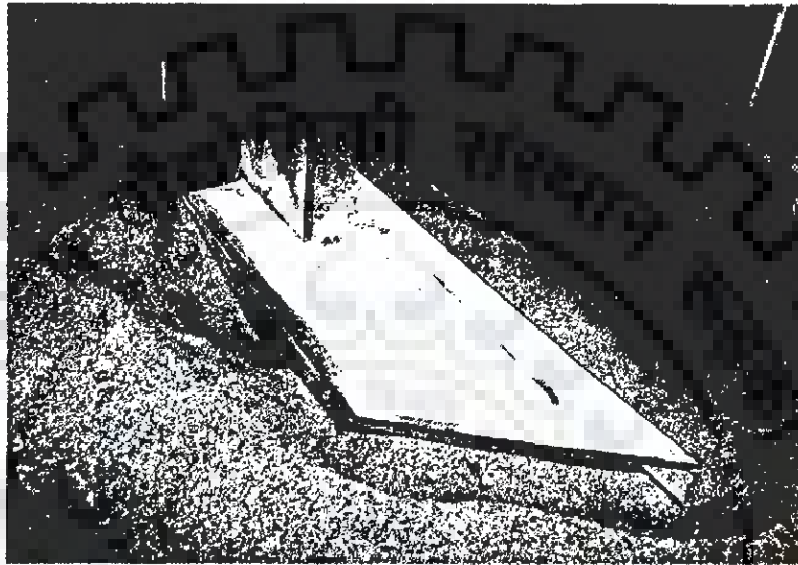


Fig. 5.29 Scour pattern for rectangular vane with collar AF2.5
 ($F_r = 0.25$, $d_{50} = 0.405$ mm, contour interval in cm)



**Plate 5.11 Scour pattern for rectangular vane with collar AF2.5
($F_r = 0.25$, $d_{50} = 0.405$ mm)**

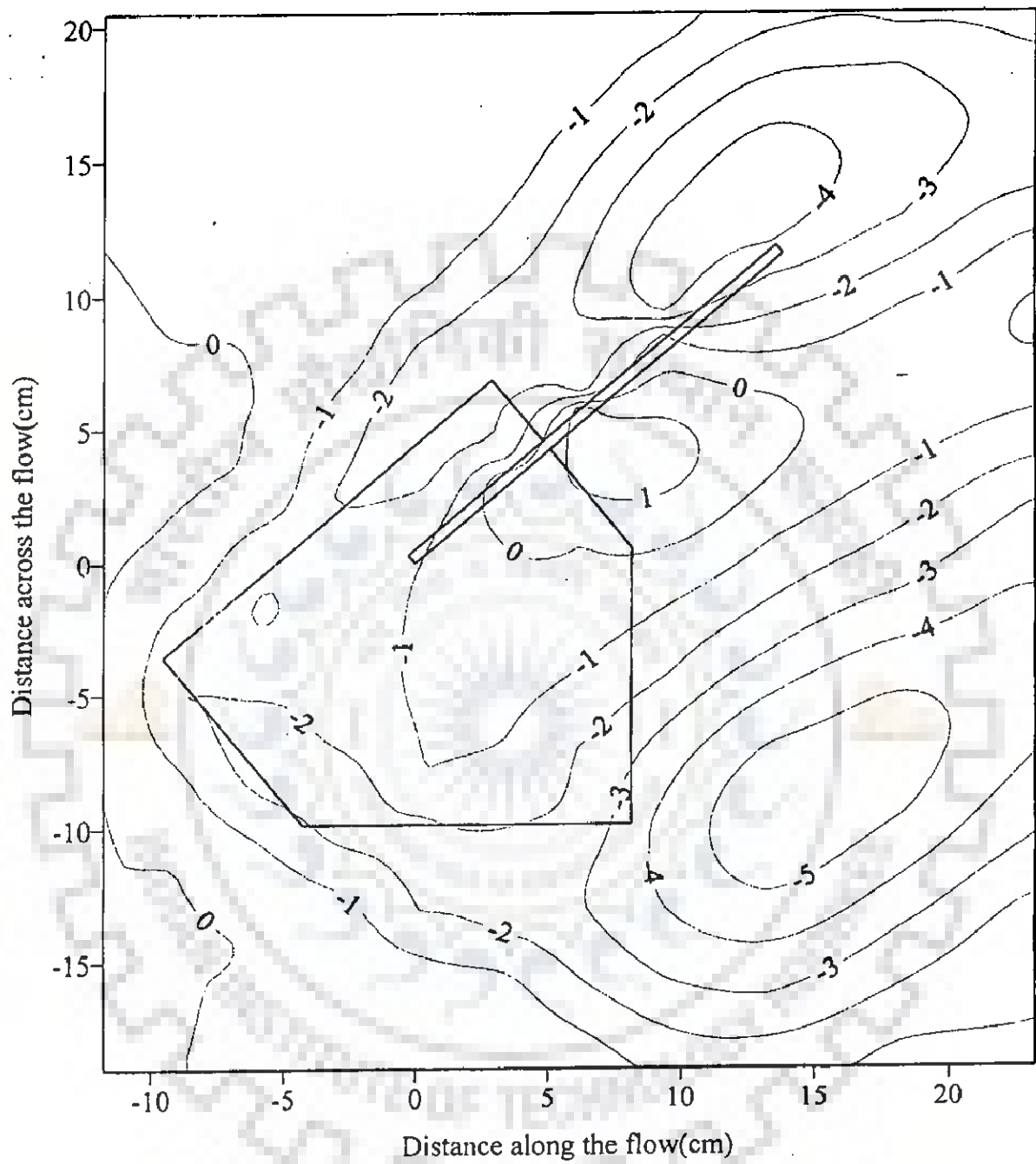


Fig. 5.30 Scour pattern for rectangular vane with collar AF2.6
 ($F_r = 0.25$, $d_{50} = 0.405$ mm, contour interval in cm)



**Plate 5.12 Scour pattern for rectangular vane with collar AF2.6
($F_r = 0.25$, $d_{50} = 0.405$ mm)**

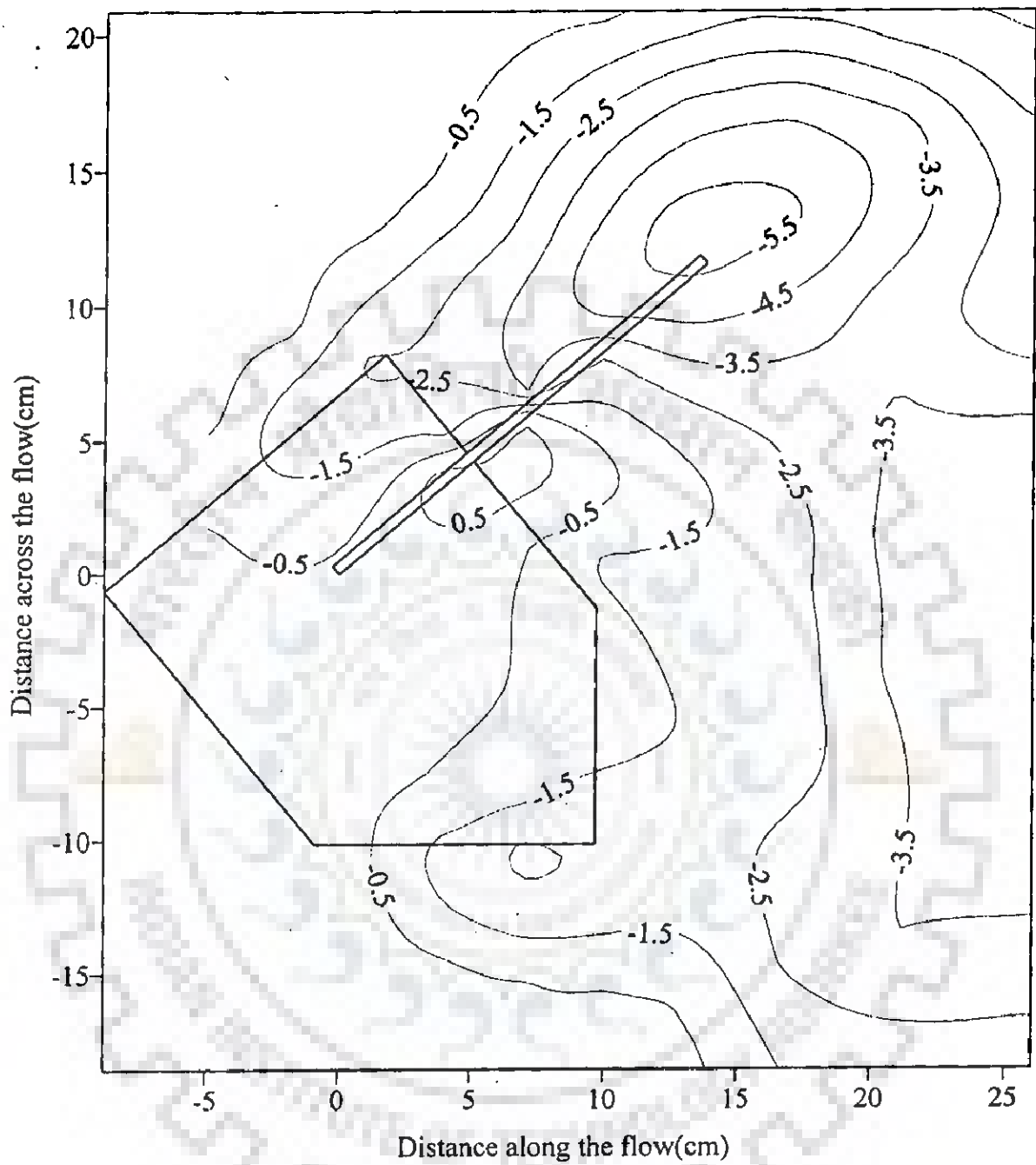


Fig. 5.31 Scour pattern for rectangular vane with collar AF2.7
 ($F_r = 0.25$, $d_{50} = 0.405$ mm, contour interval in cm)



**Plate 5.13 Scour pattern for rectangular vane with collar AF2.7
($F_r = 0.25$, $d_{50} = 0.405$ mm)**

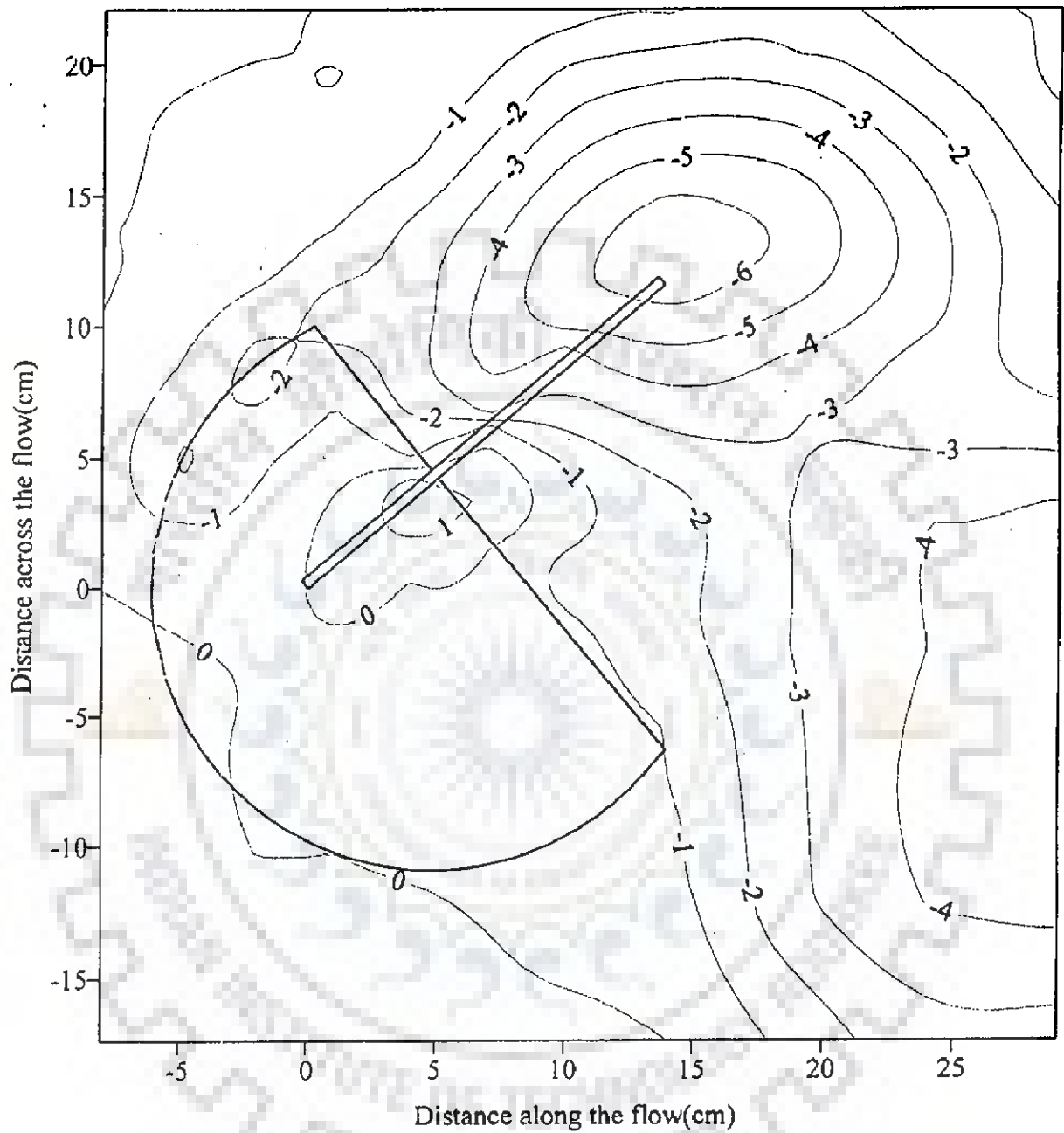
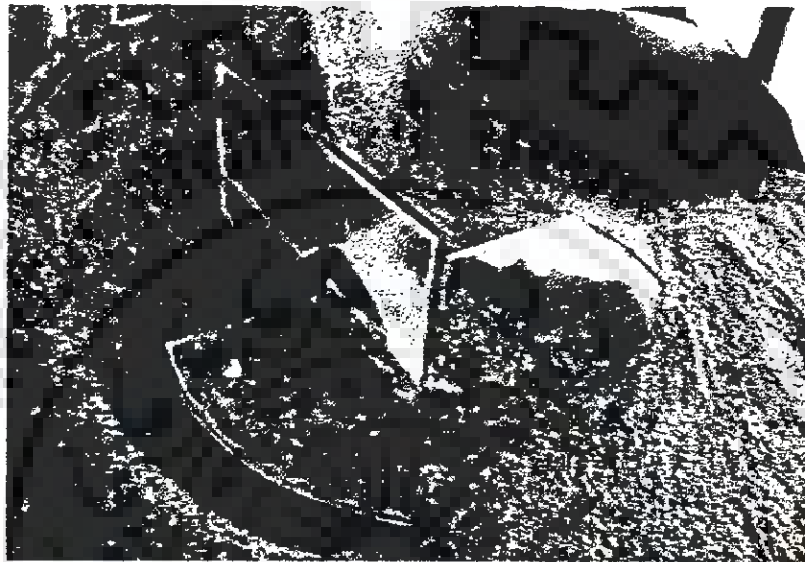


Fig. 5.32 Scour pattern for rectangular vane with collar AF2.8
 ($F_r = 0.25$, $d_{50} = 0.405$ mm, contour interval in cm)



**Plate 5.14 Scour pattern for rectangular vane with collar AF2.8
($F_r = 0.25$, $d_{50} = 0.405$ mm)**

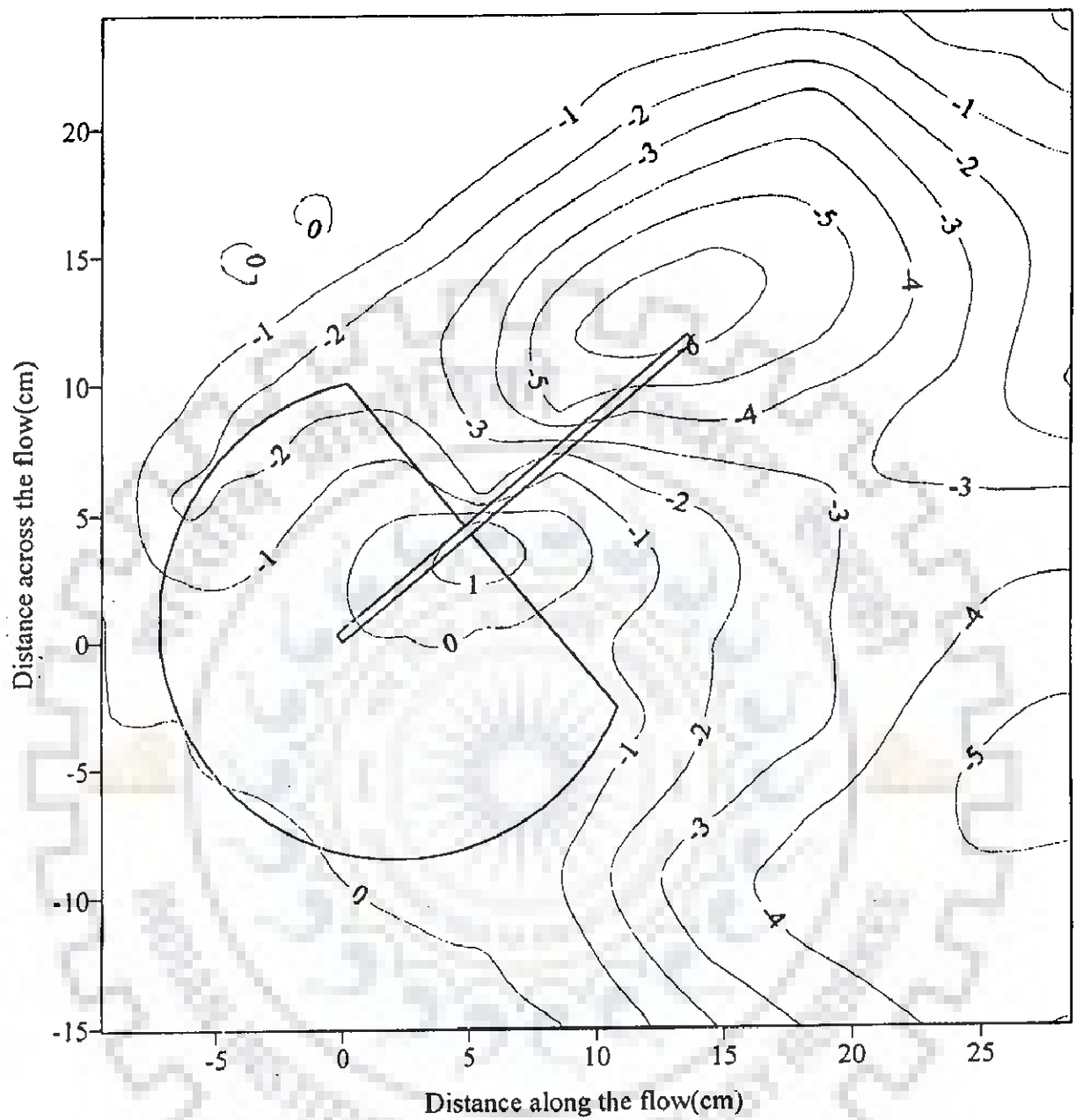
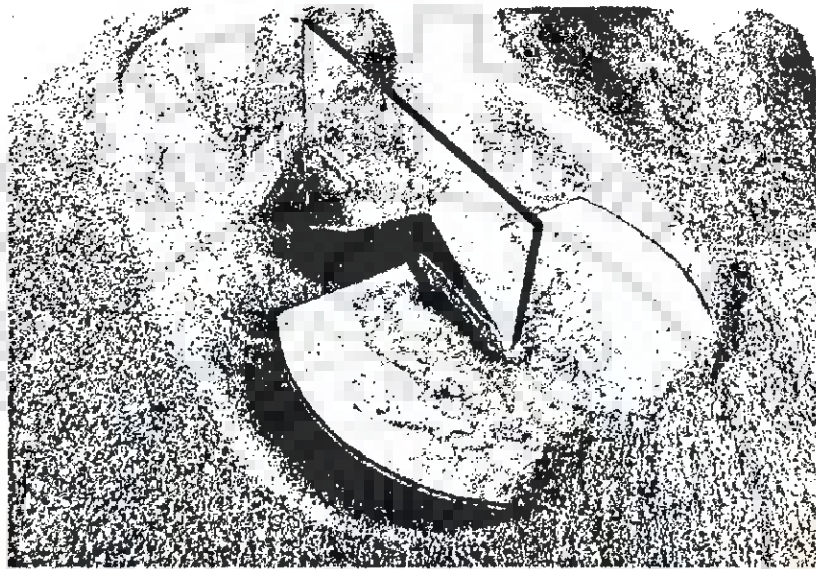


Fig. 5.33 Scour pattern for rectangular vane with collar AF2.9
 ($F_r = 0.25$, $d_{50} = 0.405$ mm, contour interval in cm)



**Plate 5.15 Scour pattern for rectangular vane with collar AF2.9
($F_r = 0.25$, $d_{50} = 0.405$ mm)**

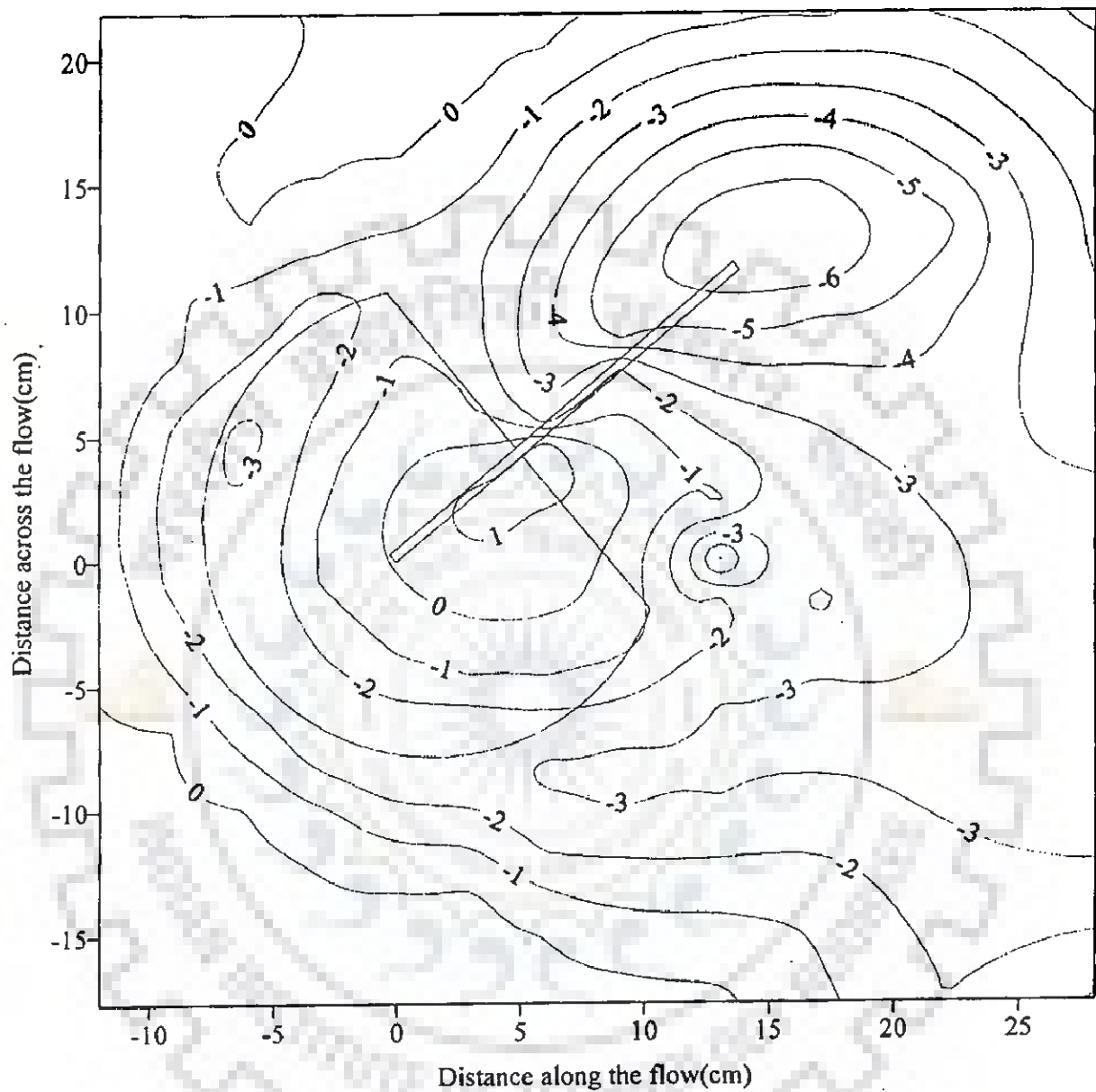
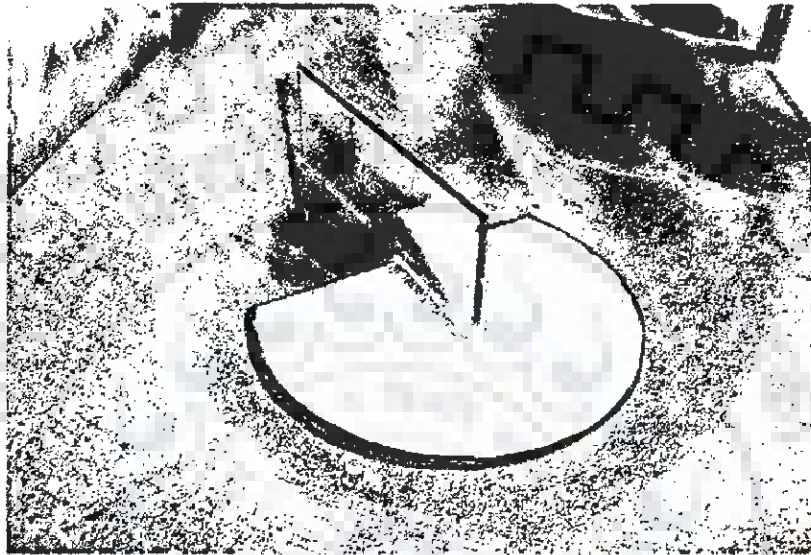


Fig. 5.34 Scour pattern for rectangular vane with collar AF2.10
 ($F_r = 0.25$, $d_{50} = 0.405$ mm, contour interval in cm)



**Plate 5.16 Scour pattern for rectangular vane with collar AF2.10
($F_r = 0.25$, $d_{50} = 0.405$ mm)**

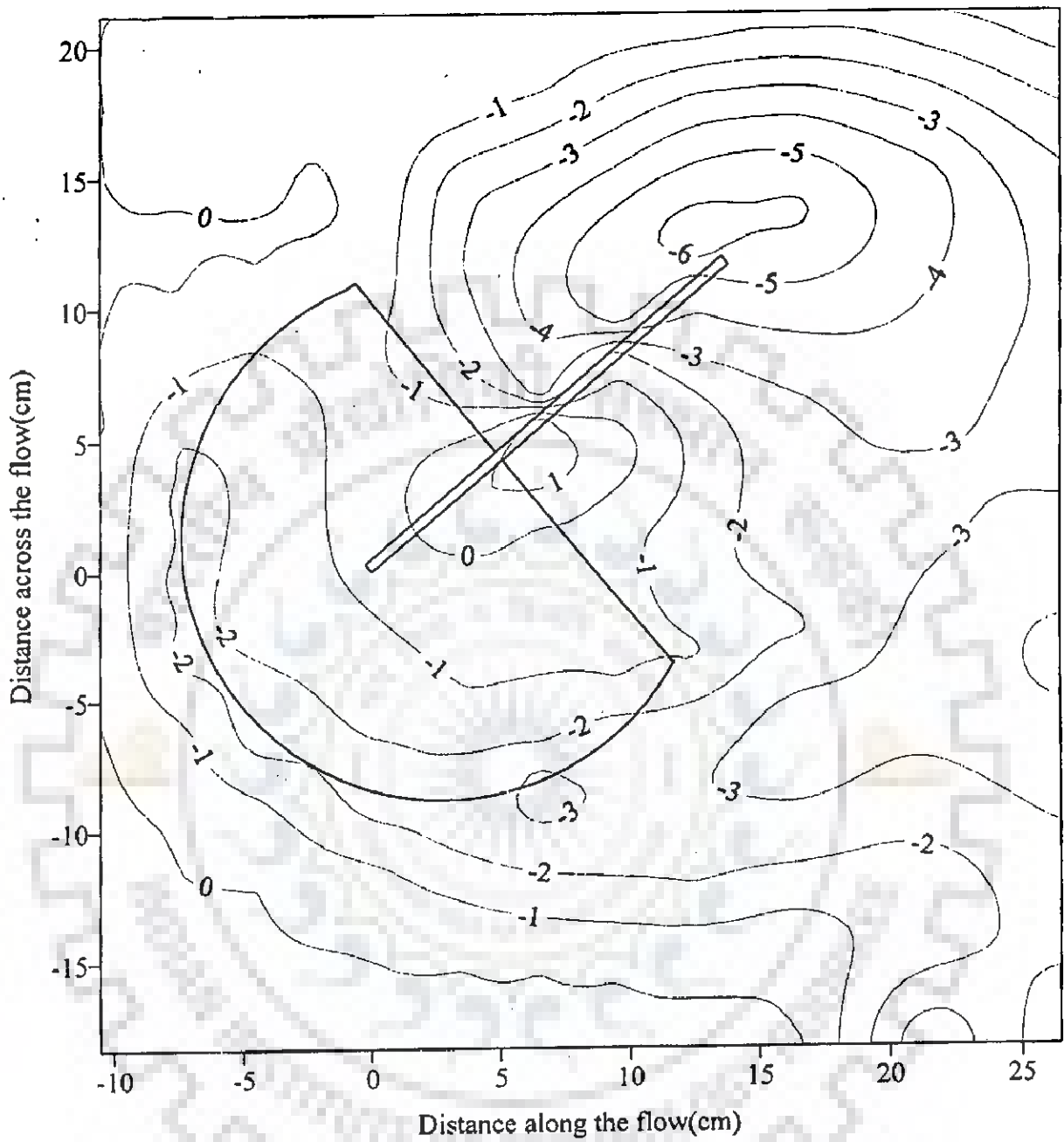


Fig. 5.35 Scour pattern for rectangular vane with collar AF2.11
 ($F_r = 0.25$, $d_{50} = 0.405$ mm, contour interval in cm)



**Plate 5.17 Scour pattern for rectangular vane with collar AF2.11
($F_r = 0.25$, $d_{50} = 0.405$ mm)**

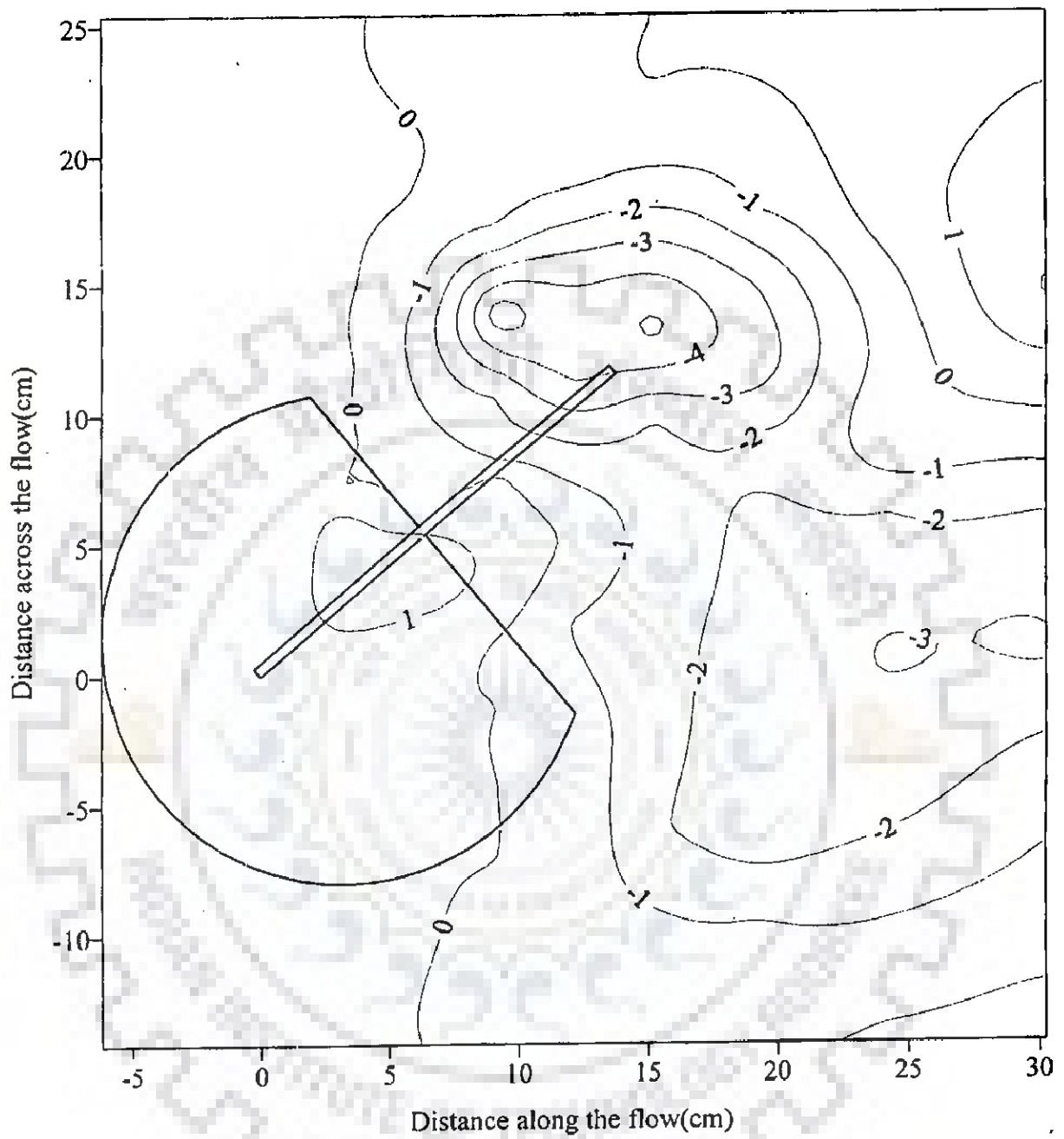


Fig. 5.36 Scour pattern for rectangular vane with collar AF2.12
($F_r = 0.25$, $d_{50} = 0.405$ mm, contour interval in cm)

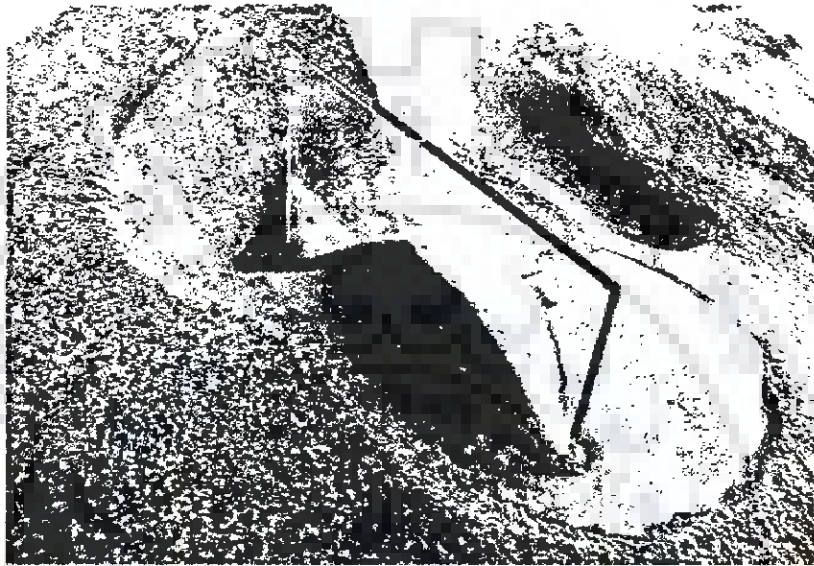


Plate 5.18 Scour pattern for rectangular vane with collar AF2.12
($F_r = 0.25$, $d_{50} = 0.405$ mm)

5.4.3.2 Trapezoidal vane (3H:2.5V)

Based on the above findings, only circular shapes of collars (Collar sizes BF2.1 to BF2.3, Figs. 5.37 to 5.39 and Plates 5.19 to 5.21) were tried for trapezoidal vane (3H:2.5V). From the Figs. 5.37 to 5.39 and Plates 5.19 to 5.21, it can be seen that any of the collar sizes from BF2.1 to BF2.3 was not found fit to be accepted as the most effective. The dimensions of the collar were again improved as the collar size BF2.4 (Fig. 5.40) and it was found more effective to some extent. It was found that collar size BF2.5 (Fig. 5.41 and Plate 5.22) is the most effective. It can be noted that AF2.12 and BF2.5 have the similar shapes and dimensions.



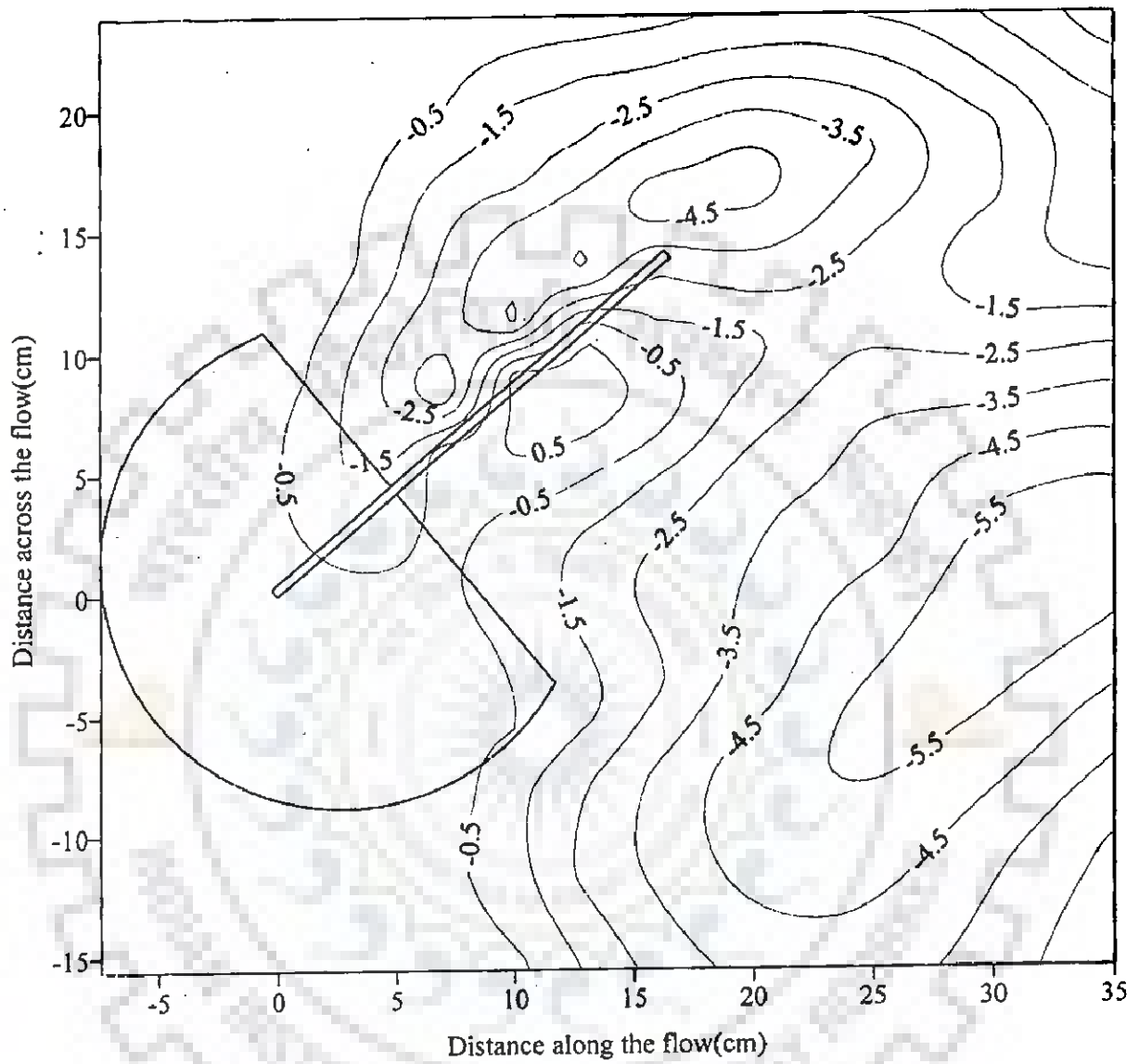
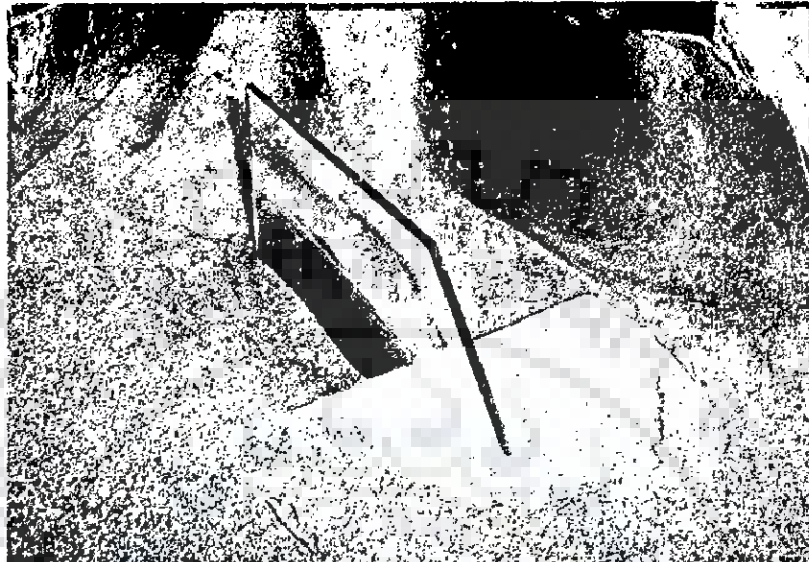
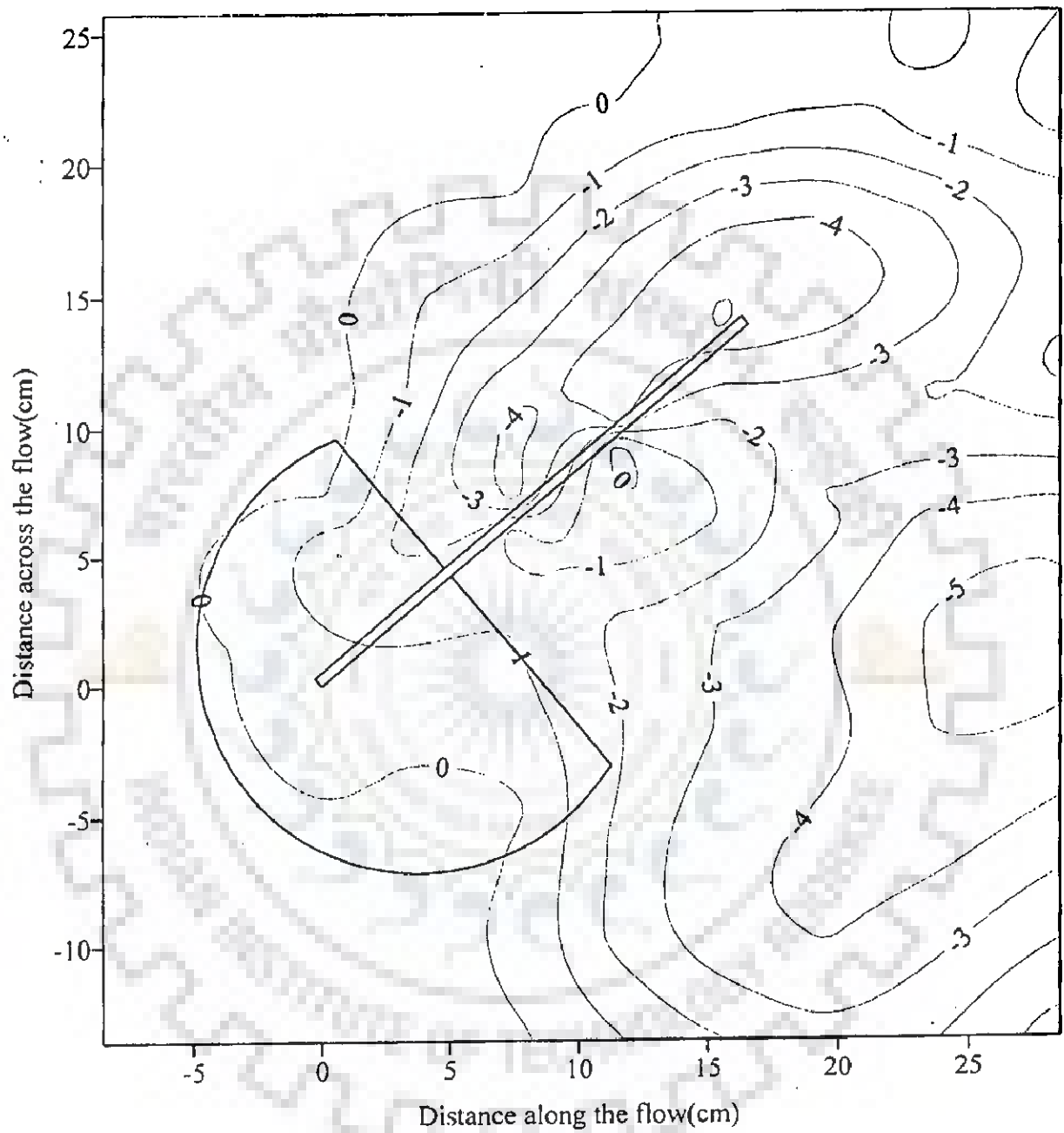


Fig. 5.37 Scour pattern for trapezoidal vane (3H:2.5V) with collar BF2.1
 ($F_r = 0.25$, $d_{50} = 0.405$ mm, contour interval in cm)



**Plate 5.19 Scour pattern for Trapezoidal vane (3H:2.5V) with collar BF2.1
($F_r = 0.25$, $d_{50} = 0.405$ mm)**



**Fig. 5.38 Scour pattern for trapezoidal vane (3H:2.5V) with collar BF2.2
($F_r = 0.25$, $d_{50} = 0.405$ mm, contour interval in cm)**

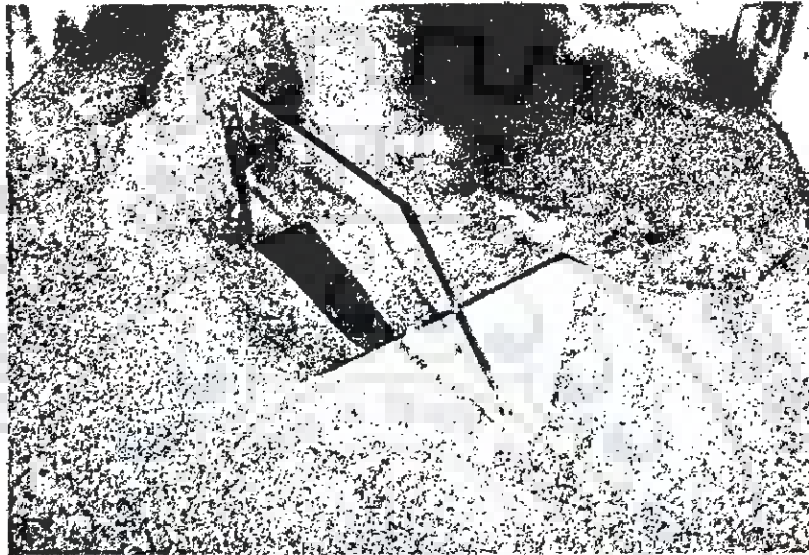


**Plate 5.20 Scour pattern for Trapezoidal vane (3H:2.5V) with collar BF2.2
($F_r = 0.25$, $d_{50} = 0.405$ mm)**

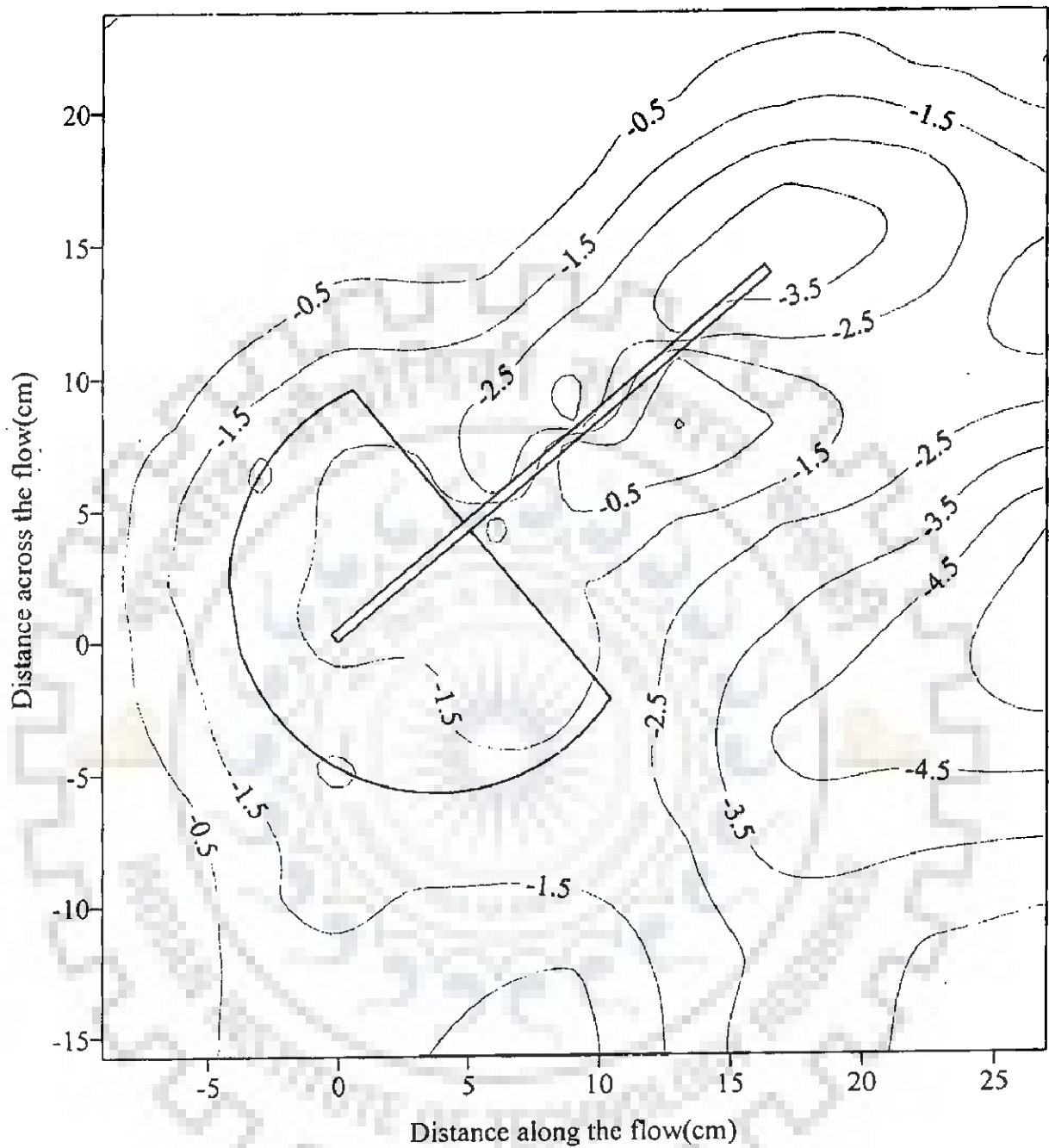
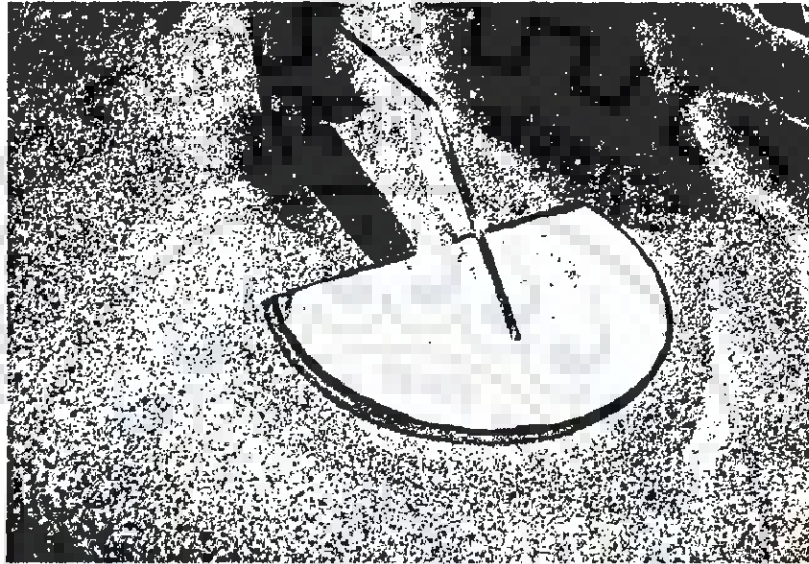
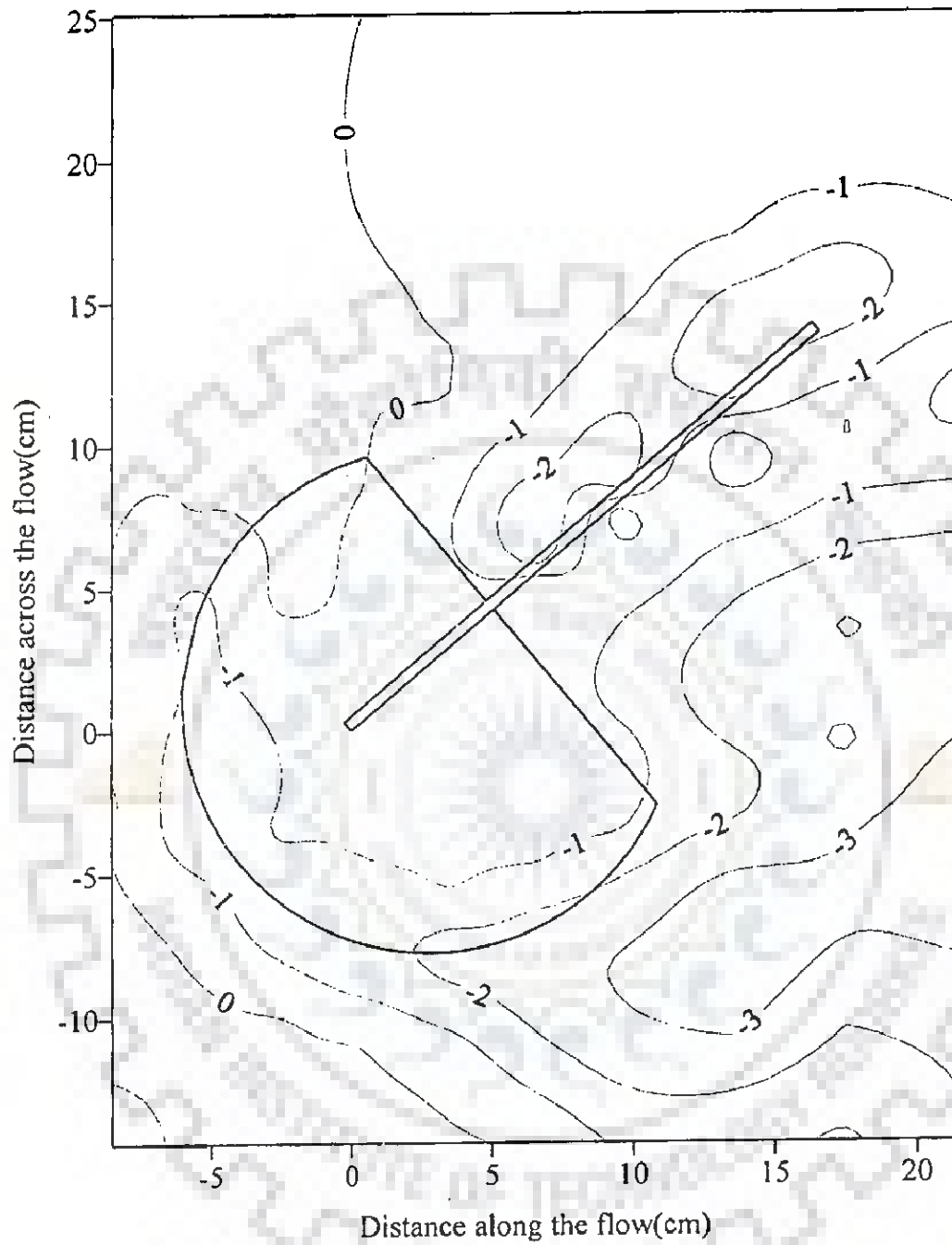


Fig. 5.39 Scour pattern for trapezoidal vane (3H:2.5V) with collar BF2.3
 ($F_r = 0.25$, $d_{50} = 0.405$ mm, contour interval in cm)



**Plate 5.21 Scour pattern for trapezoidal vane (3H:2.5V) with collar BF2.3
($F_r = 0.25$, $d_{50} = 0.405$ mm)**



**Fig. 5.40 Scour pattern for trapezoidal vane (3H:2.5V) with collar BF2.4
($F_r = 0.25$, $d_{50} = 0.405$ mm, contour interval in cm)**

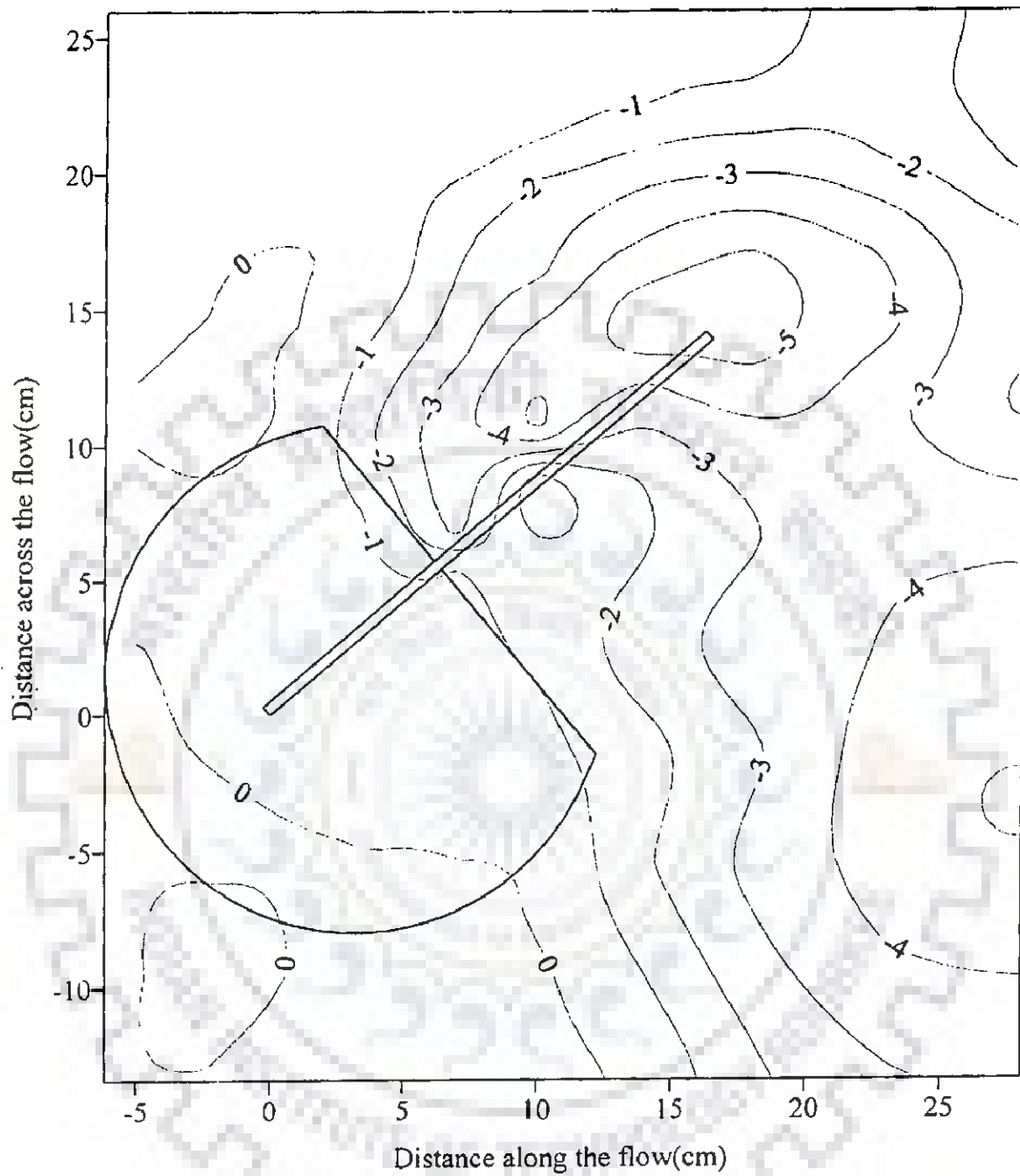


**Fig. 5.41 Scour pattern for trapezoidal vane (3H:2.5V) with collar BF2.5
 ($F_r = 0.25$, $d_{50} = 0.405$ mm, contour interval in cm)**

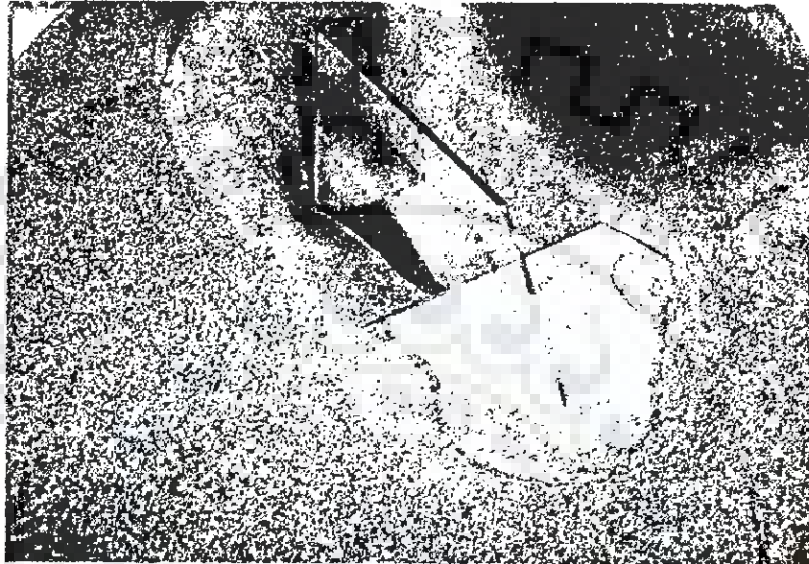


**Plate 5.22 Scour pattern for trapezoidal vane (3H:2.5V) with collar BF2.5
($F_r = 0.25$, $d_{50} = 0.405$ mm)**

5.4.4 Experiments at Froude Number 0.13 and d_{50} as 0.405 mm

5.4.4.1 Rectangular vane

The most effective collar size AF1.8 was also tested for rectangular vane at Froude number 0.13 with median size of sediment 0.405mm and was found most effective (Fig. 5.42 and Plate 5.23).

5.4.4.2 Trapezoidal vane (3H:2.5V)

From the Fig. 5.43 and Plate 5.24, it can be seen that collar size AF1.8 was most effective for trapezoidal vane (3H:2.5V) at Froude number 0.13 with median size of sediment 0.405 mm.



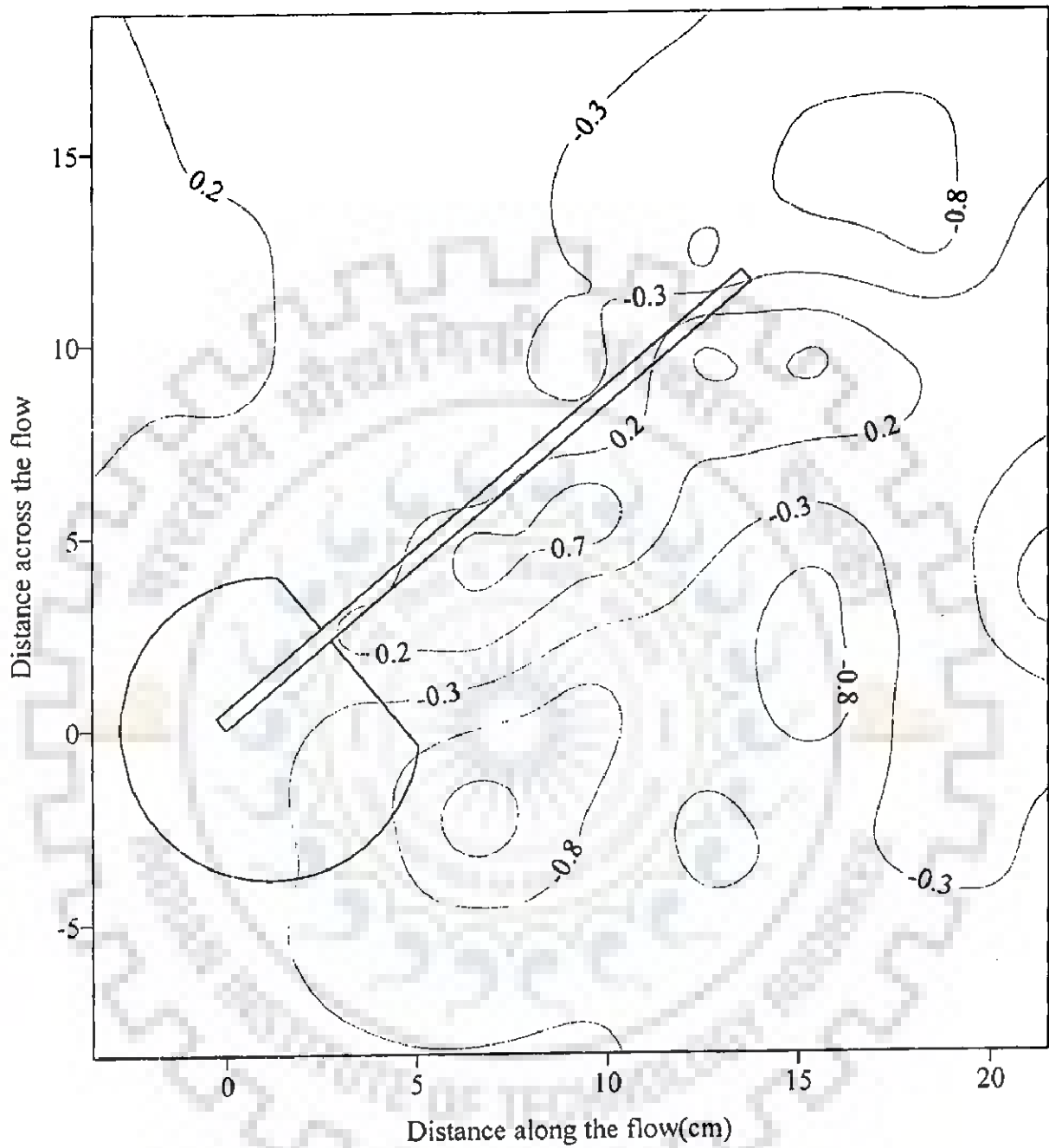
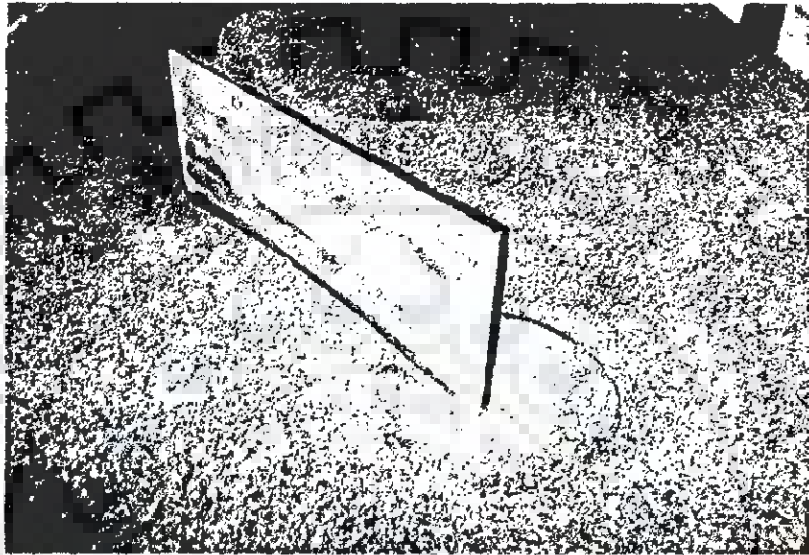


Fig. 5.42 Scour pattern for rectangular vane with collar AF1.8
 ($F_r = 0.13$, $d_{50} = 0.405$ mm, contour interval in cm)



**Plate 5.23 Scour pattern for rectangular vane with collar AF1.8
($F_r = 0.13$, $d_{50} = 0.405$ mm)**

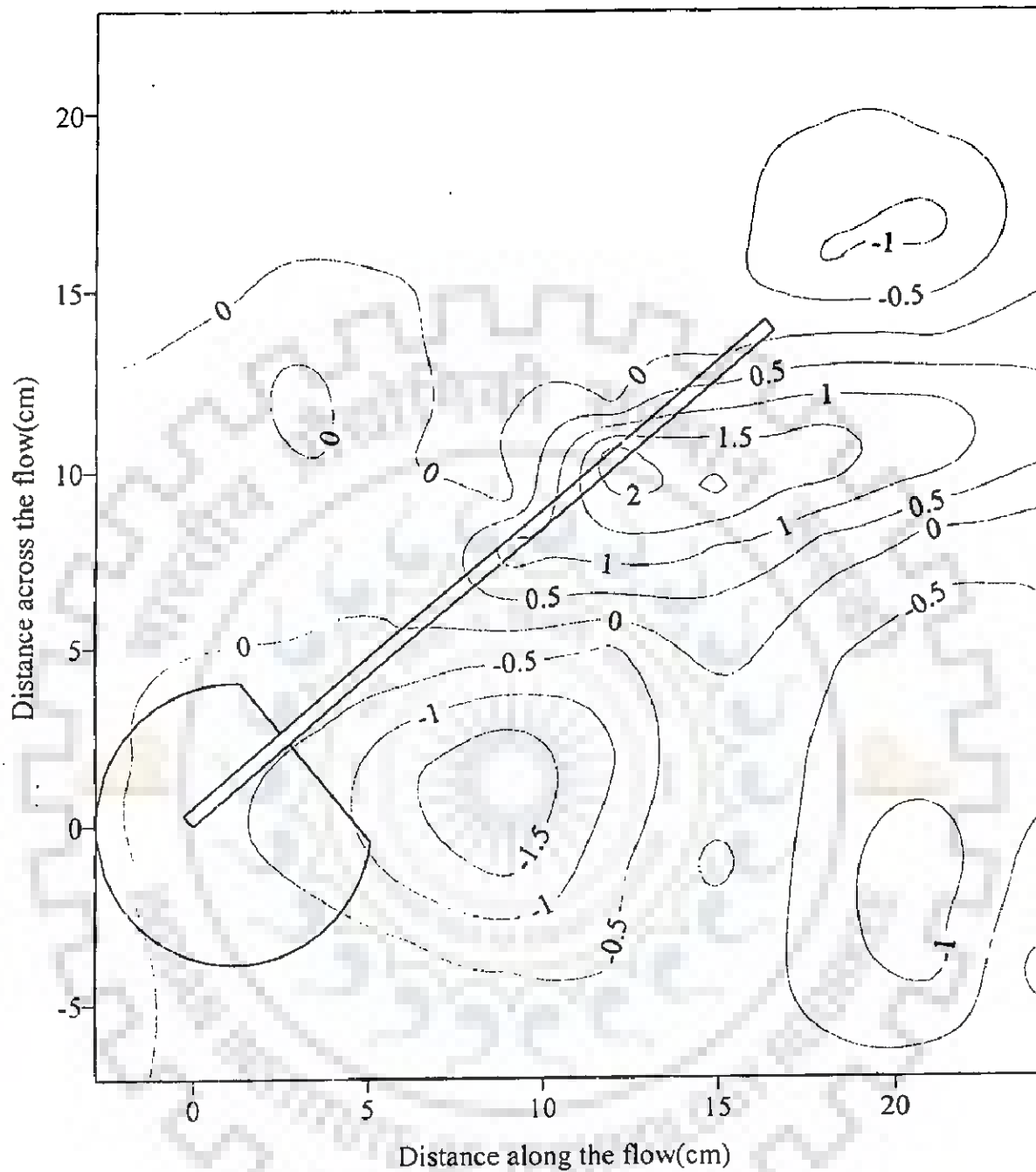
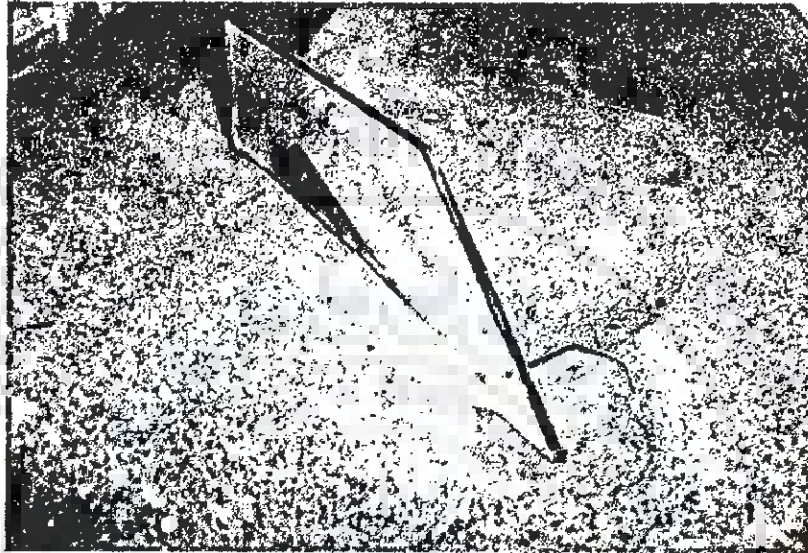


Fig. 5.43 Scour pattern for trapezoidal vane (3H:2.5V) with collar BF1.14
 ($F_r = 0.13$, $d_{50} = 0.405$ mm, contour interval in cm)



**Plate 5.24 Scour pattern for trapezoidal vane (3H:2.5V) with collar BF1.14
($F_r = 0.13$, $d_{50} = 0.405$ mm)**

5.5 RESULTS

Noncircular collar size AF1.7 (Fig. 5.7 and Plate 5.1) and collar size BF1.13 (Fig. 5.21 and Plate 5.3) was found most effective for rectangular vane and trapezoidal vane (3H:2.5V) respectively at Froude number 0.13 with median size of sediment 0.225mm. The circular shape of collar was found most effective for rectangular vane and trapezoidal vane (3H:2.5V) at Froude number 0.25 with median size of sediment 0.405mm. Therefore, circular shape of collar was again tried for rectangular and trapezoidal vane (3H:2.5V) at Froude number 0.13 with median size of sediment 0.225mm and it was found that circular collar size AF1.8 and BF1.14 are most effective for rectangular and trapezoidal vane (3H:2.5V) respectively at Froude number 0.13 with median size of sediment either 0.225mm or 0.405mm. It can be noted that AF1.8 and BF1.14 have same dimensions. Collar size AF2.12 and BF2.5 are most effective for rectangular and trapezoidal vane (3H:2.5V) respectively at Froude number 0.25 with median size of sediment either 0.225mm or 0.405mm. Collar size AF2.12 and BF2.5 have the similar dimensions. Collar size BF1.8 and BF2.5 are also most effective for trapezoidal vanes with taper angles 1H:1V and 4H:2V at Froude numbers 0.13 and 0.25 respectively with both types of sediment 0.225mm and 0.405mm. Summary of the most effective collars for different cases considered has been presented in Table 5.2.

Table 5.2: Summary of most effective collars

Case	Fr.	Vane type	Collar shape	d_{50} (mm)	Collar size
1	0.13	Rectangular	Noncircular	0.225	AF1.7
2	0.13	Rectangular	Circular	0.225	AF1.8
3	0.13	Rectangular	Circular	0.405	AF1.8
4	0.13	Trapezoidal (3H;2.5V)	Noncircular	0.225	BF1.13
5	0.13	Trapezoidal (3H;2.5V)	Circular	0.225	BF1.14
6	0.13	Trapezoidal (3H;2.5V)	Circular	0.405	BF1.14
7	0.25	Rectangular	Circular	0.225	AF2.12
8	0.25	Rectangular	Circular	0.405	AF2.12
9	0.25	Trapezoidal (3H;2.5V)	Circular	0.225	BF2.5
10	0.25	Trapezoidal (3H;2.5V)	Circular	0.405	BF2.5
11	0.25	Trapezoidal (1H;1V)	Circular	0.225	BF2.5
12	0.25	Trapezoidal (1H;1V)	Circular	0.405	BF2.5
13	0.25	Trapezoidal (4H;2V)	Circular	0.225	BF2.5
14	0.25	Trapezoidal (4H;2V)	Circular	0.405	BF2.5

5.6 PROTOTYPE FIELD STUDY

It was observed that the variation of Froude number in the prototype field test area of the Solani river near Roorkee was in the range of 0.05 to 0.1 and the median size of sediment in the river was 0.200 mm (Chapter 3). Therefore, it was decided to conduct test on the collar size that was found to be the most effective amongst all at the Froude number 0.13 and sediment size 0.225 mm in the laboratory flume. The dimensions of the most effective size of collar can be represented in terms of either H or d where H is the vane height and d is the flow depth. First the dimensions of collar have been provided in terms of H . The location of collar was fixed at $0.05H$ below the bed level of river. The variation of water depth was found between 80cm and 120cm. Therefore, the height of the trapezoidal vane ($3H:2.5V$) was taken as 40cm to get minimum degree of submergence of 0.50 at minimum depth of flow of 80 cm. Two numbers of trapezoidal vanes, one with most effective collar size BF1.13 and the other without collar was installed in the prototype test area of Solani river. The aspect ratio of the prototype trapezoidal vane was 0.33, which is similar to that of the models used in laboratory experiments. The installation depth of vane was provided as 40cm and two pipes were driven into the river bed to support the submerged vane as already described earlier in Chapter 3. Before and after the flood, the magnitude of scour depth near the leading edge of both the vanes was measured by using dumpy level. The measurements of discharge and scour were made in the Solani river as already described in Chapter 3. Plates 5.25 to 5.34 show the different photographs relating to field trials. From the prototype field study, it was found that the performance of collar size BF1.13 was very effective compared to that of the vane without collar.

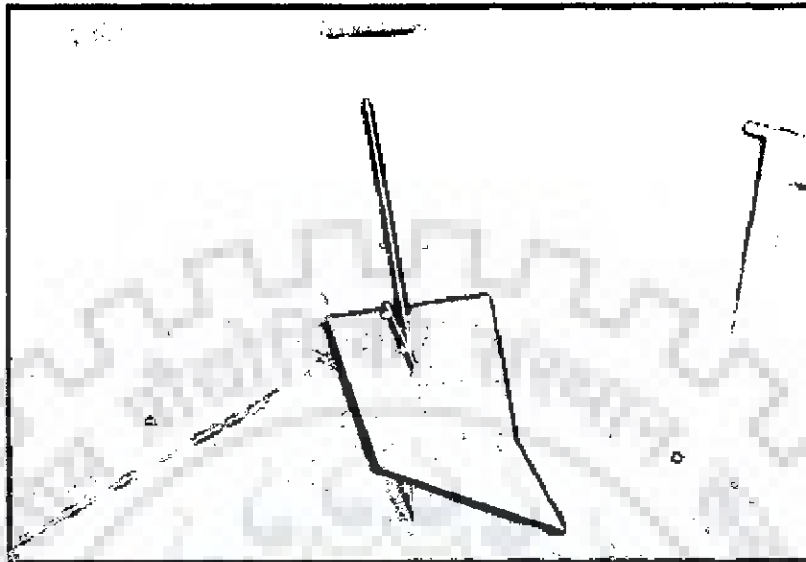


Plate 5.25 Trapezoidal vane with collar before installation in Solani river

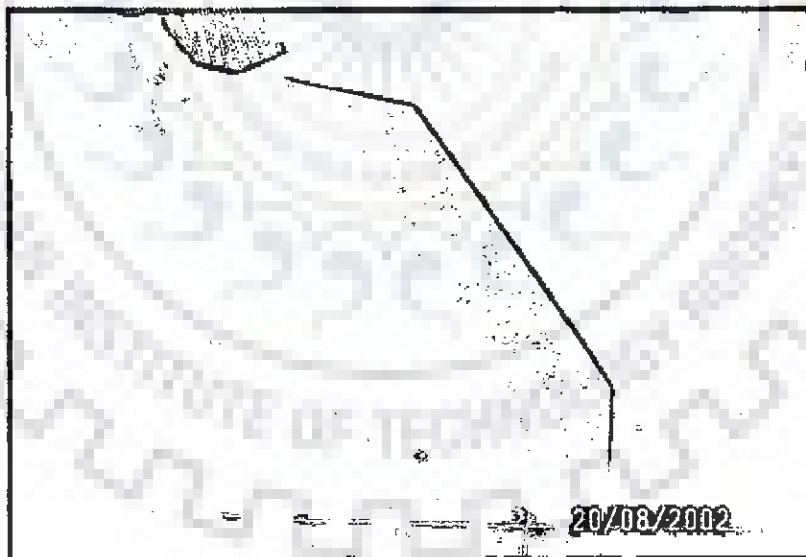


Plate 5.26 Trapezoidal vane without collar before installation in Solani river



Plate 5.27 Augured end of pipe to facilitate driving in Solani river



Plate 5.28 Pipe is being driven in Solani river to support the vanes



Plate 5.29 Trapezoidal vane with collar in the process of installation in Solani river



Plate 5.30 Bed profile in the vicinity of vane is being measured by dumpy level in Solani River



Plate 5.31 Trapezoidal vanes with and without collar installed in Solani river



Plate 5.32 Availability of water in Solani river on the day vanes installed



Plate 5.33 Vanes are fully submerged during the flood in Solani river

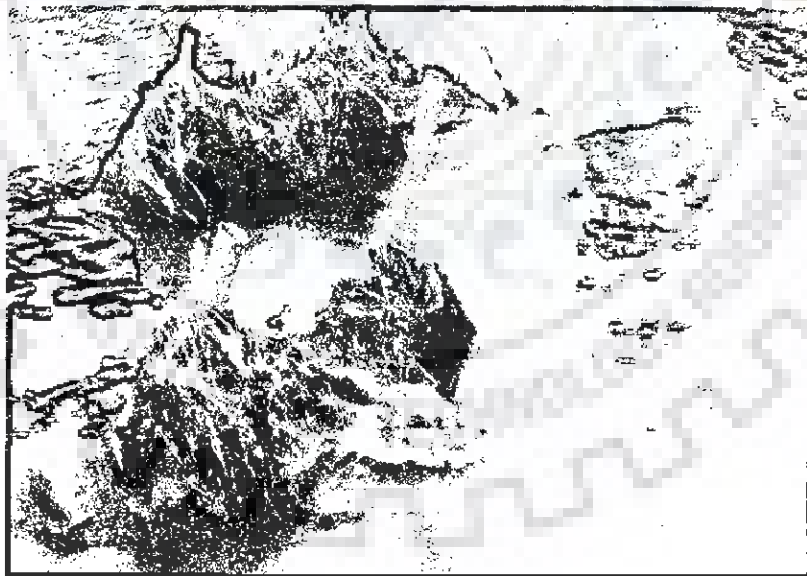


Plate 5.34 Sediment deposited on vanes after flood in Solani river

Therefore, it becomes apparent that height of the vane works out as an important parameter in fixing the collar size. The prevailing flows in the Solani river during the floods of 2002 provided permit study practically for one Froude number only, therefore; the dimensions of only one collar could possibly be tested in the prototype.

5.7 SUMMARY

In this chapter, the results obtained from laboratory and field experiments in respect of submerged vanes with collar have been presented for two conditions of Froude numbers, two sediment sizes and two types of vanes, viz rectangular and trapezoidal. In addition, two types of collar shapes namely circular and noncircular have been also explored to obtain the most effective size and shape of collar. Considering the fact that to date no information is available on shape and size of collars for submerged vanes, the present results provide positively certain basis for further improvements in the collar shape and its dimensions.

VARIATION OF STRENGTH OF VORTEX

6.1 GENERAL

Reduction of local scour at the leading edge of submerged vanes also depends upon the shape of submerged vanes. Thus, it was intended to identify the optimal angle of attack for different shapes of vane in respect of reduction of local scour. For identical hydraulic conditions, all these vanes were tested for different angles of attack such as 30° , 35° , 40° , 45° and 50° . Strength of vortex was measured as per Marelius and Sinha's (1998) approach. Strength of vortices has been calculated in terms of moment of momentum.

6.2 ASSESSMENT OF STRENGTH OF VORTEX

For this purpose, $3\text{cm} \times 3\text{cm}$ grids across the flume have been taken at the distance of 15 cm downstream from the centre of the vanes. At each grid points all the components of velocity were measured using ADV (Acoustic Doppler Velocimeter). The velocity at each grid point is the representative velocity of the grid area $3\text{cm} \times 3\text{cm}$. Fig. 6.1 shows the layout of grids in flow area cross-section. Velocity near the wall of the flume was not considered for the calculation of strength of vortex in order to neglect the wall effect on the generation of secondary flow due to the submerged vanes. Centre of vortex was observed at $z=0.9H$. The origin was taken at the mid of the average vane length at initial bed level in this chapter. For a mass m concentrated at point A (Fig. 6.2), one can write the following expression for moment of momentum, MOM_A .

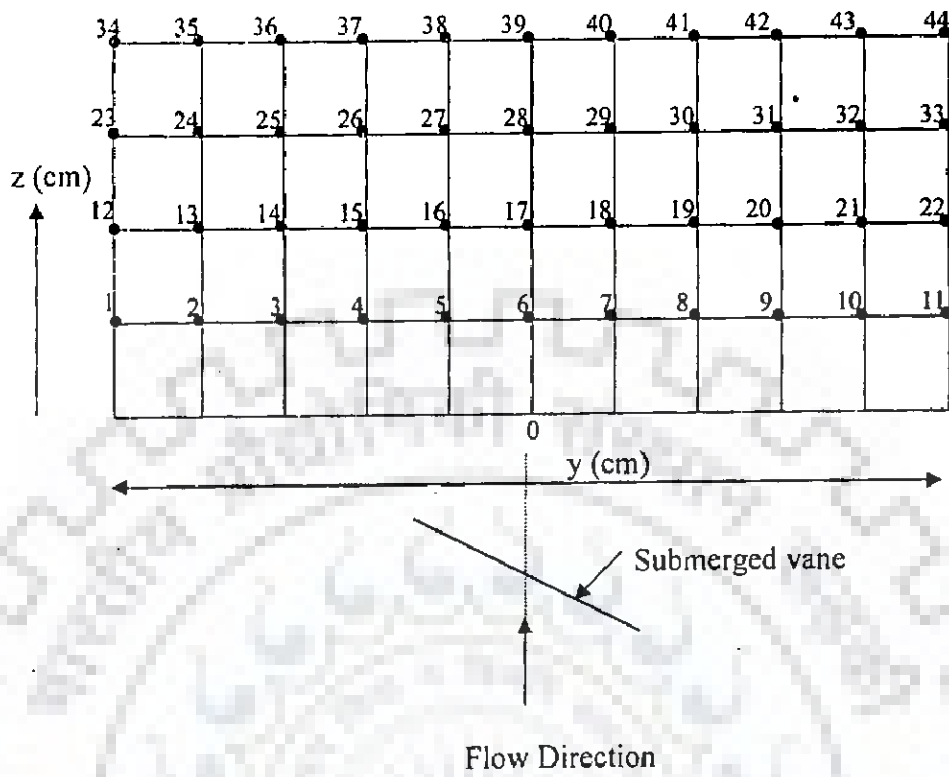


Fig. 6.1 Grid points for the collection of data

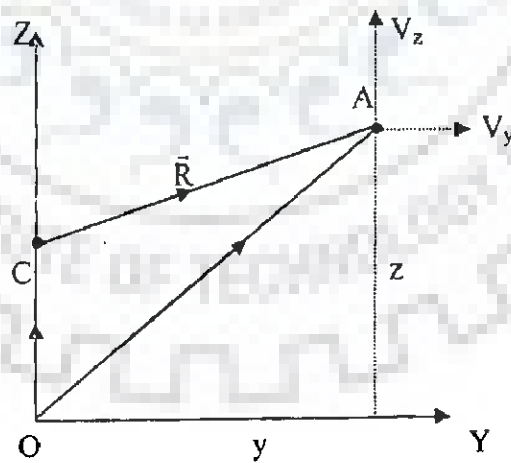


Fig. 6.2 Definition sketch for velocity vectors

$$\text{MOM}_A = (\text{mass}) (\vec{R} \times \vec{V}) \quad (6.1)$$

In eq. (6.1), \vec{R} represents the location vector of point A with respect to centre of vortex C and is given as $C\vec{A}$

The location vector of point A with respect to origin O is given as $O\vec{A}$,
where,

$$O\vec{A} = y\vec{j} + z\vec{k} \quad (6.2)$$

In eq. 6.2, y and z are coordinates of grid points and \vec{j} and \vec{k} are unit vectors along Y and Z directions, respectively. With the centre of vortex at C, one can write

$$O\vec{C} = 0.9H \vec{k} \quad (6.3)$$

where, H = Height of vane and C = Centre of vortex

From eqs. (6.2) and (6.3), location vector of point A with respect to point C, can be written as

$$\begin{aligned} \vec{R} &= O\vec{A} - O\vec{C} \\ &= y\vec{j} + z\vec{k} - 0.9H\vec{k} \\ &= y\vec{j} + (z - 0.9H)\vec{k} \end{aligned} \quad (6.4)$$

Thus, MOM of mass m at point A with respect to centre of vortex C, can be expressed as

$$\begin{aligned} \text{MOM}_A &= m \left\{ \left[y\vec{j} + (z - 0.9H)\vec{k} \right] \times \left(V_y\vec{j} + V_z\vec{k} \right) \right\} \\ &= m \vec{i} [y V_z - (z - 0.9H) V_y] \\ &= m \vec{i} [y V_z + \{-(z - 0.9H)\} V_y] \end{aligned} \quad (6.5)$$

In eq. (6.5), \vec{i} indicates the direction of MOM along the direction of flow of fluid (here water). In eq. 6.5, $(m y V_z)$ is MOM due to vertical velocity and $\{-m (Z-0.9H) V_y\}$ is MOM due to transverse velocity.

For grid area of 3 cm × 3cm and 1 cm length of flume with ρ as 1 gm/cm³, mass m can be computed as

$$m = 1 \times 3 \times 3 \times 1 = 9 \text{ gm} \quad (6.6)$$

Using eqs. (6.5) and (6.6), one can write

$$\text{MOM}_A \text{ as } = 9 \bar{i} [y \sqrt{z} + \{-(z - 0.9H)\} \sqrt{y}] \quad (6.7)$$

Thus, total MOM can be expressed as

$$\text{Total MOM} = \sum_{i=1}^{44} \text{MOM}_i \quad (6.8)$$

In Table 6.1, MOM at different grid points has been presented.

6.3 OPTIMAL ANGLE OF ATTACK

6.3.1 Rectangular Vanes

T/d ratios used by different investigators have been presented in Chapter 2. While planning the experiments on rectangular vanes there were two main considerations. The first one was the influence of angle of attack and the second consideration was related to T/d ratio and its likely influence on variability of MOM.

For this reason, a set of fifteen experiments covering five values of angle of attack ranging from 30° to 50° and three values of T/d ratio ranging from 0.6 to 0.75 were considered.

For each value of T/d ratio, the variation of MOM with respect to angle of attack is shown in the Figs. 6.3 to 6.6. It can be seen from these Figs. that MOM initially increases with angle of attack, reaches a certain maximum value and after that it declines.

Although the angle of attack at which the MOM is close to the optimum can be very well judged from these Figs. and happens to be close to 40° , it is considered desirable to obtain the value of optimum angle of attack using calibrated best fit curve within the range of angle of attack between 35° to 45° . With reference to Fig. 6.3, the equation of calibrated curve is obtained as

$$\text{MOM} = -0.074\alpha^2 + 5.8619\alpha - 109.89, R^2 = 1.0 \quad (6.9)$$

Table 6.1: Moment of momentum at different nodes

Grid points	Coordinates		Velocity		Moment of Momentum
	Symbols	Values	Vy	Vz	
1	Y_1, Z_1	2.5H, 0.5H	V_{y1}	V_{z1}	$9H[2.5V_{z1} + 0.4V_{y1}]$
2	Y_2, Z_2	2H, 0.5H	V_{y2}	V_{z2}	$9H[2V_{z2} + 0.4V_{y2}]$
3	Y_3, Z_3	1.5H, 0.5H	V_{y3}	V_{z3}	$9H[1.5V_{z3} + 0.4V_{y3}]$
4	Y_4, Z_4	1H, 0.5H	V_{y4}	V_{z4}	$9H[1V_{z4} + 0.4V_{y4}]$
5	Y_5, Z_5	0.5H, 0.5H	V_{y5}	V_{z5}	$9H[0.5V_{z5} + 0.4V_{y5}]$
6	Y_6, Z_6	0H, 0.5H	V_{y6}	V_{z6}	$9H[0V_{z6} + 0.4V_{y6}]$
7	Y_7, Z_7	-0.5H, 0.5H	V_{y7}	V_{z7}	$9H[-0.5V_{z7} + 0.4V_{y7}]$
8	Y_8, Z_8	-1H, 0.5H	V_{y8}	V_{z8}	$9H[-1V_{z8} + 0.4V_{y8}]$
9	Y_9, Z_9	-1.5H, 0.5H	V_{y9}	V_{z9}	$9H[-1.5V_{z9} + 0.4V_{y9}]$
10	Y_{10}, Z_{10}	-2H, 0.5H	V_{y10}	V_{z10}	$9H[-2V_{z10} + 0.4V_{y10}]$
11	Y_{11}, Z_{11}	-2.5H, 0.5H	V_{y11}	V_{z11}	$9H[-2.5V_{z11} + 0.4V_{y11}]$
12	Y_{12}, Z_{12}	2.5H, 1H	V_{y12}	V_{z12}	$9H[2.5V_{z12} + (-0.1)V_{y12}]$
13	Y_{13}, Z_{13}	2H, 1H	V_{y13}	V_{z13}	$9H[2V_{z13} + (-0.1)V_{y13}]$
14	Y_{14}, Z_{14}	1.5H, 1H	V_{y14}	V_{z14}	$9H[1.5V_{z14} + (-0.1)V_{y14}]$
15	Y_{15}, Z_{15}	1H, 1H	V_{y15}	V_{z15}	$9H[1V_{z15} + (-0.1)V_{y15}]$
16	Y_{16}, Z_{16}	0.5H, 1H	V_{y16}	V_{z16}	$9H[0.5V_{z16} + (-0.1)V_{y16}]$
17	Y_{17}, Z_{17}	0H, 1H	V_{y17}	V_{z17}	$9H[0V_{z17} + (-0.1)V_{y17}]$
18	Y_{18}, Z_{18}	-0.5H, 1H	V_{y18}	V_{z18}	$9H[-0.5V_{z18} + (-0.1)V_{y18}]$
19	Y_{19}, Z_{19}	-1H, 1H	V_{y19}	V_{z19}	$9H[-1V_{z19} + (-0.1)V_{y19}]$
20	Y_{20}, Z_{20}	-1.5H, 1H	V_{y20}	V_{z20}	$9H[-1.5V_{z20} + (-0.1)V_{y20}]$
21	Y_{21}, Z_{21}	-2H, 1H	V_{y21}	V_{z21}	$9H[-2V_{z21} + (-0.1)V_{y21}]$
22	Y_{22}, Z_{22}	-2.5H, 1H	V_{y22}	V_{z22}	$9H[-2.5V_{z22} + (-0.1)V_{y22}]$
23	Y_{23}, Z_{23}	2.5H, 1.5H	V_{y23}	V_{z23}	$9H[2.5V_{z23} + (-0.6)V_{y23}]$
24	Y_{24}, Z_{24}	2H, 1.5H	V_{y24}	V_{z24}	$9H[2V_{z24} + (-0.6)V_{y24}]$
25	Y_{25}, Z_{25}	1.5H, 1.5H	V_{y25}	V_{z25}	$9H[1.5V_{z25} + (-0.6)V_{y25}]$
26	Y_{26}, Z_{26}	1H, 1.5H	V_{y26}	V_{z26}	$9H[1V_{z26} + (-0.6)V_{y26}]$
27	Y_{27}, Z_{27}	0.5H, 1.5H	V_{y27}	V_{z27}	$9H[0.5V_{z27} + (-0.6)V_{y27}]$
28	Y_{28}, Z_{28}	0H, 1.5H	V_{y28}	V_{z28}	$9H[0V_{z28} + (-0.6)V_{y28}]$
29	Y_{29}, Z_{29}	-0.5H, 1.5H	V_{y29}	V_{z29}	$9H[-0.5V_{z29} + (-0.6)V_{y29}]$
30	Y_{30}, Z_{30}	-1H, 1.5H	V_{y30}	V_{z30}	$9H[-1V_{z30} + (-0.6)V_{y30}]$
31	Y_{31}, Z_{31}	-1.5H, 1.5H	V_{y31}	V_{z31}	$9H[-1.5V_{z31} + (-0.6)V_{y31}]$
32	Y_{32}, Z_{32}	-2H, 1.5H	V_{y32}	V_{z32}	$9H[-2V_{z32} + (-0.6)V_{y32}]$
33	Y_{33}, Z_{33}	-2.5H, 1.5H	V_{y33}	V_{z33}	$9H[-2.5V_{z33} + (-0.6)V_{y33}]$
34	Y_{34}, Z_{34}	2.5H, 2H	V_{y34}	V_{z34}	$9H[2.5V_{z34} + (-1.1)V_{y34}]$
35	Y_{35}, Z_{35}	2H, 2H	V_{y35}	V_{z35}	$9H[2V_{z35} + (-1.1)V_{y35}]$
36	Y_{36}, Z_{36}	1.5H, 2H	V_{y36}	V_{z36}	$9H[1.5V_{z36} + (-1.1)V_{y36}]$
37	Y_{37}, Z_{37}	1H, 2H	V_{y37}	V_{z37}	$9H[1V_{z37} + (-1.1)V_{y37}]$
38	Y_{38}, Z_{38}	0.5H, 2H	V_{y38}	V_{z38}	$9H[0.5V_{z38} + (-1.1)V_{y38}]$
39	Y_{39}, Z_{39}	0H, 2H	V_{y39}	V_{z39}	$9H[0V_{z39} + (-1.1)V_{y39}]$
40	Y_{40}, Z_{40}	-0.5H, 2H	V_{y40}	V_{z40}	$9H[-0.5V_{z40} + (-1.1)V_{y40}]$
41	Y_{41}, Z_{41}	-1H, 2H	V_{y41}	V_{z41}	$9H[-1V_{z41} + (-1.1)V_{y41}]$
42	Y_{42}, Z_{42}	-1.5H, 2H	V_{y42}	V_{z42}	$9H[-1.5V_{z42} + (-1.1)V_{y42}]$
43	Y_{43}, Z_{43}	-2H, 2H	V_{y43}	V_{z43}	$9H[-2V_{z43} + (-1.1)V_{y43}]$
44	Y_{44}, Z_{44}	-2.5H, 2H	V_{y44}	V_{z44}	$9H[-2.5V_{z44} + (-1.1)V_{y44}]$

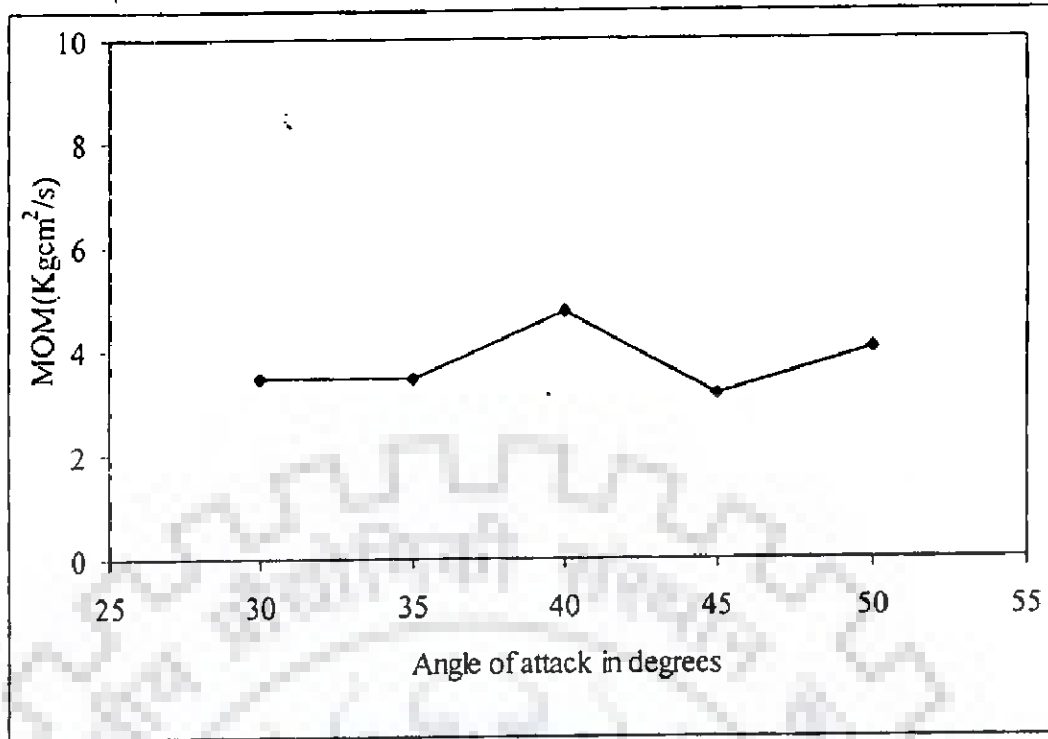


Fig. 6.3 Optimal angle of attack for rectangular vane ($T/d = 0.60$)

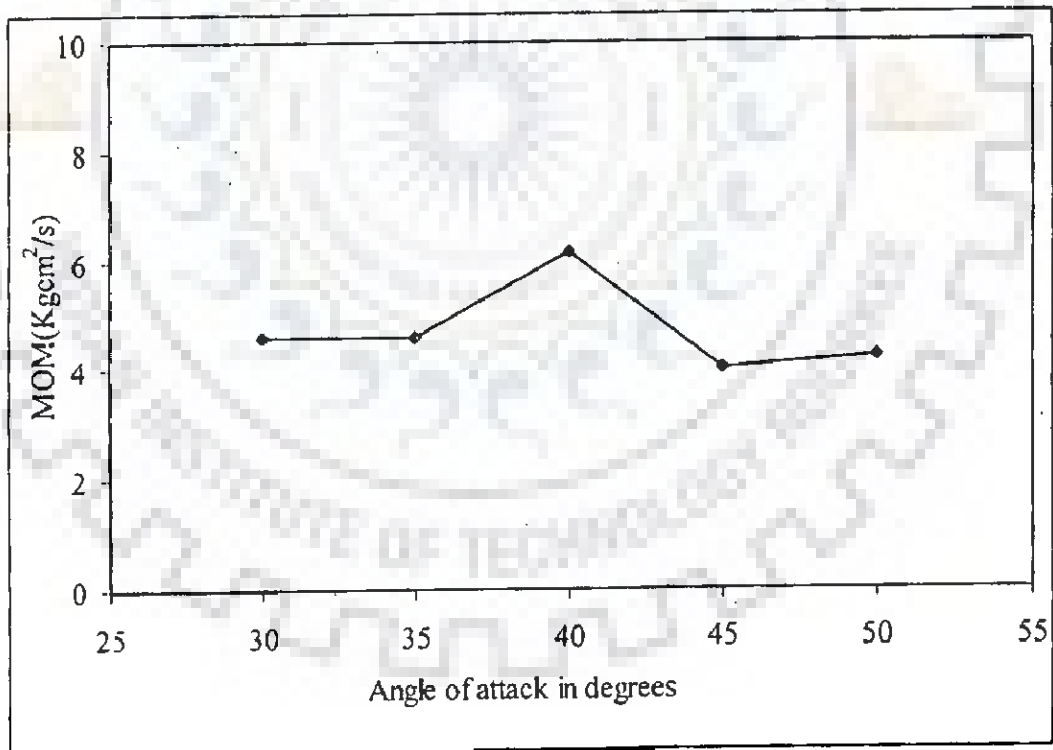


Fig. 6.4 Optimal angle of attack for rectangular vane ($T/d = 0.67$)

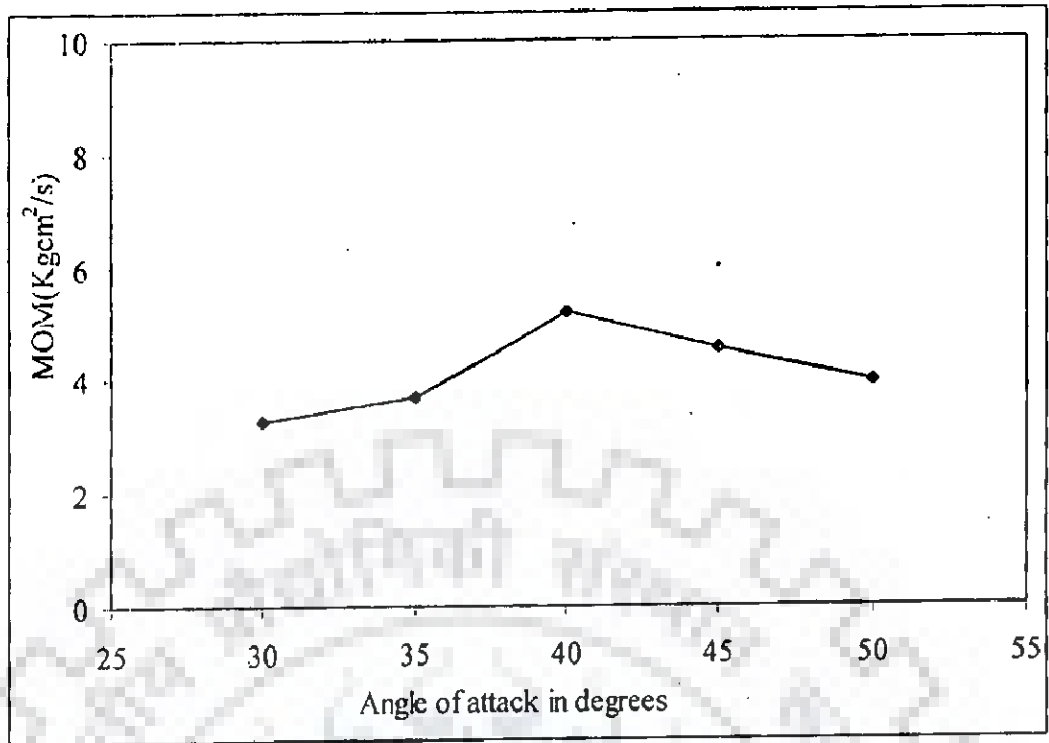


Fig. 6.5 Optimal angle of attack for rectangular vane ($T/d = 0.75$)

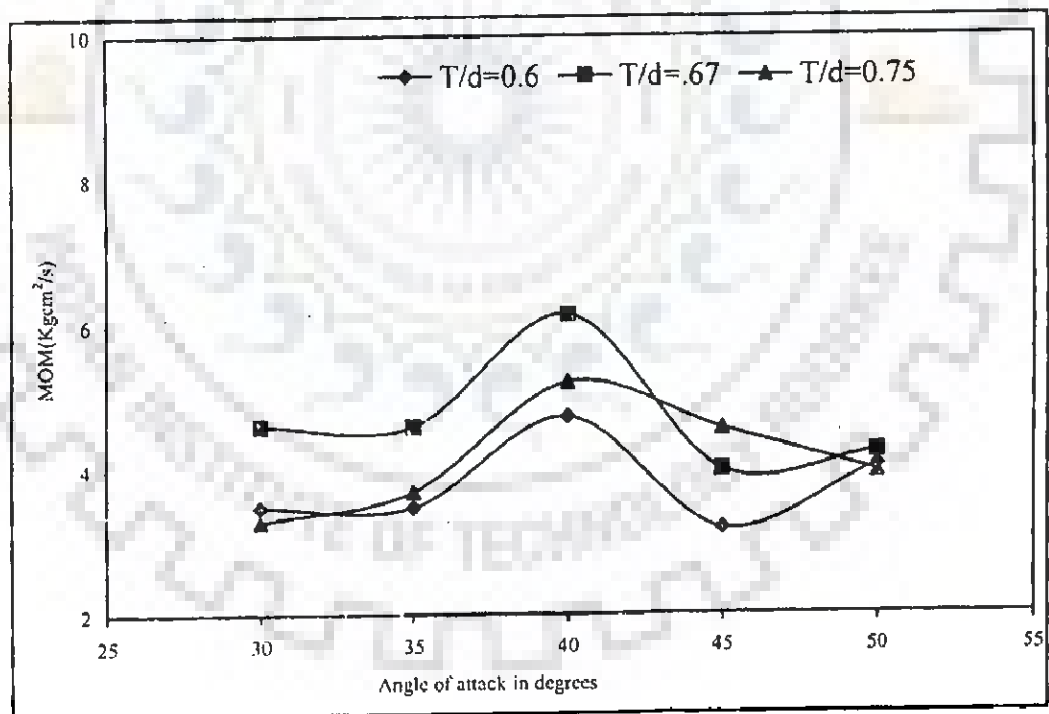


Fig. 6.6 Optimal angle of attack for rectangular vane at different T/d

Similar equations have been obtained in case of Fig. 6.4 and 6.5. For Fig. 6.4, the calibrated equation is

$$\text{MOM} = -0.043\alpha^2 + 3.531\alpha - 67.166, R^2 = 1.0 \quad (6.10)$$

Similarly, for Fig 6.5, the calibrated equation is

$$\text{MOM} = -0.0562\alpha^2 + 4.4632\alpha - 83.936, R^2 = 1.0 \quad (6.11)$$

Using equation 6.9, the optimum angle of attack can be obtained by using the following condition

$$\frac{\partial(\text{MOM})}{\partial\alpha} = 0 \quad (6.12)$$

and

$$\frac{\partial^2(\text{MOM})}{\partial\alpha^2} = (-) \text{ ve} \quad (6.13)$$

Using eqs. (6.12) and (6.13) in case of eqs. (6.9), (6.10) and (6.11), yields the optimum angle of attack for different values of T/d, as given in Table 6.2. It can be seen from this Table that optimum angle does not appear sensitive to T/d values.

Table 6.2: Computation of optimal α for rectangular vane

Figs.	MOM	$\frac{d(\text{MOM})}{d\alpha}$	$\frac{d^2(\text{MOM})}{d\alpha^2}$	α	T/d
6.3	$-0.074\alpha^2 + 5.8619\alpha - 109.89$	$-0.148\alpha + 5.8619$	-0.148	39.6	0.60
6.4	$-0.043\alpha^2 + 3.531\alpha - 67.166$	$-0.086\alpha + 3.531$	-0.086	41.06	0.67
6.5	$-0.0562\alpha^2 + 4.4632\alpha - 83.936$	$-0.1124\alpha + 4.4632$	-0.1124	39.71	0.75

6.3.1.1 Dimensional Considerations

One can see from Figs. 6.3 to 6.5 that MOM is a dimensional quantity whereas α and T/d are dimensionless quantities. Thus, it was considered desirable to maintain consistency in terms of representing variations of dimensionless MOM with angle of

attack. MOM can be considered to depend on a wide range of variables, such as α , H , L , d , ρ_w , g , μ , t , vane shape etc. Thus, in a functional form, the dependence of MOM in terms of these variables can be written as follows.

$$\text{MOM} = f(\alpha, H, L, d, \rho_w, g, \mu, t, \text{vane shape}) \quad (6.14)$$

Using eq. 6.14 and Buckingham π theorem, a large number of dimensionless π terms can be evolved.

Basically, the development of secondary flows is also related to the linear momentum (LM). Thus, it was considered desirable to use this parameter as the basis for making MOM dimensionless. The following dimensionless groups were attempted as follows.

$$\pi_1 = \frac{\text{MOM}}{\text{LM} \times d} = \text{MOM}^* \quad (6.15)$$

$$\pi_2 = \frac{\text{MOM}}{\text{LM} \times H} = \text{MOM}^{**} \quad (6.16)$$

where, LM is given as $\text{LM} = \rho_w A U$

The variation of these dimensionless terms has been shown in the Figs. 6.7 and 6.8. An attempt was made to consider the variation of dimensionless moment of momentum as given by MOM^* vs angle of attack for different T/d ratio. Fig. 6.7 is one such typical plot, which further supports the view that optimum angle of attack is 40° and T/d also has a role to play in the magnitude of MOM. Of course, this influence does not seem to be proportional as the curves corresponding to T/d value of 0.67 and 0.75 are very close to each other.

For example, for a change in T/d values from 0.6 to 0.75 (nearly 25% variation), the optimum angle changes from 39.6° to 41.06° (< 5% variation). It must be noted at this point that the MOM can be sensitive to a variety of factors, such as the variations in the Froude numbers. In case of Figs. 6.3 to 6.5, every possible attempt was made to maintain

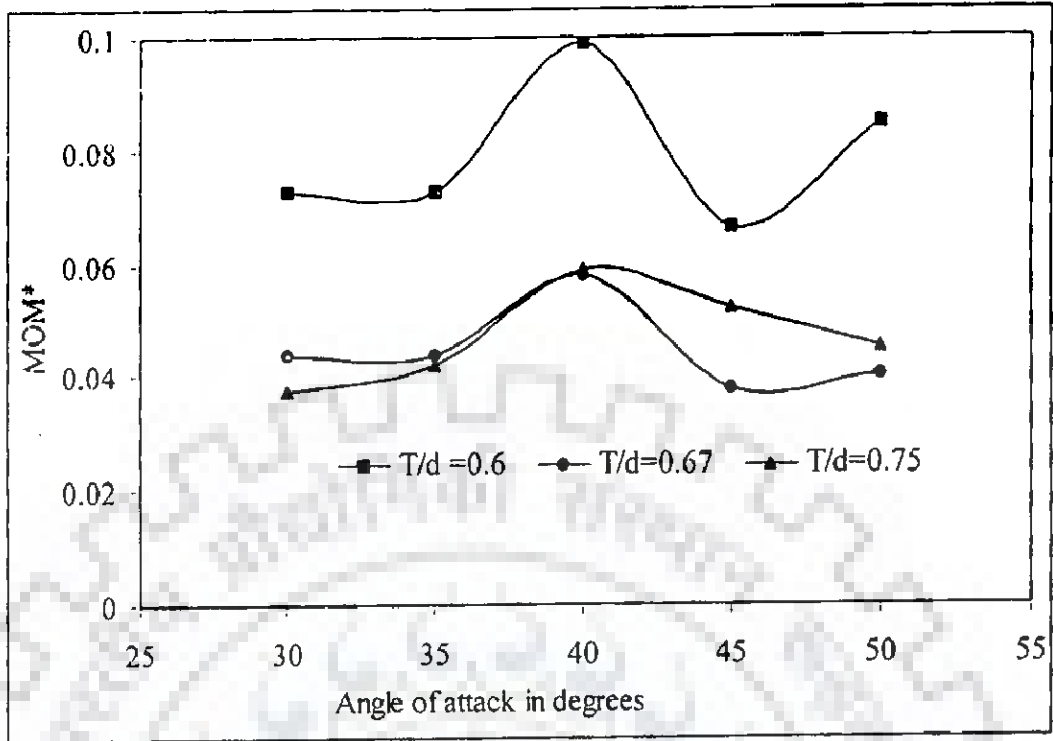


Fig 6.7 Comparison of MOM^* for rectangular vanes at different T/d

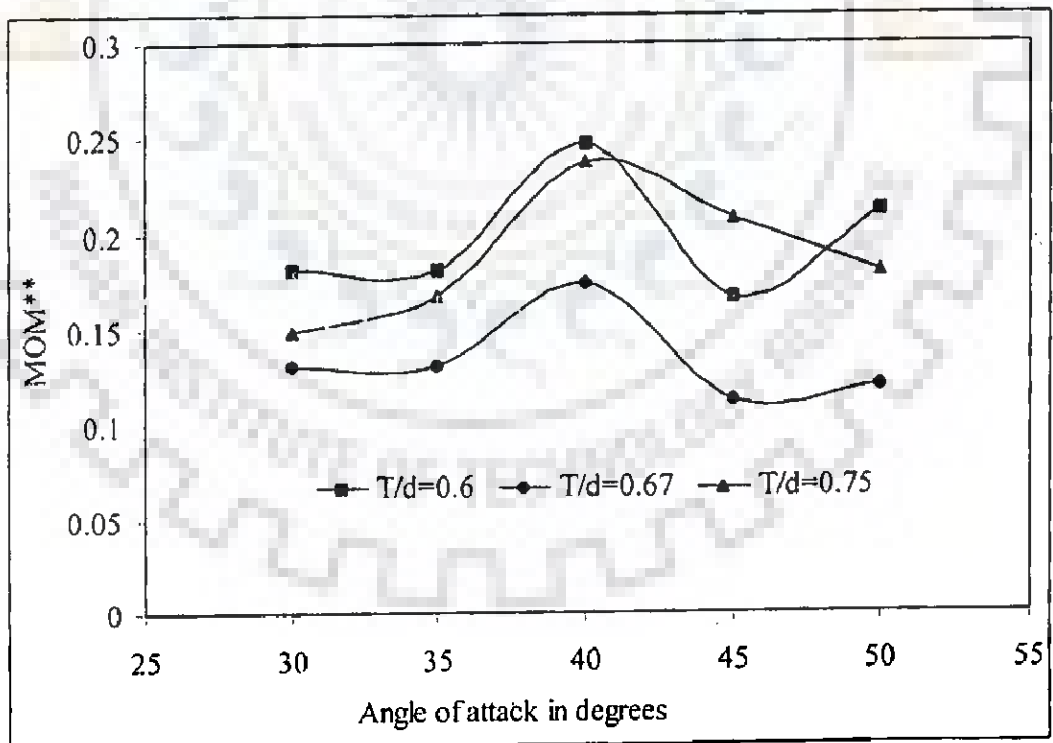


Fig 6.8 Comparison of MOM^{**} for rectangular vanes at different T/d

other experimental conditions same. However, the interesting fact is that in each of these figures, the variation of MOM follows nearly the similar trend of variability with angle of attack. It is pertinent to note that the optimum angle of attack with and without collars remains very close to each other. Thus introduction of collar, in no way reduces the strength of vortex and this is very important for advocating the use of submerged vanes with collar.

6.3.2 Vanes With Alternative Shapes

In Chapter 4, it has already been observed that vanes with alternative shapes, i.e. double curve type I, double curve type II, J1 and J2 are effective in reducing the scour around the submerged vanes to some extent. With this in view, experiments were undertaken to study the following two issues: the first was variability of MOM with angle of attack and the second was to assess how the MOM in case of different types of vanes varies with respect to MOM in case of rectangular vane. To meet these objectives, the results in respect of experiments having T/d as 0.67 are analysed and presented. From the Figs. 6.9 to 6.12, it can be seen that the optimum angle of attack for double curve type I, double curve type II, J1 and J2 type vanes is very close to 45° . In case of Figs. 6.3 and 6.9 to 6.12, every possible attempt was made to maintain the other experimental conditions same. However, it can be noted that the maximum strength of vane-induced vortex in terms of MOM is greater in case of rectangular vane than that of the double curve type I, double curve type II, J1 and J2. The possible reason behind it has been explained in later part of this chapter.

Although the angle of attack at which the MOM is close to the optimum can be very well judged from these figures and happens to be close to 45° , it is considered desirable to obtain the value of optimum angle of attack using calibrated best fit curve

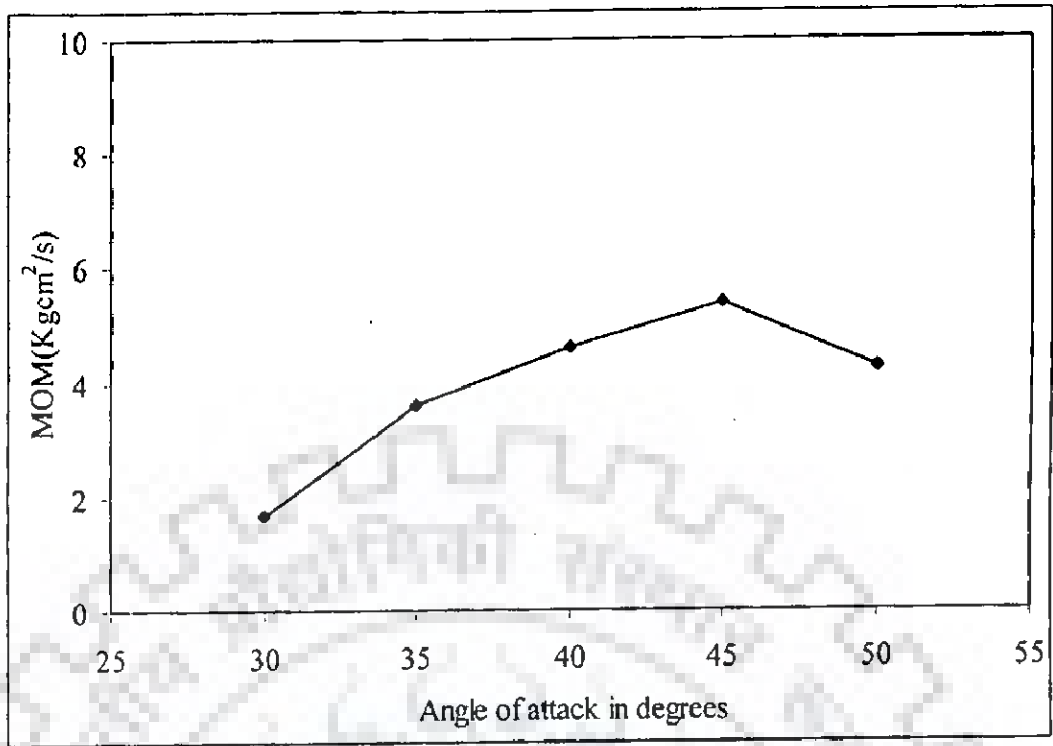


Fig. 6.9 Optimal angle of attack for double curve type I vane ($T/d = 0.67$)

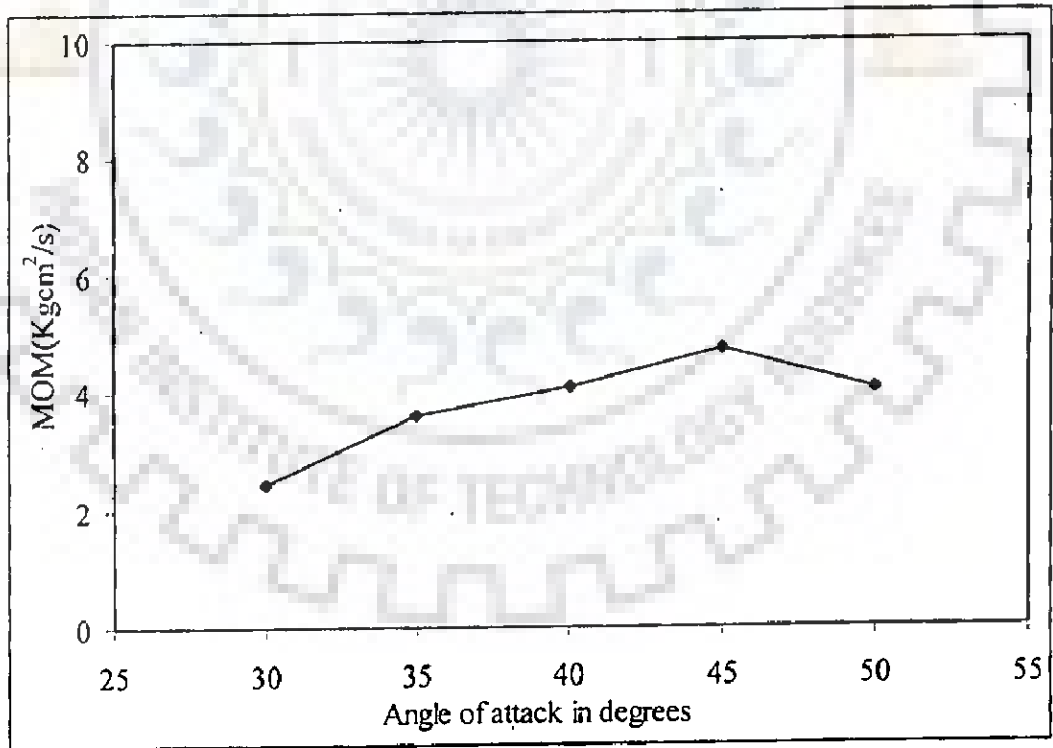


Fig. 6.10 Optimal angle of attack for double curve type II vane ($T/d = 0.67$)

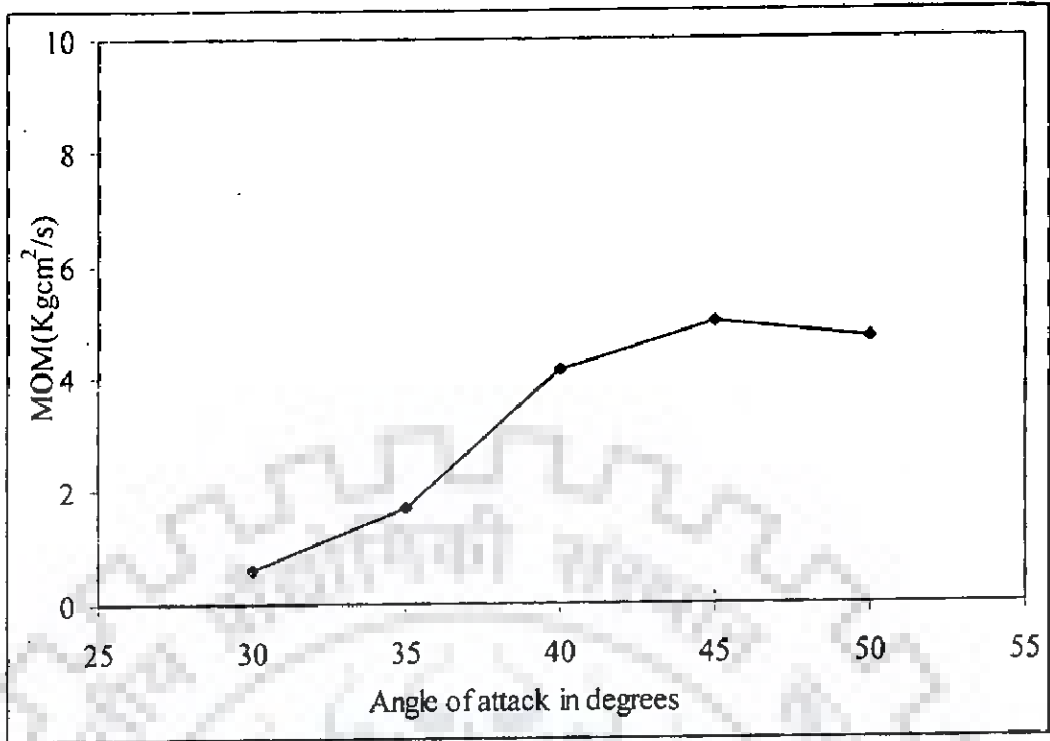


Fig. 6.11 Optimal angle of attack for J1 type vane ($T/d = 0.67$)

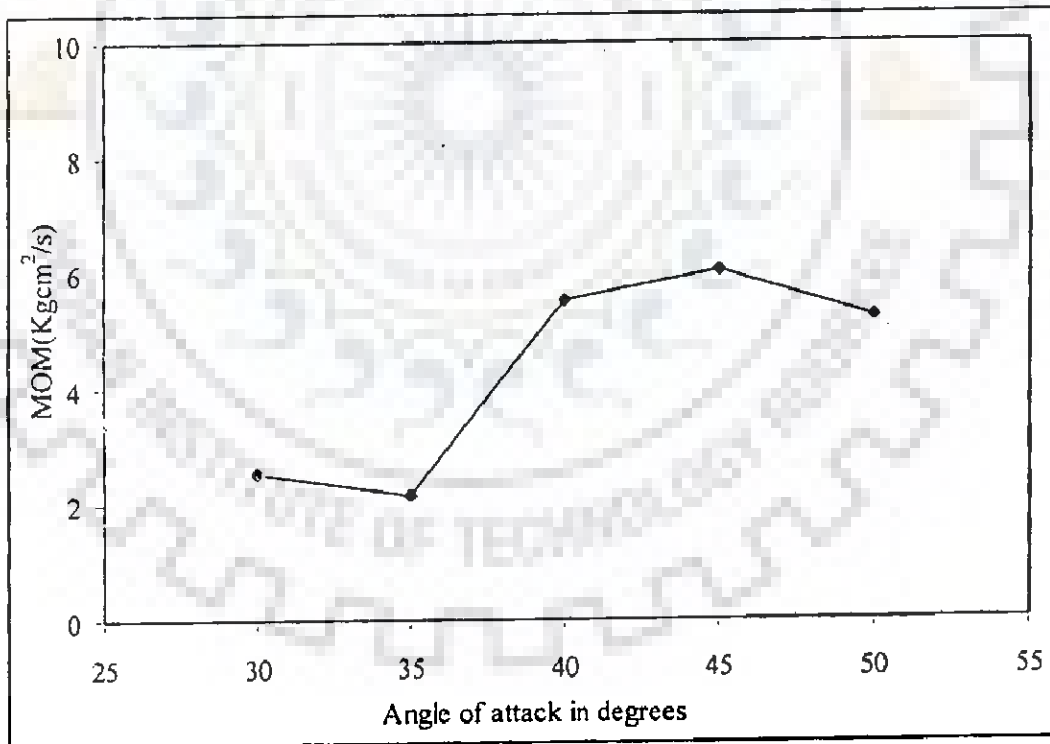


Fig. 6.12 Optimal angle of attack for J2 type vane ($T/d = 0.67$)

within the range of angle of attack between 40° to 50° . With reference to Fig. 6.9, the equation of calibrated curve is obtained as

$$\text{MOM} = -0.0372\alpha^2 + 3.3144\alpha - 68.45, R^2 = 1.0 \quad (6.17)$$

Similar equations have been obtained in case of Figs. 6.10, 6.11 and 6.12. For Fig. 6.10, the calibrated equation is

$$\text{MOM} = -0.027\alpha^2 + 2.4279\alpha - 49.805, R^2 = 1.0 \quad (6.18)$$

Similarly, for Fig. 6.11, the calibrated equation is

$$\text{MOM} = -0.023\alpha^2 + 2.1288\alpha - 44.209, R^2 = 1.0 \quad (6.19)$$

Similarly, for Fig. 6.12, the calibrated equation is

$$\text{MOM} = -0.0266\alpha^2 + 2.3649\alpha - 46.558, R^2 = 1.0 \quad (6.20)$$

Using eqs. (6.12) and (6.13) in case of equations (6.17), (6.18), (6.19) and (6.20), yields the optimum angle of attack for same values of T/d, as given in Table 6.3. It can be seen from this Table that optimum angle changes from 44.45° to 46.28° ($< 5\%$ variation).

Table 6.3: Computation of optimal α for curved vanes

Figs.	MOM	$\frac{d(\text{MOM})}{d\alpha}$	$\frac{d^2(\text{MOM})}{d\alpha^2}$	α	T/d
6.9	$-0.0372\alpha^2 + 3.3144\alpha - 68.45$	$-0.0744\alpha + 3.3144$	-0.0744	44.55	0.67
6.10	$-0.027\alpha^2 + 2.4279\alpha - 49.805$	$-0.054\alpha + 2.4279$	-0.054	44.96	0.67
6.11	$-0.023\alpha^2 + 2.1288\alpha - 44.209$	$-0.046\alpha + 2.1288$	-0.046	46.28	0.67
6.12	$-0.0266\alpha^2 + 2.3649\alpha - 46.558$	$-0.0532\alpha + 2.3649$	-0.0532	44.45	0.67

6.4 EFFECT OF ASPECT RATIO

It can be seen from the Fig. 6.13 that rectangular vanes are most effective in producing higher value of dimensionless MOM*. For this reason, the effect of aspect ratio, defined as H/L has been studied for rectangular vanes only. It is apparent from the Fig. 6.14 that aspect ratio of a submerged vane also plays a vital role for the generation of strength of vane induced secondary circulation and it increases with decrease of aspect ratio. Generation of vortex starts right from the leading edge and it is amplified till it reaches the trailing edge. After passing over the trailing edge, the strength of vortex goes on reducing. It was found that the strength of vortex of rectangular vanes of aspect ratio 0.33 is about 7 times that of aspect ratio 0.5 and vane of aspect ratio 0.25 is about 10 times that of aspect ratio 0.5 (Fig. 6.14).

6.5 EFFECT OF TAPER ANGLE

In the preceding section, the use of rectangular vanes has been advocated and for the similar reasons the influence of taper angle has been studied with respect to rectangular vanes only. In Chapter 3, tapered rectangular vane (called trapezoidal vane) has been described. Here, three tapered angles such as 1H:1V, 3H:2.5V and 4H:2V have been considered. When the taper angle is 90° , it becomes rectangular vane. The Fig. 6.15 shows the variation of dimensionless MOM* with respect to taper angle at the optimal angle of attack, 40° .

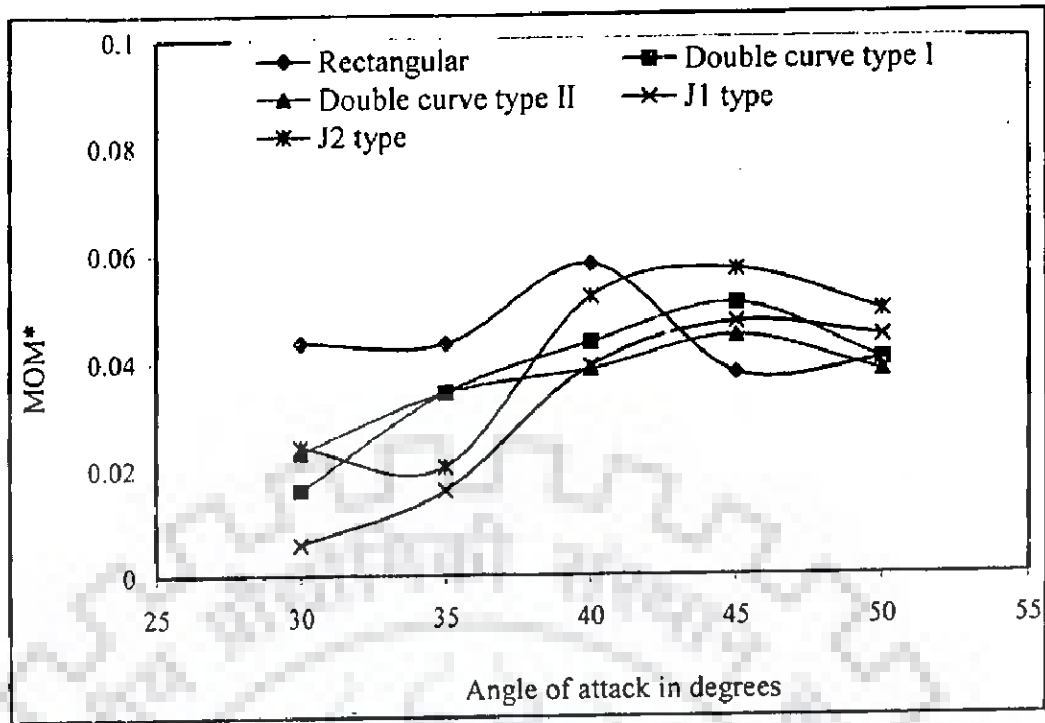


Fig. 6.13 Comparison of MOM^* for different types of vanes ($T/d = 0.67$)

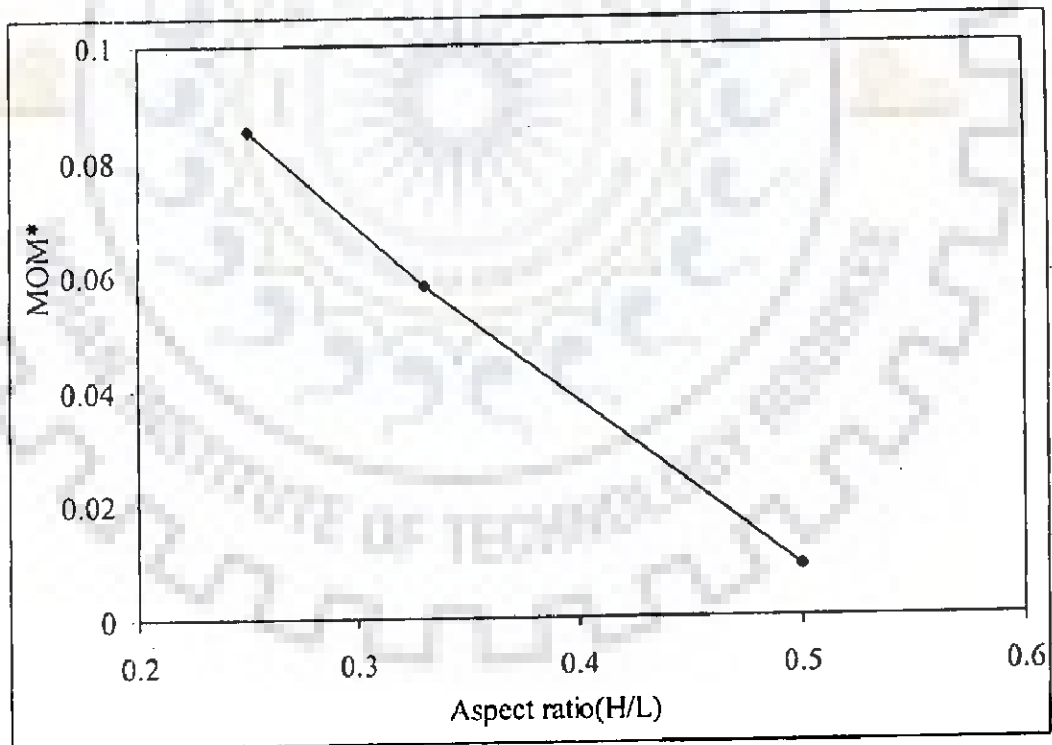


Fig. 6.14 Effect of aspect ratio of rectangular vane on MOM^* ($T/d = 0.67$)

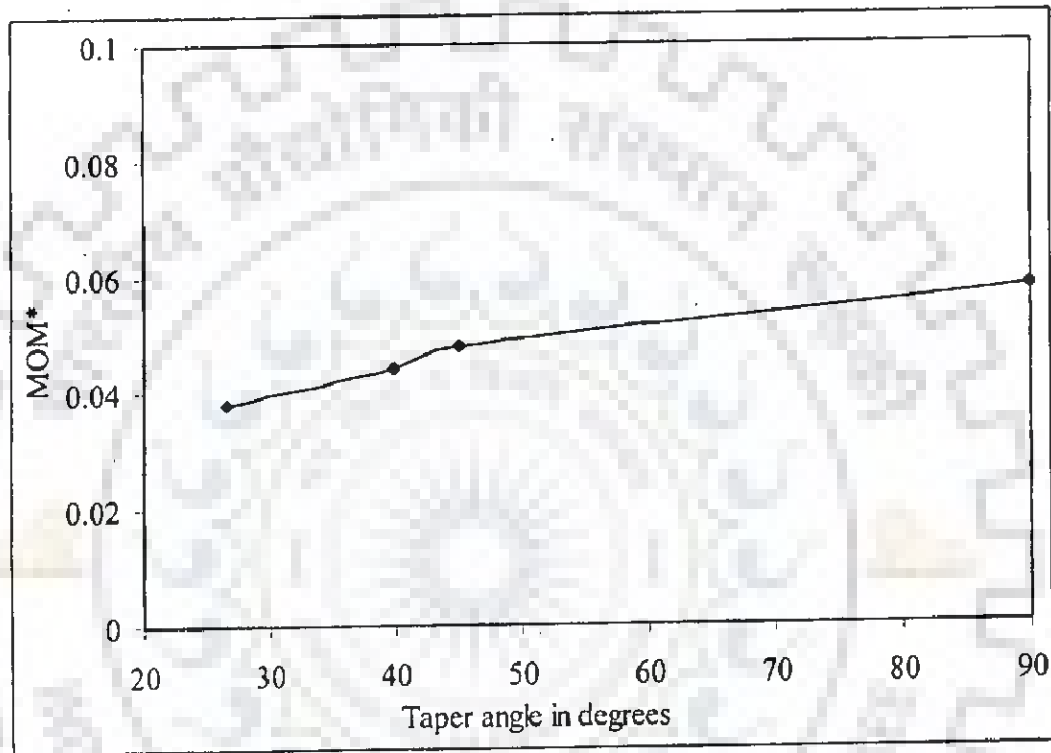


Fig. 6.15 Effect of taper angle on MOM* ($\alpha = 40^\circ$, $T/d = 0.67$)

6.6 CHANGE OF PRESSURE SIDES IN CURVED VANES

The experiments were performed on non-uniform sand of size 0.225 mm. For describing strength of vortex in terms of moment of momentum (MOM), Marelius and Sinha (1998), have identified the optimal angle of attack for rectangular vanes to be very close to 40° . In this research, optimal angle of attack for rectangular vane with collar is found to be still 40° (Figs. 6.3 to 6.5). At optimal angle of attack, it was observed that local scour hole increases the strength of rectangular vane induced secondary circulation by about 4% in the same flow conditions. Thus, introduction of collar at the leading edge of rectangular vane reduces the maximum strength of rectangular vane induced vortex by only small percentages; however, the maximum strength of vortex is still significantly high. Optimal angle of attack for curved vanes is close to 45° .

Behaviour of flow changes, when it enters from zone I to zone II, in case of curved vanes (Fig. 6.16). High and low pressure sides of a zone are replaced by low and high pressure sides respectively when the flow enters zone II to from zone I.

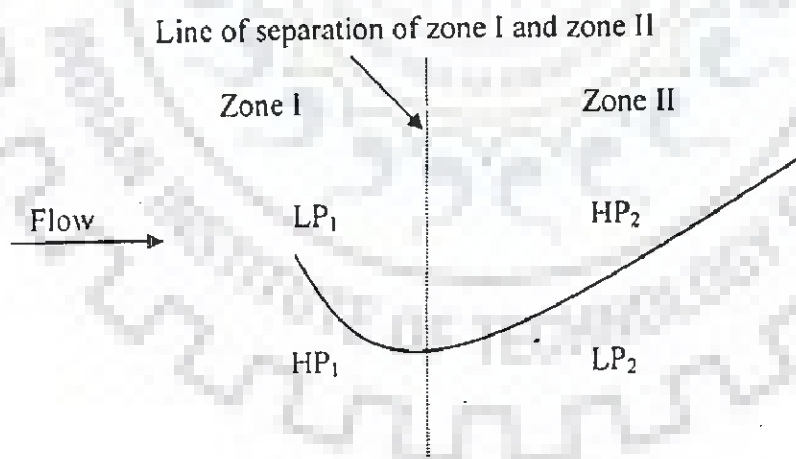


Fig. 6.16 Change of pressure sides in curved vanes

Therefore, the strength of vortex of flow is reduced by the generation of secondary flow in zone I which acts in opposite direction to that of zone II.

The vortices produced in zone I and zone II will be of opposite direction to each other, therefore strength of vortex generated in zone II will be reduced by the amount that produced in zone I and probably due to this reason, the efficiency of curved vanes will have a lesser value than that of rectangular vane if they have the same size and fluvial parameters.

6.7 SUMMARY

In this chapter, the results in respect of angle of attack and likely influence of variability of MOM in case of rectangular vane have been presented. In addition, dimensional considerations in respect of dependence of MOM have been explored. The optimal angle of attack of different curved shapes of submerged vane viz double curve type I, double curve type II, J1 and J2 types have been explored. The effects of aspect ratio and taper angle on MOM with respect to rectangular vanes have also been explored. Change of pressure sides in curved vanes is also identified.

DIKE FORMATION AND DECAY OF STRENGTH OF VORTEX WITH DOWNSTREAM

7.1 GENERAL

With the use of submerged vanes in straight channels, dikes (heaps of sediment) may form in the downstream of vanes. Knowing the layout of dikes may be helpful in deciding the magnitude of protected area. For this reason, a study on dike formation is also aimed and presented here. Similarly, another parameter of interest is the variation of strength of vortex. It is well established that vane induced strength of vortex reduces with downstream region of submerged vane. However, there is not enough information available regarding the trend of variation of MOM in the downstream of submerged vanes of different types. With this in view, the streamwise reduction of strength of vortex has been studied at an angle of attack of 40° . For identical hydraulic conditions, strength of vortex was measured for rectangular submerged vane with and without collar.

In addition, this was also identified in case of trapezoidal vanes with collar for three taper angles such as 1H:1V, 3H:2.5V and 4H:2V. Strength of vortex was measured as per the previous Chapter 6. This Chapter dwells upon primarily on the physical process of dike formation, which may give some indications for deciding upon the location of submerged vanes with respect to the river bank. In addition, it presents the trend of variation of strength of vortex in different conditions.

7.2 FORMATION OF DIKES

7.2.1 Formation of Dikes Downstream of Vane

Dike formation process was observed invariably in all the experiments performed in this study. However, the magnitude of it varied widely. Commonly, it was observed to be more pronounced at higher value of Froude number, i.e. 0.25. At the lower Froude number value of 0.13, the dike formation was negligible. The probable cause for this may be ascribed to the generation of lower strength of vortex which might have led to the lesser scour as well as reduced deposition of sediments needed for formation of dike.

At higher Froude number of 0.25, it was observed that there is also considerable development of local scour hole at the trailing edge of the submerged vanes (Plate 7.1). Based on these observations, Table 7.1 is developed. Table 7.1 gives an idea about the distance from the trailing edge of the submerged vanes for the area to be protected. The origin was taken at the trailing edge of vane at initial bed level (Fig. 7.1). It is also apparent from Figs. 7.2 to 7.7 that the formation of dike is curvilinear in case of both rectangular and trapezoidal vanes and follows a nonlinear equation (Table 7.2). Plate 7.2 shows a typical formation of dike downstream of vane.

Table 7.1: Distance of protected area from the trailing edge of vanes

Types of vanes with collar	Distance in terms of H
Vertical leading edge (Rectangular)	2.75
Trapezoidal (1H:1V)	3
Trapezoidal (3H:2.5V)	4
Trapezoidal (4H:2V)	3

Table 7.2: Modelled equations for dike formations for different taper angles

Figs.	Taper angles	Modelled equations
7.3	vertical leading edge	$-0.001x^2 - 0.0557x + 0.7104, R^2 = 0.7651$
7.4	1H:1V	$0.0004x^2 - 0.1704x + 1.6095, R^2 = 0.9766$
7.5	3H:2.5V	$0.0024x^2 - 0.1579x + 1.5292, R^2 = 0.9475$
7.6	4H:2V	$-0.0018x^2 - 0.0516x + 0.579, R^2 = 0.8744$

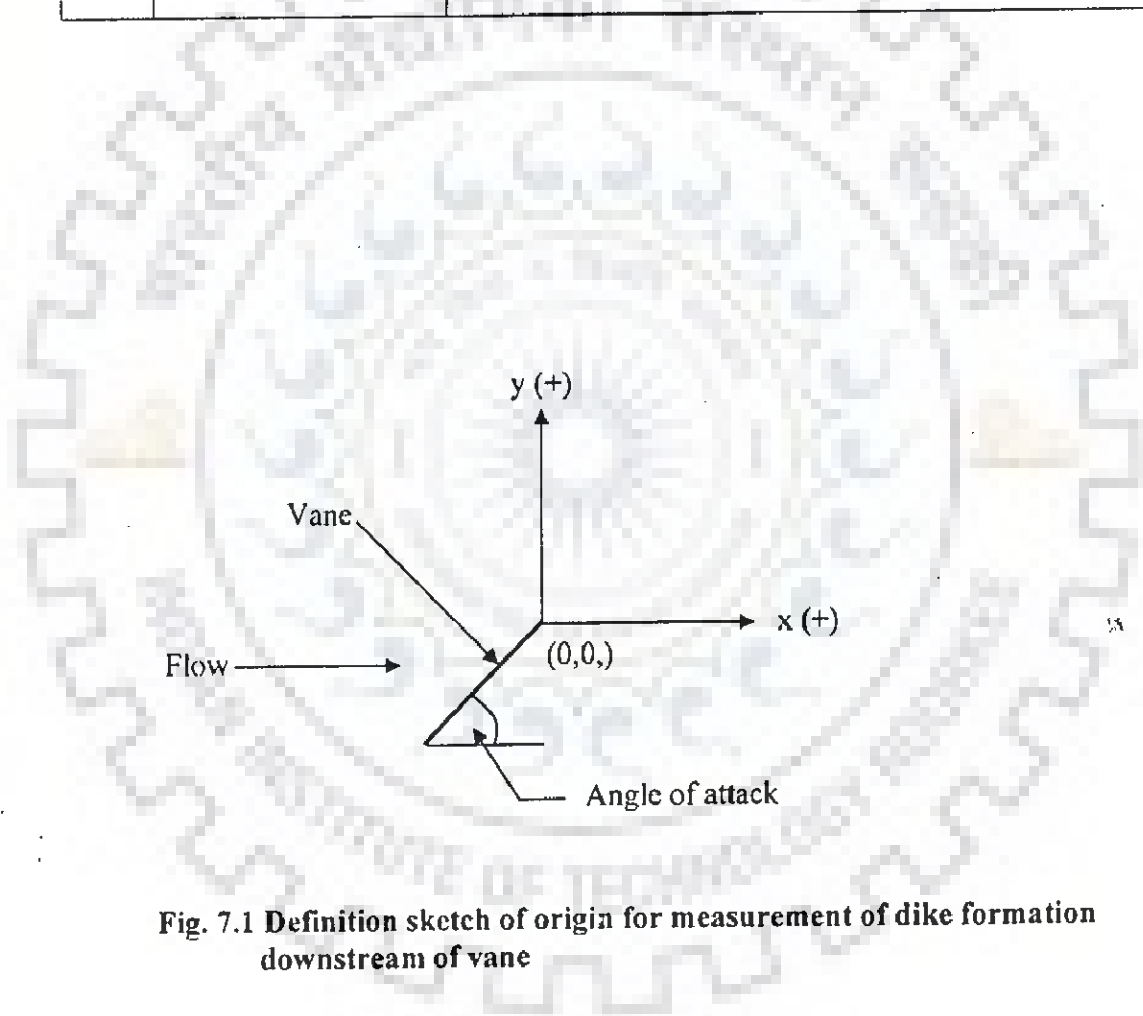


Fig. 7.1 Definition sketch of origin for measurement of dike formation downstream of vane

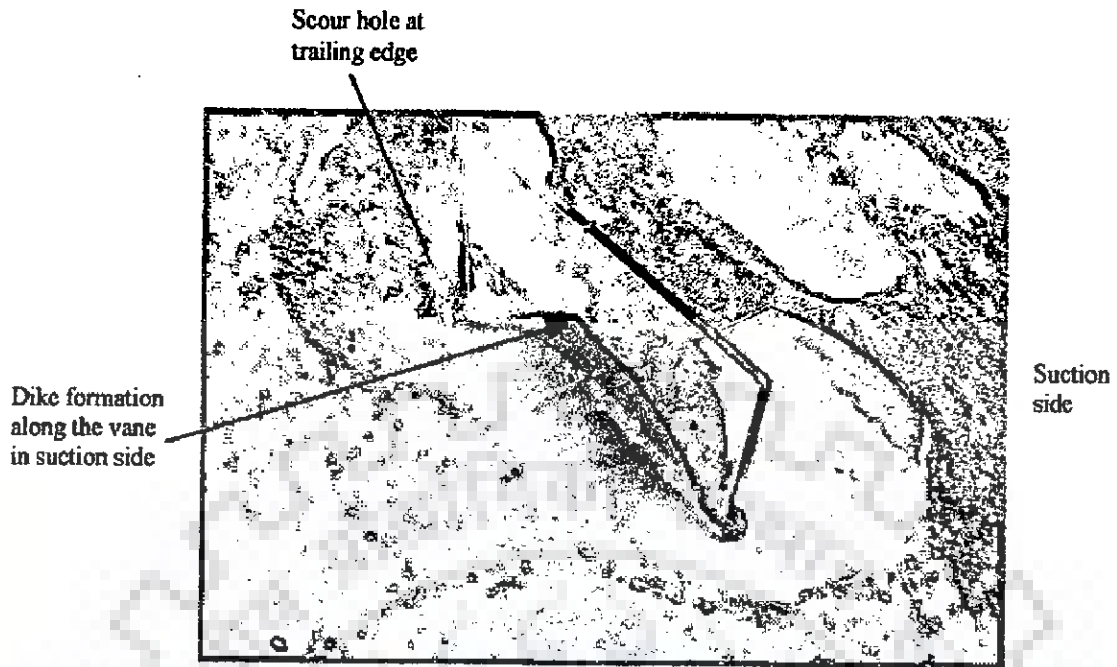


Plate 7.1 Scour hole at trailing edge of rectangular vane and dike formation along it in suction side ($F_r = 0.25$, $d_{50} = 0.405$ mm)



Plate 7.2 Dike formation in downstream of vane ($F_r = 0.25$, $d_{50} = 0.405$ mm)

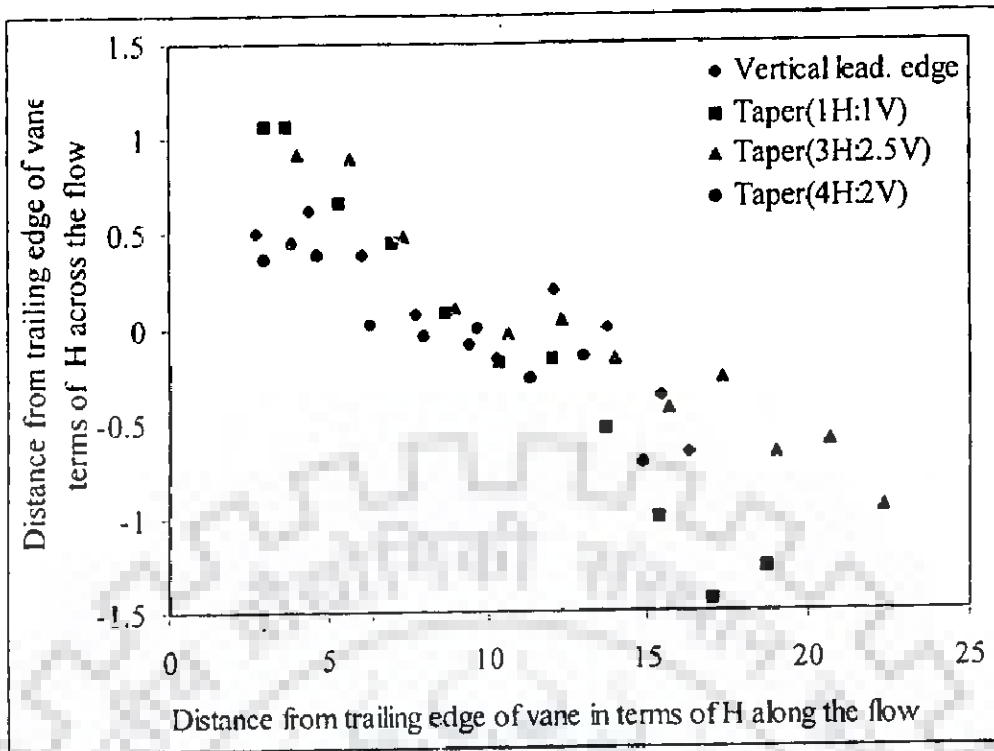


Fig. 7.2 Scattering of dike alignment across the flow with different taper angles

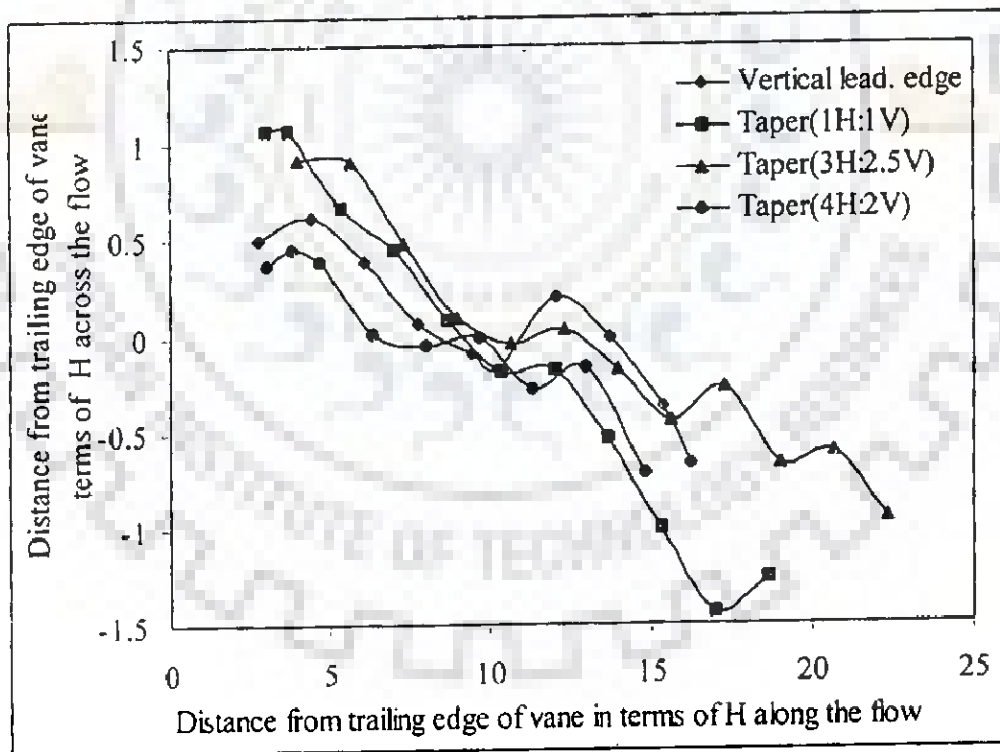


Fig. 7.3 Dike alignment across the flow with different taper angles

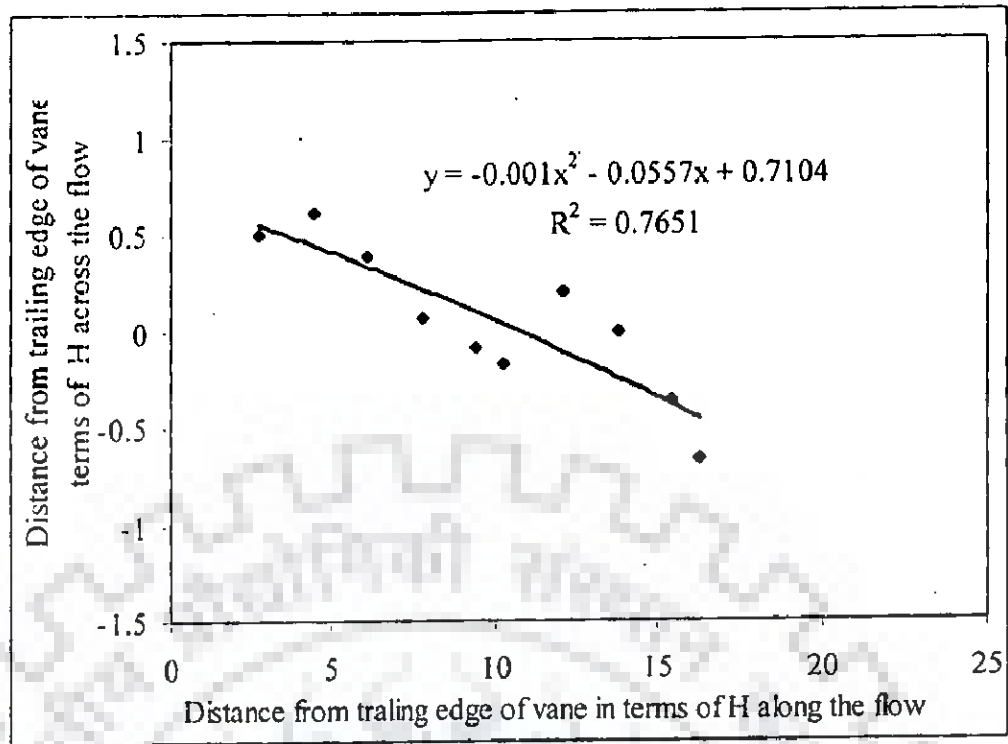


Fig. 7.4 Dike alignment across the flow with vertical leading edge vane

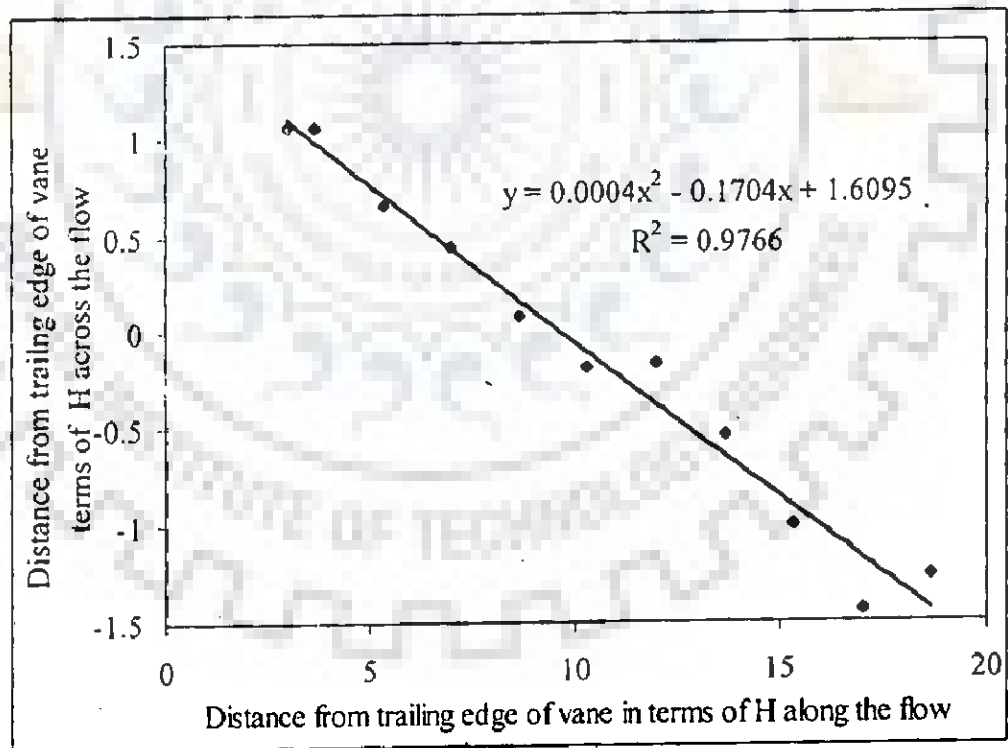


Fig. 7.5 Dike alignment across the flow with taper angle (1H:1V)

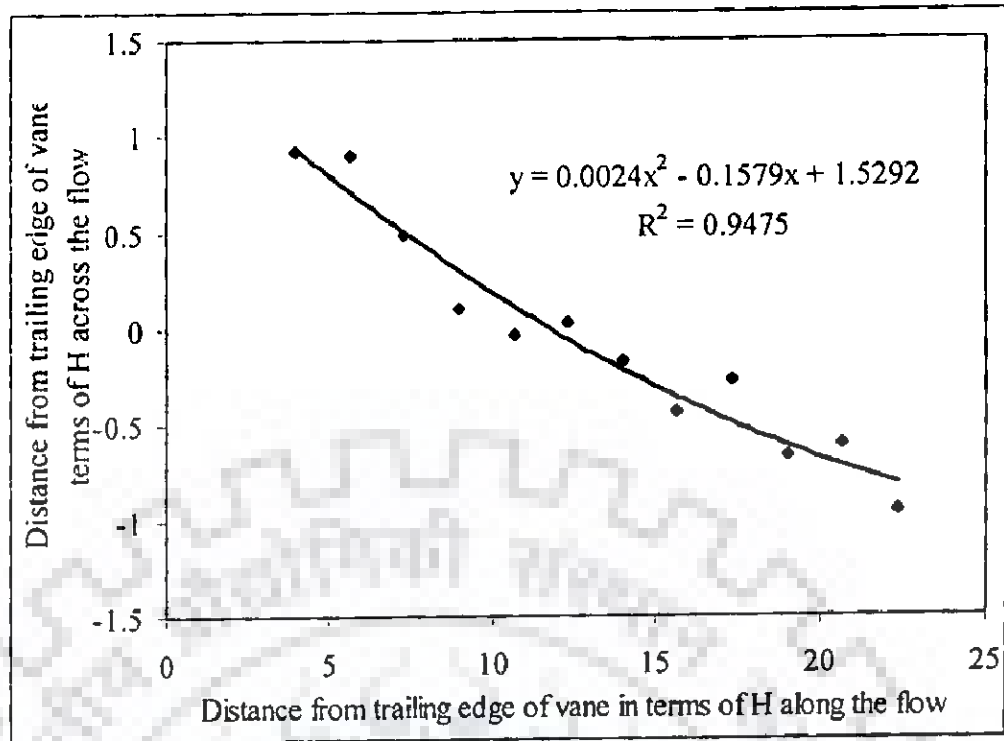


Fig. 7.6 Dike alignment across the flow with taper angle (3H:2.5V)

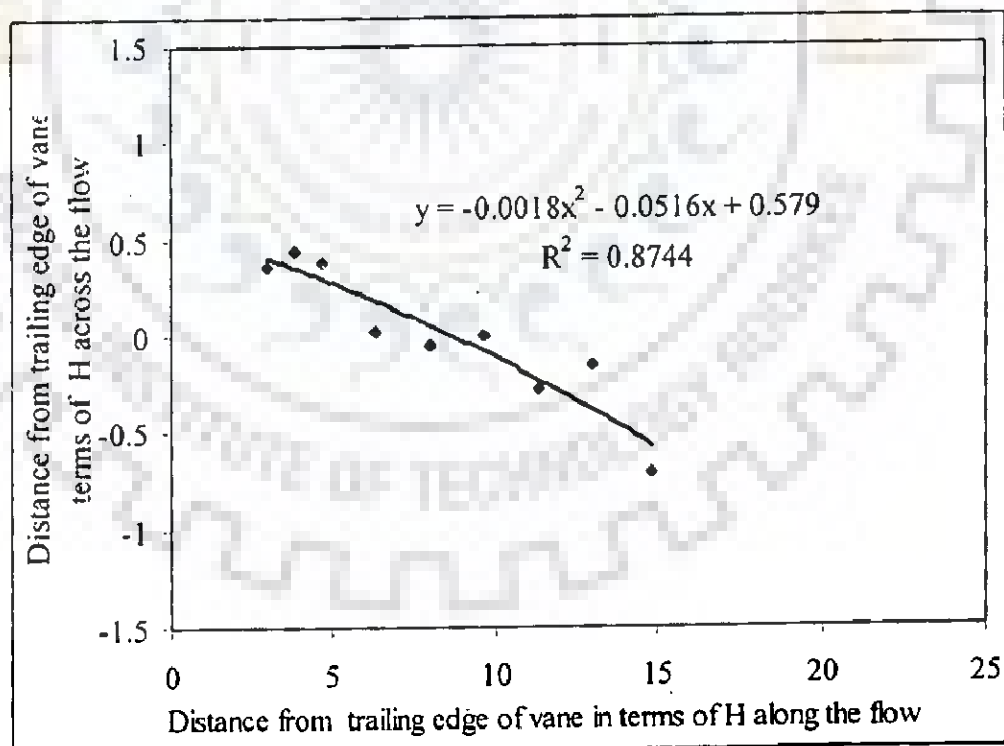


Fig. 7.7 Dike alignment across the flow with taper angle (4H:2V)

7.2.2 Formation of Dike along the Vane in Suction Side

From the experimental observations, it was found that there was not significant scour along the vane in its suction side even at higher Froude number 0.25 (Plate 7.1). The origin was taken at the leading edge of vane at initial bed level (Fig. 7.8). At Froude number 0.25, the scour profile along the vane looked like some sort of normal distribution with all the taper angles. Fig. 7.9 shows a typical plot of the nature of dike formation along the rectangular vane in suction side across the flow. The formation of dike along the vane in suction side takes the shape as per the following equation

$$z = 0.0368x^4 - 0.4008x^3 + 0.9387x^2 + 0.0207x - 0.8639, \quad R^2 = 0.9751 \quad (7.1)$$

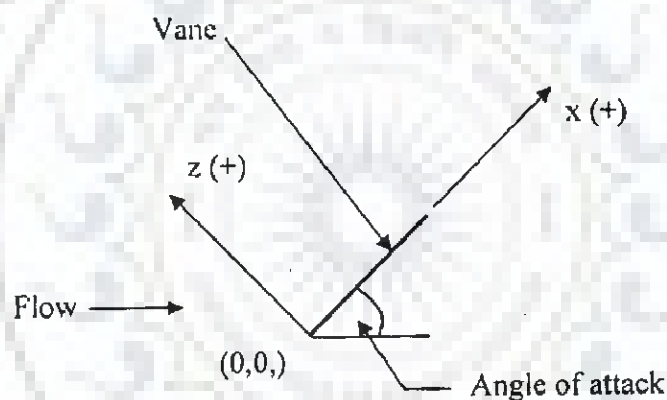


Fig. 7.8 Definition sketch of origin for formation of dike formation along the vane

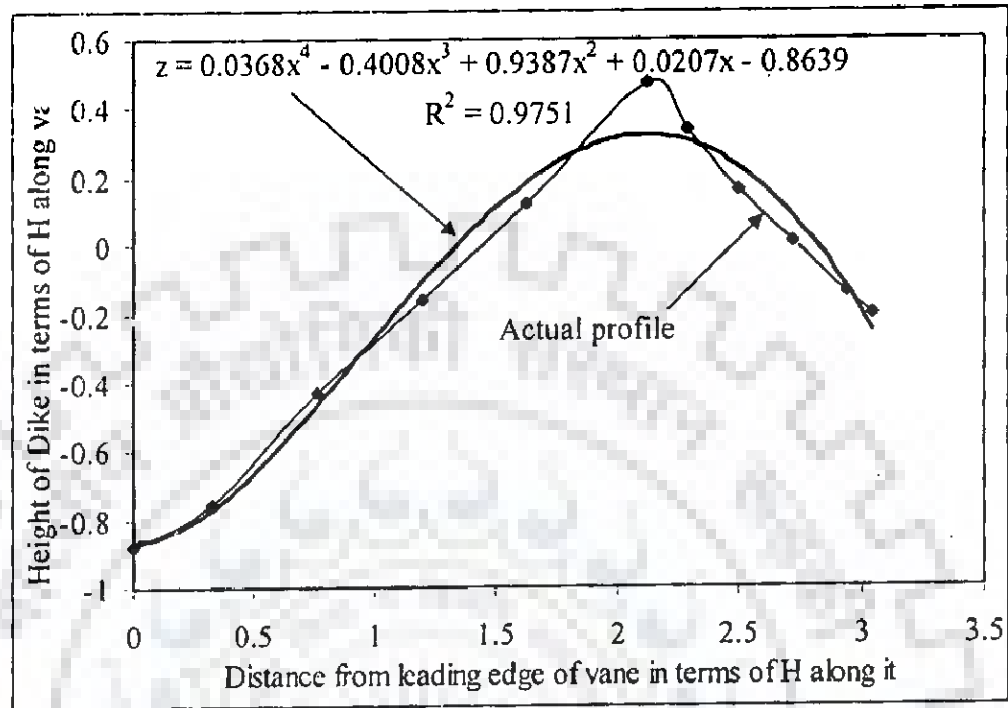


Fig. 7.9 Dike alignment along the rectangular vane in suction side (in vertical plane)

7.3 STREAMWISE DECAY OF STRENGTH OF VORTEX

For this purpose, 5 cm × 5 cm grids across the flume have been taken at the downstream distances of 10H, 20H, 30H and 40H from the centre of vane. At every grid point, all the three components of velocity were measured using ADV. Strength of vortex was evaluated at two Froude numbers, namely 0.13 and 0.25.

Streamwise decay of strength of vortex due to rectangular vane with and without collar, and the trapezoidal vanes with collar considering different taper angles have been experimentally investigated at Froude numbers of 0.13 and 0.25. The experimental programme has been explained in Chapter 3. It is apparent from Figs. 7.10 to 7.19 that there is great deal of uncertainty regarding decay of vane induced secondary circulation with downstream from the vane. It was observed that the centre of vortex goes up with downstream distance from the vane. Due to the constraint of available discharge in the laboratory, the possible water depth at Froude number of 0.25 was maintained at 14 cm. All the three components of velocity can possibly be measured by using the down looking probe of ADV only at a vertical elevation of 5 cm depth below the water surface. It was observed from the experimental data that all the transverse velocity components below 5 cm water depth from water surface and near the streamwise centre line of the vanes are directed towards the high pressure side of the vanes. Therefore, it was relevant to consider the centre of vortex in the zone of 5 cm water depth from the water surface. As exact centre of vortex was not known, three arbitrary centre of vortices were considered at the heights of 10 cm (i.e. 1.67H), 11 cm (i.e. 1.83H), and 12 cm (i.e. 2H) from the initial bed level of sediment along the streamwise centre line of vanes.

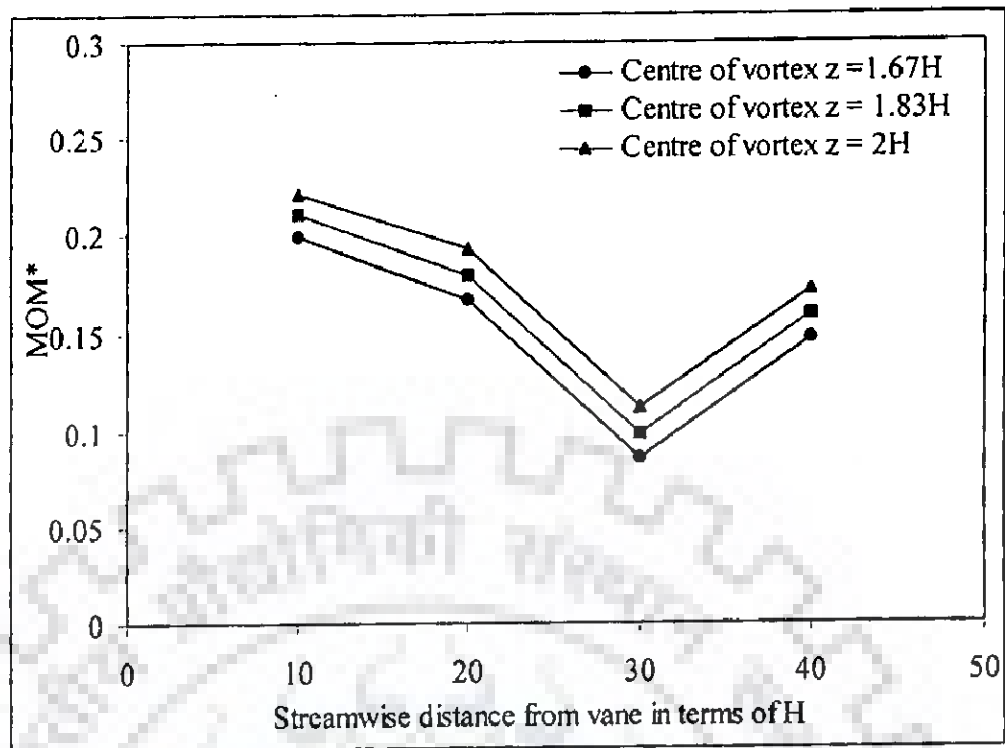


Fig. 7.10 Streamwise variation of MOM* for rectangular vane without collar at Fr 0.13

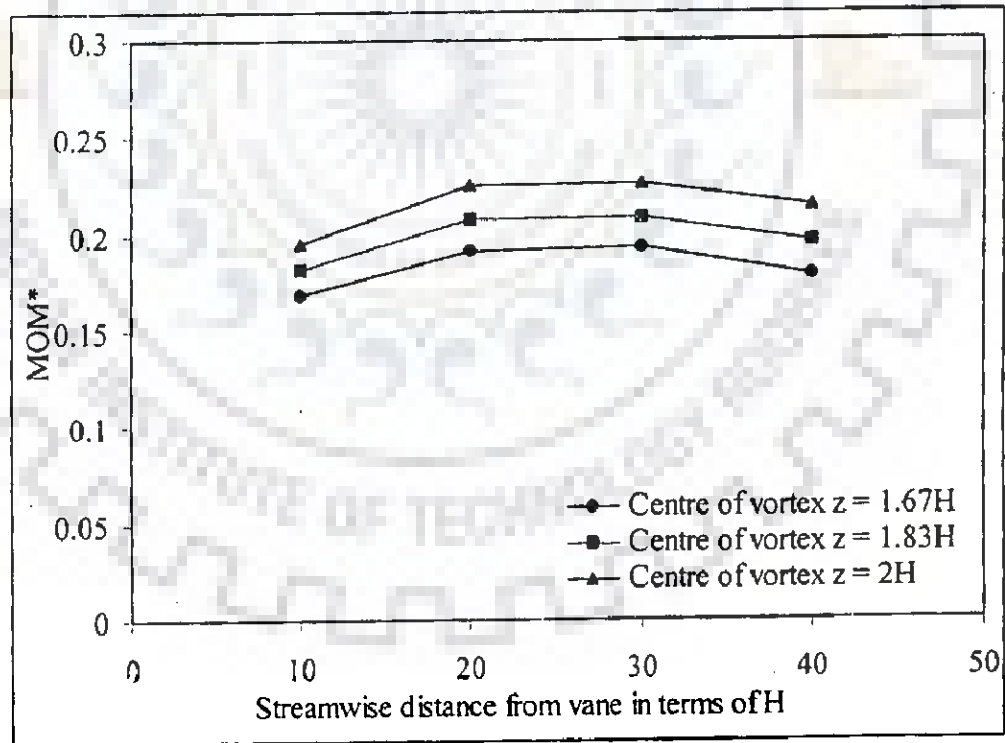


Fig. 7.11 Streamwise variation of MOM* for rectangular vane with collar at Fr 0.13

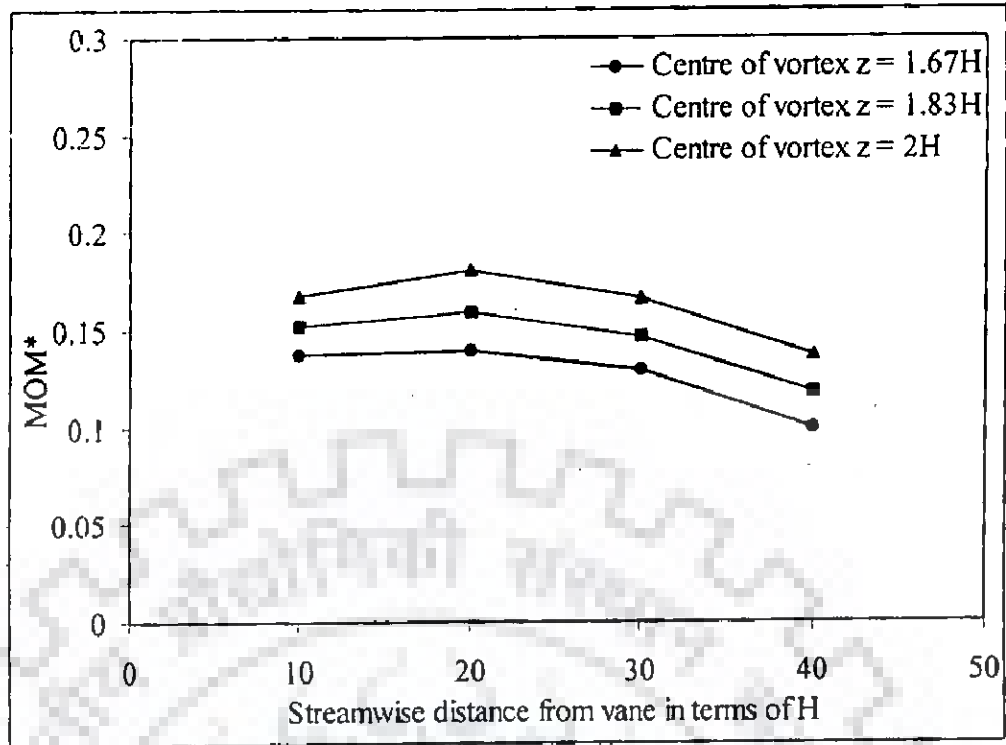


Fig. 7.12 Streamwise variation of MOM* for trapezoidal (1H:1V) vane with collar at Fr 0.13

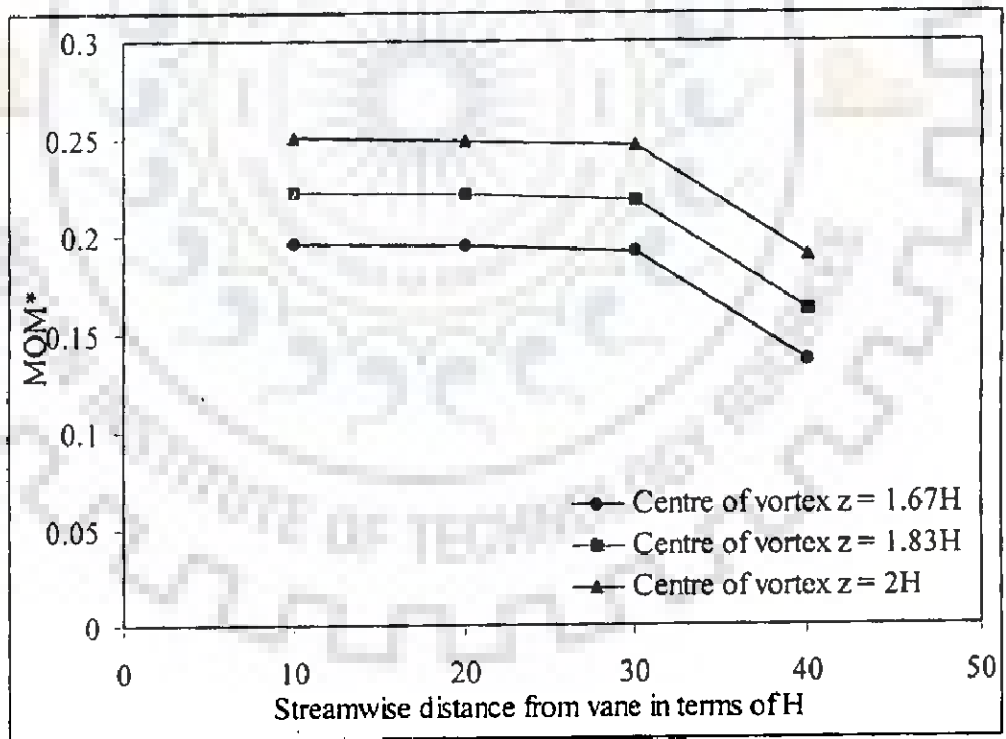


Fig. 7.13 Streamwise variation of MOM* for trapezoidal (3H:2.5V) vane with collar at Fr 0.13

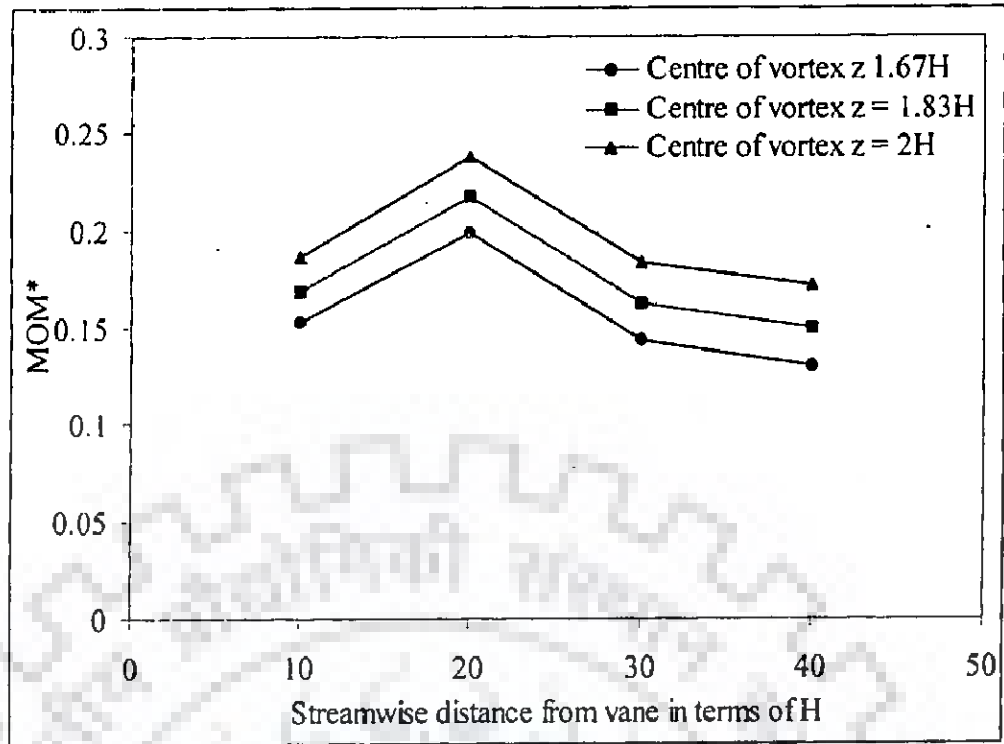


Fig. 7.14 Streamwise variation of MOM* for trapezoidal (4H:2V) vane with collar at Fr 0.13

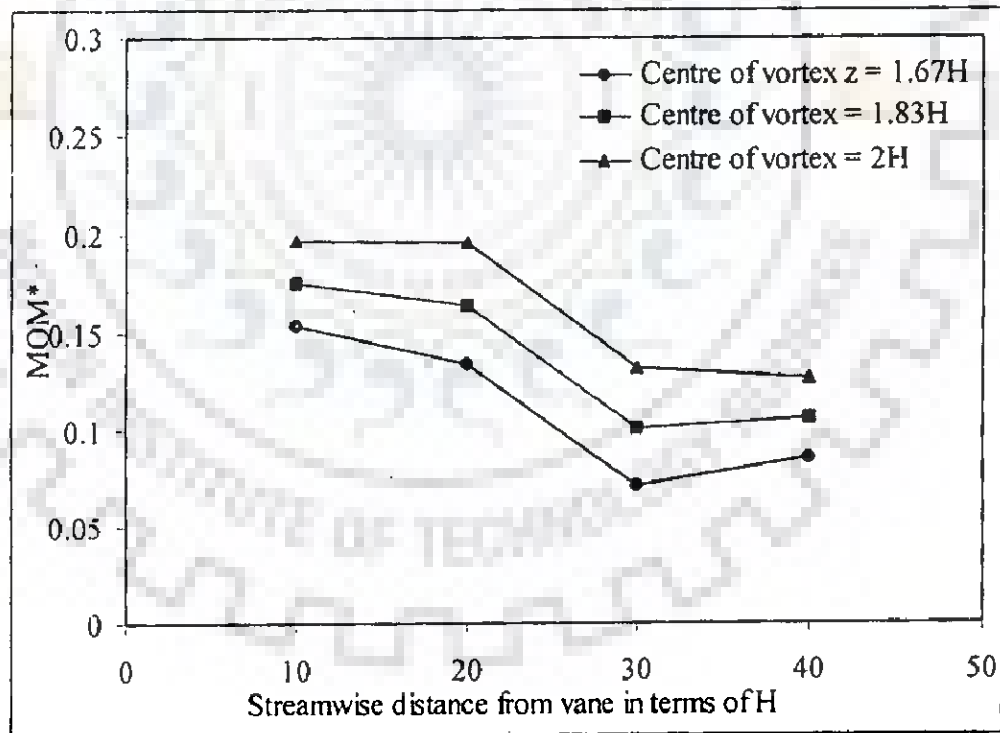


Fig. 7.15 Streamwise variation of MOM* for rectangular vane without collar at Fr 0.25

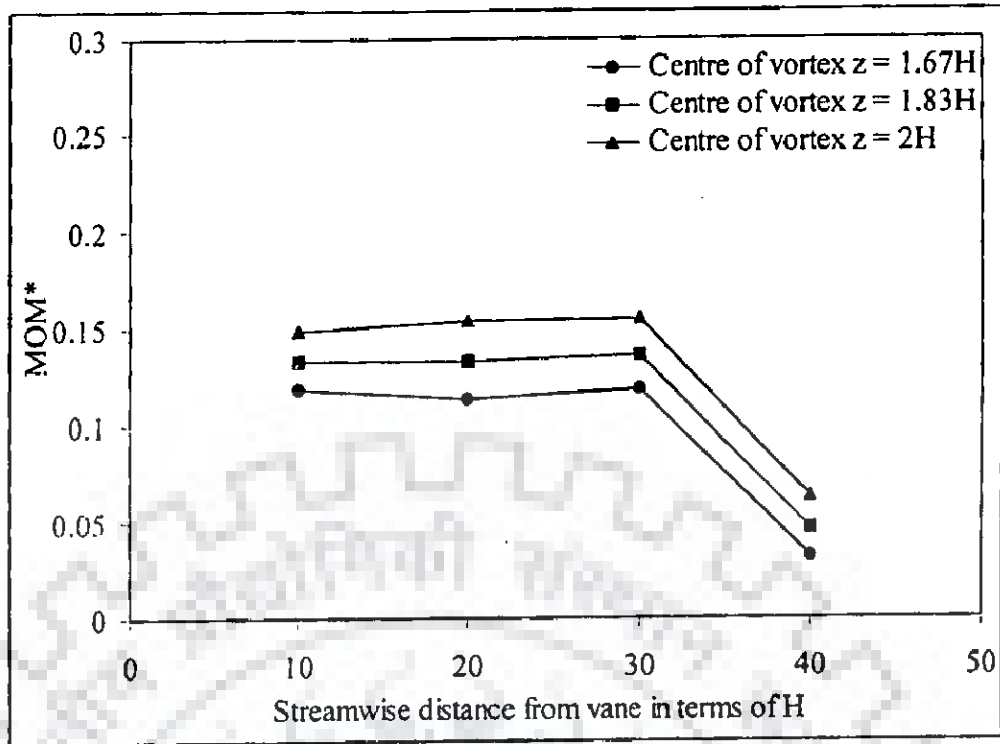


Fig. 7.16 Streamwise variation of MOM* for rectangular vane with collar at Fr 0.25

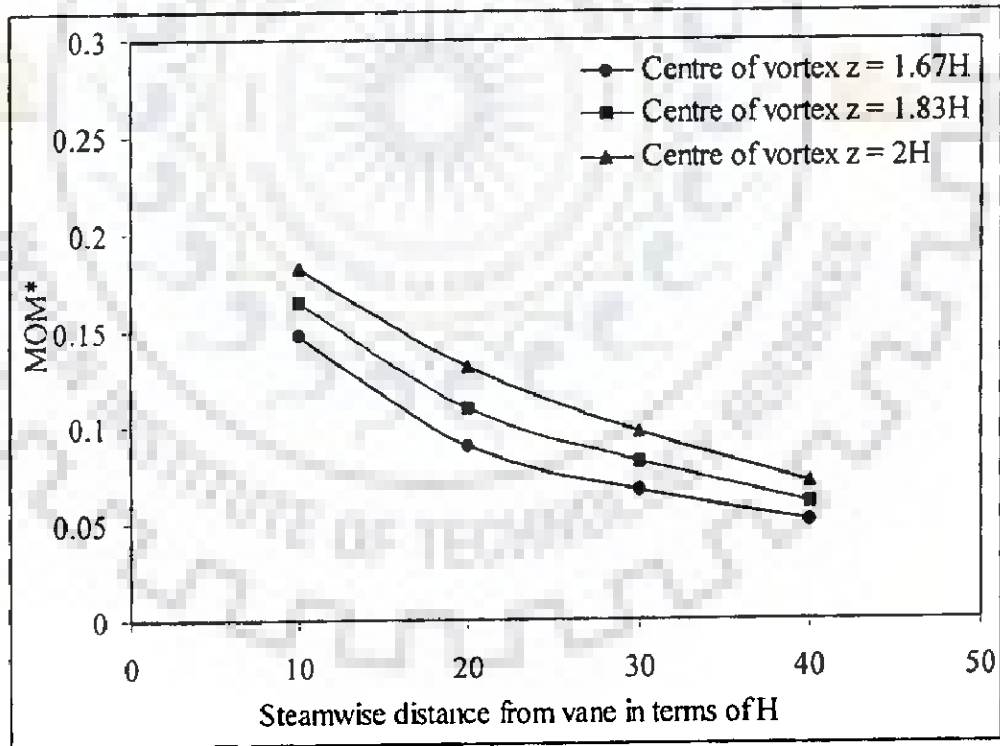


Fig. 7.17 Streamwise variation of MOM* for trapezoidal vane (1H:1V) with collar at Fr 0.25

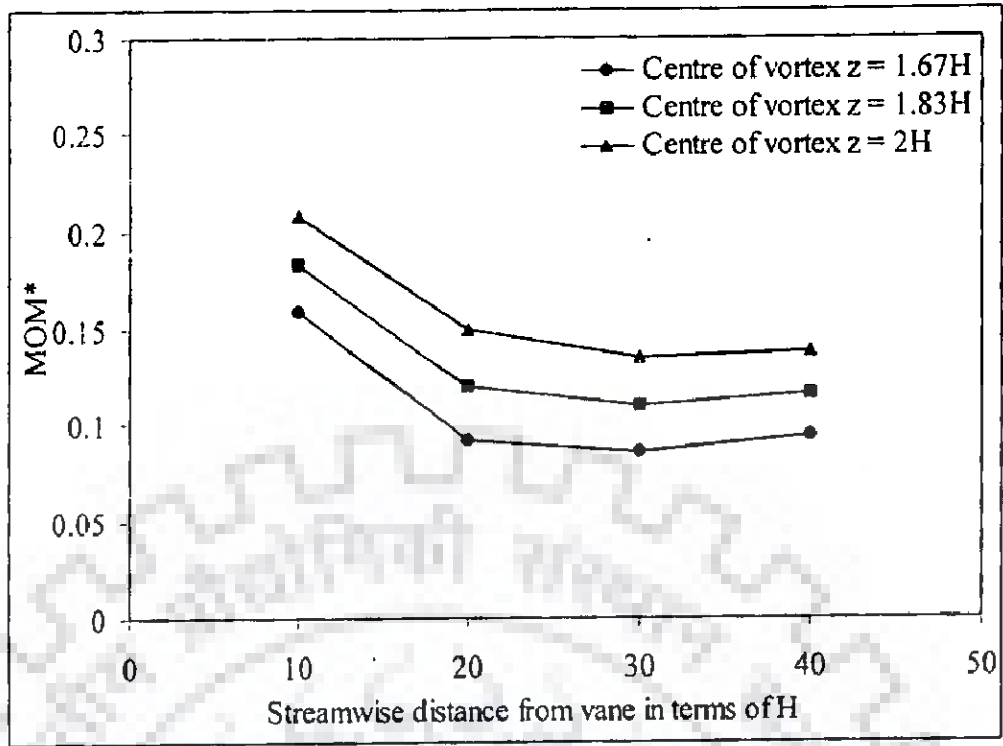


Fig. 7.18 Streamwise variation of MOM^* for trapezoidal vane (3H:2.5V) with collar at Fr 0.25

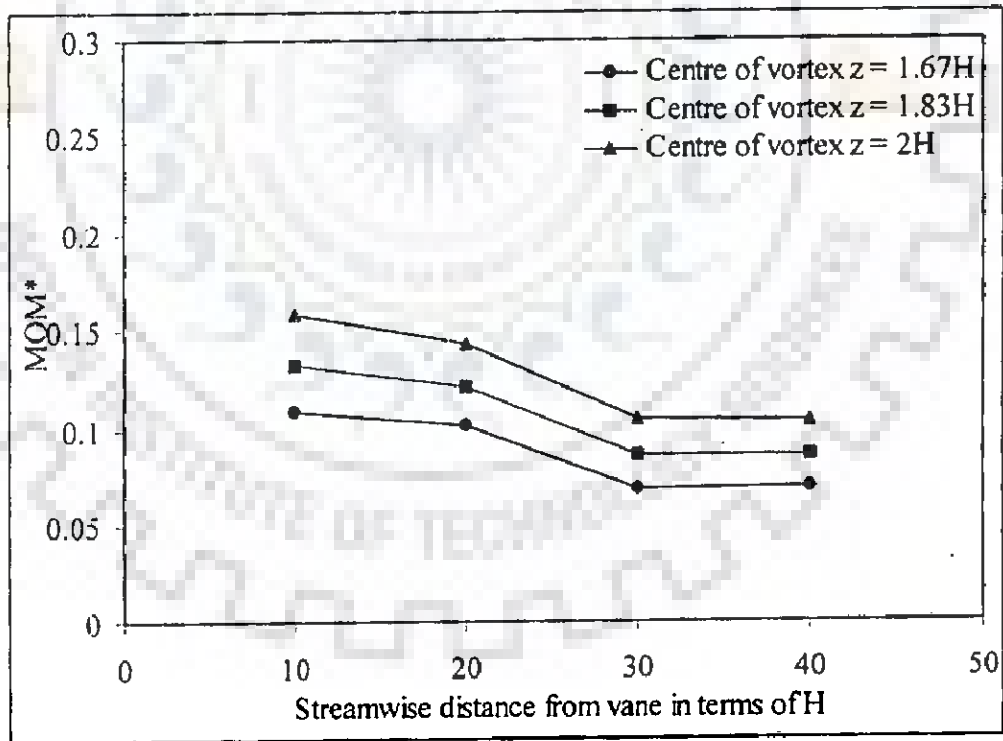


Fig. 7.19 Streamwise variation of MOM^* for trapezoidal vane (4H:2V) with collar at Fr 0.25

Therefore, variation of vane induced secondary circulation in terms of dimensionless MOM^* at center of vortex $1.67H$, $1.83H$ and $2H$ have been shown in Figs. 7.10 to 7.19. It can be seen that all the plots are parallel at centre of vortex $1.67H$, $1.83H$ and $2H$. This is due to the constant value of dimensionless MOM^* as a result of vertical velocity components. As the variation of strength of vortex with downstream distance is not consistent, any attempt to model the variation of MOM with distance was considered to be not prudent. Nevertheless, Figs. 7.10 to 7.19 indicate that the path of horse shoe vortex is not parallel to channel bed. It can be seen from Fig. 7.10 that the value of MOM^* display an abrupt rising trend again from $30H$ to $40H$. Similarly, in Figs. 7.11, 7.12 & 7.14, MOM^* increases from $10H$ to $20H$. Such deviations simplify the fact that centre of vortex does not remain constant. In fact, Figs 7.10 to 7.19 indicate very clearly that MOM^* computations are highly sensitive to the centre of vortex. Unfortunately, literature is silent about this important aspect and the earlier investigators including Odgaard and Wang (1991) and Marelius and Sinha (1998) have assumed the centre of vortex to be fixed at a certain height from the bed and this fact is not supported from the present work. Nevertheless, it is appropriate to mention here that strength of vortex does decrease with the increase in the downstream distance.

7.4 SUMMARY

In this Chapter, results in respect of dike formation in downstream of rectangular and trapezoidal vane with collar have been presented for Froude number of 0.25 with median size of sediment as 0.405 mm. In addition, a typical dike formation along the rectangular vane in suction side is also presented. Considering the fact that to date no information is available on location of centre of vortex with downstream of vane, the present results provide certain informations on the decay of strength of vortex with downstream of vane.

GENERAL REMARKS, CONCLUSIONS & FUTURE WORK

8.1 GENERAL REMARKS

The present work is primarily concerned with the evolution of suitable configuration of collars so that local scour around submerged vanes is restricted to a benign level at a given angle of attack. For vanes to be highly effective; the angle of attack is to be kept around 40° to 45° . However, at such angle of attack the scour at the leading edge of the vane may be sizable enough to cause dislodgement of the vanes. Thus, estimation of scour is equally important. For these reasons, there were three aspects for planning of the present work have been envisaged, viz, (i) observations of scour around submerged vanes and based on it, identification of maximum scour;(ii) identification of suitable shapes of collars so that destabilising scour does not occur around the vanes and no threat is posed to stability of vanes; and (iii) variation of strength of vortices measured in terms of moment of momentum.

To achieve these objectives of the study, vanes of different shapes including rectangular, nonrectangular and curvilinear portions have been considered. Experiments have been conducted only for the values of Froude numbers 0.13 and 0.25, so that user can have some basis for interpolating collar size at an intermediate value of Froude number within the range from 0.13 to 0.25. In reality, the flow conditions may not correspond to a fixed value of Froude number. Thus, depending on the range of Froude numbers likely to be encountered at a specific site, user can interpolate the collar dimensions. Although, it is agreed at this point that it may be necessary to narrow down

the range of Froude number values for planning of future experiments in order to achieve economy in providing collars.

The sediment size may play an important role in identification of effective collar shape. In the present study, only two sediment sizes of 0.225 mm and 0.405 mm have been studied. However, it has not been possible to further refine the collar shapes in terms of these sediment sizes. For example, when the configured collar shape corresponding to Froude number 0.13 and sediment size 0.405 mm was used in case of sediment size of 0.225 mm, it was found to be equally effective. Thus, as a part of future investigations, the influence of sediment size on collar shape needs to be explored. It may be possible that because of the variation of sediment size in the narrow range from 0.225 mm to 0.405 mm, the same collar shape has been efficacious. However, considering the fact that scour phenomenon is dependent on sediment size also, as apparent from the literature, this aspect needs to be studied in detail at a later stage.

Strength of vane induced vortices has been studied in terms of moment of momentum. For this purpose, moment of momentum is made dimensionless. The study has considered influence of a variety of parameters. However, the effect of incidence angle or angle of attack in line with the findings of earlier investigators.

Based on the present work, the following observations can be put forth in the form of conclusions.

8.2 CONCLUSIONS

1. Based on experiments with different types of submerged vanes, it has been observed that maximum scour occurs at the leading edge of rectangular vanes under identical flow conditions. Relatively, lesser scour has been observed at the leading edge of curved and trapezoidal vanes.

2. For rectangular vanes, the following relationship holds good

$$\frac{D_{sc}}{d} = 3.5675 F_r^{1.3761}$$

In this expression, D_{sc} represents computed scour depth, d = flow depth and F_r = Froude number

3. Trials with collar shape indicate that for $Fr = 0.13$, the collar shape can be circular or noncircular. However, at $Fr = 0.25$, the effective collar shape is interestingly observed to be circular. The dimensions of collar for these two values of Froude numbers and different types of submerged vanes are summarized in Chapter 5.

4. In Solani river, the Froude number varied between 0.05 to 0.1 in field trial test area. Therefore, the most effective size of collar obtained at Froude number 0.13 was tested and scour was observed to be considerably reduced. This indicates that collar shape obtained from laboratory experiments can be used in field conditions to achieve stability of vanes.

5. A dimensionless moment of momentum (MOM) concept has been introduced to study the vane induced secondary circulation. Using this concept, variations of dimensionless moment of momentum with respect to a variety of parameters have been studied. It has been observed that the optimal angle of attack for rectangular vane with collar is very close to 40° , which is notably the same for the rectangular vane without collar (Marelius and Sinha, 1998). In case of rectangular vane,

- optimal angle of attack does not appear to be sensitive to degree of submergence (T/d).
- 6 Strength of vane induced secondary circulation is also influenced by tapering of the leading edge of rectangular vane and its aspect ratio. Dimensionless MOM^* decreases with decrease of angle and it considerably increases with decrease of aspect ratio (H/L).
 - 7 Decay of vane induced secondary circulation with downstream distance from vane does not display definite pattern. However, the vane induced residual circulation has normally considerable value even at $40H$ distance from the rectangular and trapezoidal vanes at optimal angle of attack.
 - 8 Centre of vane induced vortex does not appear to be at a fixed height from the bed. This fact is supported from the variation of MOM^* with downstream distance. Also, centre of vortex is found to influence MOM^* computations.
 - 9 At Froude number 0.13, the vane induced process of dike formation is insignificant where as at Froude number 0.25, it has considerable formation. Formation of dike does not follow the linear shape but is has somewhat curvilinear shape bended towards suction side.
 - 10 Based on economic analysis, it was found that collar is a better option as scour retarding device than that of riprap with filter.

8.3 FUTURE SCOPE OF WORK

1. The most effective collar obtained at Froude number 0.25 and circular shape of collar at Froude number 0.13 has to be tested in field.
2. Detailed economic analysis is required for collar size at different higher Froude numbers and at different particle sizes.
3. Vanes with collar in arrays should be investigated to get important design parameters. Collar for vane should be also optimized in curvilinear channels.
4. A methodology for evaluation of centre of vortex needs to be developed.
5. Sediment concentration may influence the density of fluid to be used in MOM computations. This aspect needs further considerations.
6. Collar dimensions in relation to bed material size needs to be quantified.
7. Range of Froude numbers can be further narrowed down for obtaining collar size.
8. Further detailed investigation is required on the streamwise decay of vane induced vortex at the optimal angle of attack for both straight and curved channels, for clear water and sediment-laden flows.
9. In-depth experimental studies on the dike formation process with sediment-laden flow are suggested.

REFERENCES

1. Ab. Ghani, A. and Nalluri, C. (1996). "Development of pier-scour equations using field data." Proc., Tenth Congress-Asian and Pacific Division of IAHR, Longkawi Island, Malaysia, Vol.1, pp295-302.
2. Arora, A.K., Ranga Raju, K.G. and Garde, R.J. (1986). "Resistance to flow and velocity distribution in rigid boundary channels carrying sediment laden flow", Journal of Water Resources Research, Vol.22, No.6, pp943-951.
3. Barkdoll, B.D., Ettema, R. and Odgaard, A.J. (1999). "Sediment control at lateral diversions: limits and enhancements to vane use", Journal of Hydraulic Engineering, ASCE, Vol.125, No.8, pp862-870.
4. Barkdoll, B. (1999). Discussion on the paper "Experimental investigation of flow past submerged vanes" by Marelius, F. and Sinha, S. K. (1998), Journal of Hydraulic Engineering, ASCE, Vol.125, No.8, pp896-898.
5. Bathurst, James C., Thorne, Collin R. and Hey, Richard D. (1979). "Secondary flow and shear stress at River bends", Journal of Hydraulic Division, ASCE, Vol. 105, No. HY10, pp1277-1295.
6. Best, J. L. and Bristow, C.S. (Editors), "Braided Rivers", Geological Society Special Publication No. 75.
7. Bettess, R. (1995). Discussion on the paper "Sediment feed and recirculating flumes: Fundamental difference", by Parker, G.(1993), Journal of Hydraulic Engineering, ASCE, Vol.121, No.3, pp-292-293.
8. Chiew, Y.M. (1992). "Scour protection at bridge piers" Journal of Hydraulic Engineering, ASCE, Vol. 118, No. 9, pp1260-1269.

9. Garde, R. J. Subramanya, K. and Nambudripad, K.D. (1961). "Study of scour around spur-dikes", Journal of Hydraulic Division, ASCE, Vol.87, No. HY6, pp23-37.
10. Garde, R. J. and Mirajagaoker, A.G. (1983). "Engineering Fluid Mechanics", Nem Chand and Bros. Roorkee, India.
11. Garde, R. J. and Ranga Raju, K.G. (1985). "Mechanics of Sediment Transportation and Alluvium Stream Problems", Second Edition, Willey Eastern Limited, New Age International Publishers Limited, New Delhi (India).
12. Garde, R. J., Subramanya, K. and Nambudripad, K.D. (1963). Closure on the paper "Study of scour around spur-dikes", Journal of Hydraulic Division, ASCE, Vol.89, No. HY 1, pp167-175.
13. Graf, W.H. (1998). "Fluvial Hydraulics: Flow and transport process in channels of simple geometry, in collaboration with M.S.Altinakar, John Wiley & Sons (England).
14. Gugten, C.A. van der (1982). Discussion on the paper. "Scour around bridge piers at high flow velocities" by Jain, S.C. and Fischer, E. E. (1980), Journal of Hydraulic Division, ASCE, Vol. 108, No. HY2, pp292-298.
15. Guy, B.T., Dickinson W.T. and Rudra, R.P. (1992). "Comparison of fluvial sediment transport equations as applied to shallow overland flow", Transactions of the ASAE, Vol.35, No.2, pp545-555.
16. Holmes, Pat, Baldock, Tom (1999). "Seepage effects of sediment transport by waves and currents" In: Elsevier 26th International Conference on Coastal Engineering, Copenhagen Denmark, Vol.3, pp3601-3614.

17. Housner, G.W. and Hudson, D.E. "Applied Mechanics Dynamics", Second Edition, D. Van Nostrand Company, Inc. Princeton, New Jersey.
18. Jain, S.C. (1981). "Maximum clear-water scour around circular piers", Journal of Hydraulic Division, ASCE, Vol.107, No. HY5, pp611-626.
19. Jain, S.C. and Fischer, E. E. (1980). "Scour around bridge piers at high flow velocities". Journal of Hydraulic Division, ASCE, Vol.106, No. HY11, pp1827-1842.
20. Jansen, P. Ph. et al. (1979). "Principles of River Engineering", Pitman Publishing Limited, London, U.K.
21. Johnson, P.A., Hey, R.D., Tessier, M. and Rosgen, D.L. (2001). "Use of vanes for control of scour at vertical wall abutments", Journal of Hydraulic Engineering, ASCE, Vol.127, No.9, pp772-778.
22. Kala, N.M. (1974). "Analysis of resistance to flow in open channels with artificial roughness elements", M.E. Dissertation, University of Roorkee, India.
23. Kumar, V., Ranga Raju, K.G. and Vittal, N. (1999). "Reduction of local scour around bridge piers using slots and collars", Journal of Hydraulic Engineering, ASCE, Vol.125, No.12, pp1302-1305.
23. Lauchlen, C. S. and Melville, B. W. (2001). "Riprap protection at bridge piers", Journal of Hydraulic Engineering, ASCE, Vol.127, No.5, pp412-418.
24. Lauren, E. (1992). Discussion on the paper, "Sediment management with submerged Vanes. II: Applications" by Odgaard, A.J. and Wang, Y. (1991), Journal of Hydraulic Engineering, ASCE, Vol.118, No.5, pp827-828.

- 26 Laursen, M. (1963). "An analysis of Relief bridge scour", Journal of Hydraulic Division, ASCE, Vol.89, No. HY3, pp93-118.
- 27 Manandhar, P.K. (1999). "Experimental investigation of submerged vanes as anti bank erosion measures", M.E. Dissertation, University of Roorkee, India.
- 28 Manual on "River behaviour management and training" C.B.I.P. publication No. 204 Vol. I and II (1989).
- 29 Marelius, F. (2001). "Vane applications and induced flow", Ph.D. Thesis, Royal Institute of Technology, Stockholm, Sweden.
- 30 Marelius, F. and Sinha, S.K. (1998). "Experimental investigation of flow past submerged vanes", Journal of Hydraulic Engineering, ASCE, Vol.124, No.5, pp542-545.
- 31 Marelius, F. and Sinha, S.K. (1999). Closure on the paper "Experimental investigation of flow past submerged vanes", Journal of Hydraulic Engineering, ASCE, Vol.125, No.8, pp898-899.
- 32 Melville, B.W. (1997). "Pier and abutment scour: integrated approach", Journal of Hydraulic Engineering, ASCE, Vol.123, No.2, pp125-136.
- 33 Melville, B.W. and Chiew, Y.M. (1999). "Time scale for local scour at bridge piers", Journal of Hydraulic Engineering, ASCE, Vol.125, No.1, pp59-65.
- 34 Melville, B.W. and Sutherland, A.J. (1988). "Design method for local scour at bridge piers", Journal of Hydraulic Engineering, ASCE, Vol.114, No.10, pp1210-1226.
- 35 Modi, P.N. and Seth, S.M. (1989). "Hydraulics and Fluid Mechanics", Ninth edition, Standard Book House, Delhi (India).

- 36 Muste, N. and Patel, V.C. (1997). "Velocity profiles for particles and liquid in open-channel flow with suspended sediments", *Journal of Hydraulic Engineering*, ASCE, Vol.123, No.9, pp742-751.
- 37 Nakato, T., Kennedy, J.F. and Baurely, D. (1990). "Pump-station intake-shoaling control with submerged vanes", *Journal of Hydraulic Engineering*, ASCE, Vol.116, No.1, pp119-128.
- 38 Neill, C.R. and Chaplin, T.K. (1962). Discussion on the paper "Study of Scour around spur-dikes" by Garde, R.J., Subramanya, K. and Nambudripad, K.D. (1961), *Journal of Hydraulic Division*, ASCE, Vol.88, No. HY2, pp191-192.
- 39 Odgaard A.J. (1982). "Bed characteristics in alluvial channel bends", *Journal of Hydraulic Division*, ASCE, Vol.108, No.HY11, pp1268-1281.
- 40 Odgaard, A.J. (1981). "Transverse bed slope in alluvial channel bends", *Journal of Hydraulic Division*, Vol.107, No.HY12, pp1677-1694.
- 41 Odgaard, A.J. (1986a). "Meander flow model. I: Development", *Journal of Hydraulic Engineering*, ASCE Vol.112, No.12, pp1117-1136.
- 42 Odgaard, A.J. (1986b). "Meander flow model II: Applications", *Journal of Hydraulic Engineering*, ASCE, Vol.112, No.12, pp1137-1150.
- 43 Odgaard, A.J. (1989b). "River-meander model. II: Applications", *Journal of hydraulic Engineering*, ASCE, Vol.115, No.11, pp1451-1464.
- 44 Odgaard, A.J. (1989a). "River-meander model. I: Development", *Journal of Hydraulic Engineering*, ASCE, Vol.115, No.11, pp1433-1450.
- 45 Odgaard, A.J. and Kennedy, J.F. (1983). "River-bend bank protection by submerged vanes", *Journal of Hydraulic Engineering*, ASCE, Vol.109, No.8, pp1161-1173.

- 46 Odgaard, A.J. and Mosconi, C.E. (1987).“Stream bank protection by Submerged vanes”, Journal of Hydraulic Engineering, ASCE, Vol.113, No.4, pp520-536.
- 47 Odgaard, A.J. and Spoljaric, A. (1986).“Sediment Control by submerged vanes” Journal of hydraulic engineering, ASCE, Vol.112, No.12, pp1164-1181.
- 48 Odgaard, A.J. and Wang, Y. (1992). Closure on the paper “Sediment management with submerged vanes II: Applications”. Journal of Hydraulic Engineering, ASCE, Vol.118, NO.5, pp828-830.
- 49 Odgaard, A.J. and Wang, Y. (1991).“Sediment management with submerged vanes. I: Theory” Journal of Hydraulic Engineering, ASCE, Vol.117, No.3, pp267-283.
- 50 Odgaard, A.J. and Wang, Y. (1991).“Sediment management with submerged vanes. II: Applications”, Journal of Hydraulic Engineering, ASCE, Vol.117, No.3, pp284 -302.
- 51 Osman, A.K. and Thorne, C.R. (1988).“Riverbank stability analysis. I: Theory”, Journal of Hydraulic Engineering, ASCE, Vol.114, No.2, pp134 -150.
- 52 Parker, G. (1993).“Sediment feed and recirculating flumes: Fundamental difference”, Journal of Hydraulic Engineering, ASCE, Vol.119, No.11, pp1192-1204.
- 53 Parker, G. and Wilcock, R. (1995). Closure on the paper “Sediment feed and recirculating flumes: Fundamental difference” by Parker, G. (1993), Journal of Hydraulic Engineering, ASCE, Vol.121, No.3, pp293-294.

- 54 Posey, C.J. (1994). "Tests for scour protection for bridge piers", Journal of Hydraulic Division, ASCE, Vol.100, No.HY12, pp1773-1783.
- 55 Quick, M.C. (1990). "Analysis of spiral vortex and vertical slot vortex drop shafts", Journal of Hydraulic Engineering, ASCE, Vol.116, No.3, pp309-325.
- 56 Ranga Raju, K.G. (1981). "Flow through open channel", Tata McGraw Hill Publishing Company Ltd., New Delhi, India.
- 57 Raudkivi, A.J. (1986). "Functional trends of scour at bridge piers", Journal of Hydraulic Engineering, ASCE Vol.112, No.1, pp1-13.
- 58 Remillieux, M. (1970). Unpublished general report on "Brahmaputra river training investigation", French Technical Cooperation with India, Economic Commission for Asia and the Far East, National Hydraulics Laboratory, 6 Quai Watier-78, Chatou - France.
- 59 Report (Unpublished) on "Method of transverse circulation completments relative to the surface panels" by Department laboratoire national D'Hydraulique, 6 Quai Watier-Chatou-(Seine et Dise), November,1962
- 60 Richards, K. (1982). "Rivers", Methuen and Co. Ltd., London, UK.
- 61 Shah, S.R. (2002). "Study of scour around permeable spurs", Ph.D. Thesis, Indian Institute of Technology, Roorkee (India).
- 62 Shen, H.W., Schneider, V.R. and Karaki, S. (1969). "Local scour around bridge piers", Journal of Hydraulic Division, ASCE, Vol. 95, No.HY6, pp1919-1940.
- 63 Shethy, A.V.N. (1996). "Computerised Design of Iowa vanes for river bank protection", M.E. Special problem, University of Roorkee, India.

- 64 Singh, C.P., Setia, B. and Verma, D.D.S.(2000).“Effect of collar sleeve combination on scour around a circular pier”, International conference on Recent Advances in Hydraulics and Water Resources Engineering, HYDRO 2000.
- 65 Sinha, A.K. (1993).“Comparative study of solid and permeable spurs”, M.E. Dissertation, University of Roorkee, India.
- 66 Sinha, S.K. and Marelius, F. (2000).“Analysis of flow past submerged vanes”, Journal of Hydraulic Research, IAHR, Vol.38, No.1, pp65-71.
- 67 Stevens, M.A., Gasser, M.M. and Saad, M.B.A. (1991).“Wake vortex scour at bridge piers”, Journal of Hydraulic Engineering, ASCE, Vol.117, No.7, pp891-904.
- 68 Streeter, V.L. (1962).“Fluid Mechanics”, Third Edition, McGraw-Hill book Company, INC.
- 69 Swamee, P.K. and Mittal, M.K. (1976).“An explicit equation for critical shear stress in alluvial streams”, Journal of Irrigation and Power, CBIP, April, pp237-239.
- 70 Swamee, P.K. and Ojha, C.S.P. (1991).“Bed-load and suspended-load transport of nonuniform sediments”, Journal of Hydraulic Engineering, ASCE, Vol.117, No.6, pp774-787.
- 71 Thorne, C.R. and Osman, A.M. (1988).“Riverbank stability analysis. II: Applications”, Journal of Hydraulic Engineering, Vol.114, No.2, pp151-172.
- 72 Umbrell, E.R., Young, G.K., Stein, S.M., and Jones, J.S. (1998),“Clear-Water contraction scour under bridges in pressure flow”. Journal of Hydraulic Engineering, ASCE, Vol. 124, No.2, pp236-240.

- 73 Vittal, N., Kothiyari, U.C. and Haghghat, M. (1994).“Clear-water scour around bridge pier group”, Journal of Hydraulic Engineering, ASCE, Vol.120, No.11, pp1309-1318.
- 74 Wang, Y. and Odgaard, A.J. (1993).“Flow control with vorticity”, Journal of Hydraulic Research, IAHR, Vol.31, No.4, pp549-562.
- 75 Wang, Y., Odgaard, A.J., Melville, B.W. and Jain, S.C. (1996).“Sediment control at water intakes”, Journal of Hydraulic Engineering, ASCE, Vol.122, No.6, pp353-356.
- 76 Yeh, Keh-chia and Kennedy, J.F. (1993).“Moment model of nonuniform channel-bend flow. I: Fixed beds”, Journal of Hydraulic Engineering, ASCE, Vol.119, No.7, pp776-795.
- 77 Yeh, Keh-Chia and Kennedy, J.F. (1993).“Moment model of nonuniform channel bend flow II: Erodible beds”, Journal of Hydraulic Engineering, ASCE, Vol.119, No.7, pp796-815.
- 78 Zimmermann, C. and Kennedy, J.F. (1978).“Transverse bed slopes in curved alluvial streams”, Journal of Hydraulic Division, ASCE, Vol.104, No.HY1, pp33-48.

**COST COMPARISON OF RIPRAP WITH FILTER
VIS A VIS COLLAR**

This Appendix contains the cost comparison riprap with filter vis a vis collar at $F_r = 0.13$ and 0.25 with median size of sediment 0.225mm . A sample of computation of maximum collar area corresponding to the cost of riprap with filter is presented for rectangular vane at $F_r = 0.13$ and median size of sediment as 0.225 mm .

A.1 COMPUTATIONS RELATED TO FROUDE NUMBER 0.13

Using Tables 4.2 and 4.3 of Chapter 4,

For $F_r = 0.13$ and $d_{50} = 0.225\text{ mm}$,

$R_1 = 7.7\text{ cm}$, $R_2 = 0.4 R_1 = 3.1\text{ cm}$, $h_1 = 3.5\text{ cm}$ and

$$h_2 = \frac{h_1 R_2}{R_1 - R_2} = 2.4\text{ cm.}$$

$$l_1 = \sqrt{(h_1 + h_2)^2 + R_1^2} = 9.7\text{ cm}$$

$$l_2 = \sqrt{h_1^2 + R_2^2} = 3.9\text{ cm}$$

From eq. 4.14,

$$\text{Vol}_{os} = \frac{1}{3} \{ R_1^2 (h_1 + h_2) - R_2^2 h_2 \} = 342.2\text{ cm}^3$$

From eq. 4.18

$$A_r = \pi (R_1 l_1 - R_2 l_2) + \pi R_2^2 = 226.9\text{ cm}^2$$

From eq. 4.16 and prevailing rate r_r , Rs.1,000/m³ at Roorkee

$$C_r = \text{Vol}_s r_r = \text{Rs.}0.34$$

From eq. 4.17 and prevailing rate r_f , Rs.35/m² at Roorkee

$$C_f = A_f r_f = \text{Rs. } 0.79$$

From eq. 4.15

$$C_{rf} = C_r + C_f = \text{Rs. } 1.13$$

From eq. 4.13 and prevailing rate r_s , Rs.20,000/m³ at Roorkee

$$C_c = r_s \gamma_s \text{Vol}_c$$

or,

$$\text{Vol}_c = \frac{C_c}{r_s \gamma_s} = 7.197 \times 10^{-6} \text{ m}^3$$

From eq. 4.12 and t , 0.4 mm

$$\text{Vol}_c = t A_c$$

$$A_c = \frac{\text{Vol}_c}{t} = 180 \text{ cm}^2$$

The net area (excluding the area of groove for vane) of most effective collar size AF1.8 or BF1.14 is 25.76 cm², whereas the maximum permissible area from the above computations is 180 cm²; hence the application of collar as scour retarder for submerged vane is more economical than riprap with filter.

EXPERIMENTAL DATA RELATING TO PERFORMANCE EVALUATION OF SUBMERGED VANES WITH COLLAR

This Appendix contains the experimental data collected in River Engineering Laboratory, Water Resources Development Training Centre, Indian Institute of Technology Roorkee, India. The data presented here have been used in Chapter 5 of this thesis. The Fig. B.1 indicates the sign convention and axes.

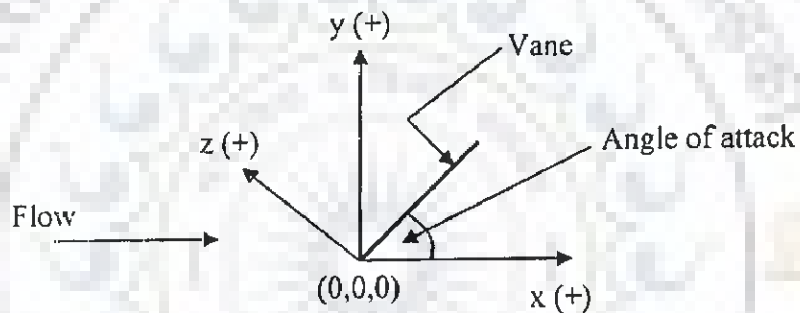


Fig. B.1 Definition sketch of origin for measurement of scour pattern

Origin = leading edge of vane at initial bed level

Table B.1: Experimental data for rectangular vane
 ($F_r = 0.13$, $d_{50} = 0.225$ mm, Collar size AF1.1)

I			II			III		
x	y	z	x	y	z	x	y	z
(cm)	(cm)	(cm)	(cm)	(cm)	(cm)	(cm)	(cm)	(cm)
-4	-3	-0.05	4	-2	-0.55	14	-4	-0.1
-4	-1	-0.7	4	0	-0.2	14	-2	-0.05
-4	1	-1.15	4	2	0.6	14	0	-0.2
-4	3	0	4	2.5	0.65	14	2	-0.35
-2	-5	-0.2	4	4	0.15	14	4	-0.2
-2	-3	-1.15	6	-6	-0.1	14	6	0.4
-2	-1	-2.1	6	-4	0.7	14	8	1.2
-2	-1	-2.15	6	-2	0.5	14	11	0.4
-2	3	-1.1	6	0	0.5	14	12	-0.2
-2	5	0.05	6	2	1.4	14	14	0.1
-1	-6	-0.1	6	4	1.7	16	-8	0.1
-1	-4	-1	6	6	0.15	16	-6	0.35
-1	-2	-2	8	-6.5	-0.1	16	-4	0.25
-1	-1	-2.55	8	-5	-0.4	16	-2	-0.1
-1	0	0.1	8	-3	0.25	16	0	-0.85
-1	1.5	-2.35	8	-1	0.5	16	1	-1.1
-1	3	-1.2	8	1	0.75	16	4	-0.85
-1	5	0	8	3	1.6	16	6	-0.1
0	-6	-0.1	8	5.5	1.8	16	8	-0.55
0	-4	-0.8	8	7	0.1	16	10	0.8
0	-2	-2.15	10	-7.5	-0.15	16	12	-0.4
0	-1	-2.3	10	-6	-0.9	16	14	0.05
0	0	-2.1	10	-4	-1.15	18	-9	-0.1
0	1	-2.4	10	-2	-0.6	18	-6	-0.1
0	2	-1.65	10	0	0.05	18	-3	-0.1
0	4	0.05	10	2	0.5	18	-1	-0.2
1	-5.5	0.05	10	4	1.15	18	1	-0.3
1	-5	-0.5	10	6	1.7	18	3	0.05
1	-3	-1.3	10	7.5	1.3	18	5	0.1
1	-2	-1.9	10	9	0.14	18	7	0.1
1	-1	-1.8	12	-8.5	-0.2	18	9	0.15
1	0	-1.5	12	-7	-0.8	18	10.5	0.45
1	1	-1.7	12	-5	-1.5	18	12	-0.4
1	2	-1.1	12	-4	-1.5	18	14	-0.85
1	4	0.1	12	-2	-1	18	16	-0.05
2	-6.5	0.1	12	0	-0.4	18	18	-2.9
2	-5	-0.25	12	2	0.4	21	8	0.1
2	-3	-1	12	4	0.95	21	10	0.15
2	-0.5	-1	12	6	1.4	21	12	0.3
2	1	-0.5	12	8	1.45	21	14	0.05
2	3	-0.1	12	9	0.7	21	16	0.3
2	5	0.1	12	11	0.15	21	18	0.5
4	-6	-0.1	14	-8	-0.1	21	20	0.1
4	-4	0.4	14	-6	-0.5			

Table B.2: Experimental data for rectangular vane
 ($F_r = 0.13$, $d_{50} = 0.225$ mm, Collar size AF1.2)

I			II			III		
x (cm)	y (cm)	z (cm)	x (cm)	y (cm)	z (cm)	x (cm)	y (cm)	z (cm)
-2	-3	0	6	2	1.55	18	-4	0.55
-2	-2	-0.2	6	4	0.5	18	-2	0.4
-2	-1	-0.55	6	5	0.25	18	0	-0.2
-2	0	0	6	7	0.15	18	2	-1
-2	0.5	-0.4	8	-6.5	0	18	4	-0.9
-2	1	-0.2	8	-5	-0.1	18	6	0.4
-2	2	0.1	8	-3	0	18	8	1.25
-1	-3	-0.2	8	-1	0.05	18	9	1.45
-1	-2	-0.65	8	1	0.55	18	11	0.1
-1	-1.5	-0.7	8	3.5	1.45	20	-5	0.1
-1	-1	-0.7	8	5	0.7	20	-3	0.15
-1	-0.5	-0.45	8	7	0.25	20	-1	-0.4
-1	0	0.2	8	9	0.15	20	1	-1.05
-1	0.5	-0.25	10	-7	-0.1	20	3	-0.9
-1	1	-0.4	10	-5	-0.4	20	5	-0.2
-1	2	-0.35	10	-3	-0.1	20	7	0.5
-1	3	0.1	10	-1	0.3	20	8.5	1.1
0	-4	-0.15	10	1	0.7	20	10	0.4
0	-3	-0.7	10	3	0.9	20	12	0.1
0	-2.5	-0.75	10	5	0.9	22	-3	0.1
0	-2	-0.8	10	7	0.7	22	-1	-0.1
0	-1.5	-0.65	10	9	0.35	22	1	-0.2
0	-1	-0.35	10	11	0.15	22	3	-0.05
0	0	0.05	12	-8	-0.1	22	5	0.2
0	1	0	12	-6	-1.2	22	7	0.5
0	2	-1.15	12	-4	-1.1	22	8.5	0.75
0	2.5	-0.3	12	-2	-0.5	22	9	0.4
0	3	-0.2	12	0	0	22	11	0.2
0	3.5	0.1	12	2	0.3	22	13	0.15
0	4	0.1	12	4	0.6	24	-2	0.15
1	-5	-0.2	12	6	0.8	24	0	0.2
1	-4	-0.7	12	8	1.1	24	2	0.3
1	-3	-0.8	12	9	0.6	24	4	0.4
1	-2	-0.55	12	11	0.3	24	6	0.1
1	0	0.1	12	13	0.2	24	8	0.21
1	1	0.1	14	-8.5	0	24	10	0.2
1	2.5	0.1	14	-7	-0.9	24	12	0.1
1	3	0.1	14	-5	-1.45	26	-2	0.2
1	4	0.1	14	-4	-1.55	26	0	0.2
2	-5.5	-0.2	14	-2	-0.9	26	2	-0.15
2	-5	-0.6	14	0	-0.5	26	4	-0.4
2	-4	-1.1	14	2	0.3	26	5	-0.35
2	-3	-0.7	14	4	0.35	26	8	0.15
2	-2	-0.3	14	6	0.55	26	9	0.25
2	-1	-0.2	14	8	1.1	26	11	0.4
2	0	0.15	14	10	0.7	26	13	0.15
2	1	0.6	14	12	0.25	28	-2	0.1
2	2	0.15	14	14	0.1	28	0	-0.75
2	3	0.2	16	-8	0	28	2	-0.1
4	-6.5	-0.1	16	-6	-0.1	28	4	0.1
4	-5	-1.05	16	-4	-0.2	28	6	0.15
4	-3.5	-1.5	16	-2	0	28	8	0.25
4	-2	-0.7	16	0	-0.3	28	10	0.6
4	0	0.2	16	2	-0.4	28	12	0.1
4	1.5	1.1	16	4	0	30	-2	0.1
4	2.5	0.65	16	6	0.6	30	0	0.2
4	4	0.25	16	8	0.85	30	2	0.2
4	6	0.15	16	10	1	30	4	0.2
6	-7	-0.1	16	12	0.2	30	6	0.2
6	-5	-0.6	16	14	0.2	30	8	0.2
6	-3	-1.15	18	-9.5	0	30	10	0.15
6	-2	-1.2	18	-8	0.4	30	12	0.15
6	0	0.05	18	-6	0.5			

Table B.3: Experimental data for rectangular vane
 $(F_r = 0.13, d_{50} = 0.225 \text{ mm}, \text{Collar size AF1.3})$

I			II			III		
x (cm)	y (cm)	z (cm)	x (cm)	y (cm)	z (cm)	x (cm)	y (cm)	z (cm)
-3	-3	0.05	2	2.5	-0.35	13	0	0.35
-3	-1	-0.2	2	3.5	0.1	13	2	0
-3	0	-0.1	2	4.5	0.25	13	4	0.1
-3	1	0	2	5.5	0.25	13	6	0.6
-3	2	0.1	3	-7	0	13	8	1.3
-3	3	0.1	3	-6	-0.35	13	10	0.35
-3	4	0.15	3	-5	-1	13	12	0.3
-2	-3	0	3	-4	-0.9	13	14	0.3
-2	-1	-0.45	3	-3	-1.2	15	-8	0
-2	0	-0.4	3	-2	-0.8	15	-6	0.35
-2	1	-0.3	3	-1	-0.2	15	-4	0.5
-2	2	-0.1	3	0	0.35	15	-2	0.2
-2	4	0.2	3	1	1	15	0	-0.3
-1	-3.5	0	3	2	0.95	15	2	-0.1
-1	-3	-0.3	3	3	0.35	15	4	0.35
-1	-2	-0.5	3	4	0.25	15	6	0.35
-1	-1.5	-0.5	3	5	0.2	15	8	0.85
-1	-1	-0.6	5	-7	0.05	15	9	1.1
-1	0	-0.8	5	-5	-0.9	15	10	0.7
-1	0.5	-0.95	5	-3	-1.4	15	12	-0.05
-1	0.75	-0.9	5	-1	-0.1	15	14	0.2
-1	1.5	-0.8	5	1	1.2	17	-8	0.1
-1	2.5	-0.35	5	2	1.6	17	-6	0.1
-1	3.5	0.1	5	3.5	0.5	17	-4	0.1
-1	4.5	0.25	5	5	0.3	17	-2	-0.3
0	-5	0	5	7	0.3	17	0	-0.45
0	-4	-0.65	7	-7	0.05	17	2	-0.1
0	-2.75	-0.55	7	-5	0	17	4	0.45
0	-2	-1.35	7	-3	-0.7	17	6	0.6
0	-1.5	-0.3	7	-1	-0.35	17	8	0.8
0	-1	-0.3	7	1	1	17	10	0.65
0	-0.5	-0.2	7	2.5	1.4	17	12	0.2
0	0	-0.35	7	4	0.8	17	14	0.2
0	0.5	-0.6	7	5	0.2	19	-3	0.1
0	1	-0.7	7	6	0.3	19	-1	0
0	1.5	-0.9	7	8	0.3	19	1	0.1
0	1.5	-0.95	9	-7	0	19	3	0.1
0	2.5	-0.7	9	-5	0.15	19	5	-0.4
0	3.5	0.1	9	-3	0.5	19	7	0
0	4.5	0.3	9	-1	0.25	19	9	0.7
1	-6	0	9	1	0.25	19	9.75	0.9
1	-5	-0.1	9	3	0.8	19	11	0.35
1	-4	-1.15	9	4.5	1.1	19	13	0.2
1	-3	-0.9	9	6	0.35	21	-2.5	0.2
1	-2.5	-0.6	9	8	0.35	21	-1	-0.05
1	0	0.1	9	10	0.35	21	1	-0.15
1	0.5	0.3	11	-8	0.1	21	3	-0.5
1	2	-0.7	11	-6	-0.9	21	4	-0.5
1	3	-0.3	11	-4	-0.5	21	5	-0.2
1	4	0.35	11	-2	0.1	21	7	0.2
1	5	0.3	11	0	0.45	21	9	0.6
1	6	0.2	11	2	0.55	21	11	0.2
2	-6	-0.05	11	4	0.6	23	-2	0.2
2	-5	-0.45	11	6.5	1.2	23	0	0.2
2	-4	-0.95	11	8	0.9	23	2	0.1
2	-3	-1.25	11	10	0.35	23	4	0.2
2	-2	-0.5	11	12	0.3	23	6	0.25
2	-1.5	-0.45	13	-8	0.05	23	8	0.4
2	-0.5	0.2	13	-6	-0.8	23	10	0.2
2	0.5	0.55	13	-4	-0.75			
2	1	0.95	13	-2	-0.3			

Table B.4: Experimental data for rectangular vane

$(F_r = 0.13, d_{50} = 0.225 \text{ mm}, \text{Collar size AF1.4})$

I			II			III		
x	y	z	x	y	z	x	y	z
(cm)	(cm)	(cm)	(cm)	(cm)	(cm)	(cm)	(cm)	(cm)
-1.5	-6.3	0	5.5	-7.8	0.3	13.5	1.2	-0.45
-1.5	-4.8	-1	5.5	-5.8	0.35	13.5	3.2	-0.2
-1.5	-2.8	-0.95	5.5	-3.8	0	13.5	5.2	0.35
-1.5	-1.3	0.1	5.5	-1.8	-0.45	13.5	7.2	1
-1.5	0.2	0.4	5.5	0.2	0.7	13.5	9.2	1.25
-1.5	2.2	0.2	5.5	2.2	1.35	13.5	10.2	1
0	-6.8	0	5.5	4.2	1.12	13.5	12.2	0.2
0	-4.8	-1.45	5.5	5.2	0.3	13.5	13.7	-0.3
0	-3.8	-1.7	5.5	7.2	0.25	13.5	14.7	0.3
0	-1.8	-0.75	7.5	-7.8	0.1	13.5	16.2	0.3
0	-1.3	-0.2	7.5	-5.8	0.05	15.5	-3.8	0.15
0	0.2	0.2	7.5	-3.8	0.2	15.5	-1.8	-0.1
0	2.2	0.15	7.5	-1.8	-0.1	15.5	0.2	0.35
0	4.2	0.2	7.5	0.2	0.3	15.5	2.2	0.3
1	-7.3	-0.1	7.5	2.2	1.3	15.5	4.2	0.4
1	-5.8	-1.1	7.5	3.7	1.55	15.5	6.2	0.5
1	-3.8	-1.65	7.5	5.7	1.1	15.5	8.2	0.9
1	-2.8	-1.65	7.5	7.2	0.4	15.5	10.2	0.85
1	-1.8	-0.8	7.5	9.2	0.3	15.5	12.2	-0.4
1	-1.3	-0.45	9.5	-8.3	0.1	15.5	14.2	-0.65
1	-0.8	-0.05	9.5	-6.3	-0.7	15.5	16.2	0.3
1	1.2	0.3	9.5	-4.8	-0.4	17.5	-2.8	0.35
1	3.2	0.2	9.5	-2.8	-0.05	17.5	-0.8	0.35
1	5.2	0.2	9.5	-0.8	0.1	17.5	1.2	0.6
2	-7.8	0	9.5	1.2	0.5	17.5	3.2	0.3
2	-5.8	-0.8	9.5	3.2	0.8	17.5	5.2	0.3
2	-3.8	-1.3	9.5	5.7	1.65	17.5	7.2	0.3
2	-2.3	-1.1	9.5	6.7	1.55	17.5	9.2	0.35
2	-1.8	-0.7	9.5	9.2	0.4	17.5	11.2	0.35
2	-1.3	-0.4	11.5	-8.3	0.1	17.5	13.2	-0.6
2	-0.8	-0.5	11.5	-6.8	0.3	17.5	15.2	0.3
2	-0.3	-0.35	11.5	-4.8	0.2	17.5	17.2	0.3
2	2.2	0.2	11.5	-2.8	-0.05	19.5	-2.8	0.2
2	4.2	0.2	11.5	-0.8	-0.2	19.5	-0.8	-0.05
2	6.2	0.3	11.5	1.2	-0.55	19.5	1.2	0.2
3.5	-7.8	0.2	11.5	3.2	-0.3	19.5	3.2	0.3
3.5	-5.8	0	11.5	5.2	0.5	19.5	5.2	0.3
3.5	-3.8	-0.65	11.5	7.2	1.6	19.5	7.2	0.3
3.5	-1.8	-0.5	11.5	8.7	1.1	19.5	9.2	0.3
3.5	0.2	0.39	11.5	10.2	0.35	19.5	11.2	0.6
3.5	2.2	0.9	11.5	12.2	0.35	19.5	13.2	0.3
3.5	3.2	0.3	13.5	-3.8	0.25	19.5	15.2	0.55
3.5	5.2	0.25	13.5	-1.8	-0.7	19.5	17.2	0.3
3.5	7.2	0.3	13.5	-0.8	-0.8			

Table B.5: Experimental data for rectangular vane
 $(F_r = 0.13, d_{50} = 0.225 \text{ mm}, \text{Collar size AF1.5})$

I			II			III		
x (cm)	y (cm)	z (cm)	x (cm)	y (cm)	z (cm)	x (cm)	y (cm)	z (cm)
-3.5	-5.7	0	3.5	-10.7	-0.1	13.5	6.3	-0.3
-3.5	-3.7	0	3.5	-9.7	-0.15	13.5	9.3	1.35
-3.5	-1.7	0	3.5	-7.7	-1.3	13.5	10.9	0.75
-3.5	0.3	0.05	3.5	-5.7	-1.8	13.5	11.8	-0.05
-3.5	0.3	0.1	3.5	-3.7	-1.2	13.5	14.3	0
-2.5	-5.7	-0.05	3.5	-1.7	0	13.5	17.3	0.1
-2.5	-4.7	0	3.5	0.3	0.75	17.5	-12.7	-0.15
-2.5	-3.7	0	3.5	1.3	1.25	17.5	-11.7	-0.1
-2.5	-2.7	-0.2	3.5	2.6	0.9	17.5	-10.7	-0.8
-2.5	-1.7	-0.45	3.5	3.8	0	17.5	-9.7	-1.25
-2.5	-0.7	-0.6	3.5	5.3	0.05	17.5	-8.7	-1.4
-2.5	0.3	-0.65	3.5	7.3	0.1	17.5	-7.7	-1.6
-2.5	1.3	-0.5	5.5	-10.7	-0.1	17.5	-6.7	-1.3
-2.5	2.3	0.1	5.5	-8.7	-1.25	17.5	-5.7	-1
-2.5	3.3	0.1	5.5	-6.7	-1.8	17.5	-4.7	-0.4
-1.5	-6.7	-0.05	5.5	-4.7	-2.3	17.5	-2.7	-0.25
-1.5	-5.7	-0.05	5.5	-2.7	-0.95	17.5	0.3	-0.5
-1.5	-4.7	-0.05	5.5	-0.7	0.15	17.5	3.3	-0.7
-1.5	-3.7	-0.7	5.5	1.8	1.6	17.5	6.3	-0.4
-1.5	-2.7	-0.8	5.5	4.1	0.4	17.5	10.3	0.9
-1.5	-1.7	-0.9	5.5	5.3	0.1	17.5	12.3	-0.2
-1.5	-1	-0.9	5.5	7.3	0	17.5	14.3	-1.1
-1.5	0.9	-0.85	5.5	9.3	0.1	17.5	15.3	-1.35
-1.5	1.8	-0.75	8.5	-11.7	-0.1	17.5	16.3	-1
-1.5	2.8	0.1	8.5	-9.7	-0.4	17.5	17.3	0
-1.5	3.8	0.1	8.5	-7.7	-1	17.5	19.3	0.1
0	-7.7	-0.1	8.5	-5.7	-1.35	21.5	-12.7	-0.2
0	-6.7	-0.15	8.5	-3.7	-1.5	21.5	-10.7	0.2
0	-5.7	-0.75	8.5	-1.7	-1.3	21.5	-7.7	0.35
0	-4.7	-0.8	8.5	0.3	-0.45	21.5	-4.7	0
0	-3.7	-1.4	8.5	2.3	0.6	21.5	-1.7	0.1
0	-2.9	-1.3	8.5	3.8	1.15	21.5	1.3	-0.2
0	-2.2	-0.35	8.5	6.3	0.35	21.5	4.3	-0.2
0	-1.2	-3.5	8.5	8.3	0.1	21.5	7.3	-0.2
0	0	0.05	8.5	10.3	0	21.5	10.3	0.65
0	0.3	0.05	8.5	12.3	0.1	21.5	12.8	1
0	1.3	0.05	11.5	-11.7	-0.15	21.5	14.3	0.15
0	2.1	-0.3	11.5	-8.7	0.1	21.5	16.3	-0.2
0	3.3	0.1	11.5	-5.7	0.1	21.5	18.3	0.4
0	4.3	0.1	11.5	-2.7	-0.1	21.5	19.3	0.3
1.5	-8.7	-0.1	11.5	0.3	-0.35	21.5	21.3	0.1
1.5	-7.7	-0.6	11.5	3.3	-0.25	26.5	-12.7	-0.1
1.5	-6.7	-1	11.5	6.3	0.7	26.5	-9.7	-0.1
1.5	-5.7	-1.15	11.5	8.5	1.7	26.5	-6.7	-0.1
1.5	-4.7	-0.9	11.5	10.3	0.15	26.5	-3.7	-0.2
1.5	-3.7	-1.3	11.5	13.3	0	26.5	-0.7	-0.2
1.5	-3	-1.55	11.5	16.3	0.1	26.5	2.3	-0.15
1.5	-2.2	-1.1	13.5	-11.7	-0.1	26.5	5.3	-0.2
1.5	-1.7	-0.8	13.5	-8.7	-0.2	26.5	8.3	-0.15
1.5	-0.95	-0.4	13.5	-5.7	0.2	26.5	11.3	0.15
1.5	1.9	-0.1	13.5	-2.7	0.3	26.5	14.8	1.25
1.5	3.3	-0.1	13.5	0.3	-0.05	26.5	18.3	0.1
1.5	5.3	0.1	13.5	3.3	-0.55	26.5	21.3	0.1

Table B.6: Experimental data for rectangular vane
 ($F_r = 0.13$, $d_{50} = 0.225$ mm, Collar size AF1.6)

I			II			III		
x	y	z	x	y	z	x	y	z
(cm)	(cm)	(cm)	(cm)	(cm)	(cm)	(cm)	(cm)	(cm)
-4	-6	0	2	-5	-1.8	14	4	0.15
-4	-4	0.05	2	-4	-2.05	14	7	0.55
-4	-2	0.1	2	-3	-1.3	14	10	0.95
-4	0	0.05	2	-2	-0.55	14	12	-0.15
-4	2	0.15	2	-1	0	14	13	-0.25
-3	-5	0.05	2	0	0.3	14	14	0.05
-3	-4	0.05	2	1	0.75	14	15	0.15
-3	-3	0.05	2	2	0.15	14	16	-0.05
-3	-2	0.1	2	3	0.1	14	17	-0.05
-3	-1	0	2	4	0.15	14	18	0.15
-3	0	-0.3	2	5	0.25	17	-11	0.05
-3	1	0.05	2	6	0.15	17	-8	-1.3
-3	2	0.15	4	-9	-0.05	17	-6	-1.05
-2	-5	-0.05	4	-7	-1.05	17	-4	-0.4
-2	-4	0	4	-5	-1.65	17	-1	-0.3
-2	-3	-0.05	4	-3	-1.35	17	2	-0.65
-2	-2	-0.45	4	-1	-0.05	17	5	-1
-2	-1	-0.75	4	1	1.3	17	8	-0.45
-2	0	-0.55	4	2.8	0.85	17	11	0.3
-2	1.4	0.05	4	4	0.2	17	13	-1.15
-2	2	0.25	4	6	0.2	17	15	-1.2
-2	3	0.15	4	8	0.2	17	17	-0.45
-1	-6	0	6	-10	0	17	19	0.15
-1	-5	-0.2	6	-8	-0.5	17	21	0.15
-1	-4	-0.8	6	-6	-0.95	22	-11	0.05
-1	-3	-0.85	6	-4	-1.25	22	-8	0.45
-1	-2	-0.95	6	-2	-0.95	22	-5	0.5
-1	-1	-0.75	6	0	0.25	22	-2	-0.1
-1	0	0.15	6	2	1.4	22	1	-0.6
-1	1	0.15	6	4	0.95	22	4	-0.1
-1	2.2	0.15	6	6	0.25	22	7	0.05
-1	3	0.25	6	8	0.25	22	10	1.05
-1	4	0.2	6	10	0.15	22	11	1.4
0	-7	-0.05	8	-10	0.05	22	13	0.75
0	-6	-0.6	8	-8	-1.2	22	15	0.2
0	-5	-1.35	8	-6	-0.85	22	17	0.5
0	-4	-1.2	8	-4	-0.45	22	19	0.55
0	-3	-1.15	8	-2	-0.35	22	21	0.1
0	-2	-0.85	8	0	0.15	22	23	0.15
0	-1	0.15	8	2	1.05	26	-7	-0.05
0	0	0.15	8	4	1.3	26	-4	-0.1
0	3	0.3	8	6	1.05	26	-2	-0.75
0	4	0.25	8	7	0.2	26	0	-0.85
0	5	0.25	8	9	0.25	26	2	0.05
0	6	0.15	8	11	0.15	26	4	0.15
1	-8	-0.05	10	-10	0.15	26	7	-0.1
1	-7	-0.2	10	-8	-1.05	26	10	0.25
1	-6	-1.05	10	-6	-1.7	26	12	0.4
1	-5	-1.7	10	-4	-0.85	26	14	0.65
1	-4	-1.55	10	-2	-0.45	26	16	0.15
1	-3.4	-1.3	10	0	-0.25	26	18	0.15
1	-3	-1.15	10	2	0.35	26	20	0.15
1	-2	-0.75	10	4	1.25	30	-7	-0.05
1	0	0.15	10	6	1.8	30	-4	0.35
1	2	0.05	10	8	2.25	30	-1	0.2
1	3	0.15	10	9	0.35	30	2	0.05
1	4	0.3	10	11	0.25	30	6	-0.1
1	5	0.25	10	13	0.15	30	10	0.05
1	6	0.2	14	-11	0.05	30	12	0.25
2	-9	0	14	-8	0.1	30	14	0.25
2	-8	-0.05	14	-5	0.2	30	16	0.4
2	-7	-0.7	14	-2	0.25	30	18	0.35
2	-6	-1.25	14	1	0.15	30	20	0.15

Table B.7: Experimental data for rectangular vane
 ($F_r = 0.13$, $d_{50} = 0.225$ mm, Collar size AF1.7)

I			II			III		
x	y	z	x	y	z	x	y	z
(cm)	(cm)	(cm)	(cm)	(cm)	(cm)	(cm)	(cm)	(cm)
-3	-3.9	0	4.5	0.1	1.05	16.5	3.1	-1.35
-3	-1.9	-0.1	4.5	1.1	1.4	16.5	6.1	-1.1
-3	0.1	-0.2	4.5	2.8	0.7	16.5	9.7	0.4
-3	2.1	0	4.5	4.1	0.1	16.5	11.1	-0.4
-2	-4.9	-0.1	4.5	6.1	0.1	16.5	13.1	-1.7
-2	-3.9	0	4.5	8.1	0.05	16.5	14.1	-1.85
-2	-2.9	-0.1	7.5	-10.9	-0.2	16.5	15.1	-1.75
-2	-1.9	0	7.5	-8.9	-1.15	16.5	16.1	-1.1
-2	-0.9	0	7.5	-6.9	-1.7	16.5	17.1	-0.6
-2	0.1	0	7.5	-4.9	-2	16.5	18.1	-0.05
-2	1.1	-0.4	7.5	-2.9	-1.7	16.5	19.1	0
-2	2.1	-0.1	7.5	-0.9	-0.6	19.5	-11.9	-0.2
-2	3.1	0.05	7.5	1.1	0.5	19.5	-9.4	-0.9
-1	-5.9	0	7.5	4.1	1.5	19.5	-6.9	-0.6
-1	-4.9	-0.1	7.5	5.1	1.5	19.5	-3.9	-0.8
-1	-3.9	-0.05	7.5	7.1	0.1	19.5	-0.9	-1.2
-1	-1.9	0	7.5	9.1	0	19.5	2.1	-1.45
-1	0.1	0	10.5	-10.9	-0.2	19.5	5.1	-1.15
-1	1.75	-0.28	10.5	-8.9	-0.65	19.5	8.1	-0.1
-1	2.6	-0.05	10.5	-6.9	-1.05	19.5	9.3	0.4
-1	3.6	0	10.5	-4.9	-1.2	19.5	11.1	-0.2
0.5	-6.9	-0.05	10.5	-2.9	-1.4	19.5	13.1	-1.1
0.5	-5.9	-0.05	10.5	-0.9	-1.3	19.5	15.1	-0.5
0.5	-4.9	-0.1	10.5	1.1	-0.95	19.5	17.1	0.4
0.5	-4	-0.2	10.5	3.1	-0.1	19.5	19.1	0.25
0.5	-0.5	-0.2	10.5	5.1	0.85	19.5	21.1	0
0.5	0.1	0	10.5	8.1	1.6	25.5	-9.9	-0.2
0.5	1.1	0	10.5	9.6	0.1	25.5	-6.9	0.1
0.5	2.1	-0.4	10.5	11.1	0	25.5	-3.9	0
0.5	3.1	-0.05	10.5	13.1	0	25.5	-0.9	0
0.5	4.1	0.1	13.5	-11.9	-0.2	25.5	2.1	-0.1
0.5	6.1	0.05	13.5	-9.9	0	25.5	5.1	-0.2
2.5	-8.9	-0.2	13.5	-6.9	-0.1	25.5	8.1	0.3
2.5	-7.9	-0.2	13.5	-3.9	-0.2	25.5	11.2	1.8
2.5	-6.9	-0.8	13.5	-0.9	-0.5	25.5	13.1	0.9
2.5	-5.9	-1	13.5	2.1	-0.7	25.5	15.1	0.25
2.5	-4.9	-1.25	13.5	5.1	-0.5	25.5	19.1	0
2.5	-3.9	-0.7	13.5	8.1	0.6	30.5	-10.9	-0.1
2.5	-2.9	-0.45	13.5	9.1	1	30.5	-6.9	-0.1
2.5	-0.9	0.1	13.5	11.1	-0.1	30.5	-2.9	-0.3
2.5	0.1	0.6	13.5	12.1	-0.85	30.5	1.1	-1
2.5	1.1	0.75	13.5	13.1	-1.2	30.5	5.1	-1.2
2.5	2.1	-0.15	13.5	14.1	-1.1	30.5	9.1	-0.4
2.5	3.1	-0.1	13.5	15.1	-0.8	30.5	12.2	0.9
2.5	4.1	-0.05	13.5	16.1	-0.1	30.5	13.1	0.45
2.5	5.1	0.3	13.5	17.1	-0.05	30.5	14.1	0.3
2.5	6.1	0.05	13.5	19.1	0	30.5	15.1	0.1
4.5	-9.9	-0.15	16.5	-11.9	-0.2	30.5	16.1	0.2
4.5	-7.9	-1.2	16.5	-8.9	-0.1	30.5	17.1	-0.1
4.5	-5.9	-1.75	16.5	-5.9	-0.6	30.5	18.1	-0.1
4.5	-3.9	-1.45	16.5	-2.9	-0.6	30.5	20.1	0
4.5	-1.9	-0.4	16.5	0.1	-1			

Table B.8: Experimental data for rectangular vane

($F_r = 0.13$, $d_{50} = 0.225$ mm, Collar size AF1.8)

I			II			III		
x	y	z	x	y	z	x	y	z
(cm)	(cm)	(cm)	(cm)	(cm)	(cm)	(cm)	(cm)	(cm)
-4.5	-7.5	-0.05	4.5	1.5	0.53	11.5	13.5	-0.19
-4.5	-4.5	0.03	4.5	3.5	0.11	11.5	16.5	-0.17
-4.5	-1.5	0.04	4.5	4.5	0.11	15.5	-7.5	-0.16
-4.5	1.5	0.03	4.5	7.5	0.11	15.5	-4.5	-0.39
-4.5	4.5	0.11	4.5	10.5	0.02	15.5	-1.5	-0.69
-4.5	7.5	0.04	4.5	13.5	-0.05	15.5	1.5	-0.65
-4.5	10.5	0.04	7.5	-7.5	-0.09	15.5	4.5	0.11
-1.5	-7.5	-0.09	7.5	-4.5	-0.04	15.5	7.5	0.11
-1.5	-4.5	-0.04	7.5	-1.5	-0.45	15.5	9.5	0.61
-1.5	3.5	-0.06	7.5	1.5	0.32	15.5	12.5	-0.5
-1.5	6.5	0.05	7.5	3	0.86	15.5	13.5	-0.89
-1.5	9.5	0.03	7.5	6	-0.04	15.5	16.5	-0.26
-1.5	12.5	0.11	7.5	7.2	0.31	19.5	-7.5	-0.17
1.5	-7.5	-0.14	7.5	9.5	0.03	19.5	-4.5	-0.29
1.5	-4.5	-0.29	7.5	12.5	-0.06	19.5	-1.5	-0.39
1.5	0.9	-0.04	7.5	15.5	-0.09	19.5	1.5	-0.29
1.5	2.1	-0.15	11.5	-7.5	-0.38	19.5	4.5	-0.79
1.5	4.5	0.11	11.5	-4.5	-0.37	19.5	7.5	-0.39
1.5	7.5	0.11	11.5	-1.5	-0.29	19.5	10.5	0.51
1.5	10.5	0.02	11.5	1.5	-1.18	19.5	13.5	-0.45
1.5	13.5	0.03	11.5	4.5	-0.39	19.5	14.5	-0.89
4.5	-7.5	-0.16	11.5	7.5	0.86	19.5	17.5	-0.25
4.5	-4.5	-0.26	11.5	9.5	0.41			
4.5	-1.5	-0.35	11.5	10.5	-0.19			

Table B.9: Experimental data for trapezoidal vane (3H:2.5V)
 ($F_r = 0.13$, $d_{50} = 0.225$ mm, Collar size BF1.1)

I			II			III		
x (cm)	y (cm)	z (cm)	x (cm)	y (cm)	z (cm)	x (cm)	y (cm)	z (cm)
-2.5	-3.6	0	7.5	-0.6	-0.7	16.5	19.4	0.2
-2.5	-1.6	0.05	7.5	1.4	-0.6	17.5	-2.6	0.2
-2.5	-0.6	-0.5	7.5	3.4	0	17.5	-0.6	0.3
-2.5	0.4	-0.45	7.5	5.8	1.5	17.5	1.4	0.05
-2.5	1.4	-0.2	7.5	6.9	0.45	17.5	3.4	-0.6
-2.5	2.4	0.1	7.5	9.4	0.45	17.5	5.4	-0.3
-2.5	4.4	0.2	7.5	11.4	0.3	17.5	7.4	0.45
0	-4.6	0	10.5	-7.1	0	17.5	9.4	1.55
0	-3.6	0	10.5	-5.6	0.2	17.5	11.4	0.6
0	-2.6	-0.65	10.5	-3.6	0.1	17.5	13.4	0.8
0	-1.95	-0.85	10.5	-1.6	0	17.5	15.6	0.3
0	-1.6	-1.25	10.5	0.4	-0.2	17.5	17.4	0.2
0	-1.1	-1.6	10.5	2.4	-0.4	17.5	19.4	0.1
0	-0.6	-1.6	10.5	4.4	-0.25	19.5	0.4	0.2
0	0.6	-1.9	10.5	6.4	1	19.5	2.4	0.25
0	0.9	-1.75	10.5	8.4	1.6	19.5	4.4	0.35
0	1.6	-1.3	10.5	9.4	0.45	19.5	6.4	0.6
0	2.4	-0.75	10.5	11.4	0.45	19.5	8.4	1.05
0	3.4	0.05	10.5	13.4	0.3	19.5	10.4	0.6
0	4.4	0.2	13.5	-6.6	0	19.5	12.4	0.6
0	5.4	0.25	13.5	-4.6	-1	19.5	14.4	0.85
1.5	-5.6	0	13.5	-2.6	-0.5	19.5	16.4	-0.05
1.5	-4.4	0	13.5	-0.6	-0.1	19.5	17.2	-0.45
1.5	-3.6	-0.7	13.5	1.4	0.05	19.5	18.4	0.2
1.5	-2.6	-0.7	13.5	3.4	0.1	21.5	0.4	0.15
1.5	-1.6	-0.75	13.5	5.4	0.75	21.5	2.4	-0.55
1.5	-0.6	-0.9	13.5	7.4	1.65	21.5	4.4	-0.45
1.5	0.9	-0.3	13.5	9.7	2.6	21.5	6.4	0.1
1.5	1.8	-0.6	13.5	10.7	2.2	21.5	8.4	0.4
1.5	2.9	-0.2	13.5	12.4	0.45	21.5	10.4	0.7
1.5	3.9	0.3	13.5	16.4	0.2	21.5	12.4	0.2
1.5	5.4	0.2	16.5	-6.6	0.1	21.5	14.4	0.55
4.5	-6.1	0	16.5	-4.6	0.3	21.5	16.4	0.15
4.5	-4.6	-1.2	16.5	-2.6	0.35	21.5	18.4	0.2
4.5	-2	-1.95	16.5	-0.6	0.2	23.5	0.4	0.2
4.5	-0.6	-1.7	16.5	1.4	0.2	23.5	2.4	0.35
4.5	1.4	-0.6	16.5	3.4	-0.4	23.5	4.4	0.3
4.5	3.1	0.4	16.5	5.4	0	23.5	6.4	0.25
4.5	4.25	0.4	16.5	7.4	0.8	23.5	8.4	0.2
4.5	6.4	0.3	16.5	9.8	1.7	23.5	10.4	0.4
4.5	8.4	0.3	16.5	11.4	0.85	23.5	12.4	0.2
7.5	-6.6	0	16.5	13.4	1	23.5	14.4	0.35
7.5	-4.6	-0.35	16.5	15.4	0.4	23.5	16.4	0.15
7.5	-2.6	-0.55	16.5	17.4	0.1	23.5	18.4	0.2

Table B.10: Experimental data for trapezoidal vane(3H:2.5V)
($F_r = 0.13$, $d_{50} = 0.225$ mm, Collar size BF1.2)

I			II			III		
x	y	z	x	y	z	x	y	z
(cm)	(cm)	(cm)	(cm)	(cm)	(cm)	(cm)	(cm)	(cm)
-1.25	-6.7	0	4.75	3	0.4	18.75	-4.7	0.1
-1.25	-4.7	0	4.75	4.3	0.2	18.75	-2.7	-0.1
-1.25	-2.7	0	4.75	6.3	0.1	18.75	-0.7	-0.7
-1.25	-0.7	0.05	4.75	8.3	0.2	18.75	1.3	-0.35
-1.25	1.3	0	7.75	-3.7	0	18.75	3.3	-0.3
0	-8.7	-0.15	7.75	-1.7	0	18.75	5.3	0.1
0	-7.7	0	7.75	0.3	-0.7	18.75	7.3	0.7
0	-6.7	0	7.75	2.3	-0.65	18.75	9.3	0.85
0	-5.7	-0.9	7.75	4.3	0.45	18.75	11.3	0.35
0	-4.7	-1.2	7.75	5.3	1	18.75	13.3	0.4
0	-3.7	-0.8	7.75	7.3	0.2	18.75	15.3	0.35
0	-2.7	-0.8	7.75	9.3	0.1	18.75	17.3	0.2
0	-2.1	-0.5	7.75	11.3	0.2	18.75	19.3	0.1
0	-1.9	-0.55	10.75	-2.7	0	19.75	-3.7	0.1
0	0	0	10.75	-0.7	-0.7	19.75	-1.7	-0.75
0	1.3	0.1	10.75	1.3	-0.4	19.75	-0.5	-0.9
0	2.3	0.1	10.75	3.3	-0.05	19.75	1.3	-0.6
0	4.3	0.1	10.75	5.3	0.65	19.75	4.3	-0.4
1	-7.7	-0.1	10.75	7.3	1.6	19.75	7.3	0.6
1	-6.7	-0.05	10.75	9.3	0.2	19.75	9.1	0.95
1	-5.7	-1.1	10.75	11.3	0.2	19.75	11.3	0.45
1	-4.7	-1.45	13.75	-3.7	0	19.75	14.3	0.6
1	-3.7	-1.25	13.75	-0.7	-0.65	19.75	16.3	0.2
1	-2.7	-1	13.75	0.8	-1.45	19.75	18.3	0.2
1	-2.1	-0.95	13.75	2.3	-1.1	23.75	-3.7	0.6
1	-1.7	-0.8	13.75	4.3	-0.55	23.75	-1.7	-0.4
1	-1	-0.5	13.75	6.3	0.6	23.75	0.3	0.2
1	-0.7	0.1	13.75	8.3	1.8	23.75	3.3	0.35
1	1.3	-0.25	13.75	10.3	1.3	23.75	6.3	0.4
1	2.3	-0.05	13.75	12.3	0.2	23.75	9.3	0.8
1	4.3	0.1	13.75	14.3	0.2	23.75	10.1	0.85
2.75	-6.7	-0.05	16.75	-3.7	0	23.75	13.3	0.2
2.75	-4.7	-0.9	16.75	-1.7	-0.25	23.75	16.3	0.2
2.75	-2.7	-1.2	16.75	0.3	-0.4	23.75	19.3	0.2
2.75	-0.7	-1.2	16.75	2.3	-0.05	25.75	-2.7	0.1
2.75	1.3	-0.2	16.75	4.3	0.2	25.75	0.3	0.2
2.75	3.3	0.1	16.75	6.3	0.6	25.75	3.3	-0.15
2.75	5.3	0.1	16.75	8.7	1.8	25.75	6.3	0.05
4.75	-5.7	0.05	16.75	10.3	0.7	25.75	9.3	0.4
4.75	-3.7	0	16.75	12.3	0.5	25.75	12.3	0.2
4.75	-1.7	-1.1	16.75	14.8	0.2	25.75	15.3	0.2
4.75	0.3	-1	16.75	16.3	0.1	25.75	18.3	0.15
4.75	2.3	0.2	16.75	18.3	0.2			

Table B.11: Experimental data for trapezoidal vane (3H:2.5V)
($F_r = 0.13$, $d_{50} = 0.225$ mm, Collar size BF1.3)

I			II			III		
x (cm)	y (cm)	z (cm)	x (cm)	y (cm)	z (cm)	x (cm)	y (cm)	z (cm)
-2.5	-9.7	0	3.5	-4.7	-1.4	15.5	-12.7	0.05
-2.5	-7.7	0	3.5	-2.7	-0.4	15.5	-10.7	-0.65
-2.5	-5.7	0.05	3.5	-1.7	0.1	15.5	-9.7	-0.85
-2.5	-3.7	0.15	3.5	-0.7	0.25	15.5	-7.7	-0.25
-2.5	-1.7	0.15	3.5	1.3	0.25	15.5	-5.7	-0.45
-1.5	-7.7	-0.05	5.5	-11.7	-0.05	15.5	-3.7	-0.45
-1.5	-6.7	0.05	5.5	-9.7	-1.45	15.5	-1.7	-0.15
-1.5	-5.7	-0.1	5.5	-7.7	-1.95	15.5	0.3	-0.25
-1.5	-4.7	-0.3	5.5	-5.7	-2.15	15.5	2.3	0.3
-1.5	-3.7	0.15	5.5	-3.7	-1.85	15.5	4.3	1.25
-1.5	-2.7	0.15	5.5	-1.7	-0.65	15.5	6.3	2.15
-1.5	-1.7	0.15	5.5	-0.2	-0.1	15.5	8.3	1.5
-1.5	-0.7	0.15	5.5	1.3	0.25	15.5	10.3	0.35
-0.5	-8.7	-0.05	5.5	3.3	0.25	15.5	12.3	0.35
-0.5	-7.7	-0.05	7.5	-12.7	-0.05	15.5	14.3	0.25
-0.5	-6.7	-0.15	7.5	-10.7	-0.9	17.5	-12.7	0.15
-0.5	-5.7	-0.5	7.5	-8.7	-1.45	17.5	-9.7	0.25
-0.5	-4.7	0.2	7.5	-6.7	-1.6	17.5	-6.7	-0.3
-0.5	-3.7	0.2	7.5	-4.7	-1.75	17.5	-3.7	-0.65
-0.5	-2.7	0.15	7.5	-2.7	-1.45	17.5	-0.7	-0.25
-0.5	-1.7	0.2	7.5	-0.7	-0.6	17.5	2.3	0.05
-0.5	-0.7	0.15	7.5	1.5	0.65	17.5	5.3	0.75
-0.5	0.3	0.15	7.5	3.3	0.3	17.5	7.3	1.7
0	-8.7	-0.05	7.5	5.3	0.25	17.5	10.3	0.95
0	-7.7	-0.1	10.5	-12.7	0	17.5	12.3	0.25
0	-6.4	-0.6	10.5	-10.7	-0.25	17.5	14.3	0.15
0	-5.7	-0.65	10.5	-8.7	-0.3	17.5	16.3	0.25
0	-4.85	-0.45	10.5	-6.7	0.05	21.5	-10.7	0.15
0	-3.7	0.15	10.5	-4.7	0	21.5	-7.7	0.35
0	-2.7	0.15	10.5	-2.7	0.05	21.5	-4.7	0.8
0	-2.2	0.2	10.5	-0.7	0.2	21.5	-1.5	0.55
0	-1.2	0.2	10.5	1.3	0.8	21.5	1.3	0.35
0	-0.2	0.15	10.5	3.7	2.3	21.5	4.3	0.55
0	0.8	0.15	10.5	6.3	0.45	21.5	7.3	0.85
1.5	-9.7	-0.05	10.5	8.3	0.25	21.5	10.3	0.75
1.5	-8.7	-0.65	10.5	10.3	0.25	21.5	13.3	-0.35
1.5	-7.7	-0.95	12.5	-13.2	0.05	21.5	14.3	0.25
1.5	-6.7	-1.25	12.5	-11.7	-0.55	21.5	16.3	0.25
1.5	-5.8	-1.05	12.5	-9.7	0.1	23.5	-10.7	0.15
1.5	-5.2	-0.75	12.5	-7.7	0.4	23.5	-7.7	0.15
1.5	-4.7	-0.5	12.5	-5.7	0.5	23.5	-4.7	0.25
1.5	-3.7	0.15	12.5	-3.7	0.2	23.5	-1.7	0.2
1.5	-2.4	0	12.5	-1.7	0.35	23.5	1.3	0.2
1.5	-1.2	0.15	12.5	0.3	0.8	23.5	4.3	0.25
1.5	-0.2	1.15	12.5	2.3	1.4	23.5	7.3	0.3
1.5	0.8	1.15	12.5	4.3	2.35	23.5	10.8	0.65
3.5	-11.7	-0.05	12.5	5.8	2.15	23.5	13.3	0.15
3.5	-10.7	-0.05	12.5	7.3	0.2	23.5	15.3	0.25
3.5	-8.7	-1.45	12.5	9.3	0.3	23.5	17.3	0.25
3.5	-6.7	-2.05	12.5	11.3	0.3			

Table B.12: Experimental data for trapezoidal vane (3H:2.5V)
($F_r = 0.13$, $d_{50} = 0.225$ mm, Collar size BF1.4)

I			II			III		
x	y	z	x	y	z	x	y	z
(cm)	(cm)	(cm)	(cm)	(cm)	(cm)	(cm)	(cm)	(cm)
-0.75	-8.5	0	8.25	-2.5	-1.9	19.25	6.5	0.3
-0.75	-6.5	0	8.25	-0.5	-1.8	19.25	10.5	2.3
-0.75	-4.5	0.1	8.25	1.5	-1.2	19.25	13.5	1.2
-0.75	-2.5	0.1	8.25	3.5	-0.3	19.25	16.5	-0.05
-0.75	-0.5	0.3	8.25	5.5	1	19.25	17.5	-0.1
-0.75	1.5	0.15	8.25	6.5	1.4	19.25	18.5	0.2
-0.75	3.5	0.25	8.25	8.5	0.4	19.25	20.5	0.2
-0.75	5.5	0.3	8.25	10.5	0.35	19.25	22.5	0.3
0	-6.5	0.02	8.25	12.5	0.35	21.25	-11	0.2
0	-5.5	0.1	11.25	-10.5	0.1	21.25	-8.5	0.5
0	-4.5	-0.15	11.25	-8.5	0	21.25	-5.5	0.6
0	-3.5	0.1	11.25	-6.5	0.2	21.25	-2.5	0.15
0	-2.5	0.1	11.25	-4.5	-0.05	21.25	-1	-0.05
0	-1.5	0.3	11.25	-2.5	-0.3	21.25	0.5	0.45
0	0	0.3	11.25	-0.5	-0.4	21.25	3.5	-0.05
0	2.5	0.2	11.25	1.5	-0.45	21.25	6.5	0.4
0	4.5	0.2	11.25	3.5	-0.2	21.25	9.5	1.3
0	6.5	0.35	11.25	5.5	0.4	21.25	11	2.2
1.25	-8.5	0.05	11.25	7.5	1.7	21.25	12.5	1.2
1.25	-7.5	-0.75	11.25	9	2.4	21.25	15.5	0.4
1.25	-6.5	-0.8	11.25	10.5	0.35	21.25	18	-1.05
1.25	-5.5	-0.9	11.25	12.5	0.35	21.25	20.5	0.2
1.25	-4.5	-1.05	14.25	-11	0.2	21.25	22.5	0.2
1.25	-3.5	-0.9	14.25	-10	-0.85	21.25	24.5	0.3
1.25	-2.5	-0.6	14.25	-9	-1.5	23.25	-11	0.3
1.25	-1.7	-0.4	14.25	-7.5	-1.3	23.25	-8.5	0.2
1.25	-1	-0.2	14.25	-5.5	-0.55	23.25	-4.5	0.1
1.25	-0.5	0.25	14.25	-3.5	0.15	23.25	0	-0.4
1.25	1.5	0.1	14.25	-1.5	0.8	23.25	2.5	0.4
1.25	3.5	0.3	14.25	0.5	0.7	23.25	5.5	0.3
1.25	5.5	0.3	14.25	2.5	0.5	23.25	8.5	0.8
3.25	-10.5	0.1	14.25	4.5	0.45	23.25	10.75	1.7
3.25	-8.5	-1	14.25	6.5	0.95	23.25	12.5	1.1
3.25	-6.5	-1.5	14.25	8.5	2.3	23.25	15.5	0.4
3.25	-4.5	-1.95	14.25	9.9	2.95	23.25	18.5	-0.5
3.25	-2.5	-1.55	14.25	11	2.4	23.25	20	-0.9
3.25	-0.5	-0.75	14.25	12.5	0.45	23.25	21.7	0.25
3.25	1	-0.3	14.25	14.5	0.3	23.25	23.5	0.3
3.25	2.1	0.2	14.25	16.5	0.3	27.25	-7.5	0.2
3.25	3.5	0.35	16.25	-11.5	0.15	27.25	-3.5	0.45
3.25	5.5	0.35	16.25	-8.5	-0.65	27.25	0.5	0.3
3.25	7.5	0.35	16.25	-6.5	-1.3	27.25	2.5	0.02
5.25	-11.5	0.05	16.25	-3.5	-0.35	27.25	6.5	0.35
5.25	-10.2	-1.05	16.25	-0.5	0.4	27.25	10.5	0.45
5.25	-8.5	-1.2	16.25	2.5	0.7	27.25	13.5	0.8
5.25	-6.5	-1.55	16.25	5.5	0.5	27.25	17.5	0.25
5.25	-4.5	-2.1	16.25	8.5	1.9	27.25	21.5	0.9
5.25	-2.5	-2.15	16.25	9.3	2.3	27.25	24.5	0.3
5.25	-0.5	-1.4	16.25	11.5	1.4	27.25	27.5	0.35
5.25	1.5	-0.35	16.25	13.5	1.2	29.25	-6.5	0.2
5.25	3.5	0.05	16.25	15.5	0.3	29.25	-2.5	0.4
5.25	5.5	0.4	16.25	17.5	0.2	29.25	1.5	0.35
5.25	7.5	0.3	16.25	19.5	0.3	29.25	5.5	0.35
5.25	9.5	0.35	19.25	-11	0.2	29.25	9.5	0.45
5.25	11.5	0.35	19.25	-8.5	0.4	29.25	13.5	0.8
8.25	-10.5	0.05	19.25	-5.5	0.4	29.25	17.5	0.3
8.25	-8.5	-0.05	19.25	-2.5	-0.4	29.25	21.5	0.3
8.25	-6.5	-0.85	19.25	0.5	0.7	29.25	26.5	0.3
8.25	-4.5	-1.4	19.25	3.5	-0.1			

Table B.13: Experimental data for trapezoidal vane (3H:2.5V)
 ($F_r = 0.13$, $d_{50} = 0.225$ mm, Collar size BF1.5)

I			II			III		
x (cm)	y (cm)	z (cm)	x (cm)	y (cm)	z (cm)	x (cm)	y (cm)	z (cm)
-2.5	-9.5	0	9.5	-3.5	-0.9	24.5	-8.5	0.2
-2.5	-7.5	0.05	9.5	-1.5	-0.8	24.5	-6.5	0.4
-2.5	-5.5	0.1	9.5	0.5	-0.05	24.5	-4.5	-0.15
-2.5	-3.5	0.2	9.5	2.5	1.15	24.5	-2.5	-0.5
-2.5	-1.5	0.2	9.5	3.5	1.7	24.5	-0.5	-0.3
-1.5	-10.5	0	9.5	4.5	0.3	24.5	1.5	-0.35
-1.5	-9.5	0	9.5	6.5	0.25	24.5	3.5	-0.25
-1.5	-8.5	0	9.5	8.5	0.25	24.5	5.5	0.1
-1.5	-7.5	0.1	12.5	-12.5	0.1	24.5	7.5	0.7
-1.5	-6.5	-0.2	12.5	-10.5	-0.2	24.5	9.5	1.8
-1.5	-5.5	-0.05	12.5	-8.5	0	24.5	11.5	0.8
-1.5	-4.5	-0.05	12.5	-6.5	0.2	24.5	13.5	0
-1.5	-3.5	0.2	12.5	-4.5	-0.3	24.5	15.5	0.15
-1.5	-2.5	0.1	12.5	-2.5	-0.9	24.5	17.5	0.3
-1.5	-1.5	0.2	12.5	-0.5	-0.85	24.5	19.5	0.2
0	-11.5	0	12.5	1.5	-0.1	27.5	-6.5	0.3
0	-10.5	-0.3	12.5	3.5	1.3	27.5	-4.5	0
0	-9.5	-0.8	12.5	5.5	2.1	27.5	-2.5	-0.4
0	-8.5	-0.6	12.5	7.5	0.35	27.5	-0.5	-0.15
0	-7.5	-0.55	12.5	9.5	0.3	27.5	2.5	-0.1
0	-6.5	-0.9	12.5	11.5	0.2	27.5	5.5	0.25
0	-5.5	-1.3	15.5	-11.5	0.2	27.5	7.5	0.6
0	-4.5	-0.8	15.5	-9.5	0.2	27.5	9.5	1
0	-3.5	0.2	15.5	-7.5	0	27.5	11	1.45
0	-2.5	0.2	15.5	-5.5	-0.2	27.5	13.5	0.45
0	-1.5	0.2	15.5	-3.5	-0.7	27.5	15.5	0.35
0	-0.5	0.2	15.5	-1.5	-0.7	27.5	17.5	0.2
1.5	-13.5	0	15.5	0.5	-0.25	27.5	19.5	0.2
1.5	-11.5	-0.9	15.5	2.5	0.7	30.5	-6.5	0.2
1.5	-9.5	-1.5	15.5	4.5	2.1	30.5	-4.5	0.4
1.5	-7.5	-1.15	15.5	6.5	2.95	30.5	-1.5	0.1
1.5	-6.4	-1.6	15.5	8	2.5	30.5	1.5	-0.1
1.5	-5.5	-1.4	15.5	10.5	0.35	30.5	4.5	-0.45
1.5	-4.5	-0.8	15.5	12.5	0.25	30.5	7.5	-0.6
1.5	-3.5	-0.3	15.5	14.5	0.25	30.5	9	-0.4
1.5	-2	-0.1	18.5	-10.5	0.2	30.5	10.5	0.6
1.5	-0.5	0.3	18.5	-8.5	0.25	30.5	11.4	1.35
1.5	1.5	0.2	18.5	-6.5	0.25	30.5	13.5	0.6
1.5	3.5	0.2	18.5	-4.5	0.05	30.5	15.5	0.2
3.5	-14.5	0	18.5	-2.5	-0.15	30.5	17.5	0.2
3.5	-12.5	-1.4	18.5	-0.5	-0.15	33.5	-6.5	0.3
3.5	-10.5	-1.7	18.5	1.5	0.2	33.5	-4.5	0.2
3.5	-8.5	-1.95	18.5	3.5	1.15	33.5	-2.5	0.35
3.5	-6.5	-1.8	18.5	5.5	1.55	33.5	-0.5	0.15
3.5	-4.5	-1.3	18.5	7.5	1.9	33.5	1.5	-0.05
3.5	-2.5	-0.2	18.5	9.5	2.25	33.5	3.5	0.15
3.5	-1.5	0.15	18.5	11	1.35	33.5	5.5	0.25
3.5	0.5	0.2	18.5	12.74	0.3	33.5	7.5	0.7
3.5	2.5	0.2	18.5	14.5	0.3	33.5	9.5	1.4
6.5	-13.5	0.1	18.5	16.5	0.25	33.5	11.5	1.55
6.5	-11.5	-0.25	21.5	-9.5	0.1	33.5	13.5	0.5
6.5	-9.5	-1.5	21.5	-7.5	0.1	33.5	15.5	0.35
6.5	-7.5	-2	21.5	-5.5	-0.25	33.5	17.5	0.25
6.5	-5.5	-1.95	21.5	-3.5	-0.6	36.5	-6.5	0.25
6.5	-3.5	-1.2	21.5	-1.5	-0.75	36.5	-3.5	0.3
6.5	-1.5	-0.4	21.5	0.5	-0.9	36.5	-0.5	0.3
6.5	0.5	-0.3	21.5	2.5	-0.5	36.5	2.5	0.3
6.5	2.5	0.3	21.5	4.5	0.35	36.5	5.5	0.4
6.5	4.5	0.25	21.5	6.5	0.6	36.5	7.5	0.7
6.5	6.5	0.25	21.5	8.5	1.55	36.5	9.5	0.3
9.5	-13.5	0.1	21.5	9.5	2.1	36.5	12.5	0.45
9.5	-11.5	0.35	21.5	11.5	0.75	36.5	15.5	0.35
9.5	-9.5	0.4	21.5	13.5	0.1	36.5	18.5	0.2
9.5	-7.5	0.15	21.5	15.5	0.34	36.5	21.5	0.2
9.5	-5.5	-0.5	21.5	17.5	0.2			

Table B.14 Experimental data for trapezoidal vane (3H:2.5V)

$(F_r = 0.13, d_{50} = 0.225 \text{ mm}, \text{Collar size BF1.6})$

I			II			III		
x	y	z	x	y	z	x	y	z
(cm)	(cm)	(cm)	(cm)	(cm)	(cm)	(cm)	(cm)	(cm)
-1.75	-7.1	0	3.25	7.9	0.1	15.25	4.9	-0.1
-1.75	-5.1	0	6.25	-10.1	0	15.25	6.9	0
-1.75	-3.1	-0.05	6.25	-8.1	-0.05	15.25	8.9	1.15
-1.75	-1.1	0	6.25	-6.1	-0.75	15.25	11.5	2.8
-1.75	-0.1	0	6.25	-4.1	-1.6	15.25	12.9	2.55
-1.75	0.9	0	6.25	-2.1	-1.9	15.25	14.1	0.05
-1.75	2.9	0	6.25	-0.1	-2	15.25	15.9	0.05
-1.75	4.9	0.1	6.25	1.9	-1	15.25	17.9	0.1
0	-8.1	0	6.25	3.9	-0.25	18.25	-6.1	0
0	-7.1	0	6.25	4.7	-0.25	18.25	-4.1	0.3
0	-6.1	-1.05	6.25	6.1	0	18.25	-2.1	-0.95
0	-5.1	-1.1	6.25	7.9	0.05	18.25	-0.5	-1.29
0	-4.1	-1.25	6.25	9.9	0.05	18.25	0.9	-0.8
0	-3.1	-1.5	9.25	-9.1	0.05	18.25	2.9	-0.1
0	-2.1	-1.3	9.25	-7.1	0.05	18.25	4.9	-0.4
0	-1.1	-0.5	9.25	-5.1	0.25	18.25	7.4	-0.7
0	0	-0.05	9.25	-3.1	-0.6	18.25	6.9	-0.1
0	0.9	-0.1	9.25	-1.1	-1.3	18.25	8.9	0.65
0	1.9	-0.1	9.25	0.9	-1.75	18.25	10.9	2.25
0	3.9	0.1	9.25	2.9	-1.05	18.25	12.9	1.15
0	5.9	0.1	9.25	4.9	-0.3	18.25	14.9	1
1.25	-8.1	0	9.25	7.4	1.1	18.25	16.9	0.1
1.25	-7.1	-1	9.25	8.9	0.1	18.25	18.9	0.05
1.25	-6.1	-1.6	9.25	10.9	0	18.25	20.9	0.1
1.25	-5.1	-1.9	9.25	12.9	0	21.25	-7.1	0.1
1.25	-4.1	-1.9	12.25	-7.1	0	21.25	-4.1	0.48
1.25	-3.1	-1.9	12.25	-5.9	-0.15	21.25	-1.1	0.15
1.25	-2.1	-1.78	12.25	-4.1	-0.2	21.25	1.9	-0.45
1.25	-1.1	-0.95	12.25	-2.1	-0.85	21.25	4.9	0.1
1.25	-0.1	-0.75	12.25	-0.1	-0.73	21.25	7.9	0.7
1.25	1.4	-0.4	12.25	1.9	-0.1	21.25	10.8	1.95
1.25	2.4	-0.3	12.25	3.9	0.1	21.25	13.9	-0.1
1.25	3.4	0	12.25	5.9	0.31	21.25	16.9	-0.05
1.25	4.9	0	12.25	7.9	1.05	21.25	19.9	0
1.25	6.9	0.1	12.25	9.9	1.8	24.25	-4.1	0.15
3.25	-9.1	0	12.25	11.4	0.1	24.25	-1.1	0.1
3.25	-7.1	-1.5	12.25	12.9	0.05	24.25	1.9	0.1
3.25	-5.1	-2.15	12.25	14.9	0	24.25	4.9	0.15
3.25	-3.1	-2.35	15.25	-7.1	0.05	24.25	7.9	0.15
3.25	-1.1	-1.71	15.25	-4.6	-0.7	24.25	10.6	1.1
3.25	0.4	-1.2	15.25	-3.1	-0.55	24.25	12.9	0.7
3.25	1.9	-0.65	15.25	-1.1	-0.25	24.25	15.9	0.2
3.25	3.9	-0.05	15.25	0.9	0.45	24.25	18.9	0.1
3.25	5.9	0.05	15.25	2.9	0.25			

Table B.15: Experimental data for trapezoidal vane (3H:2.5V)
 ($F_r = 0.13$, $d_{50} = 0.225$ mm, Collar size BF1.7)

I			II			III		
x	y	z	x	y	z	x	y	z
(cm)	(cm)	(cm)	(cm)	(cm)	(cm)	(cm)	(cm)	(cm)
-4.75	-4	0.1	5.25	-2	-1.85	17.25	2	-1
-4.75	-2	0.1	5.25	0	-1.1	17.25	4	-0.9
-4.75	0	0.1	5.25	2	-0.75	17.25	6	-0.45
-4.75	2	0.1	5.25	3.7	0.15	17.25	8	0.5
-4.75	4	0.1	5.25	5	0.25	17.25	10	1.85
-4.75	6	0.1	5.25	7	0.35	17.25	12.5	3.1
-2.75	-5	0.05	5.25	9	0.25	17.25	14	2.1
-2.75	-4	0.1	5.25	11	0.15	17.25	15.5	0.15
-2.75	-3	0.1	8.25	-10	0.25	17.25	17	0.15
-2.75	-2	-0.4	8.25	-8	0.2	17.25	19	0.1
-2.75	-1	-0.85	8.25	-6	0	20.25	-7	0.2
-2.75	0	-0.95	8.25	-4	-1	20.25	-5	0.2
-2.75	1	-0.8	8.25	-2	-1.5	20.25	-3	-0.25
-2.75	2	-0.6	8.25	0	-1.8	20.25	-1	-0.95
-2.75	3	-0.3	8.25	2	-1.5	20.25	1	-1.1
-2.75	4	0.1	8.25	4	-0.5	20.25	3	-0.9
-2.75	5	0.1	8.25	6	0.4	20.25	5	-0.75
0	-7	0.05	8.25	7.5	0.3	20.25	7	-0.2
0	-6	0	8.25	9	0.25	20.25	9	0.5
0	-5	-0.75	8.25	11	0.2	20.25	11	1.5
0	-4	-0.8	8.25	13	0.15	20.25	13	2.8
0	-3	-1	11.25	-9	0.25	20.25	15	2
0	-2	-2	11.25	-7	0.6	20.25	17	0.7
0	-1	-2.1	11.25	-5	0.5	20.25	19	0.1
0	0.5	-2.35	11.25	-3	-0.1	20.25	21	0.1
0	1	-2.1	11.25	-1	-0.75	23.25	-5	0.2
0	1.75	-1.6	11.25	1	-1.1	23.25	-3	0.25
0	3	-0.9	11.25	3	-0.9	23.25	-1	0.29
0	4	-0.35	11.25	5	-0.4	23.25	1	-0.65
0	5	0.15	11.25	7	0.55	23.25	3	-1.15
0	6	0.15	11.25	9	1.5	23.25	5	-0.6
0	7	0.1	11.25	10.5	0.25	23.25	7	0
0	-9	0.2	11.25	12	0.25	23.25	9	0.1
2.25	-8	0.1	11.25	14	0.1	23.25	11	1
2.25	-7	-0.5	14.25	-9	0.25	23.25	13	2.25
2.25	-6	-0.9	14.25	-7	0.1	23.25	15	1.6
2.25	-5	-1.1	14.25	-5	-0.4	23.25	17	0.7
2.25	-4	-0.85	14.25	-3	-0.6	23.25	19	0.2
2.25	-3	-0.85	14.25	-1	-1.3	23.25	21	0.1
2.25	-2	-1.2	14.25	1	-1.7	26.25	-4	0.2
2.25	-1	-0.95	14.25	3	-0.8	26.25	-2	0.25
2.25	0	-0.75	14.25	5	-1.2	26.25	0	0.45
2.25	1	-0.3	14.25	7	-0.2	26.25	2	0.5
2.25	2.2	-0.8	14.25	9	1.25	26.25	4	0.45
2.25	3	-0.45	14.25	11	2	26.25	6	0.35
2.25	4	0	14.25	13	0.2	26.25	8	0.25
2.25	5	0.3	14.25	15	0.25	26.25	10	0.2
2.25	6	0.2	14.25	17	2.1	26.25	12	1.15
2.25	7	0.15	17.25	-7	0.2	26.25	14	1.7
5.25	-10	0.1	17.25	-5.5	-0.5	26.25	16	1.1
5.25	-8	-0.85	17.25	-4	-0.4	26.25	18	0.4
5.25	-6	-1.35	17.25	-2	-0.55	26.25	20	0.2
5.25	-4	-1.9	17.25	0	-0.85	26.25	22	0.1

Table B.16: Experimental data for trapezoidal vane(3H:2.5V)
($F_r = 0.13$, $d_{50} = 0.225$ mm, Collar size BF1.8)

I			II			III		
x	y	z	x	y	z	x	y	z
(cm)	(cm)	(cm)	(cm)	(cm)	(cm)	(cm)	(cm)	(cm)
-3.75	-8.5	-0.1	3.25	-11.5	0	15.25	14	0.1
-3.75	-6.5	0	3.25	-9.5	-1.1	15.25	16.5	0.05
-3.75	-4.5	0	3.25	-7.5	-1.9	15.25	19.5	0
-3.75	-2.5	0	3.25	-5.5	-2.45	18.25	-5.5	0.1
-3.75	-0.5	0	3.25	-3.5	-2.7	18.25	-2.5	0.15
-3.75	1.5	0.05	3.25	-1.5	-1.5	18.25	-0.5	-0.85
-2.75	-8.5	0	3.25	2.5	-1	18.25	2.5	-0.71
-2.75	-7.5	0	3.25	3.5	0.1	18.25	5.5	-0.05
-2.75	-6.5	-0.4	3.25	5.5	0.15	18.25	8.5	0.8
-2.75	-5.5	-0.6	3.25	7.5	0.05	18.25	11.5	1.95
-2.75	-4.5	-0.8	6.25	-11.5	0.1	18.25	13.5	2.5
-2.75	-3.5	-0.3	6.25	-9.5	-0.1	18.25	16.5	0.75
-2.75	-2.5	0	6.25	-7.5	-0.8	18.25	19.5	0
-2.75	-1.5	0	6.25	-5.5	-1.15	18.25	22.5	0
-2.75	-0.5	0	6.25	-3.5	-1.65	21.25	-3.5	0
-2.75	0.5	0.05	6.25	-1.5	-1.4	21.25	-0.5	-0.45
-2.75	1.5	0.05	6.25	0.5	-1.15	21.25	2.5	-0.85
-2.75	2.5	0.05	6.25	2.5	-0.3	21.25	5.5	-1.05
-1.75	-8.5	0	6.25	4.5	-0.5	21.25	8.5	-0.3
-1.75	-7.5	-0.05	6.25	6.5	0.1	21.25	11.5	1.35
-1.75	-6.5	-0.75	6.25	8.5	0.05	21.25	14.2	2.6
-1.75	-5.5	-1.1	6.25	10.5	0.05	21.25	16.5	1.25
-1.75	-4.5	-1.2	9.25	-11.5	0.05	21.25	19.5	0.5
-1.75	-3.5	-0.85	9.25	-8.5	0.2	21.25	22.5	0
-1.75	-3	-0.5	9.25	-5.5	0.2	24.25	-4.5	0.05
-1.75	-2.5	0	9.25	-2.5	-0.3	24.25	-1.5	0.05
-1.75	1.5	0	9.25	0.5	-1.2	24.25	1.5	-0.95
-1.75	2.5	0.05	9.25	2	-1.8	24.25	4.5	-1.1
-1.75	3.5	0	9.25	4.5	-1	24.25	7.5	0.15
0	-9.5	-0.05	9.25	7.5	0.55	24.25	10.5	1.25
0	-8.5	-0.05	9.25	9	0.25	24.25	12.8	2.3
0	-7.5	-1.05	9.25	11.5	0.05	24.25	15.5	1.35
0	-6.5	-1.15	9.25	14.5	0.05	24.25	18.5	0.1
0	-5.5	-1.5	12.25	-12	0.15	24.25	21.5	-0.85
0	-4.5	-1.6	12.25	-9.5	0.1	24.25	22.5	0
0	-3.8	-1.25	12.25	-6.5	-0.1	24.25	24.5	0
0	-3.5	-1.15	12.25	-3.5	-0.45	25.25	-2.5	0.1
0	-2.5	-1.2	12.25	-0.5	-0.85	25.25	2.5	-0.9
0	-1.5	-0.95	12.25	2.5	-1	25.25	7.5	-0.3
0	-1	-0.9	12.25	4	-2	25.25	11.5	1.85
0	0.5	-0.05	12.25	6.5	-0.2	25.25	13.5	1.75
0	2	-0.05	12.25	9.5	1.9	25.25	16.5	0.4
0	3.5	0.1	12.25	11.5	0.15	25.25	18.5	-0.25
0	5.5	0	12.25	14.5	0.1	25.25	21	-1.1
2.25	-11.5	0	12.25	17.5	0	25.25	22.5	0.15
2.25	-10.5	0	15.25	-11.5	0.15	25.25	24.5	0
2.25	-8.5	-1.55	15.25	-8.5	0.15	29.25	-1.5	0
2.25	-6.5	-2.35	15.25	-5.5	0.15	29.25	3.5	-0.3
2.25	-4.5	-2.65	15.25	-2.5	-0.3	29.25	8.5	-0.2
2.25	-2.5	-1.85	15.25	0.5	-0.35	29.25	12.5	1.1
2.25	-1.8	-1.5	15.25	3.5	-1.1	29.25	14	0.75
2.25	2.5	-0.1	15.25	6.5	0.05	29.25	15	1.15
2.25	4.5	0.2	15.25	9.5	1.55	29.25	18.5	0.25
2.25	6.5	0.1	15.25	11.15	2.5	29.25	23.5	0.35
2.25	8.5	0	15.25	13	2.2	29.25	27.5	0

Table B.17: Experimental data for trapezoidal vane(3H:2.5V)
($F_r = 0.13$, $d_{50} = 0.225$ mm, Collar size BF1.9)

I			II			III		
x	y	z	x	y	z	x	y	z
(cm)	(cm)	(cm)	(cm)	(cm)	(cm)	(cm)	(cm)	(cm)
0	-5	0.1	6	1.5	-0.85	18	5	-0.25
0	-4	0.1	6	3	-0.4	18	7	0.55
0	-3	0.05	6	4	-0.05	18	9.5	1.3
0	-2	0	6	5.5	0.1	18	11	1
0	-1	0	6	7	0.2	18	13	0.5
0	0	0	6	9	0.1	18	14.5	0.4
0	1	0	8	-3	0.05	18	15.5	0.05
0	2	0	8	-1	-0.55	18	17	0.1
0	3	0.2	8	1.5	-1.45	18	19	0.1
0	4	0.2	8	3	-1.1	20	1	0
0	5	0.15	8	5	-0.3	20	3	-0.1
2	-4	0	8	6	0.25	20	4.5	-0.6
2	-3	0.05	8	7	0.15	20	6	-0.2
2	-2	0	8	9	0.05	20	8	0.25
2	-1	0	8	11	0.1	20	10	1.1
2	0	0	11	-3	0.1	20	12	-0.3
2	1	0	11	-1	0	20	14	0.9
2	2	-0.1	11	1	-0.3	20	16	-0.15
2	3	0	11	3	-0.2	20	17	-0.55
2	4	0.2	11	5	0.1	20	18	0
2	5	0.2	11	7	0.3	20	20	0.1
2	6	0.15	11	8.5	0.5	22	2	0
4	-4	0.05	11	10	0.2	22	4	0.15
4	-3	0.05	11	12	0.1	22	6	0.25
4	-2	0.1	14	-1	0.1	22	8	0.35
4	-1	-0.15	14	1	-0.5	22	10	0.35
4	0	0	14	3	-0.6	22	12	0.4
4	1	0	14	5	-0.65	22	14	0.5
4	2.65	0	14	7	0.1	22	16	-0.2
4	4	0.15	14	9	1.2	22	18	-1.05
4	5	0.2	14	11	1.8	22	20	0.05
4	6	0.15	14	12	0.1	22	22	0.1
5	-3	-0.1	14	14	0.1	25	8	0
5	-1	-0.1	15	-1	0.1	25	10	0.1
5	0	-0.3	15	1.65	-0.85	25	12	0.15
5	1	-0.5	15	5.5	-0.85	25	14	-0.1
5	2	-0.45	15	8	0.75	25	16	0
5	3.8	0	15	10.75	1.85	25	18	0
5	5	0.15	15	12	1	25	20	0.4
5	7	0.1	15	13	0.1	25	22	0.15
6	-3	0.05	15	15	0.1	25	24	0.1
6	-1	-0.15	18	1	0.1			
6	0.5	-0.9	18	3	0.1			

Table B.18: Experimental data for trapezoidal vane(3H:2.5V)
($F_r = 0.13$, $d_{50} = 0.225$ mm, Collar size BF1.10)

I			II			III		
x	y	z	x	y	z	x	y	z
(cm)	(cm)	(cm)	(cm)	(cm)	(cm)	(cm)	(cm)	(cm)
-2.75	-3.5	0	6.25	-8.5	-0.8	18.25	6.5	0.6
-2.75	-1.5	-0.1	6.25	-6.5	-1.55	18.25	9.5	1.7
-2.75	-0.5	-0.4	6.25	-4.5	-1.7	18.25	10.8	2.4
-2.75	0.5	-0.3	6.25	-3.5	-1.8	18.25	12.5	2.2
-2.75	2.5	0	6.25	-1.5	-1.1	18.25	15.5	0.5
-1.75	-4.5	0	6.25	0.5	-0.8	18.25	16.5	-0.4
-1.75	-3.5	0	6.25	2.5	-0.1	18.25	19.5	0
-1.75	-2.5	-0.3	6.25	4.5	0.6	21.25	-11.5	0.15
-1.75	-1.5	-0.7	6.25	6	0.15	21.25	-8.5	0.1
-1.75	-0.5	-1.1	6.25	7.5	0.05	21.25	-5.5	0
-1.75	0.5	-0.9	6.25	9.5	0	21.25	-2.5	-0.4
-1.75	1.5	-0.55	9.25	-11.5	0.05	21.25	0.5	-0.3
-1.75	2.5	0.05	9.25	-8.5	-1.25	21.25	3.5	-0.5
-1.75	4.5	0	9.25	-5.5	-2.15	21.25	6.5	-0.3
0	-5.5	0	9.25	-2.5	-2.25	21.25	9.5	0.6
0	-4.5	-0.05	9.25	0.5	-1.95	21.25	12.5	1.95
0	-3.5	-0.6	9.25	3.5	-0.75	21.25	15.5	0.3
0	-2.5	-1.15	9.25	7.5	1.4	21.25	18.5	-1.15
0	-1.5	-1.45	9.25	8.5	0.15	21.25	19.5	-0.9
0	-0.5	-1.2	9.25	11.5	0.05	21.25	20.5	0
0	0.5	-0.9	12.25	-10.5	0.05	21.25	23.5	0
0	1	-1	12.25	-7.5	-0.5	24.25	-12.5	0
0	2	-0.8	12.25	-4.5	-0.82	24.25	-8.5	0.4
0	3.5	0	12.25	-1.5	-1.3	24.25	-4.5	0.2
0	5.5	0.05	12.25	1.5	-1.4	24.25	-0.5	-0.3
1.25	-8.5	0	12.25	4.5	-0.8	24.25	2.5	-0.85
1.25	-6.5	0	12.25	7.5	0.6	24.25	5.5	-0.85
1.25	-5.5	-0.45	12.25	10	2.2	24.25	8.5	-0.5
1.25	-4.5	-0.5	12.25	11.5	0.1	24.25	11.5	0.7
1.25	-3.5	-0.8	12.25	14.5	0	24.25	13.5	1.7
1.25	-2.7	-1.25	15.25	-11.5	0.05	24.25	16.5	0
1.25	-2.3	-1.4	15.25	-8.5	0	24.25	19.5	-1
1.25	-1.5	-0.9	15.25	-5.5	0.1	24.25	20.5	-0.75
1.25	-0.5	-0.4	15.25	-2.5	0.2	24.25	21.5	0
1.25	1.5	-0.7	15.25	0.5	0	24.25	22.5	0
1.25	2.5	-0.2	15.25	3.5	-0.1	24.25	23.5	0.05
1.25	3.5	0.1	15.25	6.5	0.2	29.25	-2.5	0
1.25	5.5	0	15.25	9.5	1.85	29.25	1.5	0.1
3.25	-9.5	0	15.25	11.5	3.1	29.25	5.5	0
3.25	-7.5	-0.5	15.25	12.7	2.7	29.25	9.5	0
3.25	-5.5	-1.4	15.25	13.5	0	29.25	12.5	0.7
3.25	-3.5	-0.9	15.25	16.5	0	29.25	14	1.3
3.25	-1.5	-0.25	18.25	-12	0.1	29.25	16.5	0.25
3.25	-0.5	-0.35	18.25	-10.5	-1.1	29.25	19.5	0.3
3.25	0.5	0	18.25	-8.5	-1.4	29.25	21.7	0.8
3.25	1.5	0	18.25	-5.5	-0.7	29.25	23.5	0.3
3.25	3.1	0.1	18.25	-2.5	0.3	29.25	24.5	0.05
3.25	5.5	0	18.25	0.5	0.6			
6.25	-10.5	0	18.25	3.5	0.4			

Table B.19: Experimental data for trapezoidal vane(3H:2.5V)
($F_r = 0.13$, $d_{50} = 0.225$ mm, Collar size BF1.11)

I			II			III		
x (cm)	y (cm)	z (cm)	x (cm)	y (cm)	z (cm)	x (cm)	y (cm)	z (cm)
-3	-5.5	0	6	1.5	-1.15	21	0.5	0
-3	-3.5	0	6	4.3	0.4	21	3.5	-0.35
-3	-1.5	-0.1	6	5.5	-0.05	21	6.5	-0.65
-3	0.5	-0.15	6	7.5	0	21	9.5	0.1
-3	2.5	0	9	-8.5	-0.1	21	12.5	1.55
-3	4.5	0	9	-6.5	-0.75	21	14.9	2.4
-1	-6.5	-0.1	9	-4.5	-0.85	21	17.5	1.1
-1	-5.5	-0.05	9	-2.5	-1	21	20.5	0.6
-1	-4.5	-0.27	9	-0.5	-0.5	21	27.5	0
-1	-3.5	-0.7	9	1.5	-2	25	-12.5	0
-1	-2.5	-0.95	9	3.5	-1.1	25	-9.5	0.3
-1	-1.5	-1.6	9	5.5	-0.1	25	-6.5	0.3
-1	-0.5	-1.95	9	7	0.1	25	-3.5	0.25
-1	0.5	-1.8	9	8.5	-0.1	25	-0.5	-0.95
-1	1.5	-1.5	9	10.5	0	25	2.5	-0.9
-1	2.5	-1	12	-9.5	0	25	5.5	-1.65
-1	3.5	-0.05	12	-6.5	-0.7	25	7	-1.7
-1	4.5	-0.05	12	-3.5	-1.9	25	9.5	-1
-1	5.5	0	12	-0.5	-2.1	25	12.5	0.3
0.75	-6.5	-0.1	12	2.5	-2.3	25	15.5	1.3
0.75	-5.5	-0.45	12	5.5	-1.4	25	18.5	0.7
0.75	-4.5	-1.05	12	8.5	0.6	25	21.5	-0.8
0.75	-3.5	-0.75	12	11	-0.3	25	22.5	-0.85
0.75	-2.5	-1.3	12	13.5	0	25	23.5	0
0.75	-1.5	-2.2	16	-9.5	0	25	24.5	0
0.75	-0.5	-2.25	16	-6.5	-0.2	28	-8.5	0
0.75	0.5	-2.35	16	-3.5	-0.25	28	-5.5	0.3
0.75	1.5	-1.9	16	-0.5	-0.85	28	-2.5	0.05
0.75	2	-1.55	16	2.5	-1	28	0.5	0
0.75	3	-0.9	16	5.5	-0.6	28	2.5	0
0.75	4	-0.3	16	8.5	0.35	28	5.5	-0.9
0.75	5	0	16	11.5	1.7	28	8.5	-0.85
0.75	6	0	16	13.5	1.1	28	11.5	-0.05
3	-7.5	-0.1	16	14.5	0	28	14.5	0.5
3	-6.5	-0.4	16	17.5	0	28	16.5	1
3	-5.5	-1.35	19	-10.5	0.05	28	19.5	-0.35
3	-1.5	-1.65	19	-7.5	-0.4	28	22.5	-0.85
3	-3.5	-1.45	19	-4.5	-0.5	28	24.5	0.1
3	-2.5	-1.2	19	-1.5	0.25	33	-8.5	0
3	-1.6	-1.1	19	1.5	0.1	33	-4.5	0.25
3	-0.5	-0.9	19	4.5	-0.1	33	-0.5	0
3	0.5	-0.7	19	7.5	0.3	33	3.5	0.05
3	1.5	-0.6	19	10.5	1.5	33	4.5	-0.85
3	2.5	-0.6	19	13.5	2.45	33	6.5	-0.9
3	3.5	-0.3	19	16.5	0.85	33	8.5	0
3	4.5	-0.1	19	19.5	0.3	33	12.5	0.5
3	5.5	0	19	22.5	0	33	16.5	1.4
6	-7.5	-0.1	21	-11.5	0.1	33	19.5	0.7
6	-6.5	-0.1	21	-8.5	-0.9	33	23.5	0.5
6	-4.5	-1	21	-6.5	-0.85	33	25	0
6	-2.5	-2.15	21	-4.5	-0.9			
6	-0.5	-2.2	21	-2.5	-0.4			

Table B.20: Experimental data for trapezoidal vane (3H:2.5V)
($F_r = 0.13$, $d_{50} = 0.225$ mm, Collar size BF1.12)

I			II			III		
x	y	z	x	y	z	x	y	z
(cm)	(cm)	(cm)	(cm)	(cm)	(cm)	(cm)	(cm)	(cm)
-3.5	-6.5	-0.2	3.5	-0.5	-1.65	18.5	22.5	-0.1
-3.5	-4.5	-0.1	3.5	0.5	-1.3	22.5	-13.5	-0.1
-3.5	-2.5	0.05	3.5	1.5	-1.15	22.5	-12	-0.75
-3.5	-0.5	0.05	3.5	2.3	-1.5	22.5	-10	0.15
-3.5	1.5	0.1	3.5	3.5	-0.95	22.5	-6	-1.6
-3.5	3.5	0.1	3.5	5.5	-0.35	22.5	-3.5	-0.4
-2.5	-6.5	-0.2	3.5	7.5	0.25	22.5	-0.5	-0.4
-2.5	-5.5	-0.1	3.5	9.5	0.2	22.5	3.5	-0.6
-2.5	-4.5	-0.6	3.5	11.5	0.05	22.5	7.5	-0.15
-2.5	-3.5	-0.7	6.5	-12.5	-0.1	22.5	11.5	1.35
-2.5	-2.5	-0.6	6.5	-10.5	-0.95	22.5	15.15	3.2
-2.5	-1.5	-0.55	6.5	-8.5	-2.1	22.5	18.5	1.8
-2.5	-0.5	-0.7	6.5	-6.5	-2.7	22.5	22.5	0.05
-2.5	0.5	-0.5	6.5	-4.5	-3.4	22.5	25	-0.05
-2.5	1.5	-0.4	6.5	-3	-3.55	27.5	-14.5	0
-2.5	2.5	0	6.5	-1.5	-3.35	27.5	-8.5	-0.25
-2.5	3.5	0.15	6.5	0.5	-2.15	27.5	-2.5	1.15
-2.5	4.5	0.1	6.5	2.5	-1.25	27.5	0.5	0.75
-1.5	-6.5	-0.15	6.5	4	-0.8	27.5	4.5	-0.01
-1.5	-5.5	-0.3	6.5	4.9	-1	27.5	8.5	-0.35
-1.5	-4.5	-1.25	6.5	6	0.15	27.5	12.5	1.15
-1.5	-3.5	-1.45	6.5	7.5	0	27.5	16.5	1.9
-1.5	-2.5	-1.1	6.5	9.5	0.05	27.5	20.5	0.4
-1.5	-1.5	-0.7	6.5	11.5	0	27.5	23	-0.1
-1.5	-0.5	-0.7	9.5	-11.5	-0.1	27.5	25	0.2
-1.5	0.5	-1.1	9.5	-8.5	-0.9	31.5	-14.5	0.15
-1.5	0.7	-1	9.5	-5.5	-2.2	31.5	-12	0.5
-1.5	2	-0.4	9.5	-2.5	-2.75	31.5	-8	-1.4
-1.5	3	-0.3	9.5	0.5	-2.9	31.5	-5	0.2
-1.5	4	-0.15	9.5	3.5	-2.1	31.5	-2.5	0.3
-1.5	5	0.15	9.5	6.5	-0.4	31.5	-0.3	-0.65
-1.5	6.5	0.05	9.5	7.7	0.05	31.5	0.5	-0.1
0	-7.5	-0.2	9.5	9	0	31.5	3.5	-1.25
0	-6.5	-0.3	9.5	11.5	0.05	31.5	7.5	-1.35
0	-5.5	-0.5	9.5	14.5	0	31.5	11.5	-0.6
0	-4.5	-0.8	12.5	-12.5	-0.1	31.5	16.5	1.25
0	-3.5	-0.85	12.5	-9.5	-0.85	31.5	20.5	0.8
0	-2.5	-0.6	12.5	-6.5	-0.8	31.5	25	-0.1
0	-1.5	-0.1	12.5	-3.5	-1.1	35.5	-14.5	-0.1
0	-0.5	-0.1	12.5	-0.5	-1.6	35.5	-10.5	0.3
0	2	-0.7	12.5	2.5	-1.9	35.5	-6.5	0.1
0	3	-0.55	12.5	5.5	-1.55	35.5	-2.5	-0.05
0	4	-0.4	12.5	8.5	-0.3	35.5	-1.7	-0.65
0	5	-0.1	12.5	10.5	0.15	35.5	-0.5	-0.2
0	6	0.15	12.5	11.5	-0.1	35.5	3.5	-1.6
0	7.5	0.05	12.5	14.5	0	35.5	7.5	-2.1
1.5	-10.5	-0.2	12.5	17.5	-0.05	35.5	11.5	-1.2
1.5	-9.5	-0.25	15.5	-12.5	-0.1	35.5	17.5	1.7
1.5	-8.5	-0.35	15.5	-9.5	-1.7	35.5	21.5	0.3
1.5	-7.5	-0.7	15.5	-6.5	-1.5	35.5	25	0
1.5	-6.5	-1.2	15.5	-3.5	-1.6	41.5	-13.5	0
1.5	-5.5	-1.3	15.5	-0.5	-2	41.5	-9.5	0.05
1.5	-4.5	-1.4	15.5	2.5	-2.3	41.5	-3.5	-0.15
1.5	-3.5	-1.1	15.5	5.5	-2.35	41.5	-1.5	0.05
1.5	-2.5	-0.9	15.5	8.5	-1.25	41.5	2.5	-0.25
1.5	-1.5	-1.1	15.5	11.7	0.9	41.5	6.5	0.15
1.5	-0.5	-1.1	15.5	13	0.55	41.5	10.5	0.5
1.5	0.5	-1.2	15.5	14.5	-0.2	41.5	14.5	1.7
1.5	1.5	-1.1	15.5	17.5	0.05	41.5	17	2.7
1.5	2.5	-1.25	15.5	20.5	0	41.5	20.5	1
1.5	3.5	-0.95	18.5	-13.5	-0.1	41.5	25	0.25
1.5	4.5	-0.3	18.5	-10.5	0.15	47.5	-7.5	-0.15
1.5	5.5	-0.1	18.5	-7	-1.55	47.5	-2.5	0.05
1.5	6.5	0.1	18.5	-4.5	-1.7	47.5	1.5	-0.15
3.5	-13.5	-0.1	18.5	-1.5	-1.85	47.5	6.5	-0.15
3.5	-11.5	-0.9	18.5	3.5	-2.2	47.5	11.5	-0.15
3.5	-9.5	-1.1	18.5	7.5	-1.8	47.5	14.5	0.4
3.5	-7.5	-1.8	18.5	11	0.05	47.5	16.5	1.45
3.5	-5.5	-2.05	18.5	14.5	1.8	47.5	19.5	0.45
3.5	-3.5	-2.2	18.5	17.5	0.8	47.5	22.5	0.15
3.5	-1.5	-2	18.5	20.5	0	47.5	25	0.1

Table B.21: Experimental data for trapezoidal vane (3H:2.5V)
($F_r = 0.13$, $d_{50} = 0.225$ mm, Collar size BF1.13)

I			II			III		
x (cm)	y (cm)	z (cm)	x (cm)	y (cm)	z (cm)	x (cm)	y (cm)	z (cm)
-1.25	-7.9	0.05	3.75	-5.9	-0.6	20.75	-10.9	-0.4
-1.25	-5.9	0	3.75	-3.9	-1.4	20.75	-7.9	0.3
-1.25	-4.4	-0.35	3.75	-1.9	-1.3	20.75	-4.9	0.5
-1.25	-7.9	0	3.75	1.6	-0.35	20.75	-1.9	0
-1.25	-0.9	-0.1	3.75	3.1	-0.2	20.75	1.1	0.1
-1.25	1.1	-0.3	3.75	5.1	0.1	20.75	4.1	-0.1
-1.25	3.1	0	3.75	7.1	0.1	20.75	7.1	0.2
-1.25	5.1	0.1	5.75	-12.9	-0.1	20.75	10.1	1.2
0	-7.9	0	5.75	-10.9	-1.25	20.75	13.5	2.7
0	-6.9	0	5.75	-8.9	-1.1	20.75	16.1	1.15
0	-5.9	-0.4	5.75	-6.9	-1.25	20.75	19.1	0.7
0	-4.9	-0.95	5.75	-4.9	-1.8	20.75	22.1	0.1
0	-3.9	-1.1	5.75	-2.9	-1.8	24.75	-13.9	0
0	-3.2	-1.1	5.75	-0.9	-1.8	24.75	-9.9	-1.4
0	-2.9	-0.9	5.75	1.1	-0.5	24.75	-7.9	-1.25
0	-2.4	-0.5	5.75	3.6	0.35	24.75	-4.9	0
0	-0.9	-0.3	5.75	5.1	0.1	24.75	-1.9	-0.2
0	0.1	-0.3	5.75	7.1	0.2	24.75	1.1	-0.55
0	2.1	-0.25	5.75	9.1	0.1	24.75	4.1	-0.95
0	3.1	-0.1	8.75	-12.9	0.1	24.75	7.1	-0.75
0	4.1	0.1	8.75	-9.9	-0.05	24.75	10.1	0.3
0.75	-7.9	0	8.75	-6.9	-1.27	24.75	14.1	2.7
0.75	-6.9	0	8.75	-3.9	-1.95	24.75	17.1	1.2
0.75	-5.9	-0.6	8.75	-0.9	-2.4	24.75	21.1	0.1
0.75	-4.9	-1.15	8.75	2.1	-1.3	30.75	-13.9	0.1
0.75	-3.9	-1.4	8.75	5.1	-0.3	30.75	-10.4	-0.05
0.75	-3.1	-1.25	8.75	6.1	-0.55	30.75	-5.9	0.3
0.75	-2.4	-0.9	8.75	7.6	0.3	30.75	-2.9	0.7
0.75	-1.9	-0.65	8.75	11.1	0.2	30.75	0.1	0.2
0.75	-0.9	-0.3	8.75	14.1	0.1	30.75	3.1	-0.05
0.75	0.1	-0.3	11.75	-10.9	0	30.75	6.1	0
0.75	1.1	-0.3	11.75	-7.9	-0.2	30.75	9.1	0.3
0.75	2.6	-0.3	11.75	-4.9	-1	30.75	12.1	1.4
0.75	3.6	0	11.75	-1.9	-1.5	30.75	14.4	1
0.75	4.6	0.1	11.75	1.1	-2.05	30.75	17.1	0.85
1.75	-7.9	0.05	11.75	3.1	-2.2	30.75	20.1	0.2
1.75	-6.9	0	11.75	6.1	-1.3	30.75	24.1	0.1
1.75	-5.9	-0.75	11.75	9.1	0.6	35.75	-13.9	0.1
1.75	-4.9	-1.19	11.75	10.1	0.25	35.75	-10.9	-0.25
1.75	-3.9	-1.55	11.75	13.1	0.25	35.75	-6.9	0.2
1.75	-2.9	-1.5	11.75	17.1	0.1	35.75	-4.4	-0.2
1.75	-1.9	-0.9	15.75	-10.9	0	35.75	-1.9	0.3
1.75	-0.9	-0.7	15.75	-7.9	-0.75	35.75	1.1	0.05
1.75	0.1	-0.3	15.75	-4.9	-1.4	35.75	4.1	-0.55
1.75	1.1	-0.3	15.75	-0.9	-1.6	35.75	7.6	-0.9
1.75	2.1	-0.3	15.75	3.1	-1.3	35.75	11.1	-0.1
1.75	3.1	-0.3	15.75	7.1	-0.15	35.75	13.1	0.7
1.75	3.6	-0.1	15.75	10.6	1.4	35.75	15.1	0.1
1.75	4.6	0.1	15.75	12.5	0.6	35.75	18.1	0.5
1.75	5.6	0.1	15.75	13.6	0.3	35.75	22.1	0.2
3.75	-11.9	0.1	15.75	17.1	0.15	35.75	24.6	0.1
3.75	-9.9	-0.8	15.75	21.1	0.1			
3.75	-7.9	-0.65	20.75	-12.9	0			

Table B.22: Experimental data for trapezoidal vane (3H:2.5V)
 ($F_r = 0.13$, $d_{50} = 0.225$ mm, Collar size BF1.14)

I			II			III		
x	y	z	x	y	z	x	y	z
(cm)	(cm)	(cm)	(cm)	(cm)	(cm)	(cm)	(cm)	(cm)
-5.5	-8.6	-0.1	5.5	-0.6	-1.05	15.5	5.4	-0.2
-5.5	-4.6	0	5.5	2.4	-0.95	15.5	8.4	1.4
-5.5	-0.6	-0.05	5.5	4.2	-0.2	15.5	11.4	1.9
-5.5	3.4	0	5.5	5.4	0.3	15.5	12.8	1.6
-5.5	7.4	0	5.5	8.4	0.2	15.5	14.4	-0.25
-5.5	11.4	0	5.5	11.4	0.05	15.5	16.4	0.15
-5.5	15.4	0	5.5	14.4	0	15.5	19.4	-0.1
-2.5	-6.6	-0.1	8.5	-9.6	-0.1	15.5	22.4	-0.1
-2.5	-3.6	0	8.5	-6.6	0	19.5	-10.6	0
-2.5	-0.6	-0.05	8.5	-3.6	-0.75	19.5	-7.6	-0.2
-2.5	2.4	0	8.5	-0.6	-1.55	19.5	-4.6	-0.2
-2.5	5.4	0.1	8.5	2.4	-1.7	19.5	-1.6	-0.2
-2.5	8.4	0.05	8.5	5.4	-0.1	19.5	1.4	-0.35
-2.5	11.4	0.1	8.5	6.4	0.3	19.5	4.4	-0.8
-2.5	14.4	0.1	8.5	7.9	0.2	19.5	7.4	-0.3
0	-10.6	-0.1	8.5	10.4	0.1	19.5	10.4	0.95
0	-7.6	-0.1	8.5	13.4	0.1	19.5	12.2	1.35
0	-4.6	0	8.5	16.4	0	19.5	15.4	-0.2
0	3.4	0	11.5	-10.6	0	19.5	18.4	-0.1
0	6.4	0.2	11.5	-7.6	-0.1	19.5	21.4	-0.1
0	9.4	0.15	11.5	-4.6	-0.9	24.5	-11.6	0
0	12.4	0.05	11.5	-1.6	-1.15	24.5	-8.6	-0.05
0	15.4	0.1	11.5	1.4	-1.2	24.5	-5.6	-0.7
0	18.4	0.1	11.5	4.4	-0.8	24.5	-2.6	-0.3
2.5	-9.6	-0.15	11.5	7.4	0.8	24.5	0.4	-0.55
2.5	-6.6	-0.15	11.5	9.2	1.5	24.5	3.4	-0.7
2.5	-3.6	-1	11.5	10.4	0.05	24.5	6.4	-0.9
2.5	5.4	0.25	11.5	13.4	0	24.5	9.4	-0.65
2.5	8.4	0.15	11.5	16.4	0	24.5	12.4	0.7
2.5	11.4	0.1	15.5	-9.6	-0.1	24.5	15.4	0.2
2.5	14.4	0	15.5	-6.6	-0.15	24.5	17.9	-0.8
5.5	-9.6	-0.1	15.5	-3.6	-0.55	24.5	21.4	-0.1
5.5	-6.6	-0.15	15.5	-0.6	-0.9			
5.5	-3.6	-0.2	15.5	2.4	0.1			

Table B.23 Experimental data for rectangular vane
 ($F_r = 0.25$, $d_{50} = 0.225$ mm, Collar size AF2.12)

I			II			III		
x	y	z	x	y	z	x	y	z
(cm)	(cm)	(cm)	(cm)	(cm)	(cm)	(cm)	(cm)	(cm)
-4.5	-9.2	0	7.5	-10.2	-0.1	14.5	22.3	-1.1
-4.5	-6.2	0	7.5	-7.2	-0.1	18.5	-10.2	-0.02
-4.5	-3.2	0	7.5	-4.2	-0.2	18.5	-6.2	0
-4.5	-0.2	0	7.5	1.8	0.3	18.5	-2.2	-2
-4.5	2.8	0	7.5	4.8	1.2	18.5	1.8	-2.08
-4.5	5.8	0.15	7.5	6.2	0.6	18.5	5.8	-2.7
-4.5	8.8	-0.8	7.5	7.4	-1.9	18.5	8.8	-3.75
-4.5	11.8	0.05	7.5	9.8	-2.65	18.5	11.8	-5.3
-4.5	14.8	0	7.5	12.8	-3.3	18.5	14.8	-5.2
-1.5	-10.2	-0.1	7.5	15.8	-2.95	18.5	17.8	-3.7
-1.5	-7.2	-0.1	7.5	18.8	-1.6	18.5	20.8	-2.4
-1.5	-4.2	-0.4	7.5	22.3	-0.2	18.5	22.3	-2
-1.5	-1.2	-0.4	10.5	-10.2	-0.1	23.5	-12.2	0
-1.5	6.3	-0.15	10.5	-7.2	-0.2	23.5	-9.2	0
-1.5	10.3	-1.4	10.5	-4.2	-0.13	23.5	-7.2	-0.8
-1.5	12.8	0	10.5	1.8	-0.6	23.5	-3.2	-2.4
-1.5	15.8	0.05	10.5	4.4	-0.15	23.5	0.8	-2.7
1.5	-10.2	-0.15	10.5	6.8	-1.5	23.5	4.8	-3.35
1.5	-7.2	-0.1	10.5	8.6	-2.55	23.5	7.8	-3.6
1.5	-4.2	-0.35	10.5	10.3	-4.2	23.5	10.8	-4.05
1.5	1.3	0	10.5	12.8	-4.65	23.5	13.8	-3.8
1.5	7.8	-0.15	10.5	15.8	-4	23.5	16.8	-3.25
1.5	11.3	-1.6	10.5	18.8	-2.6	23.5	19.8	-3.15
1.5	13.8	-0.53	10.5	22.3	-1.1	23.5	22.3	-2.2
1.5	16.8	0.45	14.5	-10.2	-0.1	28.5	-12.2	0
4.5	-10.2	-0.1	14.5	-7.2	0	28.5	-8.2	-0.6
4.5	-7.2	-0.2	14.5	-4.2	0	28.5	-4.2	-1.9
4.5	-4.2	-0.3	14.5	-1.2	-1	28.5	-0.2	-2.47
4.5	0.8	-0.04	14.5	1.8	-1.7	28.5	3.8	-3.2
4.5	4.3	2.3	14.5	4.8	-1.4	28.5	7.8	-2.6
4.5	7.3	-0.65	14.5	7.8	-3.3	28.5	10.8	-2.35
4.5	9.8	-2	14.5	10.8	-5.05	28.5	13.8	-2.6
4.5	12.8	-2.7	14.5	12.6	-6.4	28.5	16.8	-2.8
4.5	15.8	-1.8	14.5	14.8	-5.7	28.5	19.8	-2.3
4.5	18.8	-0.64	14.5	17.8	-3.7	28.5	22.3	-0.8
4.5	22.3	0	14.5	20.8	-1.8			

Table B.24: Experimental data for trapezoidal vane (3H:2.5V)
(Fr = 0.25, d50 = 0.225 mm, Collar size BF2.5)

I			II			III		
x	y	z	x	y	z	x	y	z
(cm)	(cm)	(cm)	(cm)	(cm)	(cm)	(cm)	(cm)	(cm)
-4	-8.6	-0.15	7	-5.6	0.07	18	-7.6	-1.9
-4	-5.6	-0.15	7	5.8	-0.7	18	-4.6	-2.6
-4	-2.6	0	7	7.1	-2.93	18	-1.6	-2.7
-4	0.4	0.1	7	10.4	-3.75	18	1.4	-3
-4	3.4	0.25	7	13.4	-3.2	18	4.4	-2.35
-4	6.4	0.35	7	16.4	-2.1	18	5.9	-1.97
-4	9.4	0.3	7	19.4	-0.85	18	8.4	-2.8
-4	12.4	0.2	7	22.4	0.2	18	11.4	-4.35
-4	15.4	0.1	10	-10.6	0	18	14.4	-6.4
-2	-8.6	-0.15	10	-7.6	-0.1	18	15.9	-7.05
-2	-5.6	-0.1	10	-4.6	-0.1	18	18.4	-5.75
-2	-2.6	-0.1	10	1.9	-1.25	18	21.4	-3.75
-2	0.4	-0.3	10	4.4	-1.8	18	22.9	-2.6
-2	4.4	-0.13	10	7.4	-0.1	23	-16.6	-0.3
-2	7.4	0.28	10	8.4	-0.3	23	-13.6	-1.95
-2	10.4	0.23	10	10.7	-5.7	23	-9.6	-3.35
-2	13.4	0.15	10	13.4	-5.1	23	-5.6	-4.05
1	-10.6	0	10	16.4	-3.75	23	-1.6	-3.95
1	-7.6	0.07	10	19.4	-2.45	23	2.4	-3.71
1	-4.6	-0.1	10	22.9	0	23	7.4	-3
1	0.8	-0.3	14	-10.6	-0.2	23	10.4	-3.27
1	10	-0.1	14	-7.6	-0.25	23	13.4	-4.9
1	11.4	-0.71	14	-4.6	-0.6	23	16.4	-5.37
1	13.4	-0.5	14	-1.6	-1.3	23	19.4	-4
1	16.4	0.1	14	1.4	-2.47	23	22.9	-2.2
1	19.4	0.1	14	4.4	-2.05	28	-16.6	-1.7
4	-10.6	0.2	14	6.4	-1	28	-11.6	-3.9
4	-7.6	0.05	14	9.4	-2.7	28	-6.6	-4.6
4	-4.6	-0.1	14	11.7	-3.95	28	-1.6	-4.63
4	3.3	-0.15	14	14.1	-6.8	28	3.4	-4.24
4	8.6	-0.63	14	16.4	-5.7	28	8.4	-2.75
4	11.4	-1.97	14	19.4	-4.02	28	10.4	-2.1
4	14.4	-1.4	14	22.4	-2.25	28	13.4	-3.1
4	17.4	0.05	14	22.9	-1.9	28	16.4	-3.3
4	20.4	0.2	18	-16.6	-0.15	28	19.4	-3.05
7	-10.6	0.1	18	-13.6	-0.3	28	22.9	-1.7
7	-7.6	0	18	-10.6	-1.2			

Table B.25: Experimental data for rectangular vane
 ($F_r = 0.25$, $d_{50} = 0.405$ mm, Collar size AF2.1)

I			II			III		
x	y	z	x	y	z	x	y	z
(cm)	(cm)	(cm)	(cm)	(cm)	(cm)	(cm)	(cm)	(cm)
-9.75	-18.3	0.04	-0.75	12.7	-1.83	11.25	9.8	-0.28
-9.75	-15.3	0.11	-0.75	15.7	-2.39	11.25	10.9	-3.22
-9.75	-12.3	0.04	-0.75	18.7	-0.29	11.25	13.7	-3.24
-9.75	-9.3	0.05	2.25	-18.3	-1.79	11.25	16.7	-1.64
-9.75	-6.3	-0.12	2.25	-15.3	-2.99	11.25	19.7	-0.29
-9.75	-3.3	-0.28	2.25	-12.3	-3.58	11.25	21.2	-0.5
-9.75	-0.3	0.01	2.25	-9.3	-2.76	14.25	-18.3	-2.88
-9.75	2.7	0.16	2.25	-6.3	-1.39	14.25	-15.3	-3.47
-9.75	5.7	0.11	2.25	-3.3	-1.75	14.25	-12.3	-4.29
-9.75	8.7	0.16	2.25	-2.3	-1.95	14.25	-9.3	-4.89
-9.75	11.7	0.08	2.25	-1.3	-2.1	14.25	-6.3	-5.39
-9.75	14.7	0.11	2.25	-0.3	-2.42	14.25	-3.3	-5.59
-9.75	17.7	0.11	2.25	0.7	-2.1	14.25	-0.3	-4.48
-6.75	-18.3	-0.06	2.25	1.7	0.11	14.25	2.7	-3.29
-6.75	-15.3	-0.06	2.25	3.9	-5.99	14.25	5.7	-1.89
-6.75	-12.3	-0.25	2.25	6.7	-5.49	14.25	8.7	-0.37
-6.75	-9.3	-1.37	2.25	9.7	-3.99	14.25	11.7	-2.5
-6.75	-6.3	-1.63	2.25	12.7	-2.18	14.25	14.7	-3.49
-6.75	-3.3	-2.53	2.25	15.7	-0.79	14.25	17.7	-2.06
-6.75	-0.3	-1.87	2.25	18.7	-0.49	14.25	20.7	-0.49
-6.75	2.7	-1.09	5.25	-18.3	-2.58	18.25	-18.3	-1.76
-6.75	5.7	-0.27	5.25	-15.3	-3.87	18.25	-14.3	-2.76
-6.75	8.7	0.01	5.25	-12.3	-4.38	18.25	-10.3	-3.55
-6.75	11.7	-0.04	5.25	-9.3	-3.95	18.25	-6.3	-4.65
-6.75	14.7	-0.09	5.25	-6.3	-2.96	18.25	-2.3	-5.5
-6.75	17.7	-0.11	5.25	-3.3	-1.79	18.25	1.7	-5.25
-3.75	-18.3	-0.22	5.25	-0.3	-0.69	13.25	5.7	-4
-3.75	-15.3	-0.33	5.25	2.7	0.44	18.25	9.7	-2.2
-3.75	-12.3	-1.24	5.25	4.7	0.78	18.25	9.8	-1.15
-3.75	-9.3	-2.52	5.25	6.3	-5	18.25	11.7	-2.4
-3.75	-8.3	-2.65	5.25	9.7	-4.15	18.25	14.7	-3.6
-3.75	-6.3	-2.4	5.25	12.7	-2.49	18.25	15.7	-3.8
-3.75	-4.3	-2.5	5.25	15.7	-1.14	18.25	17.7	-2.88
-3.75	-2.3	-2.53	5.25	18.7	-0.49	18.25	19.7	-1.4
-3.75	-0.3	-3.15	8.25	-18.3	-2.99	18.25	21.2	-0.7
-3.75	1.3	-3.09	8.25	-15.3	-4.04	23.25	-18.3	-0.7
-3.75	4.7	-2.63	8.25	-12.3	-4.86	23.25	-14.3	-0.9
-3.75	7.7	-1.94	8.25	-9.3	-5.19	23.25	-10.3	-1.45
-3.75	10.7	-1.05	8.25	-6.3	-4.43	23.25	-6.3	-3
-3.75	13.7	-0.19	8.25	-3.3	-4.33	23.25	-2.3	-4.25
-3.75	16.7	-0.23	8.25	-0.3	-2.15	23.25	1.7	-4.7
-3.75	19.7	-0.29	8.25	2.7	-1.06	23.25	4.7	-4.4
-0.75	-18.3	-0.49	8.25	5.7	0.35	23.25	7.7	-3
-0.75	-15.3	-1.96	8.25	7.2	0.11	23.25	11.2	-1.35
-0.75	-12.3	-2.04	8.25	8.9	-4.07	23.25	13.7	-2.5
-0.75	-9.3	-1.85	8.25	12.7	-2.98	23.25	16.2	-3.3
-0.75	-7.9	-2.09	8.25	15.7	-1.25	23.25	18.7	-2.1
-0.75	-6.3	-1.59	8.25	18.7	-0.33	23.25	21.2	-0.95
-0.75	-4.3	-6	11.25	-18.3	-3.04	28.25	-18.3	-0.05
-0.75	-2.3	-2.75	11.25	-15.3	-3.83	28.25	-13.3	0.4
-0.75	-1.3	-3.3	11.25	-12.3	-3.78	28.25	-8.3	-0.48
-0.75	-0.3	-3.75	11.25	-9.3	-5.33	28.25	-3.3	-0.47
-0.75	0.7	-4.15	11.25	-6.3	-5.16	28.25	1.7	-3.6
-0.75	1.7	-4.4	11.25	-3.3	-4.36	28.25	6.7	-3.46
-0.75	2.7	-4.7	11.25	-0.3	-3.33	28.25	12.2	-0.65
-0.75	3.7	-4.13	11.25	2.7	-2.2	28.25	14.7	-1.6
-0.75	6.7	-3.99	11.25	5.7	-0.67	28.25	17.7	-5.7
-0.75	9.7	-2.79	11.25	8.7	-0.07	28.25	21.2	-0.2

Table B.26: Experimental data for rectangular vane
 ($F_r = 0.25$, $d_{50} = 0.405$ mm, Collar size AF2.2)

I			II			III		
x	y	z	x	y	z	x	y	z
(cm)	(cm)	(cm)	(cm)	(cm)	(cm)	(cm)	(cm)	(cm)
-9.5	-15.4	0.1	2.5	-15.4	-1.8	11.5	-8.4	-4.7
-9.5	-12.4	-0.15	2.5	-12.4	-1.85	11.5	-5.4	-3.9
-9.5	-9.4	-0.25	2.5	-9.4	-2	11.5	-2.4	-3.05
-9.5	-6.4	-0.5	2.5	-6.4	-1.1	11.5	0.6	-1.8
-9.5	-3.4	-0.7	2.5	-3.9	-1.9	11.5	3.6	-0.8
-9.5	-0.4	-0.05	2.5	-2.4	-2.48	11.5	6.6	1
-9.5	2.6	0.25	2.5	-0.4	-2.31	11.5	7.7	1.35
-9.5	5.6	0.25	2.5	1.6	0.9	11.5	9.4	0.8
-6.5	-17.4	0.2	2.5	3.6	-2.56	11.5	10.8	-1.5
-6.5	-14.4	-0.5	2.5	4.6	-2	11.5	12.6	-1.34
-6.5	-11.4	-2.2	2.5	7.6	-0.75	11.5	15.6	-0.3
-6.5	-9.4	-2.39	2.5	10.6	0.03	11.5	18.6	-0.25
-6.5	-7.4	-2.64	2.5	13.6	0.1	15.5	-18.4	-1.7
-6.5	-5.4	-2.73	5.5	-18.4	-2.4	15.5	-14.4	-3.35
-6.5	-3.4	-2.23	5.5	-15.4	-3.2	15.5	-10.4	-5.05
-6.5	-0.9	-1.95	5.5	-12.4	-3.45	15.5	-6.4	-5.45
-6.5	1.6	-0.85	5.5	-9.4	-3.1	15.5	-2.4	-4.2
-6.5	4.6	-0.1	5.5	-6.4	-1.9	15.5	1.6	-2.8
-6.5	7.6	0.1	5.5	-3.4	-1.1	15.5	5.6	-0.9
-6.5	10.6	0.1	5.5	-1.1	-0.86	15.5	9.4	0.8
-3.5	-18.4	0.15	5.5	1.3	-0.5	15.5	12.6	-1.5
-3.5	-15.4	-0.8	5.5	4.1	0.5	15.5	14.1	-1.65
-3.5	-12.4	-1.3	5.5	5.6	-1.7	15.5	16.6	-0.8
-3.5	-8.9	-1	5.5	8.6	-1.35	15.5	19.6	-0.35
-3.5	-7.4	-1.09	5.5	11.6	0.1	20.5	-18.4	-1.2
-3.5	-5.4	-1.11	5.5	14.6	-0.1	20.5	-13.4	-2.1
-3.5	-3.4	-1.86	5.5	17.6	-0.1	20.5	-8.4	-3.45
-3.5	-1.4	-2.79	8.5	-18.4	-2.8	20.5	-3.4	-4.2
-3.5	1.6	-2.63	8.5	-15.4	-4.1	20.5	1.6	-4.1
-3.5	4.6	-1.5	8.5	-12.9	-4.8	20.5	6.6	-1.95
-3.5	7.6	0.05	8.5	-10.4	-4.1	20.5	10.9	-0.2
-3.5	10.6	0.1	8.5	-7.4	-3.55	20.5	14.6	-1.45
-0.5	-18.4	0.05	8.5	-4.4	-2.5	20.5	17.6	-0.75
-0.5	-15.4	-0.95	8.5	-1.4	-1.4	20.5	21.1	-0.5
-0.5	-12.4	-1.3	8.5	1.6	0	25.5	-18.4	-2.39
-0.5	-9.4	-0.75	8.5	5.6	1.6	25.5	-13.4	-0.76
-0.5	-6.4	-1.4	8.5	7.1	1.3	25.5	-8.4	-0.39
-0.5	-4.4	-2.2	8.5	8.1	-1.7	25.5	-3.4	-1.69
-0.5	-2.4	-3.29	8.5	10.6	-1.25	25.5	1.6	-3.2
-0.5	-0.4	-4.67	8.5	13.6	0.1	25.5	6.6	-3.04
-0.5	1.6	-4.27	8.5	16.6	-0.2	25.5	12.2	0.07
-0.5	4.1	-2.6	8.5	19.6	-0.1	25.5	15.9	-0.54
-0.5	6.6	-0.8	11.5	-18.4	-2.35	25.5	19.6	0.44
-0.5	9.6	0.05	11.5	-15.4	-4	25.5	21.1	0.01
-0.5	12.6	0.1	11.5	-12.4	-5.4			
2.5	-18.4	-1.05	11.5	-10.9	-5.5			

Table B.27: Experimental data for rectangular vane
 ($F_r = 0.25$, $d_{50} = 0.405$ mm, Collar size AF2.3)

I			II			III		
x	y	z	x	y	z	x	y	z
(cm)	(cm)	(cm)	(cm)	(cm)	(cm)	(cm)	(cm)	(cm)
-12	-19	0.3	-3	13	0	11	-7	-5
-12	-15	0.2	0	-19	-2.8	11	-3	-3
-12	-12	0.1	0	-16	-3.8	11	1	-1.35
-12	-9	0.05	0	-12	-4.5	11	4	-0.5
-12	-6	-0.05	0	-9	-3.2	11	7.5	1.05
-12	-3	0	0	-4	-2.07	11	9.5	-0.05
-12	0	0.1	0	-2	-3.62	11	10.5	-2.85
-12	3	0.05	0	0	-4.47	11	11	-2.85
-12	6	0.05	0	2	-4.15	11	15	-1.75
-9	-19	0.3	0	4.7	-3.15	11	18	-0.4
-9	-16	0.1	0	6.5	-2.3	11	20.5	-0.35
-9	-13	-0.7	0	9	-0.45	15	-19	-3.1
-9	-10	-1.7	0	12	-0.1	15	-15	-4.5
-9	-7	-1.9	0	15	-0.1	15	-11	-5.4
-9	-4	-2	3	-19	-3.65	15	-7	-5.6
-9	-1	-1.1	3	-16	-4.5	15	-3	-4.5
-9	2	-0.05	3	-13	-5	15	1	-2.6
-9	5	0	3	-10	-4.4	15	5	-1
-9	8	0	3	-7	-2.6	15	8	0.05
-6	-19	-0.35	3	-5	-1.88	15	11	-1.7
-6	-16	-1.4	3	-3	-1.57	15	13.5	-3.25
-6	-13	-2.2	3	-1	-1.79	15	16	-2.3
-6	-10.5	-1.35	3	1	0.4	15	19	-0.55
-6	-9	-1.08	3	2.4	0	15	20.5	-0.5
-6	-7	-0.89	3	4	-3.4	20	-19	-1.3
-6	-5	-0.83	3	7	-1.8	20	-14	-3.2
-6	-3	-2.06	3	10	-0.7	20	-9	-4.5
-6	-1.5	-2.59	3	13	-0.2	20	-4	-5
-6	-0.2	-2.4	3	16	-0.2	20	1	-4.3
-6	3	-1.2	3	19	-0.3	20	6	-2.2
-6	6	-0.4	7	-19	-4.3	20	9.5	-0.3
-6	9	-0.1	7	-16	-5.1	20	12	-1.5
-6	12	0.05	7	-11	-6.1	20	14.5	-2.3
-3	-19	-1.75	7	-9	-4.9	20	17	-1.7
-3	-16	-2.8	7	-6	-3.2	20	19.5	-0.1
-3	-13	-3.7	7	-3	-1.95	20	20.5	-0.4
-3	-10	-2.55	7	0	-0.3	25	-19	0.34
-3	-8.2	-2	7	3	0.65	25	-14	-0.47
-3	-7	-1.06	7	6	0.7	25	-9	-1.8
-3	-5	-1.57	7	7	-2.8	25	-4	-3.18
-3	-3	-2.57	7	10	-2.3	25	1	-4.17
-3	-1	-3.39	7	13	-0.95	25	6	-2.89
-3	1	-3.69	7	16	-0.4	25	11	-0.16
-3	2.3	-3.3	7	20.5	-0.3	25	16	-1.15
-3	4	-2.75	11	-19	-3.95	25	20.5	0.21
-3	7	-1.25	11	-15	-5.25			
-3	10	-0.1	11	-11	-5.5			

Table B.28: Experimental data for rectangular vane
 $(F_r = 0.25, d_{50} = 0.405 \text{ mm}, \text{Collar size AF2.4})$

I			II			III		
x	y	z	x	y	z	x	y	z
(cm)	(cm)	(cm)	(cm)	(cm)	(cm)	(cm)	(cm)	(cm)
-11.5	-18.4	0.14	-2.5	5.6	-0.24	9.5	-18.4	-4.62
-11.5	-15.4	0.13	-2.5	8.6	0	9.5	-15.4	-5.57
-11.5	-12.4	0	-2.5	11.6	0.01	9.5	-12.4	-6.44
-11.5	-9.4	-0.09	-2.5	14.6	-0.05	9.5	-9.4	-6.45
-11.5	-6.4	0	-2.5	17.6	-0.19	9.5	-6.4	-4.86
-11.5	-3.4	0	-0.5	-18.4	-3.09	9.5	-3.4	-3.16
-11.5	-0.4	-0.12	-0.5	-15.4	-4.09	9.5	-0.4	-1.59
-11.5	2.6	0	-0.5	-12.4	-4.49	9.5	2.6	-0.69
-11.5	5.6	0	-0.5	-9.4	-3.15	9.5	5.6	1.55
-11.5	8.6	0	-0.5	-6.4	-2.76	9.5	8.6	2
-11.5	11.6	-0.09	-0.5	-4.4	-2.15	9.5	9.6	-1.46
-11.5	14.6	-0.19	-0.5	-2.4	-1.84	9.5	11.6	-1.08
-8.5	-18.4	0.14	-0.5	-0.4	-2.79	9.5	14.6	0
-8.5	-15.4	-0.73	-0.5	1.6	-2.47	9.5	17.6	-0.19
-8.5	-12.4	-1.67	-0.5	3.6	-1.42	9.5	21.1	-0.14
-8.5	-9.4	-2.39	-0.5	5	-1.26	13.5	-18.4	-3.56
-8.5	-6.4	-2	-0.5	7.6	-0.19	13.5	-14.4	-5.29
-8.5	-3.4	-2.23	-0.5	10.6	0.01	13.5	-10.4	-6.69
-8.5	-0.4	-0.99	-0.5	13.6	0.01	13.5	-6.4	-6.02
-8.5	2.6	0.01	-0.5	16.6	-0.07	13.5	-2.4	-3.56
-8.5	5.6	0.01	-0.5	21.1	-0.09	13.5	1.6	-1.57
-8.5	8.6	0.01	3.5	-18.4	-4.16	13.5	5.6	1
-8.5	11.6	0.01	3.5	-15.4	-4.79	13.5	8.1	2.21
-8.5	14.6	-0.07	3.5	-12.4	-5.55	13.5	12.1	-0.56
-5.5	-18.4	-1	3.5	-9.4	-4.79	13.5	15.1	-1.36
-5.5	-15.4	-2.49	3.5	-6.4	-2.86	13.5	19.1	-0.23
-5.5	-12.4	-1.68	3.5	-3.4	-2.49	13.5	21.1	-0.27
-5.5	-11	-2.09	3.5	-1.4	-1.87	18.5	-18.4	-1.16
-5.5	-9.4	-1.72	3.5	0.6	-1	18.5	-13.4	-3.76
-5.5	-7.4	-1.17	3.5	2.1	-0.59	18.5	-8.4	-5.39
-5.5	-5.4	-1.27	3.5	3.8	-1.25	18.5	-3.4	-5.08
-5.5	-3.4	-2.53	3.5	6.1	-1.69	18.5	1.6	-2.29
-5.5	-1.4	-2.74	3.5	8.6	-1.27	18.5	6.6	0.73
-5.5	-0.4	-2.27	3.5	11.6	0.01	18.5	9.1	1.81
-5.5	2.6	-0.62	3.5	14.6	-0.09	18.5	11.6	0.44
-5.5	5.6	0.01	3.5	17.6	-0.17	18.5	14.6	-1.47
-5.5	8.6	0.01	6.5	-18.4	-4.56	18.5	15.6	-1.74
-5.5	11.6	-0.05	6.5	-15.4	-5.47	18.5	17.6	-0.77
-5.5	14.6	-0.04	6.5	-12.4	-6.15	18.5	19.6	-0.06
-5.5	17.6	-0.09	6.5	-9.4	-5.59	18.5	21.1	-1.17
-2.5	-18.4	-2.29	6.5	-6.4	-3.78	23.5	-18.4	0.86
-2.5	-15.4	-3.18	6.5	-3.4	-2	23.5	-13.4	-1.29
-2.5	-12.4	-3.34	6.5	-0.4	-1.69	23.5	-8.4	-3.36
-2.5	-9.4	-2.26	6.5	2.6	-0.27	23.5	-3.4	-4.34
-2.5	-8.4	-2.49	6.5	5.6	0.26	23.5	1.6	-3.35
-2.5	-6.4	-1.65	6.5	6.8	-2.55	23.5	6.6	-0.07
-2.5	-4.4	-1.57	6.5	7.7	-2.49	23.5	10.4	1.72
-2.5	-2.4	-2	6.5	10.6	-1	23.5	12.6	0.42
-2.5	-0.4	-2.15	6.5	13.6	0.01	23.5	15.6	-0.99
-2.5	1.6	-2.13	6.5	16.6	-0.19	23.5	18.6	1.01
-2.5	2.6	-1.69	6.5	21.1	-0.25	23.5	21.1	0.41

Table B.29 Experimental data for rectangular vane
 ($F_r = 0.25$, $d_{50} = 0.405$ mm, Collar size AF2.5)

I			II			III		
x (cm)	y (cm)	z (cm)	x (cm)	y (cm)	z (cm)	x (cm)	y (cm)	z (cm)
-12.5	-20.3	0.2	-3.5	9.7	-0.25	6.5	14.7	0
-12.5	-17.3	0.1	-3.5	12.7	0.05	6.5	17.7	-0.2
-12.5	-14.3	-0.3	-3.5	15.7	0.05	6.5	19.2	-0.1
-12.5	-11.3	-0.35	-3.5	19.2	-0.1	10.5	-20.3	-5.6
-12.5	-8.3	-0.3	0	-20.3	-0.4	10.5	-16.3	-6.5
-12.5	-5.3	-0.6	0	-17.3	-3.5	10.5	-12.3	-5.4
-12.5	-2.3	0.1	0	-14.3	-3.15	10.5	-8.3	-3.2
-12.5	0.7	0.2	0	-11.3	-1.8	10.5	-4.3	-1.45
-9.5	-20.3	0.1	0	-7.8	-2.6	10.5	-2.3	-0.95
-9.5	-17.3	-1.2	0	-6.3	-2.5	10.5	0.7	-0.95
-9.5	-14.3	-2.5	0	-4.3	-3.5	10.5	4.7	1.4
-9.5	-11.3	-2.9	0	-2.3	-4.95	10.5	7.7	1
-9.5	-8.3	-2.65	0	-0.3	-5.43	10.5	9.2	1
-9.5	-5.3	-2.4	0	1.7	-5	10.5	10.2	-1.5
-9.5	-2.3	-1.75	0	3.7	-3.6	10.5	12.7	-0.8
-9.5	0.7	-0.45	0	4.7	-2.7	10.5	15.7	-0.5
-9.5	3.7	0.1	0	7.7	0.2	10.5	17.7	-0.25
-9.5	6.7	0.15	0	10.7	0.15	10.5	19.2	-0.1
-9.5	9.7	0.05	0	13.7	0	15.5	-20.3	-5.8
-9.5	12.7	0.1	0	16.7	0	15.5	-15.3	-6.9
-9.5	15.7	-0.05	0	19.2	0.05	15.5	-10.3	-6.4
-9.5	19.2	0.1	3.5	-20.3	-4.4	15.5	-5.3	-4.3
-6.5	-20.3	-0.35	3.5	-17.3	-4.95	15.5	-0.3	-2.4
-6.5	-17.3	-1.5	3.5	-14.3	-4.35	15.5	4.7	-0.35
-6.5	-13.3	-2.55	3.5	-11.3	-2.35	15.5	8.2	1.8
-6.5	-11.3	-2.4	3.5	-8.3	-1.95	15.5	10.7	0.5
-6.5	-9.3	-1.9	3.5	-6.3	-2.3	15.5	13.7	-1.3
-6.5	-7.3	-1.1	3.5	-4.3	-3.1	15.5	16.7	-2.6
-6.5	-5.3	-1.55	3.5	-2.3	-3	15.5	19.2	-2.85
-6.5	-3.3	-5.8	3.5	-0.3	-2.9	20.5	-20.3	-4.8
-6.5	-1.3	-2.45	3.5	1.7	-1.8	20.5	-15.3	-6.6
-6.5	1.7	-1.45	3.5	3.7	-2.5	20.5	-10.3	-7.5
-6.5	4.7	-0.5	3.5	6.2	-0.8	20.5	-5.3	-6.88
-6.5	7.7	0.1	3.5	8.7	-0.5	20.5	-0.3	-4.2
-6.5	10.7	0.1	3.5	11.7	0.4	20.5	4.7	-1.7
-6.5	13.7	-0.05	3.5	14.7	-0.1	20.5	9.7	0.8
-6.5	16.7	0.05	3.5	17.7	0	20.5	12.7	-0.7
-6.5	19.2	0.1	3.5	19.2	0.05	20.5	15.7	-1.8
-3.5	-20.3	-2	6.5	-20.3	-5.05	20.5	19.2	-3
-3.5	-17.3	-2.25	6.5	-17.3	-5.75	25.5	-20.3	-3.3
-3.5	-14.3	-2.35	6.5	-14.3	-5.1	25.5	-15.3	-4.35
-3.5	-11.3	-2.55	6.5	-11.3	-3.3	25.5	-10.3	-6.5
-3.5	-9.3	-2.1	6.5	-8.3	-2.2	25.5	-5.3	-6.65
-3.5	-7.3	-1.45	6.5	-6.3	-1.7	25.5	-0.3	-5.4
-3.5	-5.3	-1.65	6.5	-2.3	-2.3	25.5	4.7	-2.65
-3.5	-3.3	-2.9	6.5	2.7	-0.75	25.5	10.7	0.8
-3.5	-1.3	-3.7	6.5	5.2	0.65	25.5	13.7	-0.6
-3.5	1.2	-3.5	6.5	6.2	-1.4	25.5	16.7	-1.8
-3.5	3.7	-1.95	6.5	8.7	-1.5	25.5	17.7	-2.15
-3.5	6.7	-1.5	6.5	11.7	0.1	25.5	19.2	-1.8

Table B.30 Experimental data for rectangular vane
 ($F_r = 0.25$, $d_{50} = 0.405$ mm, Collar size AF2.6)

I			II			III		
x	y	z	x	y	z	x	y	z
(cm)	(cm)	(cm)	(cm)	(cm)	(cm)	(cm)	(cm)	(cm)
-11.75	-12	0	0.25	-19	-0.15	9.25	-1	-0.7
-11.75	-9	0	0.25	-16.5	-0.15	9.25	2	0.75
-11.75	-6	-0.15	0.25	-13	-2.05	9.25	4	1.55
-11.75	-3	0	0.25	-10	-2.25	9.25	7	0.05
-11.75	0	0.1	0.25	-8	-1	9.25	8.5	-0.75
-11.75	3	0.05	0.25	1.5	-1.3	9.25	9.5	-4.45
-8.75	-19	0	0.25	3	-2.15	9.25	10.7	-4.55
-8.75	-15	0	0.25	5.5	-2.95	9.25	13	-4.05
-8.75	-11	-0.05	0.25	8	-2.2	9.25	16	-2.8
-8.75	-8	-0.95	0.25	11	-0.65	9.25	19	-1.15
-8.75	-5	-2	0.25	14	-0.35	9.25	20.5	-0.45
-8.75	-2.5	-1.5	0.25	17	-0.45	13.25	-19	-1.35
-8.75	0	-0.25	0.25	20.5	-0.35	13.25	-16	-3.15
-8.75	3	0.1	3.25	-19	-0.15	13.25	-12	-5.2
-8.75	6	0.1	3.25	-16	-0.55	13.25	-9.5	-5.85
-8.75	9	-0.05	3.25	-13	-2.45	13.25	-7	-5.05
-8.75	12	-0.1	3.25	-9.85	-1.95	13.25	-3	-2.75
-8.75	15	-0.25	3.25	-8	-1.25	13.25	1	-0.9
-8.75	18	-0.25	3.25	-6.5	-0.95	13.25	5.5	0.35
-8.75	20.5	-0.35	3.25	1	0.05	13.25	8	-1.1
-5.75	-19	-0.05	3.25	3	0.85	13.25	11	-3.15
-5.75	-16	-0.05	3.25	4.2	-1.75	13.25	12	-4.05
-5.75	-13	-0.1	3.25	5.9	-2.05	13.25	14.1	-4.85
-5.75	-10	-1.25	3.25	9	-2.65	13.25	17	-3.7
-5.75	-8	-2.45	3.25	12	-1.3	13.25	20	-1.9
-5.75	-6	-2.55	3.25	15	-0.45	13.25	20.5	-1.45
-5.75	-4	-1.2	3.25	18	-0.45	18.25	-19	-0.55
-5.75	-2	-2.15	3.25	20.5	-0.45	18.25	-14	-2.85
-5.75	0	-1.9	6.25	-19	-0.25	18.25	-9	-5.2
-5.75	3	-0.15	6.25	-16	-1.85	18.25	-6	-5.45
-5.75	6	-0.05	6.25	-13	-2.95	18.25	-1	-2.95
-5.75	9	-0.05	6.25	-9.7	-2.25	18.25	7	0.05
-5.75	12	-0.15	6.25	-9	-2.2	18.25	10	-1.15
-5.75	15	-0.25	6.25	-7	-2.05	18.25	13	-3.05
-5.75	18	-0.35	6.25	-5	-1.25	18.25	16	-3.6
-5.75	20.5	-0.35	6.25	0.5	-0.05	18.25	19	-2.85
-2.75	-19	-0.1	6.25	5	1.45	18.25	20.5	-1.65
-2.75	-16	-0.15	6.25	5.7	1.8	23.25	-19	-0.9
-2.75	-13	-0.65	6.25	6.5	-2.7	23.25	-14	-1.25
-2.75	-10	-2.35	6.25	9	-2.95	23.25	-9	-3.45
-2.75	-8	-2.45	6.25	12	-2.75	23.25	-4	-4.5
-2.75	-6	-1.45	6.25	15	-1.75	23.25	-2	-4.35
-2.75	1	-1.35	6.25	18	-0.45	23.25	2	-3.15
-2.75	2.5	-2.2	6.25	20.5	-0.45	23.25	8.5	0.15
-2.75	5	-1.6	9.25	-19	-1.2	23.25	11	-0.1
-2.75	8	-0.35	9.25	-16	-2.8	23.25	14	-2.05
-2.75	11	-0.15	9.25	-13	-3.95	23.25	17	-2.85
-2.75	12	-0.25	9.25	-10	-4.25	23.25	20.5	-1.45
-2.75	15	-0.35	9.25	-7	-3.3			
-2.75	20.5	-0.35	9.25	-4	-1.75			

Table B.31 Experimental data for rectangular vane
 ($F_r = 0.25$, $d_{50} = 0.405$ mm, Collar size AF2.7)

I			II			III		
x	y	z	x	y	z	x	y	z
(cm)	(cm)	(cm)	(cm)	(cm)	(cm)	(cm)	(cm)	(cm)
-5	-18.6	0.3	4	-8.9	-0.79	13	-3.6	-1.7
-5	-14.6	0.1	4	1.4	0.25	13	-0.6	-2.15
-5	-10.6	0.1	4	3.3	1.4	13	2.4	-1.1
-5	-6.6	-0.1	4	5.3	-1.65	13	5.4	-1.9
-5	-2.6	-0.1	4	8.4	-2.65	13	8.4	-3.8
-5	1.4	-0.3	4	11.4	-2.15	13	10.2	-5.05
-5	2.9	-1.1	4	14.4	-0.7	13	12.9	-6.1
-5	4.4	-0.85	4	17.4	-0.2	13	14.4	-5.35
-5	5.9	-0.2	4	20.9	-0.15	13	17.4	-3.7
-5	7.4	-0.1	7	-18.6	0.1	13	20.9	-0.8
-5	11.4	-0.15	7	-15.6	-0.35	17	-18.6	-1.62
-5	15.4	0	7	-12.6	-2.15	17	-14.6	-2.69
-5	19.4	0	7	-10.3	-2.7	17	-10.6	-2.76
-2	-18.6	0.1	7	-9.6	-2.07	17	-6.6	-1.95
-2	-15.6	0.1	7	-7.8	-1.03	17	-2.6	-2.09
-2	-12.6	0	7	1.4	-0.4	17	1.4	-2.12
-2	-9.6	-0.1	7	4.4	1	17	5.4	-2.75
-2	-6.6	-0.1	7	5.9	0.35	17	9.4	-3.9
-2	3.4	-1.39	7	6.9	-3.65	17	13.4	-5.65
-2	5.4	-2.1	7	9.4	-3.8	17	17.4	-4.19
-2	7.4	-1.35	7	12.4	-2.9	17	20.9	-1.26
-2	9.4	-0.15	7	15.4	-2	21	-18.6	-1.95
-2	12.4	-0.1	7	18.4	-0.8	21	-13.6	-3.49
-2	15.4	-0.1	7	20.9	-0.2	21	-8.6	-3.39
-2	18.4	0	10	-18.6	-0.1	21	-3.6	-3.76
-2	20.9	0	10	-15.6	-0.5	21	1.4	-3.89
1	-18.6	0.1	10	-12.6	-1.95	21	6.4	-3.57
1	-15.6	0.05	10	-9.6	-2.5	21	9.4	-2.69
1	-12.6	-0.15	10	-5.6	-0.85	21	13.4	-4.04
1	-10.1	-0.4	10	-2.6	-1	21	16.4	-3.99
1	4	-1.23	10	0.4	-1.65	21	20.9	-0.59
1	5.4	-1.9	10	3.4	-0.25	26	-18.6	-1.89
1	7.9	-2.6	10	6.4	-1.5	26	-13.6	-3.36
1	10.4	-1.45	10	8.2	-2.55	26	-8.6	-4.19
1	13.4	-0.15	10	10.3	-5.3	26	-3.6	-4.26
1	16.4	-0.1	10	13.4	-4.5	26	1.4	-4.36
1	19.4	-0.1	10	16.4	-3.1	26	6.4	-3.39
1	20.9	-0.1	10	20.9	-0.3	26	9.6	-1.58
4	-18.6	0.15	13	-18.6	-0.2	26	14.4	-2.15
4	-15.6	0.05	13	-15.6	-0.65	26	17.9	-1.09
4	-12.6	-1.4	13	-12.6	-1.8	26	20.9	-0.27
4	-10.6	-1.95	13	-9.6	-2.3			
4	-9.6	-1.42	13	-6.6	-1.6			

Table B.32: Experimental data for rectangular vane
 ($F_r = 0.25$, $d_{50} = 0.405$ mm, Collar size AF2.8)

I			II			III		
x (cm)	y (cm)	z (cm)	x (cm)	y (cm)	z (cm)	x (cm)	y (cm)	z (cm)
-8	-13.4	0	4	-13.4	0.14	14	2.6	-1.44
-8	-10.4	0.16	4	-10.4	-0.07	14	6.6	-3.35
-8	-7.4	0.21	4	0.1	-0.06	14	10.6	-5.86
-8	-4.4	0.23	4	3.8	1.92	14	12.6	-6.89
-8	-1.4	0.24	4	5.1	-1.25	14	14.6	-6.26
-8	1.6	-0.33	4	7.6	-2.49	14	16.6	-4.87
-8	4.6	-0.47	4	10.6	-2.37	14	19.6	-2.84
-8	7.6	0.01	4	13.6	-2.29	14	22.1	-0.87
-8	10.6	0	4	16.6	-0.79	19	-17.4	-1.24
-8	13.6	0.01	4	19.6	-0.18	19	-12.4	-2.79
-5	-13.4	0.11	4	22.1	-0.09	19	-7.4	-2.86
-5	-10.4	0.11	7	-13.4	0.01	19	-2.4	-3.09
-5	-7.4	0.15	7	-10.4	-0.15	19	2.6	-3.09
-5	-4.4	0.17	7	1.6	0.01	19	7.6	-3.09
-5	-1.4	-0.05	7	3.6	1	19	12.6	-5.76
-5	2.6	-1	7	6.2	-0.48	19	14.6	-5.59
-5	4.6	-2.09	7	6.7	-3.49	19	16.6	-4.59
-5	5.6	-1.99	7	9.6	-4.48	19	18.6	-3.38
-5	8.6	-1	7	12.6	-4	19	20.6	-1.84
-5	11.6	-0.14	7	15.6	-2.77	19	22.1	-1.49
-5	14.6	-0.09	7	18.6	-1.34	24	-17.4	-2.59
-5	17.6	-0.09	7	22.1	-0.09	24	-12.4	-4
-2	-13.4	0.14	10	-13.4	-0.19	24	-7.4	-4.25
-2	-10.4	0	10	-10.4	-0.29	24	-2.4	-4
-2	-6.4	-0.09	10	-9.3	-0.07	24	2.6	-3.99
-2	5.6	-1.29	10	-7.4	-0.59	24	7.6	-2.19
-2	7.6	-2.28	10	-5.4	-0.58	24	10.6	-3.36
-2	9.1	-2.19	10	-2.4	-0.65	24	13.6	-3.46
-2	12.6	-0.47	10	0.6	-1.33	24	16.6	-2.56
-2	15.6	-0.09	10	3.6	-0.46	24	19.6	-1.13
-2	18.6	-0.09	10	6.6	-2.49	24	22.1	-0.19
1	-13.4	0.11	10	9.1	-3.73	29	-17.4	-2.55
1	-10.4	0.01	10	10.4	-5.77	29	-12.4	-4.23
1	-7.9	-0.17	10	13.6	-5.35	29	-7.4	-4.74
1	0.8	0.21	10	16.6	-3.85	29	-2.4	-4.27
1	7.6	-1	10	19.6	-2.29	29	2.6	-4.36
1	8.8	-1.73	10	22.1	-0.54	29	7.6	-1.79
1	10.6	-2.45	14	-17.4	0.01	29	10.6	-0.99
1	13.6	-1.07	14	-13.4	-0.46	29	13.6	-1.17
1	16.6	-0.15	14	-9.4	-0.79	29	16.6	-0.38
1	19.6	0.01	14	-5.4	-1.04	29	19.6	0.24
1	22.1	-0.09	14	-1.4	-1.75	29	22.1	0

Table B.33 Experimental data for rectangular vane
($F_r = 0.25$, $d_{50} = 0.405$ mm, Collar size AF2.9)

I			II			III		
x	y	z	x	y	z	x	y	z
(cm)	(cm)	(cm)	(cm)	(cm)	(cm)	(cm)	(cm)	(cm)
-9.5	-15.1	0.11	2.5	2.3	0.9	14.5	-15.1	-1.89
-9.5	-11.1	0.11	2.5	7.1	-0.99	14.5	-12.1	-3.19
-9.5	-7.1	0.05	2.5	9.9	-2.39	14.5	-9.1	-3.85
-9.5	-3.1	0.01	2.5	12.9	-2.66	14.5	-6.1	-2.59
-9.5	0.9	0.04	2.5	15.9	-0.85	14.5	-3.1	-2.1
-9.5	4.9	0.04	2.5	18.9	-0.1	14.5	-0.1	-1.99
-9.5	8.9	0.01	2.5	21.9	-0.09	14.5	2.9	-1.59
-9.5	12.9	-0.09	2.5	24.4	-0.19	14.5	5.9	-2.34
-9.5	16.9	-0.1	5.5	-15.1	0	14.5	8.9	-4.29
-9.5	20.9	-0.27	5.5	-12.1	0.03	14.5	11.9	-6.14
-6.5	-15.1	0.21	5.5	-10.1	-0.39	14.5	14.9	-6.17
-6.5	-12.1	0.12	5.5	-8.1	-0.39	14.5	17.9	-4.38
-6.5	-9.1	0.11	5.5	0.4	-0.09	14.5	20.9	-2.55
-6.5	-6.1	0.04	5.5	2.9	1.34	14.5	24.4	-0.09
-6.5	-3.1	0.02	5.5	4.5	1.91	18.5	-15.1	-3.09
-6.5	-1.1	-0.36	5.5	5.7	-2.26	18.5	-11.1	-4.27
-6.5	2.4	-0.93	5.5	8.9	-3.39	18.5	-7.1	-4.09
-6.5	3.9	-1.76	5.5	11.9	-3.46	18.5	-3.1	-2.69
-6.5	5.7	-2.19	5.5	14.9	-2.64	18.5	0.9	-2.89
-6.5	8.9	-0.95	5.5	17.9	-1.1	18.5	4.9	-2.89
-6.5	11.9	-0.1	5.5	20.9	-0.09	18.5	8.9	-3.48
-6.5	14.9	-0.09	5.5	24.4	-0.17	18.5	11.9	-5.19
-6.5	17.9	-0.1	8.5	-15.1	0.04	18.5	14.9	-5.69
-6.5	20.9	-0.29	8.5	-12.1	-0.39	18.5	17.9	-4.56
-3.5	-15.1	0.11	8.5	-9.1	-0.96	18.5	20.9	-3.49
-3.5	-12.1	0.12	8.5	-6.3	-0.35	18.5	24.4	-0.49
-3.5	-9.1	0.14	8.5	-5.1	-0.57	23.5	-15.1	-4.1
-3.5	-6.1	0.01	8.5	0.9	-0.39	23.5	-10.1	-4.85
-3.5	-3.1	-0.27	8.5	3.9	0.71	23.5	-5.1	-4.89
-3.5	5.9	-1.57	8.5	6.9	-1.17	23.5	-0.1	-3.86
-3.5	6.9	-2.18	8.5	8.9	-5.09	23.5	4.9	-3.49
-3.5	8.5	-2.49	8.5	11.9	-5.87	23.5	7.9	-2.19
-3.5	10.4	-1.69	8.5	14.9	-4.29	23.5	10.9	-3.29
-3.5	13.9	0.01	8.5	17.9	-2.24	23.5	13.9	-3.59
-3.5	16.9	-0.1	8.5	20.9	-0.64	23.5	15.9	-3.16
-3.5	19.9	-0.19	8.5	24.4	-0.19	23.5	17.9	-2.59
-3.5	22.9	-0.16	11.5	-15.1	-0.69	23.5	20.9	-1.09
-0.5	-15.1	0.13	11.5	-12.1	-1.79	23.5	23.9	0.41
-0.5	-12.1	0.11	11.5	-9.1	-2.68	28.5	-15.1	-3.95
-0.5	-9.1	0.01	11.5	-6.1	-1.49	28.5	-10.1	-4.54
-0.5	-7.9	-1.39	11.5	-3.1	-0.79	28.5	-5.1	-5.53
-0.5	9.9	-2.65	11.5	-0.1	-1.34	28.5	-0.1	-4.59
-0.5	12.9	-1.59	11.5	2.9	-0.59	28.5	4.9	-3.49
-0.5	15.9	0.01	11.5	5.9	-1.93	28.5	9.9	-0.86
-0.5	18.9	-0.09	11.5	8.9	-3.95	28.5	12.9	-1.37
-0.5	21.9	-0.15	11.5	11.9	-6.62	28.5	15.9	-1.56
2.5	-15.1	0.11	11.5	14.9	-5.59	28.5	18.9	-0.96
2.5	-12.1	0.11	11.5	17.9	-3.49	28.5	21.9	0.31
2.5	-9.1	-0.15	11.5	20.9	-1.76	28.5	24.4	-0.19
2.5	0.4	0.01	11.5	24.4	-0.09			

Table B.34: Experimental data for rectangular vane
 ($F_r = 0.25$, $d_{50} = 0.405$ mm, Collar size AF2.10)

I			II			III		
x	y	z	x	y	z	x	y	z
(cm)	(cm)	(cm)	(cm)	(cm)	(cm)	(cm)	(cm)	(cm)
-12	-17.7	0.4	0	-17.7	0.35	9	5.3	-0.65
-12	-13.7	0.25	0	-13.7	0.15	9	7.6	-1.8
-12	-9.7	0.1	0	-10.7	-1.3	9	9.2	-5.65
-12	-5.7	0	0	-7.85	-3	9	12.3	-5.3
-12	-1.7	-0.1	0	-4.7	-1.47	9	15.3	-3.8
-12	2.3	-0.45	0	-3.7	-1	9	18.3	-2.2
-12	6.3	-0.1	0	7.8	-0.85	9	21.8	-0.2
-12	10.3	-0.36	0	9.3	-1.36	13	-17.7	0.2
-12	14.3	-0.2	0	10.6	-2.05	13	-13.7	-1.17
-12	18.3	-0.2	0	13.3	-0.95	13	-9.7	-2.96
-12	21.8	-0.2	0	16.3	0.05	13	-5.7	-3
-9	-17.7	0.35	0	19.3	0.1	13	-1.7	-1.7
-9	-13.7	0.2	0	21.8	0.15	13	2.3	-0.9
-9	-9.7	0.1	3	-17.7	0.3	13	5.3	-2.2
-9	-6.7	0	3	-13.7	0.25	13	-1.7	-4.2
-9	-3.7	-1.3	3	-10.7	-1.4	13	0	-5.2
-9	-0.7	-2.3	3	-8.1	-3	13	12.6	-6.9
-9	2.3	-2.45	3	-6.7	-2.75	13	15.3	-5.55
-9	5.3	-2.1	3	-4.7	-1.1	13	18.3	-3.35
-9	8.3	-0.85	3	-4.2	-0.8	13	21.8	-0.65
-9	11.3	-0.95	3	2.05	1.3	17	-17.7	-0.8
-9	14.3	-0.15	3	5.8	-0.85	17	-13.7	-1.25
-9	18.3	-0.15	3	7.3	-1.2	17	-9.7	-2.75
-9	21.8	-0.15	3	10.3	-1.7	17	-5.7	-3.3
-6	-17.7	0.3	3	13.3	-1.55	17	-1.7	-1.85
-6	-13.7	0.2	3	16.3	-0.45	17	2.3	-2.45
-6	-9.7	-0.05	3	19.3	0.15	17	6.3	-3.3
-6	-6.7	-1.55	3	21.8	0.1	17	9.3	-4.7
-6	-4.2	-2.7	6	-17.7	0.3	17	12.3	-6.85
-6	-2.7	-2.94	6	-14.7	-0.1	17	13.3	-6.7
-6	0.3	-2.8	6	-11.7	-2	17	15.3	-5.89
-6	3.3	-3	6	-8.7	-3.1	17	18.3	-3.45
-6	5.3	-3.25	6	-7.2	-2.76	17	21.8	-0.85
-6	7.3	-2.3	6	-5.7	-1.8	22	-17.7	-2
-6	10.3	-1.35	6	-4.2	-0.75	22	-12.7	-2.55
-6	13.3	0	6	1.3	0.6	22	-7.7	-3.45
-6	17.3	0	6	4.6	1.7	22	-2.7	-2.75
-6	21.8	-0.1	6	5.8	-2.9	22	2.3	-3.1
-3	-17.7	0.3	6	8.3	-3.7	22	7.3	-3.75
-3	-13.7	0.15	6	11.3	-3.6	22	10.3	-4.2
-3	-10.7	-0.4	6	14.3	-2.5	22	13.3	-5.3
-3	-7.7	-2.45	6	17.3	-1.6	22	16.3	-3.6
-3	-6.7	-2.8	6	20.3	-0.03	22	19.3	-2.15
-3	-3.7	-2	6	21.8	0.2	22	21.8	-0.9
-3	-0.7	-0.88	9	-17.7	0.3	28	-17.7	-0.9
-3	1.3	-0.85	9	-14.7	-0.65	28	-12.7	-2.85
-3	4.3	-1.35	9	-11.7	-2.1	28	-7.7	-4
-3	7.3	-2.2	9	-8.7	-3.35	28	-2.7	-3.9
-3	10	-2.5	9	-5.2	-1.8	28	2.3	-3.25
-3	12.3	-1	9	-4.2	-1.2	28	7.3	-2
-3	15.3	0	9	-2.7	-0.4	28	12.3	-1.87
-3	18.3	0.05	9	-0.2	-0.4	28	17.3	-1.1
-3	21.8	0.03	9	2.3	0.2	28	21.8	0.3

Table B.35: Experimental data for rectangular vane
 ($F_r = 0.25$, $d_{50} = 0.405$ mm, Collar size AF2.11)

I			II			III		
x	y	z	x	y	z	x	y	z
(cm)	(cm)	(cm)	(cm)	(cm)	(cm)	(cm)	(cm)	(cm)
-10.5	-18.3	0.21	0	16.7	-0.15	12.5	-15.3	-0.19
-10.5	-15.3	0.11	0	18.7	-0.19	12.5	-12.3	-1.89
-10.5	-12.3	0.11	0	21.2	-0.15	12.5	-9.3	-2.92
-10.5	-9.3	0.11	3.5	-18.3	0.11	12.5	-6.3	-2.66
-10.5	-6.3	0.03	3.5	-15.3	0.01	12.5	-3.3	-0.89
-10.5	-3.3	0.01	3.5	-12.3	-1.19	12.5	-0.3	-1.79
-10.5	-0.3	-0.25	3.5	-9.3	-2.69	12.5	2.7	-1.29
-10.5	2.7	-0.19	3.5	-7.3	-2.16	12.5	5.7	-1.43
-10.5	5.7	0.11	3.5	-5.9	-1.18	12.5	8.7	-3.54
-10.5	8.7	0.01	3.5	0.3	-0.15	12.5	10.7	-4.26
-10.5	11.7	0.01	3.5	2.7	1.03	12.5	12.3	-6.66
-10.5	14.7	0.01	3.5	6.2	-0.98	12.5	14.7	-5.49
-10.5	17.7	0.01	3.5	8.7	-2.19	12.5	17.7	-3.37
-10.5	21.2	0.01	3.5	11.7	-2.98	12.5	21.2	-0.09
-7.5	-18.3	0.21	3.5	14.7	-2.69	16.5	-18.3	0.11
-7.5	-15.3	0.11	3.5	17.7	-0.54	16.5	-14.3	-0.39
-7.5	-12.3	0.01	3.5	21.2	-0.19	16.5	-10.3	-2.54
-7.5	-9.3	-0.09	6.5	-18.3	0.11	16.5	-6.3	-3.75
-7.5	-6.3	-0.68	6.5	-15.3	-0.03	16.5	-2.3	-1.89
-7.5	-3.3	-2.19	6.5	-12.3	-1.59	16.5	1.7	-2.89
-7.5	-0.3	-2.27	6.5	-9.3	-3.19	16.5	5.7	-2.67
-7.5	2.7	-2.17	6.5	-7.9	-3.16	16.5	9.7	-4.35
-7.5	4.7	-2.05	6.5	-6.3	-1.69	16.5	13.7	-6.19
-7.5	7.7	-0.89	6.5	0.9	-0.5	16.5	17.7	-3.66
-7.5	10.7	0.01	6.5	3.7	1.31	16.5	21.2	-0.45
-7.5	13.7	0.01	6.5	5.7	1.81	21.5	-18.3	-4.04
-7.5	16.7	-0.19	6.5	6.7	-3.59	21.5	-13.3	-0.99
-7.5	21.2	-0.07	6.5	9.7	-4.26	21.5	-8.3	-2.75
-4.5	-18.3	0.11	6.5	12.7	-4.24	21.5	-3.3	-3.29
-4.5	-15.3	0.04	6.5	15.7	-2.69	21.5	1.7	-2.79
-4.5	-12.3	0.01	6.5	18.7	-0.67	21.5	6.7	-3.29
-4.5	-9.3	-0.65	6.5	21.2	-0.14	21.5	11.7	-4.17
-4.5	-6.3	-2.44	9.5	-18.3	0.11	21.5	14.7	-4.39
-4.5	-3.3	-1.99	9.5	-15.3	-0.09	21.5	17.7	-2.57
-4.5	-1.3	-1.36	9.5	-12.3	-1.74	21.5	21.2	0.01
-4.5	9.1	-0.89	9.5	-9.3	-2.89	26.5	-18.3	-1.18
-4.5	11.7	0.01	9.5	-6.3	-2.49	26.5	-13.3	-2.48
-4.5	14.7	-0.09	9.5	-4.3	-1.02	26.5	-8.3	-3.37
-4.5	17.7	-0.06	9.5	-0.7	-0.58	26.5	-3.3	-4.36
-4.5	21.2	-0.14	9.5	1.7	-0.79	26.5	1.7	-3.15
0	-18.3	0.11	9.5	4.7	0.52	26.5	6.7	-2.55
0	-15.3	0.03	9.5	8.1	-1.39	26.5	9.7	-2.74
0	-12.3	-0.36	9.5	9.7	-5.79	26.5	12.7	-2.53
0	-9.3	-2.14	9.5	12.7	-5.49	26.5	14.7	-2.26
0	-8.3	-2.53	9.5	15.7	-3.77	26.5	17.7	-0.99
0	-6.3	-1.95	9.5	18.7	-1.67	26.5	21.2	0.82
0	11.1	-0.37	9.5	21.2	-0.15			
0	13.7	-0.16	12.5	-18.3	0.04			

Table B.36: Experimental data for rectangular vane
 ($F_r = 0.25$, $d_{50} = 0.405$ mm, Collar size AF2.12)

I			II			III		
x (cm)	y (cm)	z (cm)	x (cm)	y (cm)	z (cm)	x (cm)	y (cm)	z (cm)
-3.75	-14.1	0.35	6.25	14.9	-0.9	15.25	13.3	-5.24
-3.75	-10.1	0.3	6.25	17.9	-0.1	15.25	15.9	-3.6
-3.75	-6.1	0.3	6.25	20.9	0	15.25	18.9	-1.35
-3.75	-2.1	0.35	6.25	23.9	-0.15	15.25	21.9	-0.05
-3.75	1.9	0.2	6.25	25.4	-0.1	15.25	25.4	0
-3.75	5.9	0.3	9.25	-14.1	-0.1	19.25	-14.1	-0.15
-3.75	9.9	0.2	9.25	-10.1	-0.2	19.25	-10.1	-0.75
-3.75	13.9	0.15	9.25	-7.1	0	19.25	-6.1	-2.55
0	-14.1	0.3	9.25	-4.1	0	19.25	-2.1	-2.65
0	-10.1	0.2	9.25	-1.1	0	19.25	1.9	-2.35
0	-6.1	0.3	9.25	0.9	-0.15	19.25	5.9	-2.2
0	-3.1	0.3	9.25	3.9	0.75	19.25	8.9	-1.85
0	-0.1	0.3	9.25	7.4	0.3	19.25	11.9	-3.6
0	2.9	0.3	9.25	8.6	-1.5	19.25	14.9	-2.95
0	4.9	0	9.25	10.9	-2.1	19.25	17.9	-0.95
0	7.9	0.35	9.25	13.9	-5.7	19.25	20.9	-0.3
0	11.9	0.15	9.25	16.9	-1.25	19.25	23.9	0.1
0	15.9	0.15	9.25	19.9	-0.2	19.25	25.4	0.2
3.25	-14.1	0.1	9.25	22.9	-0.2	24.25	-14.1	0.15
3.25	-10.1	0.15	9.25	25.4	-0.1	24.25	-9.1	-1.1
3.25	-7.6	0.3	12.25	-14.1	-0.1	24.25	-4.1	-2.5
3.25	0.4	0.2	12.25	-10.1	-0.55	24.25	0.9	-3.05
3.25	2.4	1.4	12.25	-6.1	-0.3	24.25	5.9	-2.1
3.25	4.9	1.4	12.25	-2.1	-0.5	24.25	8.9	-0.15
3.25	5.9	1.4	12.25	1.9	-1.1	24.25	11.9	-0.7
3.25	6.9	0	12.25	5.4	-0.15	24.25	14.9	-0.3
3.25	8.9	0.15	12.25	7.9	-1.4	24.25	17.9	0.6
3.25	11.9	0.15	12.25	9.9	-2.8	24.25	20.9	0.45
3.25	14.9	0.1	12.25	11.4	-4.1	24.25	23.9	0.25
3.25	17.9	0.1	12.25	13.9	-4.4	24.25	24.9	0.3
6.25	-14.1	0	12.25	16.9	-2.4	30.25	-14.1	0.5
6.25	-10.1	0.05	12.25	19.9	-0.3	30.25	-9.1	-0.6
6.25	-7.1	0.05	12.25	22.9	-0.1	30.25	-4.1	-1.3
6.25	-4.1	0.05	12.25	25.4	-0.1	30.25	0.9	-3.15
6.25	-1.1	0.05	15.25	-14.1	-0.15	30.25	5.9	-2.1
6.25	0.9	0.2	15.25	-10.1	-0.7	30.25	14.7	2.1
6.25	2.9	1.3	15.25	-6.1	-1.9	30.25	17.9	1.5
6.25	5.05	2	15.25	-2.1	-1.5	30.25	21.9	1.2
6.25	5.9	-0.25	15.25	1.9	-1.6	30.25	25.4	0.3
6.25	8.9	-0.6	15.25	5.9	-1.35	30.25	14.7	2.1
6.25	11.9	-1.3	15.25	9.9	-2.05			

Table B.37: Experimental data for trapezoidal vane (3H:2.5V)
(Fr = 0.25, d50 = 0.405 mm, Collar size BF2.1)

I			II			III		
x	y	z	x	y	z	x	y	z
(cm)	(cm)	(cm)	(cm)	(cm)	(cm)	(cm)	(cm)	(cm)
-5	-15.6	0.41	7	23.9	0.14	20	-7.6	-5.2
-5	-11.6	0.41	10	-15.6	-0.2	20	-3.6	-3.87
-5	-7.6	0.33	10	-11.6	-1.14	20	0.4	-3.6
-5	-3.6	0.4	10	-7.6	-1.2	20	4.4	-3.17
-5	0.4	0.37	10	-5.6	-0.5	20	7.4	-2.1
-5	4.4	0.4	10	-1.6	-0.7	20	10.4	-1.24
-5	9.4	0.12	10	2.4	-1.08	20	12.4	-2.5
-5	13.4	0.2	10	6.4	0.73	20	15.4	-4.23
-5	17.4	0.06	10	9.2	0.84	20	17.4	-5.06
-5	21.4	0.14	10	11.4	-4.68	20	20.4	-3.2
-2	-15.6	0.5	10	15.4	-3.5	20	23.9	-0.5
-2	-11.6	0.4	10	17.6	-1.9	25	-15.6	-3.98
-2	-7.6	0.26	10	19.4	-1.94	25	-10.6	-4.97
-2	-5.6	0.23	10	21.4	-0.96	25	-5.6	-5.86
-2	5.4	0.2	10	23.9	0.12	25	-0.6	-5
-2	9.4	0.3	13	-15.6	-1.58	25	2.4	-3.95
-2	13.4	0.06	13	-11.6	-2.8	25	6.4	-3.69
-2	17.4	0.01	13	-7.6	-2.37	25	9.4	-2.78
-2	21.4	0.1	13	-4.6	-1.17	25	12.4	-1.8
1	-15.6	0.32	13	-0.6	-1.8	25	15.4	-2.7
1	-6.6	0.35	13	2.4	-1.6	25	18.4	-3.6
1	-2.6	0.16	13	5.4	-0.2	25	21.4	-2
1	9	-0.4	13	7.4	0.9	25	23.9	-0.39
1	12.4	0.2	13	10.9	0.36	30	-15.6	-3
1	16.4	0.1	13	13.4	-4.57	30	-10.6	-3.8
1	20.4	0	13	15.4	-4.2	30	-5.6	-5.3
1	23.9	0.06	13	18.4	-2.67	30	-0.6	-6.17
4	-15.6	0.3	13	21.4	-1.5	30	4.4	-5.27
4	-11.6	0.1	13	23.9	0.1	30	7.4	-3.66
4	-7.6	0.1	16	-15.6	-2.8	30	10.4	-2.17
4	4.4	-1.66	16	-11.6	-3.7	30	13.4	-0.6
4	5.8	-1.86	16	-7.6	-3.7	30	16.4	-1.66
4	9.4	-2.16	16	-3.6	-2.35	30	19.4	-1.58
4	13.4	-0.76	16	0.4	-2.9	30	21.4	-0.5
4	17.4	-0.4	16	4.4	-1.76	30	23.9	0.7
4	21.4	0.13	16	6.4	-0.57	35	-15.6	-1.71
4	23.9	0.1	16	8.4	0.2	35	-10.6	-2.36
7	-15.6	0.1	16	11.4	-1.54	35	-5.6	-3.81
7	-11.6	-0.28	16	13.8	-2.8	35	-0.6	-5.61
7	-8.2	0	16	16.2	-5.17	35	2.9	-6.11
7	2.4	-0.3	16	17.4	-4.4	35	4.4	-5.61
7	5.9	0	16	19.4	-3.08	35	9.4	-3.11
7	8.4	-4.4	16	21.4	-1.75	35	14.9	0.54
7	12.4	-2.84	16	23.9	-0.19	35	19.4	0.19
7	16.4	-2	20	-15.6	-3.8	35	23.9	2.24
7	20.4	-0.4	20	-11.6	-4.83			

Table B.38: Experimental data for trapezoidal vane (3H:2.5V)
 ($F_r = 0.25$, $d_{50} = 0.405$ mm, Collar size BF2.2)

I			II			III		
x	y	z	x	y	z	x	y	z
(cm)	(cm)	(cm)	(cm)	(cm)	(cm)	(cm)	(cm)	(cm)
-8.5	-13.7	0.2	7.5	1.3	-0.95	19.5	-9.7	-4.06
-8.5	-8.7	0.1	7.5	4.3	-1.1	19.5	-5.7	-4.15
-8.5	-3.7	0.25	7.5	6.05	-0.7	19.5	-1.7	-3.55
-8.5	1.3	0.3	7.5	7.3	-4.4	19.5	2.3	-3.9
-8.5	6.3	0.2	7.5	10.3	-4.25	19.5	6.3	-2.65
-8.5	11.3	0.2	7.5	13.3	-2.6	19.5	10	-2.05
-3.5	-13.7	0.3	7.5	16.3	-1.2	19.5	7.3	-3.1
-3.5	-8.7	0.1	7.5	19.3	0.2	19.5	15.3	-4.8
-3.5	-3.7	0.1	7.5	22.3	0.1	19.5	18.3	-3.8
-3.5	1.3	0	11.5	-13.7	-0.9	19.5	21.3	-1.4
-3.5	6.8	0.1	11.5	-9.7	-2.3	19.5	24.3	-0.1
-3.5	11.3	0.2	11.5	-5.7	-2.2	19.5	25.8	-0.1
-3.5	16.3	0.2	11.5	-1.7	-1.9	23.5	-13.7	-2.1
0.5	-13.7	0.35	11.5	2.3	-2.2	23.5	-9.7	-3.4
0.5	-8.7	0.2	11.5	6.3	-0.2	23.5	-5.7	-4.5
0.5	-3.7	-0.05	11.5	9.3	0.45	23.5	-1.7	-5
0.5	3.8	-1.5	11.5	10.3	-4.6	23.5	2.3	-5.05
0.5	5.3	-2.1	11.5	13.3	-4.2	23.5	6.3	-4.2
0.5	6.8	-0.1	11.5	17.3	-2.75	23.5	11.3	-1.9
0.5	9.3	0.2	11.5	19.3	-1.35	23.5	14.3	-3.2
0.5	11.3	0.35	11.5	22.3	0	23.5	15.4	-3.65
0.5	16.3	0.3	11.5	25.8	0	23.5	18.3	-2.85
3.5	-13.7	0.35	15.5	-13.7	-1.95	23.5	21.8	-0.35
3.5	-8.7	0.25	15.5	-9.7	-3.6	23.5	24.8	-1.7
3.5	-5.7	0.1	15.5	-5.7	-3.6	23.5	25.8	-1.4
3.5	-3.7	0.1	15.5	-1.7	-3.05	28.5	-13.7	-0.5
3.5	4.3	-1.7	15.5	2.3	-3.04	28.5	-8.7	-2.4
3.5	5.8	-2.3	15.5	6.3	-1.05	28.5	-3.7	-4.2
3.5	8.3	-2.02	15.5	10.3	-2	28.5	1.3	-5.55
3.5	11.3	-1.1	15.5	12.8	-3.8	28.5	6.3	-4.6
3.5	15.3	-0.85	15.5	13.8	-5.1	28.5	12.3	-0.65
3.5	19.3	0.2	15.5	16.3	-4.65	28.5	16.3	-1.75
7.5	-13.7	0.2	15.5	19.3	-2.8	28.5	19.3	-1
7.5	-10.7	-0.2	15.5	22.3	-0.2	28.5	22.3	0.75
7.5	-7.7	-0.15	15.5	25.8	-0.15	28.5	25.8	0
7.5	-4.7	0.2	19.5	-13.7	-2.7			

Table B.39: Experimental data for trapezoidal vane (3H:2.5V)
($F_r = 0.25$, $d_{50} = 0.405$ mm, Collar size BF2.3)

I			II			III		
x (cm)	y (cm)	z (cm)	x (cm)	y (cm)	z (cm)	x (cm)	y (cm)	z (cm)
-9	-15.75	0.1	0	19.25	0.1	13	-7.75	-2.3
-9	-11.75	0	3	-15.75	-0.55	13	-3.75	-2.85
-9	-7.75	0.1	3	-12.75	-1	13	0.25	-2.65
-9	-3.75	0	3	-9.75	-1.4	13	4.25	-1.75
-9	0.25	0.1	3	-6.75	-2.05	13	8.25	0.6
-9	4.25	0.05	3	-6.05	-2.3	13	10.65	-0.23
-9	8.25	0.1	3	-3.75	-1.65	13	11.75	-3.95
-9	12.25	0.2	3	-2.05	-2	13	14.25	-3.5
-9	16.25	0.2	3	4.75	-0.95	13	17.25	-2.15
-6	-15.75	0.25	3	6.25	-1.2	13	20.25	-0.55
-6	-12.75	0	3	6.75	-1.3	13	23.75	0
-6	-9.75	0.2	3	9.25	-2.05	17	-15.75	-3.4
-6	-6.75	-0.15	3	12.25	-1	17	-11.75	-2.6
-6	-3.75	-0.85	3	15.25	0	17	-7.75	-4
-6	-0.75	-1.4	3	18.25	0.1	17	-3.75	-4.7
-6	2.25	-1.8	6	-15.75	-0.2	17	0.25	-3.6
-6	5.25	-1.55	6	-12.75	-0.6	17	4.25	-2.6
-6	8.25	-0.55	6	-9.75	-1.35	17	8.45	-0.5
-6	11.25	0.2	6	-6.75	-2.05	17	11.25	-2.4
-6	14.25	0.2	6	-5.75	-2.05	17	14.25	-4.3
-6	17.25	0.2	6	-3.75	-1.4	17	17.25	-3.5
-3	-15.75	-1.4	6	-2.95	-0.95	17	20.25	-1.45
-3	-12.75	-0.95	6	3.15	-0.6	17	23.75	-0.2
-3	-9.75	-1.4	6	4.95	-0.4	22	-15.75	-2.3
-3	-6.75	-1.4	6	5.75	-3.05	22	-10.75	-2.6
-3	-3.75	-2.4	6	7.25	-3.2	22	-5.75	-4.25
-3	-1.75	-2.1	6	10.25	-2.15	22	-0.75	-5
-3	1.25	-1.65	6	13.25	-0.7	22	4.25	-3.2
-3	4.25	-2.25	6	16.25	0.1	22	9.25	-1.85
-3	6.25	-2.65	6	19.25	0.1	22	10.45	-1.5
-3	7.25	-2.5	9	-15.75	-0.15	22	14.25	-3.2
-3	10.25	-1.1	9	-12.75	-0.4	22	17.25	-3.25
-3	13.25	0.2	9	-9.75	-1.4	22	20.25	-1.3
-3	16.25	0.2	9	-6.75	-2	22	22.25	-0.2
-3	19.25	0.1	9	-3.75	-1.65	22	23.75	-0.2
0	-15.75	-1.3	9	-0.45	-1.05	27	-15.75	-1.65
0	-12.75	-1.3	9	2.25	-1.5	27	-10.75	-2.3
0	-9.75	-1.7	9	5.25	-0.4	27	-5.75	-4.2
0	-6.75	-1.75	9	7.55	0.45	27	-0.75	-6.4
0	-5.05	-2.75	9	8.25	-3.7	27	4.25	-5.5
0	-3.75	-2.3	9	9.75	-3.7	27	9.25	-2.35
0	-1.75	-1.9	9	12.25	-2.65	27	12.55	-0.45
0	-0.35	-1.2	9	15.25	-1.05	27	16.25	-1.8
0	5.75	-1.02	9	18.25	0	27	19.25	-0.9
0	7.25	-1.5	9	21.25	0	27	21.75	0.6
0	9.75	-2.1	9	23.75	0.1	27	23.75	-0.05
0	13.25	-0.65	13	-15.75	-1.7			
0	16.25	0.1	13	-11.75	-1.9			

Table B.40: Experimental data for trapezoidal vane (3H:2.5V)
($F_r = 0.25$, $d_{50} = 0.405$ mm, Collar size BF2.4)

I			II			III		
x	y	z	x	y	z	x	y	z
(cm)	(cm)	(cm)	(cm)	(cm)	(cm)	(cm)	(cm)	(cm)
-8.5	-14.4	-0.6	3.5	-11.4	-0.4	9.5	21.6	-0.2
-8.5	-10.4	0.35	3.5	-7.9	-2.4	13.5	-14.4	-1.2
-8.5	-6.4	0.25	3.5	-7.4	-2.3	13.5	-10.4	-3.15
-8.5	-2.4	0.15	3.5	-6.4	-1.6	13.5	-6.4	-3.8
-8.5	1.6	-0.05	3.5	-5.4	-0.9	13.5	-2.4	-1.65
-8.5	5.6	0	3.5	6.1	-0.9	13.5	1.6	-2.9
-8.5	9.6	0.05	3.5	8.6	-0.65	13.5	5.6	-1.6
-8.5	13.6	0.05	3.5	11.6	0	13.5	9.9	0.8
-5.5	-14.4	0.3	3.5	14.6	-0.05	13.5	11.9	-2.6
-5.5	-10.4	0.3	3.5	17.6	-0.1	13.5	14.6	-2.45
-5.5	-6.4	-0.35	6.5	-14.4	-0.05	13.5	17.6	-0.85
-5.5	-3.4	-1.8	6.5	-11.4	-1.65	13.5	20.6	-0.3
-5.5	-1.4	-1.6	6.5	-7.9	-2.6	13.5	23.6	-0.25
-5.5	0.6	-1.2	6.5	-7.3	-2.5	13.5	25.1	-0.2
-5.5	2.6	-1.1	6.5	-6.4	-2.05	17.5	-14.4	-0.85
-5.5	3.6	-1.15	6.5	-5.4	-1.45	17.5	-10.4	-2
-5.5	4.6	-1.25	6.5	-4.4	-0.85	17.5	-6.4	-3.1
-5.5	7.6	0	6.5	3.1	-0.4	17.5	-2.4	-2.75
-5.5	10.6	0	6.5	5.1	-0.1	17.5	-0.4	-1.8
-5.5	13.6	0.1	6.5	6.1	-2.8	17.5	3.6	-3.1
-2.5	-14.4	0.3	6.5	7.6	-2.75	17.5	7.6	-1.45
-2.5	-10.4	0.2	6.5	10.6	-1.15	17.5	10.6	0.1
-2.5	-7.4	-1.3	6.5	13.6	-0.1	17.5	12.6	-1.3
-2.5	-6.2	-1.8	6.5	16.6	-0.1	17.5	15.6	-2.7
-2.5	-4.4	-1.2	6.5	21.6	-0.25	17.5	18.6	-1.1
-2.5	-3.4	-0.85	9.5	-14.4	-1.1	17.5	21.6	-0.35
-2.5	4.6	0.2	9.5	-11.4	-2.5	17.5	25.1	-0.4
-2.5	7.6	0.1	9.5	-8.4	-3.1	21.5	-14.4	-1.9
-2.5	10.6	0.1	9.5	-5.4	-2.1	21.5	-10.4	-2.3
-2.5	13.6	0	9.5	-4.4	-1.6	21.5	-6.4	-3.4
0.5	-14.4	0.2	9.5	-3.4	-0.9	21.5	-2.4	-3.45
0.5	-10.4	-0.15	9.5	-2.4	-0.7	21.5	1.6	-2.75
0.5	-7.9	-2	9.5	-0.9	-0.6	21.5	5.6	-2.6
0.5	-6.4	-1.8	9.5	1.6	-1.4	21.5	9.6	-0.55
0.5	-5.4	-1.2	9.5	4.6	-0.8	21.5	11.1	0.3
0.5	6.1	-0.15	9.5	7.6	0.6	21.5	12.6	0.05
0.5	8.6	0	9.5	8.6	-2.5	21.5	15.6	-1.75
0.5	11.6	0	9.5	9.6	-2.55	21.5	18.6	-0.9
0.5	14.6	0.05	9.5	12.6	-1.6	21.5	21.6	-0.3
0.5	17.6	0	9.5	15.6	-0.5	21.5	25.1	-0.5
3.5	-14.4	0.1	9.5	18.6	-0.1			

Table B.41: Experimental data for trapezoidal vane (3H:2.5V)
($F_r = 0.25$, $d_{50} = 0.405$ mm, Collar size BF2.5)

I			II			III		
x	y	z	x	y	z	x	y	z
(cm)	(cm)	(cm)	(cm)	(cm)	(cm)	(cm)	(cm)	(cm)
-5	-13.5	0.01	7	-9.5	0.22	14	22.5	-0.99
-5	-9.5	0.01	7	-5.5	0.01	14	26	-0.26
-5	-5.5	0.01	7	4.5	-0.79	18	-13.5	-1.76
-5	-1.5	0.01	7	5.5	-0.99	18	-9.5	-2.55
-5	2.5	0.01	7	6.8	-3.24	18	-5.5	-3.26
-5	6.5	-0.17	7	8.1	-3.39	18	-1.5	-2.79
-5	10.5	0.01	7	10.5	-3.84	18	2.5	-3.56
-5	14.5	-0.09	7	13.5	-2.69	18	6.5	-2.89
-5	18.5	-0.09	7	16.5	-1.99	18	10.5	-3.77
-5	22.5	-0.17	7	18.5	-1.69	18	13.5	-5.28
-2	-13.5	0.01	7	21.5	-0.09	18	16.5	-5.39
-2	-9.5	-0.08	7	24.5	-0.19	18	19.5	-3.35
-2	-5.5	0.01	7	26	-0.19	18	22.5	-1.33
-2	6.5	-0.15	10	-13.5	0.24	18	26	-0.29
-2	10.5	0.13	10	-9.5	0.15	23	-13.5	-2.89
-2	14.5	0.01	10	-5.5	-0.09	23	-8.5	-3.99
-2	18.5	-0.09	10	0.6	-0.9	23	-3.5	-4.56
-2	22.5	-0.17	10	4.5	-1.57	23	1.5	-4.09
1	-13.5	0.11	10	8.5	0.01	23	6.5	-3.79
1	-9.5	0.01	10	10.7	-5.25	23	11.5	-3.09
1	-5.5	0.01	10	13.5	-4.59	23	14.5	-4.25
1	11	-0.13	10	16.5	-2.73	23	17.5	-3.78
1	14.5	0.01	10	19.5	-2.19	23	20.5	-1.99
1	18.5	-0.06	10	22.5	-0.25	23	23.5	-1.17
1	22.5	-0.15	10	26	-0.19	23	26	-2.09
4	-13.5	0.15	14	-13.5	-0.15	28	-13.5	-3.09
4	-9.5	0.11	14	-9.5	-0.99	28	-8.5	-4.26
4	-5.5	0.01	14	-5.5	-1.89	28	-3.5	-5.17
4	7.5	-1.19	14	-1.5	-1.57	28	1.5	-4.55
4	7.9	-1.29	14	2.5	-2.65	28	6.5	-3.85
4	10.5	-2.09	14	6.5	-1.89	28	11.5	-1.77
4	13.5	-1.25	14	9.5	-2.25	28	14.5	-2.29
4	16.5	-0.19	14	12.1	-3.79	28	17.5	-2.18
4	19.5	-0.19	14	14.5	-5.87	28	20.5	-0.76
4	22.5	-0.24	14	16.5	-4.56	28	23.5	-0.39
7	-13.5	0.21	14	19.5	-2.99	28	26	-0.39

Table B.42: Experimental data for rectangular vane
($F_r = 0.13$, $d_{50} = 0.405$ mm, Collar size AF1.8)

I			II			III		
x	y	z	x	y	z	x	y	z
(cm)	(cm)	(cm)	(cm)	(cm)	(cm)	(cm)	(cm)	(cm)
-3.5	-8.4	0	3.5	12.6	0.04	12.5	10.4	0.41
-3.5	-5.4	-0.1	6.5	-8.4	-0.29	12.5	12	-0.89
-3.5	-2.4	0	6.5	-5.4	-0.55	12.5	14.6	-0.57
-3.5	0.6	0	6.5	-2.4	-1.69	12.5	17.6	-0.34
-3.5	3.6	0.1	6.5	0.6	-0.53	15.5	-5.4	-0.44
-3.5	6.6	0.2	6.5	2.6	0.51	15.5	-2.4	-0.38
-3.5	9.6	0.31	6.5	4.6	0.91	15.5	0.6	-1.19
-3.5	12.6	0.31	6.5	5.4	0.55	15.5	3.6	-0.99
-1.5	-8.4	0.06	6.5	6.2	-0.18	15.5	6.6	-0.13
-1.5	-5.4	-0.03	6.5	7.6	-0.19	15.5	9.6	0.82
-1.5	-3.4	-0.29	6.5	10.6	-0.08	15.5	12.6	-0.69
-1.5	-0.4	0	6.5	13.6	-0.15	15.5	15.6	-0.89
-1.5	4.6	0.06	6.5	16.6	-0.08	15.5	18.6	-0.36
-1.5	7.6	0.15	9.5	-8.4	-0.24	18.5	-5.4	-0.39
-1.5	10.6	0.31	9.5	-5.4	-0.46	18.5	-2.4	-0.14
-1.5	13.6	0.21	9.5	-2.4	-0.76	18.5	0.6	0.11
0.5	-8.4	-0.17	9.5	0.6	-1.02	18.5	3.6	0.08
0.5	-5.4	-0.25	9.5	3.6	0.01	18.5	6.6	0.05
0.5	-3.9	-0.2	9.5	5.6	1.21	18.5	9.6	0.13
0.5	3.9	-0.26	9.5	7.6	-0.09	18.5	12.6	-0.99
0.5	6.6	0.13	9.5	9.3	-0.48	18.5	15.6	-0.87
0.5	9.6	0.27	9.5	11.6	-0.29	18.5	18.6	-0.56
0.5	12.6	0.24	9.5	14.6	-0.37	21.5	-5.4	-0.32
3.5	-8.4	-0.26	9.5	17.6	-0.19	21.5	-2.4	-0.37
3.5	-5.4	-0.46	12.5	-8.4	-0.45	21.5	0.6	-0.19
3.5	-3	-0.42	12.5	-5.4	-0.36	21.5	3.6	-1.23
3.5	0.3	-0.45	12.5	-2.4	-0.16	21.5	6.6	-0.49
3.5	2.6	0.43	12.5	0.6	-0.39	21.5	9.6	0.04
3.5	4.2	-0.27	12.5	3.6	-0.39	21.5	12.6	0.01
3.5	6.6	0.01	12.5	6.6	0.13	21.5	15.6	-0.42
3.5	9.6	-0.03	12.5	9.6	0.82	21.5	18.6	-0.69

Table B.43: Experimental data for trapezoidal vane (3H:2.5V)

(Fr = 0.13, d50 = 0.405 mm, Collar size BF1.14)

I			II			III		
x	y	z	x	y	z	x	y	z
(cm)	(cm)	(cm)	(cm)	(cm)	(cm)	(cm)	(cm)	(cm)
-2.00	-7.10	0.03	6.00	14.90	0.01	18.00	-1.10	-0.79
-2.00	-4.10	0.08	9.00	-7.10	-0.16	18.00	1.90	-0.62
-2.00	-1.10	0.07	9.00	-4.10	-0.49	18.00	4.90	-0.42
-2.00	1.90	0.05	9.00	-1.10	-1.65	18.00	7.90	0.31
-2.00	4.90	0.12	9.00	1.90	-1.89	18.00	10.40	1.88
-2.00	7.90	0.01	9.00	4.90	-0.29	18.00	12.90	0.51
-2.00	10.90	0.08	9.00	7.80	1.24	18.00	15.90	-1.05
-2.00	13.90	-0.05	9.00	9.30	-0.14	18.00	18.90	-0.57
0.00	-7.10	-0.05	9.00	11.90	-0.05	18.00	21.90	-0.37
0.00	-4.10	-0.09	9.00	14.90	-0.05	21.00	-7.10	-0.29
0.00	-2.60	-0.14	12.00	-7.10	-0.19	21.00	-4.10	-1.12
0.00	-1.10	-0.39	12.00	-4.10	-0.49	21.00	-1.10	-1.29
0.00	3.00	-0.29	12.00	-1.10	-0.62	21.00	1.90	-0.84
0.00	5.90	0.12	12.00	1.90	-1.04	21.00	4.90	-0.65
0.00	8.90	0.07	12.00	4.90	-0.59	21.00	7.90	-0.29
0.00	11.90	0.08	12.00	7.90	1.31	21.00	10.90	1.51
3.00	-7.10	-0.18	12.00	10.40	2.45	21.00	13.90	-0.13
3.00	-4.10	-0.05	12.00	11.90	-0.08	21.00	16.90	-1.15
3.00	-2.80	-0.29	12.00	14.90	-0.09	21.00	19.90	-0.39
3.00	2.60	-0.45	12.00	17.90	-0.17	21.00	22.90	-0.45
3.00	3.50	-0.16	15.00	-7.10	-0.29	24.00	-7.10	-0.29
3.00	5.90	0.04	15.00	-4.10	-0.05	24.00	-4.10	0.17
3.00	8.90	0.01	15.00	-1.10	0.11	24.00	-1.10	-0.29
3.00	11.90	-0.03	15.00	1.90	0.02	24.00	1.90	-0.65
3.00	14.90	0.02	15.00	4.90	0.17	24.00	4.90	-0.54
6.00	-7.10	-0.14	15.00	7.90	0.97	24.00	7.90	-0.39
6.00	-4.10	-0.19	15.00	9.50	2.11	24.00	10.90	0.71
6.00	-1.10	-1.16	15.00	12.90	0.15	24.00	13.90	0.26
6.00	1.90	-1.39	15.00	14.00	-0.35	24.00	16.90	-0.29
6.00	4.90	-0.04	15.00	16.90	-0.29	24.00	19.90	-0.17
6.00	6.30	0.01	15.00	19.90	-0.39	24.00	22.90	-0.37
6.00	8.90	0.04	18.00	-7.10	-0.29			
6.00	11.90	0.07	18.00	-4.10	-0.79			

**EXPERIMENTAL DATA RELATING TO VARIATION
OF STRENGTH OF VORTEX**

This Appendix contains the experimental data collected in River Engineering Laboratory, Water Resources Development Training Centre, Indian Institute of Technology Roorkee, India. The data presented here have been used in Chapter 6 of this thesis. The Fig. C.1 indicates the sign convention and axes.

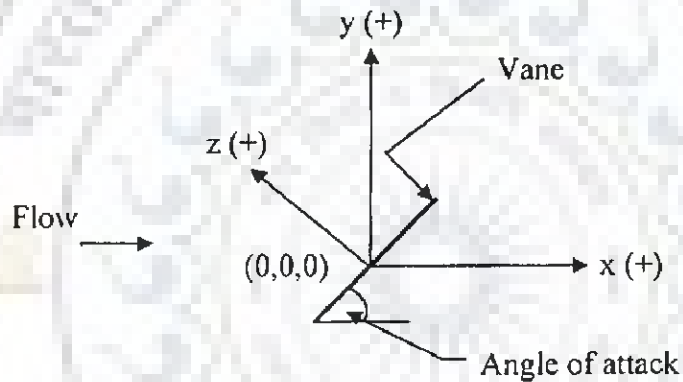


Fig. C.1 Definition sketch of origin for three dimensional velocity measurements

Origin = middle bottom edge of vane at initial bed level

Table C.1: 3D velocity components for rectangular vane (T/d = 0.60)

Angle of attack = 30°				Angle of attack = 35°			
coord. (cm)	V _x (cm/s)	V _y (cm/s)	V _z (cm/s)	coord. (cm)	V _x (cm/s)	V _y (cm/s)	V _z (cm/s)
15,-12,3	15.24	2.14	-0.59	15,-12,3	13.8	2.75	-0.72
15,-12,6	15.55	1.63	-0.9	15,-12,6	13.87	2.73	-0.68
15,-12,9	15.54	1.35	-0.81	15,-12,9	15.61	2.29	-1.13
15,-9,3	15.36	2.78	-0.78	15,-9,3	13.58	3.75	-1.22
15,-9,6	15.34	2.12	-1.39	15,-9,6	13.71	2.85	-1.04
15,-9,9	14.63	0.87	-1.16	15,-9,9	14.92	2.11	-1.68
15,-6,3	14.67	3.96	-1.35	15,-6,3	12.23	4.6	-2.75
15,-6,6	14.38	2.26	-2.27	15,-6,6	13.47	2.56	-3.07
15,-6,9	14.53	0.57	-1.47	15,-6,9	15.06	1.51	-2.1
15,-3,3	13.73	5.31	-2.9	15,-3,3	6.91	5.16	-4.65
15,-3,6	14.06	2.14	-3.71	15,-3,6	10.5	0.47	-5.45
15,-3,9	13.47	-0.44	-2.46	15,-3,9	14.05	-0.35	-2.52
15,0,3	11.31	8.25	-4.65	15,0,3	2.28	5.58	-1.53
15,0,6	12.9	-1.27	-5.99	15,0,6	5.97	-4.4	-3.04
15,0,9	14.7	-2.23	-1.74	15,0,9	14.41	-2.93	-1.19
15,3,3	9.74	9.94	3.64	15,3,3	4.11	7.66	4.67
15,3,6	12.01	-4.63	4.69	15,3,6	6.72	-3.44	2.98
15,3,9	14.89	-3.25	0.81	15,3,9	14.26	-2.87	1.5
15,6,3	8.98	3.92	2.89	15,6,3	6.34	5.34	3.05
15,6,6	12.06	1.76	3.69	15,6,6	8.3	0.84	3.96
15,6,9	13.28	-0.86	2.27	15,6,9	12.5	-0.17	2.71
15,9,3	11.71	1.95	1.29	15,9,3	11.21	1.31	1.5
15,9,6	12.78	1.4	1.94	15,9,6	12.07	1.32	1.96
15,9,9	12.81	0.19	1.73	15,9,9	11.96	1.69	1.41
15,12,3	11.38	1.05	1	15,12,3	12.19	1.17	0.87
15,12,6	12.21	0.87	1.43	15,12,6	12.05	1.79	0.92
15,12,9	12.47	0.83	1.32	15,12,9	11.42	2.43	0.91
Angle of attack = 40°				Angle of attack = 45°			
coord. (cm)	V _x (cm/s)	V _y (cm/s)	V _z (cm/s)	coord. (cm)	V _x (cm/s)	V _y (cm/s)	V _z (cm/s)
15,-12,3	15.17	3.31	-1.57	15,-12,3	15.36	2.89	-0.7
15,-12,6	14.84	2.73	-1.7	15,-12,6	16.4	2.58	-1.03
15,-12,9	14.83	1.93	-1.45	15,-12,9	17.01	1.97	-1.24
15,-9,3	15.13	4.52	-1.94	15,-9,3	14.6	3.41	-1.73
15,-9,6	15.09	3.19	-2.17	15,-9,6	14.92	2.29	-1.7
15,-9,9	14.02	1.7	-1.72	15,-9,9	16.42	1.79	-1.28
15,-6,3	14.03	5.5	-2.69	15,-6,3	11.93	4.08	-3.87
15,-6,6	14.19	3.04	-3.23	15,-6,6	13.84	1.64	-3.47
15,-6,9	14.81	1.18	-2.17	15,-6,9	15.83	0.76	-1.84
15,-3,3	12.41	7.13	-4.73	15,-3,3	5.43	2.92	-4.65
15,-3,6	13.69	2.91	-5.05	15,-3,6	9.81	-0.88	-3.75
15,-3,9	14.41	0.26	-3.27	15,-3,9	15.02	-0.26	-2.1
15,0,3	9.1	8.58	-6.99	15,0,3	1.34	2	-2.45
15,0,6	12.21	-0.71	-6.51	15,0,6	3.39	-4.17	-3.18

Contd...Table C.1: 3D velocity components for rectangular vane (T/d = 0.60)

Angle of attack = 40°				Angle of attack = 45°			
coord. (cm)	V _x (cm/s)	V _y (cm/s)	V _z (cm/s)	coord. (cm)	V _x (cm/s)	V _y (cm/s)	V _z (cm/s)
15,0,9	15.88	-1.42	-2.81	15,0,9	14.41	-2.32	-1.91
15,3,3	1.03	5.72	1.08	15,3,3	0.41	2.58	1.6
15,3,6	8.84	-4.84	-0.92	15,3,6	3.04	-3.78	1.43
15,3,9	16.83	-3.42	0.08	15,3,9	12.69	-2.54	0.6
15,6,3	7.43	9.21	7.03	15,6,3	0.85	1.63	3.93
15,6,6	11.18	-1.54	7.21	15,6,6	4.11	-1.58	3.17
15,6,9	15.3	-1.03	3.14	15,6,9	12.88	-0.5	1.61
15,9,3	10.87	5.86	0.68	15,9,3	10.9	0.14	1.21
15,9,6	13.23	2.44	3.19	15,9,6	12.51	0.43	1.98
15,9,9	13.96	0.66	2.3	15,9,9	12.46	0.68	1.38
15,12,3	11.63	2.61	1.03	15,12,3	11.36	-0.06	1.47
15,12,6	12.32	2.38	1.83	15,12,6	12.17	0.83	1.04
15,12,9	13	1.38	1.58	15,12,9	11.98	1.48	0.83
Angle of attack = 50°							
coord. (cm)	V _x (cm/s)	V _y (cm/s)	V _z (cm/s)				
15,-12,3	14.97	2.96	-0.8				
15,-12,6	15.62	2.42	-1.19				
15,-12,9	15.95	1.8	-1.07				
15,-9,3	14.45	3.85	-1.47				
15,-9,6	15.51	3.1	-2.08				
15,-9,9	15.29	1.76	-1.71				
15,-6,3	13.35	5.55	-3.78				
15,-6,6	14.31	2.98	-3.8				
15,-6,9	15.14	0.86	-2.58				
15,-3,3	10.61	5.21	-4.84				
15,-3,6	12.72	0.17	-5.87				
15,-3,9	15.42	-0.59	-3.4				
15,0,3	-0.11	2.43	-1.67				
15,0,6	7.95	-3.01	-3.91				
15,0,9	15.93	-1.72	-2.28				
15,3,3	0.31	5.13	2.04				
15,3,6	5.46	-4.09	-0.76				
15,3,9	10.21	-4.09	-0.86				
15,6,3	2.93	7.07	5.23				
15,6,6	4.76	-4.16	2.85				
15,6,9	14.98	-1.55	1.62				
15,9,3	2.62	4.84	1.39				
15,9,6	9.19	0.21	3.38				
15,9,9	13.61	0.02	1.93				
15,12,3	11.94	2.49	0.28				
15,12,6	12.39	2	1.59				
15,12,9	12.69	0.88	1.36				

**Table C.2: 3D velocity components for rectangular vane
($T/d = 0.67$)**

Angle of attack = 30°				Angle of attack = 35°			
coord. (cm)	V_x (cm/s)	V_y (cm/s)	V_z (cm/s)	coord. (cm)	V_x (cm/s)	V_y (cm/s)	V_z (cm/s)
15,-15,3	15.93	1.42	-0.41	15,-15,3	16.16	2.56	-0.41
15,-15,6	16.19	0.94	-0.51	15,-15,6	16.58	1.96	-0.72
15,-15,9	16.42	0.48	-0.55	15,-15,9	16.67	1.44	-0.57
15,-15,12	16.66	0.14	-0.52	15,-15,12	16.82	1.06	-0.26
15,-12,3	16.15	1.99	-0.46	15,-12,3	15.82	3.33	-0.44
15,-12,6	16.09	1.01	-0.71	15,-12,6	15.93	2.12	-0.69
15,-12,9	15.8	0.51	-0.56	15,-12,9	16.23	1.33	-0.56
15,-12,12	16.09	0.06	-0.54	15,-12,12	16.68	1.08	-0.27
15,-9,3	15.14	2.37	-0.49	15,-9,3	15.27	3.64	-0.91
15,-9,6	15.16	1.28	-0.88	15,-9,6	15.27	2.05	-1.1
15,-9,9	15.14	0.28	-0.79	15,-9,9	15.34	0.9	-0.72
15,-9,12	15.47	-0.32	-0.41	15,-9,12	15.71	0.3	-0.39
15,-6,3	13.52	3.11	-1.45	15,-6,3	13.69	4.49	-1.92
15,-6,6	13.67	0.89	-2.09	15,-6,6	14.41	2.16	-2.37
15,-6,9	14.68	-0.31	-1.13	15,-6,9	15.06	0.36	-1.5
15,-6,12	14.92	-0.6	-0.47	15,-6,12	15.33	0.12	-0.35
15,-3,3	13.01	5.21	-4.8	15,-3,3	12.65	7.04	-5.52
15,-3,6	13.04	-0.11	-6.03	15,-3,6	13.78	0.76	-6.43
15,-3,9	14.61	-1.77	-2.49	15,-3,9	15.38	-1.23	-2.86
15,-3,12	14.75	-1.34	-0.67	15,-3,12	15.51	-0.95	-0.46
15,0,3	6.92	6.63	-3.11	15,0,3	4.11	5.72	-4.13
15,0,6	6.71	-4.89	-3.77	15,0,6	6.24	-3.9	-4.74
15,0,9	14.67	-5.18	-1.68	15,0,9	14.22	-4.82	-1.84
15,0,12	14.56	-1.99	-0.41	15,0,12	14.59	-1.37	-0.5
15,3,3	8.06	7.13	4.32	15,3,3	5.96	6.95	4.84
15,3,6	8.67	-3.67	5.49	15,3,6	7.83	-3.82	6.17
15,3,9	12.95	-4.86	2.23	15,3,9	11.46	-4.47	2.44
15,3,12	15.13	-2.1	0.91	15,3,12	14.85	-1.74	1.17
15,6,3	8.84	2.79	2.54	15,6,3	6.74	3.24	4.01
15,6,6	12.29	0.65	3.48	15,6,6	9.46	-0.02	4.62
15,6,9	14.66	-1.01	2.77	15,6,9	15.09	-0.72	3.3
15,6,12	15	-0.71	1.3	15,6,12	15.72	-0.16	1.48
15,9,3	12.96	0.14	1.28	15,9,3	13.94	1.08	1.31
15,9,6	14.53	0.05	2.07	15,9,6	15.64	0.26	2.6
15,9,9	14.39	-0.12	1.81	15,9,9	15.49	0.25	1.95
15,9,12	14.61	0.18	0.91	15,9,12	15.25	0.92	1.03
15,12,3	13.77	-0.07	0.92	15,12,3	14.86	1.02	1.29
15,12,6	14.93	0.13	0.97	15,12,6	15.47	0.95	1.2
15,12,9	14.97	0.26	0.77	15,12,9	15.22	0.82	0.84
15,12,12	15	0.45	0.52	15,12,12	15.35	1.46	0.58
15,15,3	14.07	0.02	0.32	15,15,3	15.37	0.91	0.42
15,15,6	15.19	-0.09	0.34	15,15,6	15.44	1.04	0.39
15,15,9	15.29	0.41	0.09	15,15,9	15.39	1.31	0.27
15,15,12	15.4	0.54	0.11	15,15,12	15.33	1.52	0.15
Angle of attack = 40°				Angle of attack = 45°			
coord. (cm)	V_x (cm/s)	V_y (cm/s)	V_z (cm/s)	coord. (cm)	V_x (cm/s)	V_y (cm/s)	V_z (cm/s)
15,-15,3	14.06	1.69	-0.19	15,-15,3	16.45	3.52	-0.41
15,-15,6	15.07	1.23	-0.34	15,-15,6	16.48	2.71	-0.53
15,-15,9	14.78	1.04	-0.45	15,-15,9	16.68	2.26	-0.37
15,-15,12	15.04	0.83	-0.21	15,-15,12	16.71	1.91	-0.43
15,-12,3	14.47	1.79	-0.84	15,-12,3	14.71	3.66	-0.33
15,-12,6	15.22	1.4	-1	15,-12,6	15.66	2.68	-0.69
15,-12,9	15.42	0.94	-0.71	15,-12,9	16.71	2.44	-0.81
15,-12,12	15.29	0.8	-0.62	15,-12,12	16.23	1.87	-0.24
15,-9,3	14.67	2.25	-1.55	15,-9,3	14.1	3.91	-1.45
15,-9,6	15.27	1.56	-1.87	15,-9,6	14.81	2.53	-1.44
15,-9,9	15.83	0.91	-1.47	15,-9,9	15.58	1.84	-1.06
15,-9,12	15.54	0.73	-1.1	15,-9,12	15.98	1.66	-0.47
15,-6,3	14.65	3.75	-2.93	15,-6,3	13.33	4.96	-3.52
15,-6,6	15.64	1.79	-3.56	15,-6,6	14.91	2.32	-3.64
15,-6,9	15.79	0.36	-2.43	15,-6,9	16.09	1.23	-2.23
15,-6,12	15.98	-0.04	-1.44	15,-6,12	15.81	1.22	-0.63
15,-3,3	12.46	5.79	-6.71	15,-3,3	6.84	4.9	-5.43
15,-3,6	14.98	0.49	-6.94	15,-3,6	10.67	-0.91	-5.86
15,-3,9	16.92	-1.39	-3.51	15,-3,9	16.12	-1.28	-3.17
15,-3,12	16.29	-0.99	-1.62	15,-3,12	16.27	0.2	-0.95
15,0,3	2.7	3.72	-4.35	15,0,3	0.97	3.02	-2.93
15,0,6	9	-4.93	-6.07	15,0,6	5.5	-4.55	-5.15
15,0,9	17.41	-4.54	-2.89	15,0,9	15.8	-2.85	-2.86

Contd...Table C.2: 3D velocity components for rectangular vane
($T/d = 0.67$)

Angle of attack = 40°				Angle of attack = 45°			
coord. (cm)	V_x (cm/s)	V_y (cm/s)	V_z (cm/s)	coord. (cm)	V_x (cm/s)	V_y (cm/s)	V_z (cm/s)
15,0,12	17.07	-2.12	-0.95	15,0,12	16.33	-0.84	-0.84
15,3,3	3.43	6.41	3.95	15,3,3	0.48	4.31	1.91
15,3,6	7.84	-5.65	0.45	15,3,6	3.81	-4.67	0.43
15,3,9	15.94	-6.41	0.11	15,3,9	12.05	-5.3	-0.55
15,3,12	17.16	-2.7	0.34	15,3,12	16.58	-1.01	0.43
15,6,3	5.98	6.72	8.78	15,6,3	3.47	4.62	6
15,6,6	8.63	-2	6.68	15,6,6	4.99	-2.77	5.51
15,6,9	16.13	-3.27	3.13	15,6,9	13.93	-2.45	2.46
15,6,12	17.11	-1.56	1.46	15,6,12	16.73	-0.3	1.2
15,9,3	12.86	5.03	-1.21	15,9,3	10.62	2.35	0.84
15,9,6	15.04	2.35	3.31	15,9,6	14.2	1.48	2.81
15,9,9	16.98	-0.14	2.65	15,9,9	15.82	0.79	2.2
15,9,12	16.87	-0.36	1.5	15,9,12	15.91	1.16	1.03
15,12,3	15.48	1.71	0.71	15,12,3	15.02	1.66	0.9
15,12,6	16.81	1.67	1.42	15,12,6	15.71	1.75	1.31
15,12,9	16.88	0.99	1.4	15,12,9	15.89	1.54	1.08
15,12,12	16.7	0.63	0.97	15,12,12	15.85	1.93	0.66
15,15,3	15.91	1.5	0.86	15,15,3	15.36	1.74	0.5
15,15,6	16.59	1.25	0.94	15,15,6	16.25	1.79	0.32
15,15,9	16.72	0.98	0.81	15,15,9	16.21	1.72	0.18
15,15,12	16.52	0.84	0.63	15,15,12	15.77	2.35	0.06

Angle of attack = 50°			
coord. (cm)	V_x (cm/s)	V_y (cm/s)	V_z (cm/s)
15,-15,3	16.14	2.58	-0.19
15,-15,6	17.19	2.34	-0.52
15,-15,9	16.96	1.82	-0.49
15,-15,12	17.56	1.8	-0.5
15,-12,3	15.46	3.25	-0.54
15,-12,6	17	2.6	-1.23
15,-12,9	17.41	2.16	-0.95
15,-12,12	17.78	1.64	-0.28
15,-9,3	15.07	4.22	-1.64
15,-9,6	16.43	2.66	-2.01
15,-9,9	17.2	1.9	-1.63
15,-9,12	18.09	1.58	-0.64
15,-6,3	11.29	4.48	-4.43
15,-6,6	15.27	1.94	-4.66
15,-6,9	16.1	1.02	-2.38
15,-6,12	16.9	1.21	-1.13
15,-3,3	6.49	4.38	-4.45
15,-3,6	11.21	-1.01	-4.73
15,-3,9	17.26	-0.83	-3.19
15,-3,12	9.54	0.1	-2.13
15,0,3	0.46	3.17	-2.72
15,0,6	5.34	-3.24	-4.31
15,0,9	16.37	-2.98	-2.81
15,0,12	17.65	-0.54	-0.81
15,3,3	-1.17	2.52	-0.36
15,3,6	1.35	-5.83	-1.16
15,3,9	13.97	-3.85	-1.38
15,3,12	17.32	-0.99	-0.17
15,6,3	-0.17	2.78	4.97
15,6,6	2.83	-4.03	3.42
15,6,9	13.95	-2.83	0.63
15,6,12	17.18	-0.31	0.65
15,9,3	5.55	1.22	2.86
15,9,6	12.85	-1.33	3.21
15,9,9	16.89	-0.64	1.33
15,9,12	17.05	0.37	0.88
15,12,3	15.16	0.83	0.62
15,12,6	16.16	0.87	1.6
15,12,9	17.12	0.75	1.05
15,12,12	16.85	1.32	0.65
15,15,3	15.86	1.11	1
15,15,6	16.77	0.92	0.71
15,15,9	16.93	1.36	0.29
15,15,12	16.58	1.66	0.28

Table C.3: 3D velocity components for rectangular vane (T/d = 0.75)

Angle of attack = 30°				Angle of attack = 35°			
coord. (cm)	V _x (cm/s)	V _y (cm/s)	V _z (cm/s)	coord. (cm)	V _x (cm/s)	V _y (cm/s)	V _z (cm/s)
15,-12,2	12.05	2.67	-0.28	15,-12,2	10.96	1.82	-0.43
15,-12,4	12.55	2.64	-0.42	15,-12,4	10.89	1.67	-0.59
15,-12,6	13.01	2.59	-0.69	15,-12,6	11.39	1.56	-0.84
15,-12,8	13.21	2.38	-0.77	15,-12,8	12.21	0.93	-1.08
15,-12,10	12.95	1.94	-0.71	15,-12,10	11.49	0.37	-0.24
15,-12,12	13.06	1.63	-0.72	15,-12,12	11.92	0.78	-0.24
15,-6,2	11.8	4.49	-0.83	15,-6,2	9.24	3.99	-1.86
15,-6,4	12.22	3.79	-1.59	15,-6,4	10.74	3.09	-2.25
15,-6,6	12.04	3.24	-1.82	15,-6,6	11.15	1.89	-2.44
15,-6,8	12.14	2.35	-1.58	15,-6,8	2.08	0.14	-0.33
15,-6,10	12.22	1.86	-1.42	15,-6,10	11.29	0.57	-0.79
15,-6,12	12.44	1.11	-1.41	15,-6,12	12.05	0.39	-0.51
15,0,2	9.68	8.21	-2.56	15,0,2	4.21	6.49	-1.44
15,0,4	9.93	6.41	-4.98	15,0,4	2.77	1.48	-1.82
15,0,6	11.28	0.96	-5.16	15,0,6	4.61	-3.44	-1.86
15,0,8	12.38	0.32	-2.49	15,0,8	8.79	-4.41	-1.51
15,0,10	12.2	-0.25	-1.21	15,0,10	11.6	-1.82	-1.23
15,0,12	12.47	0.21	-0.95	15,0,12	11.79	-0.89	-0.39
15,6,2	7.18	3.89	0.99	15,6,2	3.98	2.43	0.91
15,6,4	8.66	3.81	2.54	15,6,4	6.53	1.31	3.03
15,6,6	9.49	2.79	3.27	15,6,6	8.71	-0.39	3.62
15,6,8	12.01	1.35	3.08	15,6,8	10.03	-0.77	3.02
15,6,10	11.66	0.38	1.98	15,6,10	11.38	-1.7	1.6
15,6,12	11.91	0.19	1.16	15,6,12	11.36	-0.79	1.11
15,12,2	8.99	1.86	0.72	15,12,2	9.71	0.3	0.6
15,12,4	10.15	1.71	1.12	15,12,4	9.62	0.49	0.85
15,12,6	11.11	1.68	1.24	15,12,6	10.47	0.58	0.69
15,12,8	11.43	1.57	1.26	15,12,8	10.31	0.54	0.95
15,12,10	11.33	1.27	1.48	15,12,10	11.21	0.17	0.81
15,12,12	11.98	1.05	0.87	15,12,12	11.49	0.2	0.5
Angle of attack = 40°				Angle of attack = 45°			
coord. (cm)	V _x (cm/s)	V _y (cm/s)	V _z (cm/s)	coord. (cm)	V _x (cm/s)	V _y (cm/s)	V _z (cm/s)
15,-12,2	11.68	2.11	-0.46	(15,-12,3)	11.05	2	-0.64
15,-12,4	12.03	1.82	-0.85	(15,-12,6)	11.15	1.26	-1.09
15,-12,6	12.12	1.67	-0.92	(15,-12,9)	12.31	1.24	-1.09
15,-12,8	12.66	1.35	-1.09	(15,-12,12)	12.53	1.06	-0.58
15,-12,10	12.89	1.16	-0.92	(15,-6,3)	8.87	4.03	-3.73
15,-12,12	12.75	0.98	-0.92	(15,-6,6)	10.55	-0.48	-4.09
15,-6,2	10.95	4.05	-1.7	(15,-6,9)	11.99	0.12	-1.9
15,-6,4	11.33	3.02	-2.33	(15,-6,12)	12.48	0.22	-0.85
15,-6,6	12.1	2.06	-2.58	(15,0,3)	-0.44	1.86	-1.23
15,-6,8	11.96	1.27	-2.09	(15,0,6)	2.26	-4.02	-2.17

Contd...Table C.3: 3D velocity components for rectangular vane (T/d = 0.75)

Angle of attack = 40°				Angle of attack = 45°			
coord. (cm)	V _x (cm/s)	V _y (cm/s)	V _z (cm/s)	coord. (cm)	V _x (cm/s)	V _y (cm/s)	V _z (cm/s)
15,-6,10	12.21	0.47	-1.67	(15,0,9)	11.79	-3.5	-1.02
15,-6,12	12.77	0.14	-1.41	(15,0,12)	12.56	-1.25	-0.01
15,0,2	5.99	8.46	-4.14	(15,6,3)	0.5	2.94	4.3
15,0,4	3.71	1.1	-5.04	(15,6,6)	3.28	-2.13	4.25
15,0,6	9.5	-2.41	-5.23	(15,6,9)	11.82	-0.85	2.47
15,0,8	12.95	-1.66	-3.1	(15,6,12)	12.25	-0.28	0.95
15,0,10	12.3	-1.53	-1.68	(15,12,3)	11.52	0.5	0.97
15,0,12	12.73	-1.02	-1.19	(15,12,6)	12.03	0.33	1.17
15,6,2	6.94	7.96	2.93	(15,12,9)	12.02	0.67	0.76
15,6,4	7.71	4.66	6.03	(15,12,12)	12.35	0.62	0.59
15,6,6	8.15	0.33	5.32				
15,6,8	11.49	-0.71	3.09				
15,6,10	11.62	-0.99	1.63				
15,6,12	11.6	-1	0.81				
15,12,2	9.1	1.56	0.83				
15,12,4	10.04	1.74	1.11				
15,12,6	10.46	1.13	1.54				
15,12,8	10.63	0.58	1.45				
15,12,10	11.54	0.35	0.76				
15,12,12	11.45	-0.06	0.76				
Angle of attack = 50°							
coord. (cm)	V _x (cm/s)	V _y (cm/s)	V _z (cm/s)				
(15,-12,3)	11.62	2.25	-0.71				
(15,-12,6)	12.12	1.87	-0.96				
(15,-12,9)	13.12	1.55	-1.08				
(15,-12,12)	12.48	1.24	-0.86				
(15,-6,3)	11.37	4.29	-3.28				
(15,-6,6)	12.35	2	-3.14				
(15,-6,9)	13.15	1.12	-2.2				
(15,-6,12)	13.21	0.52	-1.26				
(15,0,3)	-0.56	1.69	-1.81				
(15,0,6)	4.59	-3.76	-2.4				
(15,0,9)	13.86	-1.43	-1.54				
(15,0,12)	13.9	-0.48	-0.86				
(15,6,3)	2.96	2.93	4.01				
(15,6,6)	4.95	-2.72	2.89				
(15,6,9)	13.29	-0.64	1.15				
(15,6,12)	12.78	-0.6	0.37				
(15,12,3)	10.42	1.4	0.77				
(15,12,6)	11.07	1.24	1.35				
(15,12,9)	11.71	0.78	1.17				
(15,12,12)	11.82	0.37	0.71				

Table C.4: 3D velocity components for double curve type I vane
($T/d = 0.67$)

Angle of attack = 30°				Angle of attack = 35°			
coord. (cm)	V_x (cm/s)	V_y (cm/s)	V_z (cm/s)	coord. (cm)	V_x (cm/s)	V_y (cm/s)	V_z (cm/s)
15,-15,3	16.25	2.11	0.15	15,-15,3	16.89	2.56	-0.18
15,-15,6	17.32	1.73	0.01	15,-15,6	18.04	2.07	-0.31
15,-15,9	17.88	1.53	-0.21	15,-15,9	18.29	1.89	-0.33
15,-15,12	18.13	1.31	-0.26	15,-15,12	18.22	1.44	-0.12
15,-12,3	16.87	2.33	0.16	15,-12,3	16.7	2.42	-0.1
15,-12,6	17.87	1.88	0.06	15,-12,6	18.05	2.29	-0.29
15,-12,9	17.99	1.63	-0.06	15,-12,9	18.52	1.84	-0.4
15,-12,12	18	1.27	-0.09	15,-12,12	18.44	1.44	-0.04
15,-9,3	16.55	2.65	0.03	15,-9,3	17	2.99	0.35
15,-9,6	17.55	1.91	-0.19	15,-9,6	17.82	2.35	-0.61
15,-9,9	18.1	1.66	-0.19	15,-9,9	18.41	2.04	-0.84
15,-9,12	18.14	1.19	0.03	15,-9,12	18.49	1.23	-0.48
15,-6,3	15.98	3.06	-0.53	15,-6,3	15.75	4.36	-0.36
15,-6,6	17.53	2.18	-0.74	15,-6,6	16.35	2.87	-2.114
15,-6,9	18.31	1.7	-0.57	15,-6,9	17.38	1.68	-1.7
15,-6,12	18.57	1.2	-0.28	15,-6,12	18.56	0.89	-0.87
15,-3,3	15.6	3.86	-2.1	15,-3,3	13.82	7.32	-2.94
15,-3,6	17	2.41	-2.85	15,-3,6	16.27	2.52	-5.86
15,-3,9	18.7	0.87	-1.73	15,-3,9	16.63	0.22	-3.05
15,-3,12	18.52	0.77	-0.63	15,-3,12	19.05	-0.02	-0.83
15,0,3	6.87	6.34	-2.96	15,0,3	10.28	10.53	-1.44
15,0,6	7.46	-1.46	-4.65	15,0,6	7.94	-2.27	-1.21
15,0,9	16.98	-1.09	-1.66	15,0,9	15.77	-3.73	-1.15
15,0,12	19.09	-0.13	-0.42	15,0,12	19.42	-1.41	0
15,3,3	7.13	6.52	1.81	15,3,3	9.09	8.63	1.21
15,3,6	7.17	-2.37	2.12	15,3,6	8.84	-0.58	1.99
15,3,9	12.91	-2.35	0.77	15,3,9	13.55	-2.17	1.82
15,3,12	18.3	-0.09	-0.05	15,3,12	20.05	-1.05	1.31
15,6,3	7.67	1.75	2.93	15,6,3	5.38	4.53	4.76
15,6,6	9.56	1.24	2.42	15,6,6	5.56	-1.4	3.41
15,6,9	13.19	0.23	1.64	15,6,9	16.27	0.58	2.68
15,6,12	18.32	0.44	0.79	15,6,12	19.58	0.44	1.9
15,9,3	4.8	1.7	0.94	15,9,3	13.63	3.31	-0.51
15,9,6	10.39	1.43	1.33	15,9,6	16.99	2.84	2.1
15,9,9	17.18	1.11	1.15	15,9,9	18.81	1.97	1.89
15,9,12	18.12	1	0.55	15,9,12	19.12	1.26	1.46
15,12,3	14.11	2.19	0.87	15,12,3	14.75	3.85	1.31
15,12,6	16.45	1.64	1	15,12,6	18.27	2.82	1.4
15,12,9	17.36	1.53	0.78	15,12,9	18.46	2.3	1.35
15,12,12	17.65	1.18	0.35	15,12,12	19.17	1.83	1.15
15,15,3	13.98	1.9	0.55	15,15,3	15.23	2.89	0.74
15,15,6	16.79	1.67	0.7	15,15,6	17.16	2.55	1.12
15,15,9	17.59	1.52	0.51	15,15,9	18.14	2.27	1.11
15,15,12	17.78	1.49	0.35	15,15,12	18.53	2.12	1.06

Angle of attack = 40°				Angle of attack = 45°			
coord. (cm)	V_x (cm/s)	V_y (cm/s)	V_z (cm/s)	coord. (cm)	V_x (cm/s)	V_y (cm/s)	V_z (cm/s)
15,-15,3	15.69	0.62	-0.24	15,-15,3	16.25	2.52	-0.15
15,-15,6	16.81	0.54	-0.36	15,-15,6	17.32	2.09	-0.26
15,-15,9	17.04	0.28	-0.2	15,-15,9	17.88	1.63	-0.36
15,-15,12	16.85	0.01	-0.09	15,-15,12	18.13	1.32	-0.13
15,-12,3	16.15	1.05	-0.11	15,-12,3	16.87	3.21	-0.48
15,-12,6	16.56	0.77	-0.26	15,-12,6	17.87	2.52	-0.66
15,-12,9	16.97	0.41	-0.42	15,-12,9	17.99	1.84	-0.71
15,-12,12	16.97	0.01	-0.18	15,-12,12	18	1.25	-0.23
15,-9,3	15.62	1.45	-0.34	15,-9,3	16.55	3.61	-0.81
15,-9,6	16.42	0.9	-0.51	15,-9,6	17.55	2.81	-1.18
15,-9,9	16.31	0.3	-0.54	15,-9,9	18.1	2.15	-1.09
15,-9,12	16.74	0.02	-0.36	15,-9,12	18.14	0.99	-0.69
15,-6,3	15.27	2.6	-1.05	15,-6,3	15.98	5.13	-1.98
15,-6,6	15.84	1.67	-1.49	15,-6,6	17.53	3.39	-3.06
15,-6,9	16.84	0.36	-1.01	15,-6,9	18.31	1.52	-2.21
15,-6,12	17.5	-0.27	-0.57	15,-6,12	18.57	0.56	-1.26
15,-3,3	14.01	4.15	-3.08	15,-3,3	15.6	7.18	-5.05
15,-3,6	16.47	1.27	-4.25	15,-3,6	17	3.08	-6.13
15,-3,9	17.65	-0.97	-2.52	15,-3,9	18.7	0.29	-3.63
15,-3,12	17.57	-1.47	-0.77	15,-3,12	18.52	-0.47	-1.6
15,0,3	12.62	8.17	-2.72	15,0,3	6.87	7.72	-3.39
15,0,6	8.66	-3.43	-4.39	15,0,6	7.46	-2.61	-5.53
15,0,9	18.41	-3.79	-1.97	15,0,9	16.98	-3.93	-3.21

Contd... Table C.4: 3D velocity components for double curve type I vane
($T/d = 0.67$)

Angle of attack = 40°				Angle of attack = 45°			
coord. (cm)	V _x (cm/s)	V _y (cm/s)	V _z (cm/s)	coord. (cm)	V _x (cm/s)	V _y (cm/s)	V _z (cm/s)
15,0,12	17.84	-2.24	-0.17	15,0,12	19.09	-1.69	-1.06
15,3,3	11.77	8.19	3.54	15,3,3	7.13	9.27	4.16
15,3,6	11.18	-2.17	4.82	15,3,6	7.17	-3.98	1.52
15,3,9	16.48	-4.71	1.64	15,3,9	12.91	-4.86	0.57
15,3,12	17.68	-2.42	0.96	15,3,12	18.3	-2.03	0.52
15,6,3	7.31	4.31	3.28	15,6,3	7.67	9.22	6.19
15,6,6	8.67	1.48	3.16	15,6,6	9.56	1.46	5.54
15,6,9	17.78	-0.87	2.76	15,6,9	13.19	-1.91	2.35
15,6,12	17.83	-1.39	1.38	15,6,12	18.32	-0.71	1.37
15,9,3	14.44	1.21	0.91	15,9,3	4.8	8	0.58
15,9,6	17.09	1.35	1.88	15,9,6	10.39	1.93	2.96
15,9,9	17.07	0.11	1.67	15,9,9	17.18	1.23	2.37
15,9,12	17.36	-0.39	1.23	15,9,12	18.12	0.16	1.59
15,12,3	14.93	1.32	0.91	15,12,3	14.11	2.73	-0.2
15,12,6	16.4	0.79	1.16	15,12,6	16.45	3.01	1.58
15,12,9	17.19	0.53	1.13	15,12,9	17.36	1.95	1.92
15,12,12	17.49	-0.32	1.03	15,12,12	17.65	1.12	1.33
15,15,3	15.09	0.97	0.77	15,15,3	13.98	2.88	1.25
15,15,6	16.7	0.92	1.11	15,15,6	16.79	2.16	1.25
15,15,9	17.15	0.53	0.96	15,15,9	17.59	2.11	1.22
15,15,12	17.02	0.29	0.82	15,15,12	17.78	1.4	0.91

Angle of attack = 50°			
coord. (cm)	V _x (cm/s)	V _y (cm/s)	V _z (cm/s)
15,-15,3	15.05	2.56	0.02
15,-15,6	17.22	2.35	-0.26
15,-15,9	17.62	2.06	-0.3
15,-15,12	17.51	1.86	-0.33
15,-12,3	15.11	2.95	-0.07
15,-12,6	17.1	2.82	-0.47
15,-12,9	17.63	2.2	-0.56
15,-12,12	17.98	1.67	-0.52
15,-9,3	15.76	3.68	-0.34
15,-9,6	17.18	3.29	-0.9
15,-9,9	17.75	2.45	-1.09
15,-9,12	17.91	1.65	-0.81
15,-6,3	14.21	4.88	-1.19
15,-6,6	16.78	4.01	-2.53
15,-6,9	17.77	2.3	-2.03
15,-6,12	18.11	1.09	-1.2
15,-3,3	13.81	7.41	-3.38
15,-3,6	16.35	4.03	-6.25
15,-3,9	18.12	0.82	-3.61
15,-3,12	18.33	0.16	-1.48
15,0,3	10.5	11.83	-1.29
15,0,6	7.58	-0.34	-5.3
15,0,9	17.04	-3.84	-3.18
15,0,12	18.97	-1.04	-0.88
15,3,3	9.97	13.06	4.47
15,3,6	7.95	0.8	4.94
15,3,9	13.94	-4.57	1.25
15,3,12	18.79	-1.57	0.87
15,6,3	2.64	9.08	4.78
15,6,6	7.66	3.44	3.57
15,6,9	13.58	-0.41	3.44
15,6,12	18.5	0.11	1.94
15,9,3	12.05	3.4	-2.25
15,9,6	14.97	3.69	1.5
15,9,9	16.75	2.14	2.38
15,9,12	17.97	1.42	1.72
15,12,3	12.83	3.19	1.16
15,12,6	15.04	2.53	1.41
15,12,9	17.02	2.25	1.54
15,12,12	17.5	1.85	1.38
15,15,3	13.23	2.56	0.82
15,15,6	15.91	2.48	1.39
15,15,9	16.68	2.24	1.22
15,15,12	17.63	2.05	0.96

**Table C.5: 3D velocity components for double curve type II vane
($T/d = 0.67$)**

Angle of attack = 30°				Angle of attack = 35°			
coord. (cm)	V_x (cm/s)	V_y (cm/s)	V_z (cm/s)	coord. (cm)	V_x (cm/s)	V_y (cm/s)	V_z (cm/s)
15,-15,3	13.06	0.66	-0.26	15,-15,3	14.61	1.31	-0.29
15,-15,6	14.57	0.76	-0.47	15,-15,6	14.79	0.84	-0.51
15,-15,9	13.95	0.49	-0.23	15,-15,9	16.28	0.84	-0.66
15,-15,12	14.75	0.46	-0.42	15,-15,12	15.2	0.44	-0.19
15,-12,3	12.68	0.86	-0.49	15,-12,3	12.94	1.2	-0.25
15,-12,6	14.34	0.61	-0.77	15,-12,6	14.15	1.03	-0.45
15,-12,9	14.61	0.42	-0.83	15,-12,9	14.69	0.58	-0.54
15,-12,12	14.87	0.29	-0.79	15,-12,12	15.15	0.5	-0.31
15,-9,3	12.67	1.13	-0.29	15,-9,3	12.26	1.55	-0.3
15,-9,6	13.18	0.69	-0.26	15,-9,6	13.23	1.05	-0.36
15,-9,9	14.43	0.59	-0.53	15,-9,9	13.24	0.66	-0.52
15,-9,12	14.9	0.43	-0.51	15,-9,12	13.82	0.42	-0.64
15,-6,3	12.56	1.61	-0.44	15,-6,3	13.35	2.12	-0.73
15,-6,6	13.48	1	-0.56	15,-6,6	13.44	1.47	-1.11
15,-6,9	13.61	0.42	-0.56	15,-6,9	13.07	0.76	-0.91
15,-6,12	14.17	0.24	-0.36	15,-6,12	13.01	0.16	-0.58
15,-3,3	11.93	2.35	-1.02	15,-3,3	12.35	3.21	-1.82
15,-3,6	12.85	1.2	-1.46	15,-3,6	13.8	1.77	-2.89
15,-3,9	14.08	0.33	-1.1	15,-3,9	14.77	0.07	-1.9
15,-3,12	14.67	0.11	-0.61	15,-3,12	14.55	-0.25	-0.95
15,0,3	11.47	4.22	-3.58	15,0,3	11.65	6.03	-4.2
15,0,6	13.66	0.35	-4.07	15,0,6	11.74	-0.42	-5.76
15,0,9	14.43	-0.91	-1.78	15,0,9	14.53	-1.61	-2.52
15,0,12	14.66	-0.5	-0.63	15,0,12	14.98	-1.29	-0.81
15,3,3	8.6	5.57	-1.32	15,3,3	8.85	7.24	-1.99
15,3,6	8.07	5.11	-0.4	15,3,6	7.07	-3.84	-1.51
15,3,9	14.66	-3.15	0.04	15,3,9	13.68	-3.59	-1.32
15,3,12	15.04	-0.84	0.06	15,3,12	14.52	-2.08	0.01
15,6,3	8.16	2.29	2.86	15,6,3	9.62	5.62	3.83
15,6,6	11.37	-0.85	2.98	15,6,6	8.99	-0.47	5.61
15,6,9	15.24	-1.34	1.18	15,6,9	13.48	-3	2.2
15,6,12	14.78	-0.31	0.65	15,6,12	15.03	-1.5	0.78
15,9,3	12.43	0.5	1.01	15,9,3	11.32	1.23	0.42
15,9,6	14.67	0.14	1.28	15,9,6	14.05	0.16	2.06
15,9,9	14.63	-0.2	0.93	15,9,9	15.28	-0.44	1.56
15,9,12	13.99	0.11	0.45	15,9,12	14.44	-0.61	0.79
15,12,3	13.27	0.64	0.77	15,12,3	12.58	0.77	1.28
15,12,6	14.41	0.38	0.91	15,12,6	14.6	0.18	1.2
15,12,9	14.96	0.4	0.64	15,12,9	14.52	0.12	0.87
15,12,12	14.34	0.45	0.38	15,12,12	14.32	0.04	0.38
15,15,3	13.86	0.42	0.36	15,15,3	13.79	0.54	0.5
15,15,6	15.02	0.43	0.44	15,15,6	14.66	0.19	0.6
15,15,9	14.7	0.46	0.2	15,15,9	14.82	0.28	0.45
15,15,12	15.15	0.41	0.27	15,15,12	14.86	0.14	0.51
Angle of attack = 40°				Angle of attack = 45°			
coord. (cm)	V_x (cm/s)	V_y (cm/s)	V_z (cm/s)	coord. (cm)	V_x (cm/s)	V_y (cm/s)	V_z (cm/s)
15,-15,3	13.76	1.51	-0.18	15,-15,3	13.97	2.64	-0.5
15,-15,6	14.83	1.17	-0.29	15,-15,6	14.3	2.31	-0.61
15,-15,9	15.87	1.32	-0.5	15,-15,9	15.53	2.45	-0.77
15,-15,12	15.2	1.18	-0.22	15,-15,12	15.35	2	-0.78
15,-12,3	13.59	1.7	-0.28	15,-12,3	14.08	3.1	-0.41
15,-12,6	15.02	1.28	-0.42	15,-12,6	15.02	2.97	-0.82
15,-12,9	15.36	1.2	-0.59	15,-12,9	15.35	2.48	-0.77
15,-12,12	15.81	1.16	-0.41	15,-12,12	15.19	2.04	-0.77
15,-9,3	13.9	2.04	-0.52	15,-9,3	13.98	3.62	-0.54
15,-9,6	14.73	1.75	-0.77	15,-9,6	14.92	2.83	-0.93
15,-9,9	15.14	1.12	-0.96	15,-9,9	14.85	2.31	-0.86
15,-9,12	15.48	0.92	-0.57	15,-9,12	15.71	2.11	-0.89
15,-6,3	13.73	2.88	-0.67	15,-6,3	13.1	4.23	-0.96
15,-6,6	14.55	1.89	-1.28	15,-6,6	14.73	3.27	-1.69
15,-6,9	15.07	0.97	-1.38	15,-6,9	15.13	2.3	-1.38
15,-6,12	15.3	0.59	-0.57	15,-6,12	15.38	1.61	-0.95
15,-3,3	12.36	3.98	-2.07	15,-3,3	12.43	5.67	-2.23
15,-3,6	14.58	2.14	-3.38	15,-3,6	13.57	3.44	-3.63
15,-3,9	15.63	0.44	-2.33	15,-3,9	14.34	1.52	-2.24
15,-3,12	15.42	-0.18	-0.89	15,-3,12	15.62	1.09	-1.36
15,0,3	10.19	6.59	-5.11	15,0,3	10.49	8.25	-5.17
15,0,6	11.38	-0.58	-6.56	15,0,6	11.2	1.7	-7.66
15,0,9	16.01	-1.37	-3.31	15,0,9	15.44	-0.89	-3.72

Contd...Table C.5: 3D velocity components for double curve type II vane
($T/d = 0.67$)

Angle of attack = 40°				Angle of attack = 45°			
coord. (cm)	V _x (cm/s)	V _y (cm/s)	V _z (cm/s)	coord. (cm)	V _x (cm/s)	V _y (cm/s)	V _z (cm/s)
15,0,12	15.7	-0.94	-0.94	15,0,12	15.91	-0.56	-1.43
15,3,3	5.29	8.06	-0.36	15,3,3	3.98	8.59	-1.64
15,3,6	8.91	-4.86	-2	15,3,6	7.45	-3.55	-3.72
15,3,9	14.63	-4.91	-1.51	15,3,9	14.18	-4.91	-2.57
15,3,12	15.52	-1.84	-0.3	15,3,12	16.13	-1.7	-0.61
15,6,3	8.9	6.82	4.01	15,6,3	8.81	9.27	5.44
15,6,6	8.52	-0.57	5.5	15,6,6	9.97	-0.09	7.76
15,6,9	13.06	-3.45	2.18	15,6,9	12.04	-4	2.96
15,6,12	15.72	-1.67	0.92	15,6,12	16.03	-1.47	1.27
15,9,3	9.64	3.83	1.2	15,9,3	8.44	4.88	1.89
15,9,6	13.62	0.78	3.08	15,9,6	11.27	1.7	4.2
15,9,9	15.42	-0.56	2.02	15,9,9	14.88	0	2.78
15,9,12	15.55	-0.42	0.97	15,9,12	15.33	0.3	1.58
15,12,3	12.7	0.66	1.23	15,12,3	12.01	2.76	0.11
15,12,6	14.49	0.62	1.6	15,12,6	14.48	2.24	2.49
15,12,9	14.71	0.45	1.22	15,12,9	15.26	1.03	2.3
15,12,12	15.3	0.16	0.74	15,12,12	15.53	1.03	1.51
15,15,3	13.41	1.16	0.82	15,15,3	13.68	2.14	1.19
15,15,6	14.84	0.87	0.85	15,15,6	15.29	1.95	1.11
15,15,9	15.43	0.76	0.75	15,15,9	15.67	1.79	0.91
15,15,12	15.31	0.54	0.57	15,15,12	15.72	1.43	0.88
Angle of attack = 50°							
coord. (cm)	V _x (cm/s)	V _y (cm/s)	V _z (cm/s)				
15,-15,3	13.72	3.62	-0.5				
15,-15,6	13.89	3.02	-0.44				
15,-15,9	14.97	3.18	-0.81				
15,-15,12	14.51	2.89	-0.56				
15,-12,3	12.73	3.69	-0.31				
15,-12,6	13.53	3.19	-0.62				
15,-12,9	14.52	3.2	-0.76				
15,-12,12	14.32	2.85	-0.53				
15,-9,3	12.3	3.84	-0.4				
15,-9,6	13.4	3.49	-0.7				
15,-9,9	14.25	2.96	-0.79				
15,-9,12	14.53	2.57	-0.63				
15,-6,3	12.16	4.43	-1.03				
15,-6,6	13.86	3.81	-1.71				
15,-6,9	14.31	2.86	-1.59				
15,-6,12	14.57	2.54	-1.2				
15,-3,3	12.33	6.21	-3.01				
15,-3,6	13.66	3.89	-4.23				
15,-3,9	14.38	2.09	-2.52				
15,-3,12	15.39	0.45	-1.6				
15,0,3	8.48	7.73	-4.94				
15,0,6	10.35	0.07	-6.99				
15,0,9	15.93	-1.25	-4.11				
15,0,12	15.76	-0.7	-2				
15,3,3	3.37	8.78	-0.4				
15,3,6	6.28	-2.94	-3.41				
15,3,9	15.17	-4.38	-3.08				
15,3,12	15.76	-2.09	-1.01				
15,6,3	6.15	10.78	6.19				
15,6,6	6.09	0.3	5.86				
15,6,9	11.32	-5.31	1.36				
15,6,12	15.76	-2.21	1.02				
15,9,3	5.39	8.91	0.7				
15,9,6	7.06	3.27	4.12				
15,9,9	12.52	-0.48	3.94				
15,9,12	15.57	-0.47	1.87				
15,12,3	12.87	2.75	-1.44				
15,12,6	14.08	3.08	1.1				
15,12,9	15.03	1.79	1.99				
15,12,12	15.15	0.99	1.12				
15,15,3	13.45	1.69	0.6				
15,15,6	14.11	1.79	0.81				
15,15,9	15.03	1.81	0.94				
15,15,12	15.13	1.45	0.83				

Table C.6: 3D velocity components for J1 type vane
($T/d = 0.67$)

Angle of attack = 30°				Angle of attack = 35°			
coord. (cm)	V _x (cm/s)	V _y (cm/s)	V _z (cm/s)	coord. (cm)	V _x (cm/s)	V _y (cm/s)	V _z (cm/s)
15,-15,3	15.22	2.77	-0.2	15,-15,3	14.64	2.84	-0.28
15,-15,6	16.14	2.69	-0.38	15,-15,6	15.26	2.25	-0.32
15,-15,9	16.4	2.35	-0.51	15,-15,9	15.41	2.04	-0.26
15,-15,12	16.34	1.93	-0.65	15,-15,12	15.99	2.02	-0.27
15,-12,3	16.02	3.15	-0.25	15,-12,3	14.5	2.91	-0.21
15,-12,6	16.34	2.84	-0.51	15,-12,6	15.87	2.63	-0.52
15,-12,9	15.85	2.14	-0.47	15,-12,9	16.04	2.28	-0.46
15,-12,12	16.53	1.8	-0.34	15,-12,12	16.25	2.09	-0.52
15,-9,3	16.12	3.28	-0.09	15,-9,3	13.51	2.98	-0.15
15,-9,6	16.81	3.96	-0.39	15,-9,6	15.06	2.45	-0.36
15,-9,9	16.68	2.31	-0.4	15,-9,9	15.78	2.35	-0.3
15,-9,12	15.58	1.53	-0.09	15,-9,12	15.95	1.9	-0.42
15,-6,3	14.81	3.76	-0.51	15,-6,3	12.79	3.38	-0.88
15,-6,6	15.38	3.03	-0.55	15,-6,6	13.13	2.56	-1.35
15,-6,9	15.31	2.18	-0.53	15,-6,9	15.3	2.14	-1.22
15,-6,12	16.02	1.41	-0.22	15,-6,12	16.06	1.68	-0.55
15,-3,3	10.22	5.9	-1.9	15,-3,3	12.02	4.63	-2.74
15,-3,6	10.21	0.3	-4.03	15,-3,6	13.82	2.13	-3.8
15,-3,9	14.65	-0.19	-1.26	15,-3,9	15.29	0.78	-2.11
15,-3,12	15.19	0.17	0.11	15,-3,12	15.57	1.08	-0.77
15,0,3	9.03	5.93	1.23	15,0,3	9.43	7.07	-3.38
15,0,6	7.02	-1.53	2.37	15,0,6	10.25	-0.65	-4.5
15,0,9	12.12	-2.45	1.16	15,0,9	16.6	-1.51	-2.1
15,0,12	14.46	0.18	0.85	15,0,12	15.95	0.35	-0.65
15,3,3	8.55	2.14	1.54	15,3,3	7.46	6.59	1.3
15,3,6	11.42	0.76	3.12	15,3,6	8.09	-2.43	1.46
15,3,9	14.52	0	2.46	15,3,9	16.42	-1.97	0.32
15,3,12	15.21	0.96	1.33	15,3,12	16.43	0.15	0.2
15,6,3	13.06	0.72	1.52	15,6,3	8.05	3.31	2.72
15,6,6	14.47	0.8	2.3	15,6,6	10.39	0.67	3.22
15,6,9	14.84	1.17	2.15	15,6,9	16.25	0.29	2
15,6,12	15.57	1.68	1.34	15,6,12	16.27	0.69	0.64
15,9,3	14.36	0.99	1	15,9,3	13.66	1.86	0.76
15,9,6	15.17	1.22	1.01	15,9,6	15.89	1.48	1.65
15,9,9	15.54	1.69	0.82	15,9,9	16.31	1.3	1.33
15,9,12	14.95	2.19	0.69	15,9,12	16.29	1.56	0.63
15,12,3	14.87	0.67	0.52	15,12,3	14.95	1.79	1.05
15,12,6	15.07	0.94	0.68	15,12,6	15.89	1.79	0.95
15,12,9	14.74	1.62	0.5	15,12,9	16.15	1.82	0.56
15,12,12	15.11	2.44	0.41	15,12,12	16.33	1.69	0.22
15,15,3	12.88	4.13	-1.13	15,15,3	15.21	1.86	0.34
15,15,6	13.81	2.87	-1.78	15,15,6	15.98	1.73	0.33
15,15,9	14.6	1.54	-1.24	15,15,9	16.1	1.96	0.13
15,15,12	15.38	1.19	-0.32	15,15,12	16.07	2.05	-0.13
Angle of attack = 40°				Angle of attack = 45°			
coord. (cm)	V _x (cm/s)	V _y (cm/s)	V _z (cm/s)	coord. (cm)	V _x (cm/s)	V _y (cm/s)	V _z (cm/s)
15,-15,3	15.87	1.72	-0.12	15,-15,3	2.28	-0.39	-2.5
15,-15,6	16.94	1.66	-0.43	15,-15,6	2.16	-0.81	-2.5
15,-15,9	17.11	1.34	-0.5	15,-15,9	1.99	-0.67	-2.5
15,-15,12	16.05	0.88	0.18	15,-15,12	1.71	-0.56	-2.5
15,-12,3	14.76	1.9	-0.31	15,-12,3	2.91	-0.38	-2
15,-12,6	15.97	1.32	-0.76	15,-12,6	2.34	-0.77	-2
15,-12,9	16.36	1.05	-0.71	15,-12,9	1.9	-0.86	-2
15,-12,12	16.29	0.98	-0.36	15,-12,12	1.46	-0.67	-2
15,-9,3	14.96	2.38	-0.44	15,-9,3	3.39	-0.45	-1.5
15,-9,6	15.4	1.93	-0.97	15,-9,6	2.75	-0.94	-1.5
15,-9,9	16.08	1.16	-0.87	15,-9,9	1.81	-1	-1.5
15,-9,12	15.85	0.61	-0.6	15,-9,12	1.2	-0.82	-1.5
15,-6,3	13.85	3.48	-1.65	15,-6,3	4.47	-1.4	-1
15,-6,6	14.54	2.27	-2.37	15,-6,6	3.27	-2.67	-1
15,-6,9	15.45	0.67	-1.6	15,-6,9	1.62	-2	-1
15,-6,12	15.8	0.5	-0.98	15,-6,12	0.76	-1.1	-1
15,-3,3	12.82	5.27	-3.61	15,-3,3	6.3	-3.82	-0.5
15,-3,6	14.5	1.38	-5.5	15,-3,6	2.88	-5.93	-0.5
15,-3,9	16.2	-0.84	-2.82	15,-3,9	0.25	-3.48	-0.5
15,-3,12	16.77	-0.8	-0.89	15,-3,12	-0.34	-1.34	-0.5
15,0,3	8.37	8.26	-1.64	15,0,3	9.88	-2.3	0
15,0,6	10.05	-3.03	-4.27	15,0,6	-0.64	-3.96	0
15,0,9	15.42	-4.4	-2.17	15,0,9	-3.63	-3.34	0

Contd...Table C.6: 3D velocity components for J1 type vane
(T/d = 0.67)

Angle of attack = 40°				Angle of attack = 45°			
coord. (cm)	V _r (cm/s)	V _θ (cm/s)	V _z (cm/s)	coord. (cm)	V _r (cm/s)	V _θ (cm/s)	V _z (cm/s)
15,0,12	16.79	-2.1	-0.09	15,0,12	-1.75	-0.81	0
15,3,3	8.81	7.08	-4.32	15,3,3	16.22	3.32	0.5
15,3,6	9.43	-2.12	3.97	15,3,6	-0.67	3.31	0.5
15,3,9	12.42	-4.48	0.92	15,3,9	-4.38	0.72	0.5
15,3,12	17.25	-2.24	1.24	15,3,12	-2.3	0.94	0.5
15,6,3	5.53	6.09	-4.1	15,6,3	6.48	3.71	1
15,6,6	7.47	-0.13	3.49	15,6,6	2.57	7.03	1
15,6,9	15.4	0.06	2.46	15,6,9	-0.93	3.26	1
15,6,12	17.1	-1.06	1.59	15,6,12	-0.7	1.84	1
15,9,3	14.17	2.39	-0.86	15,9,3	2.2	-0.59	1.5
15,9,6	16.65	1.76	1.62	15,9,6	1.52	3.67	1.5
15,9,9	17.04	1.06	1.67	15,9,9	-0.44	4.27	1.5
15,9,12	16.86	0.26	1.45	15,9,12	0.75	1.61	1.5
15,12,3	15.93	1.25	0.75	15,12,3	1.13	0.86	2
15,12,6	16.65	1.31	1.01	15,12,6	1.65	1.1	2
15,12,9	16.96	1.11	1.01	15,12,9	1.45	1.39	2
15,12,12	16.89	0.74	0.98	15,12,12	1.39	0.86	2
15,15,3	16.28	0.5	0.45	15,15,3	1.4	0.66	2.5
15,15,6	16.8	1.19	0.52	15,15,6	1.61	0.83	2.5
15,15,9	16.86	1.33	0.5	15,15,9	1.4	0.79	2.5
15,15,12	16.28	1.23	0.58	15,15,12	1.62	0.42	2.5

Angle of attack = 50°			
coord. (cm)	V _r (cm/s)	V _θ (cm/s)	V _z (cm/s)
15,-15,3	15.37	2.93	-0.33
15,-15,6	16.19	2.63	-0.56
15,-15,9	16.22	2.28	-0.53
15,-15,12	16.6	1.68	-0.6
15,-12,3	15.74	3.19	-0.35
15,-12,6	16.44	2.84	-0.71
15,-12,9	16.62	2.35	-0.74
15,-12,12	16.49	1.49	-0.65
15,-9,3	15.73	3.81	-0.35
15,-9,6	15.19	3	-0.68
15,-9,9	16.69	2.24	-0.93
15,-9,12	15.84	1.16	-0.88
15,-6,3	13.9	4.49	-1.19
15,-6,6	14.02	3	-2.32
15,-6,9	15.04	1.3	-1.62
15,-6,12	15.59	0.63	-0.9
15,-3,3	11.65	6.31	-2.88
15,-3,6	13	2.61	-4.84
15,-3,9	15.1	0.13	-2.9
15,-3,12	15.37	-0.1	-1.01
15,0,3	8.42	8.72	-2.82
15,0,6	5.9	0.12	-5.08
15,0,9	13.38	-3.08	-3.59
15,0,12	14.98	-1.63	-0.56
15,3,3	6.48	8.5	1.51
15,3,6	-1.44	-0.5	1.68
15,3,9	9.34	-5.21	-0.54
15,3,12	15.55	-2.64	0.54
15,6,3	6.52	5.41	4.93
15,6,6	7.47	3.12	5.01
15,6,9	9.19	-3.95	3.38
15,6,12	14.89	-2.12	2.58
15,9,3	6.52	3.04	-0.83
15,9,6	9.66	3.24	2.34
15,9,9	12.99	-0.44	2.45
15,9,12	15.09	0.75	1.61
15,12,3	14.17	1.08	0.23
15,12,6	14.72	1.37	2.37
15,12,9	14.79	1.07	2.45
15,12,12	14.76	1.44	1.64
15,15,3	14.62	0.7	0.78
15,15,6	14.73	0.61	0.75
15,15,9	14.58	1.19	0.96
15,15,12	14.53	2.7	0.58

**Table C.7: 3D velocity components for J2 type vane
(T/d = 0.67)**

Angle of attack = 30°				Angle of attack = 35°			
coord. (cm)	V _x (cm/s)	V _y (cm/s)	V _z (cm/s)	coord. (cm)	V _x (cm/s)	V _y (cm/s)	V _z (cm/s)
15,-15,3	14.46	1.76	-0.18	15,-15,3	15.87	3.81	-0.3
15,-15,6	15.12	1.61	-0.4	15,-15,6	16.4	3.69	-0.58
15,-15,9	15.56	1.41	-0.43	15,-15,9	17.32	3.71	-0.75
15,-15,12	15.91	1.35	-0.28	15,-15,12	17.1	3.52	-0.37
15,-12,3	14.26	2.12	-0.32	15,-12,3	15.82	4.21	-0.31
15,-12,6	15.14	1.58	-0.63	15,-12,6	16.67	3.64	-0.65
15,-12,9	15.56	1.37	-0.81	15,-12,9	17.06	3.5	-0.76
15,-12,12	15.1	1.25	-0.36	15,-12,12	17.2	3.21	-0.44
15,-9,3	13.31	1.98	-0.26	15,-9,3	16.44	4.78	-0.4
15,-9,6	13.99	1.75	-0.45	15,-9,6	16.35	4.06	-0.85
15,-9,9	15	1.47	-0.54	15,-9,9	17.63	3.58	-1.07
15,-9,12	14.47	1.16	-0.32	15,-9,12	16.4	2.91	-0.45
15,-6,3	12.38	2.85	-0.91	15,-6,3	12.37	4.73	-1.42
15,-6,6	13.3	1.96	-0.92	15,-6,6	14.08	4.11	-2.1
15,-6,9	13.93	1.19	-1.09	15,-6,9	15.22	2.79	-1.68
15,-6,12	14.34	0.72	-0.55	15,-6,12	16.07	2.34	-0.67
15,-3,3	11.13	3.66	-1.6	15,-3,3	11.46	6.5	-3.3
15,-3,6	12.14	1.99	-3.35	15,-3,6	13.64	2.77	-5.16
15,-3,9	13.36	0.1	-1.89	15,-3,9	15.34	1.38	-2.42
15,-3,12	14.34	0.25	-0.77	15,-3,12	15.91	1.7	-0.97
15,0,3	10.63	6.58	-3.42	15,0,3	6.49	8.13	-1.86
15,0,6	7.65	-1.04	-4.62	15,0,6	8.72	-1.64	-2.74
15,0,9	14.93	-2.51	-2	15,0,9	15.91	-1.68	-1.91
15,0,12	14.56	-0.65	-0.48	15,0,12	15.8	0.77	0.64
15,3,3	8.74	6.37	2.33	15,3,3	8.06	9.36	4.15
15,3,6	8.53	-0.99	4.23	15,3,6	10.33	-0.01	4.34
15,3,9	13.46	-3.23	0.78	15,3,9	15.01	-2.58	0.78
15,3,12	14.3	-0.86	0.51	15,3,12	16.19	0.47	0.75
15,6,3	7.91	2.68	2.12	15,6,3	8.12	4.74	2.21
15,6,6	11.01	0.74	3.36	15,6,6	9.8	2.47	3.95
15,6,9	14.58	-0.22	1.99	15,6,9	15.7	1.12	2.75
15,6,12	14.59	0.02	0.68	15,6,12	16.03	1.47	1.18
15,9,3	10.37	0.68	0.83	15,9,3	13.17	1.94	0.71
15,9,6	13.26	0.75	1.67	15,9,6	15.29	2.64	1.9
15,9,9	13.8	0.51	1.38	15,9,9	16.05	2.49	1.6
15,9,12	14.22	0.7	0.83	15,9,12	15.66	2.23	0.94
15,12,3	13.26	1.18	0.7	15,12,3	13.95	2.84	1.14
15,12,6	14.22	1.11	0.68	15,12,6	15.71	2.73	1.07
15,12,9	14.09	1.05	0.54	15,12,9	15.56	2.84	0.83
15,12,12	14.41	1.03	0.26	15,12,12	15.66	2.71	0.34
15,15,3	13.63	0.83	0.38	15,15,3	14.93	2.57	0.47
15,15,6	14.35	1.04	0.38	15,15,6	15.42	2.73	0.52
15,15,9	14.41	1.17	0.33	15,15,9	15.53	2.83	0.58
15,15,12	14.52	1.01	0.15	15,15,12	15.56	2.89	0.4
Angle of attack = 40°				Angle of attack = 45°			
coord. (cm)	V _x (cm/s)	V _y (cm/s)	V _z (cm/s)	coord. (cm)	V _x (cm/s)	V _y (cm/s)	V _z (cm/s)
15,-15,3	15.4	1.62	-0.4	15,-15,3	15.7	2.1	-0.66
15,-15,6	15.84	1.14	-0.81	15,-15,6	16.22	1.57	-0.88
15,-15,9	15.78	0.82	-0.83	15,-15,9	16.71	1.36	-1.01
15,-15,12	16.52	0.42	-0.79	15,-15,12	16.41	0.67	-1.04
15,-12,3	15.52	1.71	-0.47	15,-12,3	16.05	2.58	-0.49
15,-12,6	15.91	1.17	0.8	15,-12,6	15.54	2.14	-0.94
15,-12,9	15.99	0.78	-0.85	15,-12,9	15.99	1.12	-0.93
15,-12,12	16.45	0.55	-0.71	15,-12,12	16.81	0.69	-0.73
15,-9,3	13.73	1.97	-0.41	15,-9,3	15.15	3.09	-0.7
15,-9,6	15.57	1.63	-1.05	15,-9,6	16.11	2.21	-1.16
15,-9,9	15.81	0.8	-1.2	15,-9,9	15.65	0.84	-1.1
15,-9,12	16.3	0.26	-0.74	15,-9,12	16.09	0.28	-1.11
15,-6,3	14.02	3.36	-1.42	15,-6,3	15.21	4.23	-1.65
15,-6,6	15.1	1.67	-2.64	15,-6,6	15.06	2.59	-2.69
15,-6,9	15.82	0.19	-1.98	15,-6,9	15.84	0.66	-2.06
15,-6,12	16	-0.44	-0.88	15,-6,12	16.24	-0.12	-1.16
15,-3,3	13.32	5.64	-3.32	15,-3,3	12.95	6.39	-3.13
15,-3,6	14.34	1.53	-6	15,-3,6	12.68	2.7	-6.09
15,-3,9	15.66	-1.19	-3.02	15,-3,9	15.35	-1.05	-3.74
15,-3,12	16.02	-1.64	-1.21	15,-3,12	15.91	-1.37	-1.19
15,0,3	8.29	8.83	-1.82	15,0,3	8.65	9.29	-1.74
15,0,6	7.25	-1.43	-4.87	15,0,6	6.26	-0.63	-4.2
15,0,9	15.39	-4.79	-3.17	15,0,9	12.63	-4.65	-3.01

Contd...Table C.7: 3D velocity components for J2 type vane
(T/d = 0.67)

Angle of attack = 40°				Angle of attack = 45°			
coord. (cm)	V _x (cm/s)	V _y (cm/s)	V _z (cm/s)	coord. (cm)	V _x (cm/s)	V _y (cm/s)	V _z (cm/s)
15,0,12	16.62	-2.95	-0.87	15,0,12	15.98	-2.91	-0.66
15,3,3	8.49	9.35	3.25	15,3,3	8.53	9.66	2.66
15,3,6	8.07	-1.79	3.61	15,3,6	6.71	-0.92	3.2
15,3,9	11.46	-5.34	0.49	15,3,9	10.2	-4.84	1.77
15,3,12	16.55	-3.05	0.39	15,3,12	15.07	-3.03	0.97
15,6,3	6.99	4.32	2.71	15,6,3	9.22	6.94	2.6
15,6,6	9.91	1.19	5.14	15,6,6	8.24	0.57	4.93
15,6,9	12.75	-2.79	3.52	15,6,9	10.44	-1.43	3.21
15,6,12	16.22	-1.78	1.68	15,6,12	15.97	-1.46	2.31
15,9,3	11.97	2.79	-0.29	15,9,3	9.75	1.6	0.48
15,9,6	14.73	1.35	2.75	15,9,6	13.08	-0.33	2.65
15,9,9	16.1	-0.32	2.56	15,9,9	15.35	-0.63	2.87
15,9,12	16.19	-0.52	1.62	15,9,12	15.45	-0.29	2.16
15,12,3	14.88	0.48	1.04	15,12,3	13.3	-0.01	1.18
15,12,6	15.98	0.78	1.29	15,12,6	15.3	0.02	1.79
15,12,9	16.34	0.43	1.17	15,12,9	15.91	0.24	1.63
15,12,12	15.76	0.55	0.98	15,12,12	15.52	0.84	1.07
15,15,3	14.88	0.7	0.71	15,15,3	14.46	-0.19	0.71
15,15,6	15.92	0.54	0.79	15,15,6	15.8	0.15	0.76
15,15,9	16.48	0.56	0.73	15,15,9	15.56	0.45	0.72
15,15,12	16.12	0.68	0.62	15,15,12	14.02	0.83	0.42
Angle of attack = 50°							
coord. (cm)	V _x (cm/s)	V _y (cm/s)	V _z (cm/s)				
15,-15,3	15.12	2.45	-0.44				
15,-15,6	15.06	2.17	-0.76				
15,-15,9	15.4	2.06	-0.75				
15,-15,12	16.33	1.71	-0.62				
15,-12,3	14.86	2.8	-0.47				
15,-12,6	15.26	2.32	-0.93				
15,-12,9	15.72	1.75	-0.88				
15,-12,12	16.76	1.63	-0.85				
15,-9,3	14.93	3.48	-0.67				
15,-9,6	15.16	2.51	-1.33				
15,-9,9	16.16	1.91	-1.44				
15,-9,12	15.85	1.35	-1.12				
15,-6,3	13.44	4.77	-1.9				
15,-6,6	14.98	3.25	-2.91				
15,-6,9	15.3	1.29	-2.49				
15,-6,12	16.13	0.71	-1.57				
15,-3,3	12.64	7.46	-4.41				
15,-3,6	13.3	2.51	-6.56				
15,-3,9	15.68	0.23	-3.38				
15,-3,12	16.64	-0.4	-2.14				
15,0,3	5.15	9.4	-1.99				
15,0,6	6.79	-0.94	-5.26				
15,0,9	14.61	-1.02	-4				
15,0,12	16.73	-2.1	-1.57				
15,3,3	6.96	10.37	3.3				
15,3,6	4.77	-1.51	2.42				
15,3,9	11.76	-5.38	-0.07				
15,3,12	16.81	-2.53	0.07				
15,6,3	4.01	4.24	4.64				
15,6,6	9.07	4.89	6.66				
15,6,9	10.53	-2	3.34				
15,6,12	16.87	-1.61	1.68				
15,9,3	7.52	4.9	-1.92				
15,9,6	10.06	3.98	1.88				
15,9,9	14.7	0.11	3.15				
15,9,12	16.57	0.07	1.62				
15,12,3	13.87	1.66	0.07				
15,12,6	15.55	2.17	1.42				
15,12,9	16.45	1.44	1.72				
15,12,12	16.73	0.93	1.17				
15,15,3	15.12	1.44	0.73				
15,15,6	16.79	1.71	0.85				
15,15,9	17.01	1.55	0.73				
15,15,12	16.61	1.43	0.53				

Table C.8: 3D velocity components for rectangular vane with different aspect ratio
(Angle of attack = 400, T/d = 067)

Aspect ratio = 0.25				Aspect ratio = 0.5			
coord. (cm)	Vx (cm/s)	Vy (cm/s)	Vz (cm/s)	coord. (cm)	Vx (cm/s)	Vy (cm/s)	Vz (cm/s)
15,-15,3	15.33	1.23	-0.48	15,-15,3	15.64	4.13	-0.21
15,-15,6	16.42	0.97	-0.99	15,-15,6	16.29	3.65	-0.55
15,-15,9	16.48	0.5	-1	15,-15,9	16.47	3.21	-0.57
15,-15,12	16.59	0.1	-0.71	15,-15,12	16.24	2.74	-0.17
15,-12,3	14.94	1.86	-0.68	15,-12,3	15.04	4.37	-0.17
15,-12,6	15.79	1.14	-1.23	15,-12,6	15.6	3.76	-0.27
15,-12,9	16.22	0.59	-1.13	15,-12,9	15.67	3.04	-0.35
15,-12,12	16.66	0.04	-0.92	15,-12,12	15.96	2.64	-0.17
15,-9,3	14.76	2.68	-1.3	15,-9,3	13.78	4.51	-0.41
15,-9,6	15.38	1.24	-1.93	15,-9,6	14.58	3.57	-0.66
15,-9,9	15.85	0.2	-1.91	15,-9,9	15.36	2.84	-0.59
15,-9,12	15.83	-0.5	-1.15	15,-9,12	15.81	2.56	-0.25
15,-6,3	14.1	4.4	-2.82	15,-6,3	13.19	5.44	-1.42
15,-6,6	15.05	1.81	-3.93	15,-6,6	14.79	3.77	-2
15,-6,9	15.7	-0.59	-2.91	15,-6,9	15.36	2.43	-1.07
15,-6,12	16.23	-1.12	-1.77	15,-6,12	15.46	2.13	-0.3
15,-3,3	10.78	7.13	-6.2	15,-3,3	11.45	7	-3.93
15,-3,6	12.5	-0.75	-8.19	15,-3,6	10.4	1.63	-4.63
15,-3,9	16.29	-2.47	-4.58	15,-3,9	15.55	0.92	-1.95
15,-3,12	16.5	-2.37	-1.98	15,-3,12	15.87	1.78	-0.27
15,0,3	2.18	7.04	-2.64	15,0,3	4.98	5.88	-2.61
15,0,6	6.26	-3.36	-5.08	15,0,6	4.84	-1.96	-2.07
15,0,9	15.47	-5.91	-3.5	15,0,9	12.46	-1.4	-1.2
15,0,12	16.74	-4.21	-1.44	15,0,12	16.08	1.1	0.15
15,3,3	1.28	6.46	1.28	15,3,3	3.92	2.91	4.3
15,3,6	4.91	-4.42	-1.13	15,3,6	5.19	-2.44	3.21
15,3,9	13.73	-7.9	-0.99	15,3,9	13.63	-1.29	0.87
15,3,12	17.18	-4.94	-0.1	15,3,12	16.36	1.17	0.52
15,6,3	7.21	8.98	7.09	15,6,3	8.77	1.35	1.08
15,6,6	7.39	-0.72	6.87	15,6,6	14.38	0.91	2.43
15,6,9	11.65	-5.9	3.29	15,6,9	15.98	0.56	1.65
15,6,12	17.02	-4.09	1.82	15,6,12	15.81	1.79	0.71
15,9,3	5.15	5.24	2.72	15,9,3	13.8	1.16	1.05
15,9,6	9.32	3.11	6.19	15,9,6	16.17	1.41	1.36
15,9,9	13.22	-1.27	4.83	15,9,9	16.02	1.63	0.86
15,9,12	16.07	-1.86	2.54	15,9,12	15.27	2.58	0.83
15,12,3	14.1	2	-0.44	15,12,3	15.98	1.8	0.82
15,12,6	15.08	1.54	2.06	15,12,6	16.59	2.06	0.53
15,12,9	15.4	0.37	2.62	15,12,9	15.95	2.17	0.34
15,12,12	15.74	-0.37	1.78	15,12,12	15.28	3.08	0.47
15,15,3	14.22	0.71	1	15,15,3	16.41	2.3	0.16
15,15,6	15.48	0.54	1.16	15,15,6	17.06	2.66	0.2
15,15,9	15.78	0.45	1.25	15,15,9	16.61	2.69	-0.14
15,15,12	15.7	0.12	0.91	15,15,12	11.85	2.21	-0.28

Table C.9: 3D velocity components for trapezoidal vane with different taper angles(Angle of attack = 400, T/d = 0.67)

Taper angle (1H:1V)				Taper angle (3H:2.5V)			
coord. (cm)	Vx (cm/s)	Vy (cm/s)	Vz (cm/s)	coord. (cm)	Vx (cm/s)	Vy (cm/s)	Vz (cm/s)
15,-15,3	15.68	2.11	-0.51	15,-15,3	16.45	2.75	-0.74
15,-15,6	15.66	1.53	-0.8	15,-15,6	16.64	2.21	-0.85
15,-15,9	16.5	1.19	-0.84	15,-15,9	15.73	1.29	-0.61
15,-15,12	16.02	0.85	-0.6	15,-15,12	15.53	1.11	-0.45
15,-12,3	15.03	2.54	-0.5	15,-12,3	14.73	2.61	-0.63
15,-12,6	15.81	1.65	-0.69	15,-12,6	14.7	1.73	-0.53
15,-12,9	15.79	0.89	-0.78	15,-12,9	15.17	1.22	-0.75
15,-12,12	15.93	0.83	-0.55	15,-12,12	15.43	0.75	-0.47
15,-9,3	15.14	3.38	-1	15,-9,3	14.44	3.5	-1.24
15,-9,6	15.65	2.12	-1.34	15,-9,6	15.08	2.07	-1.68
15,-9,9	15.94	1.08	-1.13	15,-9,9	15.22	1.13	-1.14
15,-9,12	15.82	0.4	-0.77	15,-9,12	15.45	0.51	-0.75
15,-6,3	14.97	4.67	-2.01	15,-6,3	13.2	5.4	-2.85
15,-6,6	15.02	2.19	-2.65	15,-6,6	14.89	2.51	-4.65
15,-6,9	15.59	0.52	-1.87	15,-6,9	15.81	0.51	-2.64
15,-6,12	15.56	0.02	-0.78	15,-6,12	16.19	0.09	-1.28
15,-3,3	11.23	6.68	-4.17	15,-3,3	6.58	6.59	-4.12
15,-3,6	10.34	-0.49	-6.24	15,-3,6	6.25	-0.36	-4.65
15,-3,9	14.55	-1.1	-2.39	15,-3,9	14.55	-2.18	-3.44
15,-3,12	16.44	-0.78	-1.05	15,-3,12	15.55	-1	-1.35
15,0,3	1.66	5.54	-1.75	15,0,3	3.65	6.43	-0.55
15,0,6	3.28	-4.35	-3.5	15,0,6	2.66	-3.05	-2.44
15,0,9	14.59	-4.97	-1.93	15,0,9	11.58	-4.26	-1.73
15,0,12	16.65	-1.85	-0.49	15,0,12	16.21	-2.01	-0.74
15,3,3	3.35	6.57	3.21	15,3,3	4.4	5.83	3.54
15,3,6	4.8	-5.14	3	15,3,6	4.17	-3.6	2.04
15,3,9	14.35	-4.71	1.21	15,3,9	11.03	-3.96	0.36
15,3,12	16.71	-1.77	0.71	15,3,12	16.64	-1.73	0.14
15,6,3	5.27	3.89	4.12	15,6,3	3.96	4.3	4.21
15,6,6	7.01	-0.97	4.02	15,6,6	5.13	-1.68	3.8
15,6,9	16.31	-1.25	2.56	15,6,9	14.8	-2.1	1.52
15,6,12	16.44	-0.7	1.26	15,6,12	16.23	-0.81	0.76
15,9,3	13.06	0.81	0.77	15,9,3	13.47	0.69	-0.27
15,9,6	14.7	-0.01	2.52	15,9,6	15.12	0.35	1.71
15,9,9	16.06	0.12	1.9	15,9,9	15.95	-0.1	1.42
15,9,12	15.7	0.17	1.29	15,9,12	16.3	0	0.65
15,12,3	13.25	0.61	1.07	15,12,3	14.5	0.83	0.93
15,12,6	14	0.18	1.42	15,12,6	15.34	0.24	0.99
15,12,9	14.84	0.28	1.07	15,12,9	16.07	0.4	0.77
15,12,12	15.38	0.68	0.95	15,12,12	15.93	0.44	0.46
15,15,3	13.96	0.62	0.72	15,15,3	14.62	0.82	0.64
15,15,6	14.78	0.81	0.8	15,15,6	15.59	0.35	0.2
15,15,9	14.53	0.75	0.68	15,15,9	15.68	0.48	0.2
15,15,12	14.77	0.91	0.51	15,15,12	15.97	0.61	0.07

Contd...Table C.9: 3D velocity components for trapezoidal vane with different taper angles(Angle of attack = 400, T/d = 0.67)

Taper angle (4H:2V)			
coord. (cm)	Vx (cm/s)	Vy (cm/s)	Vz (cm/s)
15,-15,3	15.79	3.49	-0.39
15,-15,6	16.33	2.75	-0.55
15,-15,9	16.49	2.38	-0.54
15,-15,12	16.43	1.83	-0.09
15,-12,3	15.41	3.99	-0.81
15,-12,6	16.91	3.78	-1.25
15,-12,9	16.5	2.67	-0.79
15,-12,12	16.79	1.97	-0.58
15,-9,3	16.65	5.4	-0.95
15,-9,6	15.59	3.29	-1.39
15,-9,9	16.16	2.2	-1.23
15,-9,12	16.3	1.67	-0.6
15,-6,3	14.69	6.81	-2.47
15,-6,6	15.16	3.17	-4.46
15,-6,9	16.32	1.45	-2.5
15,-6,12	16.59	1.08	-0.88
15,-3,3	8.4	7.65	-4.37
15,-3,6	8.07	0.51	-4.83
15,-3,9	16.46	-1.6	-3.76
15,-3,12	16.75	-0.01	-0.8
15,0,3	2.49	6.69	-0.46
15,0,6	3.19	-1.94	-3.94
15,0,9	12.39	-3.93	-2.69
15,0,12	17.29	-0.97	-0.25
15,3,3	4.31	8.82	6.15
15,3,6	3.97	-0.57	3
15,3,9	10.59	-4.63	0.8
15,3,12	17.62	-0.9	1.12
15,6,3	1.44	7.58	2.69
15,6,6	4.82	2.34	4.74
15,6,9	13.08	-0.87	2.98
15,6,12	17.18	0.45	2.11
15,9,3	15.27	1.81	-1.1
15,9,6	15.2	3.69	1.69
15,9,9	16.7	2.03	2.21
15,9,12	16.7	1.81	1.84
15,12,3	16.32	1.79	0.79
15,12,6	16.41	2.03	1.21
15,12,9	16.47	2.51	1
15,12,12	16.79	2.5	0.88
15,15,3	16.35	2.19	0.54
15,15,6	16.62	2.61	0.42
15,15,9	16.31	2.55	0.38
15,15,12	16.53	2.84	0.38

EXPERIMENTAL DATA RELATING TO DIKE FORMATION AND DECAY OF STRENGTH OF VORTEX WITH DOWNSTREAM

This Appendix contains the experimental data collected in River Engineering Laboratory, Water Resources Development Training Centre, Indian Institute of Technology Roorkee, India. The data presented here have been used in Chapter 7 of this thesis. The Fig. D.1 indicates the sign convention and axes.

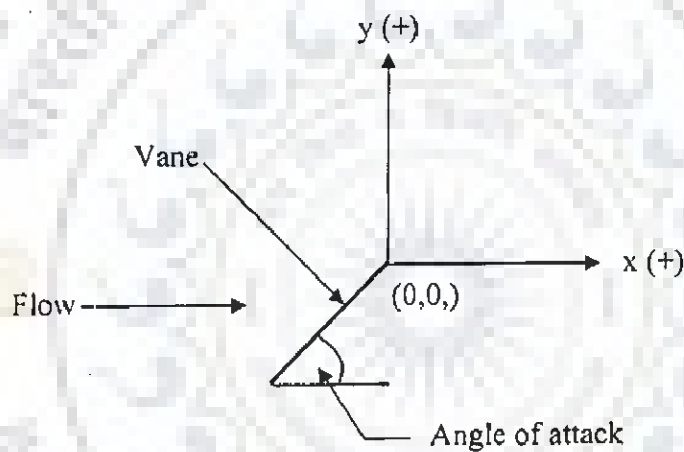


Fig. D.1 Definition sketch of origin for measurement of dike formation downstream of vane

Origin = Trailing edge of vane at initial bed level

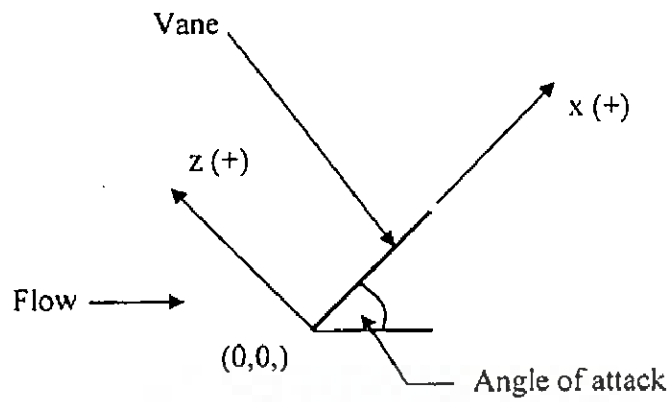


Fig. D.2 Definition sketch of origin for measurement of dike formation along the vane

Origin = Leading edge of vane at initial bed level

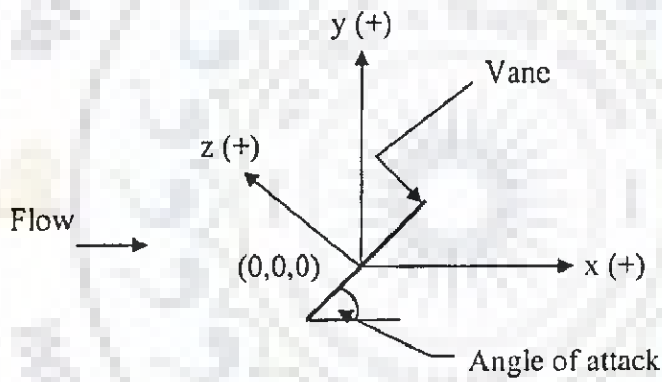


Fig. D.3 Definition sketch of origin for three dimensional velocity measurements

Origin = Middle bottom edge of vane at initial bed level

Table D.1: Experimental data relating to dike formation for rectangular and trapezoidal vanes

Rectangular vane		Trapezoidal vane					
		1H:1V		3H:2.5V		4H:2V	
x (cm)	y (cm)	x (cm)	y (cm)	x (cm)	y (cm)	x (cm)	y (cm)
16.5	3	18	6.4	24	5.5	18	2.2
26.5	3.7	22	6.4	34	5.4	23	2.7
36.5	2.3	32	4	44	2.9	28	2.3
46.5	0.4	42	2.7	54	0.6	38	0.1
56.5	-0.55	52	0.5	64	-0.2	48	-0.3
61.5	-1	62	-1.1	74	0.2	58	0
72.5	1.2	72	-1	84	-1	68	-1.65
82.5	0	82	-3.2	94	-2.6	78	-0.95
92.5	-2.2	92	-6	104	-1.6	89	-4.3
97.5	-4	102	-8.6	114	-4		
		112	-7.6	124	-3.6		
				134	-5.7		

Table D.2: Experimental data relating to dike formation along the rectangular vane in suction side (Angle of attack = 400, $F_r = 0.25$, $T/d = 0.57$)

Distance from the leading edge along the flow (cm)	Height of dike from initial bed level (cm)
0	-5.27
1.5	-4.52
3.5	-2.57
5.5	-0.97
7.5	0.73
9.75	2.83
10.5	2.03
11.5	0.98
12.5	0.08
13.5	-0.82
14	-1.22

**Table D.3: 3D velocity components for rectangular vane without collar
(Angle of attack = 400, Fr = 0.13, T/d = 0.57)**

10H				20H			
coord.	V _x	V _y	V _z	coord.	V _x	V _y	V _z
(cm)	(cm/s)	(cm/s)	(cm/s)	(cm)	(cm/s)	(cm/s)	(cm/s)
(-20, 3)	16.28	1.47	-1.51	(-20, 3)	16.95	1.46	-1.5
(-20, 8)	16.73	1.23	-0.13	(-20, 8)	17.14	1.11	0.06
(-15, 3)	17.15	1.56	-1.61	(-15, 3)	17.95	1.59	-1.66
(-15, 8)	17.18	1.44	-1.24	(-15, 8)	17.93	1.13	-0.2
(-10, 3)	16.51	1.58	-1.27	(-10, 3)	16.88	1.78	-1.4
(-10, 8)	17.05	1.2	-0.11	(-10, 8)	17.47	1.19	-0.21
(-5, 3)	17.86	2.13	-2.04	(-5, 3)	17.25	1.74	-1.67
(-5, 8)	17.63	1.28	-0.71	(-5, 8)	16.96	1.24	-0.56
(0, 3)	16.6	2.73	-3.46	(0, 3)	17.22	2.44	-2.08
(0, 8)	17.24	0.2	-1.94	(0, 8)	16.37	1.18	-1.27
(5, 3)	12.73	0	0	(5, 3)	15.29	0	0
(5, 8)	14.42	-1.73	-2.54	(5, 8)	15.03	0.56	-2.59
(10, 3)	8.92	0	0	(10, 3)	12.97	0	0
(10, 8)	12.61	-3.78	1.23	(10, 8)	12.34	-1.95	-1.13
(15, 3)	10.97	2.87	1.95	(15, 3)	13.75	3.73	1.08
(15, 8)	14.76	-0.29	2.1	(15, 8)	13.34	-1.43	1.41
(20, 3)	14.55	1.54	-0.05	(20, 3)	13.48	1.95	-0.27
(20, 8)	16.43	1.23	0.57	(20, 8)	13.44	0.24	1.3
30H				40H			
coord.	V _x	V _y	V _z	coord.	V _x	V _y	V _z
(cm)	(cm/s)	(cm/s)	(cm/s)	(cm)	(cm/s)	(cm/s)	(cm/s)
(-20, 3)	16.11	1.07	-1.65	(-20, 3)	14.93	0.84	-1.48
(-20, 8)	16.26	0.71	-0.07	(-20, 8)	15.26	0.86	-0.16
(-15, 3)	17.26	1.06	-1.52	(-15, 3)	15.36	1.31	-1.47
(-15, 8)	17.52	0.62	-0.2	(-15, 8)	17.19	1.05	-1.58
(-10, 3)	16.79	1.19	-1.49	(-10, 3)	15.8	1.18	-1.27
(-10, 8)	17.23	0.93	-0.29	(-10, 8)	16.84	1.01	-0.25
(-5, 3)	17.11	1.58	-1.33	(-5, 3)	15.91	1.4	-1.38
(-5, 8)	17.18	1.08	-0.55	(-5, 8)	16.28	1.1	-0.34
(0, 3)	16.72	2.06	-2.01	(0, 3)	16.32	2.03	-1.6
(0, 8)	15.44	0.94	-1	(0, 8)	15.69	1.14	-1.51
(5, 3)	15.66	0	0	(5, 3)	15.97	0	0
(5, 8)	14.51	0.73	-2.38	(5, 8)	13.79	0.74	-0.94
(10, 3)	14.18	0	0	(10, 3)	14.53	0	0
(10, 8)	13.36	-0.23	-2.34	(10, 8)	13.54	0.08	-0.24
(15, 3)	14.42	3.55	-1.95	(15, 3)	14.41	2.53	-0.29
(15, 8)	13.62	-0.22	-1.78	(15, 8)	13.81	0.1	0.98
(20, 3)	13.07	1.92	-0.09	(20, 3)	12.09	1.62	-0.62
(20, 8)	13.75	1	1.2	(20, 8)	13.06	0.76	0.84

Table D.4: 3D velocity components for rectangular vane with collar
 (Angle of attack = 400, Fr = 0.13, T/d = 0.57)

10H				20H			
coord.	V _x	V _y	V _z	coord.	V _x	V _y	V _z
(cm)	(cm/s)	(cm/s)	(cm/s)	(cm)	(cm/s)	(cm/s)	(cm/s)
(-20, 3)	16.92	1.71	-1.7	(-20, 3)	16.59	1.83	-1.64
(-20, 8)	17.2	1.38	-0.1	(-20, 8)	16.39	1.54	-0.27
(-15, 3)	17.25	2.06	-1.3	(-15, 3)	17.25	2.01	-1.29
(-15, 8)	17.09	1.42	0.03	(-15, 8)	17.31	1.57	0.06
(-10, 3)	17.4	2.1	-1.25	(-10, 3)	17.43	2.26	-1.16
(-10, 8)	17.22	1.52	0.16	(-10, 8)	17.59	1.62	0.24
(-5, 3)	17.61	2.43	-1.55	(-5, 3)	17.74	2.57	-1.46
(-5, 8)	17.34	1.58	-0.25	(-5, 8)	17.68	1.75	-0.26
(0, 3)	17.39	3	-3.3	(0, 3)	17.65	3.12	-2.18
(0, 8)	17.56	0.72	-1.53	(0, 8)	16.79	1.56	-1.07
(5, 3)	11.27	0	0	(5, 3)	15.76	0	0
(5, 8)	14.58	-1.99	-2.77	(5, 8)	14.53	0.43	-1.59
(10, 3)	11.55	0	0	(10, 3)	13.32	0	0
(10, 8)	13.32	-3.53	2.21	(10, 8)	13.31	-1.5	-0.59
(15, 3)	13.06	2.62	1.34	(15, 3)	13.91	3.51	0.94
(15, 8)	16.2	0.58	1.6	(15, 8)	14.11	-1.26	2.11
(20, 3)	16.24	1.6	-1.12	(20, 3)	14.45	1.63	0.12
(20, 8)	17.18	1.51	0.48	(20, 8)	15.54	1.28	0.96
30H				40H			
coord.	V _x	V _y	V _z	coord.	V _x	V _y	V _z
(cm)	(cm/s)	(cm/s)	(cm/s)	(cm)	(cm/s)	(cm/s)	(cm/s)
(-20, 3)	16.68	1.35	-1.92	(-20, 3)	16.12	1.51	-1.43
(-20, 8)	16.91	1.3	-0.22	(-20, 8)	16.4	1.53	0.04
(-15, 3)	17.62	1.77	-1.67	(-15, 3)	17.16	1.91	-1.63
(-15, 8)	17.53	1.45	0	(-15, 8)	17.49	1.48	-0.26
(-10, 3)	17.2	1.83	-1.67	(-10, 3)	17.5	1.94	-1.72
(-10, 8)	17.43	1.27	-0.25	(-10, 8)	17.66	1.8	-0.4
(-5, 3)	17.63	1.98	-1.8	(-5, 3)	17.2	2.47	-1.73
(-5, 8)	17.99	1.69	-1.58	(-5, 8)	16.67	1.49	-0.43
(0, 3)	17.56	2.55	-1.98	(0, 3)	16.93	2.62	-2.02
(0, 8)	16.11	1.32	-0.98	(0, 8)	15.55	1.35	0.65
(5, 3)	16.22	0	0	(5, 3)	15.7	0	0
(5, 8)	14.46	0.68	-1.13	(5, 8)	14.2	0.84	-1.04
(10, 3)	15.44	0	0	(10, 3)	15.03	0	0
(10, 8)	13.74	-0.31	0.07	(10, 8)	14.27	0.49	-0.17
(15, 3)	15.53	3.17	-0.02	(15, 3)	14.59	2.53	1.01
(15, 8)	14.57	0.06	1.28	(15, 8)	14.46	0.84	1.16
(20, 3)	13.91	1.96	0.3	(20, 3)	13.12	1.37	0.14
(20, 8)	14.58	1.27	0.96	(20, 8)	13.97	1.15	0.21

Table D.5: 3D velocity components for trapezoidal vane (1H:1V)
 (Angle of attack = 400, Fr = 0.13, T/d = 0.57)

10H				20H			
coord.	V _x	V _y	V _z	coord.	V _x	V _y	V _z
(cm)	(cm/s)	(cm/s)	(cm/s)	(cm)	(cm/s)	(cm/s)	(cm/s)
(-20, 3)	18.03	1.7	-0.14	(-20, 3)	18.12	1.74	-0.13
(-20, 8)	18.46	1.68	0.03	(-20, 8)	18.83	1.68	0.09
(-15, 3)	18.65	2.19	-0.16	(-15, 3)	18.85	2.12	-0.17
(-15, 8)	18.66	1.81	-0.01	(-15, 8)	18.54	1.84	-0.09
(-10, 3)	18.44	2.1	-0.12	(-10, 3)	17.75	2.35	-0.08
(-10, 8)	18.6	1.67	-0.14	(-10, 8)	18.12	2.02	-0.45
(-5, 3)	18.08	2.77	-0.68	(-5, 3)	17.19	2.8	-0.32
(-5, 8)	18.03	1.59	-0.69	(-5, 8)	16.45	2.12	-1
(0, 3)	15.56	3.56	-2.96	(0, 3)	15.73	3.49	-1
(0, 8)	15.72	-0.33	-2.45	(0, 8)	14.6	1.46	-1.24
(5, 3)	11.08	0	0	(5, 3)	14.59	0	0
(5, 8)	12.1	-3.16	-0.76	(5, 8)	13.25	0.13	-0.54
(10, 3)	12.77	0	0	(10, 3)	13.79	0	0
(10, 8)	14.14	-1.99	2.87	(10, 8)	13.93	0.02	1.03
(15, 3)	16.71	2.12	0.24	(15, 3)	12.85	1.99	0.88
(15, 8)	17.93	1.69	1.17	(15, 8)	15.01	0.8	1.21
(20, 3)	17.09	1.67	-0.03	(20, 3)	14.63	1.62	-0.16
(20, 8)	18.53	1.99	0.22	(20, 8)	16.85	1.7	0.07
30H				40H			
coord.	V _x	V _y	V _z	coord.	V _x	V _y	V _z
(cm)	(cm/s)	(cm/s)	(cm/s)	(cm)	(cm/s)	(cm/s)	(cm/s)
(-20, 3)	16.65	1.75	-0.04	(-20, 3)	17.79	1.45	-0.21
(-20, 8)	17.78	1.88	-0.16	(-20, 8)	18.64	1.6	0.02
(-15, 3)	16.85	1.84	0.31	(-15, 3)	18.23	1.87	0.05
(-15, 8)	18.39	1.78	-0.17	(-15, 8)	18.65	1.67	0.03
(-10, 3)	16.91	1.99	0.21	(-10, 3)	17.92	1.98	0.04
(-10, 8)	17.54	1.98	-0.3	(-10, 8)	18	1.54	0.13
(-5, 3)	16.95	2.52	0.05	(-5, 3)	17.9	2.2	-0.07
(-5, 8)	16.4	1.93	-0.61	(-5, 8)	17.17	1.76	-0.25
(0, 3)	16.37	2.83	-0.66	(0, 3)	17.2	2.56	-0.34
(0, 8)	15	1.23	-0.81	(0, 8)	16.38	1.52	-0.6
(5, 3)	16.54	0	0	(5, 3)	16.7	0	0
(5, 8)	14.94	0.48	-0.7	(5, 8)	15.74	1.08	-0.53
(10, 3)	16.2	0	0	(10, 3)	16.11	0	0
(10, 8)	15.79	0.11	1.09	(10, 8)	16.32	0.73	-0.01
(15, 3)	14.8	2.27	0.98	(15, 3)	14.65	2.04	0.63
(15, 8)	15.87	1.06	1.25	(15, 8)	15.91	1.12	0.73
(20, 3)	15.7	1.13	-0.01	(20, 3)	14.85	1.38	-0.15
(20, 8)	16.26	1.2	0.28	(20, 8)	16.21	1.57	-0.06

Table D.6: 3D velocity components for trapezoidal vane (3H:2.5V)
 (Angle of attack = 400, Fr = 0.13, T/d = 0.57)

10H				20H			
coord.	V _x	V _y	V _z	coord.	V _x	V _y	V _z
(cm)	(cm/s)	(cm/s)	(cm/s)	(cm)	(cm/s)	(cm/s)	(cm/s)
(-20, 3)	18.96	3	-1.17	(-20, 3)	19.93	3.01	-1.34
(-20, 8)	18.9	2.42	0.02	(-20, 8)	17.8	-0.85	0.67
(-15, 3)	19.15	3.13	-0.94	(-15, 3)	19.74	3.2	-1.26
(-15, 8)	18.98	2.65	0.2	(-15, 8)	19.78	2.39	0.21
(-10, 3)	19.05	3.45	-1.07	(-10, 3)	19.3	3.28	-1.21
(-10, 8)	18.43	2.61	0.31	(-10, 8)	18.72	2.23	0.24
(-5, 3)	18.39	4.17	-1.68	(-5, 3)	18.89	3.95	-1.52
(-5, 8)	18.28	2.52	-0.95	(-5, 8)	16.91	2.66	-0.48
(0, 3)	15.2	4.98	-2.32	(0, 3)	16.6	3.71	-0.49
(0, 8)	13.55	0.83	-1.97	(0, 8)	15.19	1.74	-0.46
(5, 3)	11.93	0	0	(5, 3)	15.67	0	0
(5, 8)	12.64	-1.54	-0.07	(5, 8)	14.73	0.99	-0.11
(10, 3)	12.65	0	0	(10, 3)	15.39	0	0
(10, 8)	14.99	-0.67	2.81	(10, 8)	15.34	0.68	1.03
(15, 3)	16.49	2.86	-0.7	(15, 3)	14.74	3.29	-0.22
(15, 8)	17.8	2.09	1.15	(15, 8)	16.13	1.65	1.23
(20, 3)	17.34	2.77	-1.29	(20, 3)	14.41	2.82	-0.58
(20, 8)	18.25	2.44	0.26	(20, 8)	16.59	2.42	0.61
30H				40H			
coord.	V _x	V _y	V _z	coord.	V _x	V _y	V _z
(cm)	(cm/s)	(cm/s)	(cm/s)	(cm)	(cm/s)	(cm/s)	(cm/s)
(-20, 3)	19	2.95	-1.54	(-20, 3)	18.23	2.4	-1.4
(-20, 8)	19.39	2.21	-0.34	(-20, 8)	16.65	2.14	-0.21
(-15, 3)	19.18	2.61	-1.44	(-15, 3)	18.56	2.55	-1.36
(-15, 8)	19.07	2.36	-0.33	(-15, 8)	18.34	2.41	-0.17
(-10, 3)	18.43	3.07	-1.24	(-10, 3)	17.77	3.15	-1.42
(-10, 8)	18.71	2.27	-0.06	(-10, 8)	17.69	2.38	-0.12
(-5, 3)	18.25	3.52	-1.3	(-5, 3)	17.73	3.17	-1.32
(-5, 8)	17.35	2.4	-0.13	(-5, 8)	16.15	2.12	-0.19
(0, 3)	17.02	3.3	-0.27	(0, 3)	16.47	2.8	-0.39
(0, 8)	16.11	1.93	-0.41	(0, 8)	15.85	1.94	-0.51
(5, 3)	17.16	0	0	(5, 3)	16.27	0	0
(5, 8)	15.75	1.44	-0.45	(5, 8)	15.62	1.62	-0.24
(10, 3)	16.25	0	0	(10, 3)	15.67	0	0
(10, 8)	16.04	1.29	0.68	(10, 8)	15.86	1.76	-0.87
(15, 3)	14.71	2.94	-0.48	(15, 3)	13.3	2.49	-0.88
(15, 8)	15.87	1.74	0.71	(15, 8)	14.98	1.72	0.56
(20, 3)	14.42	2.43	-0.96	(20, 3)	13.52	2.05	-1.3
(20, 8)	15.98	2.09	0.26	(20, 8)	14.65	2.07	-0.97

Table D.7: 3D velocity components for trapezoidal vane (4H:2V)
 (Angle of attack = 40°, Fr = 0.13, T/d = 0.57)

10H				20H			
coord.	V _x	V _y	V _z	coord.	V _x	V _y	V _z
(cm)	(cm/s)	(cm/s)	(cm/s)	(cm)	(cm/s)	(cm/s)	(cm/s)
(-20, 3)	18.65	1.83	-0.19	(-20, 3)	16.26	1.69	-2.35
(-20, 8)	19.37	2	0.05	(-20, 8)	17.8	1.73	-0.35
(-15, 3)	19.38	2.08	-0.04	(-15, 3)	17.02	1.75	-0.29
(-15, 8)	19.84	1.87	0.13	(-15, 8)	18.42	1.8	-0.32
(-10, 3)	19.47	2.39	-0.13	(-10, 3)	17.76	1.99	-0.2
(-10, 8)	18.74	1.91	0	(-10, 8)	18.63	1.97	-0.41
(-5, 3)	18.03	2.96	-0.62	(-5, 3)	18.9	2.87	-0.64
(-5, 8)	18.33	1.83	-0.86	(-5, 8)	18.18	2.02	-0.94
(0, 3)	16.12	3.58	-2.91	(0, 3)	17.42	3.26	-1.44
(0, 8)	16.66	0.44	-2.76	(0, 8)	16.12	1.72	-1.31
(5, 3)	11.12	0	0	(5, 3)	15.15	0	0
(5, 8)	12.51	-2.13	-1.45	(5, 8)	13.66	0.05	-0.98
(10, 3)	11.95	0	0	(10, 3)	14.03	0	0
(10, 8)	14.43	-2.62	2.47	(10, 8)	13.75	-0.95	1.13
(15, 3)	14.11	2.51	1.09	(15, 3)	13.97	2.92	1.44
(15, 8)	16.43	1.11	1.4	(15, 8)	15.35	0.36	1.54
(20, 3)	15.54	1.65	0.33	(20, 3)	14.67	1.75	0.18
(20, 8)	17.72	1.89	0.23	(20, 8)	17.11	1.72	0.22
30H				40H			
coord.	V _x	V _y	V _z	coord.	V _x	V _y	V _z
(cm)	(cm/s)	(cm/s)	(cm/s)	(cm)	(cm/s)	(cm/s)	(cm/s)
(-20, 3)	17.04	1.37	-0.12	(-20, 3)	17.52	1.6	-0.43
(-20, 8)	18.35	1.38	-0.27	(-20, 8)	18.23	1.59	-0.33
(-15, 3)	16.93	1.48	0.17	(-15, 3)	17.3	1.77	-0.22
(-15, 8)	19.12	1.48	0.14	(-15, 8)	18.88	1.73	-0.42
(-10, 3)	17.28	1.68	0.1	(-10, 3)	17.37	1.91	-0.13
(-10, 8)	19	1.98	-0.21	(-10, 8)	18.34	1.84	-0.33
(-5, 3)	17.58	2.29	0.06	(-5, 3)	18.15	2.32	-0.19
(-5, 8)	17.68	1.94	-0.48	(-5, 8)	17.84	1.92	-0.28
(0, 3)	17.59	2.72	-0.51	(0, 3)	17.57	2.71	-0.47
(0, 8)	16.14	1.62	-0.9	(0, 8)	16.43	1.6	-0.56
(5, 3)	16.46	0	0	(5, 3)	17.12	0	0
(5, 8)	15.29	1.13	-0.77	(5, 8)	15.82	1.25	-0.68
(10, 3)	15.64	0	0	(10, 3)	17.1	0	0
(10, 8)	15.2	0.27	0.69	(10, 8)	16.29	1.88	0.04
(15, 3)	15.32	3.09	1.25	(15, 3)	15.87	2.35	0.65
(15, 8)	15.23	0.89	1.48	(15, 8)	16.6	1.19	0.71
(20, 3)	13.58	1.77	0.43	(20, 3)	15.56	1.44	-0.15
(20, 8)	15.14	1.78	0.54	(20, 8)	16.17	1.66	0.12

Table D.8: 3D velocity components for rectangular vane without collar
(Angle of attack = 40°, Fr = 0.25, T/d = 0.57)

10H				20H			
coord.	V _x	V _y	V _z	coord.	V _x	V _y	V _z
(cm)	(cm/s)	(cm/s)	(cm/s)	(cm)	(cm/s)	(cm/s)	(cm/s)
(-20, 3)		3.25	-0.83	(-20, 3)		3.96	-1.06
(-20, 8)		3.64	-0.36	(-20, 8)		4.32	0.24
(-15, 3)		4.03	-0.51	(-15, 3)		5.12	-0.23
(-15, 8)		3.34	-0.55	(-15, 8)		4.63	0
(-10, 3)		4.86	-1.69	(-10, 3)		6.11	0.63
(-10, 8)		2.79	-2.41	(-10, 8)		4.31	-0.81
(-5, 3)		8.32	-2.32	(-5, 3)		7.17	0.23
(-5, 8)		0.14	-3.28	(-5, 8)		3.84	-0.14
(0, 3)		10.58	2.68	(0, 3)		9.75	-0.04
(0, 8)		-3.79	1.59	(0, 8)		3.93	0.19
(5, 3)		0	0	(5, 3)		0	0
(5, 8)		1.15	4.66	(5, 8)		4.35	3.36
(10, 3)		0	0	(10, 3)		0	0
(10, 8)		5.29	0.34	(10, 8)		6.01	0.54
(15, 3)		5.59	-2.06	(15, 3)		3.95	-2.11
(15, 8)		3.54	0.1	(15, 8)		4.48	-0.9
(20, 3)		-0.78	-0.85	(20, 3)		4.52	-0.83
(20, 8)		4.23	0.9	(20, 8)		3.5	0.11
30H				40H			
coord.	V _x	V _y	V _z	coord.	V _x	V _y	V _z
(cm)	(cm/s)	(cm/s)	(cm/s)	(cm)	(cm/s)	(cm/s)	(cm/s)
(-20, 3)		3.21	2.23	(-20, 3)		3.3	-1.78
(-20, 8)		4.51	0.77	(-20, 8)		3.73	-0.86
(-15, 3)		4.63	1.41	(-15, 3)		3.37	-1.18
(-15, 8)		5.07	0.8	(-15, 8)		3.39	-0.55
(-10, 3)		6.96	1.66	(-10, 3)		3.03	1.23
(-10, 8)		5.49	0.14	(-10, 8)		4.25	0.15
(-5, 3)		8.33	-0.1	(-5, 3)		3.35	-0.18
(-5, 8)		5.23	-0.27	(-5, 8)		4.22	0.32
(0, 3)		8.1	0.1	(0, 3)		2.7	-1.29
(0, 8)		4.96	0.28	(0, 8)		4.03	0.23
(5, 3)		0	0	(5, 3)		0	0
(5, 8)		4.36	1.16	(5, 8)		3.56	0.63
(10, 3)		0	0	(10, 3)		0	0
(10, 8)		3.88	0.79	(10, 8)		3.6	0.19
(15, 3)		3.43	-1.67	(15, 3)		3.15	-1.13
(15, 8)		4.01	-0.74	(15, 8)		3.67	-0.1
(20, 3)		4.12	-1.29	(20, 3)		1.04	-1.35
(20, 8)		3.5	-0.61	(20, 8)		3.57	-0.47

Table D.9: 3D velocity components for rectangular vane with collar
 (Angle of attack = 400, Fr = 0.25, T/d = 0.57)

10H				20H			
coord.	V _x	V _y	V _z	coord.	V _x	V _y	V _z
(cm)	(cm/s)	(cm/s)	(cm/s)	(cm)	(cm/s)	(cm/s)	(cm/s)
(-20, 3)		2.21	-1.67	(-20, 3)		2.48	-2.22
(-20, 8)		1.92	-0.11	(-20, 8)		2.57	-0.44
(-15, 3)		2.92	-1.26	(-15, 3)		2.67	-1.56
(-15, 8)		2.23	-0.15	(-15, 8)		2.7	-0.38
(-10, 3)		3.66	-1.89	(-10, 3)		3.72	-1.62
(-10, 8)		2.64	-1.09	(-10, 8)		3.14	-1.19
(-5, 3)		5.37	-3.46	(-5, 3)		4.98	-1.45
(-5, 8)		2.23	-2.69	(-5, 8)		2.79	-1.46
(0, 3)		6.65	-3.99	(0, 3)		6.31	-0.44
(0, 8)		0.71	-3.4	(0, 8)		2.98	-0.86
(5, 3)		0	0	(5, 3)		0	0
(5, 8)		-4.03	3.4	(5, 8)		3.23	2.93
(10, 3)		0	0	(10, 3)		0	0
(10, 8)		2.32	3.58	(10, 8)		4.41	3.25
(15, 3)		2.55	-2.64	(15, 3)		1.63	-3.24
(15, 8)		3.25	-0.14	(15, 8)		3.59	-0.88
(20, 3)		2.45	-1.4	(20, 3)		2.57	-1.31
(20, 8)		2.56	-0.05	(20, 8)		2.93	-0.86
30H				40H			
coord.	V _x	V _y	V _z	coord.	V _x	V _y	V _z
(cm)	(cm/s)	(cm/s)	(cm/s)	(cm)	(cm/s)	(cm/s)	(cm/s)
(-20, 3)		2.03	-2.42	(-20, 3)		2.58	-1.78
(-20, 8)		2.61	-0.83	(-20, 8)		2.95	-0.45
(-15, 3)		2.82	-2.09	(-15, 3)		3.26	-0.45
(-15, 8)		2.69	-0.97	(-15, 8)		3.15	-0.26
(-10, 3)		3.4	-0.08	(-10, 3)		3.27	-0.2
(-10, 8)		3.16	-0.23	(-10, 8)		3.03	0.27
(-5, 3)		4.13	0.58	(-5, 3)		3.55	-1.21
(-5, 8)		3.69	-0.02	(-5, 8)		3.01	0.24
(0, 3)		3.01	-0.4	(0, 3)		3	-1.37
(0, 8)		3.3	1	(0, 8)		3.17	0.21
(5, 3)		0	0	(5, 3)		0	0
(5, 8)		3.06	2.36	(5, 8)		2.29	0.2
(10, 3)		0	0	(10, 3)		0	0
(10, 8)		3.08	1.35	(10, 8)		2.44	0.37
(15, 3)		1.25	1.03	(15, 3)		-0.06	-2.99
(15, 8)		2.9	0.01	(15, 8)		2.63	-0.51
(20, 3)		3.46	-1.49	(20, 3)		1.04	-3.12
(20, 8)		3	-0.55	(20, 8)		1.59	-1.58

Table D.10: 3D velocity components for trapezoidal vane (1H:1V)
 (Angle of attack = 400, Fr = 0.25, T/d = 0.57)

10H				20H			
coord.	V _x	V _y	V _z	coord.	V _x	V _y	V _z
(cm)	(cm/s)	(cm/s)	(cm/s)	(cm)	(cm/s)	(cm/s)	(cm/s)
(-20, 3)		2.13	-1.88	(-20, 3)		1.26	1
(-20, 8)		2.29	-0.94	(-20, 8)		3.14	0.15
(-15, 3)		1.52	0.02	(-15, 3)		3.58	0.18
(-15, 8)		2.02	-0.67	(-15, 8)		3.79	-0.08
(-10, 3)		2.33	0.46	(-10, 3)		4.6	1.2
(-10, 8)		2.29	-0.9	(-10, 8)		3.96	-0.03
(-5, 3)		5.21	1.12	(-5, 3)		5.33	0.45
(-5, 8)		1.6	-0.94	(-5, 8)		3.67	-0.5
(0, 3)		5.74	2.28	(0, 3)		6.09	-0.2
(0, 8)		0.73	-0.48	(0, 8)		3.9	-0.03
(5, 3)		0	0	(5, 3)		0	0
(5, 8)		1.13	3.05	(5, 8)		3.23	-0.11
(10, 3)		0	0	(10, 3)		0	0
(10, 8)		5.91	4.12	(10, 8)		2.68	1.2
(15, 3)		3.06	1.8	(15, 3)		1.35	0.47
(15, 8)		5.19	0.72	(15, 8)		2.48	0.58
(20, 3)		2.17	0.2	(20, 3)		3.27	0.63
(20, 8)		3.54	0.45	(20, 8)		2.33	-0.53
30H				40H			
coord.	V _x	V _y	V _z	coord.	V _x	V _y	V _z
(cm)	(cm/s)	(cm/s)	(cm/s)	(cm)	(cm/s)	(cm/s)	(cm/s)
(-20, 3)		2.34	-0.47	(-20, 3)		0.44	-1.02
(-20, 8)		3.05	-0.4	(-20, 8)		1.73	-0.16
(-15, 3)		2.76	0.51	(-15, 3)		1.17	-0.25
(-15, 8)		3.25	0.06	(-15, 8)		1.49	0
(-10, 3)		2.35	0.31	(-10, 3)		0.54	0.86
(-10, 8)		3.32	-0.04	(-10, 8)		2.09	0.77
(-5, 3)		2.45	0.61	(-5, 3)		1.16	0.19
(-5, 8)		2.8	0.12	(-5, 8)		2.28	0.7
(0, 3)		3.15	0.51	(0, 3)		2.19	0.33
(0, 8)		2.41	0	(0, 8)		2.08	0.61
(5, 3)		0	0	(5, 3)		0	0
(5, 8)		2.34	0.41	(5, 8)		1.97	0.75
(10, 3)		0	0	(10, 3)		0	0
(10, 8)		2.18	0.6	(10, 8)		1.72	0.87
(15, 3)		1.62	0.71	(15, 3)		1.43	0.7
(15, 8)		2.31	0.46	(15, 8)		1.96	0.97
(20, 3)		1.95	-0.37	(20, 3)		1.93	-0.1
(20, 8)		2.17	-0.7	(20, 8)		1.91	-0.38

Table D.11: 3D velocity components for trapezoidal vane (3H:2.5V)
 (Angle of attack = 400, Fr = 0.25, T/d = 0.57)

10H				20H			
coord.	V _x	V _y	V _z	coord.	V _x	V _y	V _z
(cm)	(cm/s)	(cm/s)	(cm/s)	(cm)	(cm/s)	(cm/s)	(cm/s)
(-20, 3)		2.64	-0.62	(-20, 3)		3.77	0.23
(-20, 8)		3.57	0.42	(-20, 8)		4.45	0.41
(-15, 3)		3.08	0.43	(-15, 3)		3.6	1.92
(-15, 8)		3.51	0.56	(-15, 8)		4.6	0.95
(-10, 3)		4.75	-0.22	(-10, 3)		5.64	2.32
(-10, 8)		4.21	-0.29	(-10, 8)		4.85	0.96
(-5, 3)		7.57	-0.9	(-5, 3)		7.1	1.9
(-5, 8)		3.28	-1.42	(-5, 8)		5.46	0.5
(0, 3)		8.25	0.84	(0, 3)		7.68	-0.02
(0, 8)		0.98	-1.51	(0, 8)		5.25	0.16
(5, 3)		0	0	(5, 3)		0	0
(5, 8)		0.2	1.9	(5, 8)		5.16	1.29
(10, 3)		0	0	(10, 3)		0	0
(10, 8)		4.34	4.86	(10, 8)		4.65	3.19
(15, 3)		3.13	1.44	(15, 3)		2.17	-0.82
(15, 8)		3.96	0.24	(15, 8)		4.44	0.49
(20, 3)		4.93	0.06	(20, 3)		3.4	-1.27
(20, 8)		4.77	1.19	(20, 8)		4.44	0.44
30H				40H			
coord.	V _x	V _y	V _z	coord.	V _x	V _y	V _z
(cm)	(cm/s)	(cm/s)	(cm/s)	(cm)	(cm/s)	(cm/s)	(cm/s)
(-20, 3)		2.97	-2.85	(-20, 3)		3.71	-1.53
(-20, 8)		3.96	0.26	(-20, 8)		4.01	-0.62
(-15, 3)		5.15	4.07	(-15, 3)		3.43	-1.22
(-15, 8)		4.07	1.23	(-15, 8)		4.05	-0.1
(-10, 3)		3.92	1.72	(-10, 3)		3.03	-0.91
(-10, 8)		4.83	0.79	(-10, 8)		3.92	-0.33
(-5, 3)		4.62	-0.48	(-5, 3)		4.26	-0.69
(-5, 8)		4.75	0.58	(-5, 8)		4.12	0.23
(0, 3)		5.62	-0.76	(0, 3)		4.14	-0.21
(0, 8)		4.69	0.71	(0, 8)		4.01	0.33
(5, 3)		0	0	(5, 3)		0	0
(5, 8)		5.12	1.63	(5, 8)		3.52	0.65
(10, 3)		0	0	(10, 3)		0	0
(10, 8)		3.95	1.7	(10, 8)		3.61	0.6
(15, 3)		2.18	0.6	(15, 3)		2.52	-1.46
(15, 8)		3.79	0.74	(15, 8)		3.96	0.24
(20, 3)		2.8	-1.23	(20, 3)		2.84	-2.25
(20, 8)		3.12	-0.67	(20, 8)		3.19	-0.89

Table D.12: 3D velocity components for trapezoidal vane (4H:2V)
 (Angle of attack = 400, Fr = 0.25, T/d = 0.57)

10H				20H			
coord.	V _x	V _y	V _z	coord.	V _x	V _y	V _z
(cm)	(cm/s)	(cm/s)	(cm/s)	(cm)	(cm/s)	(cm/s)	(cm/s)
(-20, 3)		2.82	0.35	(-20, 3)		2.37	-1.13
(-20, 8)		2.96	-0.16	(-20, 8)		3.08	-0.51
(-15, 3)		4	-0.22	(-15, 3)		2.79	0.12
(-15, 8)		2.55	-0.38	(-15, 8)		3.24	-0.84
(-10, 3)		4.28	2.86	(-10, 3)		3.77	1.23
(-10, 8)		2.83	-0.29	(-10, 8)		3.46	-0.83
(-5, 3)		6.38	0.69	(-5, 3)		5.79	1.35
(-5, 8)		5.29	-0.82	(-5, 8)		3.24	0.07
(0, 3)		9.47	0.38	(0, 3)		5.07	0.31
(0, 8)		3.73	-1.57	(0, 8)		3.9	0.04
(5, 3)		0	0	(5, 3)		0	0
(5, 8)		3.28	4.28	(5, 8)		3.3	1.45
(10, 3)		0	0	(10, 3)		0	0
(10, 8)		5.2	1.42	(10, 8)		2.94	1.1
(15, 3)		2.12	-1.25	(15, 3)		1.36	0.75
(15, 8)		3.89	-0.78	(15, 8)		3.06	-0.14
(20, 3)		2.51	0.28	(20, 3)		2.96	-0.68
(20, 8)		3.68	0.1	(20, 8)		3.42	-0.55
30H				40H			
coord.	V _x	V _y	V _z	coord.	V _x	V _y	V _z
(cm)	(cm/s)	(cm/s)	(cm/s)	(cm)	(cm/s)	(cm/s)	(cm/s)
(-20, 3)		1.75	0.29	(-20, 3)		2.44	-0.24
(-20, 8)		2.83	-0.29	(-20, 8)		3.12	-0.54
(-15, 3)		3.22	-0.13	(-15, 3)		2.33	-0.41
(-15, 8)		3.3	-0.45	(-15, 8)		3.14	-0.57
(-10, 3)		3.22	0.07	(-10, 3)		2.62	-0.07
(-10, 8)		3.39	-0.07	(-10, 8)		3.21	-0.33
(-5, 3)		3.49	0.97	(-5, 3)		3.02	0.02
(-5, 8)		3.5	-0.02	(-5, 8)		3.36	0.05
(0, 3)		3.99	0.32	(0, 3)		3.36	0.28
(0, 8)		3.13	0.21	(0, 8)		2.81	0.15
(5, 3)		0	0	(5, 3)		0	0
(5, 8)		2.49	1.13	(5, 8)		2.65	0.32
(10, 3)		0	0	(10, 3)		0	0
(10, 8)		2.55	0.8	(10, 8)		2.44	0.37
(15, 3)		1.76	-0.1	(15, 3)		2.18	-0.48
(15, 8)		2.81	-0.52	(15, 8)		2.81	-0.15
(20, 3)		2.44	-0.52	(20, 3)		2.29	-0.81
(20, 8)		2.75	-0.6	(20, 8)		2.48	-0.63